

FORECASTING EARTHQUAKE LOSSES IN PORT SYSTEMS

A Dissertation
Presented to
The Academic Faculty

by

Lindsay Ivey Burden

In Partial Fulfillment
of the Requirements for the Degree
Doctor of Philosophy in the
School of Civil and Environmental Engineering

Georgia Institute of Technology
February 2012

FORECASTING EARTHQUAKE LOSSES IN PORT SYSTEMS

Approved by:

Dr. Glenn J. Rix, Advisor
School of Civil and Environmental
Engineering
Georgia Institute of Technology

Dr. Reginald DesRoches
School of Civil and Environmental
Engineering
Georgia Institute of Technology

Dr. Dominic Assimaki
School of Civil and Environmental
Engineering
Georgia Institute of Technology

Dr. Alan Erera
School of Industrial Systems
Engineering
Georgia Institute of Technology

Mr. Stuart D. Werner
President
*Seismic Systems and Engineering
Consultants*

Date Approved: February 17th, 2012

For my parents, who taught me to live life by following my passions. I know you were hoping I'd be passionate about music, but it turned out to be earthquakes.

ACKNOWLEDGEMENTS

When I began my PhD program at Georgia Tech, the completion of my dissertation was merely a distance dream. Now that actually finishing has become reality, as I look back upon my journey it is apparent that I could have never gotten here on my own. There are numerous people that have helped me to get to this point and I would like to express my appreciation to them.

First and foremost, I would like to thank Dr. Glenn Rix. I feel extremely privileged that you are my advisor because seismic risk analysis is but a fraction of what I've learned from you. You have taught me by example how to be well respected within the academic profession, and that achieving any goal takes hard work, patience, and persistence. To my committee members Dr. Dominic Assimaki, Dr. Reginald DesRoches, Dr. Alan Erera, and Stu Werner: Thank you. Your insights and comments have greatly improved the quality of my work, and I appreciate your time and dedication.

My research would have never been possible without the contributions of my fellow graduate students within the Ports Grand Challenge Project. Antonios, Varun, Rachelle, Emily, Aykagan, Ben, and Laura: thank you for your hard work, and hopefully you get some satisfaction in knowing that I have read each of your theses. A special thanks should be granted to Yu-Shiu Lin because your help in integrating the BQCSP program into the Risk Analysis was invaluable. Also, an extra special thanks needs to be granted to Abdollah Shafieezadeh. Of everyone, you were most privy to my bouts of impatience while we waited for data, and I would like to thank you for your expedience in processing that data once you received it. Moreover, I would like to thank you for answering each and every one of my many questions.

I would like to acknowledge the project sponsors. The material presented in this research is based upon work supported by the NEESR program of the National Science Foundation under Grants No. CMS-0530478 and CMS-0402490, Project Title "NEESR-

GC: Seismic Risk Mitigation for Port Systems". Any opinions, findings, and conclusions or recommendations expressed in this material are those of the author and do not necessarily reflect the views of NSF.

My journey to graduation would not have been nearly as enjoyable if not for the professors and my fellow students in the Geotechnical department. Because of you, I can look back fondly on my experience at Tech. This sentiment is especially applicable to Robert Hurt and Nortey Yeboah, I very much enjoyed our random lunch trips and football Saturdays in the South. To Laura Spencer: After I visited Tech during recruitment weekend in 2006, I knew two things for certain: 1.) I was going to be a yellowjacket, and 2.) We would be great friends. Your friendship was a huge part of what made grad school so enjoyable for me, and I thank you for that.

Finally, I'd like to thank my entire family for their continual support, and I'd like you to know that your influences have shaped my life path. Granddad Pete thank you for letting me use your tools and cultivating my desire to design and build. Dad, thank you for raising me as a proper nerd. My analytical mind is a byproduct of yours. Mom, because of you, I've gotten up every morning with a smile on my face and looked them in the eye. The woman I am today is a byproduct of you. To my husband Derek: Thank you for never doubting or questioning my goals. Your love and support has helped me to finally achieve a lifelong dream and I consider myself lucky to be on life's journey with you.

TABLE OF CONTENTS

ACKNOWLEDGEMENTS.....	V
LIST OF TABLES.....	XII
LIST OF FIGURES	XV
LIST OF ABBREVIATIONS.....	XXV
SUMMARY	XXVII
1. INTRODUCTION	1
1.1. Motivation.....	1
1.2. Objectives and Scope.....	6
1.3. Dissertation Outline	7
2. LITERATURE REVIEW	9
2.1. Historical Examples of Earthquake Damage in Ports.....	9
2.1.1. Historical Earthquake Occurrences in Ports	9
2.1.2. Common Modes of Damage	10
2.1.2.1. Wharves	10
2.1.2.2. Cranes	13
2.1.2.3. Embankments.....	14
2.1.2.4. Utility and Transportation Lifelines.....	15
2.2. Review of Current Design Guidelines	16
2.2.1. PIANC	17
2.2.2. Port of Los Angeles Code	19
2.2.3. American Society of Civil Engineers	22
2.2.3.1. Geotechnical Hazards	24
2.2.3.2. Force-based Analysis and Design.....	25
2.2.3.3. Displacement-based Analysis and Design	26
2.2.3.4. Ancillary Components (Cranes)	26
2.2.4. Liftech Crane Guidelines	27
2.3. Prior Studies in Risk Assessment	28
2.3.1. Werner and Taylor, 2004	28
2.3.1.1. Overview of acceptable risk approach.....	29
2.3.1.2. Results.....	34
2.3.2. Pachakis and Kiremidjian, 2004	36
2.3.2.1. Assessment.....	36
2.3.2.2. Results.....	39
2.3.3. Na and Shinozuka, 2009	40
2.3.3.1. Response of Quay Walls.....	40

2.3.3.2.	Effects of Spatial Variation in Soil Parameters in the Performance of Port Structures.....	41
2.3.3.3.	Simulation-based Port Losses.....	42
2.4.	Gaps in Knowledge.....	44
3.	SEISMIC RISK ASSESSMENT FRAMEWORK.....	47
3.1.	Performance-Based Engineering.....	47
3.1.1.	Performance-Based Earthquake Engineering and Uncertainty.....	47
3.1.2.	Previous Methods for Assessing Performance.....	48
3.1.3.	PEER Framework.....	53
3.1.3.1.	Response, Damage, and Loss Models.....	54
3.1.3.2.	Fragility Curves.....	55
3.2.	Risk Analysis Framework Applicable to this Study.....	56
3.2.1.	Probabilistic Analysis.....	61
3.2.1.1.	Conventional Monte Carlo Sampling.....	61
3.2.1.2.	Stratified Monte Carlo Sampling.....	66
3.2.2.	Scenario-Based Analysis.....	69
3.2.3.	Intensity-Based Analysis.....	70
3.3.	Seismic Hazard.....	70
3.3.1.	Earthquake Rupture Forecast.....	71
3.3.2.	Ground Motion Prediction Equation.....	72
3.3.3.	Ground Motion Spatial Correlation Model.....	72
3.3.3.1.	Spatial Correlation.....	72
3.3.3.2.	Spectral Correlation.....	75
3.3.4.	Intra-event and Inter-event Residuals.....	76
3.4.	Component Fragility.....	77
3.4.1.	Ground Motion Database.....	77
3.4.2.	Embankment Response.....	82
3.4.2.1.	Embankment Modeling Overview.....	82
3.4.2.2.	Soil Mitigation Options.....	85
3.4.2.3.	Embankment Model Shortcomings.....	88
3.4.2.4.	Transfer Functions.....	89
3.4.3.	Wharf Response.....	103
3.4.3.1.	Wharf Model.....	103
3.4.3.2.	Wharf Damage Measures.....	113
3.4.3.3.	Wharf Repair Cost and Time.....	113
3.4.3.4.	Calculation of Repair Requirements.....	122
3.4.3.5.	Operational Status of the Wharf.....	123
3.4.4.	Crane Response.....	128
3.4.4.1.	Crane Modeling Overview.....	128
3.4.4.2.	Crane Damage Measures.....	130
3.4.4.3.	Crane Fragility Curves.....	131
3.4.4.4.	Crane Repair Cost and Time.....	133
3.4.4.5.	Operational Status of the Cranes.....	134
3.4.4.6.	Crane Damping.....	135
3.5.	System Fragility.....	135

3.5.1.	Ship Arrival Schedule.....	135
3.5.2.	Arriving Ship Data.....	142
3.5.3.	Berth and Quay Crane Scheduling Program.....	144
3.5.3.1.	Summary of Operational Modeling and Generated Statistics.....	147
3.5.3.2.	Example	148
3.5.3.3.	Arrival Stream.....	151
3.5.3.4.	Berth and Crane Utilization	152
3.5.3.5.	Displaced Ships.....	152
3.5.3.6.	TEU Statistics	153
3.5.4.	Effect of Earthquake Disruption on Shipping Operations	154
3.6.	Operational Modeling Using Regression.....	159
3.6.1.1.	Run GHI Residuals and Comparison of Runs	164
3.6.1.2.	Operational Regression Model with the Risk Analysis Program ...	168
3.6.2.	Calculation of Business Interruption Losses.....	168
3.6.3.	Operational Mitigation Options	169
3.7.	Total Cost.....	170
3.7.1.	Mean Rate of Exceedance.....	171
3.7.2.	Mean and Variance of Annual Loss.....	173
4.	RISK ANALYSIS FRAMEWORK AS APPLIED TO A HYPOTHETICAL PORT	175
4.1.	Hypothetical Port Configuration.....	175
4.2.	Example Earthquake	180
4.3.	Evaluation of Results for Entire Earthquake Sample	180
4.3.1.1.	PGV and SA Data	181
4.3.1.2.	Total Cost Data	188
4.3.1.3.	Conclusions.....	191
4.4.	Probabilistic Analysis Results.....	197
4.4.1.	Earthquake Sample Size	197
4.4.2.	Exceedance Results.....	201
4.4.2.1.	Repair Cost Exceedance Curves	202
4.4.2.2.	Business Interruption Loss Curves	203
4.4.2.3.	Total Cost Curves	204
4.4.3.	Sample Summary Statistics.....	207
4.4.4.	Exceedance Curve Sample Calculations.....	209
4.4.4.1.	Probability of a Specific Loss	209
4.4.4.2.	Loss Associated with a Specific Return Period	210
4.4.4.3.	Exposure Time Calculations	211
4.5.	Scenario-Based Analysis Results.....	212
4.6.	Intensity-Based Analysis Results.....	216
4.7.	Sources of Uncertainty.....	221
4.7.1.1.	Control: Using the Mean of All Sources of Uncertainty	222
4.7.1.2.	Ground Motion.....	226
4.7.1.3.	Spatial Correlation	228
4.7.1.4.	Crane Repair Requirements	230
4.7.1.5.	Wharf Repair Requirements	233

4.7.1.6.	Operational Regression Model	235
4.7.1.7.	Comparison of All Sources of Uncertainty	238
4.8.	Comparison with Previous Studies	240
4.8.1.	Werner and Taylor	241
4.8.1.1.	Cost	242
4.8.1.2.	Number of Ships Scheduled	242
4.8.1.3.	Port Capacity	242
4.8.1.4.	Comparison	243
4.8.2.	Pachakis and Kiremidjian	247
4.8.2.1.	Ship Traffic	247
4.8.2.2.	Berth Assignment and Crane Allocation	248
4.8.2.3.	Service Times	248
4.8.3.	Linear Calculation of BIL	249
5.	MITGATION OPTIONS	258
5.1.	Geotechnical Options	258
5.2.	Structural Options	265
5.2.1.	Crane Improvements	265
5.3.	Repair Options	272
5.3.1.	Repair Incentives	273
5.3.2.	Varying Mobilization Time	278
5.3.3.	Repair Sequencing	281
5.4.	Operational Options	283
5.5.	Economic Analysis of Alternative Options	285
5.6.	Economic Analysis	286
5.6.1.	Cost Benefit Analysis	286
5.6.1.1.	Cost of Installing Vertical Drains	287
5.6.1.2.	Calculation of Benefits	288
5.6.1.3.	Calculation of Cost/Benefit	289
5.6.1.4.	Conclusion	289
5.6.2.	Mean-Variance Analysis	290
5.6.3.	Stochastic Dominance	292
5.7.	Planning for Port Emergency Response Operations	293
5.8.	Calibration of Current Seismic Design	294
6.	APPLICATION OF RISK ANALYSIS FRAMEWORK TO OTHER PORTS	298
6.1.	Hazard-related Issues	298
6.2.	Component-related Issues	299
6.2.1.	Wharf and Embankment	300
6.2.1.1.	Other possible embankments	300
6.2.1.2.	Embankment Performance in Past Earthquakes	300
6.2.1.3.	Embankment Modeling	300
6.2.1.4.	Other Possible Wharf Configurations	301
6.2.1.5.	Wharf Performance in Past Earthquakes	302
6.2.1.6.	Developing Fragility Curves	302

6.2.2.	Crane.....	304
6.2.2.1.	Other Possible Crane Configurations.....	304
6.2.2.2.	Crane Performance in Past Earthquakes.....	305
6.2.2.3.	Developing Fragility Curves.....	306
6.3.	System-related Issues.....	306
7.	SUMMARY, CONCLUSIONS, AND FUTURE WORK	308
7.1.	Summary and Conclusions	308
7.2.	Impact of Research	311
7.3.	Recommendations for Future Work.....	312
A.	APPENDIX A – CALIBRATION OF OPERATIONAL MODEL	315
A.1.	Stopping Criteria within the Operational Model	315
A.2.	Stopping Criteria Based on Repair Periods	319
B.	APPENDIX B – GROUND MOTIONS.....	324
C.	APPENDIX C – MARINE EXCHANGE OF SOUTHERN CALIFORNIA	346
	REFERENCES	391

LIST OF TABLES

Table 2.1 Examples of Earthquake-Induced Damage to Port Facilities	9
Table 2.2 Acceptable level of damage in PIANC performance-based design (from (PIANC 2001)).....	17
Table 2.3 – Performance grades S, A, B, and C (from (PIANC 2001))	18
Table 2.4 – Types of Analyses Related to Performance Grades (from (PIANC 2001)) ..	18
Table 2.5 – Minimum Seismic Hazard and Performance Requirements from (ASCE 2011)	23
Table 2.6 Combinations of Berth Seismic upgrade Options that Pass the MVC (Werner and Taylor 2004).....	35
Table 3.1 California Blue Book Performance Goals	49
Table 3.2 Excerpt from Earthquake Rupture Forecast.....	71
Table 3.3 NGA and SIM Ground Motion Summary Table	79
Table 3.4 Soil Properties for Liquefiable Embankment Profile (from (Vytiniotis et al. 2011)).....	85
Table 3.5 Dafalias and Manzari constitutive model constants (From Vytiniotis 2005)..	88
Table 3.6 – Soil Properties.....	95
Table 3.7 Description of NGA Motions Used in Transfer Function Validation.	100
Table 3.8 – Root Mean Square Errors between Response Spectra.....	103
Table 3.9 Wharf Damage States for Pile Damage (1) (Lehman et al. 2009) from (Werner and Cooke 2009).....	114
Table 3.10 Wharf Damage States for Pile Damage (2) (Lehman et al. 2009) from (Werner and Cooke 2009).....	114
Table 3.11 Repair Cost and Time Summary – Pile damage (Lehman et al. 2009) from (Werner and Cooke 2009).....	115
Table 3.12 Wharf Damage States for Deck Damage (Earthquake Engineering Research Institute (EERI) 1990; Werner 1998) from (Werner and Cooke 2009).....	116

Table 3.13 Repair Cost and Time Summary – Deck damage (Lehman et al. 2009) from (Werner and Cooke 2009).....	117
Table 3.14 Wharf Damage States for Crane Rail / Collector Trench Damage (Lehman et al. 2009) from (Werner and Cooke 2009).....	118
Table 3.15 Repair Cost and Time Summary – crane rail / collector trench damage (Lehman et al. 2009) from (Werner and Cooke 2009)	119
Table 3.16 Wharf Damage States for Relative Movement of Crane Rail and Wharf Deck (Earthquake Engineering Research Institute (EERI) 1990; Werner and Dickenson 1996) from (Werner and Cooke 2009).....	120
Table 3.17 Repair Cost and Time Summary – Relative Movement of Crane Rail and Wharf Deck (Lehman et al. 2009) from (Werner and Cooke, 2009).....	120
Table 3.18 Example of Port System Operational Status.....	124
Table 3.19 Number of Ships Able to Dock for Each Repair Sequence.....	126
Table 3.20 Crane Repair Costs and Time	134
Table 3.21 Terminal Data from the Port of Los Angeles and the Port of Long Beach from March-August of 2008.....	136
Table 3.22 K-S Test Results	138
Table 3.23 Arrival Stream for the First 100 Days after an Earthquake	142
Table 3.24 TEU Statistics by month.....	143
Table 3.25 Example Sampled Ship.....	144
Table 3.26 Excerpt of Operational Modeling Statistics Output.....	149
Table 3.27 Number of Weeks Each Earthquake Scenario Was Run	154
Table 3.28 BQCSP Model Test Runs	160
Table 3.29 – Multivariate Regression Results	163
Table 3.30 – Comparison of Correlations for Runs ABD and GHI.....	165
Table 3.31 – Business Interruption Costs	169
Table 4.1 Separation Distances (h in km) between Terminals in the Hypothetical Port.	178
Table 4.2 – Spatial Correlation Coefficients for Hypothetical Port.....	179

Table 4.3 Hypothetical Port Terminal Specifications.....	179
Table 4.4 Example Earthquake and Loss Data Generated by Risk Analysis Program...	180
Table 4.5 – Instances of Crane Damage per Terminal.....	197
Table 4.6 – Exceedance Value Reference.....	200
Table 4.7 – Mean Inter-arrival Times for All Terminals	204
Table 4.8 – Summary Statistics for Exposure time of 20 years.....	212
Table 4.9 - Intensity Based Scenario Inputs	217
Table 4.10 – Mean Maximum Repair Times for OLE and CLE	220
Table 4.11 – Description of Uncertainty Runs	221
Table 4.12 Ship Capacity for Comparison Example	244
Table 4.13 Scheduled Arrivals vs. Capacity for Terminal A.....	245
Table 4.14 Ship Arrival Stream – Ship lengths and TEUs	246
Table 4.15 Calculation of Linear TEU Losses Using Components and Berths Not Available – Earthquake #3.....	252
Table 5.1 – Installation Costs per Terminal for PVDs.....	288
Table 5.2 – Average Repair Costs and BIL with Drains	288
Table 5.3 – Average Repair Costs and BIL: Baseline	288
Table 5.4 – Wharf Repair Costs and BIL Saved Through Drain Upgrade	289
Table 5.5 – B-C Ratio for PVD Installation	289
Table 5.6 – Repair Costs and Times for OLE and CLE at hypothetical port	296
Table 6.1 Damage and Repair Time Fragility Curves from (FEMA 2003).....	304
Table 6.2 – Fragility and Restoration Parameters of HAZUS Damage States for Unanchored/Rail Mounted Port Cranes from (FEMA 2003)	306
Table A.1 Number of Weeks Required to Return to Normal Operation	323

LIST OF FIGURES

Figure 1.1 Container traffic in US ports (from AAPA data)	1
Figure 1.2 The largest container ports in the US on the USGS seismic hazard map.....	2
Figure 1.3 Partially submerged container crane at the Port-au-Prince Port (photo courtesy of (Riddle 2010)).....	4
Figure 1.4 - Hypothetical Berth	5
Figure 2.1 Deformation/failure modes of gravity quay walls (from (PIANC 2001)).....	11
Figure 2.2 Typical modes of failure for anchored sheet piles (from (PIANC 2001))	12
Figure 2.3 Common deformation/failure modes of pile-supported wharves (from (PIANC 2001)).....	12
Figure 2.4 – Crane Deformation Modes: a.) Widening between Legs, b.) Narrowing between Legs due to Rocking, c.) Tilting of Crane from Differential Settlement, and d.) Overturning of One Leg Due to Rocking/Sliding (from (PIANC 2001))	13
Figure 2.5 – a.) Lateral Spreading: Port de Port-Au-Prince (Photo by (Rix, 2010)) and b.) Crane Settlement: 1985 Chile Earthquake (from (Werner 1998)).....	15
Figure 2.6 – Kobe, Japan, 7 months after the 1995 Kobe Earthquake (from (Brundsdon, 1995)).....	16
Figure 2.6 Berths included in the Port of Oakland WESP Seismic Risk Reduction Project (Werner and Taylor 2004)	29
Figure 2.7 Risk Assessment Approach for the Port of Oakland (Werner and Taylor 2004)	30
Figure 2.8 Operations/System Seismic Risk Analysis procedure for estimating business interruption losses (Werner and Taylor 2004).....	33
Figure 2.9 Port Terminal (after (Pachakis and Kiremidjian 2004)).....	37
Figure 2.10 Typical section of damage criteria for a quay wall (From (Na et al. 2008)).	41
Figure 2.11 Statistics for 130 RHD responses (From (Na and Shinozuka 2009)).....	42
Figure 2.12 Loss estimation methodology (from (Na and Shinozuka 2009))	43
Figure 2.13 System fragility curves for (a) original and (b) retrofitted structure (From (Na and Shinozuka 2009))	44

Figure 3.1 Combinations of earthquake hazard and performance levels as proposed by Vision 2000 (from (SEAOC 1995)).	50
Figure 3.2 Performance Assessment Process (Applied Technology Council 2006)	52
Figure 3.3 Illustration of Performance Prediction Processes using PEER Terminology (after (Kramer and Mitchell 2006))	54
Figure 3.4 - Relationship between Response Relationship, Uncertainty and Fragility Curves	56
Figure 3.5 Graphical representation of equation 3.2.	57
Figure 3.6 - Risk Analysis Framework	60
Figure 3.7 Probability mass for entire ERF population	62
Figure 3.8 Histogram of conventionally-Monte-Carlo-sampled earthquakes	64
Figure 3.9 Magnitude vs. percent of total earthquake sample for conventional Monte Carlo sampling (100 = red, 1000 = blue, 10000 = green)	65
Figure 3.10 Histogram of magnitudes using stratified MC sampling for 100, 1000, and 10000 earthquakes	68
Figure 3.11 Port of Oakland.	73
Figure 3.12 Inter vs. Intra-event spatial correlations	74
Figure 3.13 Frequency response of numerical differentiation filter	78
Figure 3.14 Response spectra for entire suite of ground motions.	81
Figure 3.15 Moment magnitude vs. closest distance to the rupture.	81
Figure 3.16 Example of embankment section analyzed with pile nodes (from (Vytiniotis 2010)).	83
Figure 3.17 Soil Profile – Liquefiable soil (after (Vytiniotis et al. 2011)).	84
Figure 3.18 Prefabricated vertical drain and triangular installation pattern from (Howell et al. 2011)	86
Figure 3.19 Soil Profile – Liquefiable soil with prefabricated vertical drains (after (Vytiniotis et al. 2011)).	87
Figure 3.20 Directional reference for the wharf.	89
Figure 3.21 Input rock motions (X and Y) for NGA1642	90

Figure 3.22 Comparison of Rock input motion response spectra and the Pseudo-transfer function	93
Figure 3.23 Soil Profile for Transfer Function Validation	96
Figure 3.24 Horizontal soil motions (X and Y) from OPENSEES.....	97
Figure 3.25 Comparison of target response spectrum and OPENSEES-generated response spectrum for the out-of-plane direction.	98
Figure 3.26 Response spectra produced via the RSPMATCH program.....	99
Figure 3.27 Time histories for X_{soil} (R), Y_{soil} (B), and computed Y_{soil} (G) for NGA1642.	100
Figure 3.28 Response spectra for Y_{soil} (B), and computed Y_{soil} (G) for NGA0897.	101
Figure 3.29 Time histories for Y_{soil} (B), and computed Y_{soil} (G) for NGA0897.	102
Figure 3.30 Response spectra for Y_{soil} (B), and computed Y_{soil} (G) for NGA0779.	102
Figure 3.31 Time histories for Y_{soil} (B), and computed Y_{soil} (G) for NGA0779.	103
Figure 3.32 Typical 1960's Wharf.....	104
Figure 3.33 Interacting components that comprise the numerical wharf model (from (Werner and Rix 2008)).....	105
Figure 3.34 Conversion from 2D to 3D wharf model (from (Shafieezadeh 2011))	107
Figure 3.35 Typical configurations of common pile-deck connections: (a) embedded dowel with outward bent bars, (b) embedded dowel with T-headed bars, (c) extended pile, and (d) extended strand.	108
Figure 3.36 Macroelement schematic showing input, output, and components (from (Varun 2010)).....	110
Figure 3.37 Wharf and crane rail response during NGA1057: (a) profile of the maximum curvature ductility demand and (b) final deformed shape of the wharf (from (Shafieezadeh 2011))	111
Figure 3.38 Component fragility curves for (a) pile section, (b) pile-deck connections, and (c) relative movement of the wharf with respect to the landside crane rail (solid lines are the fragility estimates and dashed lines are the corresponding 90% confidence boundaries). (from (Shafieezadeh 2011)).....	112
Figure 3.39 – Calculated Correlation Factors between Adjacent Wharf Segments	122
Figure 3.40 Repair Sequencing Example.....	125

Figure 3.41 Histogram of Ship Lengths.....	127
Figure 3.42 Container Crane Schematic	130
Figure 3.43 Fragility curves for J100 container crane, assuming portal uplift theory seismic demand model (from Kosbab 2010).	132
Figure 3.44 Fragility curves for LD100, assuming portal uplift theory seismic demand model. (Kosbab 2010).....	132
Figure 3.45 Fragility curves for LD50, assuming portal uplift theory seismic demand model. (Kosbab 2010).....	133
Figure 3.46 Port of Los Angeles Inter-arrival Time Distribution.....	137
Figure 3.47 Port of Long Beach Inter-arrival Time Distribution.....	138
Figure 3.48 Linear Regression Models: Weighted (blue) vs. Un-weighted (red)	140
Figure 3.49 Berth length vs. ship length.	141
Figure 3.50 Berth length vs. TEU Capacity.....	141
Figure 3.51 Crane allocation example: berth (from (Erera, 2008))	146
Figure 3.52 Crane allocation example: sequential assignments	146
Figure 3.53 Crane allocation example: simultaneous berth and crane model assignment	147
Figure 3.54 Wharf and crane repair times for example earthquake scenario	148
Figure 3.55 Ship Arrivals, Dwell Time, and Delays per week	151
Figure 3.56 Berth and Crane Utilization per Week	152
Figure 3.57 # and Percent of Displaced Ships per Week.....	153
Figure 3.58 TEUs Handled, Lost and % Lost per week	154
Figure 3.59 Final Berth Utilization Comparison of Earthquake Scenarios	155
Figure 3.60 Final Crane Utilization Comparison of Earthquake Scenarios.....	155
Figure 3.61 Final TEU Statistic Comparison of Earthquake Scenarios.....	156
Figure 3.62 TEUs Lost Statistic Comparison of Earthquake Scenarios	157
Figure 3.63 Final Total Dwell Time Statistic Comparison of Earthquake Scenarios.....	158

Figure 3.64 – Probit Regression Equation for Combination of Runs G, H, and I	162
Figure 3.65 Wharf Time vs. TEU Loss.....	163
Figure 3.66 – Plot of Residuals for Probit Regression Equation	165
Figure 3.67 – Residual Plots for Multivariate Regression Equation Variables	167
Figure 3.68 Inverse cumulative distribution function (from (NIST 2011)).....	172
Figure 3.69 Mean rate of exceedance plot example	173
Figure 4.1- Hypothetical port location: A.) Map Location, B.) Aerial view.	176
Figure 4.2 - Hypothetical Port	177
Figure 4.3 Histogram of terminal separation distances	178
Figure 4.4 – a.) PGV vs. Repair Time for the wharf, b.) SA vs. Repair Time for the cranes	182
Figure 4.5 – a.) PGV Vs. Cost, b.) Spectral Acceleration vs. Cost: Terminal A.....	184
Figure 4.6 – a.) PGV Vs. Cost, b.) Spectral Acceleration vs. Cost: Terminal B.....	185
Figure 4.7 – a.) PGV Vs. Cost, b.) Spectral Acceleration vs. Cost: Terminal C.....	186
Figure 4.8– a.) PGV Vs. Cost, b.) Spectral Acceleration vs. Cost: Terminal D.....	187
Figure 4.9 – Repair Time vs. Repair cost for Wharf and Crane	188
Figure 4.10 - Total Cost Plots a.) PGV vs. Total Cost, b.) SA vs. Total cost.....	189
Figure 4.11 – Ratios of BIL/Total Repair Cost.....	191
Figure 4.12 Fragility curves for LD100, assuming portal uplift theory seismic demand model. (Kosbab 2010).....	193
Figure 4.13 - Component fragility curves for (a) pile section, (b) pile-deck connections, and (c) relative movement of the wharf with respect to the landside crane rail (solid lines are the fragility estimates and dashed lines are the corresponding 90% confidence boundaries). (from (Shafieezadeh 2011)).....	194
Figure 4.14 – PGV vs. Repair Cost per Terminal.....	195
Figure 4.15 – SA vs. Crane Repair Cost Comparison per Crane Type	196
Figure 4.16 – Empirical (10000-EQ sample) and Reference Hazard Curve Comparison: Terminal A	198

Figure 4.17 – a.) MRE curves for total cost among 2 different 100,000 earthquake baseline runs as compared to a 10,000-earthquake run (in red), and b.) The empirically calculated hazard curve for PGV vs. the reference hazard curve (red) for the run represented by the red MRE curve in a.): Terminal A.....	199
Figure 4.18 – Comparison of RC, BIL, and TC Exceedance Curves: Terminal A	201
Figure 4.19 - Repair Cost Exceedance Curves: All Terminals.....	202
Figure 4.20- Business Interruption Loss Exceedance Curves: All Terminals.....	203
Figure 4.21 – MRE of Total Losses and One-sided Confidence Intervals: All Terminals	206
Figure 4.22 – Summary Statistics: Repair Cost.....	207
Figure 4.23 – Summary Statistics: Business Interruption Loss	208
Figure 4.24 – Summary Statistics: Total Cost	209
Figure 4.25 - Finding the Probability of Exceeding a Specific Loss.....	210
Figure 4.26 - Finding the Loss Associated with a Specific Return Period.....	211
Figure 4.27 – Exceedance Results for Scenario-based example run a.) Repair Cost, b.) Business Interruption Loss, and c.) Total Loss.....	215
Figure 4.28 – Sample Statistics of Scenario-Based Run: Total Cost.....	216
Figure 4.29 – Exceedance Results for OLE and CLE example runs a.) Repair Cost, b.) Business Interruption Loss, and c.) Total Loss.....	218
Figure 4.30 – Sample Statistics of OLE and CLE Run: Total Cost.....	220
Figure 4.31 – Total Cost Uncertainty Comparison: Control – Using only Mean Values.....	223
Figure 4.32 – Total Cost Uncertainty Comparison: Mean Values, Terminal A	224
Figure 4.33 – a.) Repair Cost and b.) Business Interruption Loss Uncertainty Comparison: Mean Values, Terminal A.....	225
Figure 4.34 – Total Cost Uncertainty Comparison: Ground Motion.....	226
Figure 4.35 – a.) Repair Cost and b.) Business Interruption Loss Uncertainty Comparison: Ground Motion.....	227
Figure 4.36 – Total Cost Uncertainty Comparison: Spatial Correlation	229

Figure 4.37 – a.) Repair Cost and b.) Business Interruption Loss Uncertainty Comparison: Spatial Correlation.....	230
Figure 4.38 – Total Cost Uncertainty Comparison: Crane Repair Requirements	231
Figure 4.39 – a.) Repair Cost and b.) Business Interruption Loss Uncertainty Comparison: Crane Repair Requirements	232
Figure 4.40 – Total Cost Uncertainty Comparison: Wharf Repair Requirements.....	233
Figure 4.41 – a.) Repair Cost and b.) Business Interruption Loss Uncertainty Comparison: Wharf Repair Requirements.....	234
Figure 4.42 – Illustration of Uncertainty within the Operational regression Model’s calculation of TEUs. (Red = mean and distribution)	235
Figure 4.43 – Total Cost Uncertainty Comparison: Regression Analysis	236
Figure 4.44 – a.) Repair Cost and b.) Business Interruption Loss Uncertainty Comparison: Regression Analysis	237
Figure 4.45 – Comparison of Uncertainty Runs Terminals A, B, C, and D	240
Figure 4.46 Terminal A and B – BIL Comparison Example	244
Figure 4.47 Wharf and Crane Repair Times for Example Earthquake Scenario #3	249
Figure 4.48 – TEUs Handled per Week in EQ 3 and No Damage Scenarios	250
Figure 4.49 TEUs Handled per Week with (berth,crane) Availability: Earthquake 3	251
Figure 4.50 TEUs Handled per Week: Earthquake 1	253
Figure 4.51 TEUs Handled per Week: Earthquake 2	254
Figure 4.52 TEUs Handled per Week: Earthquake 4	254
Figure 4.53 TEUs Handled per Week: Earthquake 5	255
Figure 5.1 – MRE of Wharf Repair Costs With and Without Drains: Terminal A	259
Figure 5.2 – MRE of Wharf Repair Costs With and Without Drains: Terminal B	259
Figure 5.3 – MRE of Wharf Repair Costs With and Without Drains: Terminal C	260
Figure 5.4 – MRE of Wharf Repair Costs With and Without Drains: Terminal D	260
Figure 5.5 – MRE of Repair Costs With and Without Drains: All Terminals.....	261

Figure 5.6 – MRE of Business Interruption Losses With and Without Drains: All Terminals	262
Figure 5.7 – MRE of Total Losses With and Without Drains: All Terminals.....	263
Figure 5.8 – MRE of Total Losses With and Without Drains: Terminal A.....	263
Figure 5.9 – MRE of Total Losses With and Without Drains: Terminal B.....	264
Figure 5.10 – MRE of Total Losses With and Without Drains: Terminal C.....	264
Figure 5.11 – MRE of Total Losses With and Without Drains: Terminal D.....	265
Figure 5.12 – MRE of Crane Repair Costs With and Without Crane Upgrade: Terminal A	266
Figure 5.13 – MRE of Crane Repair Costs With and Without Crane Upgrade: Terminal B	266
Figure 5.14 – MRE of Crane Repair Costs With and Without Crane Upgrade: Terminal D	267
Figure 5.15 - MRE of Crane Repair Costs With and Without Crane Upgrade: All Terminals	269
Figure 5.16 - MRE of Total Costs With and Without Crane Upgrade: All Terminals...	270
Figure 5.17 - MRE of BIL With and Without Crane Upgrade: Terminal A	271
Figure 5.18 - MRE of BIL With and Without Crane Upgrade: Terminal B.....	271
Figure 5.19 - MRE of BIL With and Without Crane Upgrade: Terminal D	272
Figure 5.20 – MRE of Repair Costs Baseline and Repair Time Decrease: All Terminals	274
Figure 5.21– MRE of BIL Baseline and Repair Time Decrease: All Terminals.....	275
Figure 5.22 – MRE of Total Cost Baseline and Repair Time Decrease: All Terminals.	276
Figure 5.23 – MRE of Total Cost Baseline and Repair Time Decrease: Terminal A	276
Figure 5.24 – MRE of Total Cost Baseline and Repair Time Decrease: Terminal B.....	277
Figure 5.25 – MRE of Total Cost Baseline and Repair Time Decrease: Terminal C.....	277
Figure 5.26 – MRE of Total Cost Baseline and Repair Time Decrease: Terminal D	278
Figure 5.27 – MRE of Total Cost Baseline and Mobilization Variation: Terminal A ...	279

Figure 5.28 – MRE of Total Cost Baseline and Mobilization Variation: Terminal B....	280
Figure 5.29 – MRE of Total Cost Baseline and Mobilization Variation: Terminal C....	280
Figure 5.30 – MRE of Total Cost Baseline and Mobilization Variation: Terminal D ...	281
Figure 5.31 – Terminal Example: Repair Sequencing.....	281
Figure 5.32 – MRE of BIL Baseline and Repair Sequencing Variation: All Terminals	282
Figure 5.33 – MRE of Total Cost Baseline and Repair Sequencing Variation: All Terminals	283
Figure 5.34 – MRE of Losses: Force Majeure.....	285
Figure 5.35 – Mean Variance of Total Cost: Terminal B	291
Figure 5.36 – Stochastic Dominance Comparison of Mitigation Options: Terminal B .	293
Figure 5.37 – Reference curve for PGV vs. Annual Rate of Exceedance	295
Figure 6.1 – Common Wharf Structures (from (PIANC 2001)).....	302
Figure 6.2 – Histogram of the Maximum Width (# of containers) of Surveyed US Container Cranes.....	305
Figure A.1 Earthquake 1: Utilization statistics for full and half stopping criteria.....	316
Figure A.2 Earthquake 1: TEU statistics for full and half stopping criteria	317
Figure A.3 Earthquake 2: Utilization statistics for full and half stopping criteria.....	318
Figure A.4 Earthquake 3: Utilization statistics for full and half stopping criteria.....	318
Figure A.5 Earthquake 4: Utilization statistics for full and half stopping criteria.....	319
Figure A.6 TEU statistic comparison of earthquake scenarios.....	320
Figure A.7 Total dwell time statistic comparison of earthquake scenarios	321
Figure A.8 Berth utilization comparison of earthquake scenarios.....	322
Figure A.9 Crane utilization comparison of earthquake scenarios	322
Figure B.1 NGA 0033, 0145, 0150.....	325
Figure B.2 NGA 0448, 0451, 0472.....	326
Figure B.3 NGA 0632, 0648, 0649.....	327

Figure B.4 NGA 0669, 0676, 0684.....	328
Figure B.5 NGA 0739, 0751, 0753.....	329
Figure B.6 NGA 0779, 0791, 0802.....	330
Figure B.7 NGA 0810, 0897, 0954.....	331
Figure B.8 NGA 0969, 0982, 0983.....	332
Figure B.9 NGA 1008, 1012, 1013.....	333
Figure B.10 NGA 1014, 1023, 1031.....	334
Figure B.11 NGA 1035, 1055, 1057.....	335
Figure B.12 NGA 1085, 1086, 1642.....	336
Figure B.13 NGA 1794, 2374, 2393.....	337
Figure B.14 NGA 2397, 2399, 2490.....	338
Figure B.15 NGA 2498, 2658, 2716.....	339
Figure B.16 NGA 2804, 2967, 2871.....	340
Figure B.17 NGA 2883, 3008, 3016.....	341
Figure B.18 NGA 3353, 3361, 3469.....	342
Figure B.19 NGA 3474, 3507, SIM 0001.....	343
Figure B.20 SIM 0002, 0003, 0004	344
Figure B.21 SIM 0005, 0006, 0007	345

LIST OF ABBREVIATIONS

NEES	Network for Earthquake Engineering Simulation
TCLEE	Technical Council for Lifeline Earthquake Engineering
ATC	Applied Technology Council
FEMA	Federal Emergency Management Agency
PBEE	Performance-based earthquake engineering
PEER	Pacific Earthquake Engineering Research Center
DV	Decision variable
DM	Damage measure
EDP	Engineering demand parameter
IM	Intensity measure
PSHA	Probabilistic seismic hazard analysis
WESP	Wharf and Embankment Strengthening Program
SRRP	Seismic risk reduction planning
PGA	Peak ground acceleration
PGV	Peak ground velocity
PGD	Peak ground displacement
SA	Spectral Acceleration
MVC	Mean variance criterion
TEU	Twenty foot equivalent units
FOSM	First order second moment
PIANC	International Navigation Association
MOTEMS	Marine Oil Terminal Engineering and Maintenance Standard
COV	Coefficient of variation
RHD	Residual horizontal displacements
ERF	Earthquake rupture forecast
GMPE	Ground motion prediction equation
NGA	Next-Generation Attenuation of ground motions
SSI	Soil structure interaction

TF	Transfer function
K-S Test	Kolmogorov-Smirnov Test
2D	Two dimensional
3D	Three dimensional
MRE	Mean Rate of Exceedance
J100	Modern Jumbo Crane
LD100	Heritage Jumbo Crane
LD50	Heritage Compact Crane
MXSOCAL	Marine Exchange of Southern California
BIL	Business Interruption Loss
POLA	Port of Los Angeles
POLB	Port of Long Beach
BQCSP	Berth and Quay Crane Scheduling Program

SUMMARY

Ports play a critical role in transportation infrastructure, but are vulnerable to seismic hazards. Downtime and reduced throughput from seismic damage in ports results in significant business interruption losses for port stakeholders. Current risk management practices only focus on the effect of seismic hazards on individual port structures. However, damage and downtime of these structures has a significant impact on the overall port system's ship handling operations and the regional, national, and even international economic impacts that result from extended earthquake-induced disruption of a major container port. Managing risks from system-wide disruptions resulting from earthquake damage has been studied as a central element of a Grand Challenge project sponsored by the National Science Foundation Network for Earthquake Engineering Simulation (NEES) program. The following thesis presents the concepts and methods developed for the seismic risk management of a port-wide system of berths. In particular the thesis discusses the framework used to calculate port losses: the use of spatially correlated ground motion intensity measures to estimate damage to pile-supported marginal wharves and container cranes of various configurations via fragility relationships developed by project team members, repair costs and downtimes subsequently determined via repair models for both types of structures, and the impact on cargo handling operations calculated via logistical models of the port system. Results are expressed in the form of loss exceedance curves that include both repair/replacement costs and business interruption losses. The thesis also discusses how the results from such an analysis might be used by port decision makers to make more informed decisions in design, retrofit, operational, and other seismic risk management options.

1 INTRODUCTION

1.1 Motivation

Seaports are an integral part of the current world infrastructure. Global trade has consistently increased in the past (see Figure 1.1) and once the economy fully rebounds, it should continue to increase.

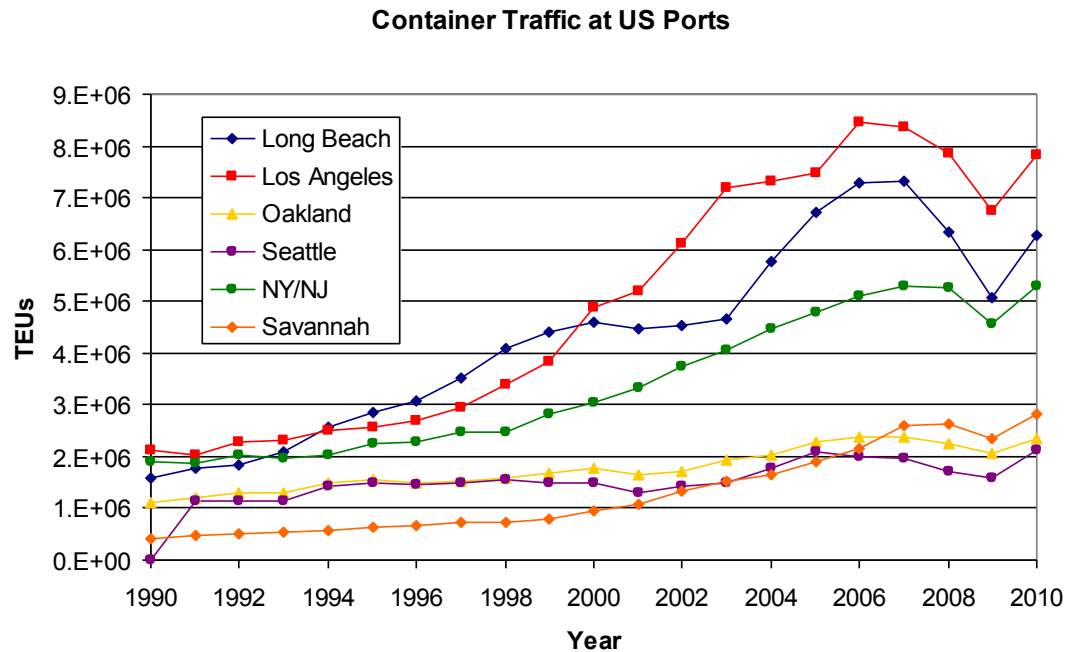


Figure 1.1 Container traffic in US ports (from AAPA data)

The global economy depends on ports as critical nodes to load and unload cargo. However, many ports around the world and in the US are located in areas with a significant seismic hazard. Figure 1.2 maps the 10 largest container ports in the US on top of the US Geological Survey (USGS) seismic hazard map: of the ten largest ports, six of them lie in areas with significant seismic hazard.

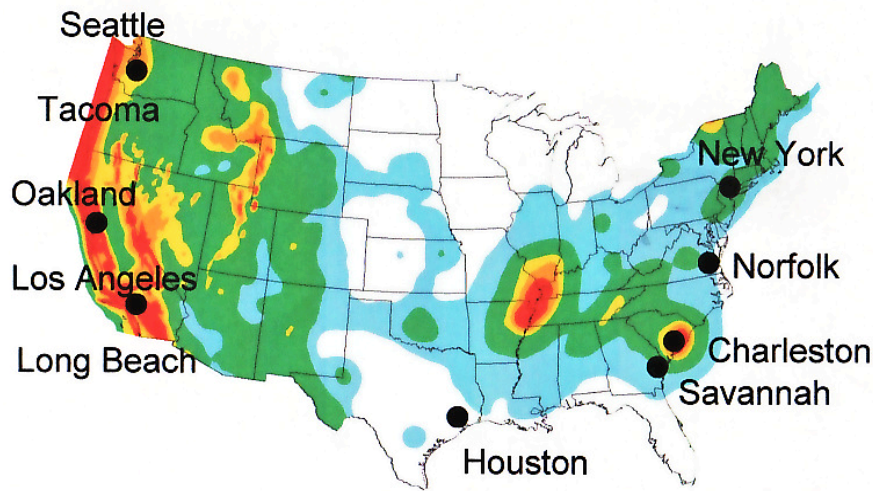


Figure 1.2 The largest container ports in the US on the USGS seismic hazard map

Unfortunately, little attention has been paid to ports and the seismic hazards that threaten to disrupt them. History has shown through the Port of Kobe in Japan, at Port-Au-Prince in Haiti, and the 2011 Japanese earthquake/tsunami that the possibility of earthquake damage should be an important consideration in a port system. In 1995 after the Hyogoken-Nanbu earthquake, the Port of Kobe suffered extensive liquefaction, wharf, and crane damage. The direct losses associated with replacing damaged facilities amounted to approximately \$5.5 billion dollars. However, the indirect losses from business interruptions, although much harder to quantify, were likely greater. Chang (2000) noted, “Once shippers were forced to invest in setting up operations elsewhere while Kobe was repairing its earthquake damage, they seemed in many cases not to have returned.” The overall impact of the earthquake demoted what was once the 6th largest container port in the world to the 55th largest port in 2007 (AAPA 2009), 12 years after the earthquake.

Japan’s economy was severely disrupted again in 2011. After the earthquake and tsunami, the Port of Tokyo took five days to recover operationally, and the ports north of Tokyo took significantly longer as many were closed or disabled for weeks and even months (Reuters 2011). It was estimated that the earthquake affected the ports that

handled approximately 7% of Japan's industrial exports, and the country lost \$3.4 billion US dollars a day in lost seaborne trade (Reuters 2011). Japan is an excellent case study on the effects of business interruption. It is very evident that business interruption losses have a lasting effect on both the economy and the port itself, so it would behoove current ports in seismically active areas to attempt to prevent fates similar to the ports in Japan.

Earthquake mitigation and planning should be considered to prevent business interruption losses, but also for emergency preparedness. The main port in Port-au-Prince Haiti was greatly affected by the January 2010 earthquake that killed hundreds of thousands of people (Werner *et al*, 2011). Approximately 50% of the port was destroyed including the main container terminal (BBC News 2010). The US Navy worked to repair the terminal and it reopened on a limited basis after nine days (CNN News 2010). However, the port's only container crane was partially submerged in water (Figure 1.3) and could not be used for unloading. Crews were forced to ferry supplies to the port and it only operated at a pre-earthquake capacity of 10% (BBC News 2010). Most of the aid sent by foreign countries had to be flown in through the Haitian airport, which was immediately overwhelmed. Many foreign aid agencies resorted to shipping goods in through the ports and airport in the Dominican Republic and then trucking the aid to Haiti (Taylor 2010). After six months, the crane remained submerged, and two floating barges had replaced the main pier, which still could not operate at pre-earthquake levels (Associated Press 2010). To date, the port has still not fully recovered. Therefore, it is important to investigate the effects of earthquakes not only on the physical structures but also the operational systems within the port.



Figure 1.3 Partially submerged container crane at the Port-au-Prince Port (photo courtesy of (Riddle 2010))

One of the main problems with the current treatment of seismic risk in ports is that currently ports do not explicitly account for seismic disruption. While engineers design individual components to withstand certain earthquake loads, little thought has been put into the sustainability of the port *system*. This could be remedied through probabilistic risk assessment, which would examine the vulnerabilities of the port components and of the port system, allowing port sustainability issues to be addressed. However, probabilistic risk assessment to date has mostly only been conducted on individual structures (buildings / bridges) or highway systems. Container ports are combination of networked individual components working together within a more complex system. Therefore, several features must be factored into the risk assessment of a port. Globally, a port is a place where cargo is transferred to and from container ships. Ships call at terminals composed of one or more berths consisting of a pile-supported

wharf structure and one or more container cranes for loading and unloading containers (Figure 1.4). Each berth contains several components whose response to earthquake ground motions must be included in a seismic risk assessment:

- 1.) Crane Response
- 2.) Wharf Response
- 3.) Soil-Structure Interaction
- 4.) Possibility of Liquefaction within Backfill

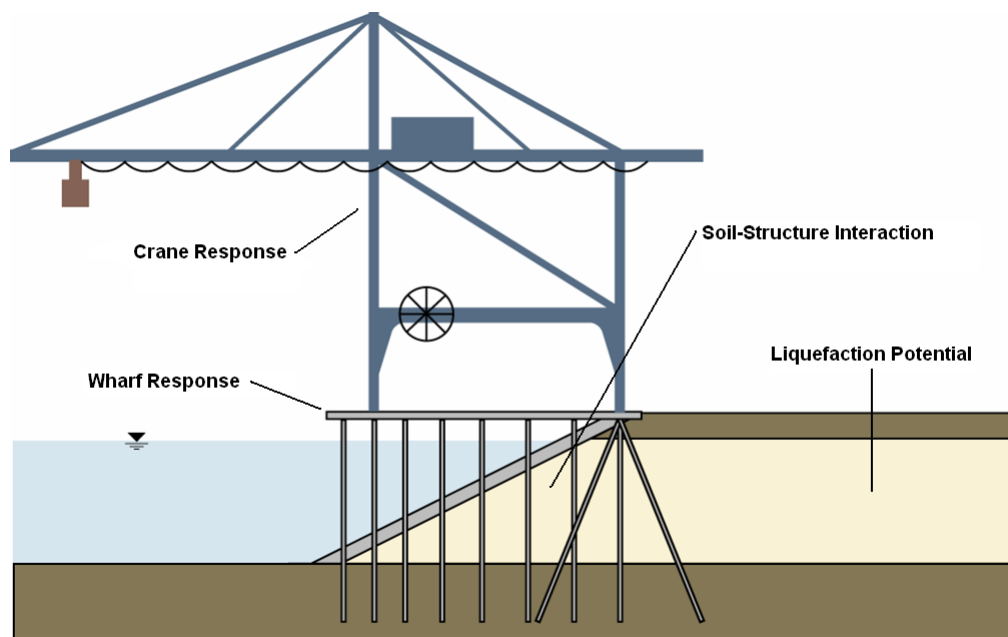


Figure 1.4 - Hypothetical Berth

Another of the main problems with current treatment of seismic risk in ports is that the earthquake design that is applied to the wharves, the cranes, and to some extent the backfill, have performance requirements that are associated with arbitrary return periods for ground motions rather than potential losses (Port of Los Angeles 2007). By ignoring the performance metrics valuable to port stakeholders, they lack the tools to make informed decisions concerning seismic risks given that potential direct and indirect losses are not explicitly considered. Perhaps this lack of knowledge has prevented some of the seismic improvements that could have been made to prevent earthquake disruption.

The seismic risk assessment of the port system proposed in the scope of this work would not only look at the port as a system, but also allow for the evaluation of performance based on metrics valuable to the stakeholders within the port; resulting in solution to the two issues that are lacking when dealing with the current seismic risk treatment in ports.

1.2 Objectives and Scope

This research is encompassed within a NEES Grand Challenge project on Seismic Risk Management for Port Systems. The project integrates the work of many researchers across the country to predict earthquake effects at a port system. Specifically, the project attempts to model the response of several port components / subcomponents (soil backfill, soil-structure interaction, wharf, pile connections, and cranes), and then use those component responses to model the port operations post-earthquake. Other researchers have completed much of the physical and computer modeling of the port components and port operations. This research aims to connect all the completed research and model the overall port. The objective will be to integrate both the components and operations into a seismic risk management framework that will focus on the performance and resilience of the port as a system. Under this focus, port stakeholders will be able to obtain port performance metrics that are more meaningful to them; therefore, they will be able to manage seismic risk more effectively, and plan for business continuity.

Research tasks within this scope include:

- Use a seismic risk analysis framework to calculate the monetary losses at a port that result from component repair and business interruption due to earthquake disruption.

- Develop a list of earthquakes with which to apply to the seismic risk framework, and examine the validity of the earthquake list.
- Integrate previously completed port component modeling into the seismic risk framework.
- Consider estimated repair requirements for various damage states of port components, and how downtime during repair periods affect wharf cargo-handling operations and throughput.
- Integrate previously completed operational modeling into the seismic risk framework.
- Examine the risk analysis results for a baseline port configuration, and also several mitigated port configurations.
- Illustrate the use of the risk analysis framework in various economic analysis applications.

1.3 Dissertation Outline

The content of the dissertation has been organized into the following chapters:

- **Chapter 2** provides an overview of the historical examples of seismic port damage, as well as a review of current seismic design guidelines, an overview of the previous research conducted on risk analysis in ports, and a discussion of the gaps in knowledge.
- **Chapter 3** overviews the methodology of the proposed risk assessment framework and suggests methods to use for the treatment of seismic hazard, component modeling and fragility, and system modeling and fragility for a hypothetical port system located in Santa Cruz, California.

- **Chapter 4** examines the results of the seismic risk framework as applied to a baseline configuration of a probabilistic, scenario-based, and intensity-based earthquake scenario of the hypothetical port. Responses of wharves, cranes, and the operational system to a sample of probabilistic earthquake events are studied to ascertain the validity of the risk analysis framework, loss exceedance curves are calculated and their uses discussed, and the sources of uncertainty within the risk framework are isolated and examined.
- **Chapter 5** examines the seismic risk framework results of various mitigated configurations of the hypothetical port, and provides direct and economic analysis comparisons of such to the baseline configuration examined in Chapter 4.
- **Chapter 6** provides a discussion of how the risk analysis framework can be applied to existing ports.
- **Chapter 7** summarizes the research while drawing conclusions, discusses the impact of the research, and suggests avenues for future study.

2 LITERATURE REVIEW

2.1 Historical Examples of Earthquake Damage in Ports

2.1.1 Historical Earthquake Occurrences in Ports

Damage to port systems from earthquakes is not an emerging problem. Seismic port damage has been documented as far back as 1923. Examining previous port damage provides valuable insight into ways in which port damage can be reduced during future earthquakes (Werner 1998). A complete list of earthquake damage to port structures during the years 1923-1995 can be found in the TCLEE monograph: Seismic Guidelines for Ports. The following table (Table 2.1) highlights some of the previously record earthquakes at port and the resulting damage from the TCLEE monograph in addition to some more recent data:

Table 2.1 Examples of Earthquake-Induced Damage to Port Facilities

EQ Location	Date	Mag.	Port	Damage	Reference
Kanto, Japan	9/1/23	8.3 (M_w)	Yokohama	Sliding, tilting and collapse of concrete block quay walls, buckling of pile supports in a steel bridge pier.	(Werner 1998)
Olympia, WA	4/13/49	7.1 (M_s)	Seattle	Damage to dock structures caused among other things by vertical displacements, displacements of filled soil materials	(Werner 1998)
Alaska	3/27/64	9.2 (M_w)	(1) Anchorage (2) Valdez (3) Whittier (4) Seward	(1) Extensive damage to pile supports, (2) Port destroyed by a landslide, (3) buckling, bending, twisting of steel pile supported piers, (4) Destroyed by landslide.	(Werner 1998)
Loma Prieta	10/17/89	6.9 (M_w)	Redwood City Richmond San Francisco Oakland	Ports experienced damage to batter piles due to lateral displacement and settlement, container cranes were damaged, liquefaction was present, and infrastructure components were damaged.	(Werner 1998)
Hyogoken Nanbu, Japan	1/17/95	6.8 (M_s)	Kobe	Extensive liquefaction of fills, seaward displacement of quay walls, vertical displacement, de-railing, overturning, and buckling of legs in cranes, infrastructure component damage.	(Werner 1998)
Haiti	1/12/10	7.0 (M_w)	Port-Au-Prince	Wide-spread liquefaction, collapse of the north wharf, damage to batter piles in the south pier, submerged cranes, and transportation infrastructure component damage.	(Werner et. al, 2011, Green et. al, 2011)

2.1.2 Common Modes of Damage

Numerous components within a port system are susceptible to earthquake damage. The most common types of damage considered apply to the wharf structures, but cranes, embankments, and utility and transportation lifelines are also commonly considered within the scope of earthquake-induced damage. The following sections outline some of the damage modes common to typical port components.

2.1.2.1 Wharves

Damage to wharf components is perhaps the damage most prominent cause of the interruption of port operations. Some common port wharf structures and their failure modes include:

Gravity Quay Walls – A gravity quay wall consists of a caisson or other rigid wall placed on the seabed. Stability of the wall is maintained through the friction at its base. Typical failure modes for quay walls during earthquakes involve seaward displacement, settlement, and tilt. Figure 2.1 shows an example of two typical failure modes. It should be noted that failure mode b was commonly seen for quay walls at the Port of Kobe during the 1995 earthquake:

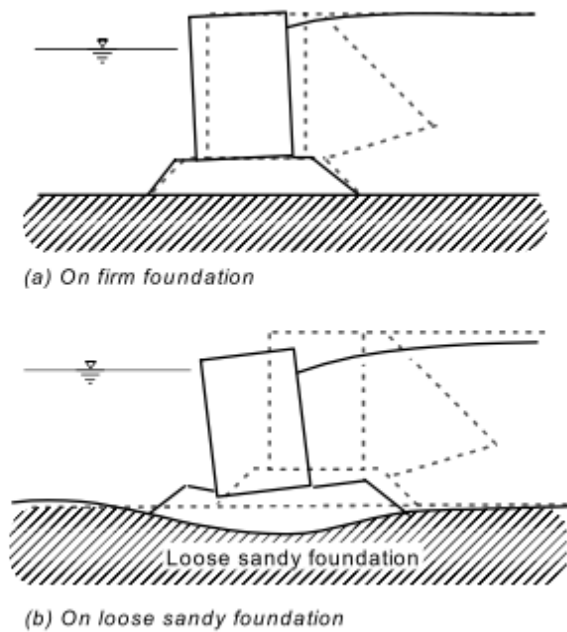


Figure 2.1 Deformation/failure modes of gravity quay walls (from (PIANC 2001))

Anchored Sheet Pile Walls – Anchored sheet pile walls are composed of a wall of sheet piles that are held in place by tie-rods and anchors. Failure modes of anchor walls are dependent upon the geometry of the wall as well as the composition of the soil backfill. Lateral displacement within loose sandy soil deposits (Figure 2.2) can affect the anchor (a), the pile wall (b), or the embedment (c):

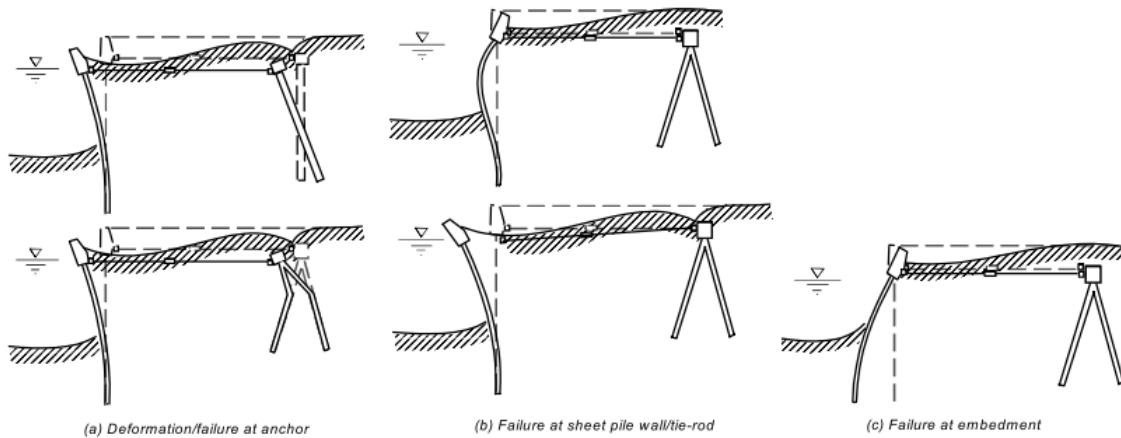


Figure 2.2 Typical modes of failure for anchored sheet piles (from (PIANC 2001))

Pile-Supported Marginal Wharves – Pile-supported marginal wharves consist of a deck supported by multiple piles embedded into a sloped embankment. Common deformations/ failure modes for this type of wharf (Figure 2.3) involve the inertial force of the deck (a), a horizontal force from the retaining wall in the backfill (b), and the lateral displacement of loose subsoil (c). In addition, significant deformations within the wharf deck connections are also a common failure mode (Werner, 1998). It should be noted that pile-supported marginal wharves are the most common type of wharf used the US.

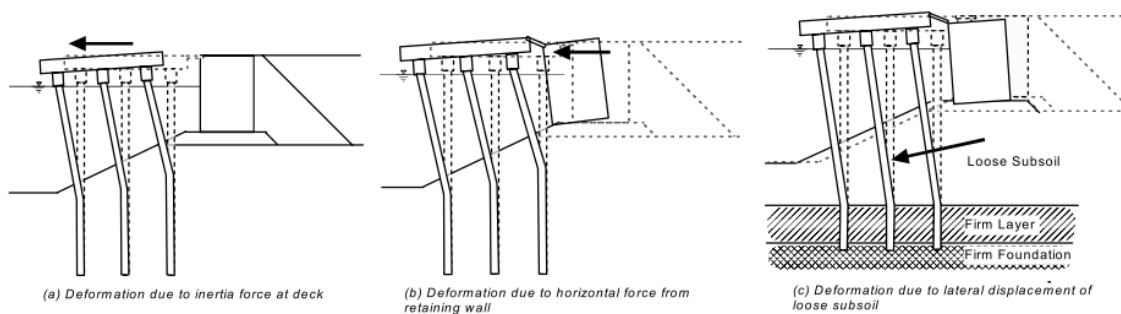


Figure 2.3 Common deformation/failure modes of pile-supported wharves (from (PIANC 2001))

2.1.2.2 Cranes

One of the most common modes of rail supported crane damage is the derailment of the crane through tipping. Generally, in this case, no serious damage occurs, and the crane can once again be operational within a matter of days (Kosbab et al. 2009). Other modes of failure include detachment or pull-out of vehicle, rupture of clamps and anchors, buckling, and overturning (PIANC 2001). Figure 2.4 illustrates some of these deformation modes:

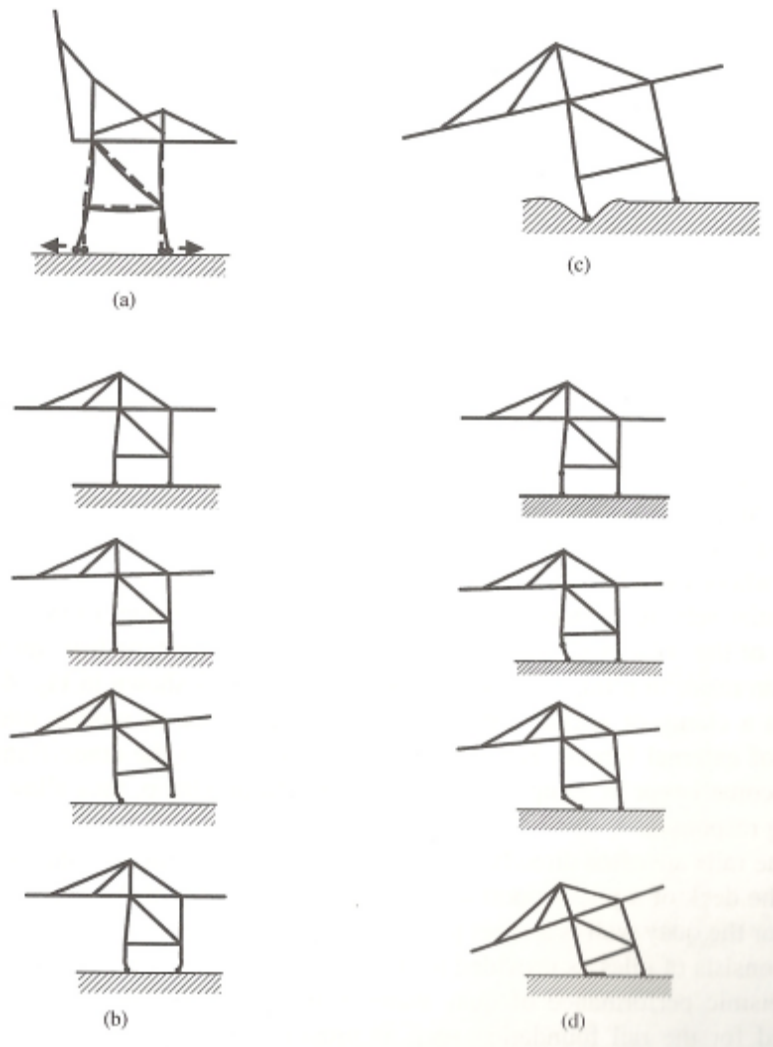


Figure 2.4 – Crane Deformation Modes: a.) Widening between Legs, b.) Narrowing between Legs due to Rocking, c.) Tilting of Crane from Differential Settlement, and d.) Overturning of One Leg Due to Rocking/Sliding (from (PIANC 2001))

2.1.2.3 Embankments

Lateral displacements, settling, embankment failures, and lateral spreading due to liquefaction are the main failure modes within wharf embankments. Shifting of the embankment itself often initiates a failure or deformation in one or more of the other port components. The photos below show some of the aforementioned failure modes in port facilities during previous earthquakes:



Figure 2.5 – a.) Lateral Spreading: Port de Port-Au-Prince (Photo by (Rix, 2010)) and b.) Crane Settlement: 1985 Chile Earthquake (from (Werner 1998))

2.1.2.4 *Utility and Transportation Lifelines*

Damage to utility and transportation lifelines impacts the post-earthquake repair and restoration efforts. Possible failure modes include the shearing or rupturing of pipelines carrying gas, water, or wastewater, the loss of power due to damaged power lines, or any damage to roadways or bridges used for port access. The Port of Kobe offers an excellent example of how lifeline damage affects the port. After the earthquake the Port of Kobe lost power which in turn caused the loss of the entire contents of every refrigerated warehouse, water lines ruptured and the service to Port Island was out for 30 days, and many of the roadways and bridges into and around the Port of Kobe were damaged and could not be used immediately (Werner 1998). In fact, repairs to the roadways and bridges continued to restrict cargo throughput even after many of the berths became operational again. Figure 2.6 shows one main roadway under repair 7 months after the Kobe earthquake whose repairs restricted the flow of cargo to and from the port.



Figure 2.6 – Kobe, Japan, 7 months after the 1995 Kobe Earthquake (from (Brundsdon, 1995))

2.2 Review of Current Design Guidelines

2.2.1 PIANC

In 2001 the International Navigation Association (PIANC) introduced a set of international guidelines for seismic design. The guidelines examined port systems, both large and small, across the globe and identified two levels of earthquake motions at which designs will be calculated:

Level 1 (L1) – level of earthquake motions likely to occur during the life-span of a structure.

Level 2 (L2) – the level of earthquake motions associated with infrequent rare events

Acceptable levels of damage from each of these design motions are specified by the users/owners of the facility under one of the following degrees of Table 2.2.

Table 2.2 Acceptable level of damage in PIANC performance-based design (from (PIANC 2001))

Acceptable level of damage	Structural	Operational
Degree I : Serviceable	Minor or no damage	Little or no loss of serviceability
Degree II: Repairable	Controlled damage**	Short-term loss of serviceability***
Degree III: Near collapse	Extensive damage in near collapse	Long-term or complete loss of serviceability
Degree IV: Collapse****	Complete loss of structure	Complete loss of serviceability

* Considerations: Protection of human life and property, functions as an emergency base for transportation, and protection from spilling hazardous materials, if applicable, should be considered in defining the damage criteria in addition to those shown in this table.

** With limited inelastic response and/or residual deformation

*** Structure out of service for short to moderate time for repairs

**** Without significant effects on surroundings

Performance of the actual structure is then defined by a performance grade S, A, B, or C according an acceptable level of damage defined at each of the levels of earthquake motions (Table 2.3):

Table 2.3 – Performance grades S, A, B, and C (from (PIANC 2001))

Performance grade	Design earthquake	
	Level 1(L1)	Level 2(L2)
Grade S	Degree I: Serviceable	Degree I: Serviceable
Grade A	Degree I: Serviceable	Degree II: Repairable
Grade B	Degree I: Serviceable	Degree III: Near collapse
Grade C	Degree II: Repairable	Degree IV: Collapse

Performance grades for structures are chosen either by the operator/user or based on the importance of the structure. The seismic performance of that structure is then evaluated by comparing a response parameter calculated from simplified, simplified-dynamic or dynamic analyses with the response parameter of the damage criteria specified for the selected performance grade. If the results of the analysis do not meet the damage criteria, this indicates that the proposed design or existing structure analyzed should be modified.

The PIANC guidelines suggest that the chosen method for analysis be appropriate to the performance grade chosen. For example, if a structure is to be examined at performance grade S, it will require a more sophisticated model. Table 2.4 shows the type of analysis most appropriate for each performance grade:

Table 2.4 – Types of Analyses Related to Performance Grades (from (PIANC 2001))

Type of analysis	Performance grade			
	Grade C	Grade B	Grade A	Grade S
Simplified analysis: Appropriate for evaluating approximate threshold level and/or elastic limit and order-of-magnitude displacements.				
Simplified dynamic analysis: Of broader scope and more reliable. Possible to evaluate extent of displacement/stress/ductility/strain based on assumed failure modes.				
Dynamic analysis : Most sophisticated. Possible to evaluate both failure modes and extent of displacement/stress/ductility/strain.				
Index:				
	Standard/final design			
	Preliminary design or low level of excitations			

2.2.2 Port of Los Angeles Code

The design considerations for the Port of Los Angeles (POLA), which were based on the Marine Oil Terminal Engineering and Maintenance Standards (MOTEMS) seismic design guidelines for marine oil terminals, establishes minimum wharf and crane design criteria that is meant to protect public safety in the event of rare intense ground shaking, and also aims to reduce the risk of economic losses through the implementation of performance criteria for structures in the event of moderate and large ground motions. Many of the existing wharves at POLA are pile-supported marginal wharves and the structural system analyzed within the code is based on a strong beam (deck), weak column (piles) frame concept. The following is some general criteria assumed in the analysis of the port structures based on the current POLA designs (Port of Los Angeles 2007):

- 1.) Structural System - for the structural system expects that the wharf shall be designed as a ductile moment-resisting frame consisting of a reinforced concrete deck supported by vertical piles. All elements of the deck shall be

capacity-protected to resist loading from piles, and the expansion joints will provide accommodation of thermal expansion.

- 2.) Piles – Uncoupled inertial and kinematic loading of piles shall be considered. Seismic piles are expected to have fully ductile performances with special pile-deck connection detailing. Secondary seismic piles do not need to be fully ductile, and have less stringent detailing of pile-deck connections. Battered piles shall not be used for the design of new wharves or for the replacement of damaged wharves. Any steel pipe piles should meet local buckling requirements in accordance with the applicable standards.
- 3.) Concrete Cover – A 3 in. (minimum) concrete cover should be placed on wharf beams, slabs, piles, and all concrete placed against the soil, except for headed reinforcing bars such as pile dowels or shear stirrups. Here the cover can be reduced to 2.5 in. (at the top surface only).
- 4.) Crane Rails – Crane rails should be connected to beams by supported vertical piles, and should be connected horizontally by a continuous wharf deck, struts, or other means that controls the gauge of the rails.
- 5.) Embankment – The embankment beneath the wharf should be protected from erosion by riprap in order to prevent the migration of fines along the back of the wharf.
- 6.) Utilities and Pipelines – Flexible connections should be provided where utilities span joints, individual wharf units, or places where they span rigid and non-rigid structures. Ground surface rupture will be addressed by providing increased flexibility of utility connections that pass from the backland to the wharf.

The code uses a performance-based design approach for the design of new marginal container wharves and the evaluation of the existing container wharves. Design is based on the performance of the wharves and cranes at each of the following three ground motions:

- 1.) Operating level earthquake (OLE) – This earthquake has a 50% probability of exceedance in 50 years or a 72-year return period and it is expected that any forces and deformations of the structures or permanent embankment deformations of the wharf should not result in significant structural damage. If repairs need to be made they are expected to be visible and accessible and should not interrupt wharf operations. OLE forces and deformations should not result in any structural, electrical, or mechanical crane damage. If derailment occurs it should be repaired in a reasonable amount of time (Port of Los Angeles 2007).
- 2.) Contingency Level Earthquake (CLE) - This earthquake has a 10% probability of exceedance in 50 years or a 475-year return period. For this level earthquake it is expected that any forces and deformations of the wharf or permanent embankment deformations result in controlled inelastic structural behavior and limited permanent deformations. Temporary loss of operations is expected but should be restored within an acceptable amount of time. No design requirements exist for the cranes at this design level (Port of Los Angeles 2007).
- 3.) Ultimate Level Earthquake (ULE) – this earthquake is defined in accordance with the ASCE/SEI 7-05 Standard. This level earthquake is considered the largest designed for by the port. After this level earthquake it is expected that neither the wharf nor cranes collapse and that the wharf would still be able to support the dead load of the container cranes (Port of Los Angeles 2007).

Structures within the port are analyzed for each ground motion and performance level to determine the displacement demand and capacity. The majority of the code specifies the details of analyses conducted for the wharf structures. Specifically, the code requires modeling of the following displacements: the torsional response of the structure, the interaction between adjacent wharf units at expansion joints, and the combination of simultaneous orthogonal excitations. Possible analysis methods suggested by the code include: nonlinear static pushover analysis, modal response spectrum analysis, single mode transverse analysis, substitute structure analysis, and linear or nonlinear time-history analysis (Port of Los Angeles 2007).

In addition since permanent displacement of the embankment is a concern in ports, it is suggested that liquefaction potential, the static and pseudo-static slope stability, post-earthquake slope stability, potential for lateral spreading, potential for settlement of the embankment also be examined (Port of Los Angeles 2007). Analyses should also consider the loads introduced to the wharf by the embankment by considering soil-structure interactions, the soil behavior under lateral pile loading, and the effect of earth pressures.

2.2.3 American Society of Civil Engineers

As of January 2012, the American Society of Civil Engineers (ASCE) Standard for the Seismic Design of Port Systems has not been officially published. However, the release of this document will mark the newest standards in port design in the US. Therefore, the design practices specified within the ASCE Standard will be covered within this document.

The ASCE standard for the seismic design of ports focuses mainly on the function and design of piers and wharves supported on concrete or steel piles, but also presents design requirements for “ancillary components” (pipelines, container cranes, marine loading arms, etc.) Design requirements are based on performance requirements of three

earthquake levels: Operating Level Earthquake (OLE), Contingency Level Earthquake (CLE), and Design Earthquake (DE) at three different design classifications (high, moderate and low). Structures are given a particular design classification based on importance. High structures would be essential to the region's economy or post-event recovery, and require a level of safety beyond life-safety protection, moderate structures are considered of secondary importance to the regional economy and no essential to post-event recovery, but still require life-safety protection, and low structures include all remaining structures (ASCE 2011). The probability of exceedance and minimum performance requirement of each combination of earthquake level and design classification are located in Table 2.5:

Table 2.5 – Minimum Seismic Hazard and Performance Requirements from (ASCE 2011)

Design Classification	Seismic Hazard Level and Performance Level					
	Operating Level Earthquake (OLE)		Contingency Level Earthquake (CLE)		Design Earthquake (DE)	
	Ground Motion Probability of Exceedance	Performance Level	Ground Motion Probability of Exceedance	Performance Level	Seismic Hazard Level	Performance Level
High	50% in 50 years (72-year return period)	Minimal Damage	10% in 50 years (475-year return period)	Controlled and Repairable Damage	Design Earthquake per ASCE 7 [2.1]	Life-Safety Protection
Moderate	n/a	n/a	20% in 50 years (224-year return period)	Controlled and Repairable Damage	Design Earthquake per ASCE 7 [2.1]	Life-Safety Protection
Low	n/a	n/a	n/a	n/a	Design Earthquake per ASCE 7 [2.1]	Life-Safety Protection

The structural responses considered in Table 2.5 fall under one of three performance levels: minimal damage, controlled and repairable damage, or life-safety protection. Minimal damage is defined by when a structure exhibits near-elastic structural response and only minor or no residual deformation, serviceability of the

structure should be continued, and all materials remain contained in a manner that poses no threat to public safety. Controlled and repairable damage is defined by a structural response in a controlled and ductile manner with limited inelastic deformations at locations where repair is possible. Repairs that are necessary result in a serviceability loss less than “several months”, and again, all materials remain contained in a manner that poses no threat to public safety. Life-safety protection is the highest performance-level considered in the standard. Post-earthquake a life-safety protected structure should continue to support gravity loads, any damage occurring should not prevent egress, and materials should still be contained in a manner that does not pose a public hazard (ASCE 2011). If structures perform in the manner set forth in the previous descriptions for their specified design levels, they meet the design code for the ASCE Standard.

These design codes are tested by considering the following seismic hazards in the modeling of the wharf and ancillary components: inertial loads due to ground shaking, ground deformations associated with liquefaction and cyclic deformation of weak soils, kinematic loading due to ground deformations adjacent to piles and fault rupture effects (ASCE 2011). The following sections will discuss the seismic hazards considered and their use in the ASCE Standard’s consideration of geotechnical hazards, the force-based and displacement-based structural design models considered, and the ASCE Standard’s consideration of ancillary components, namely cranes.

2.2.3.1 Geotechnical Hazards

Liquefaction potential should be evaluated for predominantly sandy soils and non-plastic silts using current standards of practice (Martin and Lew 1999; Youd et al. 2001; California State Land Commission 2010). Liquefaction hazards warrant the evaluation of the following failure modes: flow slides of native soils or hydraulically placed fill, ground failures involving containment dikes, embankments, and slopes supporting

wharves and piers, lateral spreading of dike/embankment/slope, and post liquefaction settlement of the dike/embankment/slope and underlying foundation soils (ASCE 2011).

Sensitive fine-grained soils have also demonstrated a mobilization in large strains and a resulting loss of stiffness and strength (and ground deformations) when subject to moderate cyclic loading (ASCE 2011). Screening tools have been developed to identify fine-grained soils susceptible to liquefaction and/or large-strain development and ASCE recommends using the following references to determine susceptibility: Seed et al. (2003), Andrews and Martin (2000), Bray and Sancio (2006) and Boulanger and Idriss (2006).

In addition, it is also important to conduct soil-structure interaction evaluations to determine the lateral loads subjected to piles by any ground deformations. Load conditions considered should include the inertial loading due to the wharf deck and other contributing masses under seismic conditions which produces maximum moments in the upper portion of the piles, and the kinematic loading associated with the influence of permanent ground deformation of the piles which imposes maximum moments in the lower portion of the piles (ASCE 2011).

2.2.3.2 Force-based Analysis and Design

One possible method of analysis and design uses the force-based analytical method for equivalent lateral force analysis taken from ASCE 7 (ASCE 2005) with only minor modifications. However, the standard notes that this analysis will produce pier and wharf structures that are less economical than those designed using the displacement-based methods, and that in general, marginal wharves are not well suited to force-based design due to the large eccentricity between the center of mass and center of rigidity or the piles in the elastic range (ASCE 2011). If force-based analysis is used, the following must be considered/modeled: seismic base shear, seismic response coefficient,

fundamental structural period, pile stiffness, shear strength of concrete or pipe piles, confinement of prestressed piles, and overstrength shear force.

2.2.3.3 Displacement-based Analysis and Design

The displacement-based design approach is a more complicated approach than the force-based, but is commonly used in design codes of actual ports such as POLA and Port of Long Beach (POLB) (ASCE 2011). The displacement analysis should be based on appropriate ground motions and the physical structures modeled should represent the spatial distribution of the mass and stiffness of the structure to an extent that is adequate for the calculation of the significant features of its dynamic response. Dynamic responses typically modeled and model considerations include: moment curvature analysis, plastic rotation, plastic hinge length, in-ground plastic hinge length, plastic hinge length for pile-to-deck connections, pile depth to fixity, seismic p-delta effects, capacity analysis (non-linear static pushover), and demand analysis (modal response spectrum and nonlinear static demand) (ASCE 2011).

2.2.3.4 Ancillary Components (Cranes)

While the ASCE Standard focuses on multiple ancillary components, this section will focus on standards pertaining to the cranes. From past crane performance, ASCE recognizes that the larger, heavier and more stable modern container cranes are more susceptible to damage during earthquakes with the modern jumbo crane with a 100 ft or more gage length probably experiencing significant damage in the OLE and collapse in the CLE or DE. The ASCE Standard requires that the ancillary structures to the pier and wharf (such as the cranes) be designed to that they will not collapse in the ASCE design earthquake (DE), which corresponds to a 2475-year mean recurrence interval (MRI) design earthquake (Soderburg et al. 2009) and that seismic performance requirements be included within the decision-making process when procuring new cranes (ASCE 2011).

2.2.4 Liftech Crane Guidelines

Currently because the ASCE guidelines are not yet published, no standardized set of codes exists specifically for container cranes. Historically, either consultants or the crane manufactures have been responsible for setting performance requirements within crane design. Early container crane designs were small with lift heights of approximately 25 m above the wharf and weighed about 600-800 metric tons (Soderburg et al. 2009). Seismic loading was not considered a significant design load because cranes would tip before they could become damaged. However, modern jumbo cranes have grown in size with the increase of ship size (Kosbab 2010) . These modern cranes range in lift height from 35 m - 42 m above the wharf and weigh anywhere from 1300-1800 tons. These larger cranes require stiffer portal frames, have greater portal clearances, and are more stable, which results in larger lateral loads (Soderburg et al. 2009). Therefore, the early seismic design criteria can not be applied to modern jumbo cranes.

The new Liftech seismic design criterion specifies design requirements for a 72 year (OLE) and 475 year (CLE) earthquake. Design criteria for each earthquake include (Soderburg et al. 2009):

Operating Level Earthquake – Design criteria requires elastic design stresses in the crane structure. Any damage that may occur should be easily reparable.

Contingency Level Earthquake – The design criteria for this level earthquake considers (1) Tipping – wherein the crane is designed to tip with stresses less than 90% of the yield, and (2) Special moment frame – wherein the portal frame is designed to yield plastically. If stresses exceed 80% of yield, the member should meet the American Institute of Steel Construction (AISC) seismic detailing requirements. The performance criteria requires that collapse be prevented by specifically designing the crane to tip, designing the crane to be ductile (seismic loads are absorbed by ductile yielding), and designing the crane to be structurally isolated from the wharf (done through the introduction of an isolation joint).

2.3 Prior Studies in Risk Assessment

As seen in the previous section, the current seismic codes involving ports are all based on arbitrarily selected ground motion probabilities rather than acceptable levels of cargo throughput resilience. Any mention of throughput is vague and gives no real standard of acceptable losses from downtime. The study discussed in the following section was the first to specifically address cargo throughput within its risk evaluation, and is the framework upon which the NEES Grand Challenge framework described in this dissertation is based.

2.3.1 Werner and Taylor, 2004

Perhaps the most ambitious seismic risk assessment of a port system to date was performed by Werner and Taylor (2004) for the Port of Oakland. This project used seismic risk reduction planning consisting of acceptable-risk evaluations that could be used to guide the port's selection of a level of seismic upgrade for each of the specific berths examined. These upgrades would then be aggregated to achieve an overall level of system-wide seismic performance.

Not every berth in the Port of Oakland was upgraded within this project. Some of the berths were involved in the Wharf and Embankment Strengthening Program (WESP) and for those berths structural modifications were made to improve the strength of the wharves and to improve the seismic response. The remaining berths were not strengthened but still evaluated in the seismic risk reduction planning (SRRP). Figure 2.7 shows the layout of the examined berths within the port:

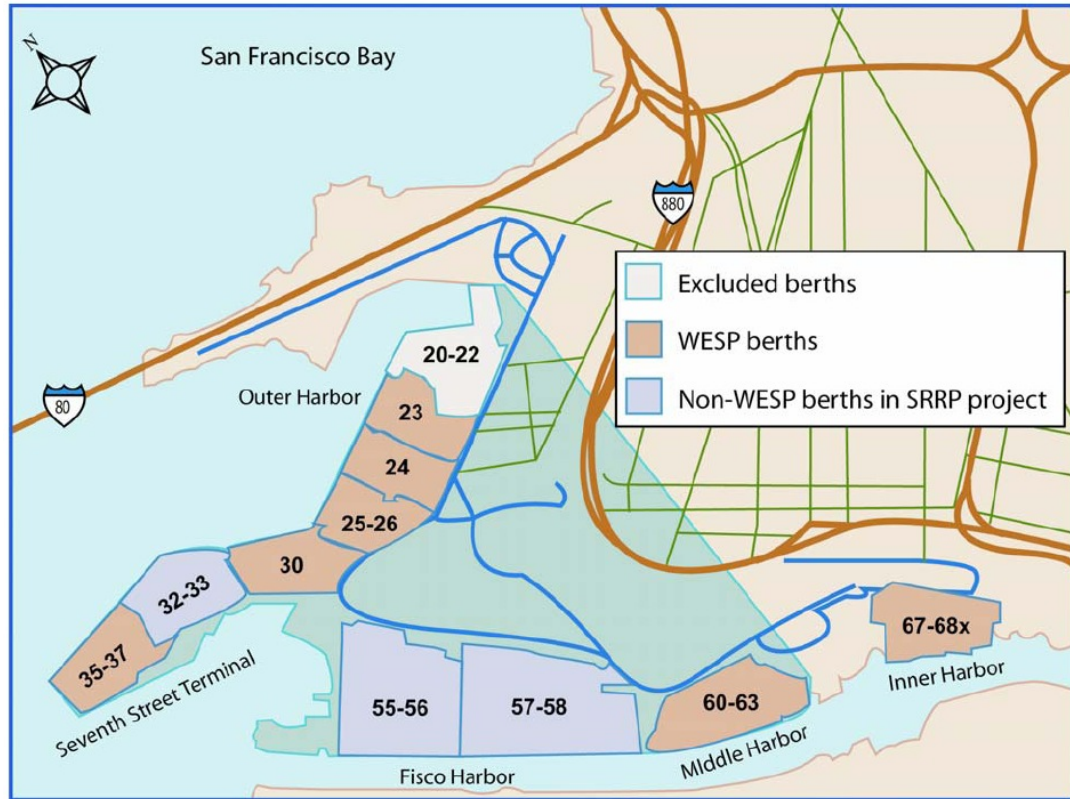


Figure 2.7 Berths included in the Port of Oakland WESP Seismic Risk Reduction Project (Werner and Taylor 2004)

2.3.1.1 Overview of acceptable risk approach

The overall goal of this analysis was to obtain an amount of “acceptable” risk within the port system. Since it is not possible to reduce the seismic risk to zero with the application of some design or upgrade, an acceptable risk is achieved. Acceptable risk can be defined by the point where the residual risks from earthquakes remain acceptable and “beyond which the economic, regulatory, legal, etc. costs of further reducing these risks are unacceptable.”(Werner and Taylor 2004) To obtain this risk, the approach adhered to the following five-step procedure:

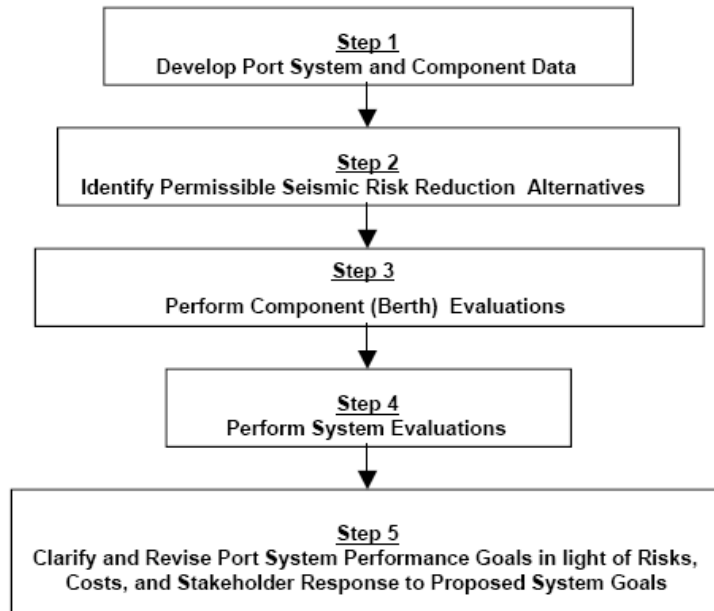


Figure 2.8 Risk Assessment Approach for the Port of Oakland (Werner and Taylor 2004)

Step 1 – Develop Port System and Component Data

The first step in the risk assessment was to gather port system data and component data from the Port of Oakland. Port system data was obtained from meetings with port financial and operations staff and consisted of data that detailed operation of the port system on a daily basis. Component data was obtained from drawings and berth plans and pertained specifically to the geometry, material properties and seismic response characteristics of both the wharf structures and the embankments.

Step 2 – Identify Permissible Seismic Risk Reduction Alternatives

For this project, seismic upgrade options were developed by structural consultants for each of the WESP berths. The sets of berths within the port were built at different times in the port's history and therefore had varying starting configurations and slightly different upgrade options. Some berths did not need a seismic upgrade (26 and 30), were damaged in the Loma Prieta earthquake and subsequently upgraded (35-37), or performed well enough in the Loma Prieta earthquake to only require small changes. For

these berths, risk reduction alternatives were not costly. However, the alternatives for the other berths varied in seismic performance upgrades and ranged from \$7.1 to \$39.1 million dollars.

Step 3 - Perform Component Evaluations

The response of each type of berth to seismic motion was evaluated through the use of vulnerability models. These models, which are essentially fragility models, related berth repair costs and post-earthquake functionality to a range of seismic hazard levels.

The first step in the vulnerability modeling was to define a range of combinations of ground shaking and permanent ground displacement demands that could occur at the site from potential regional earthquakes. Ground-motion attenuation models estimated firm-site horizontal peak ground accelerations (PGAs) for 15 levels of ground shaking. These levels corresponded to the mean and mean \pm one standard deviation for earthquakes with a moment magnitudes of 5.5, 6.2, 6.7, and 7.1 along the Hayward Fault, and $M_w = 7.9$ along the San Andreas Fault. One set of firm-site PGAs was applied to the entire port for each earthquake. To account for local soil conditions, one-dimensional, equivalent linear site response analyses with site-specific profiles were applied to corresponding firm-site ground motion time histories. Furthermore, corresponding permanent ground displacements along the depths of the piles were found by using pseudo-static stability methods and Newmark-type displacement analyses, and/or the results of FLAC dynamic finite-difference analyses.

The risk assessment for all the different berth configurations was conducted using ground motions from a walkthrough procedure (Taylor et al. 2001) that detailed the number, location, and magnitudes of earthquakes that occurred each year over a 10,000 year period. This period was chosen in view of the large number of California earthquakes. Furthermore, since the operational portion of the port system was to be examined over 10 year periods, the project would actually be modeling 1,000 samples of

10-year random walks. It was also believed that this period provided a reasonable basis for assessing the financial costs and risk patterns in step 4 for the many combinations of berth seismic upgrade options considered in this project. For each year in the walkthrough table, the following were estimated:

- The seismic hazards at the berth site
- The damageability of each berth to these hazards, along with the corresponding repair cost

Damageability of each berth was decided from a range of damage states based on the capacities of various berth components. Once the lower limit of the limit capacity was reached, a specific damage state and associated repair model was applied. When deciding between repair and replacement of damaged berth components, it was assumed that collapse (or at least 2 rows of broken piles) would require replacement, and less damage would result in repair. Furthermore, it is assumed that normal resources of materials, contractor, and labor availability exist, and that contracts for evaluating, designing, and supervising repairs could be rapidly negotiated. Repairs due to liquefaction-induced subsidence of the backfill except where it was a symptom of potential damage to the wharf itself, crane damage, electrical damage, and damage to mechanical equipment and connections were excluded from all repair scenarios. Finally, repair/replacement costs and potential downtimes were estimated by structural engineers according to the damage states and the types of repairs that needed to be made.

Step 4 – Perform System Evaluations

For each year of the walkthrough table, the following system analysis properties were calculated:

- 1.) Post-earthquake functionality of wharf and duration of repair
- 2.) The berth functionalities and how the functionality of each affected the shipping demand

3.) The economic losses from repair costs and interruption of shipping operations

The main goal of step 4 was to determine the functionality of the berth and if it was not functional, for how long it would remain that way. The functionality of the berth is determined by 1000-ft. intervals, or the average length needed to accommodate one ship. Downtimes in repair models were recorded in 1000-ft. increments and used in the estimation of system-wide business interruption losses due to earthquake damage to the berths.

Business interruption losses required its own analysis procedure that is outlined in Figure 2.9:

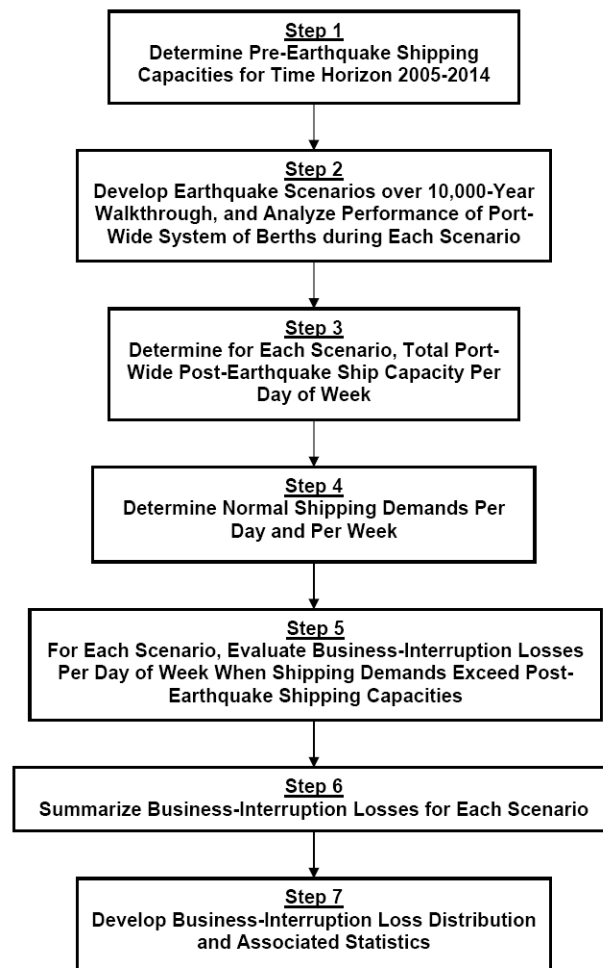


Figure 2.9 Operations/System Seismic Risk Analysis procedure for estimating business interruption losses (Werner and Taylor 2004)

Capacities and demands within the previous steps were estimated over 10-year spans by using previous shipping data supplied by port operations officers. This data was important because shipping demands not only vary by day of week but also seasonally. Therefore, it was necessary to analyze business interruptions on a day-to-day basis.

Once evaluations of all components and all component upgrade options for each year of the 10,000-year period were complete and the damage states along with repair costs were determined, the results were “aggregated to probabilistically characterize economic risks associated with each combination of upgrade options for the various berths (Werner and Taylor 2004).” Risk assessments were then conducted using a mean-variance criterion. This criterion provided an opportunity to compare options on the basis of the yield and volatility of an investment.

Step 5 – Clarify and Revise Port System Performance Goals

This step revaluated the results from the previous steps in tandem with administrative, regulatory, legal, or other constraint that might make one berth option more preferable than another. Options were improved iteratively until the optimal solution for all parties involved was decided upon.

2.3.1.2 Results

Eighty combinations of berth upgrade options were evaluated using mean-variance criterion (MVC). However some of those options were ruled out by MVC because the mean value and standard deviation of the total life-cycle cost were higher than those of at least one other combination. The combinations that passed the MVC test are listed in Table 1. Overall, seismic upgrades for Berth 30 and the 68 extensions were warranted by MVC in all cases. In the table for each combination, the option number for each upgrade is listed along with the overall normalized total cost and standard deviation of that cost. Note that an upgrade option of 0 indicates that no upgrade was made. The

baseline option (or no seismic upgrade) had a present value mean total cost of \$29.6 million and a standard deviation of \$11.2 million (not present value). While the total cost of this option is lower than all of the other options, the standard deviation is the greatest, which means that it has the greatest volatility of all the investments.

Table 2.6 Combinations of Berth Seismic upgrade Options that Pass the MVC (Werner and Taylor 2004)

Combination No.	Seismic Upgrade Levels at Each Berth					Normalized Total Cost *	Normalized Standard Deviation *
	Berths 23-25	Berth 30	Berths 60-63	Berths 67-68	Berth 68 Extension		
1	0	1	0	0	1	0.99	0.99
2	0	1	0	1	1	1.188	0.97
3	1	1	0	0	1	1.190	0.95
4	1	1	0	1	1	1.39	0.92
5	2	1	0	0	1	1.72	0.87
6	2	1	0	1	1	1.92	0.84
7	3	1	0	1	1	2.27	0.824
8	4	1	0	1	1	2.30	0.820
9	0	1	1	0	1	2.83	0.60
10	0	1	1	1	1	3.023	0.57
11	1	1	1	0	1	3.025	0.56
12	1	1	1	1	1	3.22	0.53
13	2	1	1	0	1	3.55	0.49
14	2	1	1	1	1	3.75	0.46
15	3	1	1	1	1	4.11	0.436
16	4	1	1	1	1	4.14	0.435

* Costs normalized relative to baseline combination, which corresponds to as-is (no seismic upgrade) option for all WESP berths. For this combination, total cost = \$29.6 million, and standard deviation = \$11.2 million.

2.3.2 Pachakis and Kiremidjian, 2004

While the previous study by Werner and Taylor was perhaps the most comprehensive port study to date, others have examined more specific aspects of the risk assessment procedure. Pachakis and Kiremidjian (2004) conducted a study that calculated operational losses occurring after scenario earthquakes in multi-terminal container ports. The majority of the operational losses, resulting from wharf damage, were a consequence of downtime within the terminal.

2.3.2.1 Assessment

Assessment began with an estimation of ground motions at the site using a deterministic seismic hazard analysis. Using predicted intensity measures present at the site, the damage state probabilities were calculated, and then those damage states were related to the losses that could occur. Operationally, facilities have a binary status: they are either operational or non-operational, depending on the damage state. The determination of this functional state “require[d] a system approach, where the damage states of the port components (buildings, cranes, wharves, and utilities) that contribute[d] to the cargo handling operations [were] combined through fault trees and event trees to produce the functional states of the terminals and their associated probabilities (Pachakis and Kiremidjian 2004).”

Once the functionality of a terminal was established, downtime was calculated. The port simulation took place over a time period Δt , that was large enough to include a full restoration of damage plus a length of time long enough for operations to return to a steady state. In the computation of revenue losses, the port was modeled as a queuing system wherein the ships were equivalent to customers and the berths represented the servers. The ship traffic was described by the vector process $\bar{I} \equiv \{\bar{I}_n\}, n \in N$ whose components included the ship arrival times, terminal of destination, ship type, length, and cargo to be loaded and unloaded. The simulation assumed that the change in traffic as a

result of the scenario event was beyond the scope of the study, so the process $\{\bar{I}_n\}$ was stationary, ergodic, and unaffected by the earthquake. Using these assumptions, the loss was calculated by subtracting revenue generated when an earthquake occurred, from that generated when no earthquake occurred over the period Δt .

$$E[L_d] = E_{\bar{D}}[E_{\bar{I}}[L_d|\bar{D}]] = \sum_d E_{\bar{I}_d} \left[\sum_{t=T_0}^{t=T_0+\Delta t} (R_{\bar{I}}(t) - R_{\bar{I}|\bar{d}}(t)) \right] P[\bar{D} = \bar{d}] \quad (2.2)$$

This equation asserts that the expected revenue loss due to downtime is equal to the expectation over all possible damage states of the revenue loss conditional on a particular damage state (Pachakis and Kiremidjian 2004).

The port model used in this evaluation assumed that the basic modeling unit of a port was a port terminal. A representational schematic of this unit is shown in Figure 2.10.

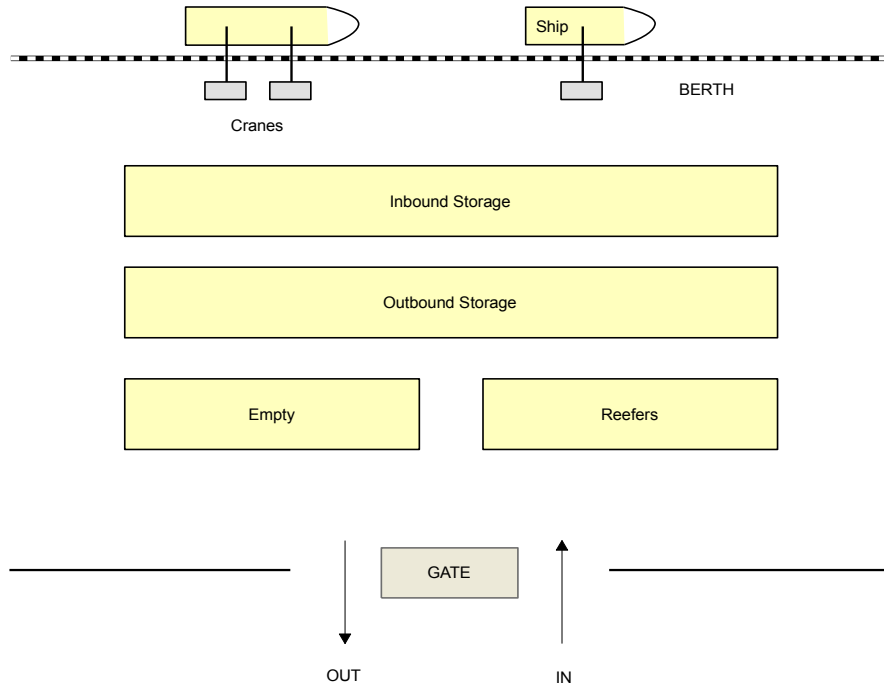


Figure 2.10 Port Terminal (after (Pachakis and Kiremidjian 2004))

Using the schematic above, port operations were assumed to take place in the following manner: Cargo is brought into the port by containerships. The quantity of this

cargo is measured in twenty-foot equivalent units (TEUs). Cargo is unloaded from a ship using one or multiple cranes (depending on ship length and availability). Some ships may then be reloaded with additional cargo kept in the terminal. Containers stored in the terminal are divided into four categories: Inbound containers, outbound containers, empty containers and refrigerated containers (reefers).

In order to analyze risk and revenue losses following a seismic event, it was necessary to obtain information about the ship traffic coming in and out of the port and how those ships were treated on a terminal operation level. For this study, the following assumptions about terminal operation were used: when a ship enters the port it is assigned a terminal and a berth. If a berth is unavailable, the ship enters a queue. Berth queues were necessary because some berths could only accommodate certain types of cargo. Therefore, cargo also had to be considered as one of the variable attributes of a berth in addition to length, water depth, and number of cranes. A berth also had to have a buffer size (or maximum amount of ships that could belong to the queue to be serviced). Once the buffer was reached, additional ships to be added to the queue would be diverted to other berths or terminals. For those ships in the queue or at the dock, the berth with the maximum number of available cranes would be chosen from a selected set of berths. As a general rule, the more containers on the ship to be processed, the more cranes that would be needed for processing. However, when waiting occurred, each ship had an assigned a waiting capacity so that if it was exceeded, the ship moved on to another terminal to be processed. These berth and crane assignment rules were used in order to minimize wait time because docking fees could accrue while a ship was docked and waiting.

During servicing, the total time spent servicing the ship was considered to be a function of the total number of TEUs, the number of cranes available, and the service rate for a given storage system. The service rate, r , was the total time docking, unloading, and reloading, over the total number of TEUs processed divided by the number of cranes:

$$r = \frac{\text{Service time}}{\left(\frac{\text{TEU}}{\text{Crane}} \right)} \quad (2.3)$$

The service rate r could then be used to determine the total service time for a ship which was evaluated as follows:

$$\sigma = \frac{\left(\text{TEU}_{\text{loaded}} + \text{TEU}_{\text{discharged}} \right)}{\# \text{ of Cranes}} * r \quad (2.4)$$

The total service time, σ , was used to calculate dockage fees which was determined by the duration of stay and the length of the ship. In addition, ships also may or may not have had to pay a number of additional fees:

- Wharfage – function of the number of TEUs loaded and discharged to and from the ship.
- Demurrage – if containers discharged from the ship or waiting to be loaded to a ship remain within the port for more than 5 days, a fee is collected per day for each TEU.
- Wharf Storage – if an owner wants to store containers at the storage facilities of a port for an extended period, there is a daily charge per TEU.
- Craneage – the tenants of a berth pay a fee each time a crane loads or unloads a TEU.

The previous port operational rules and equations were input into a computer program along with earthquake data to simulate port operations pre and post-earthquake. Then statistics of the revenue differences were calculated and weekly revenue streams for periods with and without an event were plotted.

2.3.2.2 Results

The study used the previous methodology on sample data to estimate revenue loss in a port after a severe earthquake. For the most part, these examples showed that this

methodology produced reasonable results, and that with proper planning and ship diversion, that the port can still accommodate its previous shipping demands (with some waiting time) even after earthquake damage. One of the highlights of this study was the use of sensitivity analysis. Variables affecting port operations were isolated and it was determined which variables had the greatest effect on revenue losses. Cranes and wharf damage had the greatest influence over revenue loss in this study. Their downtime was found to be significant and the accuracy of this estimation was required to get a high-quality loss estimate. It was also concluded that simulating terminals simultaneously was very important because it's easier to understand how the intelligent diversion of ships from damaged to undamaged terminals will minimize the losses after a strong earthquake.

2.3.3 Na and Shinozuka, 2009

Recently, there has also been some probabilistic risk assessment work conducted concurrent to the NEES Grand Challenge project. This work, from researchers at the University of California Irvine, has focused on the response of quay walls during earthquake excitation using the Port of Kobe as a case study, the effects of spatial variation in soil properties on the seismic performance of port structures, and simulation-based port loss estimation.

2.3.3.1 Response of Quay Walls

For the quay wall analysis, researchers conducted a case study using damage history data from the Kobe earthquake and created a 2D numerical model that represented berth PC1 which was damaged in Port Island, Kobe during the 1995 Kobe earthquake. After the Kobe earthquake the Port and Harbor Research Institute of Japan conducted an extensive survey of the seismic performance of 24 ports in the Kobe area (Na et al. 2008). Reports showed that seismic responses varied among the port structures, where the damage patterns of the quay walls ranged from large lateral movements, to

tilting, to settlements of caissons, to ground movements of the backfill in the form of lateral movements and settlements of the apron. A typical section of the damage patterns in a typical quay wall is shown in Figure 2.11.

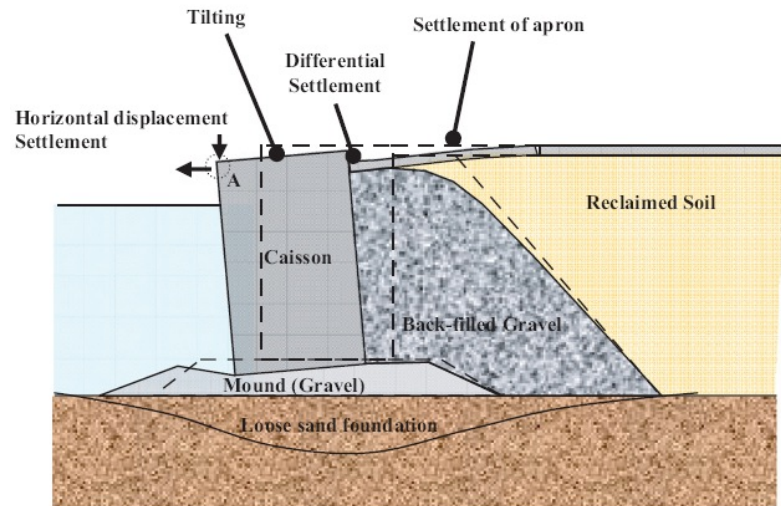


Figure 2.11 Typical section of damage criteria for a quay wall (From (Na et al. 2008))

2.3.3.2 *Effects of Spatial Variation in Soil Parameters in the Performance of Port Structures*

Ports are often susceptible to liquefaction during earthquake excitation because of the use of hydraulic fill in the backfill of the wharves. As a result, it is necessary to study the effect of liquefaction and the resulting lateral spreading on the seismic response of the wharves. Na et al (2009) specifically looks at quay walls. For this analysis, the researchers use FLAC to conduct a 2D nonlinear dynamic analysis of the soil-structure system. In the analysis, the 2D soil system is idealized as a homogeneous non-Gaussian random field. Next, a simulation algorithm was used to generate 130 digital realizations of 2D random field samples. The ground motion time history from the Kobe earthquake was applied to each of these realizations and the spatial variation of shear modulus was examined. The samples were characterized probabilistically in the Monte Carlo sense and are then compared to the response obtained under the uniform field assumption with the mean value of soil property (Na and Shinozuka 2009). The analysis found that

seismic response showed significant variation in horizontal displacement. Also, “while uniform field models generally lead to unconservative estimates of quay wall response, consideration of spatial variability of soil not only leads to better prediction of average response, but also can capture the dispersion of observed response of quay walls” (Na and Shinozuka 2009). Figure 13 illustrates the 130 response generated through the analysis. It can be seen that probability distribution of the residual horizontal displacements (RHD) of the realizations has a lognormal distribution, which could be used to predict confidence intervals of RHD response or for other statistical analysis.

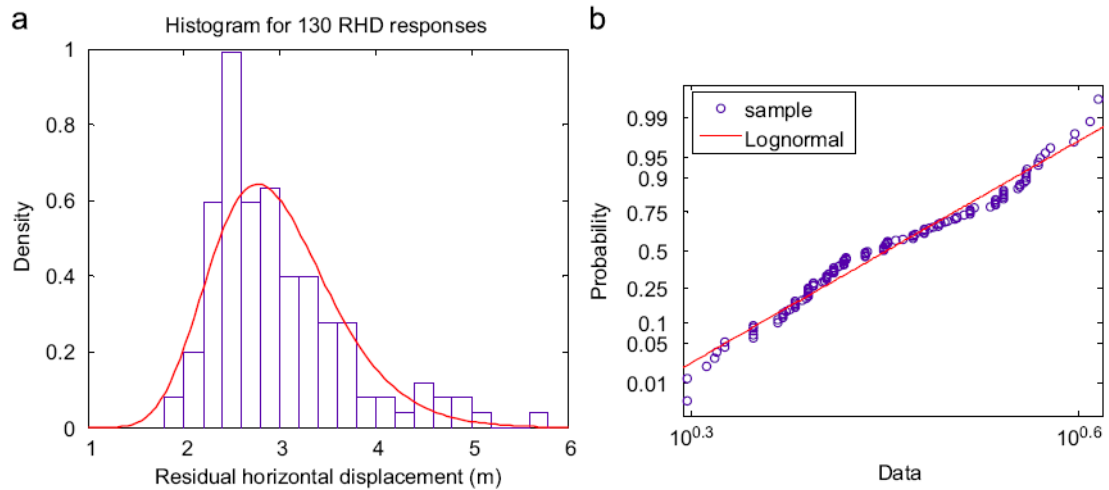


Figure 2.12 Statistics for 130 RHD responses (From (Na and Shinozuka 2009))

2.3.3.3 Simulation-based Port Losses

Loss estimation in ports is an important research avenue since most of the money lost after a large earthquake is caused by business interruption losses. As an example, in Kobe, physical damage cost \$5.5 billion whereas economic loss exceeded \$6 billion in the first 9 months after the earthquake (Na and Shinozuka 2009). Na et al (2009) provide a methodology to estimate this direct economic loss by evaluating the decreased container throughput resulting after an earthquake (Figure 2.13).

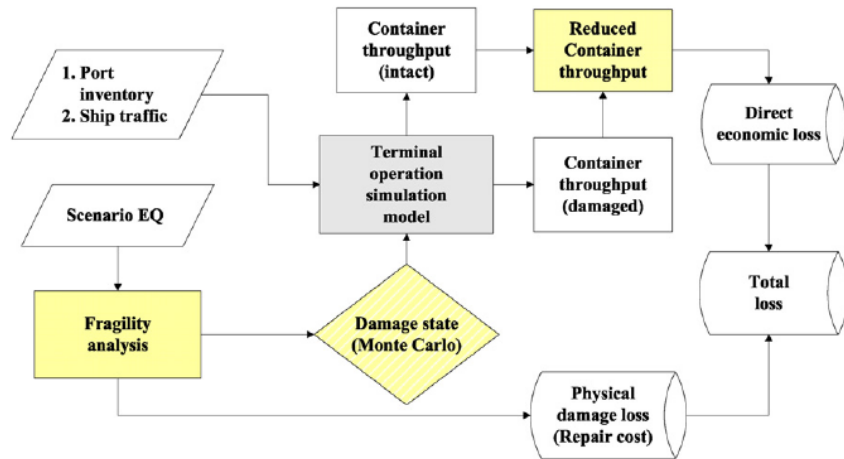


Figure 2.13 Loss estimation methodology (from (Na and Shinozuka 2009))

Calculation of throughput was conducted using a terminal operation simulation model. Development and simulation of this model was done using the software package ARENA. Inputs into this model include ship traffic, which is generated from terminal operation records, and a damage state for the berths at a terminal. Damage states were generated through a Monte Carlo simulation using quay wall fragility curves. The terminal operation simulation model is run more than once for varying states of damage within the port. The first run is done for an intact port with no damage so that a baseline (intact) container throughput can be measured. After, the model is run again including damage. This resulting throughput can be compared to the intact throughput to see how the container throughput was reduced due to the damage at the port. Direct economic loss can then be calculated using the calculated reduced throughput, port inventory information, and economic data.

Loss estimation through the use of component fragility curves provides a way to examine the fragility of the port operating system. For this study, system fragility was calculated at an existing port terminal with four berths and 13 container cranes. Damage states were independently determined probabilistically for each berth, and no damage was assumed for the container cranes. With damage states established, system restoration

times were then probabilistically calculated. Repair periods from t_{ideal} to $t_{pessimistic}$ were chosen using a random distribution and then the repair processes were simulated using a Monte Carlo approach. Loss estimation was conducted for the port in its initial and retrofitted states. Figure 2.14 provides an example of exceedance the fragility curves used to calculate losses for an original and retrofitted wharf.

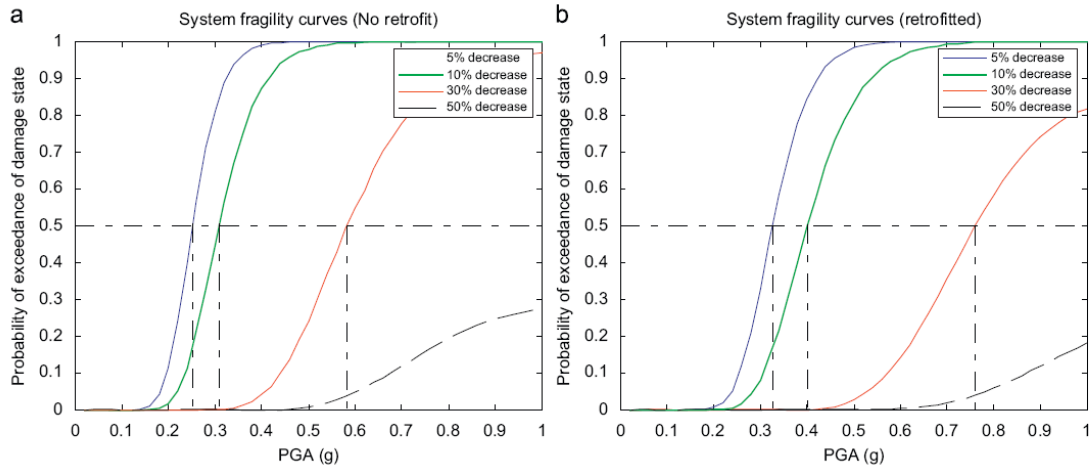


Figure 2.14 System fragility curves for (a) original and (b) retrofitted structure (From (Na and Shinozuka 2009))

2.4 Gaps in Knowledge

While much research and study has been conducted surrounding the seismic risk analysis of port systems, there is still room for improvement. The main objective of this study is to examine a US container port as a complete system using the state-of-the-art applicable engineering techniques. While the aforementioned studies have certainly assessed risk in the key port components, they fall short of a risk assessment of the port as a complete system. The Werner and Taylor study, which did the most complete job, only looked at the wharf response. The soil and wharf responses were modeled along with a few mitigation options, however there was no consideration of crane response. Furthermore, the operational losses calculated capacity decreases solely based on wharf availability. The operational treatment of ports in the Pachakis and Kiremidjian study offered an improvement since wharf and crane damage both contributed to losses, in the

calculation of damage states liquefaction hazards, soil-structure interaction, and pile-deck connections were not considered. Furthermore, the fragility curves used to determine the damage states for both the wharves and cranes were generic and not calculated by the authors. While the Na and Shinozuka studies did calculate their own fragility curves, they focused on quay walls, a type of wharf typical in Japan, and not west coast US ports. Additionally, while this study did include soil-structure interaction, it lacked consideration of cranes. Of all the port components neglected within the other studies, cranes are perhaps the most important. During the 2010 earthquake in Port-Au-Prince, Haiti, the main container crane available in port became partially submerged in the water and could not be used. Heavily damaged cranes cannot be repaired in the same way as wharves, which are built on-site. Cranes are manufactured abroad and then shipped to the port. Replacement times are lengthy and often last longer than it takes to rebuild other damaged port components (Kosbab 2010). The current port codes obviously include design requirements for both the wharves and the cranes, but they are based on arbitrary earthquake design levels and are limited in that there is no direct calculation of business interruption losses.

The seismic risk analysis developed under the NEES Grand Challenge project aims to remedy the gaps present within the previous studies by modeling the port system as completely as possible and but by also modeling spatially correlated seismic hazards in a fully probabilistic manner that is far superior to the arbitrary earthquake levels used in current designs. This project will model liquefaction hazards, soil-structure interaction, wharves (including pile-deck connections), and cranes to make fragility curves for use in the risk assessment. Additionally, operational losses will be calculated using sub-optimal tabu searches, which seek to closely replicate human decision-making. The use of state-of-the-art operational modeling is also a significant improvement because this is the first analysis conducted in which the sophistication of the operational model is equal to the sophistication at which engineered structures are modeled. Lastly, the loss calculations

generated will be used in economic analyses to illustrate the benefits of the probabilistic nature of the results to port stakeholders by comparing seismic mitigation options using meaningful metrics. While the Werner and Taylor study included mitigation and upgrade options for the wharves, the current model will also include geotechnical mitigation to prevent liquefaction, structural, construction, and operational mitigation options.

3 SEISMIC RISK ASSESSMENT FRAMEWORK

3.1 Performance-Based Engineering

Engineers evaluate structures and facilities on the basis of performance. The most widely used current performance assessments evaluate a structure's performance in a binary manner. If the structure "fails," the performance is poor or unacceptable. If however, the structure does not fail, the performance is considered satisfactory. Additionally, in practice, performance is usually evaluated using strength; a metric valid to engineers, but one that has little to no meaning to stakeholders and decision makers. Performance-based design addresses both of these issues. First, performance-based design is not binary; it can be used to evaluate structures using a continuum of performance levels. Also, performance can be evaluated by any number of metrics, including strength. For example, seismic performance-based design can measure performance in terms of potential for casualties, repair/replacement costs, or the down-time resulting from earthquake-induced damage.

3.1.1 Performance-Based Earthquake Engineering and Uncertainty

Performance-based design is also closely related with probabilistic methods of design, which means that certain levels of uncertainty are associated with its use. Probabilistic methods were first introduced into PBEE through probabilistic seismic hazard analysis and the applications of the seismic motions. However, as the field has advanced, probabilistic methods have permeated the remaining modeling techniques used in performance-based earthquake engineering methods. Predictive models "should be recognized as mathematical idealizations of reality – they are not perfect (Kramer 2008)." This imperfection is usually either a result of a simplification of a more complex problem, or the lack of understanding of the true physics of a problem. Since no model

can be perfect, uncertainties must be included and quantified within the predictive models of PBEE.

There are two basic types of uncertainties that are important in engineering. The first is aleatoric uncertainty which results from inherent or intrinsic variability seen in quantities or nature. Aleatoric uncertainty, sometimes “randomness”, cannot be reduced. The other type of uncertainty, epistemic uncertainty, results from the assumptions made in the analysis of a system and from the limitations of supporting databases for that system. Unlike aleatoric uncertainty, epistemic uncertainty can be reduced if additional knowledge of the subject or a more comprehensive analysis is used.

In the case performance-based earthquake engineering, examples of both types of uncertainty are prevalent in all aspects of design. Aleatoric uncertainties lie in the ground motions and the uncertainty of where, when, or how large an earthquake event will be. Furthermore, epistemic uncertainty is inherent in the simple fact that a model is used to predict real-life occurrences. Furthermore, epistemic uncertainty results from our inability to tell the future. When trying to quantify the losses that occur as a result of earthquakes, factors such as quantities, unit costs, future material and labor costs, interest rates, and repair times for future events are ultimately unknown. Therefore, epistemic uncertainty will influence these modeling processes.

3.1.2 Previous Methods for Assessing Performance

Performance-based design has been around for a while in some form or another. For earthquake engineering, the first performance requirements were established for buildings after the 1925 Santa Barbara earthquake (NEHRP 2009). Acceptable performance in this case prevented collapse onto the street. However, the first written performance-based design measures in its most current form was adopted in the first edition of the Structural Engineers Association of California Blue Book (SEAOC 1959)

which attempted performance-based design by qualifying three damage states and the performance goals for each:

Table 3.1 California Blue Book Performance Goals

Damage State (Level of Shaking)	Performance Goals
Minor	No damage
Moderate	No structural damage, minor non-structural
Strong	No collapse but structural and non-structural damage

Risk-based evaluation of design criteria caught on after that (Cornell 1968; Ellingwood and Ang 1974), and the first probabilistic-based seismic design code was ATC-3-06 (Applied Technology Council 1978). It was based on the probabilistic seismic hazard analysis concept from Cornell (1968), and the mapping work of Algermissen and Perkins (1976). ATC-3-06 specified levels of safety from effective peak acceleration and velocity exceedance probabilities based on the relationship between estimated and allowable interstory drifts.

The most recent building codes have kept the probabilistic nature of ATC-3-06, but have expanded performance goals by allowing multiple levels of performance at multiple hazard levels, with performance-related quantities that are closely related to damage. Vision 2000 (SEAOC 1995) was the first building code to establish procedures for new buildings using this format. In addition, it also established different performance levels for different types of buildings. As seen in Figure 3.1 below, performance levels are related to earthquake design levels by whether or not the performance at a specific design level is acceptable by design standards. Acceptable performance levels are indicated in green, whereas unacceptable performance levels are indicated in red.

		Earthquake Performance Level			
		Fully Operational	Operational	Life Safe	Near Collapse
Earthquake Design Level	Frequent (43 yrs)				
	Occasional (72 yrs)		Basic		
	Rare (475 yrs)		Essential/Hazardous		
	Very Rare (975 yrs)		Safety Critical		

Figure 3.1 Combinations of earthquake hazard and performance levels as proposed by Vision 2000 (from (SEAOC 1995)).

The graph also sets differing performance levels for three different types of structures:

Safety Critical – Structures containing large quantities of hazardous materials such as toxins, radioactive materials, or explosives that could cause significant external effects with damage to the building.

Essential/ Hazardous – Critical post-earthquake facilities such as hospitals, communications centers, police/fire stations, etc. or hazardous materials with limited impact outside the immediate vicinity of the building (i.e. refineries)

Basic – All remaining structures

For instance, after an earthquake with a design level of rare, the graph indicates that if the desired performance level was achieved, a nuclear power plant should still be fully operational, a hospital could have minor damage but its functionality should not have been affected, and a family home may have sustained moderate damage but should not have fallen down.

The efforts following Vision 2000 (FEMA 273 (Applied Technology Council 1997), FEMA 274 (Applied Technology Council 1997), FEMA 356 (American Society of Civil Engineers 2000), and ATC-40 (Applied Technology Council 1996)) use the same

performance framework, but diverge in the manner in which performance and hazard levels are defined, and in the suggested procedures for estimating force and displacement-related demands. FEMA 445, one of the most recent performance-based seismic design guidelines uses the following process to calculate losses (Also see Figure 3.2) (Applied Technology Council 2006):

- Characterize Ground Shaking Hazard – The method for applying a seismic energy to the desire component should be decided. This can be done either deterministically or probabilistically.
- Perform Structural / Nonstructural Analysis – Using engineering methods, the ground shaking should be applied to the components, and the forces or deformations occurring within the components are calculated.
- Form Structural Response Function – Next, the probable response and the intensity of shaking is calculated with respect to the ground shaking intensity using the forces and deformations from the previous analysis.
- Form Structural / Nonstructural Fragility Function - Here, probable damage to the component is estimated in light of the different levels of response that could occur.
- Form Structural / Nonstructural Damage Function – The Damage function formed in this relates specific types of damage incurred to corresponding component losses.
- Predict Loss as a Function of Damage – At this stage, all of the losses are calculated and aggregated with respect to the potential calculated damage.

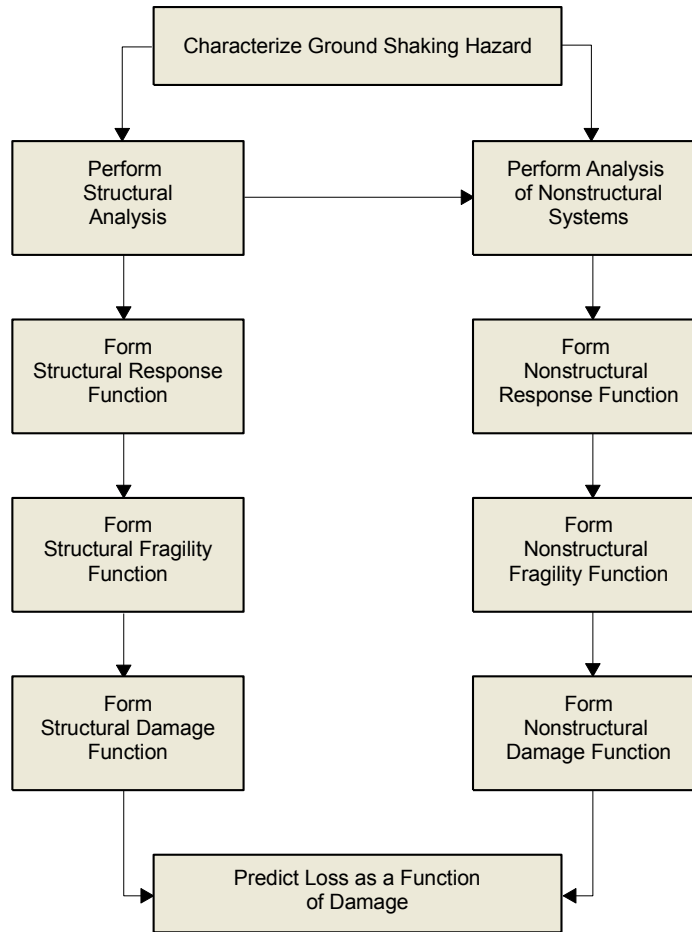


Figure 3.2 Performance Assessment Process (Applied Technology Council 2006)

It should be noted that each structural component and each nonstructural component is analyzed individually, and then each is aggregated into a final prediction of loss. Specifics of each step will be further discussed in subsequent sections. This process introduced the current goal/focus of performance-based seismic design: estimating losses. “Performance-based seismic design research from PEER and the recommendations at stakeholder’s workshop indicate that in order to fulfill its promise, a performance-based procedure must estimate expected losses from earthquake shaking and not be limited to predefined performance states” (NEHRP 2009).

3.1.3 PEER Framework

Numerous researchers have explored the possibility of using performance-based design for analysis of buildings, bridges, and even highway systems. However, because the concept in its current form is not yet used as the standard in practice, the terminology and framework used are not yet uniform. For this study, the Pacific Earthquake Engineering Research Center (PEER) framework and terminology (Porter 2006) for probabilistic risk assessment will be used:

$$\lambda(\overrightarrow{DV}) = \iiint G(\overrightarrow{DV}|\overrightarrow{DM}) \left| dG(\overrightarrow{DM}|\overrightarrow{EDP}) \right| dG(\overrightarrow{EDP}|\overrightarrow{IM}) d\lambda(\overrightarrow{IM}) \quad (3.1)$$

In equation (3.1), $G(a|b)$ denotes a complementary cumulative distribution function (CCDF) for a conditioned upon b . Overall, equation (3.1) represents the process of risk assessment that moves from ground motions to losses and can be represented by four different variables that have been conditioned upon one another. These variables make up the PEER risk analysis terminology, and are defined here:

Intensity Measure (IM) – Any of a number of ground motion parameters that characterize the level of ground motions produced by earthquake shaking (e.g., PGA, S_A , Arias intensity, etc.)

Engineering Demand Parameter (EDP) - Describes the response of the system of interest to the ground motions (e.g., excess pore pressure, interstory drift, etc.)

Damage Measures (DM) – Measure of the physical damage associated with the system response (e.g., slab cracking, wall tilt, etc.)

Decision Variables (DV) – The losses coupled with the physical damage that are of some importance to the decision makers (e.g. casualties, repair cost, downtime, etc.)

The PEER terminologies are illustrated within the framework progression in Figure 3.3:

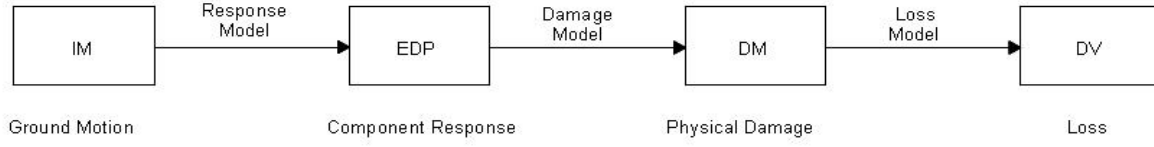


Figure 3.3 Illustration of Performance Prediction Processes using PEER Terminology (after (Kramer and Mitchell 2006))

3.1.3.1 Response, Damage, and Loss Models

For each variable, specific values are calculated from models within the PEER framework equation. As illustrated in Figure 3.3, the risk assessment process moves from the acquirement of intensity measures, to the production of engineering demand parameters, to damage measures, all the way to decision variables. This is possible through the application of three separate models that calculate the four variables from one another: a response model, a damage model, and a loss model. Furthermore, these models can be calculated independently of one another, which allow for equation (3.1) to be broken down into three separate models:

Response Model – Predicts the response of a structural system to an imposed ground motion. (i.e. get EDP from an IM):

$$\lambda_{EDP}(edp) = \int P[EDP > edp \mid IM = im] d\lambda_{IM}(im) \quad (3.1a)$$

Damage Model – Predicts the physical damage to a structure from the response of the structure. (i.e. predict DM from EDP):

$$\lambda_{DM}(dm) = \int P[DM > dm \mid EDP = edp] d\lambda_{EDP}(edp) \quad (3.1b)$$

Loss Model – Predict losses associated with some level of physical damage. (i.e. get DV from a DM):

$$\lambda_{DV}(dv) = \int P[DV > dv \mid DM = dm] d\lambda_{DM}(dm) \quad (3.1c)$$

Broken up in this manner, exceedance probability curves may be computed for EDP, DM, and DV and then interpreted in the same manner that seismic hazard curves

are computed for IM in probabilistic seismic hazard analysis (PSHA). It should be noted that while the PEER framework will be used to create the risk framework for the port system, it couldn't be used explicitly in its current form for two reasons. The first is due to the fact that the current form is meant for a single structure and does not accommodate the system dynamic of the port. Secondly, in the context of a port, the losses considered include both physical losses but also business interruption losses. The PEER framework adaptation for the port system will be further discussed and detailed in section 3.2.

3.1.3.2 Fragility Curves

One of the advantages of using a fully probabilistic risk framework like the PEER method, is that broken apart, the conditional probability terms in the equations 3.1a-3.1c can be expressed graphically as a fragility function. Fragility functions represent the variation of the mean (or median) and the uncertainty associated with the relationship between two variables as related to the conditional probability. Figure 6 illustrates this using the combination of equations 3.1a and 3.1b, where the damage model is predicting using an intensity measure instead of just the EDP. The top graph shows the mean rate of exceedance of some damage measure given the intensity measure. The fragility curves created were determined by the dispersion of DMs at a specific intensity measure. For instance, at the point in the upper graph, a low and a high dispersion are drawn. The low dispersion indicates less uncertainty and results in a steeper sloped fragility curve in the lower graph. The higher dispersion indicates more uncertainty at the point and results in a flatter fragility curve. Fragility curves will be used in this risk assessment in this form to determine the damage state of the wharves and cranes within the port based on some intensity measure.

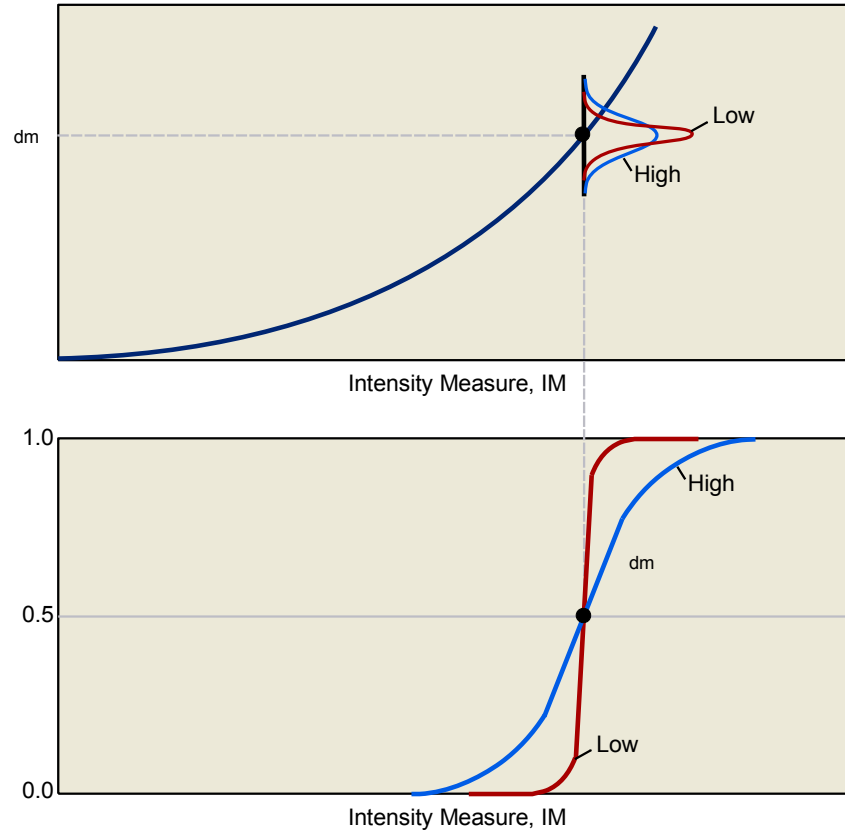


Figure 3.4 - Relationship between Response Relationship, Uncertainty and Fragility Curves

3.2 Risk Analysis Framework Applicable to this Study

While the PEER risk assessment framework discussed in section 3.1.3 provides the most currently accepted framework for risk analysis, the adopted equation cannot be used explicitly in the context of a port system. Problems arise because the PEER framework is designed for risk analysis of a singular structure (Deierlein et al. 2003), the performance of which solely depends on its ability to function. For example, a bridge is built to span and provide passage over a river. As long as the bridge remains standing and is safe to cross, it fulfills its function and satisfies a non-failure performance level. In this case, the ability to meet the desired performance objective is explicitly dependent on the structure itself. A container port is built for the purpose of loading and unloading cargo from ships. This is accomplished through the use of multiple wharves and cranes

that are interdependent. Wharves cannot perform their designated functions without cranes, and vice versa; they must work as a *system*. The performance of the port is dependent on the performance of the individual structures within the system (losses from physical damage) and also on the performance of the system itself (losses from business interruption). The matter becomes more complex because ports contain redundant systems, so that if one berth is not functional, another can be used. The entire *system* must be considered when evaluating the performance of the port, and the risk analysis framework must be modified to account for this difference.

The decision variables considered in the PEER framework are fatalities, monetary cost, or downtime. In the case of a port, downtime directly results in a monetary cost through business interruption losses. Therefore, it is necessary to treat downtime as a “damage” sustained by the port that results in a portion of the overall monetary loss. The PEER framework uses the term damage to refer to the physical damage incurred by a structure that results in some type of loss. For the port framework, damage will continue to define the purely physical damage. However, the system “damage”, whose consequence is monetary loss, will be referred to as repair requirements.

When represented graphically, an additional step is inserted into the graphical representation of the PEER equation as shown in Figure 3.5. This step examines the physical damage at the port and uses that to estimate the repair requirements (cost and downtime) for the port.

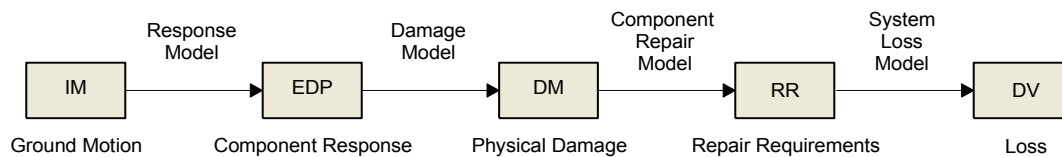


Figure 3.5 Graphical representation of equation 3.2

Mathematically, in the port risk assessment framework, this difference occurs in the damage model, which is combined with the response model to calculate the repair requirements given an intensity measure:

$$\lambda_L(l) = \iiint P[L > l | RR = rr] P[RR > rr | DM = dm] P[DM > dm | EDP = edp] P[EDP > edp | IM = im] d\lambda_{IM}(im) \quad (3.2)$$

However, equation 3.2 must be further modified before it can properly model a port system. In its current state, the equation finds the mean rate of exceedance of losses for an individual port structure such as a wharf or a crane at a single site. Ports are obviously made of structures at multiple terminals that have a measureable spatial separation. Therefore, the loss in the port system risk analysis must be calculated over the multiple sites within a port. Therefore, when modified to model the port facility, the probabilistic risk analysis equation from PEER takes on the form:

$$\lambda_j(l) = \sum_{i=1}^N \nu_i \left[\int_{RR} \int_{IM} G_{L|RR} f_{RR|IM} f_{IM|M=m_i, R=r_{i,j}} dim drr \right] \quad (3.3)$$

Equation 3.3 is used to calculate the mean annual rate of exceedance of losses occurring within the port system. Specifically, $\lambda_j(l)$ is the mean annual rate of exceedance of losses for a portfolio of terminal facilities $j = [j_1, j_2, \dots, j_j]$. Earthquake disruption is now defined over terminals because there is a spatial correlation between sites located some distance apart (see Section 3.3.3), and this is accounted for at the terminal level. N is the number of seismic source zones used in analysis, and ν_i is the mean rate of occurrence of earthquakes larger than a minimum magnitude originating in source zone i ; $G_{L|RR}$ is the complementary cumulative distribution function of the system-level losses conditional on the repair requirements at each terminal; $f_{RR|IM}$ is the

probability density function of the repair requirements at each terminal conditional on the intensity measures; and $f_{\overline{IM}|M=m_i, R=r_i}$ is the probability density function of ground motion intensity conditional on earthquake i with specific values of magnitude and distance. Equation 2 still contains the response, damage and loss models of the PEER framework, except that now the response and damage models are combined within the $f_{\overline{RR}|\overline{IM}}$ term (also seen in equation 3.2), and the loss model is described by the term $G_{\overline{L}|\overline{RR}}$.

The system dynamic of the port further dictates that to calculate the mean rate of exceedance for losses within the port system from equation 3.3, there are multiple components within the port that must be modeled. Therefore, this is done using a risk analysis framework program. Figure 3.6 maps the steps involved in the calculation of the mean rate of exceedance of losses using the program. The result involves three major steps for calculation: (1) seismic hazard calculations are used to estimate correlated earthquake ground motions at each terminal within the port complex conditional on the earthquake magnitude and distance, (2) component fragility calculations encompass the PEER response and damage models which are used to estimate not only the resulting physical damage to container wharves and cranes but also the cost and time required to repair or replace the damaged structures, and (3) system fragility, or the port operations level that estimates the port system fragility expressed as business interruption losses due to reduced container throughput and ship delays or re-routing. Each of these major steps is delineated graphically in Figure 3.6 through the use of different colored backgrounds. Subsequent explanations of each step in the figure are applied to a hypothetical port system located off the coast of Santa Cruz California as described in Section 4.1.

Considerations that must be taken into account when the risk analysis framework as applied to an existing or differing port are discussed in Chapter 6.

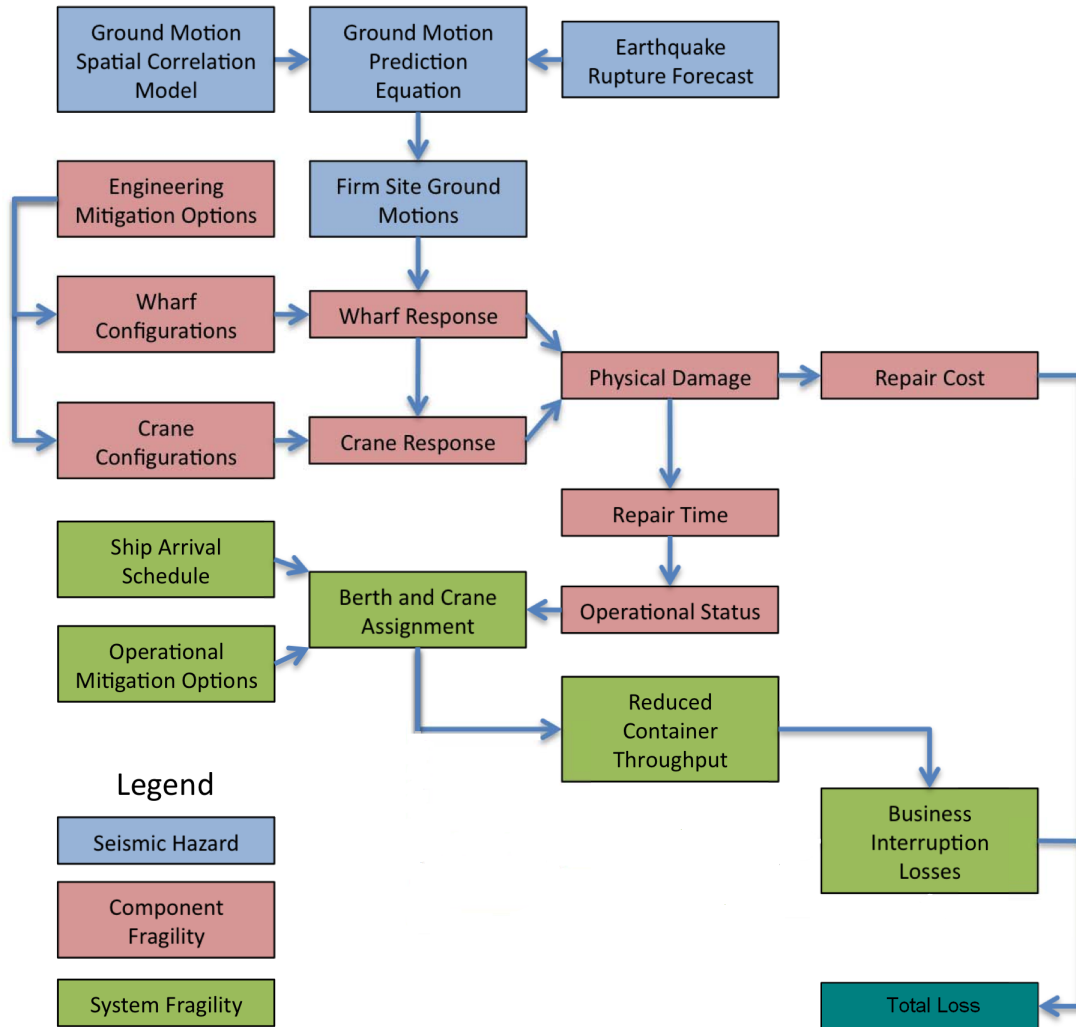


Figure 3.6 - Risk Analysis Framework

This risk analysis framework is repeatedly applied to a sample of earthquakes taken from an earthquake rupture forecast (See 3.3.1) and the total cost is calculated for each earthquake occurrence. The risk analysis framework offers four built-in options as to how earthquakes are sampled from an earthquake rupture forecast. A fully probabilistic analysis is built into the framework that allows the user to choose either

conventional or stratified Monte Carlo sampling. Additionally, earthquakes can also be sampled using a scenario-based analysis that samples earthquakes of a certain magnitude range, or using an intensity-based analysis that samples earthquakes within a specified intensity range. Several sampling methods were considered in the analysis of equation 3.1. One of the more well known methods for sampling earthquakes for use in a risk analysis is the walkthrough table method by Taylor *et al* (2001). In this method, sampled earthquakes are aggregated into a list of year-by-year earthquake occurrences throughout a region over a span of thousands of years. This method works well and offers elegance when accounting for inflation and changes in monetary value over time, but large earthquakes occur very infrequently. To capture large earthquakes that will cause large amounts of damage within the port, the walkthrough table must be at least 10,000 years long. While this approach has been used in previous studies and would clearly work, it's possible to improve the efficiency of the risk analysis and reduce the overall run time, which for a walkthrough table would be significant. Therefore, in an effort to streamline the analysis process and provide better large earthquake data within the analysis, Monte Carlo-based analysis methods were chosen as the primary method for earthquake sampling.

3.2.1 Probabilistic Analysis

3.2.1.1 Conventional Monte Carlo Sampling

Fully probabilistic earthquake catalogs are created from an earthquake rupture forecast (See 3.3.1) in one of two ways within the risk analysis program. The first method uses conventional Monte Carlo sampling. Within this method, a specific number of ruptures within the ERF are randomly sampled according to probability mass functions calculated for each rupture ($\text{pmf_rupture} = \text{rate_rupture} / \text{total_rate}$). Varying earthquake magnitudes are included within this sample according to the density function:

$$f(m) = \frac{\sum_{j=1}^{n_f} v_j f_j(m)}{\sum_{j=1}^{n_f} v_j} \quad (3.4)$$

which is calculated from the theorem of total probability where n_f equals the number of active faults in a region, v_j denotes the annual rate of recurrence for earthquakes on fault j , and $f_j(m)$ equals the density function for magnitudes of earthquakes on fault j .

In this case, the sampled earthquake catalog will be stochastically reflective of the ERF population; most of the earthquakes will be small in magnitude and very few will be large. Figure 3.7 plots the probability mass calculated for all of the earthquakes in the ERF population.

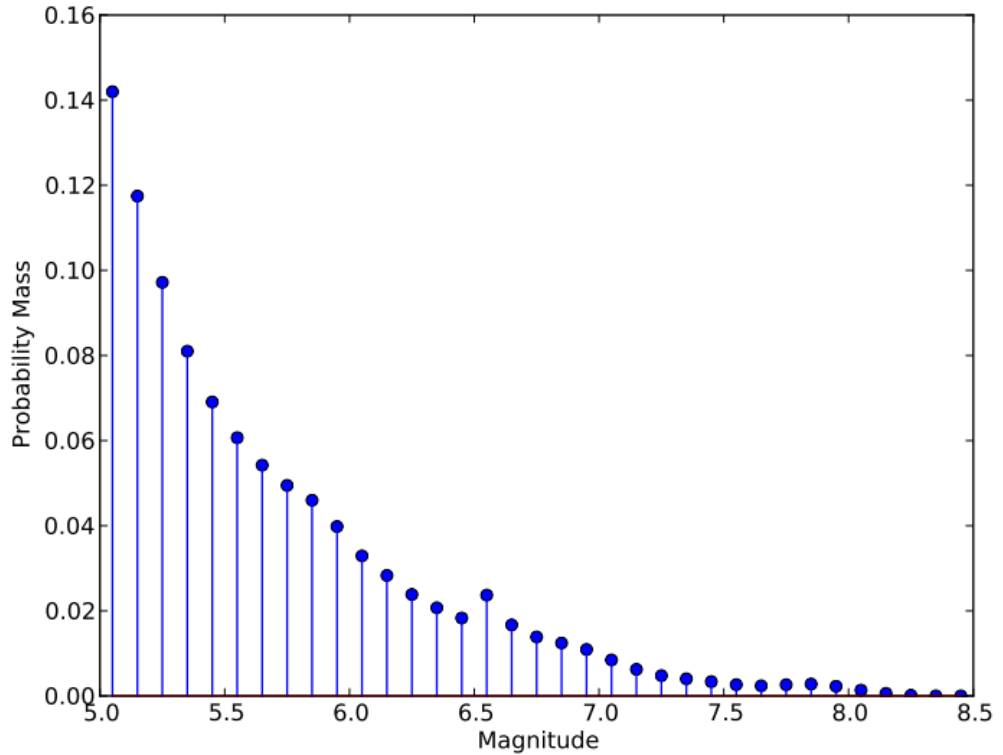
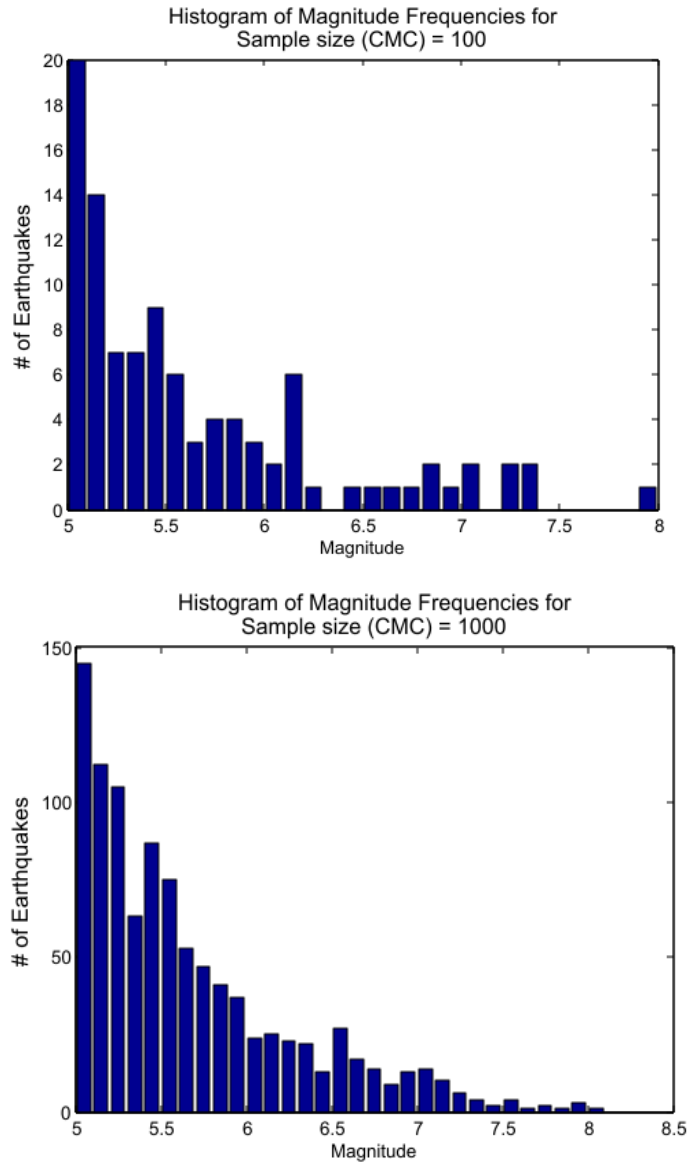


Figure 3.7 Probability mass for entire ERF population

It can be seen from Figure 3.7 that the majority of the earthquakes in the event set have small magnitudes while very few have large magnitudes. Monte Carlo sampling will reflect this distribution by randomly sampling earthquakes from the entire event set.

Figure 3.8 shows a histogram of earthquake magnitudes sampled using the conventional Monte Carlo method. The sample sizes for the 3 plots are 100, 1000, and 10000 earthquakes respectively.



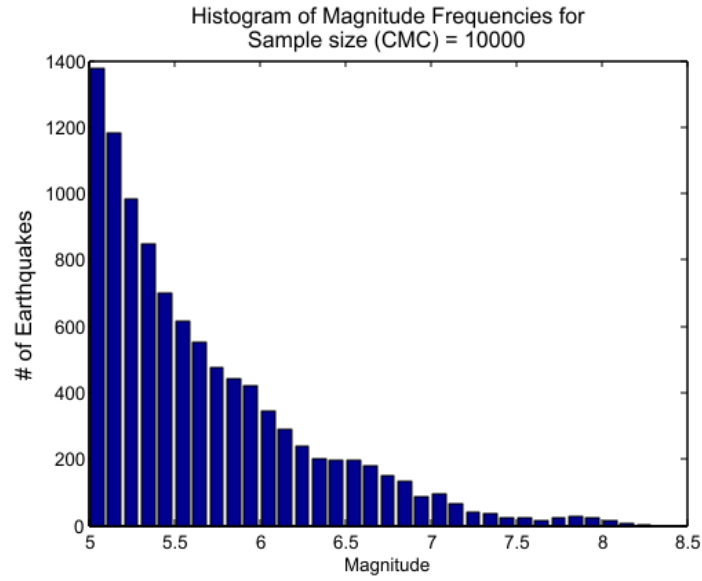


Figure 3.8 Histogram of conventionally-Monte-Carlo-sampled earthquakes

The figure above clearly shows the disadvantage in using the conventional Monte Carlo method: in order to get a sample representative of the ERF, a large number of earthquakes must be sampled. The percent of the total earthquake sample was calculated for each bar of the histogram for each of the previous sample sizes and plotted in Figure 3.9 for comparison. When compared to Figure 3.7, it is apparent that the 100-earthquake sample least represents the event set, while the 10000-earthquake sample most represents the event set.

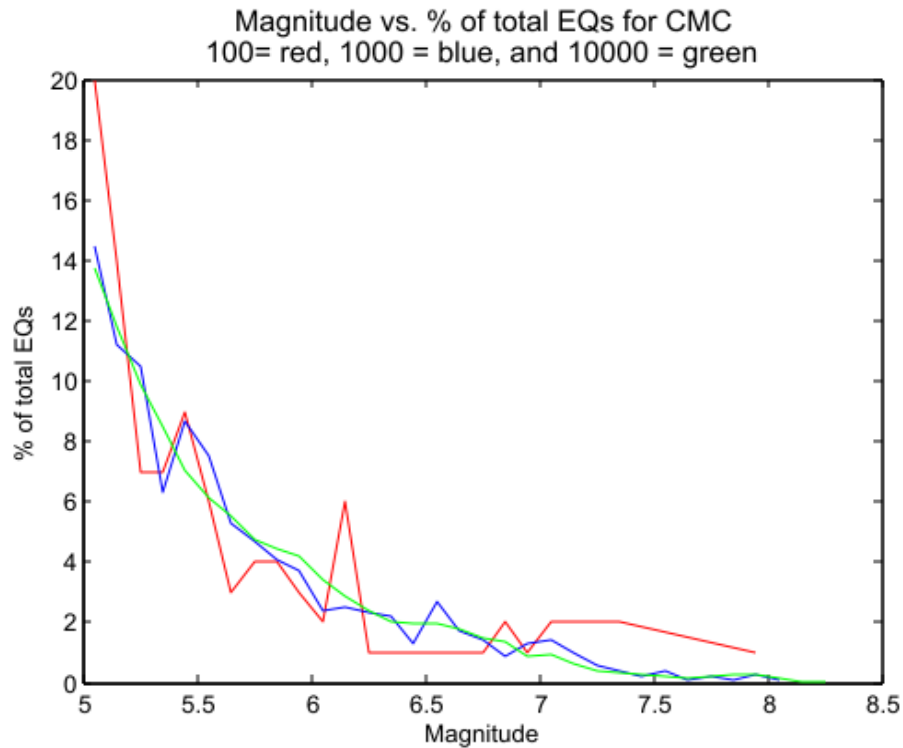


Figure 3.9 Magnitude vs. percent of total earthquake sample for conventional Monte Carlo sampling (100 = red, 1000 = blue, 10000 = green)

Conventional Monte Carlo sampling has another disadvantage: even when a large sample is used, very few large earthquakes are present within the sample. The many small earthquakes sampled produce little to no damage, which translates into little to no downtime, and this data won't provide an extensive look into the response of a port system during large events. The large earthquakes that occur infrequently in conventional Monte Carlo sampling produce significant damage, which provides better-quality data with which to use in the risk analysis. Real-life large events, like those in Kobe or Haiti, caused extensive disruption to the port system, and significant problems that port stakeholders would want to try and prevent in the future. Conventional Monte Carlo sampling won't produce enough data to properly examine these large events unless the total number of simulations is very large. Therefore, the method chosen for the risk

analysis uses Monte Carlo simulation in tandem with stratified sampling (Jayaram and Baker 2010) to preferentially sample these large events.

3.2.1.2 Stratified Monte Carlo Sampling

In the stratified sampling method for the risk analysis, earthquake magnitudes are divided into a number of strata, and each stratum corresponds to a single discrete value of magnitude. For this project, strata range between a magnitude of 5.05 to 8.45, where stratum $i+1$ has a magnitude 0.10 greater than stratum i . The ERF database is queried and ruptures are sorted according to the magnitudes of each stratum. Then ruptures are randomly sampled from each magnitude stratum. The number of samples per stratum is selected in an optimum manner as laid out in Rubinstein and Kroese (2007). If N equals the total number of samples and $N = \sum_{i=1}^m N_i$; the optimal number of samples in stratum i (N_i) is given by :

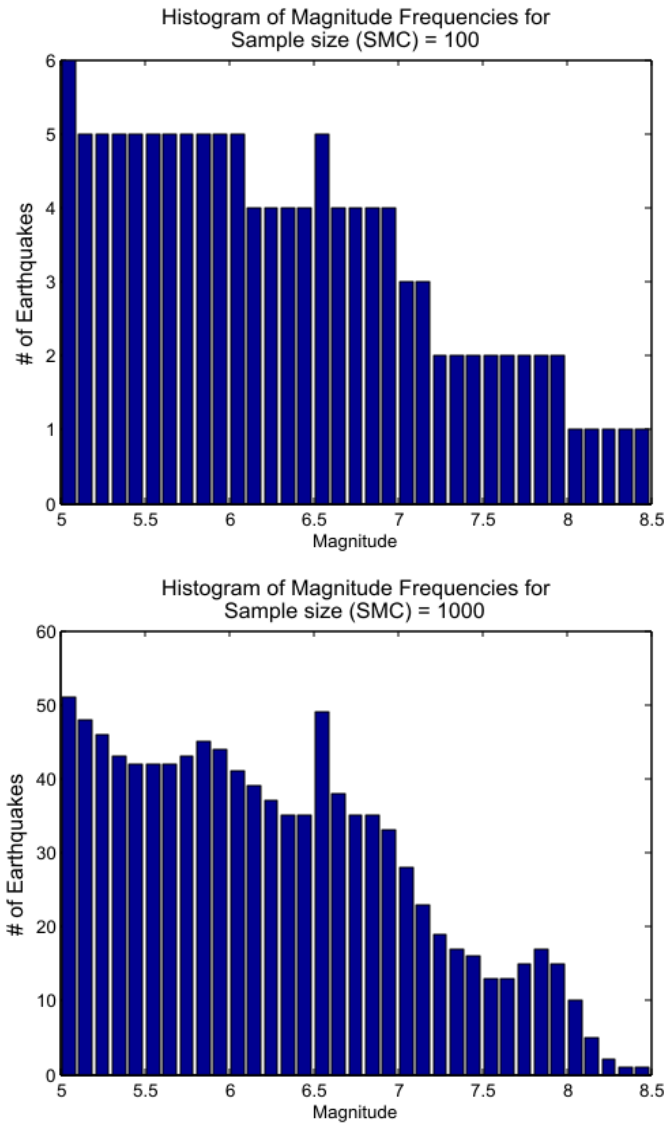
$$N_i^* = N \frac{p_i \sigma_i}{\sum_{j=1}^m p_j \sigma_j} \quad (3.5)$$

because it gives a minimal variance of the mean rate of exceedance for a specific level of loss of :

$$Var(\hat{l}^{*s}) = \frac{1}{N} \left[\sum_{i=1}^m p_i \sigma_i \right]^2 \quad (3.6)$$

For equation 3.3, p_i denotes the probability that an earthquake falls in stratum i , and σ_i is the standard deviation of the estimate value of loss. Since the standard deviation is unknown, and the ground motion intensity is one of the largest sources of variability, the standard deviation of the ground motion for stratum i is used as a proxy for the standard deviation of the estimated mean rate of exceedance for stratum i . This standard deviation is calculated for PGV using Atkinson and Boore (2008) at a magnitude equal to the stratum magnitude at an arbitrary distance of 20 km. The denominator of equation 3.5 calculates the sum of $p^* \sigma$ over every stratum. N_i earthquakes are then sampled using conventional Monte Carlo sampling from all the earthquakes within the event set

database with a magnitude equal to the magnitude of the stratum. It should be noted that within the risk analysis the value of N_i was rounded up to the nearest integer value, therefore it is possible that $N \leq \sum_{i=1}^m N_i$. Figure 3.10 shows a histogram of the magnitudes for samples of 100, 1000, and 10000 earthquakes.



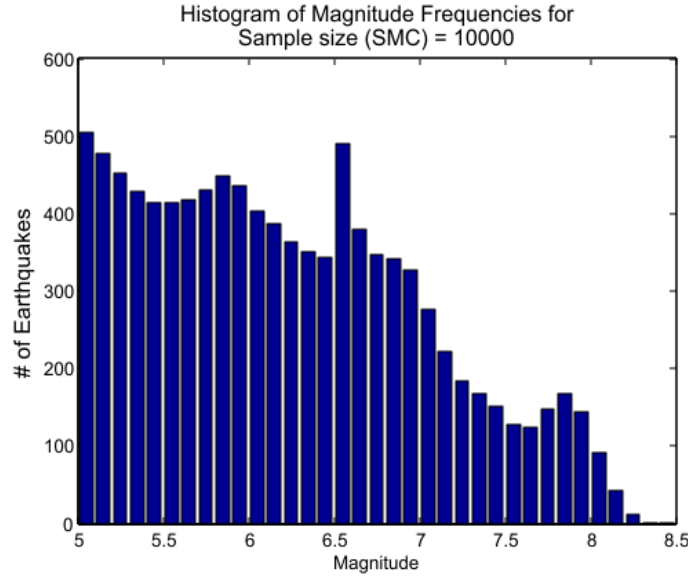


Figure 3.10 Histogram of magnitudes using stratified MC sampling for 100, 1000, and 10000 earthquakes

The benefit of this technique is that a larger number of large earthquakes are sampled. For example, 27 earthquakes with a magnitude greater than 7.0 were sampled from the 100-earthquake sample using the stratified technique, whereas only seven were sampled using conventional Monte Carlo. Additionally, stratified sampling requires fewer earthquakes to achieve the same variance of the estimated mean rate of exceedance. Therefore, when employing the stratified sampling technique the sample size could be reduced without significantly altering the uncertainty in the estimated mean rate of exceedance and overall computation time would be appreciably decreased.

However, if the magnitude distributions in Figure 3.10 are compared to Figure 3.7, it is apparent that the sampled earthquake catalog is no longer stochastically representative of the earthquake event set database. To account for this, the sampling parameters of each stratum (probability of occurrence (p_i) of stratum i and the number of strata, N , are used within the calculation of the summary statistics to reverse the stochastic misrepresentation created by the stratified sampling procedure in the following manner:

Stratum Mean :

$$mean = \sum_{i=0}^N (p_i * \bar{x}_i) \quad (3.7)$$

where \bar{x}_i equals the mean of the samples in stratum i , and the mean value of the mean rate of exceedance for a specific level of loss.

Variance of Stratum Mean:

$$Variance = \sum_{i=0}^N \left(p_i^2 * \frac{Var(x_i)}{N} \right) \quad (3.8)$$

where $var(x_i)$ equals the variance of samples in stratum i and N is the number of samples in the stratum.

Stratum Variance

$$v_s = \sum_{i=0}^N \left(p_i * \left(Var(x_i) + (\bar{x}_i - x_i)^2 \right) \right) \quad (3.9)$$

3.2.2 Scenario-Based Analysis

The scenario-based analysis built into the risk analysis program could be used to estimate port losses for a specific earthquake scenario. Scenarios could be hypothetical or based on actual earthquake events such as the 1995 Kobe or 2010 Haiti earthquakes. Within this analysis, earthquakes are conventional Monte Carlo sampled from the earthquake rupture forecast (See 3.3.1) of the port for specified range of magnitude and distance. For each scenario-based analysis, the user defines a nominal magnitude, a magnitude tolerance, a nominal distance, a distance tolerance, and the number of Monte Carlo sampled earthquakes within the sample.

To create this earthquake sample, the earthquake rupture forecast database is queried for earthquakes that match the input criteria. Next, earthquakes are randomly sampled through conventional Monte Carlo sampling from the generated list. As with stratified sampling, the earthquake sample generated from this analysis will not be stochastically representative of the overall earthquake rupture forecast. Therefore, sample parameters for the specific sample must be stored so that the mean value of the performance function can be properly calculated.

3.2.3 Intensity-Based Analysis

Like the scenario-based analysis, the intensity-based analysis within the risk analysis program can also be used to define specific scenarios. The intensity-based analysis better defines a specific earthquake scenario and if intensity information is known, should be used over the scenario-based analysis. For instance, if the user wished to model the 1995 Kobe earthquake, the scenario-based analysis only defines magnitude and distance and could include a wide range of intensity measures that may not adequately define the earthquake. However, if instead intensity values were known and used in the analysis, the losses calculated from the program would be much closer to the actual losses since intensity has a direct correlation to damage and magnitude does not.

To create the intensity-based sample, the user specifies the intensity value type, the intensity value, a coefficient of variation for that value, and the number of earthquakes to be sampled. Intensity measure types available within the analysis include peak ground acceleration (PGA), peak ground velocity (PGV), and spectral acceleration (SA). Again, like the scenario-based analysis, the earthquake rupture forecast (See 3.3.1) is queried for earthquakes that match the specified input, and then the sample is randomly sampled through Monte Carlo sampling for the number of samples specified in the input.

3.3 Seismic Hazard

Once the earthquake sample is established, the first step in calculating the mean rate of exceedance of losses requires the estimation of the intensity of the ground motions at the port components for each earthquake occurrence in the sample. This seismic hazard analysis is contained within the $f_{IM|M=m_i, R=r_i}$ term of Equation 3.3, which is the probability density function of ground motion intensity conditional on an earthquake's magnitude (m) and distance (r) from source zone i . A number of source zones are investigated and summed after multiplying the inner equation of 3.3 by the rate of occurrence of each earthquake sampled.

3.3.1 Earthquake Rupture Forecast

Since the hypothetical port is located in Santa Cruz, California, the Uniform California Earthquake Rupture Forecast, Version 2 (WGCEP 2008; WGCEP. 2008) will be used. Possible earthquake ruptures at the hypothetical port are populated into an event set list through the use of the OpenSHA program: IM_EventSetCalc version 3.0 (Feild et al. 2009). This program compiles all earthquake ruptures from the ERF within 200 km of the terminal sites, including background seismicity. Table 3.2 features an excerpt of ERF use for the hypothetical port, giving rupture rates of occurrence and magnitude for various segments of the South San Andreas and Calaveras faults.

Table 3.2 Excerpt from Earthquake Rupture Forecast

ID	Mean rate of Occurrence	Moment Magnitude	Fault
279	2.09E-05	8.15	S. San Andreas
280	1.36E-05	8.25	S. San Andreas
281	4.83E-06	8.35	S. San Andreas
282	1.08E-06	8.45	S. San Andreas
283	3.00E-05	6.55	Calaveras
284	3.00E-05	6.55	Calaveras
285	3.00E-05	6.55	Calaveras
286	3.00E-05	6.55	Calaveras
287	3.00E-05	6.55	Calaveras
288	3.00E-05	6.55	Calaveras

In addition to compiling the list of all possible earthquake ruptures, the event set calculator also finds the distance from each rupture to the terminal sites specified by the user and studied within the risk analysis. The distance is the appropriate measure (e.g., the Joyner-Boore distance) used by the ground motion prediction equation (GMPE) selected by the user. This information will be subsequently used to calculate the intensity measures using one or more ground motion prediction equations.

3.3.2 Ground Motion Prediction Equation

For a given earthquake k from the earthquake sample, a ground motion prediction equation (GMPE) is used to estimate firm-site ground motion intensity measures (calculated as lognormal random variables) at each terminal within the port. The basic form of the GMPE is:

$$\ln(Y_{jk}) = \ln(\bar{Y}_{jk}) + \varepsilon_{jk} + \eta_k \quad (3.10)$$

where Y_{jk} is the ground motion intensity measure of interest at terminal j due to earthquake k , \bar{Y}_{jk} is the median value of the intensity measure obtained from the GMPE, ε_{jk} is the intra-event residual, and η_k is the inter-event residual.

The ground motion prediction equation chosen to calculate $\ln(Y_{jk})$ for hypothetical port analysis is that of Atkinson and Boore (2008):

$$\ln \bar{Y} = F_M(M) + F_D(R_{JB}, M) + F_S(V_{S30}, R_{JB}, M) \quad (3.11)$$

Here, F_M , F_D , and F_S represent the magnitude scaling, distance function, and site amplification respectively. M is the moment magnitude, R_{JB} is the Joyner-Boore distance (Boore et al. 1997), and V_{S30} is the average shear wave velocity over the upper 30 meters.

The remainder of the GMPE, $\varepsilon_{jk} + \eta_k$, calculates the intra and inter-event residuals. The intra and inter-event residuals within the GMPE reflect the spatial correlation of ground motion intensities at closely spaced sites and the correlation of response spectral values at differing natural periods.

3.3.3 Ground Motion Spatial Correlation Model

3.3.3.1 Spatial Correlation

A study from Park *et al.* (2007) reports that ignoring or underestimating spatial correlations overestimates frequent losses and underestimates rare losses in risk analysis assessments. Spatial correlation is large for sites that are close to one another; therefore it

is important to determine this value for a port system. Boore *et al.* (2003) calculated that past 10 kilometers the spatial correlation coefficient equals zero, so distances below that will have some correlation. Terminals in ports are usually located within a five-kilometer distance of one another. For instance, the Port of Oakland (Figure 3.11) has terminals that range from 0.62-4.87 kilometers apart. Therefore, calculation of spatial correlation between terminals will be important in the port system risk assessment.

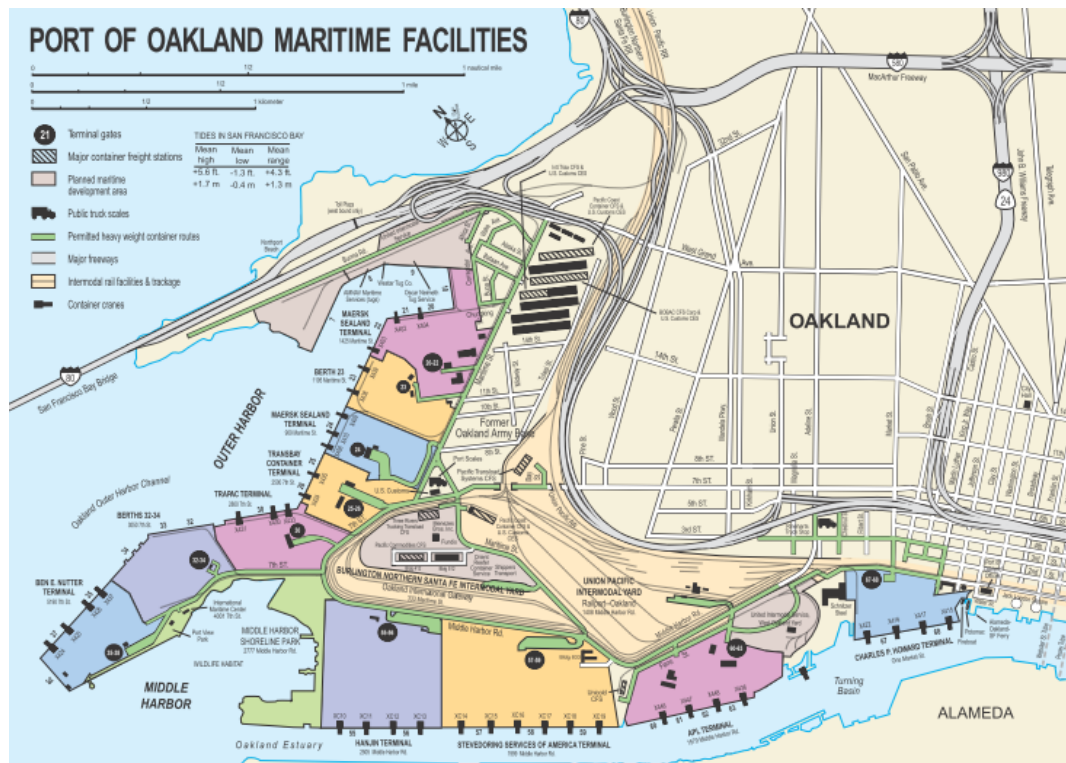


Figure 3.11 Port of Oakland

As depicted in Figure 3.12, the spatial portion of the intra-event residual describes the correlation between multiple sites and a single earthquake, while the inter-event residual describes the correlation between multiple earthquakes affecting a single site.

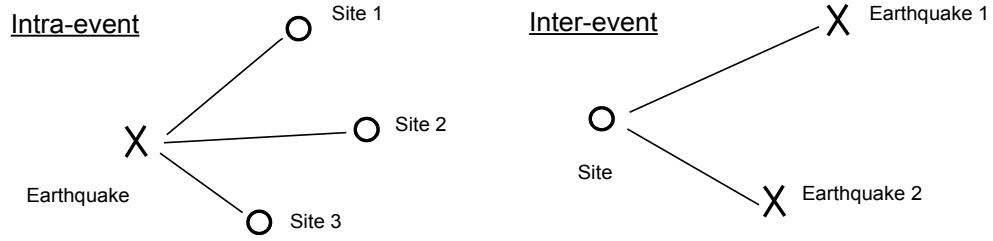


Figure 3.12 Inter vs. Intra-event spatial correlations

Analysis has shown that spatial correlation typically reduces as the separation between sites increases (Jayaram and Baker 2009). For a portfolio of sites separated by only a few kilometers (e.g., terminals within a port), the correlation is strong and it is especially important that the intra-event residual be calculated. Both the intra-event and inter-event residuals are calculated using semivariograms. Semivariograms are matrices that measure the average dissimilarity between data. In this case, the semivariogram, $\gamma(h)$, measures the dissimilarity between intensity measures separated at sites u and u' by some distance h :

$$\gamma(h) = a[1 - \rho(h)] \quad (3.12)$$

Here a and $\rho(h)$ are the sill and the correlation coefficient between Z_u and Z_{u+h} of the semivariogram, respectively. Let Z denote a spatially distributed random function where u denotes the location of a site. The sill of the semivariogram equals the variance of Z_u , and the correlation coefficient can be calculated using the following equation:

$$\rho(h) = \exp(-3h/b) \quad (3.13)$$

For equation 3.13, b is defined as the range of the semivariogram. The ranges of correlations computed at long periods (>1 sec) are quite similar. However, correlations at short periods (< 1 seconds), depend on the similarity of geologic conditions between sites, particularly V_{s30} . For the port, the geologic conditions between the terminals are fairly similar, and it is expected that V_{s30} at the sites would show clustering (Jayaram

and Baker 2009). Therefore, the range of the exponential semivariograms, b , can be predicted using the period, T and the following equations:

For short periods ($T < 1$ second):

$$b = 40.7 - 15.0T \quad (3.14a)$$

For long periods ($T \geq 1$ second):

$$b = 22.0 - 3.7T \quad (3.14b)$$

Jayaram and Baker (2009) express that the spatial correlation coefficient for PGV is approximately equal to the correlation coefficient for spectral acceleration at a period of 0.5 to 1.0 seconds. Since the intensity measures used within the risk analysis framework are PGV and spectral acceleration for a period of 1.5 seconds, when PGV is used as the intensity measure will be taken from the center of this range (0.75 s) in the calculation of the exponential semivariogram b .

3.3.3.2 Spectral Correlation

The spectral correlation portion of the intra and inter-event residual is important because the intensity measure calculated for the wharf will be PGV while the intensity measure calculated for the cranes will be spectral acceleration. Each of these calculated intensity measures will occur at different periods and must be correlated accordingly. This correlation is modeled using the following equation (Baker and Jayaram 2008):

Given T_1 and T_2 :

$$\begin{aligned} \text{If } T_{\max} < 0.109 \quad \rho_{\varepsilon(T_1), \varepsilon(T_2)} &= C_2 \\ \text{else if } T_{\min} > 0.109 \quad \rho_{\varepsilon(T_1), \varepsilon(T_2)} &= C_1 \\ \text{else if } T_{\max} > 0.2 \quad \rho_{\varepsilon(T_1), \varepsilon(T_2)} &= \min(C_2, C_4) \\ \text{else} \quad \rho_{\varepsilon(T_1), \varepsilon(T_2)} &= C_4 \end{aligned} \quad (3.15)$$

In this case, C_1 , C_2 , and C_4 are defined as follows:

$$C_1 = 1 - \cos\left(\frac{\pi}{2} - 0.366 \ln\left(\frac{T_{\max}}{\max(T_{\min}, 0.109)}\right)\right) \quad (3.16)$$

$$C_2 = \begin{cases} 1 - 0.105 \left(1 - \frac{1}{1 + e^{100T_{\max}^{-5}}} \right) \left(\frac{T_{\max} - T_{\min}}{T_{\max} - 0.0099} \right) & \text{if } T_{\max} < 0.2 \\ 0 & \text{otherwise} \end{cases} \quad (3.17)$$

$$C_4 = C_1 + 0.5 \left(\sqrt{C_3} - C_3 \right) \left(1 + \cos \left(\frac{\pi T_{\min}}{0.109} \right) \right) \quad (3.18)$$

Where:

$$C_3 = \begin{cases} C_2 & \text{if } T_{\max} < 0.109 \\ C_1 & \text{otherwise} \end{cases} \quad (3.19)$$

The above equations were calculated as a fit of the spectral correlations of the ground-motions in the Next-Generation Attenuation (NGA) database, and apply to periods between 0.01 and 10 seconds (Baker and Jayaram 2008).

3.3.4 Intra-event and Inter-event Residuals

Both the spatial and spectral correlations determined from the equations above are used to calculate the intra-event residual, where only the spectral correlation determines the inter-event residual.

The intra-event residual (ε_{jk}) is a function of both the site location (j) and the earthquake (k), therefore both the spatial and spectral correlations must be considered in its calculation. The intra-event residual is a correlated randomly sampled vector of residuals from a multi-variate standard normal distribution. This distribution can be described by creating a correlation matrix containing the product of spatial and spectral correlations for every site pair used in the calculation of the GMPE. Spatial correlation between sites u and u' will be calculated using equations 3.13-3.14b where h = the separation distance between sites u and u' , and the period $T = \sqrt{T_u * T_{u'}}$. Spectral correlation is calculated using equations 3.15-3.19 and periods T_u and $T_{u'}$.

The inter-event residual follows a univariate normal distribution and is only dependent on the spectral correlation. To create its correlation matrix, the spectral correlation is calculated for the different periods between all of the intensity measure type pairs. The inter-event residual is calculated by sampling from this distribution of spectral correlations. Once calculated, both the inter and intra- event residuals are added to the median value of the intensity measure obtained from Atkinson and Boore (2008) resulting in the final estimate of the intensity measures for earthquake k .

3.4 Component Fragility

3.4.1 Ground Motion Database

Part of the process for developing the fragility of a component is modeling the response over a wide range of possible earthquakes. For this project, a total of 63 empirical and simulated ground motions were selected for the development of fragility models for both the wharf and crane structures. Each of these motions are typical of coastal California firm-site conditions and also represent a broad range of possible earthquake magnitudes and distances to which these structures may be subjected.

Of the 63 motions, 56 are empirical motions selected from the Next-Generation Attenuation of Ground Motions (NGA) database (Chiou et al. 2008). These ground motions were selected randomly using the following criteria:

- Minimum moment magnitude (M_w): 5.5
- Distance to rupture: between 0-60 km
- Fault mechanism: Strike-slip, reverse, or reverse-oblique
- Site Class: C (“Very dense soil and soft rock”)
- Minimum usable frequency: less than 0.5 Hz
- Earthquake location: No earthquakes outside the U.S. except for the 1995 Kobe, Japan and 1999 Chi-Chi, Taiwan earthquakes, and no records from the 1983 Coalinga earthquake

In addition to these records, Paul Somerville of URS Corporation provided a list of near-fault records to be included in the suite of ground motions. Dr. Robert Graves, also of URS Corporation, provided data pertaining to simulated motions, since large-magnitude California earthquakes were not available in the NGA database. The simulated motions corresponded to $M_w = 7.8$ ShakeOut simulations of the southern San Andreas fault with distance to rupture ranges from 18-60 km within a Site Class C.

The simulated ground motion data was provided as velocity time histories. Acceleration time histories were then calculated by using backward-difference filter to numerically differentiate the velocity data:

$$\ddot{u}_j = \frac{\dot{u}_j - \dot{u}_{j-1}}{\Delta t} \quad j = 2, 3, \dots, N \quad (3.20)$$

The frequency response of the numerical differentiation filter is shown in Figure 3.13:

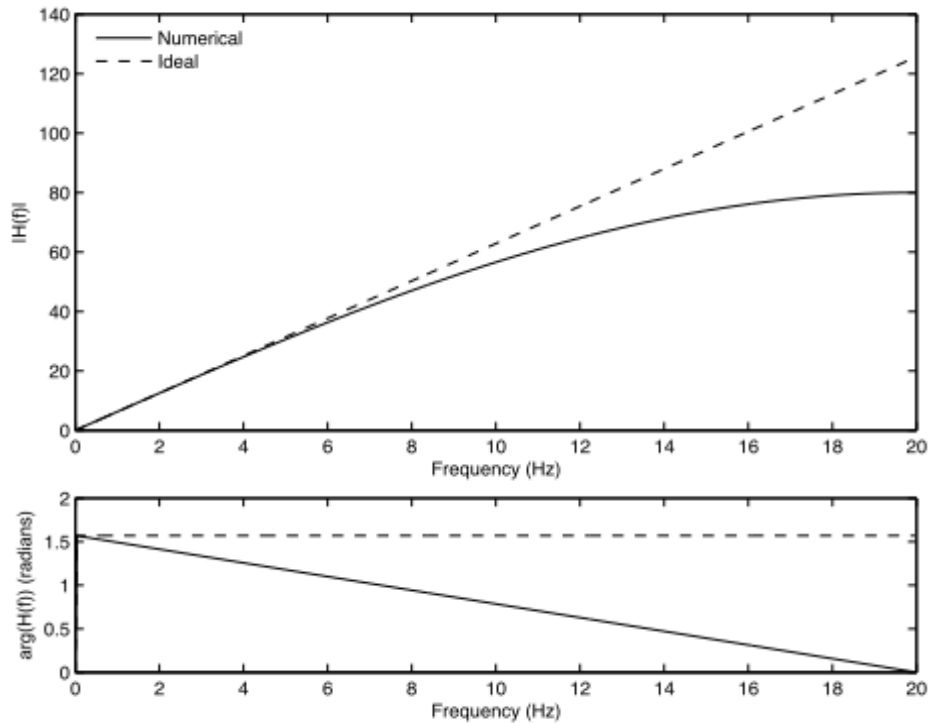


Figure 3.13 Frequency response of numerical differentiation filter

The resulting suite of ground motions is summarized in Table 3.3. Plots of the X and Y component time histories were included in Appendix B.

Table 3.3 NGA and SIM Ground Motion Summary Table

NGA Record #	Earthquake Name	Delta t (sec)	Earthquake Magnitude	PGA (g)
33	Parkfield	0.010	6.19	0.293
145	Coyote Lake	0.005	5.74	0.218
150	Coyote Lake	0.005	5.74	0.404
448	Morgan Hill	0.005	6.19	0.343
451	Morgan Hill	0.005	6.19	0.965
472	Morgan Hill	0.005	6.19	0.067
632	Whittier Narrows-01	0.020	5.99	0.137
648	Whittier Narrows-01	0.020	5.99	0.153
649	Whittier Narrows-01	0.020	5.99	0.154
669	Whittier Narrows-01	0.005	5.99	0.196
676	Whittier Narrows-01	0.005	5.99	0.161
684	Whittier Narrows-01	0.020	5.99	0.031
739	Loma Prieta	0.005	6.93	0.238
751	Loma Prieta	0.005	6.93	0.091
753	Loma Prieta	0.005	6.93	0.498
779	Loma Prieta	0.005	6.93	0.783
791	Loma Prieta	0.005	6.93	0.071
802	Loma Prieta	0.005	6.93	0.382
810	Loma Prieta	0.005	6.93	0.457
897	Landers	0.020	7.28	0.070
954	Northridge-01	0.010	6.69	0.200
969	Northridge-01	0.010	6.69	0.056
982	Northridge-01	0.005	6.69	0.764
983	Northridge-01	0.005	6.69	0.765
1008	Northridge-01	0.010	6.69	0.129
1012	Northridge-01	0.010	6.69	0.319
1013	Northridge-01	0.005	6.69	0.453
1014	Northridge-01	0.020	6.69	0.042
1023	Northridge-01	0.020	6.69	0.169
1031	Northridge-01	0.020	6.69	0.128
1035	Northridge-01	0.010	6.69	0.166
1055	Northridge-01	0.010	6.69	0.234
1057	Northridge-01	0.010	6.69	0.104
1085	Northridge-01	0.005	6.69	0.647
1086	Northridge-01	0.020	6.69	0.701
1642	Sierra Madre	0.020	5.61	0.277
1794	Hector Mine	0.010	7.13	0.150
2374	Chi-Chi, Taiwan-02	0.005	5.90	0.021
2393	Chi-Chi, Taiwan-02	0.005	5.90	0.029
2397	Chi-Chi, Taiwan-02	0.005	5.90	0.019
2399	Chi-Chi, Taiwan-02	0.005	5.90	0.046
2490	Chi-Chi, Taiwan-03	0.005	6.20	0.077
2498	Chi-Chi, Taiwan-03	0.005	6.20	0.076
2658	Chi-Chi, Taiwan-03	0.005	6.20	0.608
2716	Chi-Chi, Taiwan-04	0.005	6.20	0.032

2804	Chi-Chi, Taiwan-04	0.004	6.20	0.019
2867	Chi-Chi, Taiwan-04	0.005	6.20	0.023
2871	Chi-Chi, Taiwan-04	0.005	6.20	0.052
2883	Chi-Chi, Taiwan-04	0.005	6.20	0.031
3008	Chi-Chi, Taiwan-05	0.005	6.20	0.057
3016	Chi-Chi, Taiwan-05	0.005	6.20	0.040
3353	Chi-Chi, Taiwan-06	0.005	6.30	0.018
3361	Chi-Chi, Taiwan-06	0.005	6.30	0.037
3469	Chi-Chi, Taiwan-06	0.005	6.30	0.040
3474	Chi-Chi, Taiwan-06	0.005	6.30	0.644
3507	Chi-Chi, Taiwan-06	0.005	6.30	0.257
Broadband Simulations				
0001	Shakeout-HS1.2.0	0.025	7.80	0.250
0002	Shakeout-HS1.2.0	0.025	7.80	0.151
0003	Shakeout-HS1.2.0	0.025	7.80	0.165
0004	Shakeout-HS1.2.0	0.025	7.80	0.061
0005	Shakeout-HS1.2.0	0.025	7.80	0.119
0006	Shakeout-HS1.2.0	0.025	7.80	0.207
0007	Shakeout-HS1.2.0	0.025	7.80	0.050

Response spectra for empirical and simulated ground motions were calculated using the algorithm described in Nigam and Jennings (1969), and a summary of the acceleration response spectra for the suite of motions is shown in Figure 3.14. Figure 3.15 provides a summary of the moment magnitudes vs. the closest distance to rupture for the entire suite.

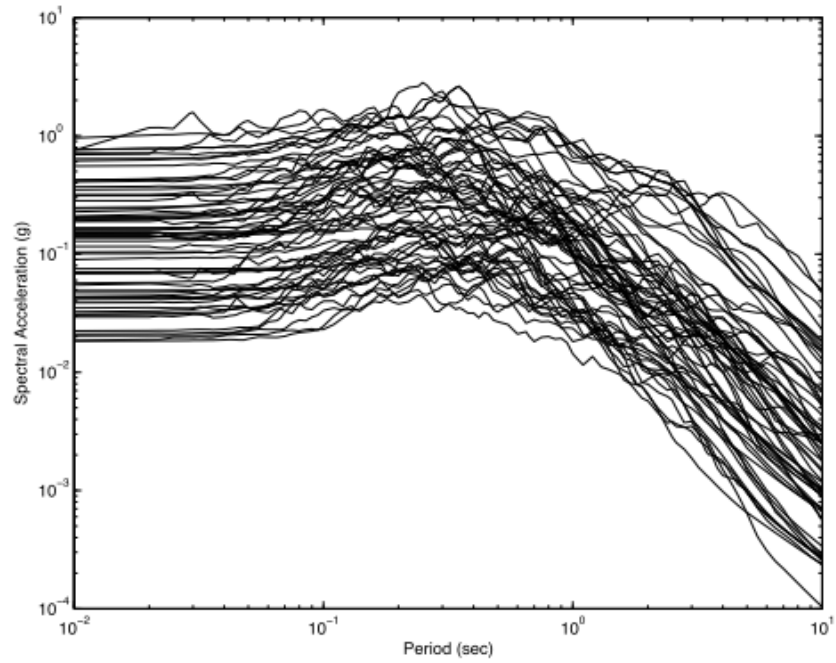


Figure 3.14 Response spectra for entire suite of ground motions

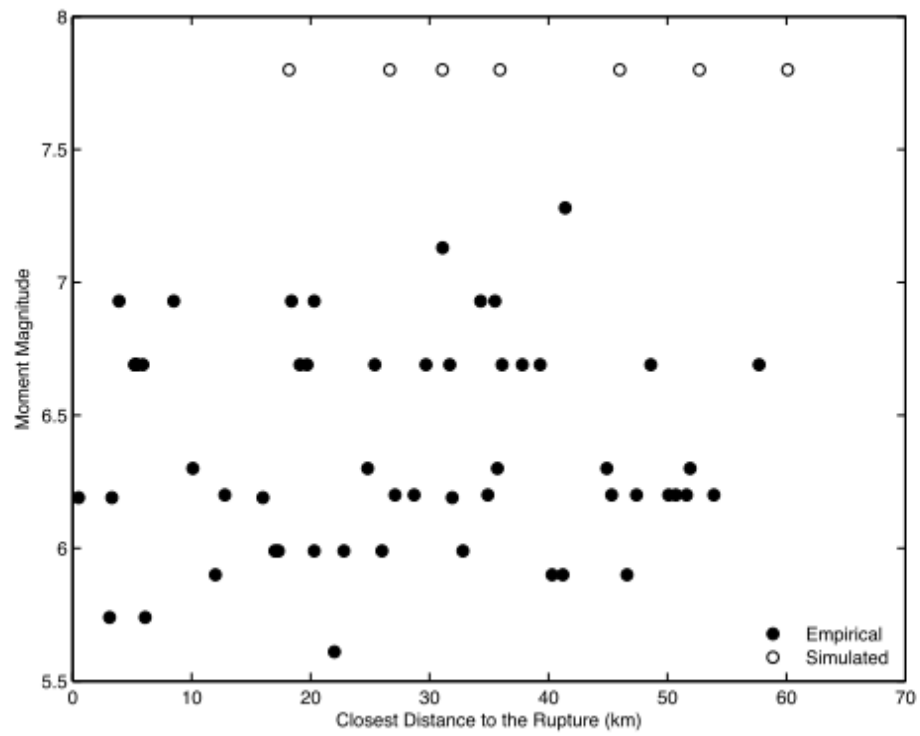


Figure 3.15 Moment magnitude vs. closest distance to the rupture

This collection of 63 ground motions was chosen as a representative sample of the wide variety of ground motions that the hypothetical port could be subject to. Consequentially, they were used to develop fragility models for the wharves and cranes within the hypothetical port. Sequentially, embankment response, soil-structure interaction, wharf response, and then crane response were modeled. Each component's individual response was also modeled to accommodate the future comparison of a number of different port mitigation options that would alter the overall fragility models of the wharves and cranes.

3.4.2 Embankment Response

3.4.2.1 Embankment Modeling Overview

Seismic slope stability is a complex design problem. The seismic response of an embankment depends on the shape of the embankment, the types of soil included within the embankment, and the level of the water table (Vytiniotis 2005). In ports, the soil backfills within embankments commonly consist of some type of hydraulic sand fill (Gallagher 2000). Therefore, liquefaction and lateral spreading become a significant concern (Hamada et al. 1996; Gallagher and Mitchell 2002). To properly estimate damage resulting from liquefaction or lateral spreading, the response of the soil embankment must be properly modeled. Within the scope of this project the embankment modeling was conducted by researchers at the Massachusetts Institute of Technology using dynamic coupled pore-pressure displacement seismic slope-stability finite element analyses (Vytiniotis et al. 2011). The numerical model of the embankment was built in OPENSEES (McKenna and Rodgers 2010) using a modified Dafalias-Manzari soil model (Dafalias and Manzari 2004). This type of model was chosen for its ability to accurately simulate the stress-strain behavior of sand during cyclic mobility events, its accurate prediction of void ratio effects, and the effects of dilation during subsequent loading and unloading paths. The model calculated displacement in the

horizontal and vertical directions, along with the pore water pressure at a number of nodes located along where the wharf piles are embedded within the embankment (see Figure 3.16). These specific nodes were chosen because the results would be used in subsequent models to estimate the soil-structure interaction between the soil and piles, and ultimately the wharf response.

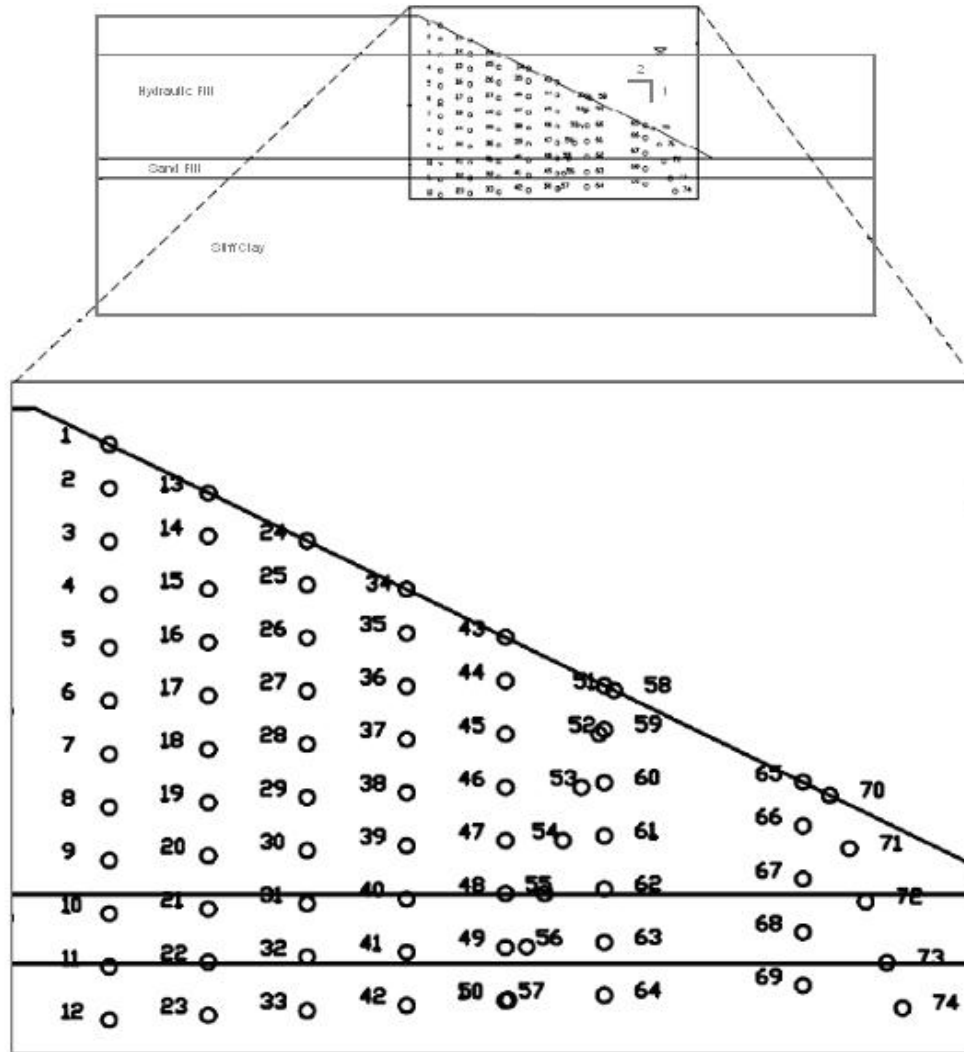


Figure 3.16 Example of embankment section analyzed with pile nodes (from (Vytiniotis 2010)).

Two different embankment responses were numerically modeled within the scope of this project: a liquefiable embankment and an embankment mitigated with vertical drains (see section 3.4.2.2).

Liquefiable Soil Embankment

Since many ports use dredged material as backfill for embankments, the possibility of liquefaction and lateral spreading within these embankments is significant. The first soil profile examined will be that of an embankment subject to liquefaction. This embankment consists of a 18.3 meter layer of hydraulic fill through which the majority of the wharf piles are embedded. The profile geometries can be found in Figure 3.17, and the soil properties for each layer are in Table 3.4.

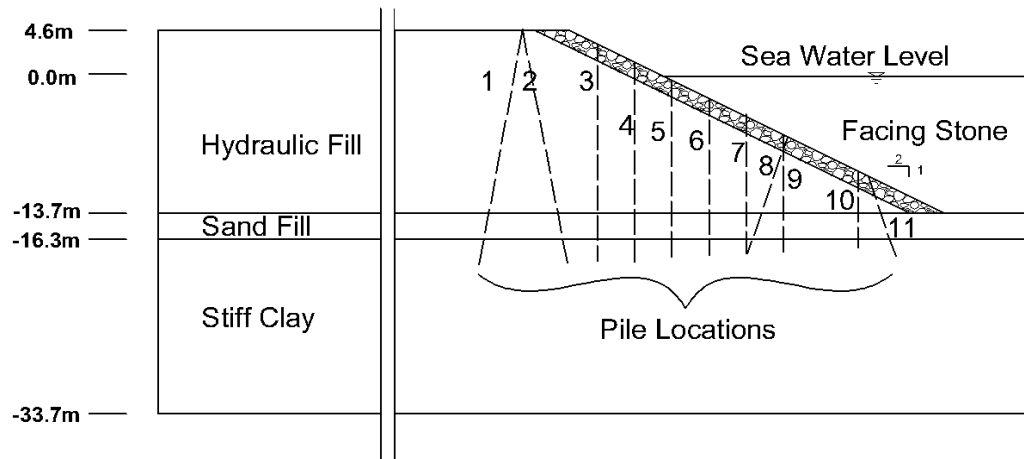


Figure 3.17 Soil Profile – Liquefiable soil (after (Vytiniotis et al. 2011)).

Table 3.4 Soil Properties for Liquefiable Embankment Profile (from (Vytiniotis et al. 2011)).

Layer	Saturated Unit Weight (Mgr/m ³)	Hydraulic Conductivity (m/s)	Main Model Parameters		
Dafalias Manzari Model					
			Calibration Material	Voids ratio	
Hydraulic Fill	1.85	3E-3	Toyoura Sand	0.825	
Sand Fill	2.05	3E-3	Toyoura Sand	0.635	
Facing Stone	1.85	3E-2	Toyoura Sand	0.673	
Visco Elastic Model					
			E (kPa)	V	ξ (%)
Stiff Clay	1.75	3E-7	282400kPa	0.412	10
Sea Water	1.00	-	0.29999999555556kPa	0.4999999777778	10

3.4.2.2 Soil Mitigation Options

Two options were examined as soil remediation possibilities within the scope of this project. In many ports, the backfill for the wharf is composed of loose sand placed as a result of dredging. This material is especially susceptible to liquefaction upon earthquake excitation. Both soil remediation possibilities could be implemented to mitigate the effects of soil liquefaction within the backfill of the wharf. The two mitigation methods studied in this project include colloidal silica gel and prefabricated vertical drains.

3.4.2.2.1 Colloidal Silica Gel

Colloidal silica gelling is a passive stabilization technique. In this method, a stabilizing material is injected into the soil at the up-gradient edge of a site. The stabilizer is then spread through the site using the natural ground water flow. Once the stabilizer has spread to the intended area, it will begin to gel and bind soil particles together; stabilizing the mass. Gel times can be predetermined based on delivery times or can be rapidly

brought on with the introduction of a catalyst (Spencer 2010). Once stabilized, soil particles are bound together and liquefaction cannot occur. However, while the colloidal silica material itself is relatively inexpensive, the injection process into existing backfill is not. Therefore, it was decided that computational time would not be spent on modeling this particular soil mitigation technique within the embankment response.

3.4.2.2.2 Prefabricated Vertical Drains

Prefabricated vertical drains are essentially corrugated plastic pipes lined with geotextile that can be placed vertically within backfill at specific intervals, and provide a conduit for the dissipation of excess pore pressure built up during earthquake excitation. The dissipation of the excess porewater pressure lessens the effects of liquefaction and alleviates lateral spreading. Figure 3.18 shows an example of a vertical drain and the pattern in which they are installed within the ground.

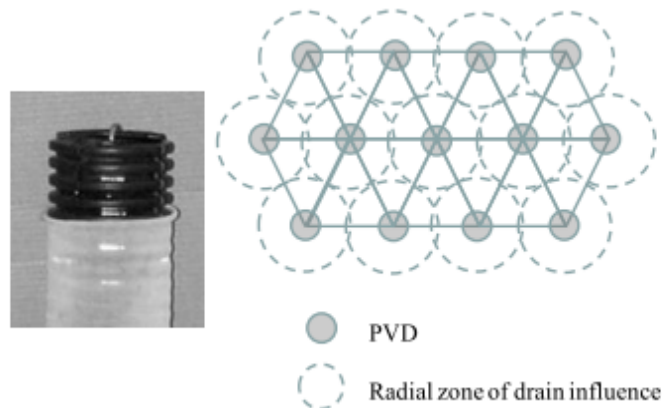


Figure 3.18 Prefabricated vertical drain and triangular installation pattern from (Howell et al. 2011)

Prefabricated vertical drains (PVDs) were chosen as the main soil remediation technique examined within the scope of this project because of their versatility and ease of implementation at existing wharf structures. Extensive physical modeling of PVDs using

centrifuge tests found that PVDs were effective in dissipating excess pore water pressure both during and after earthquake excitation. Associated deformations from liquefaction were also reduced. There was a 30-60% improvement in horizontal deformations and a 20-60% improvement in vertical settlement (Howell et al. 2011).

Like the physical models, it is expected that the embankment model with the inclusion of prefabricated vertical drains (PVDs) in the backfill will reduce the porewater pressures during earthquake excitation. The change in porewater pressure will be present within the free field, and relative displacements of soil will be lessened. The positioning of the PVDs within the embankment model geometry can be found in Figure 3.19, and the soil properties will be the same as those in the liquefiable soil embankment model (Table 3.4).

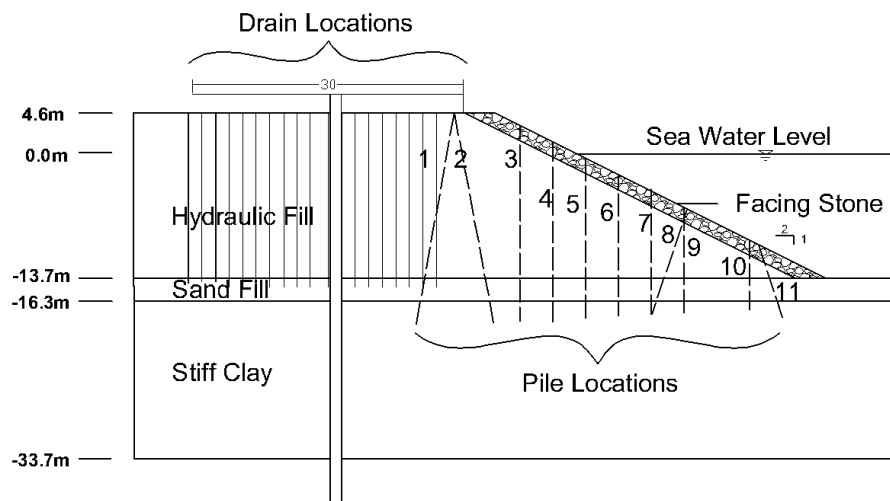


Figure 3.19 Soil Profile – Liquefiable soil with prefabricated vertical drains (after (Vytiniotis et al. 2011)).

For the Dafalias and Manzari (2004) sand model, the numerical simulations were calibrated using Toyoura sand. The sand constants used in the constitutive model can be found in Table 3.5.

Table 3.5 Dafalias and Manzari constitutive model constants (From Vytiniotis 2005).

Constant	Variable	Value	Constant	Variable	Value
Elasticity	G_0	125	Yield Surface	M	0.01
	N	0.05	Plastic Modulus	h_0	7.05
Critical State	M	1.25		c_h	0.968
	c	0.712		n^b	1.1
	λ_c	0.019	Dilatancy	A_0	0.704
	e_0	0.934		n^d	3.5
	ξ	0.7	Fabric-dilatancy tensor	z_{max}	4
				c_z	600

3.4.2.3 Embankment Model Shortcomings

The embankment analysis produces ground motions at varying soil nodes in two dimensions. However, the wharf analysis uses a three-dimensional wharf model. Therefore it was necessary to estimate ground motions for the missing dimension. One possibility considered included conducting a separate 1-D analysis to generate the needed ground motion, but this idea was rejected because it seemed impractical for a user to conduct an entirely separate 1-D analysis at multiple soil nodes in addition to the embankment analysis. Therefore, it was decided that the most practical method for generating the necessary ground motions in the third dimension was to use transfer functions to estimate the required ground motion.

The ground motion not calculated within the embankment model lies in the longitudinal or Y direction if one considers Z as vertical, and X as the transverse direction from the seaside edge to landside edge of the port (See Figure 3.20). Also, it

should be noted that since Figure 3.20 is drawn in the X-Z plane, for all subsequent descriptions of the two horizontal motions, X is the in-plane motion calculated from the embankment model, and Y is the out of plane (into the page) motion that will be calculated using transfer functions.

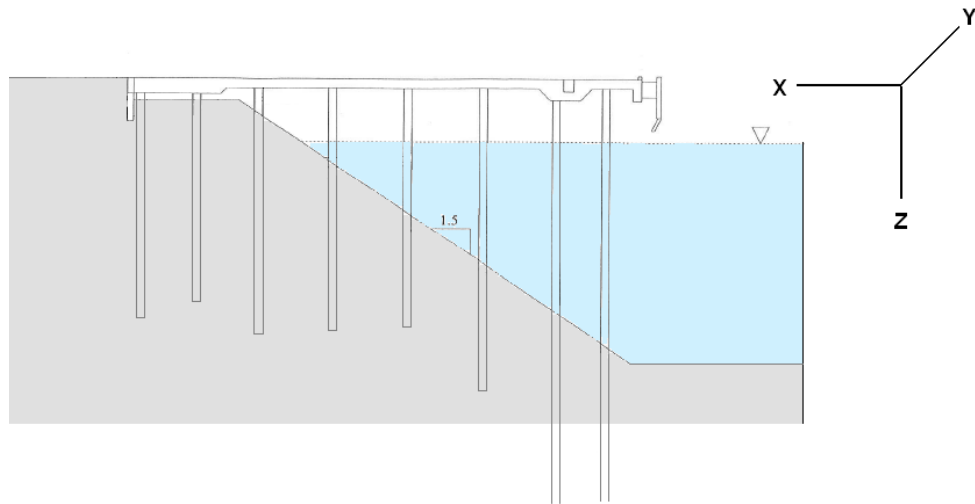


Figure 3.20 Directional reference for the wharf.

3.4.2.4 *Transfer Functions*

Multiple attempts were made to use transfer functions to calculate a reasonable estimate of the out-of-plane motion. Most attempts did not produce accurate estimates for large, highly non-linear ground motions. The method that was ultimately chosen will be termed pseudo-transfer functions. The pseudo-transfer functions are named as such because their calculation uses response spectra instead of the more traditional Fourier spectra. The pseudo-transfer function method was found to be preferable over the use of the Fourier analysis transfer function because for large motions with significant soil non-linearity, Fourier estimated out-of-plane motions were filled with noise and not

representative of true earthquake motions. The use of the pseudo-transfer function method resolves this problem.

Pseudo-transfer functions are calculated by finding the response spectrum of X_{rock} and Y_{rock} and then using equation 3.21 to calculate the ratio between the two spectra:

$$TF = \frac{Sa_{Yrock}}{Sa_{Xrock}} \quad (3.21)$$

As an example, the pseudo-transfer function will be calculated for NGA motion 1642 which can be seen in Figure 3.21:

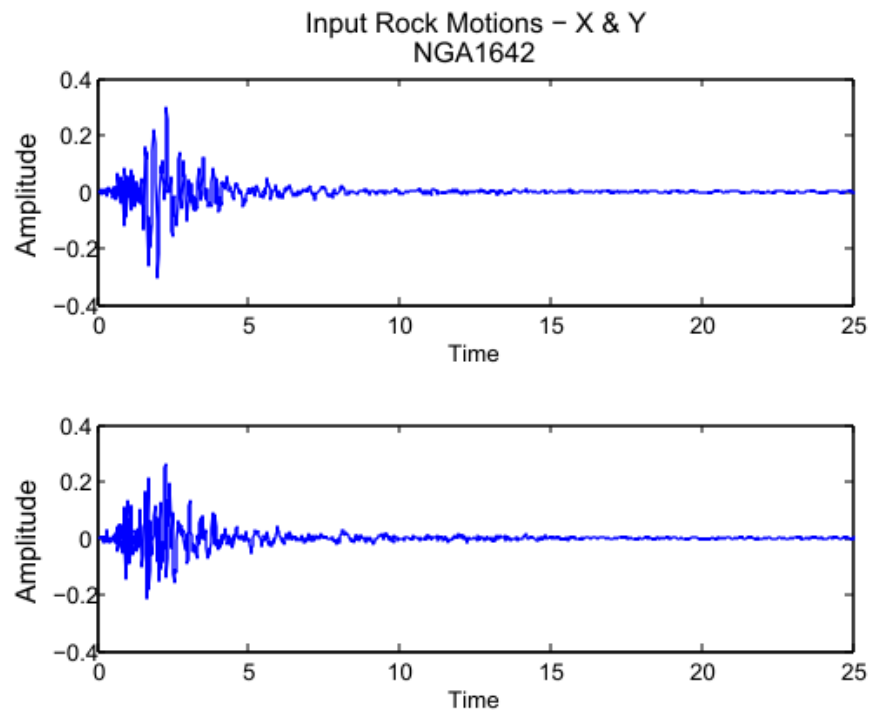
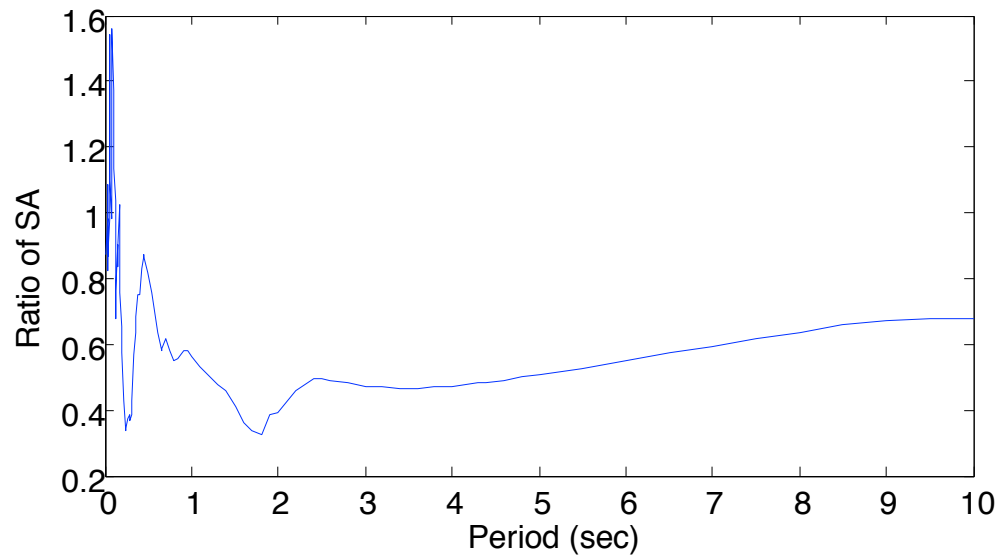
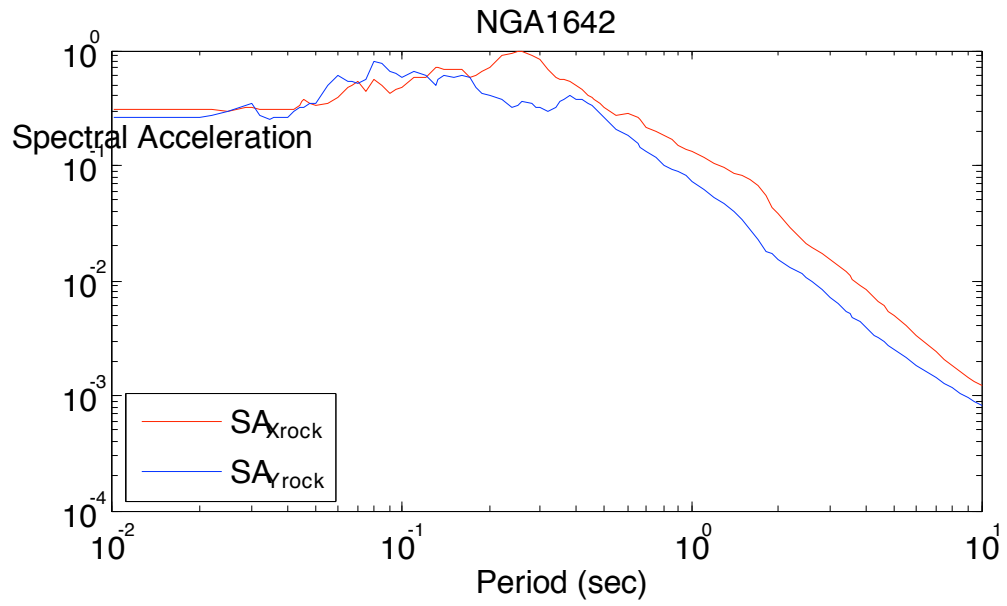


Figure 3.21 Input rock motions (X and Y) for NGA1642

First the response spectra of each motion is calculated using the algorithm developed by Nigam and Jennings (1969). In this particular case, the output is absolute

spectral acceleration at a spectral damping = 5%. Figure 3.22 shows the response spectra for both X_{rock} (in-plane) and Y_{rock} (out-of-plane) in the upper plot and then a plot of the transfer function below.

Response Spectra Rock In-Plane vs. Rock Out-of-Plane and Pseudo-Transfer Function (SA_{Yrock}/SA_{Xrock})



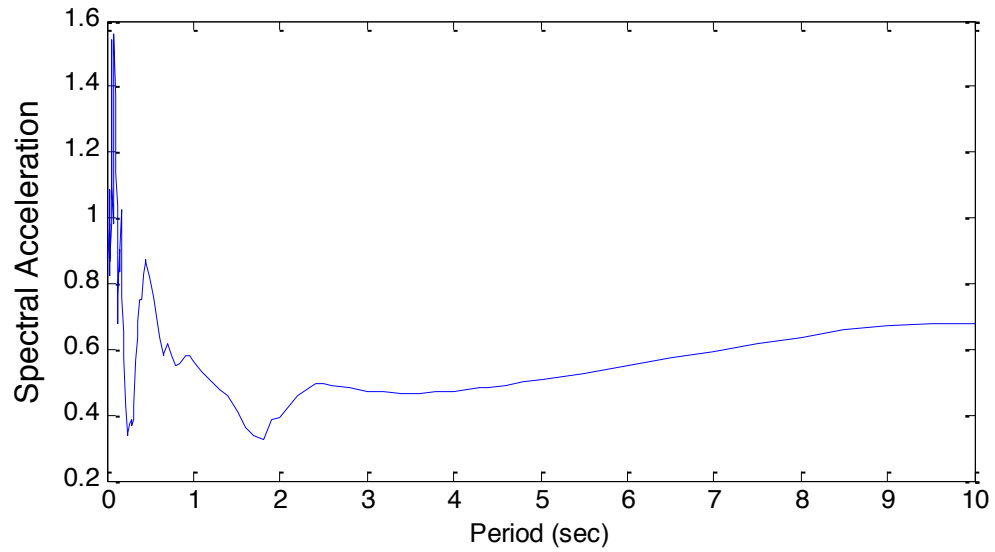
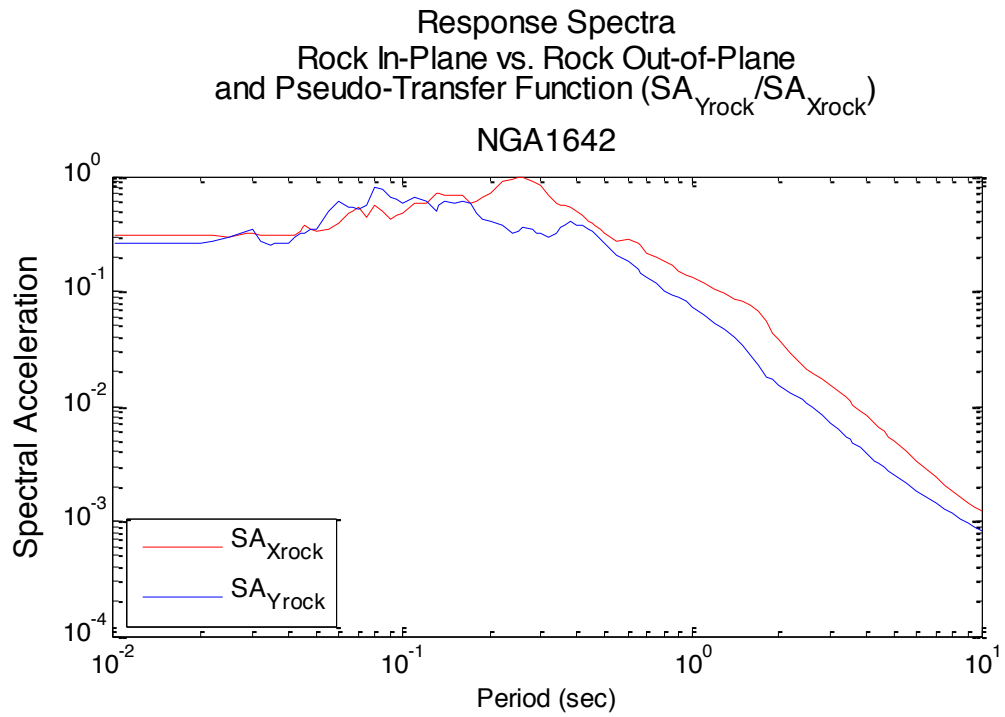


Figure 3.22 Comparison of Rock input motion response spectra and the Pseudo-transfer function

When the pseudo-transfer function is multiplied by the response spectra for the in-plane (X_{soil}) soil motion at a specified wharf node in the embankment model (Equation 3.22), it gives an estimate of the out-of-plane (Y_{soil}) response spectra (U).

$$U = Sa_{Y_{\text{soil}}} = \frac{Sa_{Y_{\text{rock}}}}{Sa_{X_{\text{rock}}}} * Sa_{X_{\text{soil}}} \quad (3.22)$$

The out-of-plane motion in the time domain is then calculated from the (Y_{soil}) response spectra estimate using a spectral matching program. The calculated response spectrum U will become the target spectrum within the program, which will spectrally match the response spectrum of the in-plane soil motion (X_{soil}) to the target spectrum U . The program can then compute an out-of-plane (Y_{soil}) soil response spectrum along with the out-of-plane soil motion in the time domain.

This process is most easily understood through an example. Therefore, for the current NGA motion 1642, calculation of the out-of-plane (Y_{soil}) time history will be made at the ground surface soil node. It is important to note that within the wharf model the X_{soil} time history generated from the embankment model is used in the transfer function method to calculate the Y_{soil} time history. However, to help check the validity of using this procedure, an OPENSEES (McKenna and Rodgers 2010) effective stress analysis for a soil profile (Figure 3.23) comparable to those used in the embankment response was conducted to generate the X_{soil} motion and a corresponding Y_{soil} motion. The OPENSEES Y_{soil} will be used to compare with the Y_{soil} computed using the transfer function. Soil properties for each layer of the soil profile used in the OPENSEES analysis are located in

Table 3.6. The soil profile and soil properties were chosen so that they closely resemble the profile and properties within the embankment model.

Table 3.6 – Soil Properties

Soil	Unit Weight (Mg/m ³)	Vs (m/s)	G	v	E	K
Upper Hydraulic Fill	1.85	103.6	1.99e ⁴	0	3.98e ⁴	1.32e ⁴
Lower Hydraulic Fill	1.85	134.3	3.34e ⁴	0	6.67e ⁴	2.22e ⁴
Sand Fill	2.05	157.4	5.08e ⁴	0	1.02e ⁵	3.39e ⁴
Clay	1.75	239.1	1.00e ⁵	0	2.00e5	6.67e ⁴

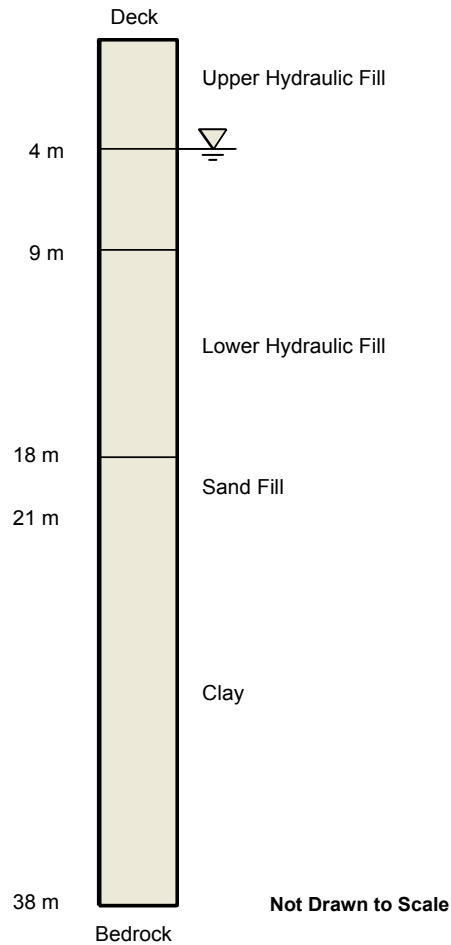


Figure 3.23 Soil Profile for Transfer Function Validation

The OPENSEES analysis conducted was an effective stress site response analysis for a layered soil profile on a 0% slope and underlain by an elastic half-space. The code used was modified from the effective stress analysis code available on the OPENSEES wiki created by McGann et al (2011). In this analysis, nine node quadrilateral elements with both displacement and pore pressure degrees of freedom enable the model to track changes in pore pressure and effective stress during earthquake excitation. The finite rigidity of the underlying elastic half space is accounted for through the use of a Lysmer-

Kuhlemeyer dashpot (1969). The horizontal ground motions produced at the surface node as a result of the earthquake excitation in this analysis can be found in Figure 3.24.

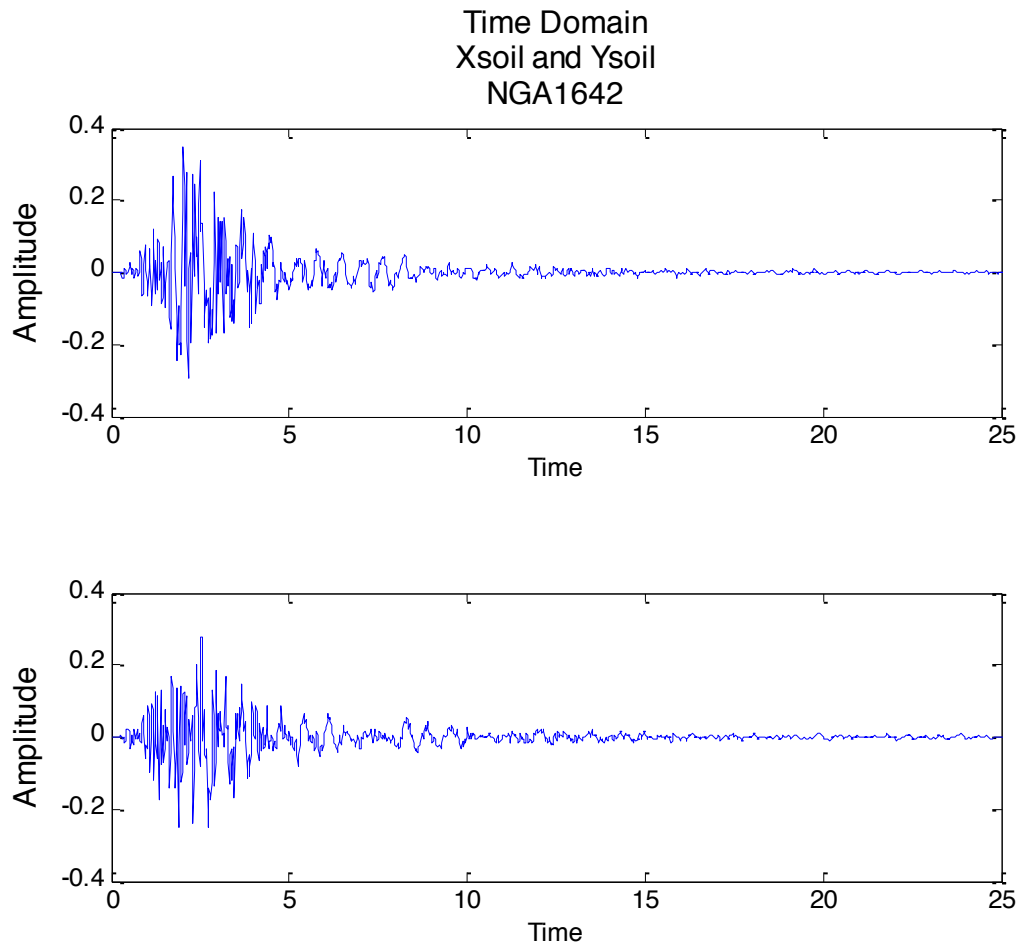


Figure 3.24 Horizontal soil motions (X and Y) from OPENSEES.

It is assumed that had the embankment model actually calculated the out-of-plane motion, it would be comparable to the motion calculated using OPENSEES. The transfer-function-calculated out-of-plane soil motion will now be calculated for comparison. Using equation 3.20 the target response spectrum U , is calculated by multiplying the transfer function by the response spectra of the in-plane soil motion calculated within the embankment model. The resulting target response spectrum is

shown in green in Figure 3.25. This figure also compares the calculated out-of-plane response spectrum to the response spectrum of the out-of-plane soil motion for NGA1642 generated in OPENSEES (blue). The two response spectra are comparable in that the root mean square error for the OPENSEES Y_{soil} curve minus the computed Y_{soil} curve equals 0.1990.

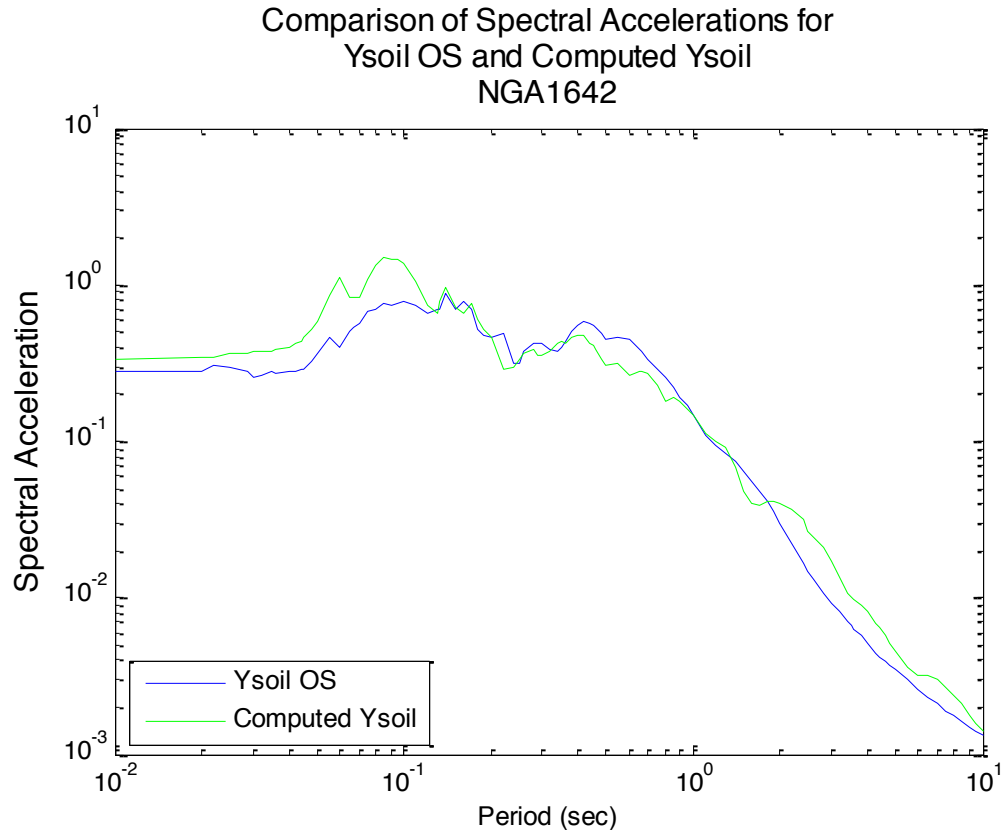


Figure 3.25 Comparison of target response spectrum and OPENSEES-generated response spectrum for the out-of-plane direction.

The estimated out-of-plane time history is extracted from the targeted response spectrum U using the time-domain spectral matching program RSPMATCH developed by Norm Abrahamson (1999). The program uses the algorithm developed by Tseng and Lilanand (1988) to match seed accelerograms to a target response spectrum by adding wavelets in the time domain. With respect to the example shown, the target response

spectrum described corresponds to the target spectrum U which was calculated in equation 3.20 using the pseudo-transfer function, and the seed accelerogram corresponds to the response spectrum of the in-plane (X) time history at the ground surface soil node calculated by the embankment model. Figure 3.26 provides an example of the response spectra calculated by the RSPMATCH program:

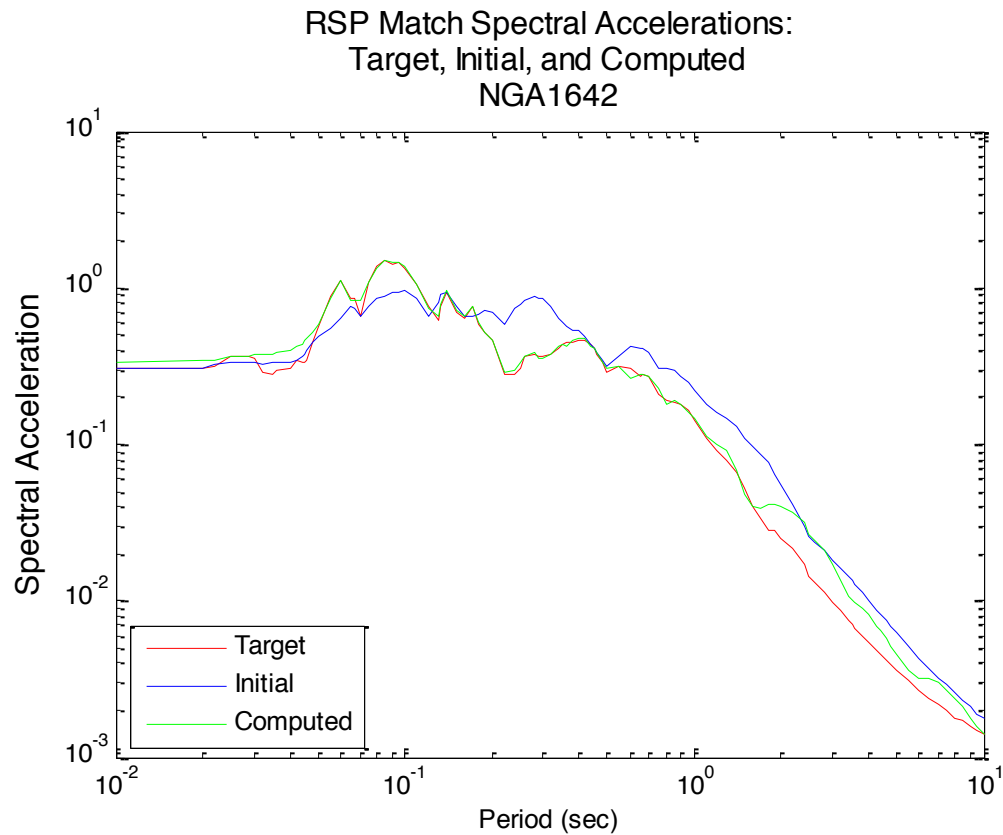


Figure 3.26 Response spectra produced via the RSPMATCH program.

The response spectra computed from the RSPMATCH program compared to those generated from the soil motions produced through OPENSEES was shown in Figure 3.25. Figure 3.27 compares the Y_{soil} time history produce by the RSPMATCHprogram from the spectra and the Y_{soil} time history from OPENSEES:

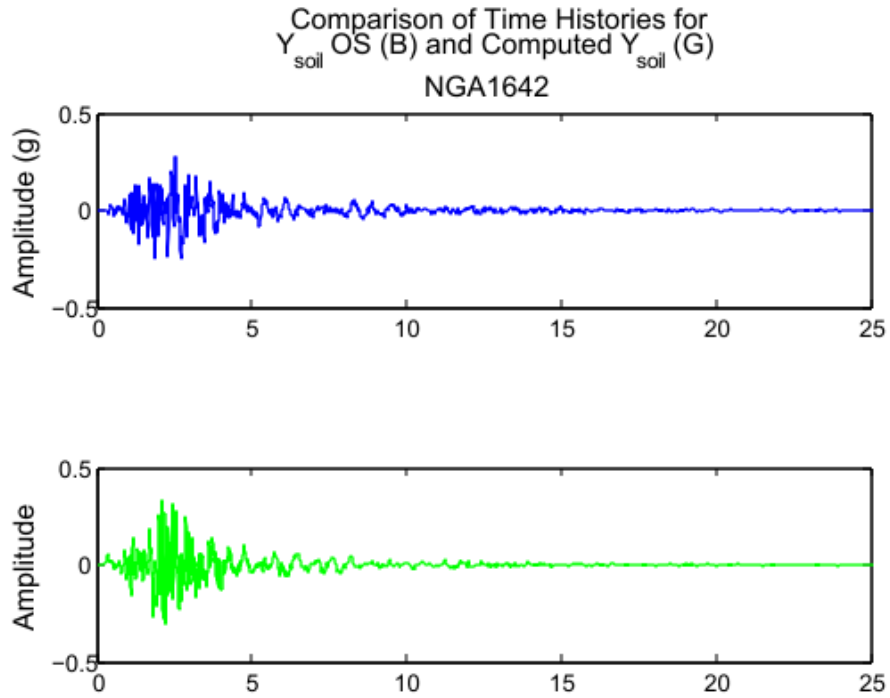


Figure 3.27 Time histories for X_{soil} (R), Y_{soil} (B), and computed Y_{soil} (G) for NGA1642.

3.4.2.4.1 Additional Pseudo-Transfer Function Validation Tests

A total of three ground motions were used to test the pseudo-transfer function method. The three motions used were NGA 0897, 1642, and 0779 and from the PGAs of each motion they represented a small, medium, and large ground motion respectively. The name and PGA of each ground motion used in testing is listed in Table 3.7.

Table 3.7 Description of NGA Motions Used in Transfer Function Validation.

Name	Size	PGA (g)
NGA0897	Small	0.070
NGA1642	Medium	0.277
NGA0779	Large	0.783

To confirm that the pseudo-transfer function method computes reasonable Y_{soil} time histories for small and large motions in addition to a medium-sized motion

(NGA1642), Figure 3.28, Figure 3.29, Figure 3.30, and Figure 3.31 show the comparison between the Y_{soil} (B), and computed Y_{soil} (G) response spectra and time histories for NGA0897 and NGA0779, Table 3.8 calculates the root mean square error between the OPENSEES and computed Y_{soil} response spectra:

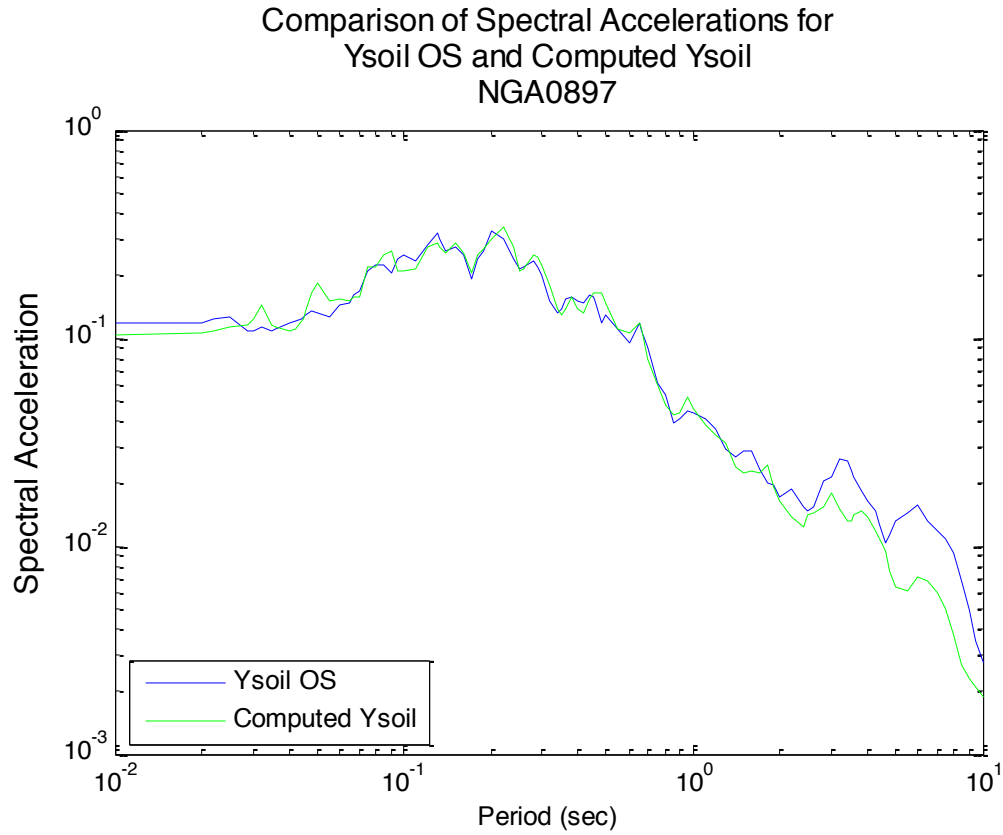


Figure 3.28 Response spectra for Y_{soil} (B), and computed Y_{soil} (G) for NGA0897.

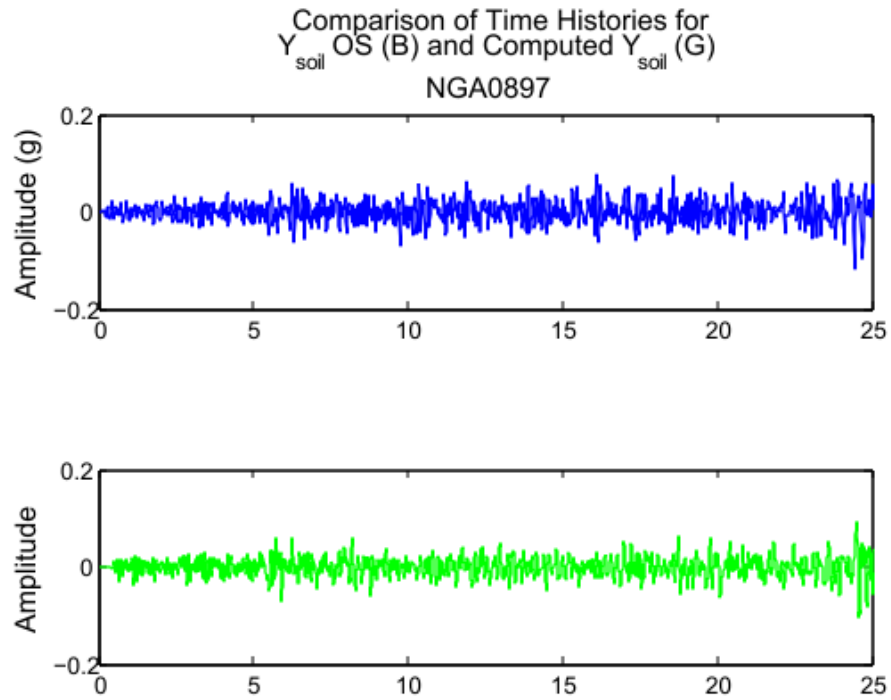


Figure 3.29 Time histories for Y_{soil} (B), and computed Y_{soil} (G) for NGA0897.

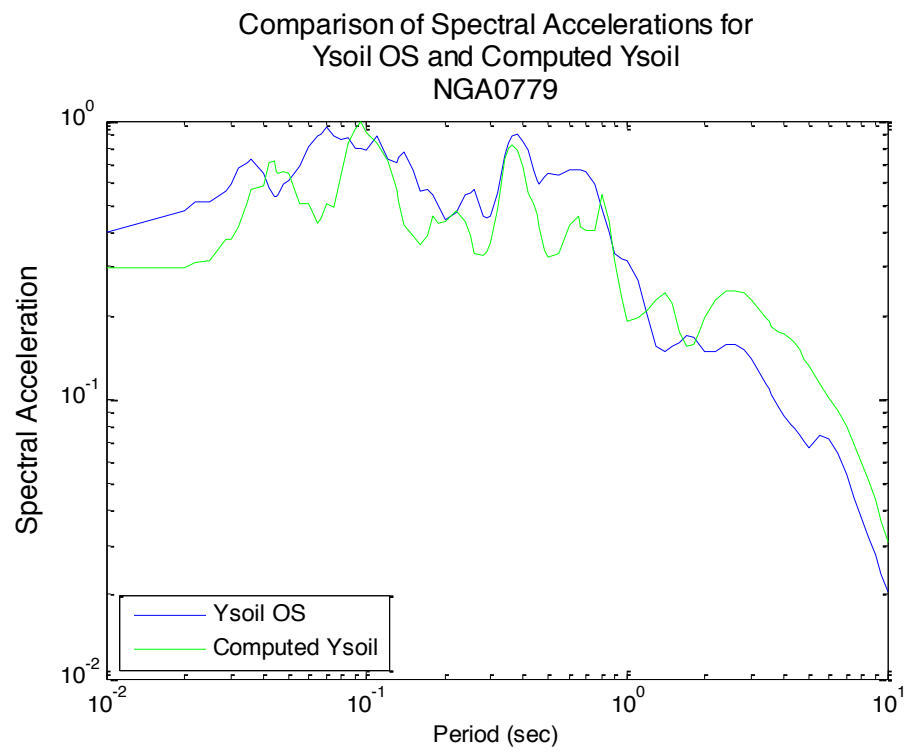


Figure 3.30 Response spectra for Y_{soil} (B), and computed Y_{soil} (G) for NGA0779.

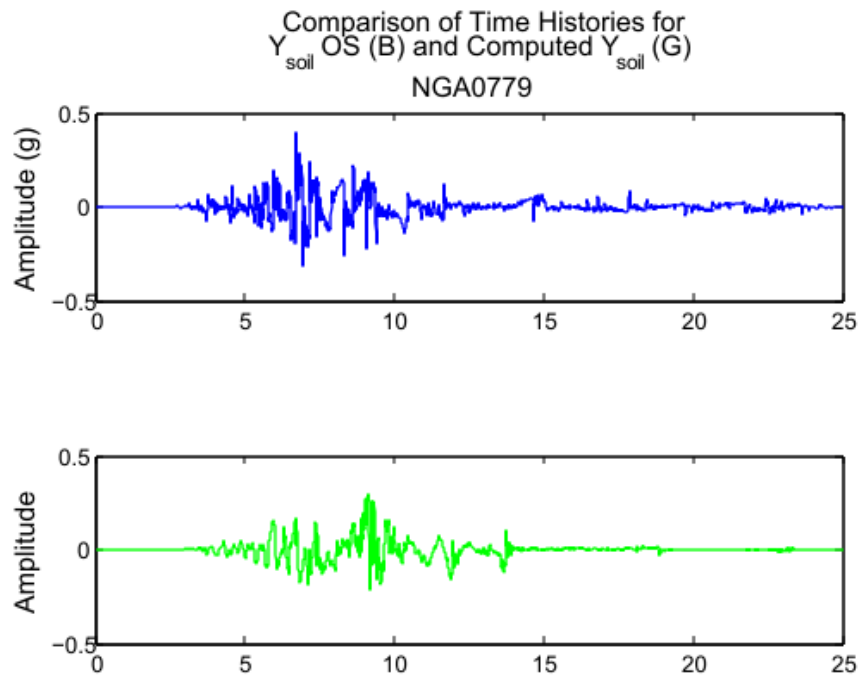


Figure 3.31 Time histories for Y_{soil} (B), and computed Y_{soil} (G) for NGA0779.

Table 3.8 – Root Mean Square Errors between Response Spectra

Earthquake Motion	RMSE
NGA 0897	0.0162
NGA 1642	0.1990
NGA 0779	0.1630

3.4.3 Wharf Response

3.4.3.1 Wharf Model

Finding the response of the wharf to earthquake excitation is a complicated but vital part in the overall risk analysis of the port. The finite element (FE) model for the wharf has been developed in OPENSEES, an object-oriented FE analysis framework (McKenna and Mcgann 2010). Models were built for both 2-D and 3-D analysis.

The wharf model combines the research of several separate investigations to develop a more advanced method in modeling wharf responses that are unique to pile

supported wharves found in west coast seaports. The following sections will overview the marginal wharf configurations analyzed within the scope of this study and highlight some of the new advances incorporated to improve the modeling of pile-deck connection failure mechanisms and the soil-structure interaction in liquefiable soils.

3.4.3.1.1 Wharf Configurations

The wharf configuration represented in this analysis accounts for some of the most commonly used wharf structures along the west coast. Many of the current west coast wharves were designed and built in the late 1960's and early 1970's using seismic design criteria much less robust than the criteria used in modern design, which makes them seismically vulnerable:

60's Designed Wharf - This wharf configuration still exists in west coast ports today, but is consistent with wharves built in the 1960's. This wharf is thought to have higher seismic vulnerability than the new construction wharf. It should also be noted that several of these types of wharves were damaged in previous earthquake events and had to be repaired (Figure 3.32).

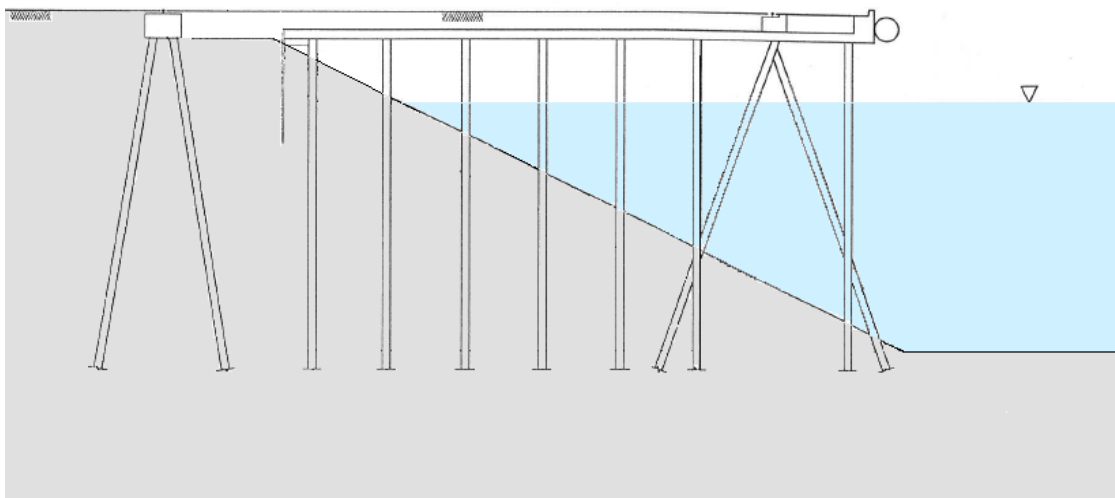


Figure 3.32 Typical 1960's Wharf

3.4.3.1.2 Physical Elements

As the details for modeling the physical elements within the wharf are described, it should be noted that subsequent details of the wharf model refer specifically to the aforementioned 1960's wharf configuration (Figure 3.32). However, all concepts and modeling techniques are essentially the same for any pile-supported marginal wharf configuration.

Figure 3.33 illustrates each of the elements that interact to produce the two-dimensional numerical strip model of the wharf: results from the embankment model, macroelements / soil springs, pile-deck connection model, and the physical elements (wharf deck and piles) of the wharf itself. The modeling techniques for the physical elements for the 2D model will be discussed first and then its translation into the 3D sense will also be discussed in this section. The remainder of the interacting elements (soil springs / macroelements and pile-deck connection model) will be discussed in separate subsequent sections.

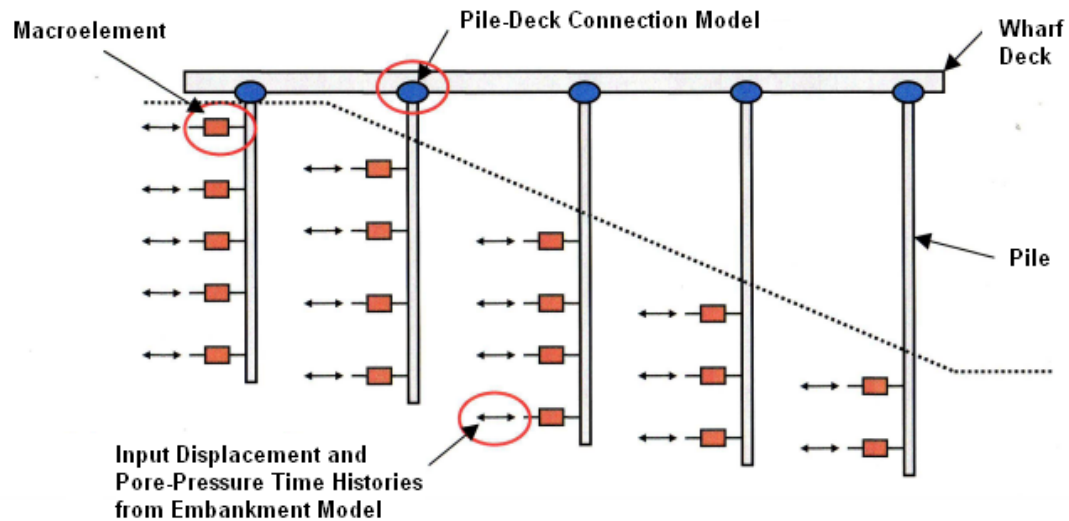


Figure 3.33 Interacting components that comprise the numerical wharf model (from (Werner and Rix 2008))

The two-dimensional wharf model uses OPENSEES to build a plain strain strip model of a specific wharf configuration. Again, subsequent explanations will refer to the 1960's wharf configuration (Figure 3.32). In this configuration, the deck is a cast-in-

place reinforced concrete slab that was found to be substantially rigid with negligible flexural deformations. Therefore, the deck is modeled using rigid beam elements. The deck is supported by two different types of piles. The bulk of the vertical load is supported by a series of pre-stressed reinforced concrete vertical piles, which, when subjected to lateral loads, resist by bending. The non-vertical piles in the wharf configuration are batter piles and account for the majority of the resistance to lateral loading. Lateral displacement of the wharf deck is accommodated by axial deformations in the batter piles, which induce tension or compression depending on the direction of displacement (Shafieezadeh et al. 2009).

The three-dimensional model builds upon the two-dimensional model by taking the 2D strip model and repeating it in the longitudinal direction. This conversion is depicted graphically in Figure 3.33. 2D wharf models are more common in practice, but for this study the 3D model was examined because there are forces and interactions considered in the 3D model that cannot be considered in a 2D model. For instance, the 3D model allows for the investigation of the response of the wharf in the longitudinal direction from the longitudinal motion (in this case calculated by the pseudo-transfer functions), the torsional response of the wharf caused by differing centers of mass and rigidity, and the boundary effects from adjacent segments (specifically pounding and shear key effects) (Figure 3.34) (Shafieezadeh 2011).

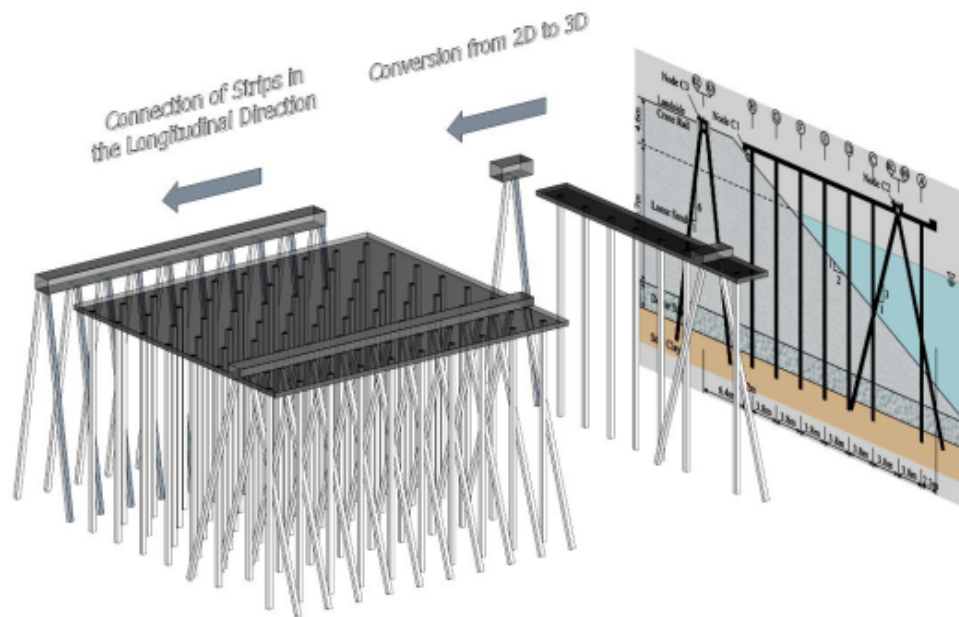


Figure 3.34 Conversion from 2D to 3D wharf model (from (Shafieezadeh 2011))

3.4.3.1.3 Pile-Deck Connections

Pile deck connections refer to the structural detailing thorough which the piles are connected to the deck. Obviously, pile-deck connections are important in both 2D and 3D modeling, but in 3D modeling forces in the longitudinal direction are also considered. Typical deck connections common in port facilities include embedded dowels, extended piles, embedded piles, and extended strand (Brackman 2009). (See Figure 3.35)

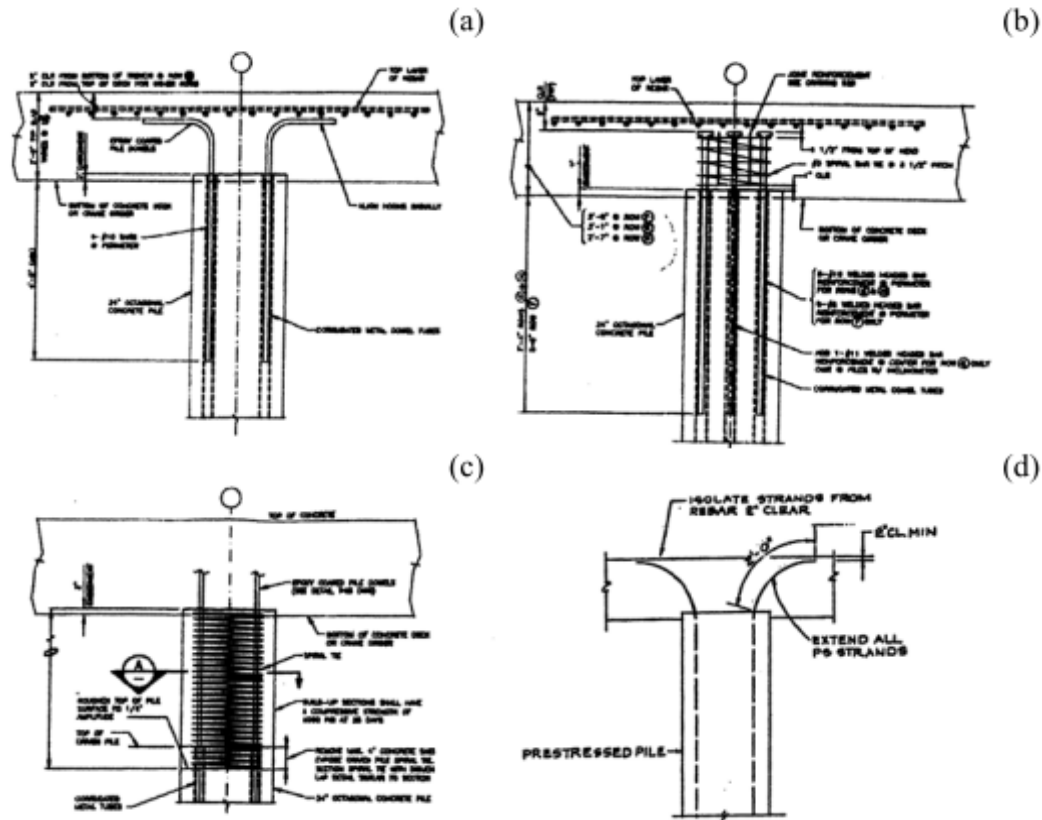


Figure 3.35 Typical configurations of common pile-deck connections: (a) embedded dowel with outward bent bars, (b) embedded dowel with T-headed bars, (c) extended pile, and (d) extended strand.

T-headed dowel bars were modeled and the non-linear behavior of the connection was calibrated against full-scale tests within the scope of this project. Therefore, T-headed dowel bar connections were used in the wharf model.

3.4.3.1.4 Soil Structure Interaction

Soil-structure interactions (SSI) are also applicable to both the 2D and 3D modeling. Again, the difference in the application to each is the consideration of the longitudinal direction in 3D modeling. Soil-structure interaction modeling is important because during earthquake excitation the flexibility of the foundation support beneath a structure alters the ground motion in the vicinity of the foundation as compared to the free field. SSI models are used to determine the actual loading experienced by the

structure foundation. For the wharf soil-structure interaction model, porewater pressure time histories and soil displacements calculated within the free field simulation of the embankment response discussed in 3.4.2 (and from the pseudo-transfer functions in the case of the longitudinal response) are input into the model at nodes along the piles. At each of these nodes, soil springs and damping elements are used to mimic the inertial, kinematic, and dissipation effects occurring during excitation.

Soil Springs

Pile-soil interaction is modeled by different types of springs for the various directions and soil layers studied. In the horizontal direction, macroelements (Varun and Assimaki 2008) model the SSI within the loose sand layer and conventional p-y springs model the SSI within the underlying dense sand and clay layers (Boulanger et al. 1999). The pile-soil interaction in the vertical direction is modeled by t-z (side) and q-z (tip) springs. P-y, t-z, and q-z soil springs are commonly used in soil-structure interaction models, and their formulation and documentation can be found in Boulanger et al. (2007).

The macroelements however, are a new and novel concept developed as part of this risk analysis research. Unlike p-y elements, the macroelements are able to capture the effects of liquefiable soil, which was a specific embankment condition tested within the port project. The macroelement is composed of a modified Bouc-Wen type hysteresis model, a coupled viscous damper and a nonlinear closure gap spring. (See Figure 3.36 for the configuration). The effect of liquefaction on the pile-soil interaction is considered by evaluating the average effective stress in the vicinity of the pile using the “liquefaction front” concept developed by Iai et al. (1992). In this approach, pore pressure generation is directly proportional to the total amount of plastic shear work done per unit volume of soil (Towhata and Ishihara 1985). The macroelement accounts for pore pressure dissipation by allowing drainage between near-field and far-field controlled by hydraulic conductivity of soil. 3D finite element simulations, large scale centrifuge tests, and field tests were used to verify the macroelement technique. Details can be found in Varun

(2010), but overall predicted results showed a close agreement to the experimental results.

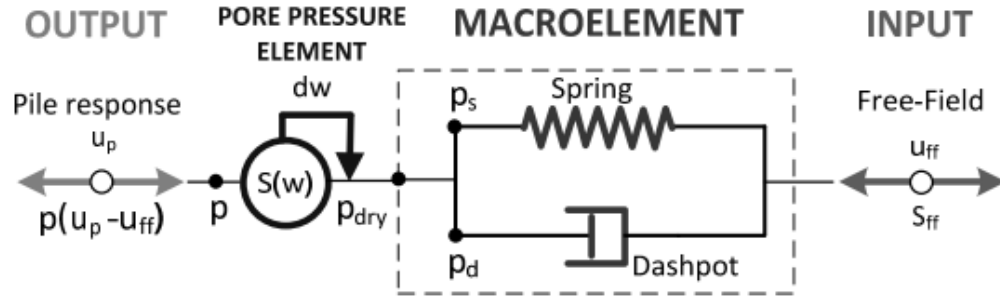


Figure 3.36 Macroelement schematic showing input, output, and components (from (Varun 2010)).

Damping

In a dynamic loading, energy dissipation is accounted for through material damping and through damping at the bearings and joints of a structure from friction. In the wharf model, structural damping in the deck, joints and piles is set at 5% (based on Rayleigh proportional damping). The material damping caused by energy dissipation through the soil is a function of small-strain damping, radiation damping, and hysteretic damping. At small strain levels, damping is usually less than 10%, and 5% damping is a widely accepted value (Ishihara 1996; Lai and Rix 1998) that will be used in this study. The energy dissipation from radiation damping was modeled using the method proposed by Gazetas and Makris (1991) for the vertical direction and by Makris and Gazetas (1992) for the lateral horizontal direction. These methods represent radiation damping as a linear dashpot in parallel with the soil spring. The damping coefficient per unit length of the pile is calculated at every pile node location (in parallel to the soil spring at that location) as:

$$c = \rho_s V_s a_0^{-1/4} Q d \quad (3.23)$$

where ρ_s is the density of the soil, V_s is the shear wave velocity of the soil, d is the pile diameter, $a_0 = \omega B / V_s$ is the normalized frequency of loading, and Q is a shape factor. In the lateral direction, $Q = 3$ (Varun 2010) and in the vertical direction $Q = \pi$ (Makris

and Gazetas 1992). The hysteretic damping cause by large nonlinear soil deformations does not need to be calculated separately because it is automatically captured by the nonlinear hysteretic force-deformation behavior of soil springs in the horizontal and vertical directions.

3.4.3.1.5 Numerical Modeling Results

Once the numerical wharf model is run, the result is a measure of damage (See 3.4.3.2) calculated at every pile node in the model caused be the specific ground motion used in that run of the numerical model. Figure 3.37 shows the result of one such run: figure (a) shows the maximum curvature ductility demand calculated along each pile, and figure (b) shows the final deformed shape of the wharf whose displacement resulted from the demand in (a).

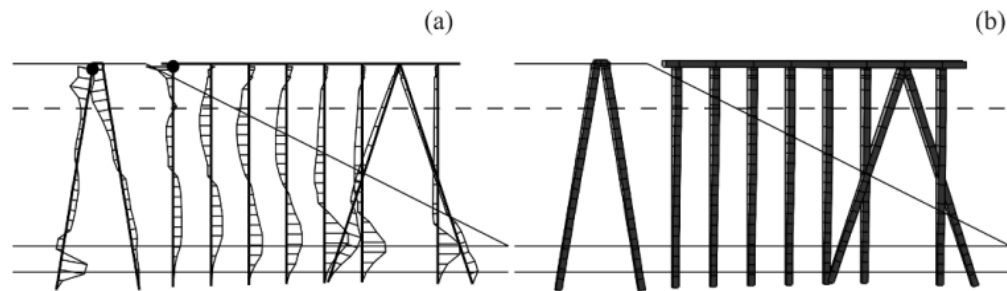


Figure 3.37 Wharf and crane rail response during NGA1057: (a) profile of the maximum curvature ductility demand and (b) final deformed shape of the wharf (from (Shafieezadeh 2011))

The full extent of this damage is then classified within a damage state. Damage is more extensively explained in 3.4.3.2, but basically damage is classified into one of three general categories: slight, moderate, or extensive. Figure 3.38 calculates component fragility curves for a 2D analysis of the piles, pile-deck connections, and relative movement of the wharf from the landside crane rail by comparing the probability of some damage state given an intensity measure. In this case the intensity measure is PGV:

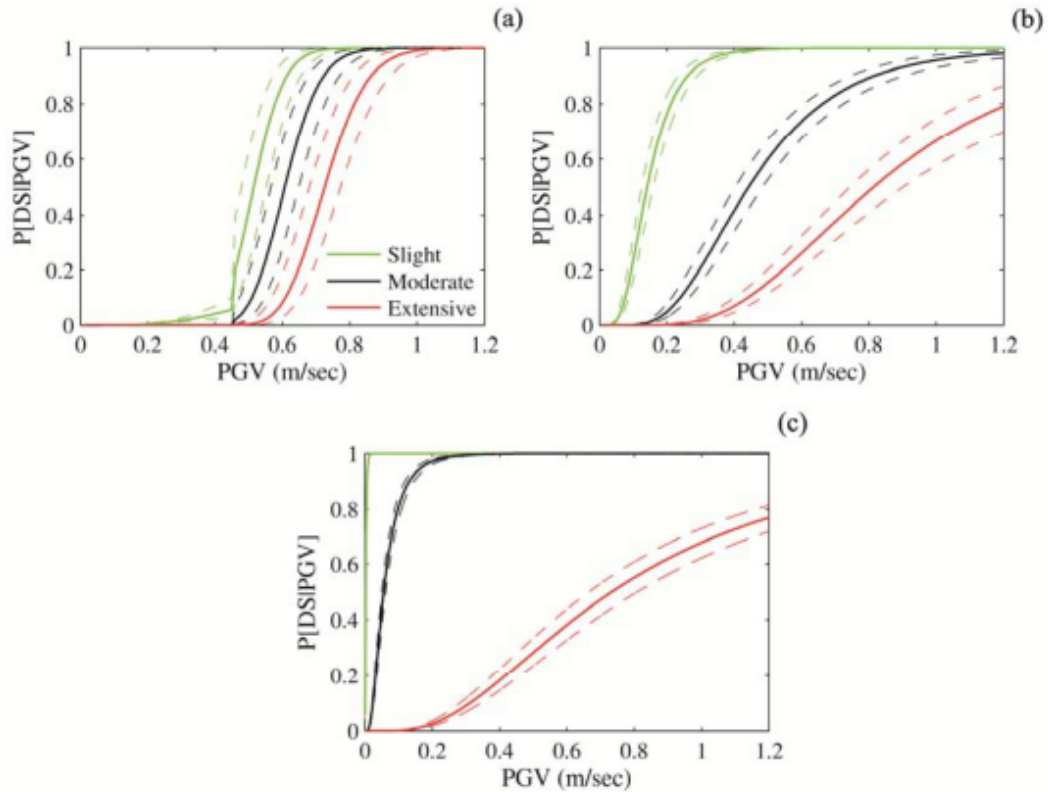


Figure 3.38 Component fragility curves for (a) pile section, (b) pile-deck connections, and (c) relative movement of the wharf with respect to the landside crane rail (solid lines are the fragility estimates and dashed lines are the corresponding 90% confidence boundaries). (from (Shafieezadeh 2011))

The damage state is used to find the repair cost and time resulting from the original earthquake excitation (See 3.4.3.4). Once the repair costs and times of damage states from every earthquake in the ground motion suite have been calculated, the losses can be aggregated within a fragility curve. This fragility curve estimates the loss produced for a pile-supported wharf given an earthquake intensity measure (PGV). The fragility curves are the ultimate goal of the wharf model because they will be used to probabilistically estimate wharf damage given the earthquake excitations within the overall risk analysis.

3.4.3.2 Wharf Damage Measures

The numerical wharf model calculates a damage measure at every node in the model. These calculated damage states help to define the damage at a given wharf section and to calculate the repair requirements for that damage. Since the port is located over an area with varying underlying soil types and wharf structures, damage will not be uniform throughout the port after a ground motion. Instead, repair costs and times are established for individual berths and then aggregated over the entire wharf.

3.4.3.3 Wharf Repair Cost and Time

The damage at each berth section will require varying degrees of repair and include varying modes of damage. Thus, each berth section will also require varying degrees of repair time. Probable damage modes at berth sections considered within the scope of this project are divided into one of four categories: pile damage, deck damage, damage to crane rails / collector trench, and relative movement of crane rail and wharf deck. The estimated costs and repair times for each of these categories is described in the following sections:

3.4.3.3.1 Pile Damage

Pile damage can account for minor to severe damage depending on the number and degree of pile damage. Possible pile damage states are explained and illustrated in

Table 3.9 and Table 3.10 and include: minimally spalled vertical piles, moderately damaged vertical piles (above or below the water) broken vertical piles, broken batter pile pair, broken pile below ground.

Table 3.9 Wharf Damage States for Pile Damage (1) (Lehman et al. 2009) from (Werner and Cooke 2009)



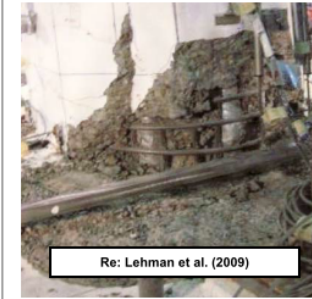

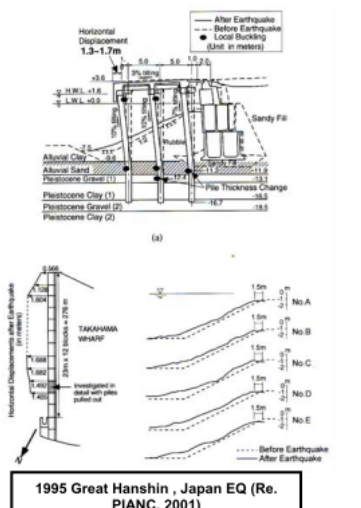
Damage State	Minimally Spalled Vertical Pile	Moderately Damaged Vertical Pile (above or below water)	Broken Vertical Pile
Symptom/Cause	Pile spalled at head due to moderate lateral displacement. No loss of vertical load carrying capacity.	Spalling and horizontal or diagonal cracking of pile's concrete cover, due to excessive bending or shear demands. Concrete core and reinforcing steel are reasonably intact, although some loss of vertical load carrying capacity has occurred. Damage is repairable.	Crushed and badly damaged pile head. Rupture and displacement along diagonal crack, due to large lateral displacement (for piles in shallow water) or P-delta effects or deck torsion (for piles in deeper water). Damage is irreparable; i.e., replacement of pile is required.
Illustration	 Re: Lehman et al. (2009)	 Re: Lehman et al. (2009)	 Re: Lehman et al. (2009)

Table 3.10 Wharf Damage States for Pile Damage (2) (Lehman et al. 2009) from (Werner and Cooke 2009)

Damage State	Broken Batter Pile Pair	Broken Pile Below Ground
Symptom/Cause	Crushed and badly damaged pile head. Rupture and displacement along diagonal crack due to large lateral displacement (for piles in shallow water) or P-delta effects or deck torsion (for piles in deeper water). Damage is irreparable; i.e., replacement of piles is required.	Wharf has residual displacement > 12 in. Inboard piles with short exposed lengths are visibly spalled/cracked all around, just under deck. Caused by excessive curvature demands at underlying liquefied soil layer between adjacent non-liquefied layers, or due of excessive sliding of overall soil embankment. Damage is irreparable; i.e., replacement of piles is required.
Illustration	 1995 Manzanillo Mexico EQ (Re Werner, 1998)	 1995 Great Hanshin, Japan EQ (Re. PIANC, 2001)

Repairs and downtimes for each type of damage can be found in Table 3.11. Note that all repair costs are in 2009 Dollars and each entry represents thousands of dollars.

For instance, the entry \$45, actually equals \$45,000 in 2009 dollars. Costs are also displayed both with and without contingencies (conting.).

Table 3.11 Repair Cost and Time Summary – Pile damage from (Werner and Cooke 2009)

Damage State	First Pile		Next few Damaged Piles					For Many Additional damaged Piles			
Description	Repair Cost (2009 Dollars)		Downtime (days)	# of Piles	Repair Cost /Pile (2009 Dollars)		Downtime (days)	# of Piles	Repair Cost /Pile (2009 Dollars)		# of Piles driven / repaired per day
	w/out conting.	w/ conting.			w/out conting.	w/ conting.			w/out conting.	w/ conting.	
Broken 24" Vertical Octagonal Pile – Not under crane rail girder - Under crane rail girder											
	\$146.1	\$268.8 ¹	67 days	Next 2- 3 piles	\$51	\$93.8	2 days/pile	≥ 4 broken piles	\$45	\$82.8	4 piles driven / day
	\$189	\$347.8 ¹	88 days		\$75	\$138	2 days/pile		\$65	\$119.6	
Broken batter Pile Pair	\$192.6	\$354.4	91 days	All further broken pairs	\$74	\$136.2	3 single piles driven per day	--	--	--	--
Minimally spalled/cracked vertical pile Above Water Below water			No downtime	Next 2- 3 spalled piles			No downtime	≥ 4 spalled piles			No downtime
	\$2.9	\$5.3			\$2.4	\$4.4			\$2.2	\$4	
	\$11.9	\$21.9			\$5.5	\$10.1			\$5.2	\$9.6	
Moderately damaged vertical pile Above Water				All further cracked				--	--	--	--




Below water	\$9.2	\$16.9	5 days	piles	\$1.3	\$2.4	3 days				
	\$15.5	\$28.5	10 days		\$10.5	\$19.3	5 days ²				
Broken Pile Below ground	Costs and downtimes to replace broken piles will be the same regardless of whether the break is above or below ground. See first 3 rows of this table. If soil sloughing has occurred and broken the piles, refer to Table 3.X for governing costs and times.										

Notes: 1.) Contingencies applied to repair design and construction costs, but not to mobilization.
2.) If damage occurs in absence of other types of damage that requires repair inspection, include 2 days of downtime for inspection.

3.4.3.3.2 Deck Damage

Much like pile damage, deck damage can attribute to minor to severe damage states depending on the area and degree of damage. Damage states for possible deck damages are explained in Table 3.12 and include: damage to underside of deck above piles, ruptured concrete shear keys, and ruptured deck caused by punch through of piles.

Table 3.12 Wharf Damage States for Deck Damage (Earthquake Engineering Research Institute (EERI) 1990; Werner 1998) from (Werner and Cooke 2009)

Damage State	Damaged Underside of Deck above Piles	Ruptured Concrete Shear Key	Ruptured Concrete Deck due to Punch Through of Piles
Symptom/Cause	Spalled concrete, and exposed and possibly bent reinforcing steel. Usually accompanies pile-head damage,	Relative movement and separation of deck segments at expansion joint, accompanied by bending and shear cracks in deck and possibly in piles as well. Crane rail unseated and bolts to deck damaged..	Failure of pile-deck connection, offset of damaged pile, and protrusion of pile through deck. Most common at batter piles and thin wharf deck, when pile-deck connection has insufficient strength and ductility to accommodate earthquake demands.
Illustration	 1989 Loma Prieta EQ (Re. Werner, 1998)	 1994 Northridge EQ (Re. Werner, 1998)	 Pile Punch-Through at Bridge Deck during 1989 Loma Prieta EQ. Appearance expected to be similar to pile punch-through that would occur at seaport wharf deck (Re. EERI, 1990).

Repair Costs and downtimes for these damage states include the repair of the deck itself, repair of the broken piles, and repair of batter pile pairs. Again, the repair cost and

time summary table (Table 3.13) lists costs in thousands of dollars as in Table 3.11, with contingencies (w/ conting.) and without contingencies (w/out conting.).

Table 3.13 Repair Cost and Time Summary – Deck damage from (Werner and Cooke 2009)

Damage State	First damage occurrence		Next few Damage Occurrences					For Many Additional damage occurrences			
Description	Repair Cost (2009 Dollars)		Downtime (days)	# of damage occurrences	Repair Cost /Pile (2009 Dollars)		Downtime (days)	# of damage occurrences	Repair Cost / Damage Location (2009 Dollars)		Downtime (days)
	w/out conting.	w/ conting.			w/out conting.	w/ conting.			w/out conting.	w/ conting.	
Damaged underside of deck above piles	\$3.2	\$5.9	No downtime	Next 2-3 occurrences	\$2.4	\$4.4	No downtime	≥ 4 locations	\$2	\$3.7	No downtime
Broken 24” Vertical Octagonal Pile – under crane-rail girder	\$16	\$29.4	8 days ¹	For all additional damaged shear keys	\$16	\$29.4	8 days ¹	--	--	--	--
Broken batter Pile Pair	\$21.4 (deck repairs only) ²	\$39.4	7 days	All additional pile punch through occurrences	\$21.4 (deck repairs only) ²	\$39.4	7 days	--	--	--	--

Notes: 1.) If damage occurs in absence of damage to other wharf components that require damage inspection, repair design, and mobilization of repair resources, increase downtime by 3 days for inspection and repair design, and by the following times for mobilization of repair resources: (a) 5 days for earthquake M < 7.0; and (b) 10 days for M ≥ 7.0.
2.) Include additional costs and downtimes for repair of piles

3.4.3.3.3 Crane Rails / Collector Trench Damage

Relative movement between crane rails and collector trenches account for more severe damage states because movement often prohibits use of the cranes through loss of power or through damage to the crane path alignment. While repair costs account for

some of the losses in such a situation, the operational losses will far exceed the repair costs. Damage states pertaining to the crane rail collector trench are dependent on the relative displacement at the expansion joints and are explained in Table 3.14 and their repair costs and downtimes are listed in Table 3.15.

Table 3.14 Wharf Damage States for Crane Rail / Collector Trench Damage from (Werner and Cooke 2009)

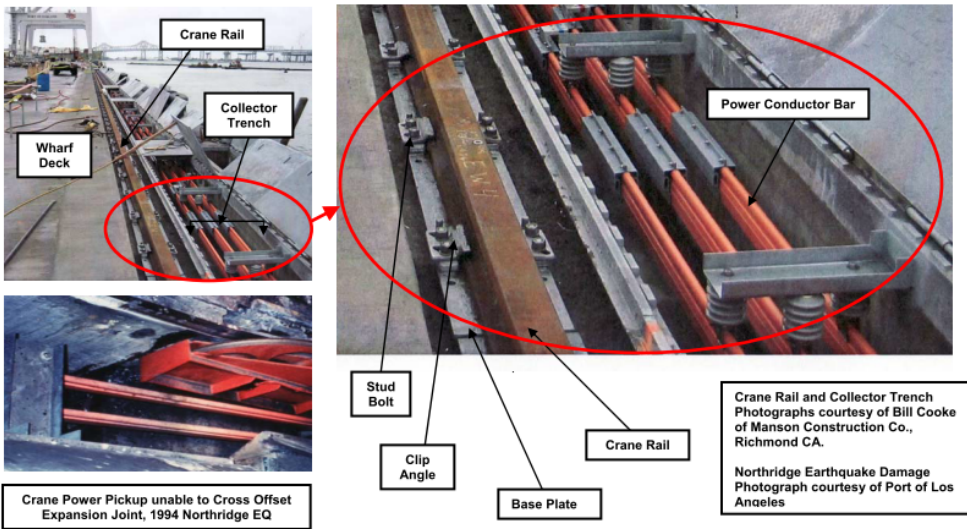
Damage State	Minor Loss of Alignment of Crane Rail and Loss of Contact between Crane and Trench Conductor Bars	Moderate Crane Rail Damage and Loss of Contact between Crane and Trench Conductor Bars	Major Crane Rail Damage, Misalignment of Crane and Trench Conductor Bars, and Damage to Collector Trench Structure
Symptom/Cause	Relative Displacement. at Expansion Jt. $\leq \frac{3}{4}$ in.	Relative Displacement. at Expansion Jt. $\frac{3}{4}$ in – 1-1/2 in..	Relative Displacement. at Expansion Jt > 1 -1/2in.
Configuration and Example of EQ Disruption	 <p>Crane Rail</p> <p>Collector Trench</p> <p>Wharf Deck</p> <p>Crane Power Pickup unable to Cross Offset Expansion Joint, 1994 Northridge EQ</p> <p>Power Conductor Bar</p> <p>Stud Bolt</p> <p>Clip Angle</p> <p>Base Plate</p> <p>Crane Rail</p> <p>Crane Rail and Collector Trench Photographs courtesy of Bill Cooke of Manson Construction Co., Richmond CA.</p> <p>Northridge Earthquake Damage Photograph courtesy of Port of Los Angeles</p>		

Table 3.15 Repair Cost and Time Summary – crane rail / collector trench damage from (Werner and Cooke 2009)

Relative Displacement (Offset) Across expansion joint (inches)	Repair Cost (2009 Dollars) ¹		Downtime (days) ^{1,2}
	w/out contingencies	w/ contingencies	
$\frac{3}{8}$ to $\frac{3}{4}$	\$7,500	\$13,800	3 days
$\frac{3}{4}$ to $1\frac{1}{2}$	\$22,500	\$41,400	9 days
$> 1\frac{1}{2}$	\$220,000	\$404,800	80 days

Notes: 1.) Damage to collector trench will occur only if shear keys along expansion joints are damaged. Therefore, costs for collector trench repair should be combined with costs for repair of shear keys (**Error! Reference source not found.**). Downtimes for shear key repairs are concurrent with downtimes for collector trench repairs.
2.) If collector trench damage occurs in absence of damage to other wharf components that require inspection, repair design, and mobilization of repair resources, increase downtime by 3 days for inspection and repair design and by the following times for mobilization of repair resources: (a) 5 days if $M < 7.0$; and (b) 10 days if $M \geq 7.0$.

3.4.3.3.4 *Relative movement of crane rail and wharf deck*

The relative movement of the crane rail and wharf deck accounts for one of the most severe types of wharf damages. Depending on the relative displacement, cranes could remain operable, or be rendered useless until repair has taken place. As with the crane rail and collector trench, the overall wharf damage state depends on the amount of relative displacement (Table 3.16). Likewise, the repair cost and downtimes also depend on displacement (Table 3.17).

Table 3.16 Wharf Damage States for Relative Movement of Crane Rail and Wharf Deck (Earthquake Engineering Research Institute (EERI) 1990; Werner and Dickenson 1996) from (Werner and Cooke 2009)




Damage State	$1/8 \text{ in.} < \Delta_h \leq 1 \text{ in.}$	$1 \text{ in.} < \Delta_h \leq 6 \text{ in.}$ (with possible comparable levels of relative settlement)	$\Delta_h > 6 \text{ in.}$ (with possible comparable levels of relative settlement)
Symptom/Cause	Relative movement of crane rail girder and wharf deck. No damage to girder or to underlying piles. Caused by shaking and liquefaction of underlying or adjacent soils.	Relative movement of landside crane rail girder and wharf deck. Cracks in girder but usually no/minor damage to supporting piles or to crane. Caused by shaking and liquefaction of underlying or adjacent soils.	Relative movement of landside crane rail girder and wharf deck. Cracks in landside crane rail girder and damage to supporting piles. Usually accompanied by significant crane damage. Caused by ground shaking and liquefaction of underlying or adjacent soils.
Illustration	 <p>Slotted clip to secure rail flange to concrete trench</p> <p>Crane rail</p> <p>Bolts thru steel clip into concrete trench</p> <p>Note. Relative movement of girder and deck is within available length of slot in clip (see Appendix B)..</p>	 <p>1989 Loma Prieta EQ (Re. EERI, 1990)</p>	 <p>1995 Great Hanshin, Japan EQ (Re. Werner and Dickenson, 1995)</p>

Table 3.17 Repair Cost and Time Summary – Relative Movement of Crane Rail and Wharf Deck from (Werner and Cooke, 2009)

Damage State	Length of damage = 300 ft.			Length of damage > 1,200 ft.		
	Repair Cost, 2009 Dollars ¹		Downtime (crane out of service) days ^{1,3}	Repair Cost, 2009 Dollars ²		Downtime (crane out of service) days ^{2,3}
Description	w/out contingencies	w/ contingencies		w/out contingencies	w/ contingencies	
Relative horiz. movement of landside crane rail and wharf that is > 1/8 in. and ≤ 1 in. ⁴	\$60,000	\$110,400	10 days	--	--	--
Relative horiz. movement of landside crane rail and wharf that is > 1 in. and ≤ 6 in. ⁴	\$104,000	\$192,100	20 days ²	--	--	--
More than 6" of relative movement of landside crane rail and wharf Repairs include new structural connection b/w deck and landside crane rail Repairs exclude new structural connection b/w deck and landside crane rail	--	--	--	\$2,004,000	\$3,687,400	140 days
	--	--	--	\$3,379,400	\$6,218,700	270 days

Notes 1.) It is assumed here that these relative horizontal movements extend over a length along the crane rail girder that is 150 ft. on either side of the expansion joint (total length = 300 ft.). However, for lengths experiencing movement different from 300 ft, increase or decrease the repair costs and downtimes proportional to the ratio of the actual length to 300 ft.
2.) It is assumed that if horizontal movements exceed 6 in. and extend over a significant length, the entire girder b/w expansion joints (1,200 ft.) will need to be replaced. Replacement of lengths differing from 300 ft, would have repair costs and downtimes increased or decreased in proportion with the ratio of the actual length to 300 ft.

- 3.) If these relative movements occur in absence of damage to other wharf components that require inspection, repair design, and mobilization of repair resources, increase downtime by 3 days for inspection and repair design and by the following times for mobilization of repair resources: (a) 5 days if $M < 7.0$; and (b) 10 days if $M \geq 7.0$.
- 4.) If relative horizontal movements are accompanied by relative vertical movements ≥ 2 in., crane rail girder will need to be replaced.

While it is intended that most occurring damage will simply be repaired, it is possible that some wharf damage will be so severe that replacement becomes more economical. In discussions with port officials, it was decided that when repair costs = 50-60% of the replacement costs for damaged wharfs, that replacement becomes a more feasible option than repair. For the confines of this study, replacement will occur over repair when repair costs are greater than or equal to 60% of the repair costs. Cost of replacement with contingencies = $\$320/\text{ft}^2$, and takes 24 months for the first 1200' segment, and 12 months for each additional segment.

Furthermore, it is important to note that several assumptions have been made in the development of the repair and replace costs/times for wharf damage. These assumptions include but are not limited to:

- 1.) Damages listed are not all encompassing; only those expected to most commonly occur.
- 2.) Damages / Repairs only apply to the pile supported wharfs common to the US West Coast.
- 3.) For cost/repair estimates, the length of one berth within the wharf is 600'.
- 4.) All costs cited are in 2009 dollars.
- 5.) Mobilization time/cost = 0 days for a $M_w < 6.0$, 5 days for $6.0 \leq M_w \leq 7.0$, and 10 for $M_w < 7.0$.
- 6.) Cost contingencies should be applied to all estimates.
- 7.) Damage to the following within the port infrastructure system is not considered: pavements in wharf backlands, electrical and mechanical lines/connections/equipment, buildings, and connecting rail or roadway systems.

3.4.3.4 Calculation of Repair Requirements

It was decided that the fragility curves calculated using the 2D wharf models would be used instead of the 3D models. After investigation, it was apparent that the torsional component did not have as pronounced an effect in the response as expected (Shafieezadeh 2011). Most of the wharf damage was a result of lateral displacements, which can be accurately captured in the 2D model. Therefore, the 2D model was used in favor of the 3D model. Use of the 2D model instead of the 3D also means that the repair requirements for deck damage and crane rail/ collector trench damage will not be considered since the torsional response in the longitudinal direction is not calculated. Therefore, only damage to the piles and the relative movement of the crane rail and wharf deck will be considered in the calculation of the repair requirements and the following fragility curves for the wharf.

However, the repair requirements and the wharf analysis described in the previous sections only apply to a single wharf segment. Each terminal is comprised of multiple wharf segments. The repair costs and repair times for all of the segments within the wharf are exponential random variables calculated from two variables: a mean cost and mean time from the tables above and a correlation factor between adjacent wharf segments.

The correlation factor between wharf segments $[i,j] = e^{-0.2*|i-j|}$. In the following terminal (Figure 3.39) if berth 1 remains wharf segment i , the rest of the berths would have the following correlation factors:

① cf = 1	② cf = 0.81	③ cf = 0.67	④ cf = 0.54	⑤ cf = 0.44
-------------	----------------	----------------	----------------	----------------

Figure 3.39 – Calculated Correlation Factors between Adjacent Wharf Segments

3.4.3.5 Operational Status of the Wharf

For each earthquake occurrence in the earthquake catalog, the component fragility curves for the wharf structures throughout the port will be used to estimate the initial damage state for each wharf section within the port system. This damage will then be repaired over some period of time before the port can once again be fully operational. During this repair time, the port cannot function at full capacity, and port operations will be modeled within the operational model to determine the effect of the reduced capacity. The operational status of the wharf must be calculated during the repair period so that the operational model has knowledge of which berth sections are available over the entire repair period. Table 3.18 shows a simplified example of how the operational status of the port's wharf and crane structures is depicted within the risk analysis. In this example, several wharf sections and cranes are damaged in the earthquake and rendered inoperative during the first few days after the earthquake. By Day 8 following the earthquake, all of the wharf sections and cranes are repaired and operational and the port has gained full functionality.

Table 3.18 Example of Port System Operational Status

			Time After Earthquake (days)									
Terminal	Wharf Section	Crane	0	1	2	3	4	5	6	7	8	...
A	1		N	N	N	N	N	N	Y	Y	Y	...
	2		N	N	N	N	Y	Y	Y	Y	Y	...
	3		Y	Y	Y	Y	Y	Y	Y	Y	Y	...

	5		Y	Y	Y	Y	Y	Y	Y	Y	Y	...
		a	N	N	N	N	N	N	N	Y	Y	...
		b	N	N	N	N	N	N	N	N	Y	...
		c	N	N	N	Y	Y	Y	Y	Y	Y	...
	
		j	Y	Y	Y	Y	Y	Y	Y	Y	Y	...

Y = Operational; N = Not Operational

For the example above and within the risk analysis, the operational status is calculated using component fragility curves, which estimate the initial damage state and the repair times for each damage state, which are predetermined from real-life data. The operational model within the risk assessment requires an account of what day each wharf section or crane becomes available for use.

The risk analysis program will apply two methods of repair sequencing within the terminals: Parallel and Series repair. Parallel sequencing is more likely and desirable of the two scenarios. Parallel sequencing assumes that all wharves and cranes in need of repair will be worked on simultaneously. Therefore the repair time with contingencies will equal the total repair time for each damaged berth. Parallel sequencing is used for all

of the runs in the results section except for the one that specifically tests the series repair sequencing.

Series repair is a more conservative option and assumes that damaged sections will not be fixed simultaneously but consecutively. For this case, the sequence in which the damaged wharf sections will be repaired must be decided in order to calculate operational status. There are several options available for deciding the series repair sequence: maximizing the longest contiguous length of berth, beginning with the berth with the shortest repair time and continuing to the longest repair time, choosing the inverse sequence of longest to shortest repair time, or attempting to maximize the number of ships able to berth at the undamaged wharf sections of the terminal. The last option coincides with the operational goal of maximizing productivity during the repair period, however the latter three options are easier to implement. Therefore, all options will be compared within the following example:

Assume that the following seven wharf sections (Figure 3.40) with the following repair times comprise a terminal. Each section is 183 meters long. Repair times equal to zero indicate immediate use, while those greater than zero indicate the number of days in which it will take a team to repair that section. Ships docking at the wharf are assumed to be 270 meters, requiring two consecutive undamaged berths to dock in the terminal.

①	②	③	④	⑤	⑥	⑦
rt = 0	rt = 0	rt = 2	rt = 0	rt = 1	rt = 3	rt = 0

Figure 3.40 Repair Sequencing Example

Three of the 7 sections are damaged: sections 3, 5, and 6. Therefore, there are $3!$ (6) repair sequences possible for repair. The repair period for these sequences equals the sum of the repair times (since they are done consecutively), which equals $2+1+3 = 6$ days. To compare the repair sequence options, every possible option will be simulated and the number of ships that are able to dock at the terminal will be calculated over the entire six-day repair period. Table 3.19 shows the results of this example.

Table 3.19 Number of Ships Able to Dock for Each Repair Sequence

Repair Sequence	Day						Total
	1	2	3	4	5	6	
3-5-6	1	2	2	2	2	3	12
3-6-5	1	2	2	2	3	3	13
5-3-6	2	2	2	2	2	3	13
5-6-3	2	2	2	3	3	3	15
6-3-5	1	1	2	2	3	3	12
6-5-3	1	1	2	3	3	3	13

The maximum number of ships is able to dock at the terminal during the repair period for sequence 5-6-3, and to maximize the productivity of the port post-earthquake, wharf sections should be repaired in that sequence. The other sequencing options previously discussed did not allow as many ships to dock at the terminal during the repair period. Repair sequences 6-5-3 and 3-5-6 corresponding to the longest and to the shortest repair time, and maximizing the longest contiguous length of wharf, respectively, allowed for a total of 12 ships to dock at the terminal during the repair period. Sequence 5-3-6 corresponds to repairing the section with the shortest repair time and then moving to the longest repair time. This sequence produced slightly better results with 13 ships allowed during the repair period. It is apparent that the best method for repair sequencing is to calculate the maximum ships able to dock at the berth during the repair period, and use

that specific sequence for repair. However, this repair sequence is the hardest to implement because every combination of repair sequence has to be calculated before the optimum sequence can be chosen. Port operators are not likely to perform a calculation of this nature. Instead they would choose a good solution that's easier to implement. For this reason, the risk analysis program will use what corresponds to sequence 5-3-6: repairing sections in order from shortest to longest repair periods.

It should be noted that though the previous example assumed a ship length of 270 meters, in actual operation, ship lengths will vary. In reality a small ship might be able to dock at only one wharf section length, thus increasing the total ship count. However, frequency of ship lengths was studied using actual shipping data for two west coasts ports over a six-month period, to produce the estimate used in the previous example. Figure 3.41 shows the frequency of ship lengths arriving at these ports.

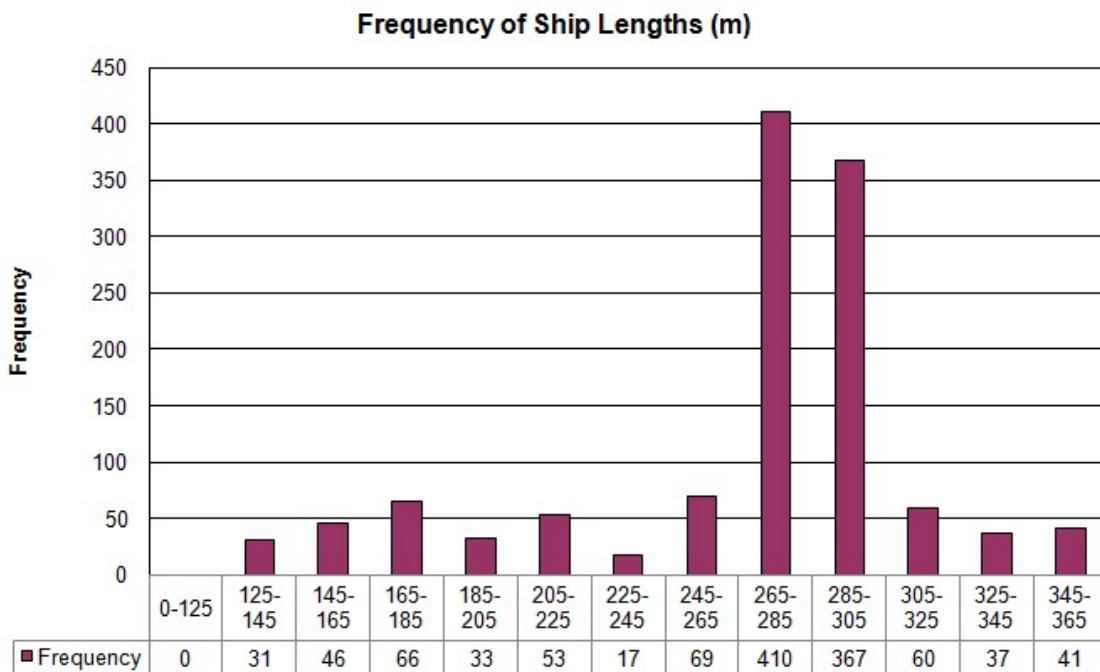


Figure 3.41 Histogram of Ship Lengths

Only 11% of the ships within the data would fit at a single wharf section, while every other ship within the data would be able to dock at two contiguous sections. Therefore for the example, ship lengths were assumed to be the average length, 270 meters.

3.4.4 Crane Response

3.4.4.1 Crane Modeling Overview

Consideration of container cranes is an added concept from most previous port risk evaluations. *Seismic Guidelines for Ports* (Werner 1998), suggests that container cranes generally perform well during earthquakes, however cranes have been growing in size and these newer, larger cranes may actually be damaged or fail during earthquakes (Kosbab 2010). Severe crane damage results in significant losses due to downtime, since completely replacing a crane takes an average of 330 days. Therefore, it was important to include crane damage within the scope of this project.

Three typical “A” frame container cranes (Figure 3.42) were considered under the scope of this project. Cranes are generally classified by their outreach (ability to service ships of certain widths), and gage width (distance between the crane rails). The following cranes range in outreach and gage width but generally represent the array of cranes used in US west-coast container ports (Schleiffarth 2008), and are therefore considered within the scope of this project:

- 1.) Modern Jumbo Crane (J100) – Represents cranes with 100 foot (30.48 m) gage lengths and outreaches ranging from largest of the Post-Panamax class cranes (18-20 containers wide) to the small to moderate cranes within the Super Post-Panamax class (21-22 containers wide), which were built circa 2000. This crane was designed without forethought of earthquake loading but “has a relatively stiff

and strong portal sway mode due to operational stiffness requirements and lifting forces” (Kosbab 2010).

2.) Heritage Jumbo Crane (LD100) – This crane type also has a 100 foot gage length and the outreach represents both small and large Post-Panamax class cranes (18-20 containers wide) cranes built circa 1980. In the original design, consideration of uplift of the crane legs in reaction to earthquake motion was accounted for though the frame was not specifically designed to withstand earthquake forces. Today, many of these cranes have been retrofitted with longer booms to service larger ships, without any further frame modifications.

3.) Heritage Compact Crane (LD50) – This crane represents those with 50 foot (15.24 m) gage lengths and outreaches similar to the smallest of the Post-Panamax class cranes built around 1970. Subsequent crane designs meant to minimize rocking and uplift were based on the response of this crane. Tipping prior to significant structural damage is common during earthquakes.

Crane modeling was conducted in OPENSEES (McKenna and Rodgers 2010) using a finite element analysis technique. Several simplified analyses were conducted to determine the most vulnerable aspects of the crane, but the modeling to develop the fragility analyses was completed three dimensionally (Kosbab et al. 2009).

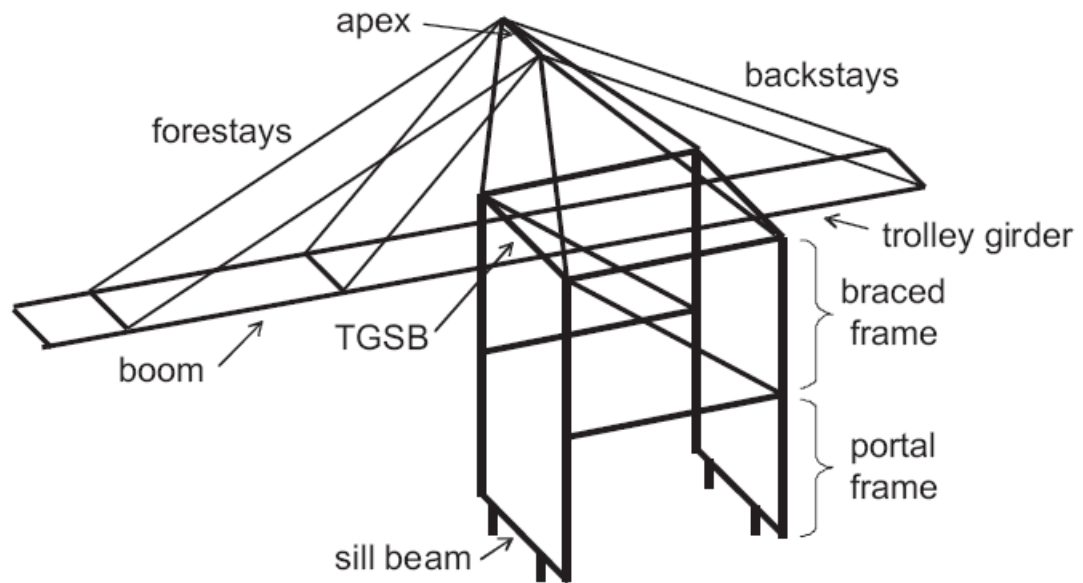


Figure 3.42 Container Crane Schematic

3.4.4.2 Crane Damage Measures

Damage states for the cranes were compiled through the use of an internal document (Liftech Inc. 2008) presenting case studies and typical repairs for container cranes along with personal communication between Liftech, Inc. and Kosbab (2010). Four damage states caused by earthquake disruption have been identified for cranes:

- 1.) Derailment – Derailment occurs when lateral loads are large enough to reduce the axial reaction of one leg to zero, thus causing the leg to be displaced from the wharf-mounted crane rail. Derailment must be repaired by using mobile cranes or jacking systems to reposition the derailed crane back onto the crane rails (Liftech Inc. 2008).
- 2.) Immediate Use – In this damage state the crane only suffers minor structural damage but is still available for use post-earthquake. Specific damage can include frame buckling or torsional movement.
- 3.) Structural Damage – In this damage state, the crane has suffered enough significant structural damage that it cannot be used immediately, but has

not collapsed. Specific damage includes severe portal deformation and local buckling.

- 4.) Complete Collapse – In this state structural damage to the crane is so severe that the structure collapses. In this situation, repairs are usually not possible, and replacement is the only option. Since most container cranes are made by one company (Shanghai Zhenhua Heavy Industry Co., Ltd. (ZPMC) controls greater than 80% of international market share (Shipping China 2009)), purchases are semi-custom and replacement of the crane can take one year or more.

3.4.4.3 Crane Fragility Curves

Fragility curves were calculated in previous research (Kosbab 2010) to represent the probability of a crane reaching a particular limit state, given that specific earthquake intensities occur. To calculate the fragility curves that follow, the following methodology was employed. First, sensitivity analyses were conducted to characterize the importance of various contributors to overall uncertainty within container cranes. Next, finite element models, seismic demand modeling, and capacity estimates were used to gain knowledge of the crane response during earthquake excitation and the most vulnerable crane components. The engineering demand parameter ultimately chosen was spectral acceleration at the fundamental period of the crane ($T=1.55$ s) for a spectral damping of 1.5%. This EDP was easily applied from the portal uplift theory used to model the seismic demand. A fragility method was employed to describe this model in which earthquake intensities were related to expected losses through the theorem of total probability. The fragility curves created are intended to be used as industry “default” curves for most cranes in existence that should be tailored to specific cranes with the use of the aforementioned methodology. The following figures (Figure 3.43-Figure 3.45) show the fragility curves for the cranes studied within the scope of this project.

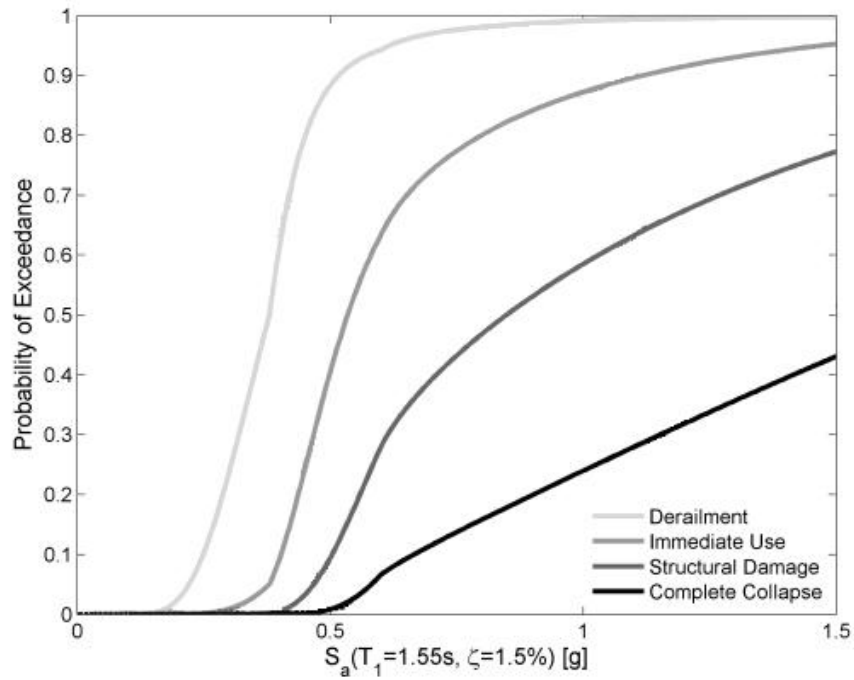


Figure 3.43 Fragility curves for J100 container crane, assuming portal uplift theory seismic demand model (from Kosbab 2010).

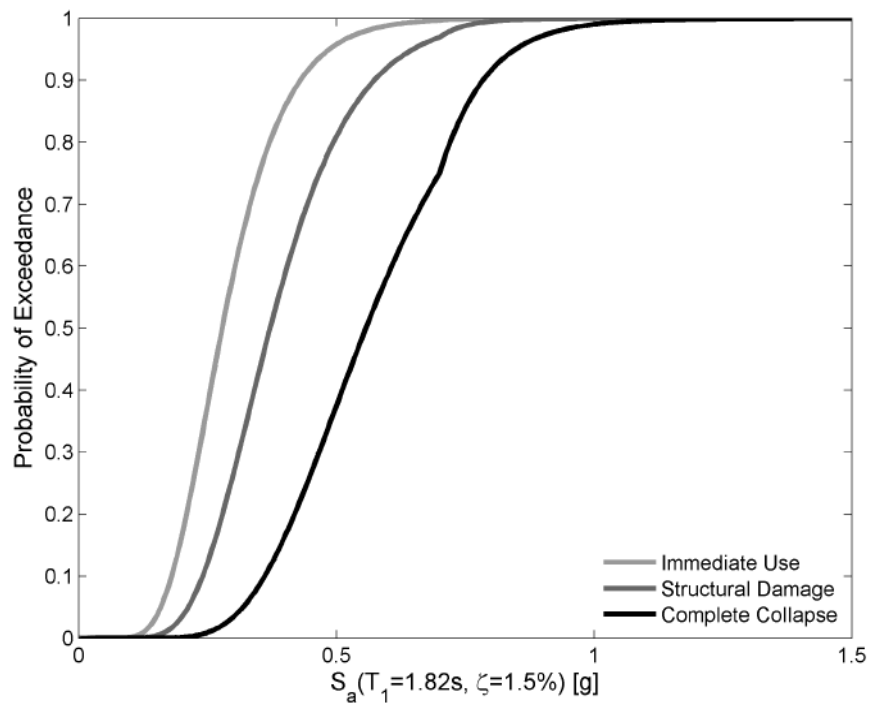


Figure 3.44 Fragility curves for LD100, assuming portal uplift theory seismic demand model. (Kosbab 2010)

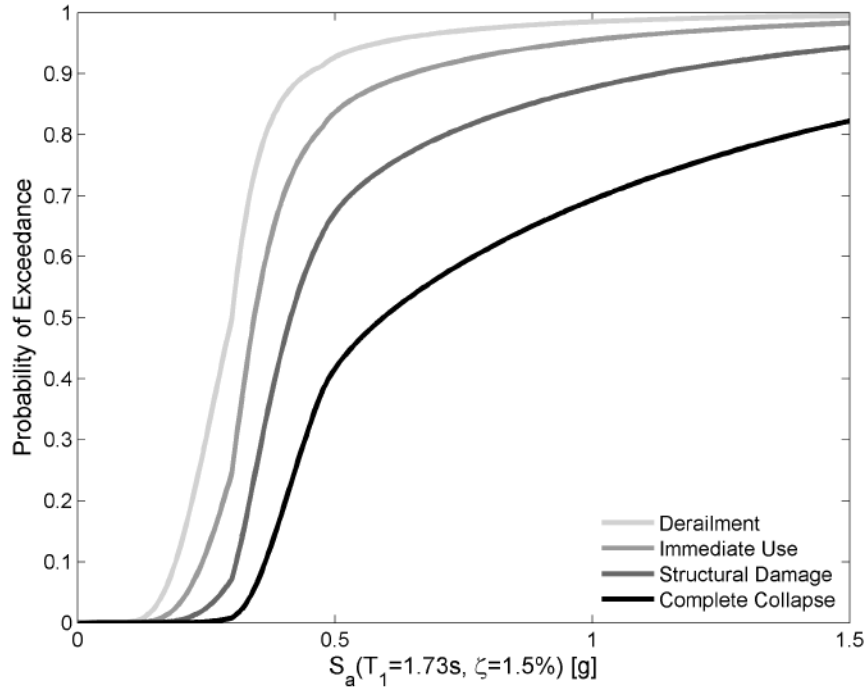


Figure 3.45 Fragility curves for LD50, assuming portal uplift theory seismic demand model. (Kosbab 2010)

By examining the fragility models above, it is easy to determine which cranes types are the most and least vulnerable to earthquakes. In order from low to high seismic vulnerability: J100, LD100, LD50. The aforementioned fragility curves were later compared to those calculated from scaled crane models (Jacobs 2010), and the agreement between the two was satisfactory.

3.4.4.4 Crane Repair Cost and Time

Repair costs and times for the cranes correspond to the damage unique to the crane. It is possible for the crane to remain undamaged but still be inoperable due to wharf damage involving the crane rails or collector trench. The crane specific damages are listed in Table 3.20 along with the mean repair costs and times. Additionally coefficients of variability are also listed with each mean to account for the uncertainties corresponding to these values. Repair costs and times for the cranes should be included within the total repair cost and time in addition to wharf damage.

Table 3.20 Crane Repair Costs and Time

Damage State	Cost (\$)	COV	Downtime (Days)	COV
Derailment	50,000	0.3	6	0.3
Immediate Use	300,000	0.5	10	0.5
Structural Damage	500,000	0.5	60	0.5
Complete Collapse	7,000,000	0.3	330	0.3

3.4.4.5 Operational Status of the Cranes

Crane operational status is binary in nature: the crane is operational, or it is not. However, as previously discussed, crane damage alone will not determine the operational status. Cranes cannot operate independent of the wharf, so the damage state of the wharf must also be taken into consideration. For instance, the crane damage state could be that of immediate use, but if a significant relative displacement between the crane rail and the collector trench has cut off the power to the crane, it cannot operate. Another scenario might include that the crane has derailed, but the berth segments on which it operates are severely damaged. Experience has shown that the most common form of crane damage is derailment, and that type of damage takes approximately 6 days to repair. However, if the berth is severely damaged, repair could take weeks, so even after the crane is operational, it could not be utilized. Both of these situations illustrate this interdependence, however in the operational model, the locations/ interdependence between the wharf and crane will not be taken into consideration. The operational status of each will instead be considered independent. For instance, if 1/3 of a wharf is unusable, but all of the cranes are functioning, it is assumed that every crane will be available for use on the usable 2/3 of the wharf despite the fact that in real life, this scenario might not always be true.

3.4.4.6 Crane Damping

It should be noted that the damping ratio of the spectral acceleration used to calculate the crane fragility curves and the damping ratio of the spectral acceleration used as an intensity measure within the risk analysis program differ. A period of 1.55 seconds and a ratio of 1.5% were used to calculate the fragility curves while a period of 1.5 s and a ratio of 5% were used as the intensity measure within the program. This change had to be made so that the spectral acceleration values could be used within the ground motion prediction equations that require damping ratios of 5%. The following equation from Newmark and Hall (1982) calculates a damping correction factor that is used within the risk analysis calculation of repair requirements to account for this difference:

$$dcf = 1.40 - 0.25 * \log(damping\ ratio\ \%)$$

3.5 System Fragility

The goal of the port operations models developed for this project is to simulate port operations decision-making by terminal operators during periods of disruption in port infrastructure. This simulation will then be used to estimate the port performance metric: container throughput. Inputs into the port operations model not only include the operational status of each of the port terminals, but also an estimation of the ship arrival schedule of the port along with the number of TEUs handled for each arriving ship. Containers that cannot be handled as throughput at the port will be counted within the business interruption loss (BIL) at the port.

3.5.1 Ship Arrival Schedule

The inputs to the port operations model include the day-by-day, port-wide system damage state and the schedule of arriving ships within the period of time beginning at the earthquake occurrence through the time when normal port operations are restored (i.e., when all of the damaged infrastructure is repaired). Ship arrivals for the hypothetical

port during this period were estimated using actual ship arrival and departure logs from March-August of 2008 for the Port of Los Angeles (POLA) and the Port of Long Beach (POLB) (Marine Exchange of Southern California 2008). The Marine Exchange of Southern California (MXSOCAL) data can be found in Appendix C. The logs for this data include 14 terminals, seven from POLA and seven from POLB. Table 3.21 lists each terminal name, the number of associated berths, the length of the terminal, the mean number of ships using that terminal per day, and the standard deviation of ships per day obtained from these logs. Location of the terminals can be determined by looking at the berth numbers. POLA terminals have numbered berths, whereas POLB berths are both lettered and numbered.

Table 3.21 Terminal Data from the Port of Los Angeles and the Port of Long Beach from March-August of 2008.

Terminal Name	Berths	Length (m)	Mean Ships/Day	σ Ships/Day
West Basin Container Terminal 1	100	365.76	0.124	0.323
West Basin Container Terminal 2	121-131	1066.8	0.366	0.545
TraPac	135-139	1234.44	0.319	0.466
Yusen	212-225	1767.84	0.422	0.593
Seaside	226-236	1432.56	0.665	0.603
APL	302-305	1219.2	0.67	0.746
APM	401-406	2191.51	1.108	0.863
SSA Terminal 1	A88-A96	1097.28	0.476	0.633
SSA Terminal 2	C60-C62	548.64	0.216	0.412
California United	E24-E26	640.08	0.135	0.342
Long Beach Container Terminal	F6-F10	838.2	0.141	0.347
International Transportation Service	G226-G236	1944.32	0.541	0.624
Pacific Container	J243-J270	1798.32	1.157	0.971
Total Terminals International	T132-T140	1524	0.757	0.87

In all, 1230 ships were logged at all terminals during this 5-month period. It has been assumed that ship arrivals are a Poisson process (Kia et al. 2000; Kia et al. 2002; Kuo et al. 2006). To check this hypothesis, a goodness of fit test was performed on the inter-arrival times (time in between each consecutive ship arrival) of ships within the two

ports. If ship arrivals are a Poisson process, then the inter-arrival times should be exponentially distributed.

A goodness of fit test was conducted on terminal inter-arrival times for both POLA and POLB. A two-sample Kolmogorov-Smirnov (K-S) test was used to compare frequencies of inter-arrival times from the port data to the expected frequencies of inter-arrival times for an exponential distribution. The null hypothesis for the test asserted that the two samples were from the same continuous distribution, and were tested to a 5% significance level. If the calculated p-value, or the probability of the MXSOCAL test statistic being at least as extreme as the one calculated using the exponential distribution, fell below 0.05, the null hypothesis would be rejected. Figure 3.46 and Figure 3.47 show the histograms scaled to a probability of occurrence and the overlying exponential distribution for each port. Results from the two-sample K-S tests can be found in Table 3.22.

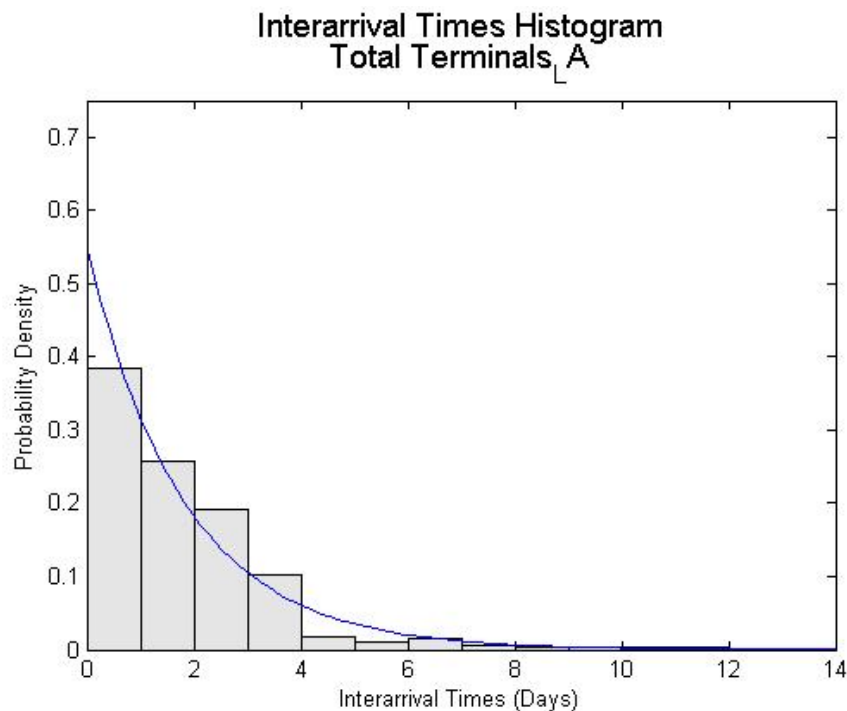


Figure 3.46 Port of Los Angeles Inter-arrival Time Distribution

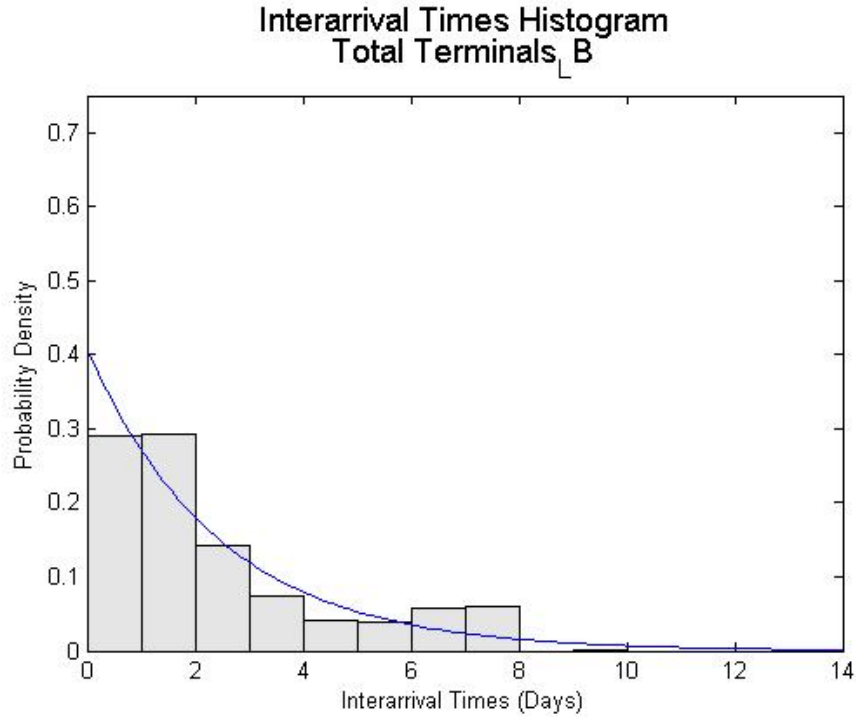


Figure 3.47 Port of Long Beach Inter-arrival Time Distribution

Table 3.22 K-S Test Results

Terminal	p-Value	KS rejected at 5%?
Port of LA	0.9971	No
Port of LB	0.2672	No
All terminals	0.8622	No

The results in Table 3.22 show that for K-S tests done for POLA and POLB, and for every terminal in the MXSOCAL data combined, none were rejected at a 5% significance level. It is apparent from the table that POLA showed a much better fit than POLB. The p-value of the POLA data is significantly higher than the p-value of the POLB data. This better fit is also apparent in the figures themselves. Despite the lower p-value for the POLB data, the combined data still has a relatively high p-value, so it is safe to assume

that inter-arrival times can be assumed to be exponential, and therefore ship arrivals can be modeled using a Poisson distribution.

Since ship arrivals can be modeled as a Poisson process, in the context of the hypothetical port, ship arrivals will be estimated as such. Ship arrivals will be generated randomly using a Poisson distribution with a mean value based on the total berth length at each of the terminals. For the shipping data collected, berth lengths and mean ship arrivals/day correlated, so they were plotted and a linear fit of the data was calculated. Since five months of data was available, the linear fit was improved by weighting data points so that those terminals that were most frequently used, received a greater weight within the linear regression model than those less frequently used. Figure 3.48 shows a comparison of the two linear models. The red line is the weighted model, and the blue line is the un-weighted model.

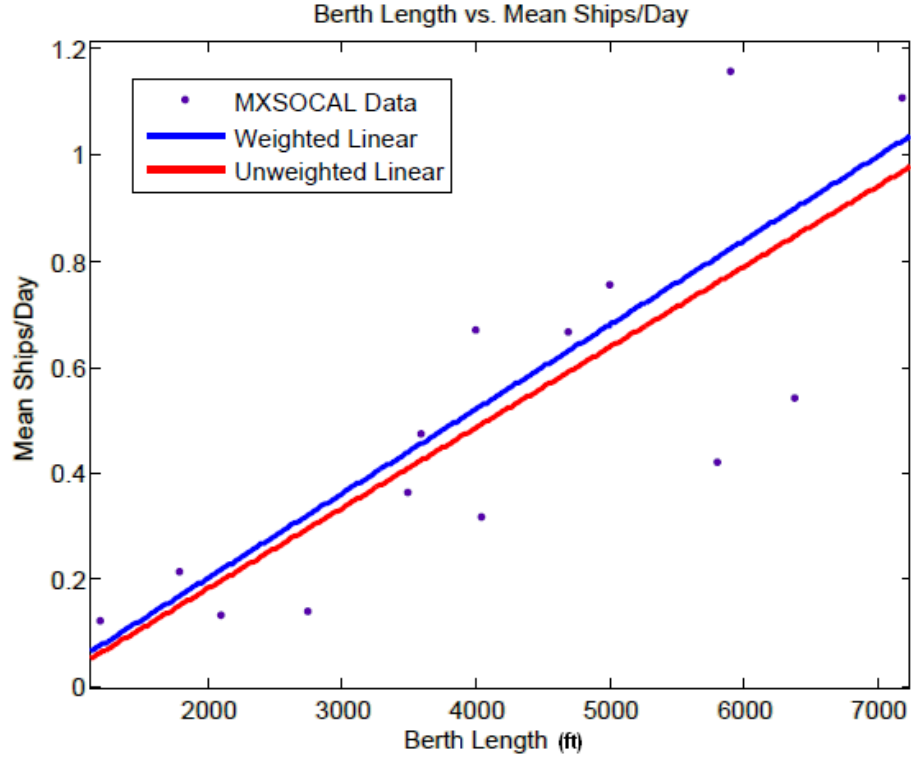


Figure 3.48 Linear Regression Models: Weighted (blue) vs. Un-weighted (red)

The formula for the linear regression model to be used in the context of this project is the weighted regression model: $f(x) = 0.000518x - 0.1124$, where $f(x)$ is the mean ships per day and x is the berth length in feet. The correlation coefficient of the fit of this equation to the MXSOCAL data is equal to 0.79. Inter-arrival times at the hypothetical port will be sampled over an exponential distribution using the inverse of the weighted regression model as the mean inter-arrival time (in days):

$$\text{mean inter-arrival time: } t_{\text{mia}} = 25087 * x^{-1.119} \quad (3.22)$$

Ships that enter the port will get ship data (length, total TEUs, etc.) from a random sampling of the MXSOCAL list. Random sampling of the ship log is possible because no correlation was found between berth length and ship length or berth length and TEU capacity (see Figure 3.49 and Figure 3.50), so it is possible that any of the ships within the shipping log could dock at any of the hypothetical berths.

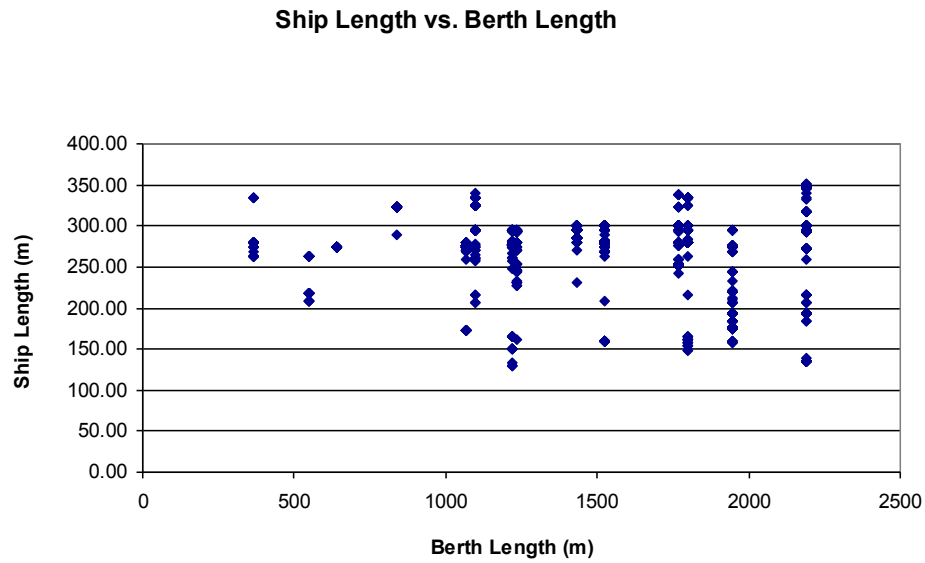


Figure 3.49 Berth length vs. ship length.

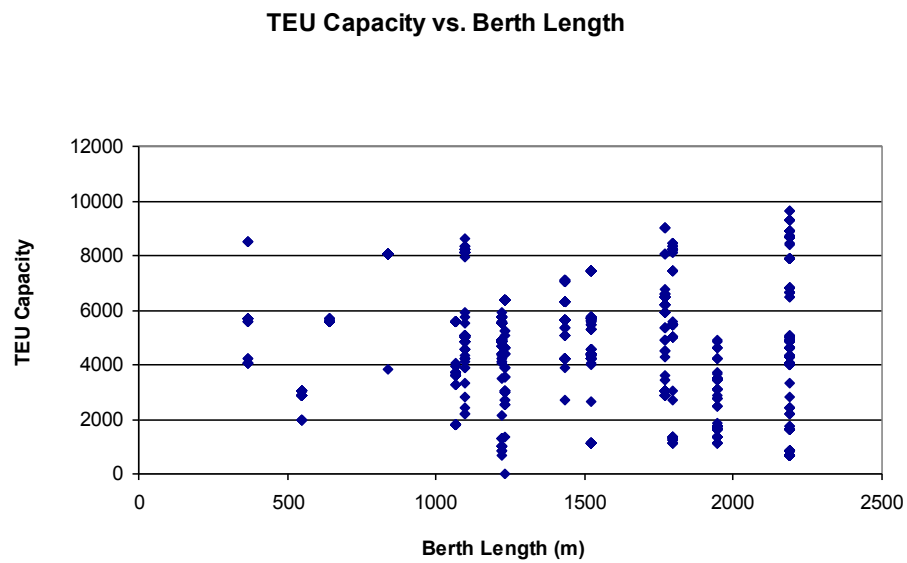


Figure 3.50 Berth length vs. TEU Capacity.

Table 3.23 shows a sample arrival stream for the port in the first 100 days after an earthquake. The data listed (decimal day after the earthquake, ship length, and TEUs loaded/unloaded) is used later in the operational model to schedule berths and cranes.

Details on how to calculate the number of TEUs loaded and unloaded can be found in 3.5.2.

Table 3.23 Arrival Stream for the First 100 Days after an Earthquake

Day	Ship Length (ft)	TEUs Loaded and Unloaded
0.39	961.66	9072
1.36	925.29	5775
2.51	904.62	5102
5.93	904.62	5161
7.33	964.65	4020
7.38	881.66	6179
12.19	1109.20	10429
16.04	983.67	9537
19.51	964.71	6936
23.62	1065.34	12680
24.07	958.74	3608
24.59	925.29	5123
25.81	824.92	2274
27.61	863.39	5794
30.53	958.25	6264
35.56	964.71	7544
40.39	520.70	1481
47.65	964.71	6701
50.41	958.02	4285
53.02	1138.09	9828
60.29	964.32	4528
66.58	925.29	3569
69.39	958.15	3692
72.32	964.35	4215
73.88	984.13	11157
74.96	1059.11	9078
78.67	964.68	6666
79.36	1134.88	8402
86.63	964.65	5915
93.89	964.68	6265
95.39	917.09	3938
95.69	1138.16	10024
96.04	711.76	4349

3.5.2 Arriving Ship Data

Once the arrival estimate determines how many ships will call at the port, the operational model requires an estimation of the amount of cargo unloaded from and loaded on to

each ship. The TEU capacity for each ship was provided while load/unload data was not provided per ship within the MXSOCAL data. However, monthly load / unload port totals were available via the individual port websites. From this data, ratios of the loaded or unloaded cargo vs. total TEU capacity (calculated by summing TEU ship capacities per month) was determined for the months in which the shipping log was monitored (See Appendix C). The total TEUs loaded and unloaded onto ships were estimated using ratios of total monthly TEUs loaded or unloaded vs. the sum of the TEU capacities over each month that the shipping log was monitored (Port of Long Beach 2010; Port of Los Angeles 2010).

Table 3.24 TEU Statistics by month.

Month	In Total (TEUs)	Out Total (TEUs)	Total (TEUs)	# of Ships	Total Capacity (TEUs)	In Total/ Capacity	Out Total/ Capacity	Total/ Capacity
March	529,526	552,421	1,081,947	196	954,013	0.56	0.58	1.13
April	612,394	549,658	1,162,051	196	940,731	0.65	0.58	1.24
May	644,168	571,691	1,215,859	205	1,082,264	0.60	0.53	1.12
June	635,131	576,825	1,211,955	192	987,618	0.64	0.58	1.23
July	649,296	612,566	1,261,862	223	1,104,344	0.59	0.55	1.14
August	691,410	637,915	1,329,325	218	1,139,703	0.61	0.56	1.17

Total	Mean		
6,208,673	0.61	0.57	1.17

The five-month shipping log was sampled using a Poisson distribution to obtain the arriving ship stream and the total TEU capacities for the arriving ships were used to calculate the total TEUs loaded and unloaded by applying the mean in/out ratios to the sampled TEU capacities to calculate the total TEUs loaded and unloaded from each incoming ship.

For example, assume that the following ship was sampled from the MXSOCAL data:

Table 3.25 Example Sampled Ship

Vessel Name	Length (m)	Beam (m)	TEU Capacity	Berth
Xin Yan Tai	279.60	40.30	5668	100

The TEUs loaded and unloaded from this ship would be calculated using the following methods:

Unloaded (rounded to the nearest integer TEU):

$$\frac{Unloaded}{TEU\ Capacity} = 0.61, \quad Unloaded = TEU\ Capacity * 0.61 = 5668 * 0.61 = 3457$$

Loaded (rounded to the nearest integer TEU):

$$\frac{Loaded}{TEU\ Capacity} = 0.57, \quad Loaded = TEU\ Capacity * 0.57 = 5668 * 0.57 = 3231$$

So then the total TEUs loaded/unloaded = 3457+3231 = 6688.

3.5.3 Berth and Quay Crane Scheduling Program

Once the number of ships arriving per day is determined, those ships will need to be assigned to a berth within the port, and assigned cranes that will unload the cargo. In current practice (Pachakis and Kiremidjian 2004; Canonaco et al. 2007; Bierwirth and Meisel 2009), berth scheduling and crane assignment is often treated as a sequential problem. First terminal operators determine the berth assignment based on berthing durations of each vessel. Next, cranes are assigned to vessels depending on the number of ships docked simultaneously at each berth. This practice for assignment can cause delays because once a ship is assigned to a berth, the number of cranes for use is finite. For this project, a method for simultaneous berth and crane scheduling was developed to prevent this crane limitation and to utilize all of the information available to port operators when scheduling cranes and berths within the port (Ak, 2008 and Lin, 2011).

In the assignment model, the berths within the ports are considered continuous structures having B equally sized sections and Q identical cranes operating along a single set of crane rails. The length of each ship docking at a berth is divided into a number holds that consists of three or four container rows. Berth section lengths are also equal to hold lengths. It is assumed that multiple ships may dock at a berth and be serviced simultaneously. Cranes may only service one hold at a time, but multiple cranes can be assigned to the same ship. Each hold requires a certain processing time for loading / unloading and a ship remains at the berth until all of the unloading / loading is finished for each ship. Furthermore it is assumed that once a ship had docked at a berth, it must remain at its original position on the berth until processing is complete. Under these assumptions, the assignment model seeks to assign cranes in a manner that minimizes the time ships spend docked at the berth and the cost associated with servicing each vessel.

The following example illustrates how crane allocation can minimize the time ships spend docked at a berth. Suppose that 3 ships have been assigned to the berth (length = 7 holds) in Figure 3.51 in the following sequence: yellow, orange, red. The yellow ship has three holds that will take 4, 0, and 2 time periods to unload respectively, the orange ship has three holds that will take 3, 3, and 2 time periods to unload respectively, and the red ship has four holds that will take 5, 2, 3 and 4 time periods to load/unload respectively. Four cranes are available for use.

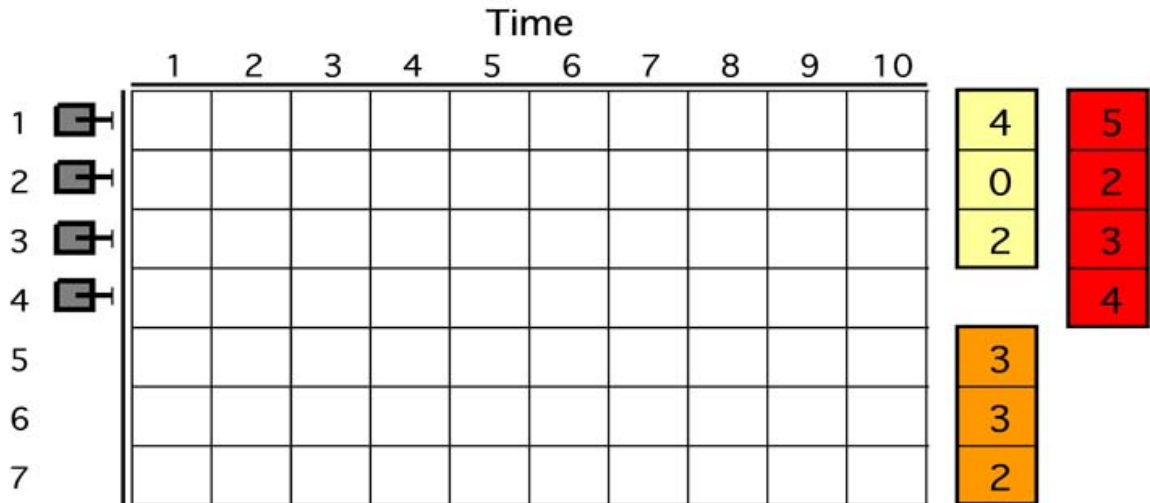


Figure 3.51 Crane allocation example: berth (from (Erera, 2008))

If cranes are assigned sequentially, cranes will be allocated to the yellow ship first, the orange ship second and the red ship last until all cargo has been loaded/unloaded. Using the time periods for loading/unloading, Figure 3.52 shows that the loading/unloading of all three ships will take a total of 9 time periods to complete.

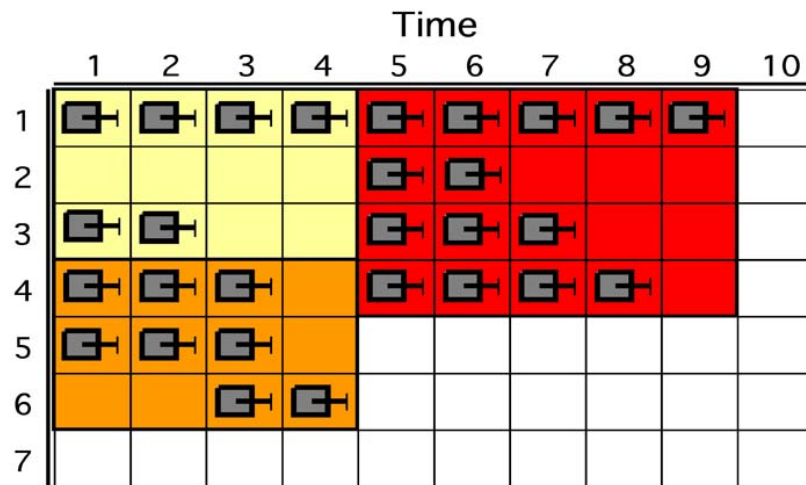


Figure 3.52 Crane allocation example: sequential assignments

However, by using the crane allocation proposed to minimize the time that ships spend docked at the berth (dwell time), the orange ship would be serviced first because it

would only take 3 time periods to finish. Once the orange ship is complete, the red ship would be serviced (Figure 3.53). The red ship begins servicing one time period prior to the start of servicing in the previous example, which results in one less time period overall to finish all three ships. This allocation is superior because it minimizes the dwell times of the ship, which in turn minimizes the cost assessed for ship servicing that is in direct proportion with the dwell times.

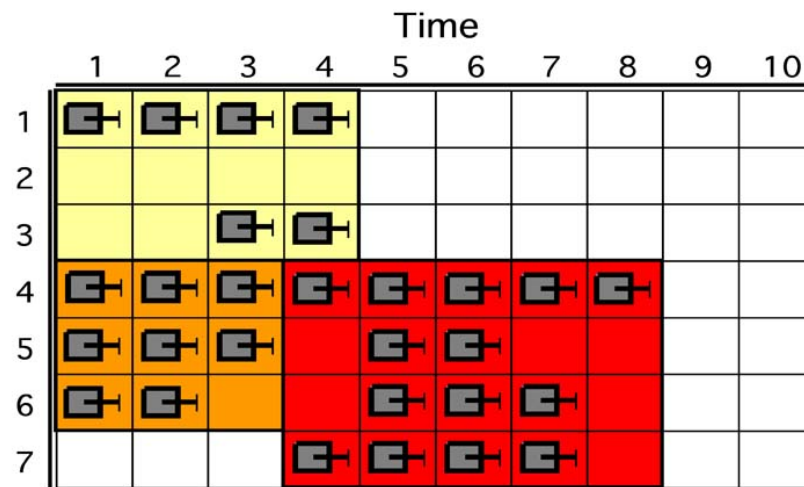


Figure 3.53 Crane allocation example: simultaneous berth and crane model assignment

3.5.3.1 Summary of Operational Modeling and Generated Statistics

In this study, an optimization-based heuristic scheduling technique (BQCSP) (Ak 2008) is used to mimic the post-earthquake operational decision-making of terminal operators. Within this technique, decisions are simulated regarding:

- (1) What arriving vessels may be turned away or will go another port
- (2) What times arriving vessels are berthed
- (3) Where they will be berthed within a particular terminal complex
- (4) Which cranes will be assigned to the vessels and when

The scheduling technique assigns post-earthquake available berth space and cranes to each ship scheduled to arrive at the port. Terminal operator decisions are mimicked since assignments maximize an objective function that balances the need to process containers quickly given available resources while avoiding excessive delay to any arriving vessels.

The technique also uses a rolling time horizon that considers the schedule of arriving vessels several days into the future; berth and crane assignments are updated daily based on the new information.

3.5.3.2 Example

The following example is meant to illustrate the full functionality of the BQCSP operational model. For this example, five different earthquake scenarios were input into the model that ranged from very little to very severe wharf and crane earthquake damage. Each scenario was applied to a single 3000-ft terminal containing five, 600-ft berth sections and six cranes. The earthquake scenario examined specifically in the next few figures is Earthquake 3, and corresponds to an earthquake that resulted in moderate wharf damage and limited crane damage (Figure 3.54). The $t = \#$ for each berth and crane corresponds to the number of days post-earthquake that it will take for that component to become fully operational. A value of $t = 0$ indicates that the component is fully operational zero days after the earthquake.

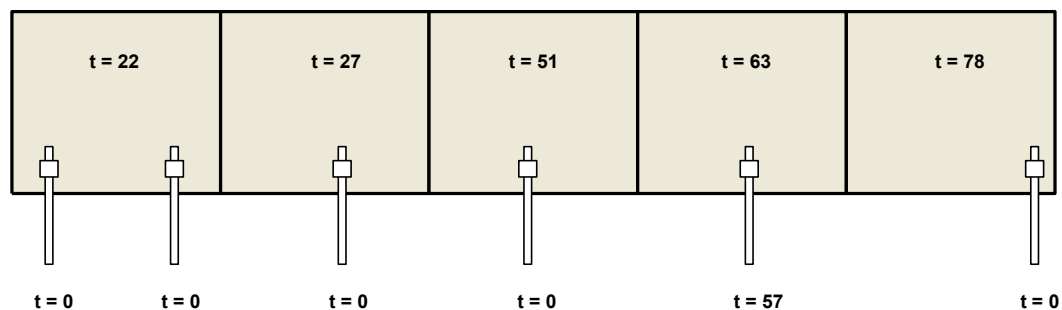


Figure 3.54 Wharf and crane repair times for example earthquake scenario

Repair information is used as input for the BQCSP operational model to assign berths and cranes over a length of time after the earthquake until the port is fully repaired and regains steady-state operations. The decisions made within the operational model are recorded in output files according to the day after the earthquake the decision was made.

Table 3.26 shows an excerpt of the first 31 days after Earthquake 3 and the decisions made within the operational model.

Table 3.26 Excerpt of Operational Modeling Statistics Output

Day	# of Displaced Ships	TEUs Lost	# of Ships That Will Berth	Total Dwell (days)	Total Delay (days)	TEUs Handled	Cranes Used per Day	Cranes Available per Day	Berth Feet Used per Day	Berth Feet Available per Day
1	1	9072	0	0	0	0	0	5	0	0
2	1	5775	0	0	0	0	0	5	0	0
3	1	5102	0	0	0	0	0	5	0	0
4	0	0	0	0	0	0	0	5	0	0
5	0	0	0	0	0	0	0	5	0	0
6	1	5161	0	0	0	0	0	5	0	0
7	0	0	0	0	0	0	0	5	0	0
8	2	10199	0	0	0	0	0	5	0	0
9	0	0	0	0	0	0	0	5	0	0
10	0	0	0	0	0	0	0	5	0	0
11	0	0	0	0	0	0	0	5	0	0
12	0	0	0	0	0	0	0	5	0	0
13	1	10429	0	0	0	0	0	5	0	0
14	0	0	0	0	0	0	0	5	0	0
15	0	0	0	0	0	0	0	5	0	0
16	0	0	0	0	0	0	0	5	0	0
17	1	9537	0	0	0	0	0	5	0	0
18	0	0	0	0	0	0	0	5	0	0
19	0	0	0	0	0	0	0	5	0	0
20	1	6936	0	0	0	0	0	5	0	0
21	0	0	0	0	0	0	0	5	0	0
22	0	0	0	0	0	0	0	5	0	0
23	0	0	0	0	0	0	0	5	0	600
24	0	0	0	0	0	0	0	5	0	600
25	2	8731	0	0	0	0	0	5	0	600
26	0	0	1	1.75	1.25	0	0	5	0	600
27	0	0	0	0	0	0	0	5	0	600
28	0	0	1	1.5	0	3920	5	5	1000	1200
29	0	0	0	0	0	3920	5	5	1000	1200
30	0	0	0	0	0	0	0	5	0	1200
31	0	0	1	1.5	0	2940	3.75	5	750	1200

The statistics recorded within the operational output are explained in greater detail below:

Day – Day refers to the day number after the earthquake. Also, it should be noted that for the purposes of crane and berth utilization within the port. One “day” is equal to four four-hour periods, or a 16-hour work day.

of Displaced Ships– Counts the number of ships within the arrival stream that cannot be accommodated at the port on a given day due to large delay times. For this example, ships will become displaced if the expected delay time is greater than 3 days.

of Ships that will Berth – Counts the number of ships that will berth on any given day.

Dwell – Calculates the total time the ship will remain in the port once it arrives

Total Delay – Calculates the delay time, or time in between when the ship arrives and when it is actually docked at a berth.

TEUs Handled – The total number of TEUs handled at the terminal for any given day.

Cranes used per day – Calculates the number of cranes used on any given day.

Note: each day is broken into four, 3-hour periods, cranes used per day is reflective of the number of cranes used in each period, divided by the total number of periods. Therefore, this statistic could have a decimal value.

Cranes Available per Day – Notes the number of cranes available to use for any given day.

Berth Feet used per Day – Notes the berth length occupied by a ship on any given day.

Berth Feet Available per Day – Notes the berth length available for occupation on any given day.

In examining Table 3.26 the BQCSP model made the decision to displace all ships until day 25, after which it began to allow ships to dock and began processing them. The statistical outputs resulting from these decisions and given in the table can then be used to calculate and plot various port performance metrics for the examined terminal. Subsequent figures display some of these possibilities: arrival and dwell time metrics, berth and crane utilization, number of ships displaced, and TEU handling metrics.

3.5.3.3 Arrival Stream

Figure 3.55 gives a visual representation of the full data set begun in Table 3.26: the number of ships berthed at the terminal each week post-earthquake, the total dwell time of ships during that same week, and the total number of days of delays experienced by ships for that week. Again, delay is the period of time between when the ship arrives and is berthed.

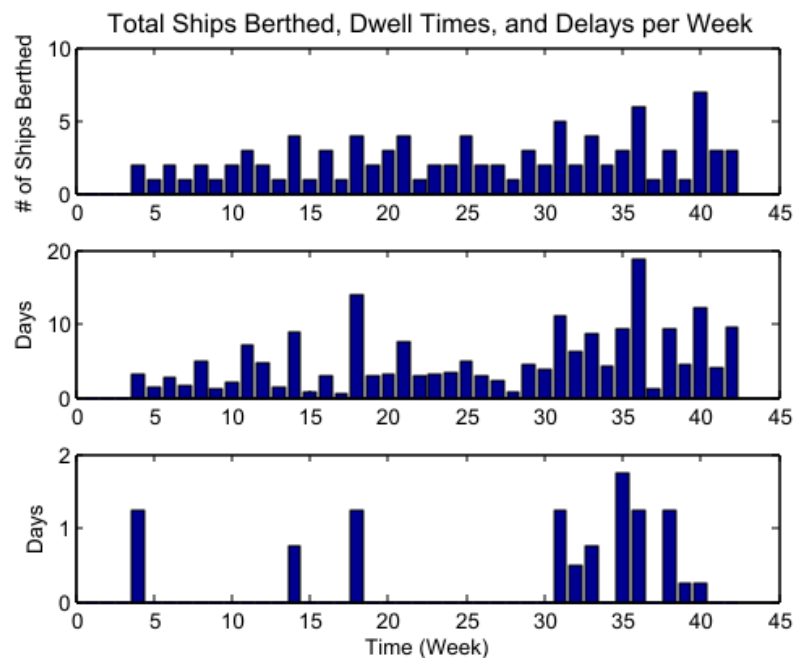


Figure 3.55 Ship Arrivals, Dwell Time, and Delays per week

3.5.3.4 Berth and Crane Utilization

Figure 3.56 shows the berth and crane utilization each week post-earthquake. Utilization was calculated as the ratio of used berth feet or cranes divided by the available berth feet or number of cranes respectively. Utilization equal to one indicates that every available berth-foot or crane was used for an entire week. In Figure 3.56 it should be noted that crane utilization rates are higher than the berth utilization rates. This indicates that for this terminal utilization is rate-limited by the number of cranes.

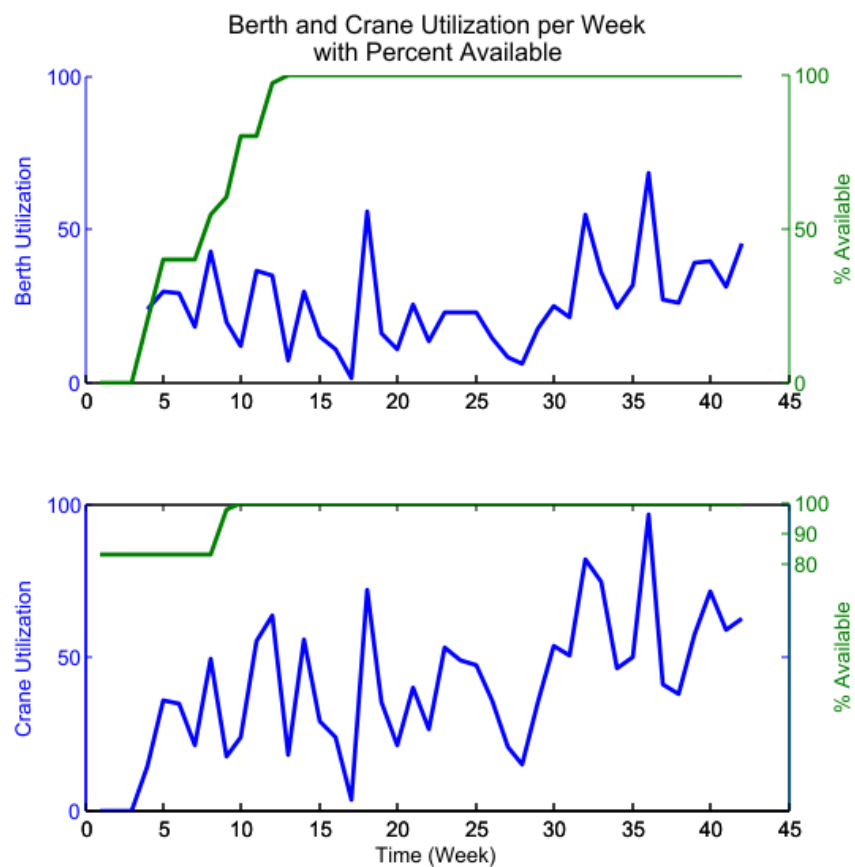


Figure 3.56 Berth and Crane Utilization per Week

3.5.3.5 Displaced Ships

After an earthquake event, if the terminal availability is so small that it cannot meet the demand of arriving ships, it becomes more economical for those ships to go to another port than to wait for an opening in the damaged port. This type of operational decision

was prevalent in the aftermath of the 1995 Kobe earthquake. Numerous ship operators had to set up operations in other ports because of the severe damage to some of Kobe's terminals. The same type of operational decision was captured within this example by assuming that if a ship would be delayed more than 3 days, it would become a displaced ship and seek out another port. Figure 3.57 shows the number and percent of displaced ships in the total ship population for each post-earthquake week.

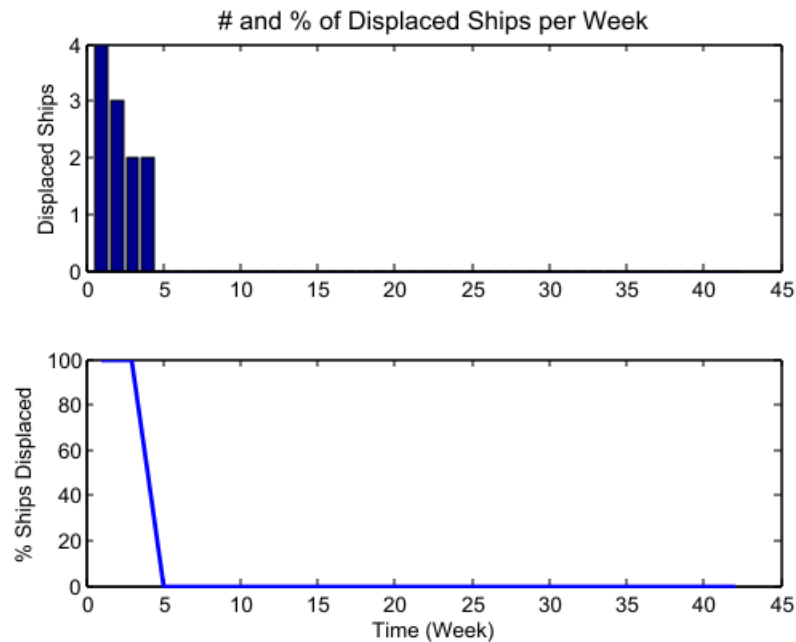


Figure 3.57 # and Percent of Displaced Ships per Week

3.5.3.6 TEU Statistics

The TEU statistics derived from this model are perhaps the most important in quantifying the losses sustained by ports after an earthquake. Figure 3.58 shows the total number of TEU handled by the port per week, the total number of TEUs lost per week, and the percent lost per week. Lost TEUs are calculated by summing the TEUs onboard displaced ships. When those ships do not use the port, it becomes a direct loss of income.

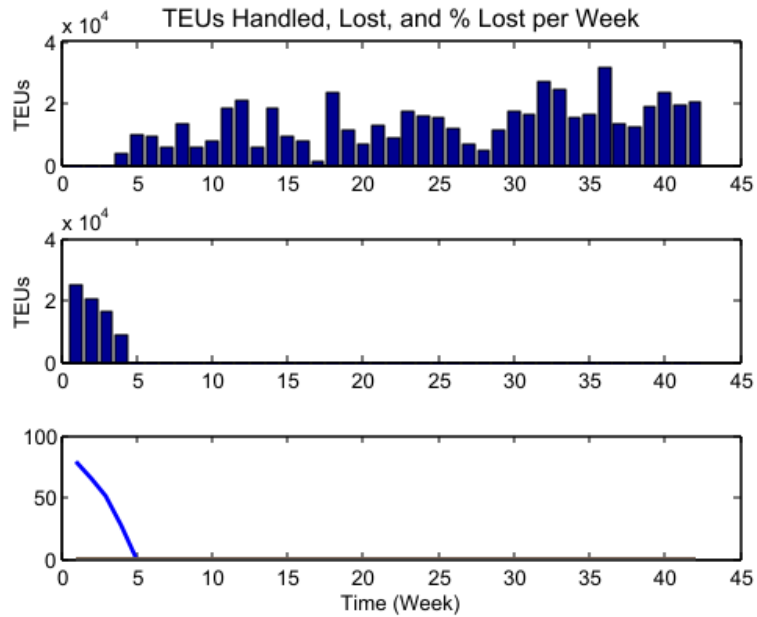


Figure 3.58 TEUs Handled, Lost and % Lost per week

3.5.4 Effect of Earthquake Disruption on Shipping Operations

Ultimately, the operational modeling was run with half-stopping criteria and a length limited by the repair period. Finalized statistics are found in Figure 3.59- Figure 3.63, and the number of weeks run in each scenario can be found in Table 3.27.

Table 3.27 Number of Weeks Each Earthquake Scenario Was Run

Earthquake	Repair Period (weeks)	Run Time (weeks)
1	0.71	2
2	4.87	5
3	11.14	12
4	11.71	12
5	48.86	50

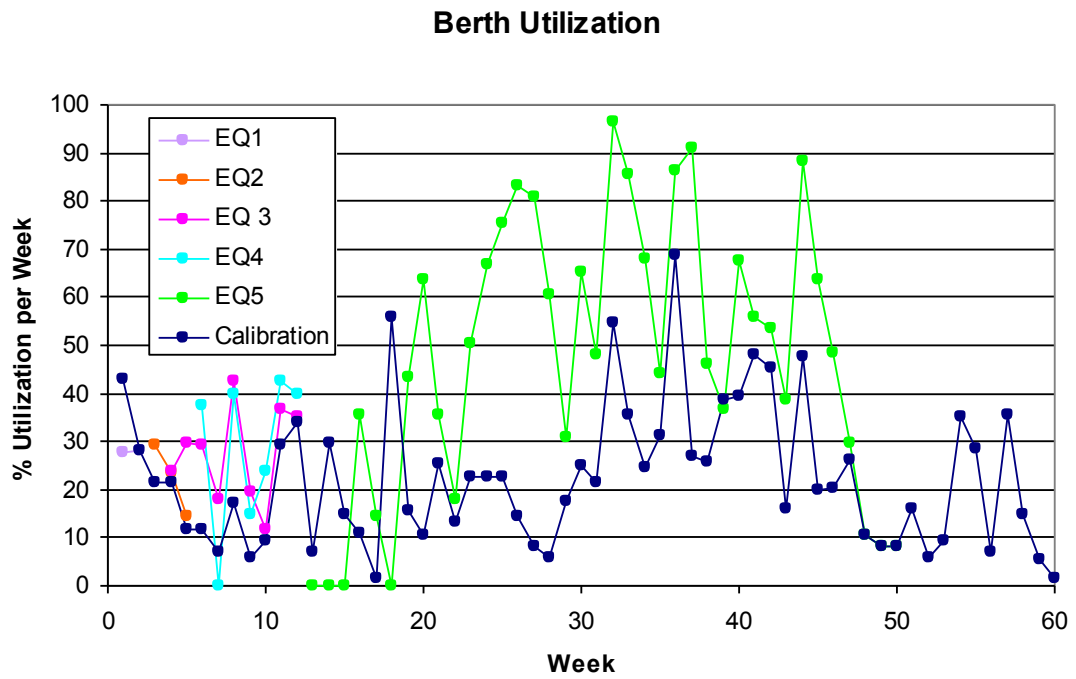


Figure 3.59 Final Berth Utilization Comparison of Earthquake Scenarios

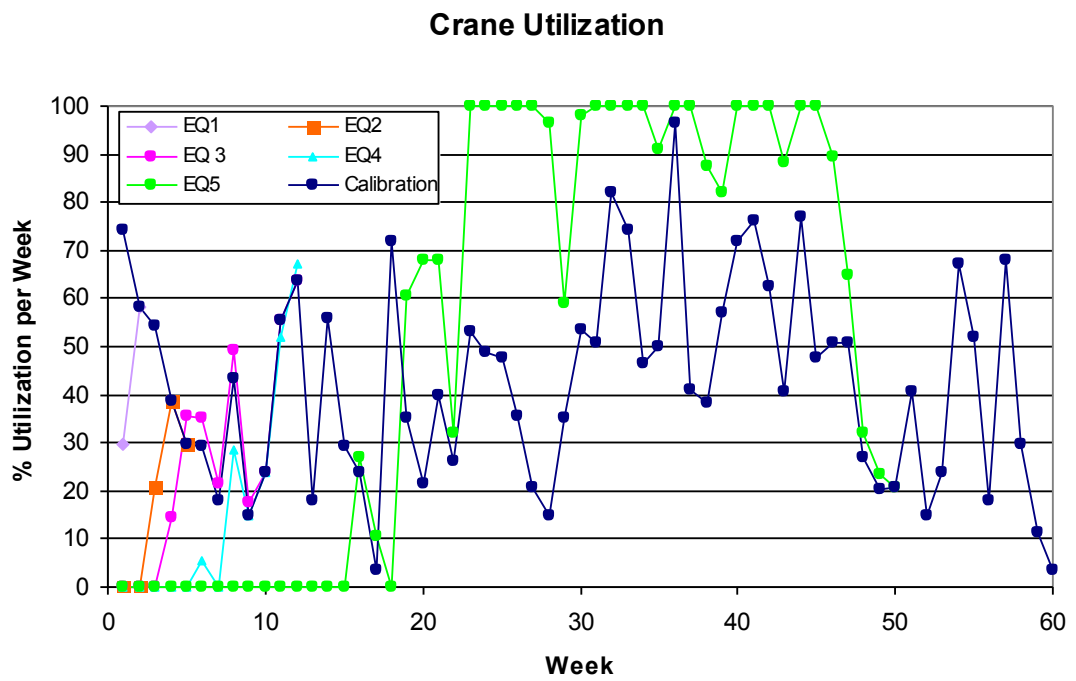


Figure 3.60 Final Crane Utilization Comparison of Earthquake Scenarios

Berth and crane utilization statistics offer insight into the trends of the other statistics because utilization depicts how the port is being used after the earthquake. In some cases what limited resources are available can accommodate the ships arriving at the port on the same scale as utilization during the calibration scenario. However at other points utilization increases dramatically because the port has limited resources to perform operational duties. For example, there are multiple instances within the crane utilization equal to 100% utilization. Here, every available crane is being used constantly for an entire week to keep up with the demand of incoming ships. When the berth utilization is compared at those weeks with 100% crane utilization, it is apparent that while high, berth utilization is never higher than the crane utilization. In fact, it is a general trend that crane utilization is consistently higher than berth utilization. This indicates that this particular port configuration is rate-limited by the cranes.

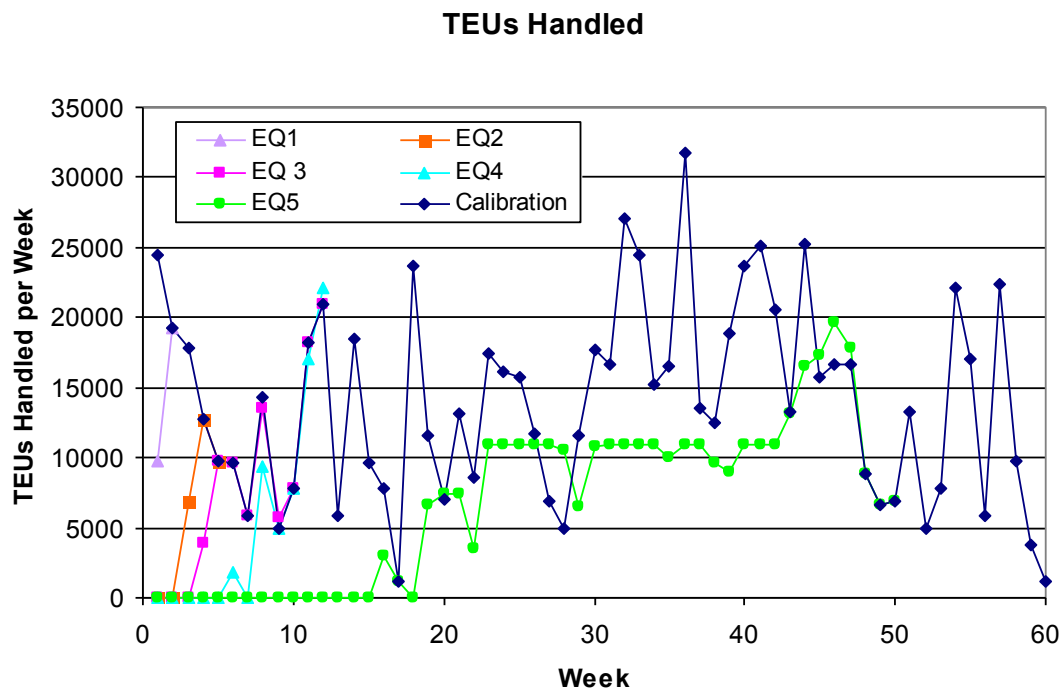


Figure 3.61 Final TEU Statistic Comparison of Earthquake Scenarios

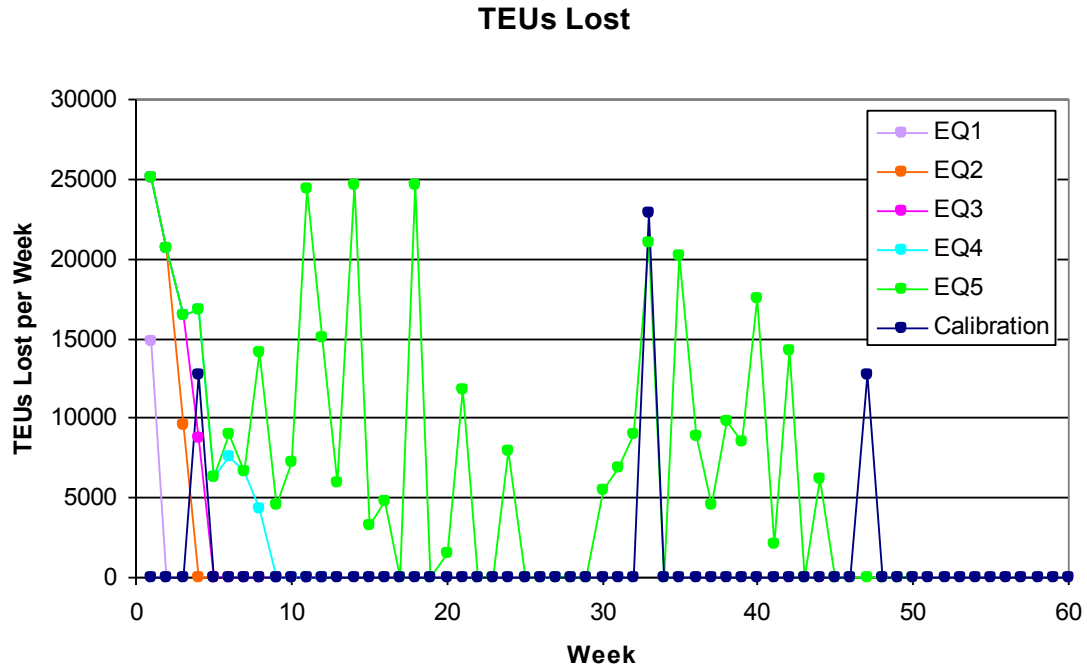


Figure 3.62 TEUs Lost Statistic Comparison of Earthquake Scenarios

Figure 3.61 clearly shows that for every earthquake scenario the number of TEUs handled is much lower than normal initially, but they eventually return to the calibration level. Obviously the initial damage and subsequent repair explains this trend. However, at some points (usually right before the earthquake run period ends), the TEUs handled during an earthquake scenario exceed those handled during normal operation (see EQ 5). This happens because the earthquake scenario has to catch up with the normal operation since there has been limited utilization during the earthquake scenario. For weeks 46-47 in EQ 5, where more TEUs are handled than in the calibration state, crane utilization is double (100%) during the earthquake than what it would be normally (50%). Therefore the port must catch-up despite the increase number of ships that get turned away during the time period (weeks 23-45) of increased utilization (See Figure 3.59). Initial increases in ship displacement seem normal, but the port is so heavily damaged by EQ 5 that resources are scarce and the port still can not meet demand even though all of its assets are being highly utilized.

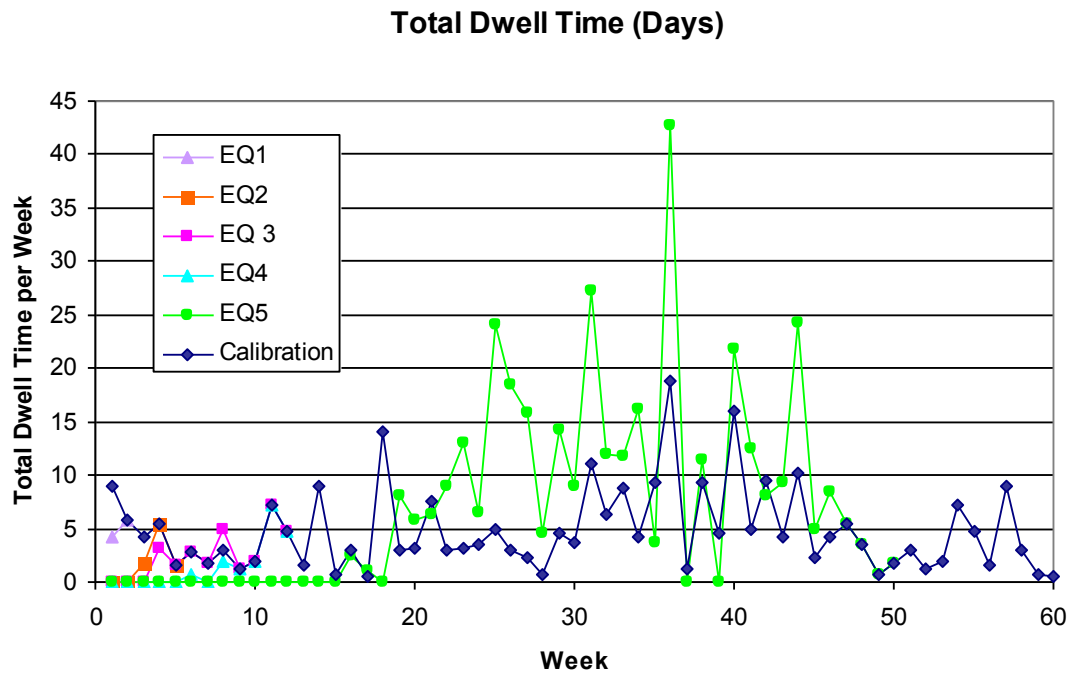


Figure 3.63 Final Total Dwell Time Statistic Comparison of Earthquake Scenarios

Dwell time reduces initially after an earthquake because many ships are displaced (Figure 3.63), and those that do come into the port can be processed quickly. However, as time passes, dwell times equal or exceed those found in normal operation. When dwell times are equal, it is likely that the available components can meet the demand. During these periods (the first few weeks) utilization is often higher than normal utilization, but that is due to the fact the every component is not yet repaired. Dwell times higher than normal indicate that the port is operational but not meeting demand. Examining EQ 5 provides a good example. Dwell times between weeks 20 – 46 are mostly greater than those found in the calibration scenario. This time period is the same as the period where utilization is significantly higher than normal (Figure 3.59), TEUs handled are lower than normal (Figure 3.61), and ships are consistently being displaced

(Figure 3.62). This trend is likely due to the fact that ships that aren't displaced are taking longer to load/unload because there is limited crane availability (see Figure 3.60).

3.6 Operational Modeling Using Regression

Several test runs were conducted using the BQCSP operational model for stratified samples of 2500 and 1000 earthquakes. However, computation time for these models was very lengthy (5+ days). Additionally, the number of samples within these models did not produce enough large earthquake samples to be stochastically representative at small mean rates of exceedance. To use the BQCSP model with the number earthquakes needed to accurately calculate small mean rates of exceedance would have required extremely long computation times. Therefore, an additional method was employed to reduce computation time of the operational model within the risk analysis framework. Using various port configurations and the thousands of earthquake occurrences run using the BQCSP model as data points, a multivariate linear regression equation was developed to replace the BQCSP model by using a number of independent variables to calculate the number of TEUs lost via a linear regression. In this analysis, the following earthquake scenarios were run using the BQCSP operational model to test the validity of using a multivariate regression equation to replace the BQCSP model:

Table 3.28 BQCSP Model Test Runs

Run	# of Earthquakes	Port Configuration
A	1000	Baseline Port Configuration
B	800	Baseline Port Configuration
C	800	Baseline, but with vertical drains at every terminal
D	1000	Baseline Port Configuration
E	1000	Baseline, but with vertical drains at every terminal
F	790	Baseline, but with only J100 type cranes
G	1000	Baseline, with repair min and max as output
H	1000	Baseline, with repair min and max as output
I	1000	Baseline, with repair min and max as output

It should be noted that the ship arrival stream and all other settings except those listed were the same for each run. In examining the data sets, TEU Losses ranged from 0 to over 1,000,000 TEUs. For the first linear regression equation applied to the data, the correlation was fairly good, but the equation yielded a y-intercept near 19,000 TEUs. The data set contained multiple instances where no TEUs were lost during earthquake occurrences. To accurately capture this result it was decided that the multivariate linear regression equation would only be used for instances when disruption caused TEU Loss (i.e. TEU Loss > 0). Therefore, a mixed distribution was employed where:

$$P[TEU > x] = (1 - P[TEU = 0]) * P[TEU > x | TEU > 0] \quad (3.23)$$

To find the probability of TEU Loss > 0, a probit model regression equation was calculated. In a probit model the dependent variable of the regression equation must be binary. For this case, instances where TEU Loss = 0 equaled zero, and instances where TEU Loss > 0 equaled one. The independent variables tested within the regression equation used to determine whether TEU Loss would be greater than zero were: the

minimum and maximum wharf repair times (t_{Wmin} and t_{Wmax}), minimum and maximum crane repair time (t_{Cmin} and t_{Cmax}), terminal length (x_T), and number of cranes (N_C). P values for the coefficients of the independent variables revealed that max and min crane repair time was not statistically significant in calculating the probability that TEU Loss > 0, so they were omitted as independent variables in the final probit regression calculation:

$$P[TEU > 0] = -7.8391 + 0.0054(x_T) + 1.7001(\ln(t_{Wmin})) + 0.9818(\ln(t_{Wmax})) - 2.1995(N_C) \quad (3.24)$$

The coefficients were calculated using the combined data from Runs G, H, and I. A further discussion of that choice and the residuals for the probit regression equation is located in 3.6.1.1.

Figure illustrates a cumulative distribution function generated using $P[TEU \text{ Loss} > 0]$ values calculated from a “modified” probit regression equation where only the wharf repair time data from runs G, H, and I are considered. The cdf is calculated using the $\ln(t_W)$ since wharf repair time is the most dominant variable in the probit regression, and the actual failure (0) or success (1) of TEU Loss > 0 of the ABD data is plotted for each earthquake instance:

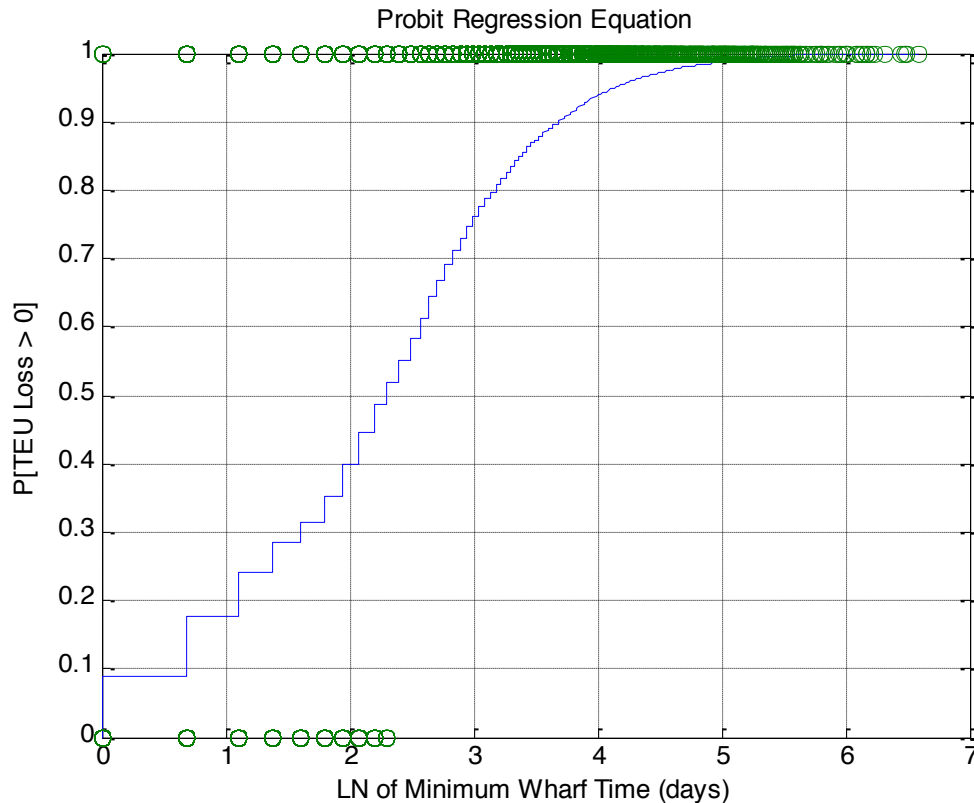


Figure 3.64 – Probit Regression Equation for Combination of Runs G, H, and I

When the TEU losses don't equal zero, they will be calculated using a multivariate linear regression equation. The independent variables within this regression were modeled after the BQCSP operational model, which uses wharf repair times, crane repair times, and terminal data (# of berths, # of cranes) as input to calculate TEU Losses. Specifically, the linear regression equation uses berth length, the maximum and minimum $\ln(\text{wharf time})$, maximum and minimum crane time, and number of cranes as independent variables, and the $\ln(\text{TEU Loss})$ as the dependent variable. The natural log of min/max wharf time and TEU Loss was used because TEU Loss and wharf time have a distinct logarithmic correlation (Figure 3.65). In addition, for the p-values of the coefficients calculated, wharf times consistently had the smallest p-values for every single run

conducted. Since it was the most influential independent variable, the logarithmic correlation was considered within the regression:

$$TEU\ Loss = e^{(6.4332+0.6881*\ln(T_{W\ min})+0.03547*\ln(T_{W\ max})+0.0007*x_T+0.00250*t_{C\ min}+0.0.0007*t_{C\ max}-0.2230*N_C)} \quad (3.25)$$

and the correlation results for equation 4.7 can be found in Table 3.29.

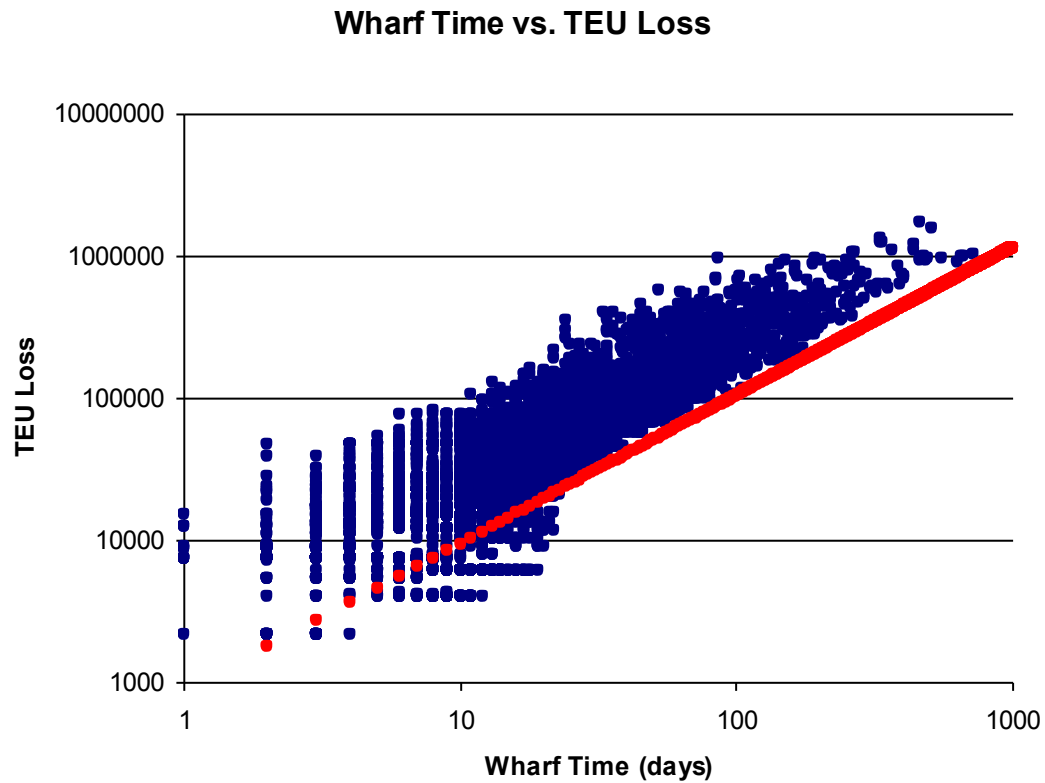


Figure 3.65 Wharf Time vs. TEU Loss

Table 3.29 – Multivariate Regression Results

		GHI
Correlation	R ²	0.79
	Error	0.49
	P-values >0.05	no

As with the probit regression equation, the final results for the multivariate regression equation are also a combination of Runs G, H, and I. Calculation of TEU Loss is predominantly a function of the wharf repair time, which consistently had the smallest

p-value in every single run. Crane repair time was the least influential independent variable and in three of the smaller runs could not be considered statistically significant. However, the p-values in these runs though > 0.05 were still relatively small, and therefore crane repair time was still used as an independent variable in the calculation of TEU Loss.

3.6.1.1 Run GHI Residuals and Comparison of Runs

For the nine runs of BQCSP data tested, all runs produced similar coefficients despite the port configuration differences. The data using vertical drains or upgraded cranes obviously produced different TEU losses, but the calculation of those losses from the examined independent variables produced similar coefficients to the baseline runs A, B, and D. For runs A-F, coefficient of determination (R^2) values ranged from 0.71-0.79 and error values were also quite similar.

In comparing all of the runs, the greatest increase in correlation between the dependent and independent variables occurred in runs G, H, and I when the minimum wharf and crane repair times were used as independent variables in addition to the maximum wharf and crane repair times. The combination of the baseline runs G, H, and I was chosen as the final data set from which to calculate the regression equations because previous runs had proved that port configuration was not an influencing factor, and the sample provided a large number of data points as well as the min and max wharf and crane repair times (Table 3.30).

Table 3.30 – Comparison of Correlations for Runs ABD and GHI

Run	ABD	GHI
Multivariate Regression Analysis		
R ² (Coefficient of Determination)	0.71	0.79
Error	0.58	0.49
Probit Regression Analysis		
sfit (Dispersion Parameter)	5.623	1.075

To further examine the correlation of the probit and multivariate regression equations, plots of the residuals for the 3057 earthquake sample in GHI are shown in Figure 3.66 and Figure 3.67. First the residuals for the probit regression equation are plotted in Figure 3.66.

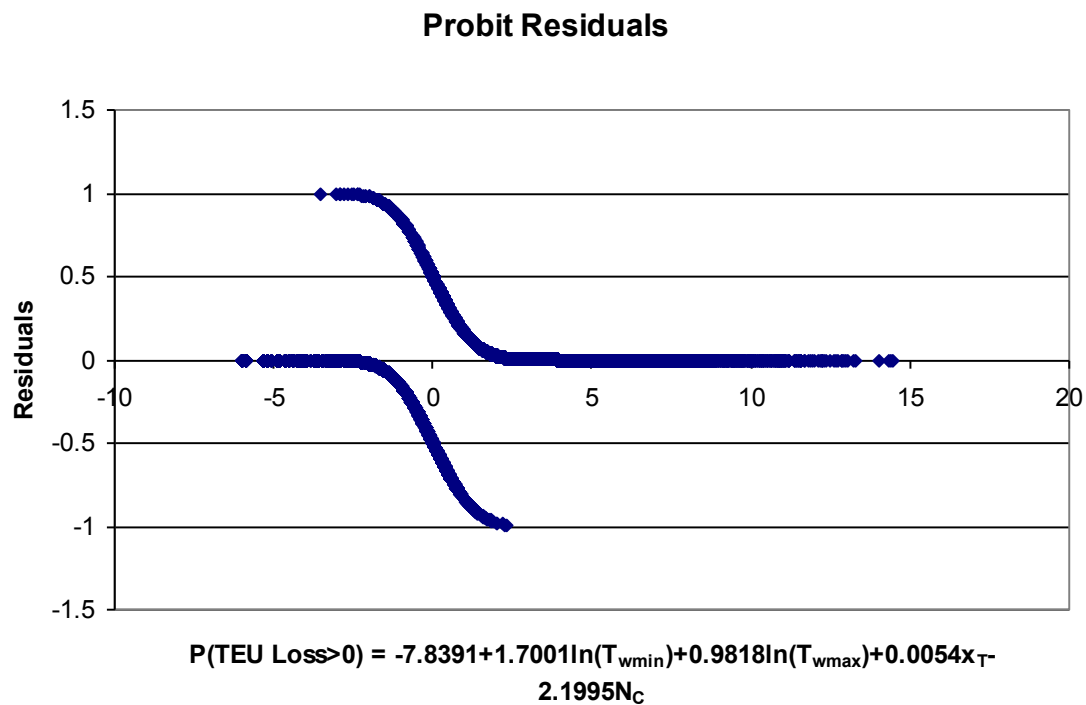
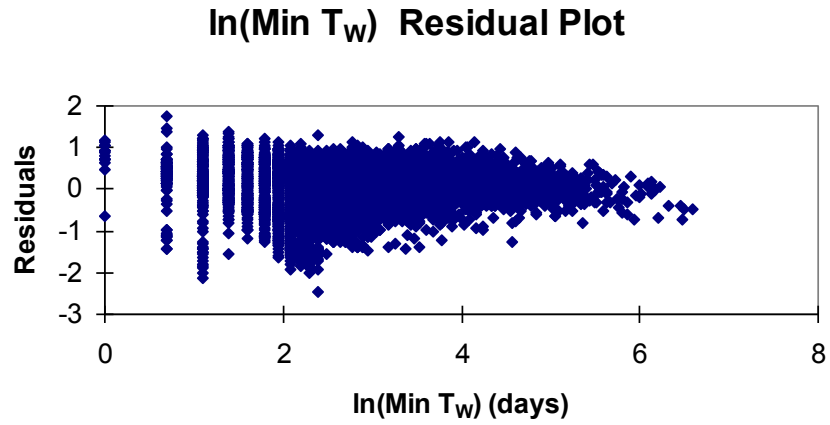


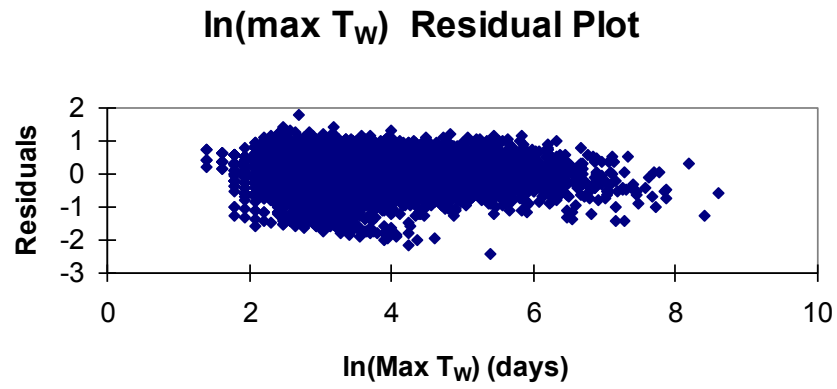
Figure 3.66 – Plot of Residuals for Probit Regression Equation

Residuals for each of the independent variables in the multivariate regression equation to determine TEU loss are shown in Figure 3.67. Notice that each has a small range from -3 to 2.

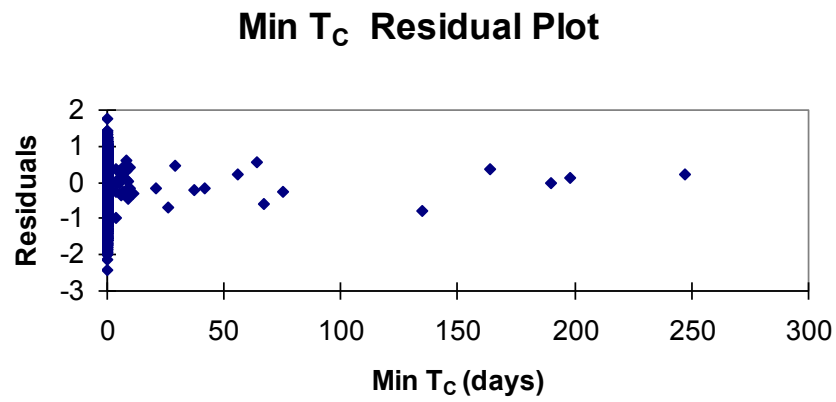
a.)



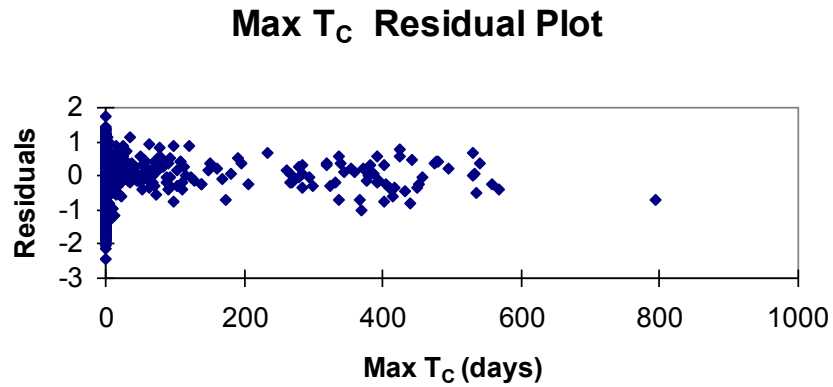
b.)



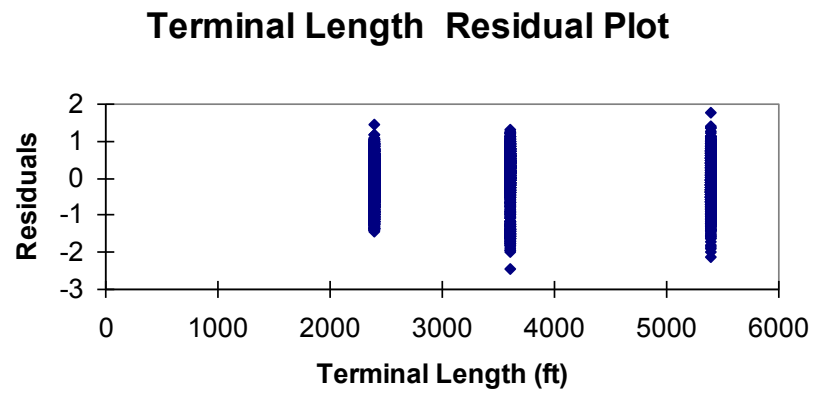
c.)



d.)



e.)



f.)

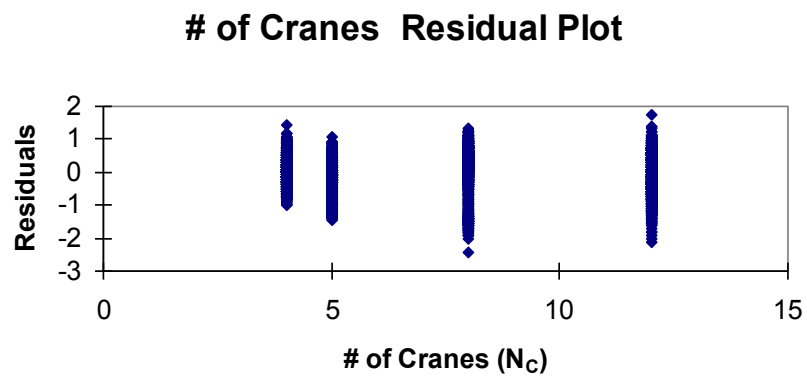


Figure 3.67 – Residual Plots for Multivariate Regression Equation Variables

3.6.1.2 Operational Regression Model with the Risk Analysis Program

Within the program the calculated operational regression model from the data in runs G, H, and I is implemented in the following context: First the probability that TEU Loss > 0 is calculated by taking the normal cumulative distribution function of the probit regression equation for the combination of Runs G, H, and I:

$$P[TEULoss > 0] = \Phi(-7.8391 + 0.0054(x_T) + 1.7001(\ln(t_{W_{min}})) + 0.9818(\ln(t_{W_{max}})) - 2.1995(N_C)) \quad (3.26)$$

A binary random number is generated from a binomial distribution based on the probability that TEU Loss > 0. If the random number generated equals 0, TEU Loss = 0. If the random number generated equals one, the TEU Loss = e^x , where x is calculated by sampling from a lognormal distribution of TEU Losses where the mean equals the TEU Loss calculated from the multivariate regression with coefficients corresponding to those found in Run ABD, and the logarithmic standard deviation equals the standard error (0.49) associated with the calculation of the regression equation:

$$\bar{x} = 6.433 + 0.688 * \ln(t_{W_{min}}) + 0.356 * \ln(t_{W_{max}}) + 0.0007 * x_T + 0.0025(t_{C_{min}}) + 0.0007(t_{C_{max}}) - 0.223(N_C) \quad (3.27)$$

3.6.2 Calculation of Business Interruption Losses

Business interruption losses should be calculated from the number of TEUs lost from the either the BQCSP or operational regression model. The cost per TEU may be estimated for each terminal within the port using financial information such as the revenue derived by the port and terminal operator for each TEU. Each of these cost values were discussed with port officials (Seeds, 2011) and can be found in Table 3.31.

Table 3.31 – Business Interruption Costs

Business Cost	\$/TEU
Revenue derived by port operator	\$100
Revenue derived by port operator	\$150

TEUs will be lost if the ships that are carrying them are turned away from the port. This could occur if a terminal is so severely damaged there are no available berths during the repair period, or if the ship has to wait an unacceptable amount of time to dock at an available berth (3 days (Seeds 2011)). Also, ships will be turned away if the terminal has to undergo wharf replacement. In this situation it is assumed that every ship scheduled to arrive at that terminal will be displaced. Therefore every TEU will be counted as a loss.

Adding these business interruption losses to the repair and/or replacement costs for wharves and cranes in each terminal yields the total port-wide losses due to damage from a given earthquake.

3.6.3 Operational Mitigation Options

Several options exist to minimize the amount of downtime experienced at a port. Total downtime can be reduced by improving the operations within the port or by reducing the downtime resulting from constructional issues. One of the operational mitigation options studied under the scope of this project deal with the assignment of ships to undamaged berths when the originally assigned berth is damaged. In handling the assignment of ships to undamaged berths, this project will examine the following options:

- 1.) Keeping the status quo- a scenario in which ships may only dock at their original destination berths despite damage.

2.) Force Majeure – Company claims over berths are dissolved and incoming ships may dock at any available berth.

These options represent the spectrum of how berthing assignments could be made after an earthquake.

The other type of mitigation option studied under the scope of this project examines the affect of decreasing the construction times or repair periods on the operational interruption experienced after an earthquake. One option decreases the downtime required for repairs by offering a bonus to construction crews to reduce the length of the repair process. For comparison, an additional scenario will be run in which mobilization time is reduced to a minimum time and increased to a maximum time. In this way it will be possible to see what effect construction crews have on business interruption losses. By studying each of these mitigation options and their effects on downtime and operational losses within the port, it will be possible to recommend those options that offer the greatest returns on investments.

3.7 Total Cost

Total cost of the losses sustained by the port system from the earthquake is calculated by adding the cost of the physical damage to the port components to the business interruption losses calculated from the operational model. This total cost is calculated for every earthquake in the earthquake catalogue by the risk analysis program and stored in a matrix with its corresponding intensity measure. This data is used to calculate mean rate of exceedance curves for cost and downtime and the mean annual losses for the port.

3.7.1 Mean Rate of Exceedance

The depending on whether exceedance curves for cost or time are calculated, mean rate of exceedance calculation requires the following exceedance data to be known:

- 1.) *data* - the total cost or total time required before the port can return to working order as a result of earthquake j in the earthquake catalog.
- 2.) *sample parameters* - to “undo” the stochastic misrepresentation of the event set created through stratified sampling, the probability p that a rate falls in stratum i (p_i), and the number of samples within each stratum (N_i) must be known. (If Monte Carlo (MC) sampling was chosen, the probability = 1 because the number of samples = the total number of samples.)
- 3.) *total rate* – the total rate of the earthquakes. When using Monte Carlo sampling the total rate is the sum of the rates of all the earthquake events in the event set. For stratified sampling, the total rate must be calculated per stratum. In this case it equals the sum of the rates in the event set that have a magnitude corresponding to the magnitude of the stratum examined.

The probability of exceedance is calculated for y occurrences, where y equals a *data* value in a vector defined from 0 to $\max(data)$ that has a number of divisions equal to the number of values in *data*. The probability of exceedance equals:

$$mpe = p_i * \left[\frac{1}{\#of\ values} \sum_{j=0}^{\#of\ values} I_{(y_j \geq y)} \right] \quad (3.28)$$

where $I_{(y_j \geq value)}$ is an indicator variable that equals one if y_j equals or exceeds some value y being examined and zero if does not. In this way the mean probability of exceedance is calculated. Variance of the mean is calculated in the same fashion:

$$variance_{mpe} = p_i^2 * \frac{\text{var}(mpe)}{\#of\ values} \quad (3.29)$$

The mean rate of exceedance is calculated by multiplying the probability exceedance values at each y by the total rate:

$$mre_y = mpe * total_rate_i \quad (3.30)$$

where the *total_rate* is the sum of all mean rates of occurrence for the earthquakes sampled in stratum *i*. If confidence intervals were required along with the mean rate of exceedance, those would be calculated by calculating the standard deviation for each stratum:

$$std = \sigma * total_rate \quad (3.31)$$

where σ is the $\sqrt{\text{variance}}$ calculated in equation 3.29. Distances from the mean for the confidence intervals can be acquired by multiplying the standard deviation by the inverse cumulative distribution function and a corresponding alpha value. For instance when the confidence interval of 90% is calculated, as in this case, $\alpha = 0.1 = (1 - 0.90)$, and the distance from the mean is calculated using: $\Pr[X \leq G(\alpha)] = \alpha$. (Johnson 1992)

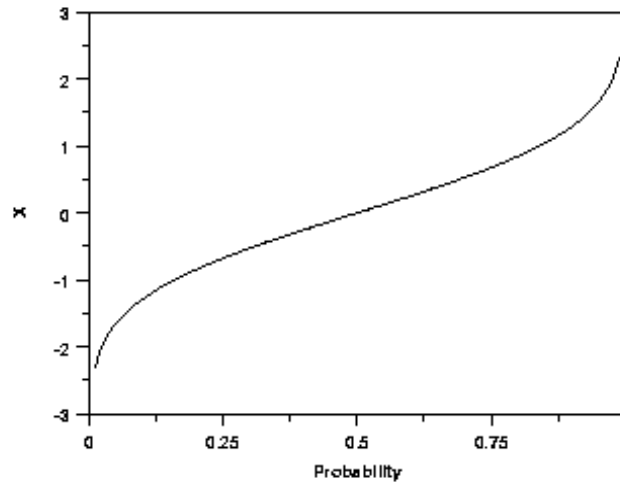


Figure 3.68 Inverse cumulative distribution function (from (NIST 2011))

The distance calculated from the mean at the confidence interval of 90% would then be added or subtracted from the mean to get the CI values needed to plot both the mean rate of exceedance and the upper and lower bounds of the confidence interval. Mean rate of exceedance plots look similar to the following (Figure 3.69):

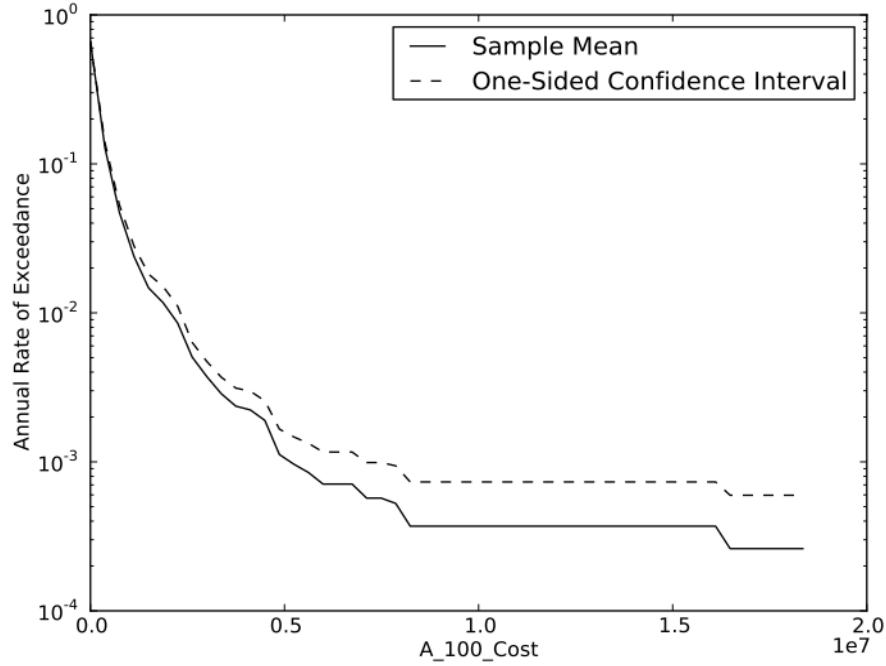


Figure 3.69 Mean rate of exceedance plot example

3.7.2 Mean and Variance of Annual Loss

Mean annual loss would be calculated using the cost mean rate of exceedance curve and integrating it over all intensity measures (calculating the area under the curve). Since the mean rate of exceedance curve exist in a discrete format, integration can be accomplished using the trapezoidal rule between discrete cost values in the mean rate of exceedance curve:

$$\int_a^b f(x) dx \approx (b-a) \frac{f(a) + f(b)}{2} \quad (3.32)$$

where a is the i th discrete point, and b is the $i+1$ th discrete point. Mean annual loss will equal the sum of the $f(x)$ values over the entire range.

Total cost of the losses sustained by the port system from the earthquake is calculated by adding the cost of the physical damage to the port components to the business interruption losses calculated from the operational model. This total cost is calculated for every earthquake in the earthquake catalogue and stored in a matrix with its

corresponding intensity measure. This data is used to calculate mean rate of exceedance curves for cost and downtime and the mean annual losses for the port.

4 RISK ANALYSIS FRAMEWORK AS APPLIED TO A HYPOTHETICAL PORT

4.1 Hypothetical Port Configuration

Due to concerns about the release of proprietary data, no existing west coast port was modeled using the risk framework. Instead, a hypothetical port was created on the coast of Santa Cruz, California (Figure 4.1) to test the risk framework. The following sections detail the parameters and response models used within the risk analysis framework to model the following hypothetical port:

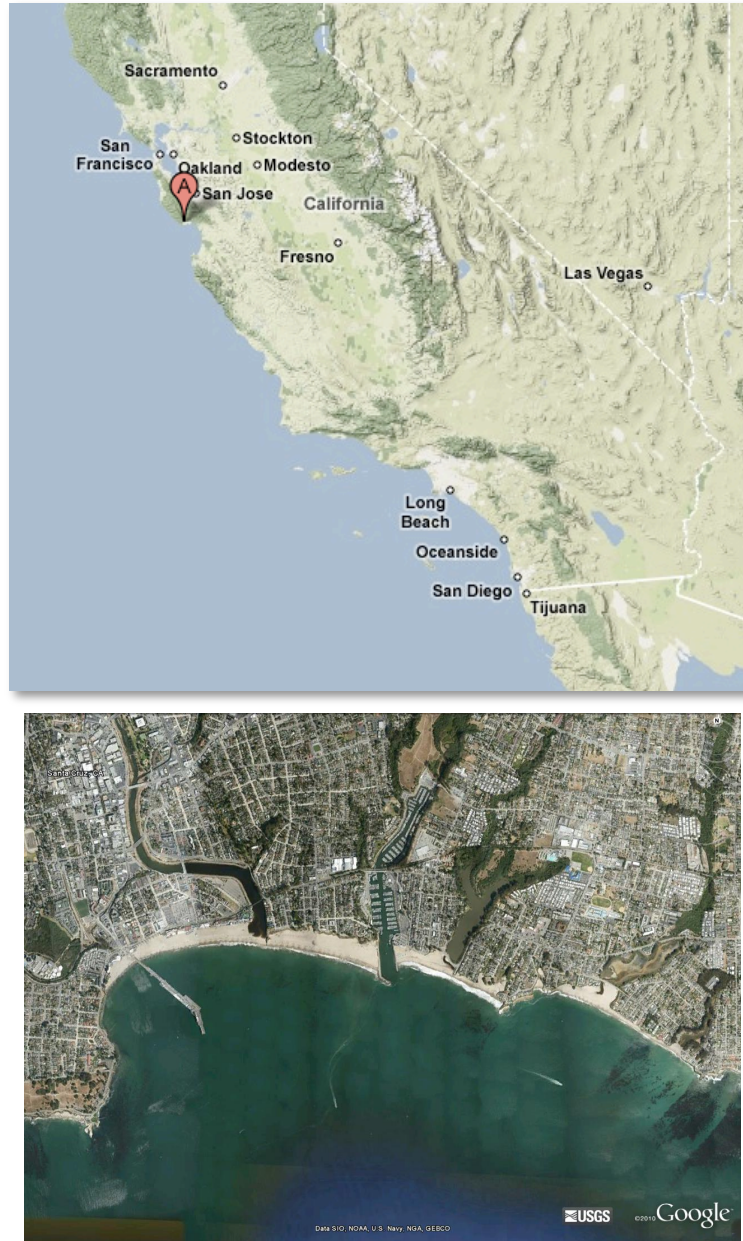


Figure 4.1- Hypothetical port location: A.) Map Location, B.) Aerial view.

The hypothetical port (Figure 4.2) consists of four terminals each with a wharf type modeled after a 1960's type wharf commonly found in US West Coast ports that are expected to have the high seismic vulnerability. The wharf type description can be found in Section 3.4.3.1. Each terminal also contains a number of one of the three specified crane types (Section 3.4.4.1) commonly found in US West Coast ports. It is also assumed that every terminal sits on liquefiable soil. (Soil profile description located in

3.4.2) The terminal lengths and number of cranes at each terminal were chosen for the hypothetical port because they are consistent with the variety of terminal lengths and corresponding crane numbers typically found in US ports ((Schleiffarth), unpublished data).



Figure 4.2 - Hypothetical Port

Terminal positions for the hypothetical port were chosen to mimic actual separation distances between terminals at west coast ports. Figure 4.3 depicts a histogram of the separation distances between container terminals in the Port of Los Angeles, Port of Long Beach, and Port of Oakland. Of the 84 separation distances measured, the average separation distance was 2.48 km, with a minimum distance of 0.62 km, a maximum distance of 5.5 km, and a median distance of 2.35 km.

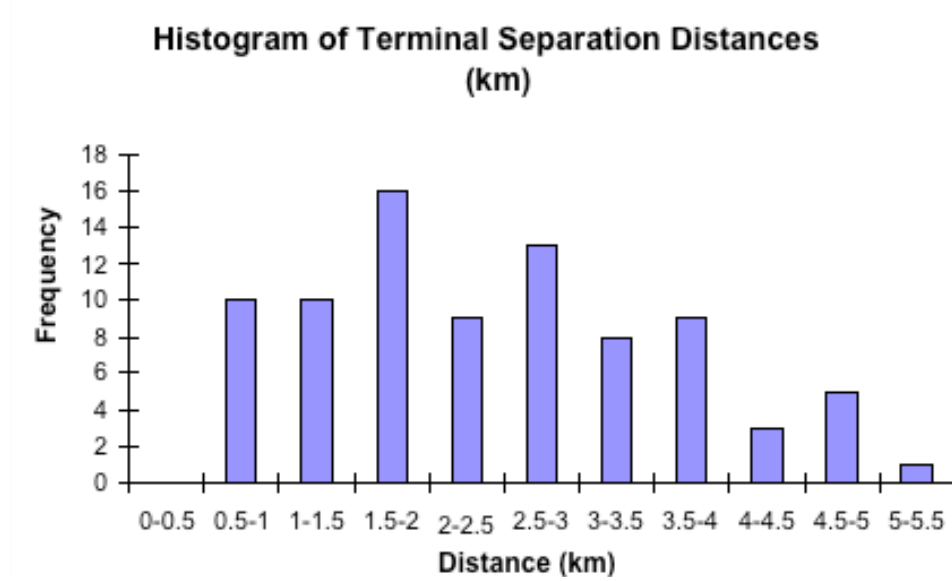


Figure 4.3 Histogram of terminal separation distances

The separation distances for the hypothetical port (Table 4.1) fall into the range of separation distances, while fitting into the natural land shapes at the hypothetical port location, and into the range of separation distances applicable to terminal sites with spatially correlated ground motions (Jayaram and Baker 2009).

Table 4.1 Separation Distances (h in km) between Terminals in the Hypothetical Port.

	A	B	C	D
A	0	0.57	1.46	3.27
B	0.57	0	1.55	3.30
C	1.46	1.55	0	1.82
D	3.27	3.30	1.82	0

The spatial correlation coefficients for the ground motions between each of the terminals can be calculated using the following equation from Jayaram and Baker (2008):

$$\rho(h) = \exp(-3h/b) \quad (4.1)$$

where $\rho(h)$ is the correlation coefficient, h is the separation distance (in kilometers), and b is the range of the exponential semivariograms. For the situation of the hypothetical port, $b = 40.7 - 15.0T$ (4.2), which applies to clustered V_{s30} values arising from the

similar soil conditions among the terminals, and short periods, $T < 1$ second. Assuming that the period T equals 0.26 seconds (the fundamental mode of the wharf in the transverse direction), and using the separation distances in the table above, the correlation coefficients between terminals would equal:

Table 4.2 – Spatial Correlation Coefficients for Hypothetical Port

	A	B	C	D
A	1	0.95	0.89	0.77
B	0.95	1	0.88	0.76
C	0.89	0.88	1	0.86
D	0.77	0.76	0.86	1

It is apparent that the terminals within the hypothetical port have fairly high correlation coefficients. All of the correlation coefficients exceed 0.76, which indicates that spatial correlation of earthquake ground motions between terminals is important, as would be expected for sites with small separation distances.

4.1.1.1.1 Baseline Configuration

Table 4.3 outlines the specifications for each terminal of the hypothetical port introduced in the previous chapter. It is assumed that due to the wharf and soil types chosen (1960's wharves on liquefiable soils) that the baseline configuration of the port will have the highest probability of seismic disruption. Latter runs of the hypothetical port will seek to use mitigation options to lessen the total losses sustained at the hypothetical port.

Table 4.3 Hypothetical Port Terminal Specifications.

Terminal	Longitude	Latitude	Length (ft)	Wharf Type	# of Cranes	Crane Type	Soil Type
A	122°1'21.97"	36°57'11.18"	2400	60's	4	LD50	L
B	122°1'23.72"	36°57'29.91"	2400	60's	5	LD100	L
C	122°0'23.23"	36°57'15.86"	5400	60's	12	J100	L
D	121°59'10.06"	36°57'23.28"	3600	60's	8	LD100	L

4.2 Example Earthquake

The risk analysis framework discussed in Chapter 3 is applied to every single earthquake in the earthquake sample for the distances to each terminal in the port. For instance, the hypothetical port has four terminals, so for a 1000-earthquake sample, the risk analysis program would calculate earthquake and loss statistics for (1000 x 4) 4000 earthquake occurrences. The calculated data includes the following:

Table 4.4 Example Earthquake and Loss Data Generated by Risk Analysis Program

Earthquake Data

Fault	Magnitude	Terminal	R Distance (km)	PGV (cm/s)	SA (T=1.5 s) (g)
N. San Andreas: SAO+SAN	7.85	A	104.36	17.89	0.0581

Loss Data

Wharf Repair Cost for Each Berth (\$)	Total Wharf Repair Cost (\$)	Wharf Repair Time (days)	Total Crane Repair Cost (\$)	Crane Repair Time (days)	BIL (\$)	Total Loss (\$)
(100,272.86, 231,938.00, 345,341.80, 226,417.75)	\$903,970	(38, 43, 56, 60)	\$0	(0,0,0,0)	\$20,831,623	\$21,735,593

From this data it is possible to see that for this specific magnitude 7.85 earthquake at Terminal A, a PGV of 0.0581 cm/s and a spectral acceleration of 0.0581 g caused a total of just under one million dollars in wharf damage and no crane damage. Specific cost and repair times at each berth are calculated. From those, the business interruption loss can be calculated. In this situation for 38 days, no berth segments are available for use, so every incoming ship must be counted as a loss. After day 38, berth segments begin to become functional until day 60 when all segments have been repaired.

4.3 Evaluation of Results for Entire Earthquake Sample

The following detailed results from the risk analysis program were generated using a stratified sampling of 10,000 earthquakes as well as a stratified sampling of

100,000 earthquakes both in conjunction with the operational regression model discussed in Section 3.6. Port configuration specifics are those of the baseline configuration described in section 4.1. A plethora on data is generated within the risk analysis program at each terminal for each earthquake instance. The following earthquake and loss data was collected and will be analyzed within a 10,000-earthquake sample: fault name, magnitude, terminal name, berth number, distance value used in the ground motion prediction equation, peak ground velocity, spectral acceleration at a period of 1.5 seconds and 5% damping, min / max wharf repair time (days), wharf repair cost, min / max crane repair time (days), crane repair cost, and business interruption loss. This data will be examined to test the functionality of the calculation methods within the risk analysis program. A 100,000-earthquake sample will be used to produce mean rate of exceedance data that was discussed in Section 3.7.1.

4.3.1.1 PGV and SA Data

The earthquake and loss data will be analyzed to check for reasonable correlations between the intensity measures used within the program and the resulting losses. The earthquake intensity measures used within the risk analysis are peak ground velocity (PGV) and spectral acceleration (SA). PGV was used as the input into the fragility models that described the wharf response and spectral acceleration was used as the input into the crane fragility models. If the risk analysis program is properly calculating repair requirements from the fragility models, the PGV should correlate well with the wharf repair time and the SA should correlate well with the crane repair time:

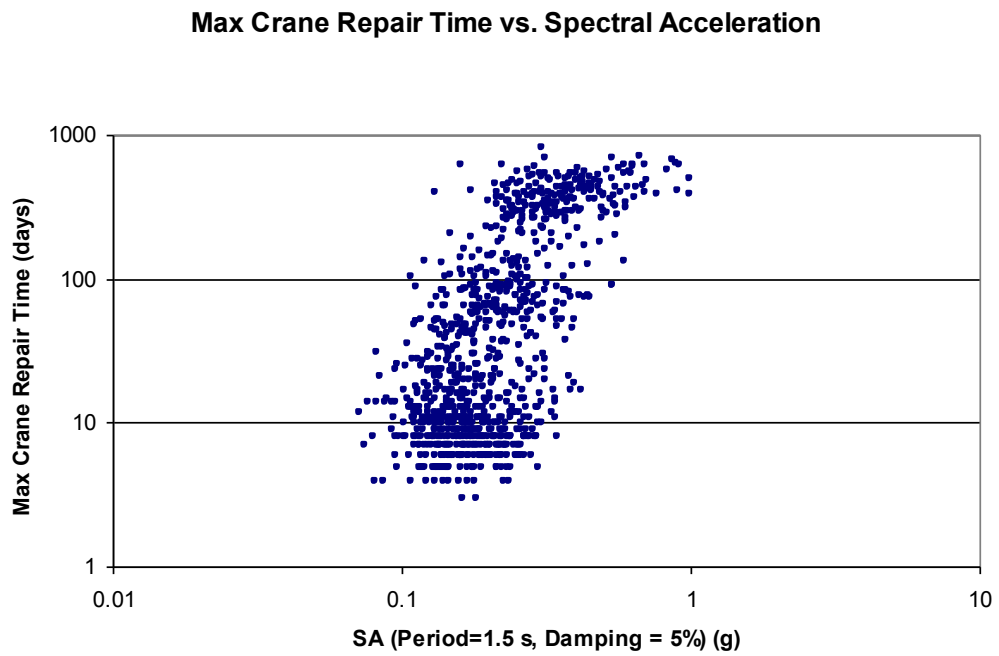
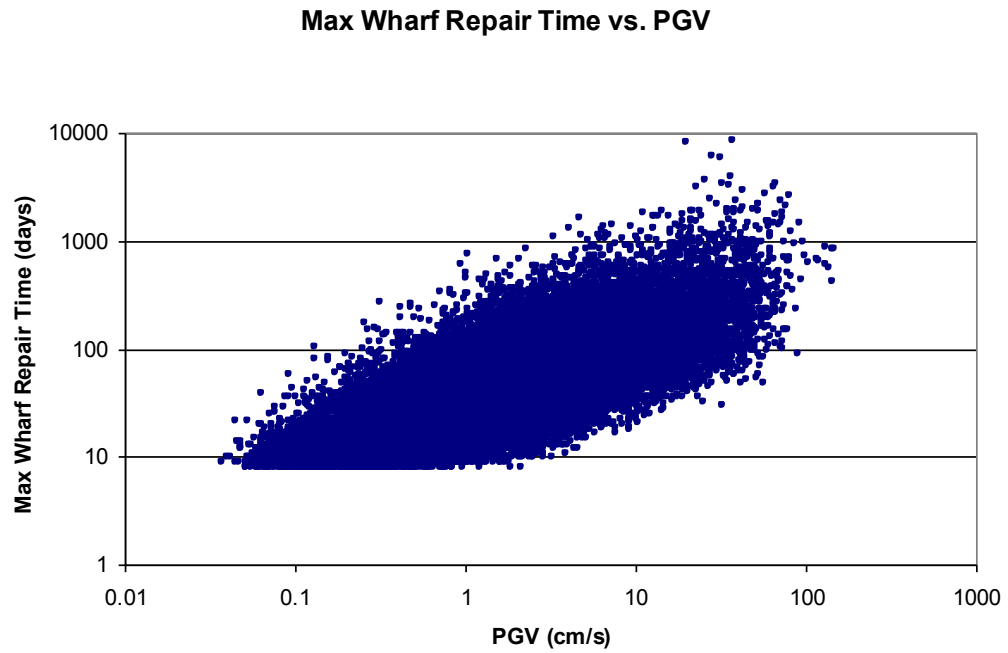


Figure 4.4 – a.) PGV vs. Repair Time for the wharf, b.) SA vs. Repair Time for the cranes

Figure 4.4 a and b show that both PGV vs. wharf repair time and SA vs. crane repair time are well correlated. Therefore one can assume that the program is in fact calculating the repair times for the wharf and cranes from the intensity measures in the positive correlation expected. One should note that both wharf and crane repair times are rounded up to the next largest integer value. This causes the bands of data that are especially apparent at small repair times. These bands also highlight the scatter in PGV and SA values for specific repair times. The rounding of repair times is partially responsible for the wide scatter in PGV and SA. However the scatter also results from the random normal distribution used to select repair times from fragility curves and the spatial correlation of repair times between berths in the terminal.

Plots of the intensity measures vs. the resulting repair costs should also be correlated since repair cost is a repair requirement calculated from the fragility curves. Furthermore, if the repair costs are correlated to the intensity measures, the business interruption losses should also be correlated to the intensity measures since BIL is calculated as a function of several variables, the most predominant of those being repair time. Figure 4.5 - Figure 4.8 plots the intensity measures vs. the repair costs and the business interruption losses (both in millions of dollars) at each terminal. Logic dictates that both of these costs should increase as the earthquake intensity measures increase:

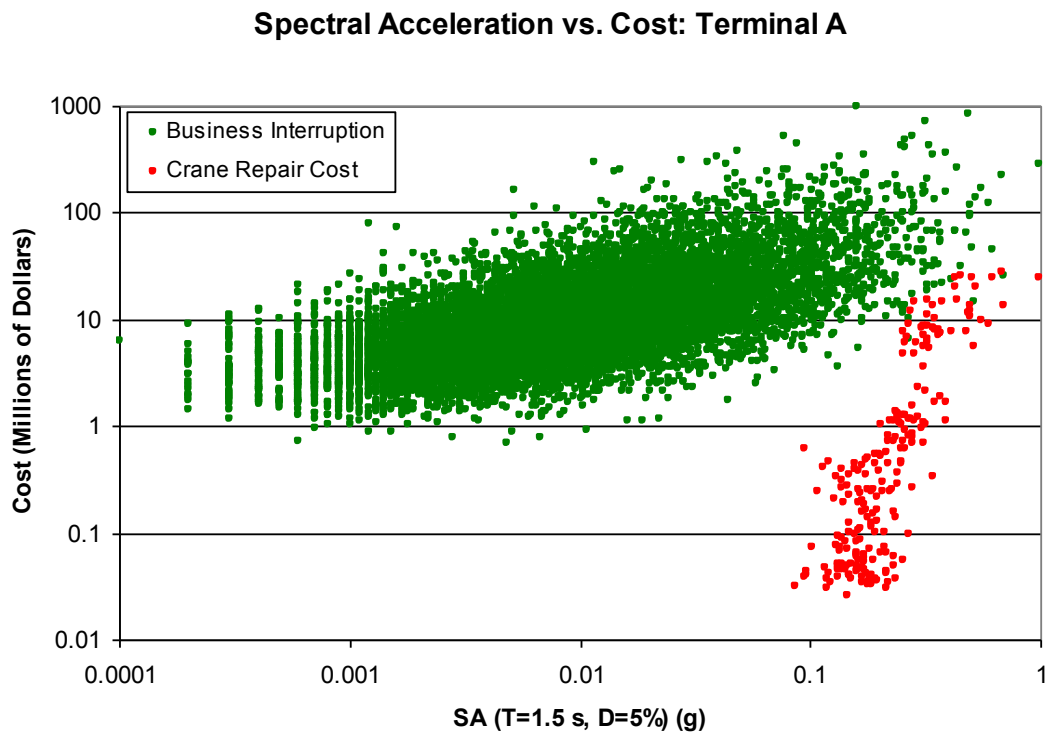
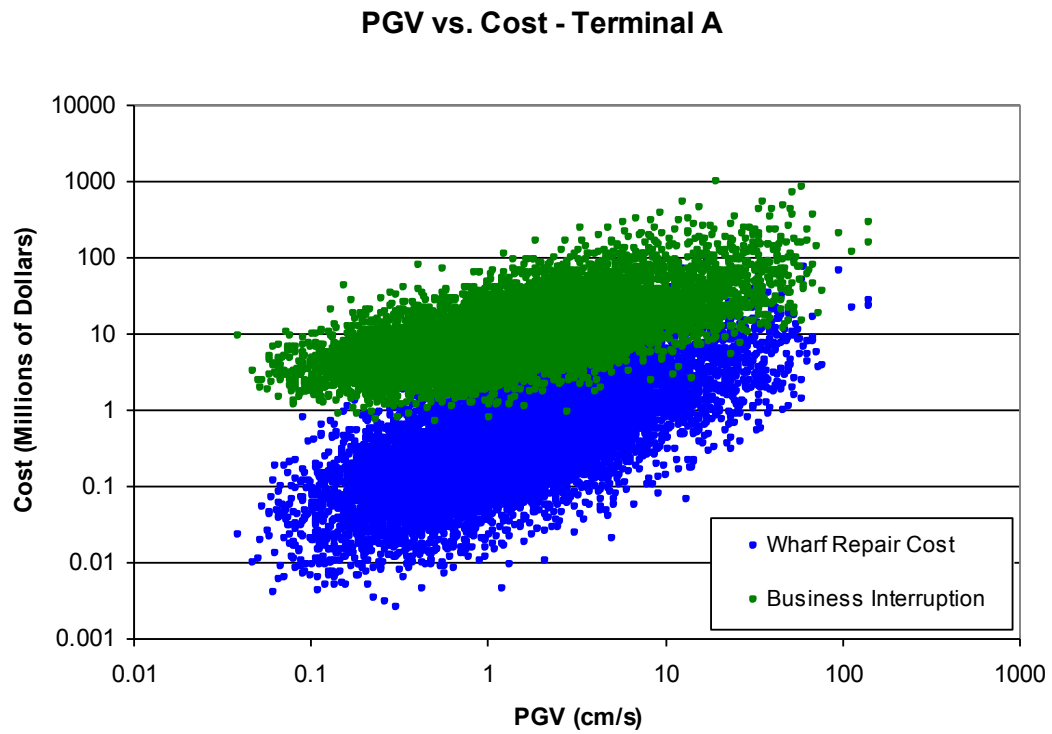


Figure 4.5 – a.) PGV Vs. Cost, b.) Spectral Acceleration vs. Cost: Terminal A

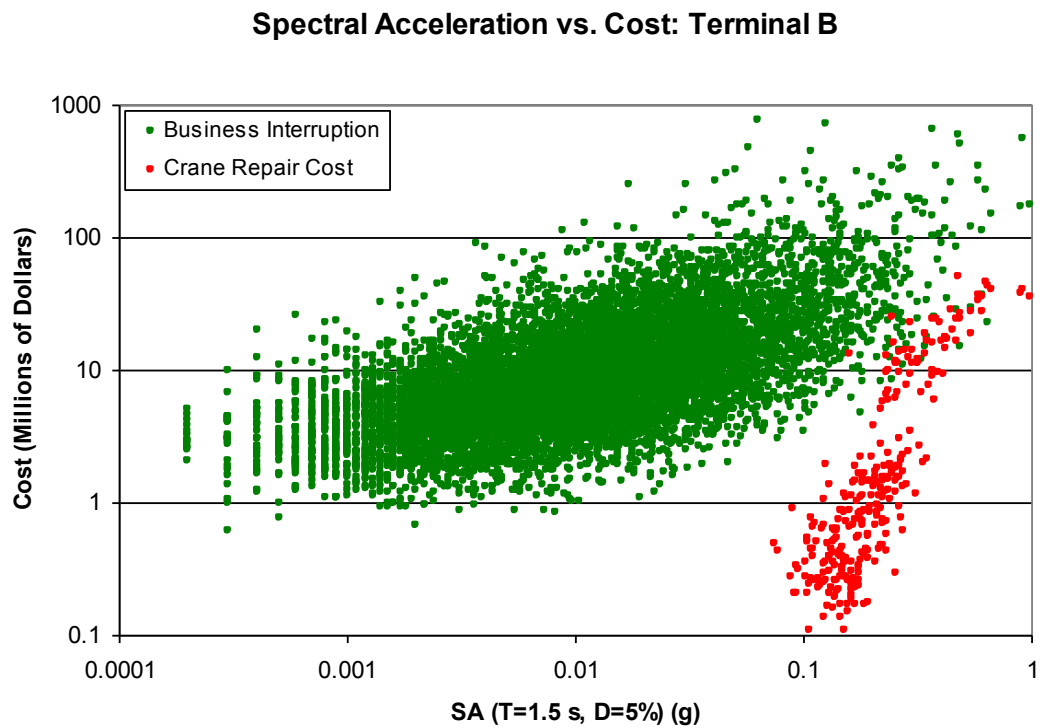
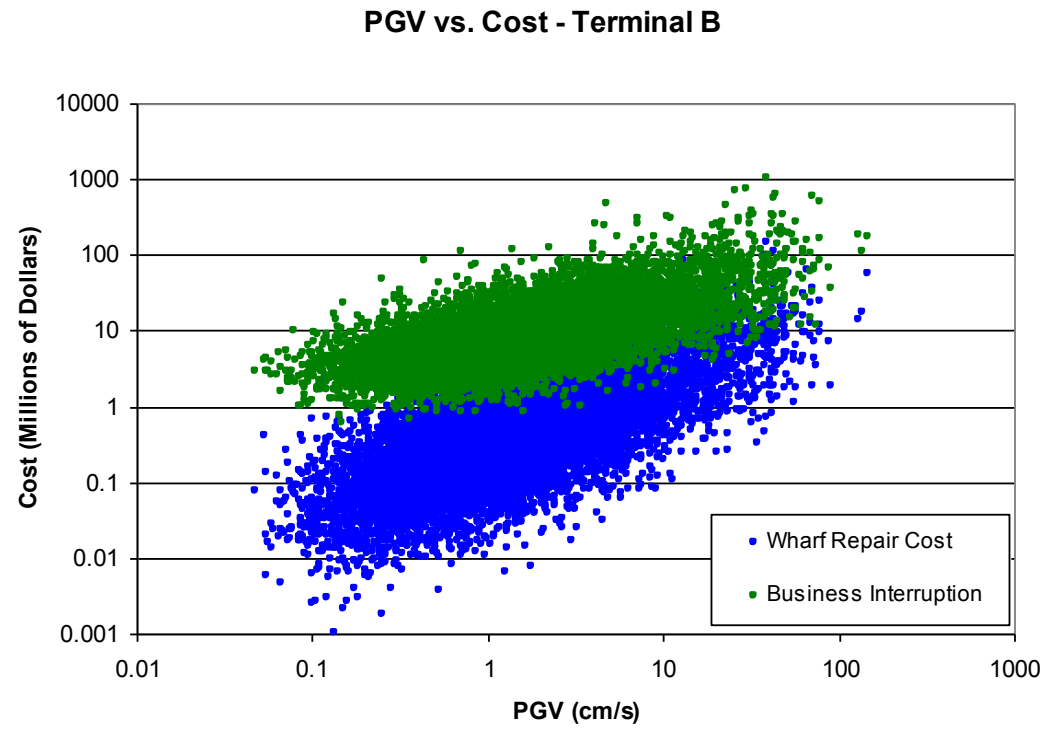


Figure 4.6 – a.) PGV Vs. Cost, b.) Spectral Acceleration vs. Cost: Terminal B

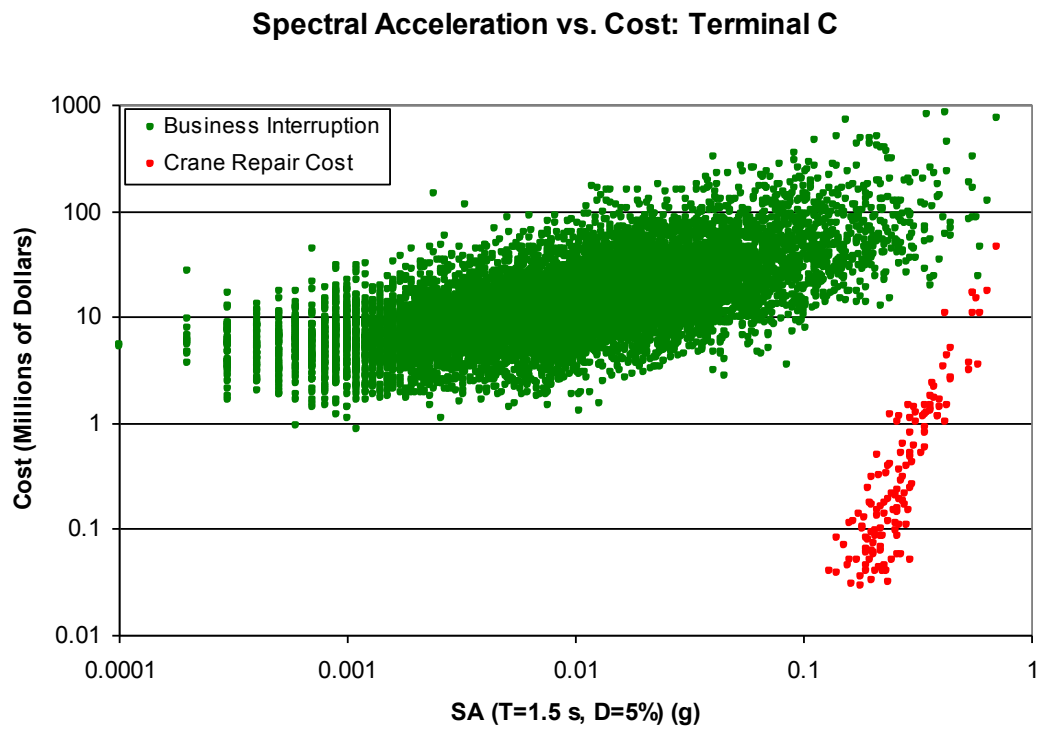
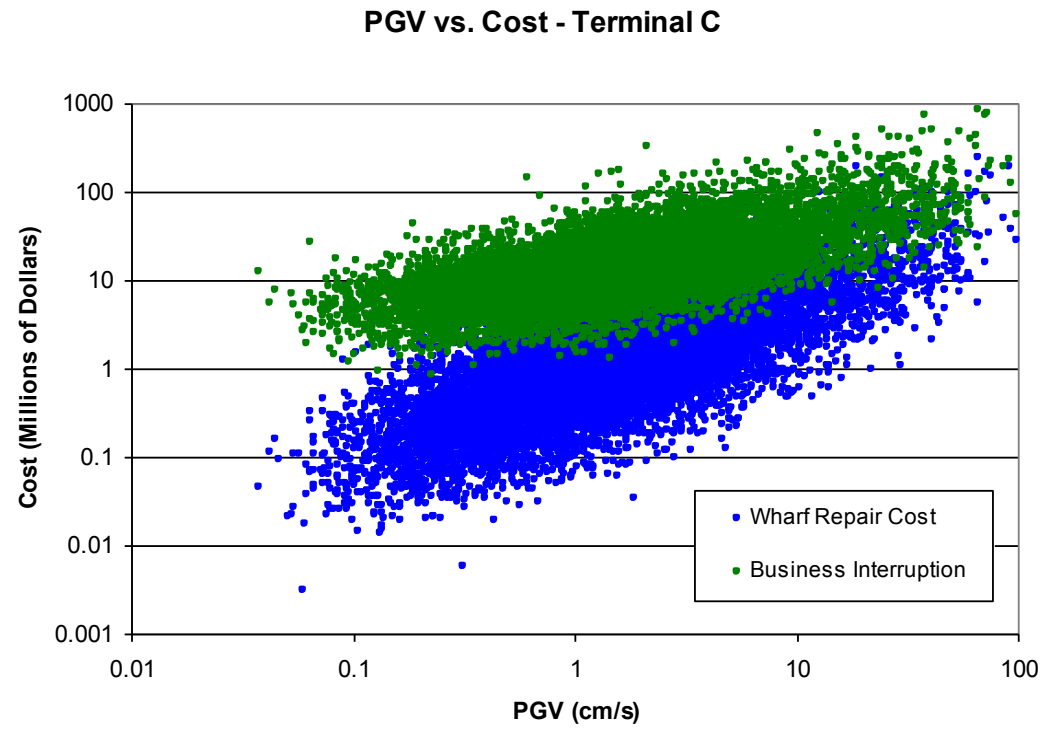


Figure 4.7 – a.) PGV Vs. Cost, b.) Spectral Acceleration vs. Cost: Terminal C

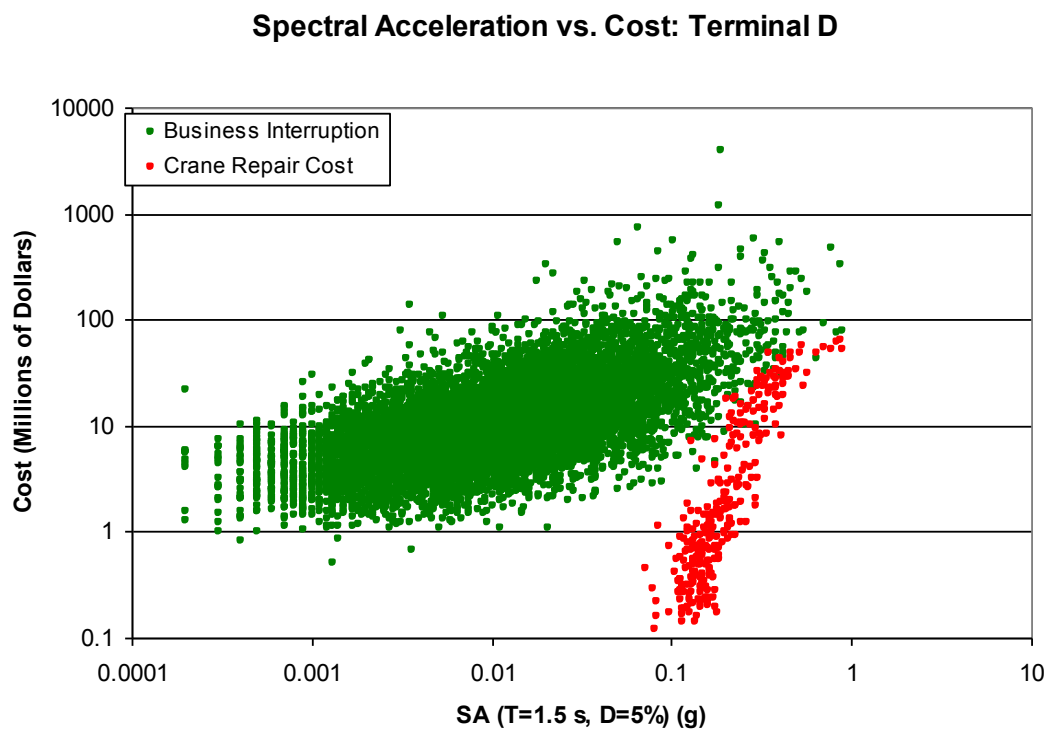
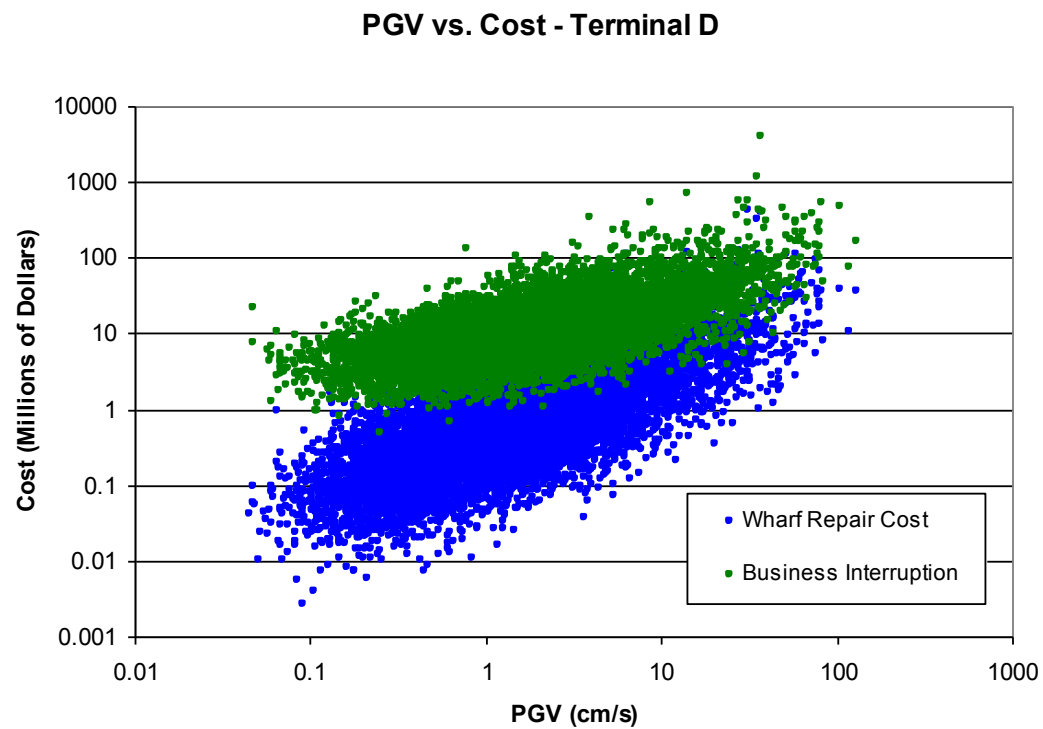


Figure 4.8– a.) PGV Vs. Cost, b.) Spectral Acceleration vs. Cost: Terminal D

As an additional check Figure 4.9 plots the relationship between repair time and repair cost. Again, logic dictates that as the repair time increases, the repair cost should also increase. Instances of wharf and crane repair are plotted in blue and red respectively:

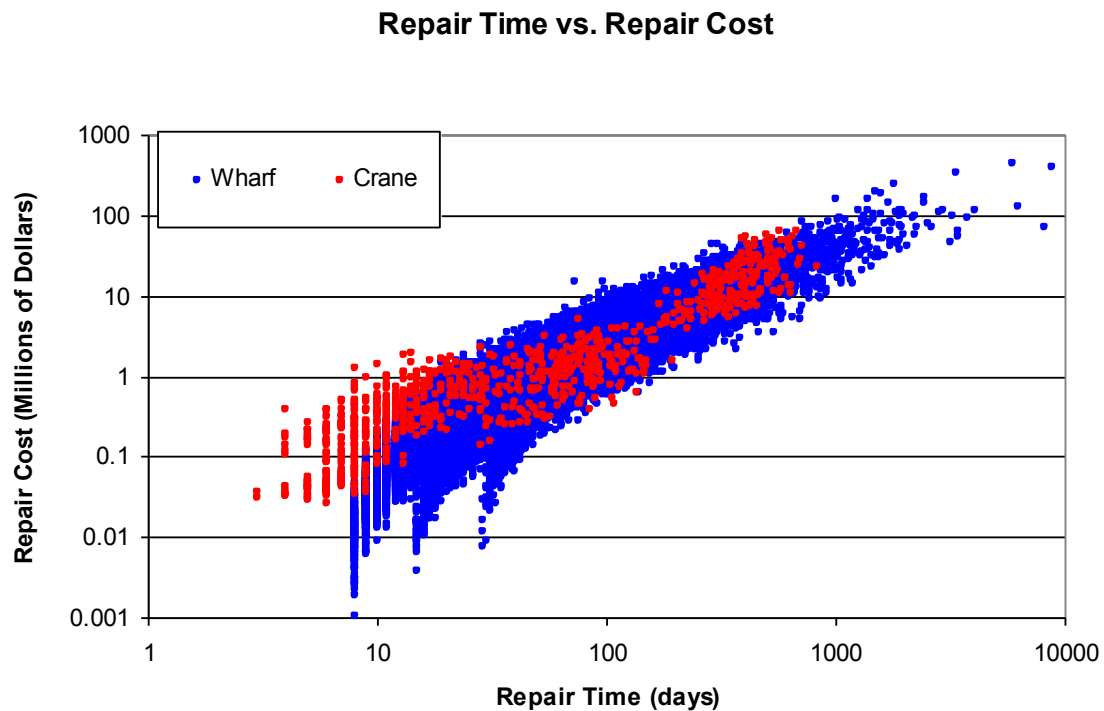


Figure 4.9 – Repair Time vs. Repair cost for Wharf and Crane

Figure 4.9 also demonstrates how damage to the wharf is more prevalent during earthquake disruption than crane damage. Each point represents an instance of damage and the number of blue points far exceeds the number of red points in the plot above.

4.3.1.2 Total Cost Data

Since repair costs and business interruption losses correlate with the intensity measures and the total cost is calculated as the sum of the repair cost and business interruption loss at each earthquake instance, it stands to reason that the total cost should also logarithmically correlate with the intensity measures. These relationships are plotted in Figure 4.10:

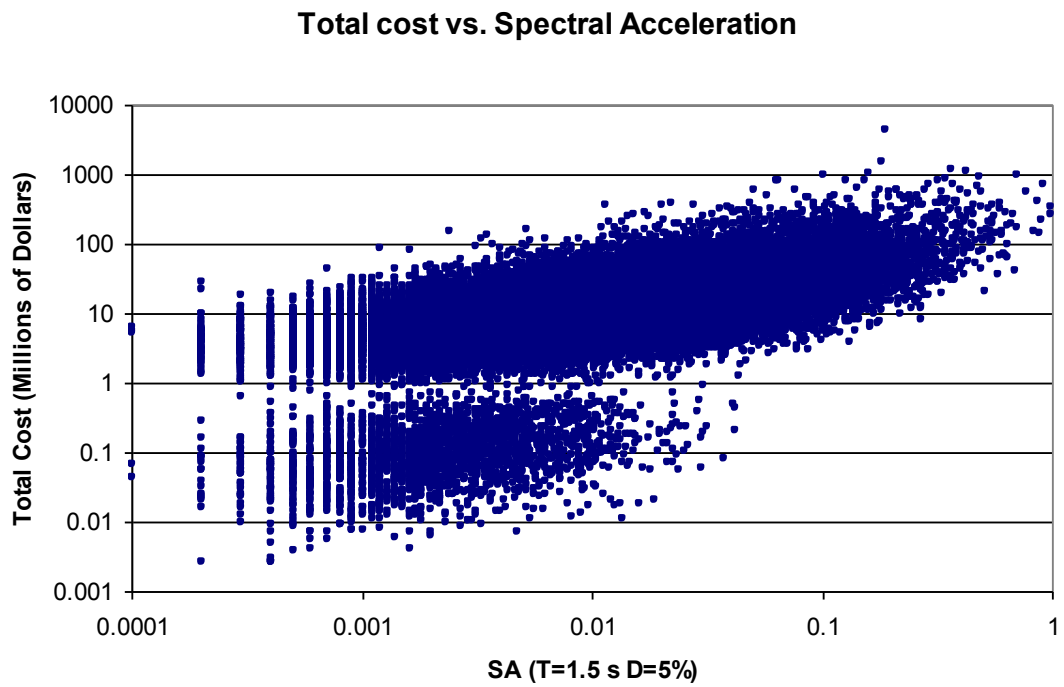
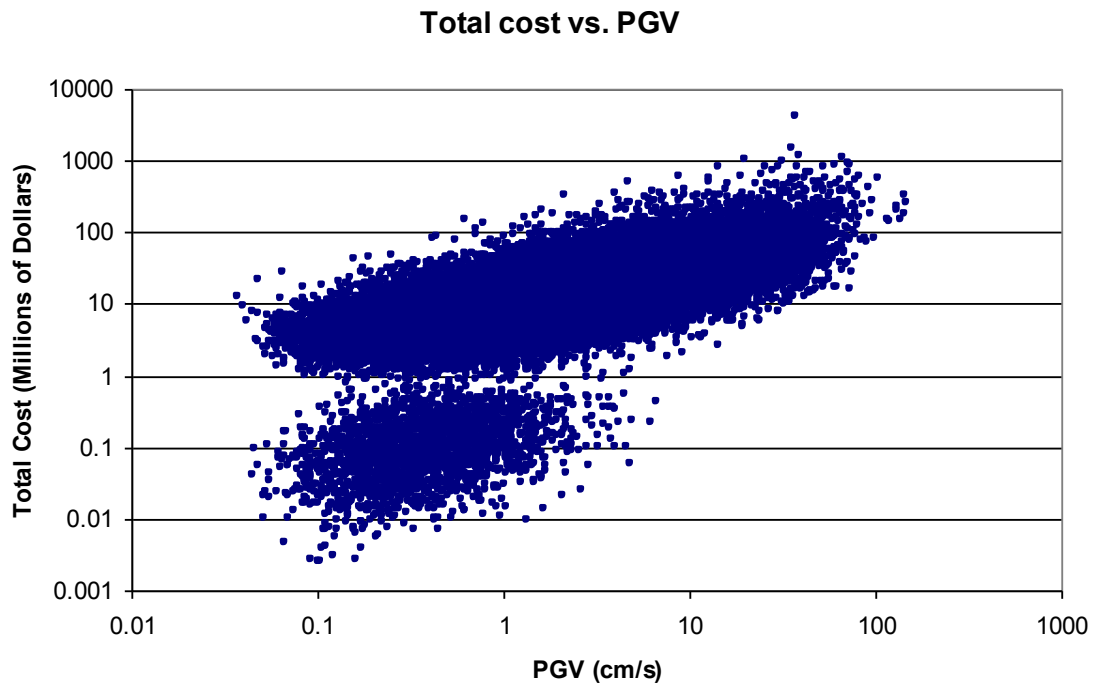


Figure 4.10 - Total Cost Plots a.) PGV vs. Total Cost, b.) SA vs. Total cost

The most noticeable feature in each of these plots is that there are two distinct clusters of correlated points. The reason for this is very simple. As described by the operational regression model (Section 3.6), multiple earthquake instances that result in no business interruption loss. Business interruption losses only occur when an arriving ship cannot be serviced within three days after arriving. In some instances the wharf and crane damage was so minor that all arriving ships could still be serviced. Therefore, the lower cluster in Figure 4.10 corresponds to instances where the business interruption loss equaled zero, and the upper cluster corresponds to instances where the business interruption loss was greater than zero.

The clusters are so distinct because the difference between no business interruption loss and a business interruption loss is the displacement of an entire ship. The ships used in the risk analysis have TEU capacities ranging from 1012 to 9310 TEUs. Since the mean number of TEUs processed by the port is calculated as $0.57 * \text{TEU capacity} + 0.61 * \text{TEU capacity}$, the mean number of TEUs lost ranges from 1194 to 10986. At a loss of \$250/TEU, that translates to \$298,500-\$2,746,500. So the gap between $\text{BIL} = 0$ and $\text{BIL} > 0$ is at least \$298,500.

The width of the lower cluster and the range of PGVs or SAs that correspond to no business interruption loss is a function of berth length. Two scenarios could occur where larger intensity values with assumed larger repair requirements would still produce no business interruption loss.

- 1.) A scenario might occur in which the intensity measures damage only a short portion of a terminal and enough berths are still available to accommodate all incoming ships. This would be likely in longer terminals.
- 2.) Shorter berths correspond to longer inter-arrival times between ships. A larger intensity measure may have cause significant damage in one part of the terminal, but as long as there's enough berth length and

cranes to service the one ship that will arrive every three to four days, there won't be a business interruption loss.

4.3.1.3 Conclusions

All of the previous plots were logarithmically correlated as was expected. However they also depict several other interesting details within the risk analysis program that should be noted:

Business interruption losses are larger than the repair costs.

This result is clearly visible in Figure 4.5 - Figure 4.8 for both intensity measures. For all earthquake instances in the 10000-earthquake sample where $BIL > 0$, the ratio of BIL to total repair cost was calculated ($BIL/Total\ Repair\ Cost$) and plotted in Figure 4.11:

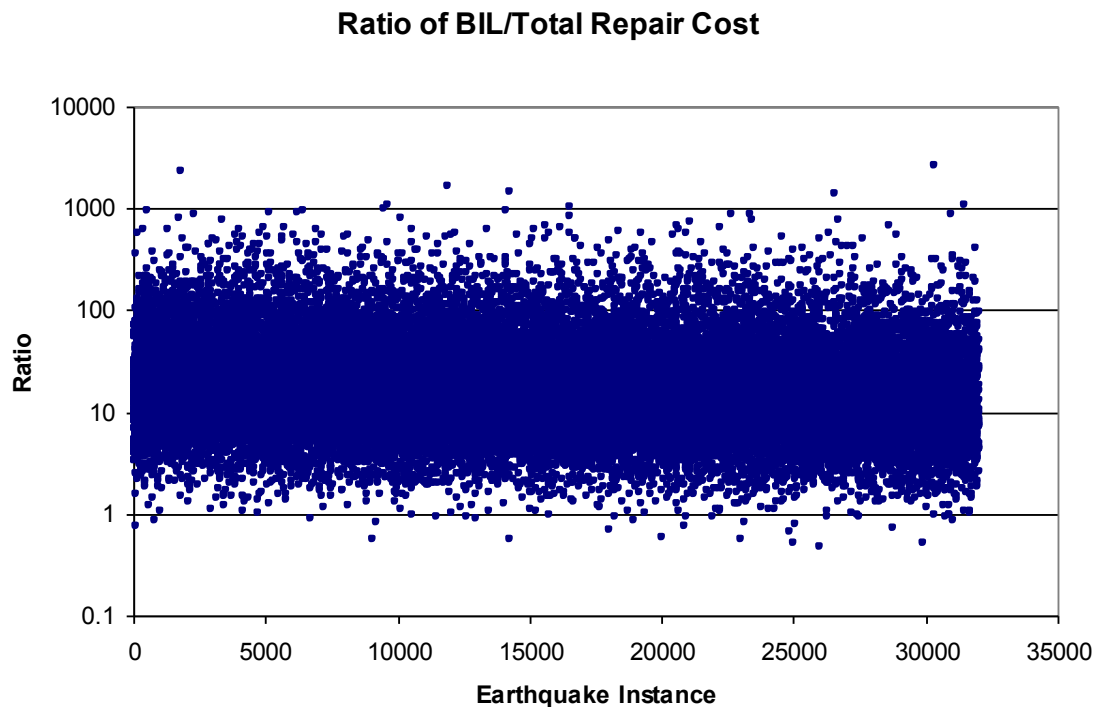


Figure 4.11 – Ratios of BIL/Total Repair Cost

While some ratios were greater than 100, of the 37,759 instances calculated most were less than 50 and the average ratio was 28.94 and the median ratio was 14.97.

Very few ratios were less than one, which would indicate that the BIL was smaller than the total repair cost. Therefore on average, the business interruption loss is almost 30 times that of the total repair cost. As suspected, the majority of the total losses experienced at ports are due to business interruption, and this result reiterates the necessity of calculating operational losses within the risk framework

4.3.1.3.1 Damage states are visible in the crane data

In the plots depicting spectral acceleration vs. cost, the crane repair costs are correlated and grouped into 3 clusters. Moreover, it is almost possible to differentiate between the different crane damage states as described in Kosbab (2010). For instance the plot for terminal A shows three distinct clusters of points. If one keeps in mind that Figure 4.5 shows the total crane repair cost (sum of all crane repairs in a terminal) it is possible to associate the elevated means of the clusters to specific damage states. The lowest cluster corresponds to the derailment damage state, which has a mean cost of \$50,000 and a COV of 0.3. The middle cluster is probably a combination of the immediate use and structural damage damage states which have a mean cost of \$300,000 and \$500,000 respectively and COVs of 0.5. The upper cluster would then correspond to the complete collapse damage state, which has a mean cost of \$7,000,000 and a COV of 0.3. The presence of specific damage states with the repair cost data further confirms that the repair requirements are being calculated correctly within the risk analysis framework.

The lack of visible damage states within the wharf repair data is due to the nature of how and the number of repair costs calculated. While different damage states exist for the wharf, they are less binary than that of the cranes. If a crane is in a certain damage state, there is a specific mean cost associated with that state. The wharf repair cost is also calculated as a function of the extent to which the berth is damaged (i.e. the number of piles damaged). However, because there are so many instances of wharf repair and the

damage states are correlated, repair costs take on large ranges of values that plot as a single correlated cluster of wharf repair costs.

4.3.1.3.2 Intensity Measures correlate well with fragility curves.

Figure 4.5b-Figure 4.8b also show that crane damage initiates at a SA value around 0.1 g and the cost increases rapidly as the SA increases. The spectral acceleration intensity measure was taken at a period of 1.5 s and a damping ratio of 5%. This damping differs from the ratio used to generate the fragility curves (1.5%) but this difference is accounted for within the risk analysis program (See 3.3.4.6). This value is consistent with the fragility curves developed in Kosbab (2010) in which crane damage initiated around the same value (Figure 4.12).

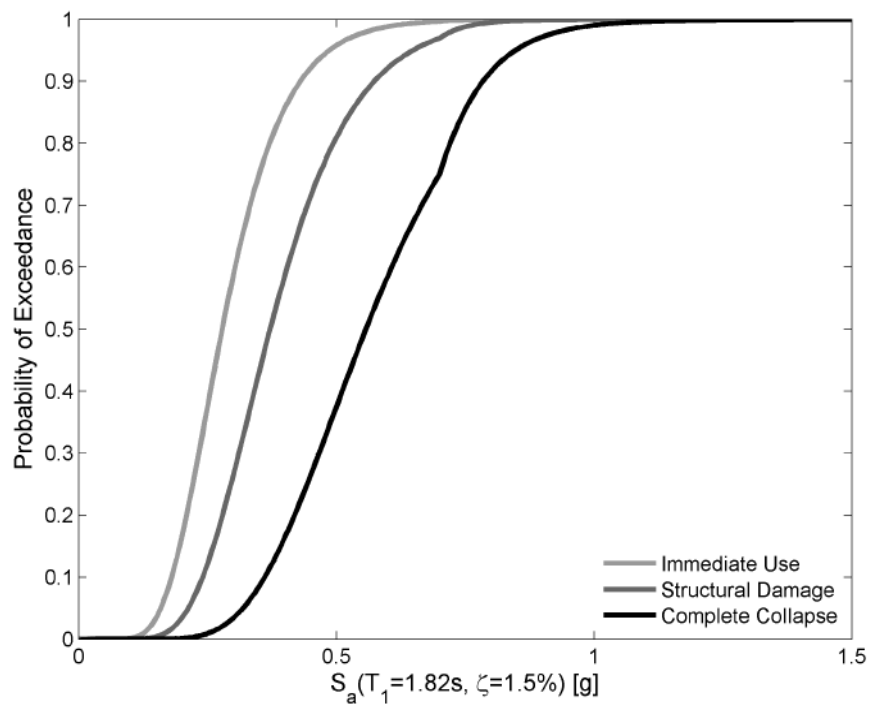


Figure 4.12 Fragility curves for LD100, assuming portal uplift theory seismic demand model. (Kosbab 2010)

Wharf repair costs in Figure 4.5-Figure 4.8 initiate at a PGV of 0.02 cm/s and logarithmically increase with increasing PGV. The fragility curves from Shafieezadeh

(2011) in Figure 4.13 depict slight damage at PGVs near 0 m/s for relative movement of the wharf with respect to the crane rail. While there are instances of damage at low PGVs that correspond to this curve, the core of the repair cluster begins near 0.1 cm/s which correspond to the curve for slight damage near 0.1 m/s for damage to pile-deck connections. One must remember that these fragility curves show the PGVs corresponding to the probability of damage for an entire wharf section, which includes 110 separate piles. It takes 0.1 m/s to initiate damage all 110 piles, however damage to a single pile would not require such a large intensity. The smaller intensity measure value of initial damage in Figure 4.5-Figure 4.8 likely corresponds to the damage of a single or small number of piles.

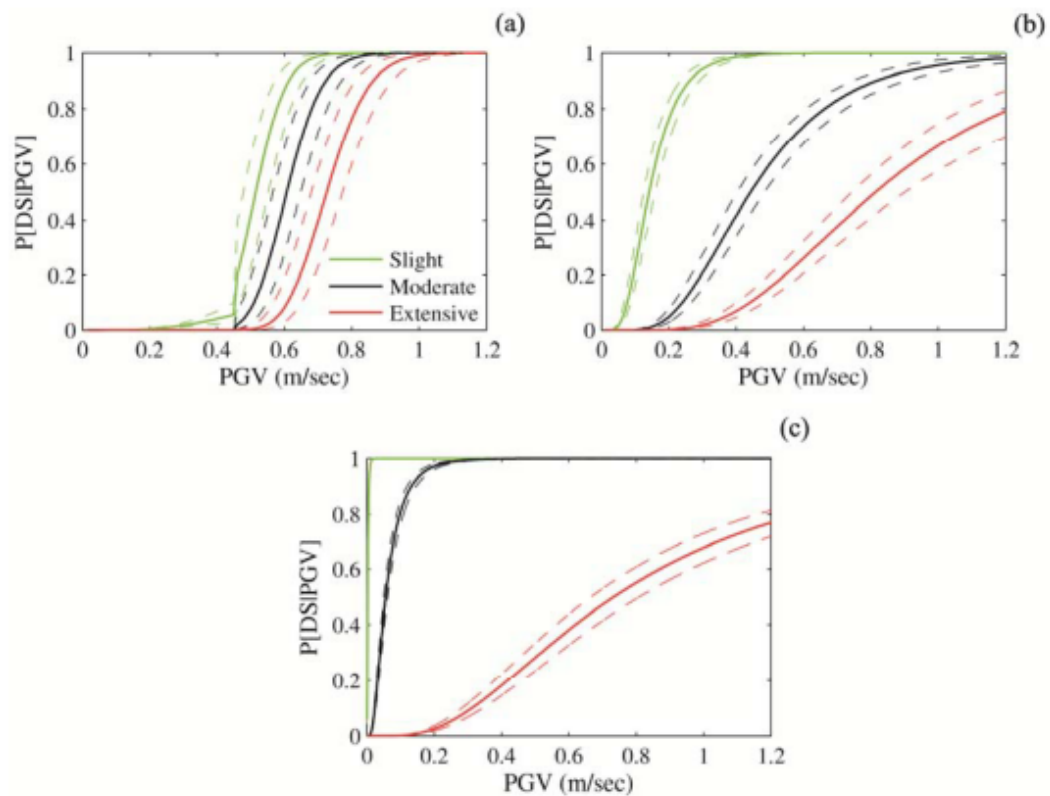


Figure 4.13 - Component fragility curves for (a) pile section, (b) pile-deck connections, and (c) relative movement of the wharf with respect to the landside crane rail (solid lines are the fragility estimates and dashed lines are the corresponding 90% confidence boundaries). (from (Shafieezadeh 2011))

Figure 4.9 proved that for the earthquakes sampled wharf damage was far more prevalent than crane damage. This of course is partially due to the fact that the number of wharf sections that can be damaged is larger than the number of cranes. However, it is still apparent that wharves seem to be more vulnerable during earthquakes when comparing the two. Figure attempts to draw conclusions about the vulnerability of the wharf at each terminal:

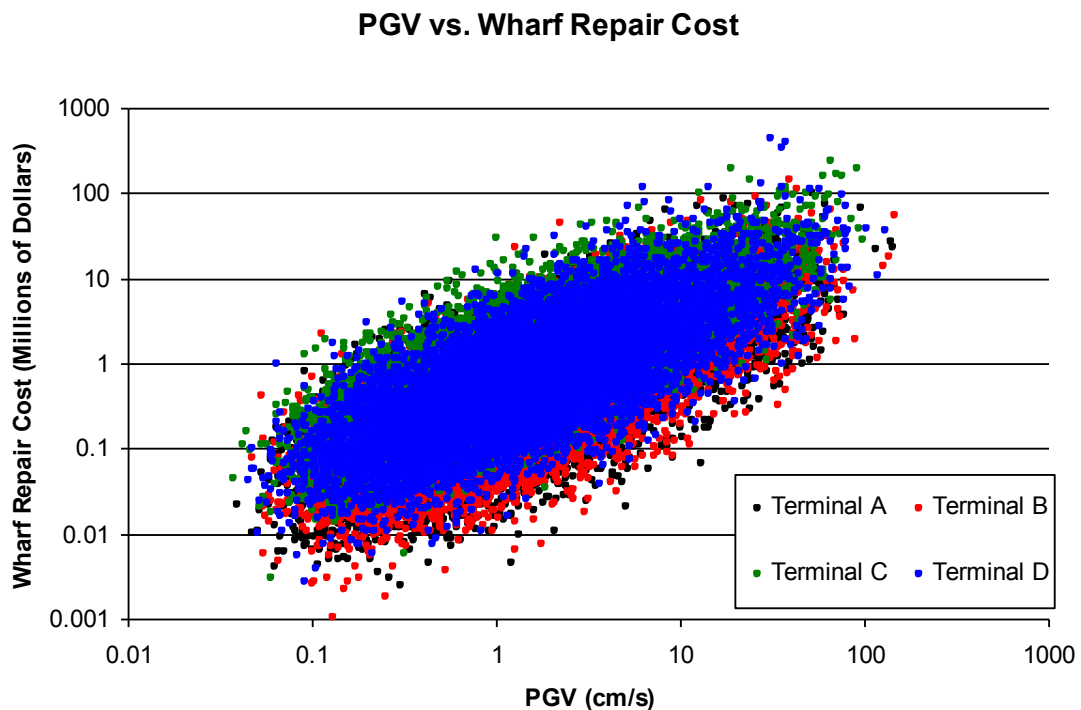


Figure 4.14 – PGV vs. Repair Cost per Terminal

However, the density of the points and the wide scatter among repair costs at specific PGVs prevent any definitive statement about the order of vulnerability among the terminals. Therefore statements of wharf vulnerability per terminal will be saved until the mean rate of exceedance curves are plotted. However, it can be said that if differences in vulnerability exist, it will be a factor of wharf length, because that is the only major difference between the four terminals. On the other hand, since there are far

less instances of crane damage it is much easier to see correlations between crane type and SA values.

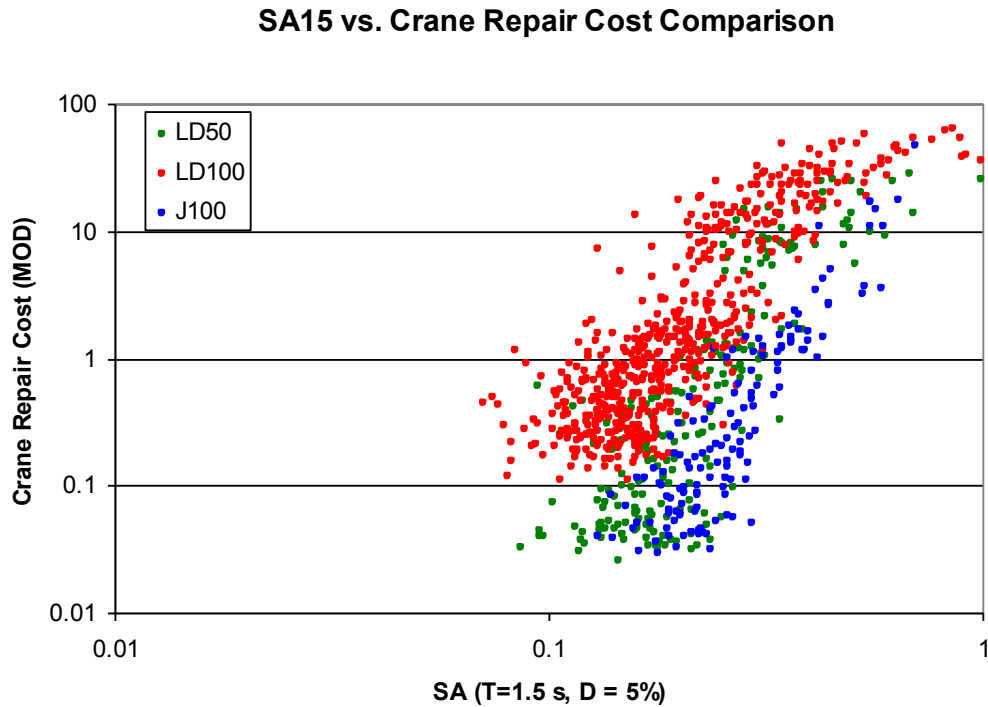


Figure 4.15 – SA vs. Crane Repair Cost Comparison per Crane Type

From Figure 4.15 it is evident that the range of SA at which damage occurs varies by crane type. The LD100 crane has the lowest range, the LD50 crane a mid-range, and the J100 the highest range. If ranked from most to least vulnerable the order would be LD100, LD50, and J100. This can also be confirmed by counting the instances of damage for each crane type for the 10019 earthquakes in this particular sample (Table 4.5) or by comparing mean rate of exceedance curves for crane damage.

Table 4.5 – Instances of Crane Damage per Terminal

Terminal	Crane Type	Instances of Damage	% of Total
A	LD50	217	2.2%
B	LD100	279	2.8%
C	J100	138	1.4%
D	LD100	298	3.0%

4.4 Probabilistic Analysis Results

4.4.1 Earthquake Sample Size

A sample size of 100,000 earthquakes implementing stratified sampling was chosen to generate mean rate of exceedance data within the risk analysis program. A sample that large was required in order to accurately calculate the annual exceedance rates less than $10e-4$ that corresponded to the largest instances of port damage/disruption.

Smaller sample sizes were tested but the results were not consistent at small annual exceedance values. A hazard curve for PGV vs. a reference hazard curve for Terminal A and a 10000-earthquake sample (Figure 4.16) confirms that MRE curves were not representative of true hazard curves at small rates of exceedance. For instance, this hazard curve begins to become unrepresentative of the reference curve at an exceedance value of about 10^{-3} . A larger earthquake sample will be used so that the MRE curves can be better defined at small rates of exceedance.

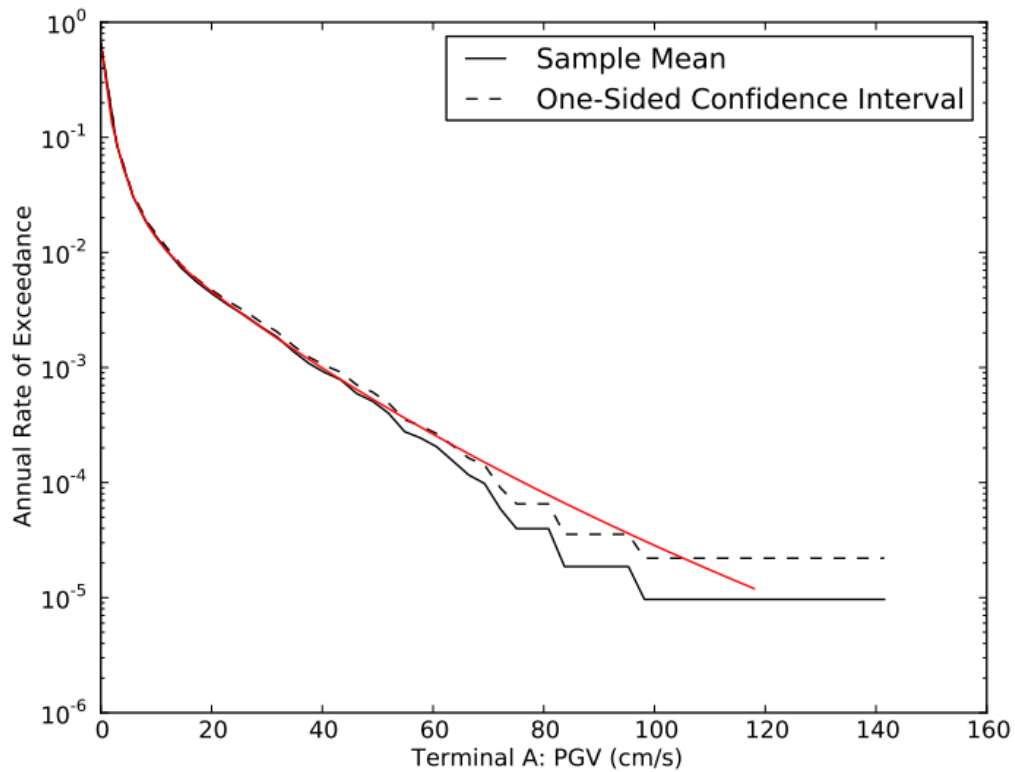


Figure 4.16 – Empirical (10000-EQ sample) and Reference Hazard Curve Comparison: Terminal A

When the 100,000 earthquake sample was implemented curves at lower rates of exceedance were better defined at smaller rates of exceedance (Figure 4.17). The following plot shows MRE curves for total cost among two different 100,000 earthquake baseline runs as compared to a 10,000-earthquake run (in red), and plot b shows the empirically calculated hazard curve for PGV vs. the reference hazard curve for the run represented by the blue MRE curve in plot a.

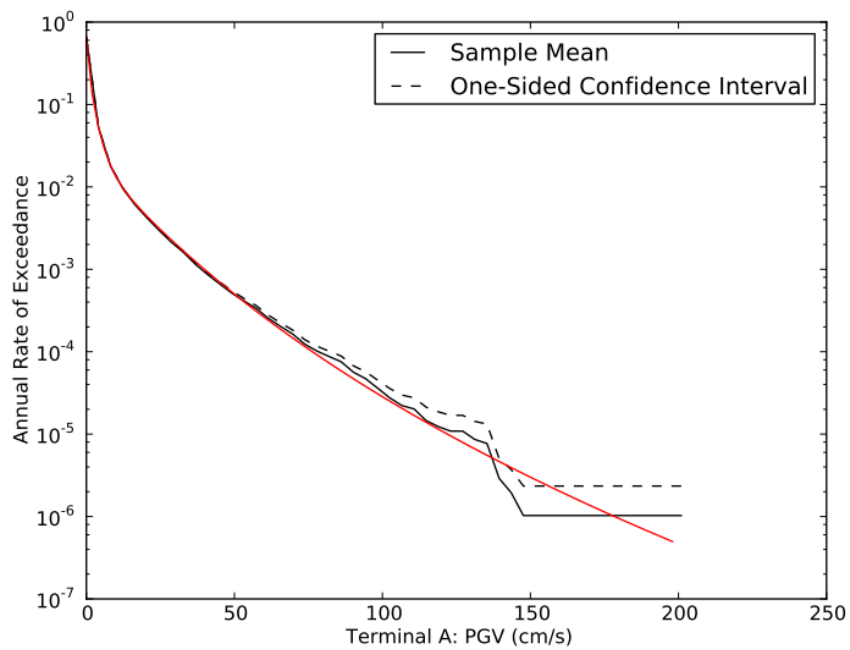
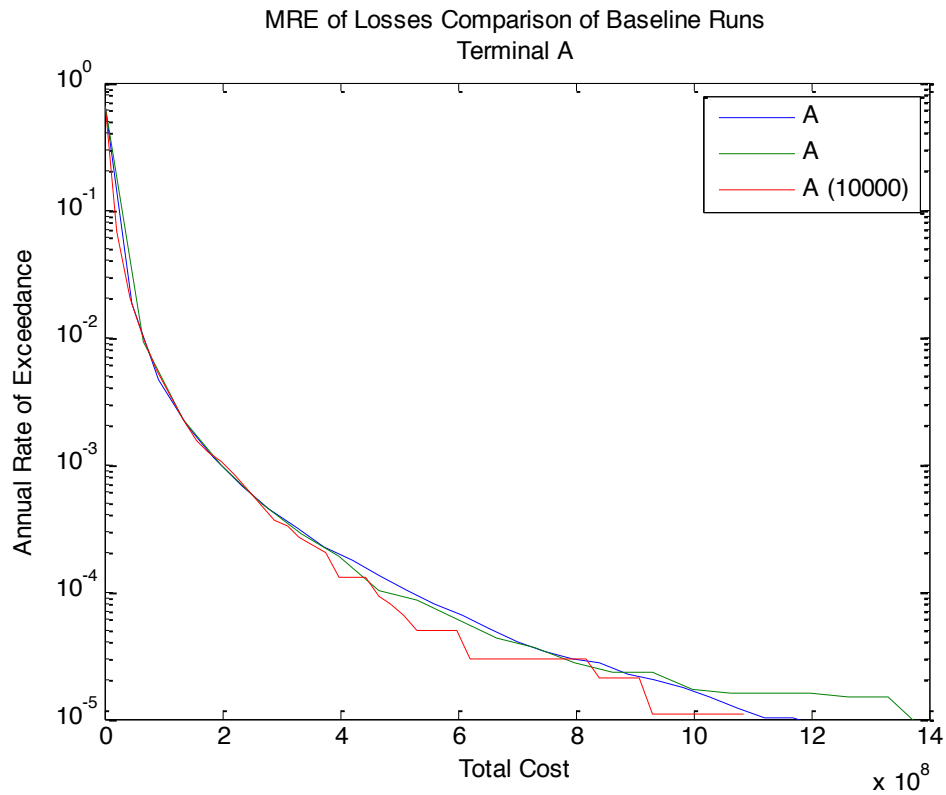


Figure 4.17 – a.) MRE curves for total cost among 2 different 100,000 earthquake baseline runs as compared to a 10,000-earthquake run (in red), and b.) The empirically calculated hazard curve for PGV vs. the reference hazard curve (red) for the run represented by the red MRE curve in a.): Terminal A

In Figure 4.17a, the 100,000-earthquake samples (blue and green) are similar in magnitude and well defined even at small rates of exceedance. The horizontal portions of the smaller sample (red) at small rates of exceedance indicate that there are not enough large earthquakes in the sample to properly define the MRE curve at very small rates of exceedance. Thus, it's obvious that the larger sample is needed. However, from Figure 4.17b, it is also possible to see that at very very small exceedance rates, the 100,000-earthquake sample also loses definition of the MRE curve. Considering the previous plots and using a sample size of 100,000 earthquakes, MRE curves up to 10^{-4} will be considered well defined, the portion of the curve between 10^{-4} and 10^{-5} will be considered moderately well defined, and any data smaller than 10^{-5} will not be considered. There aren't enough earthquakes in the 100,000-earthquake sample to properly define the curves at exceedance values less than 10^{-5} . This result is acceptable because in practice, most earthquake engineers do not consider exceedance rates for earthquakes larger than a return period of 2500 years. The data is well defined up to and slightly smaller this value. For reference, the following return periods correspond to the following exceedance rates:

Table 4.6 – Exceedance Value Reference

Return Period (years)	Annual Rate of Exceedance
10	10^{-1}
72 (OLE)	$1.4 \cdot 10^{-2}$
100	10^{-2}
475 (CLE)	$2.1 \cdot 10^{-3}$
1000	10^{-3}
2500	$4 \cdot 10^{-4}$
10000	10^{-4}
100000	10^{-5}

4.4.2 Exceedance Results

Exceedance curves are the most common results used in earthquake risk analysis. Calculation of these curves is outlined in Section 3.7.1. The exceedance curves produced to analyze the port system include curves that find the annual rate of exceedance for repair costs, business interruption losses, and total costs at each terminal.

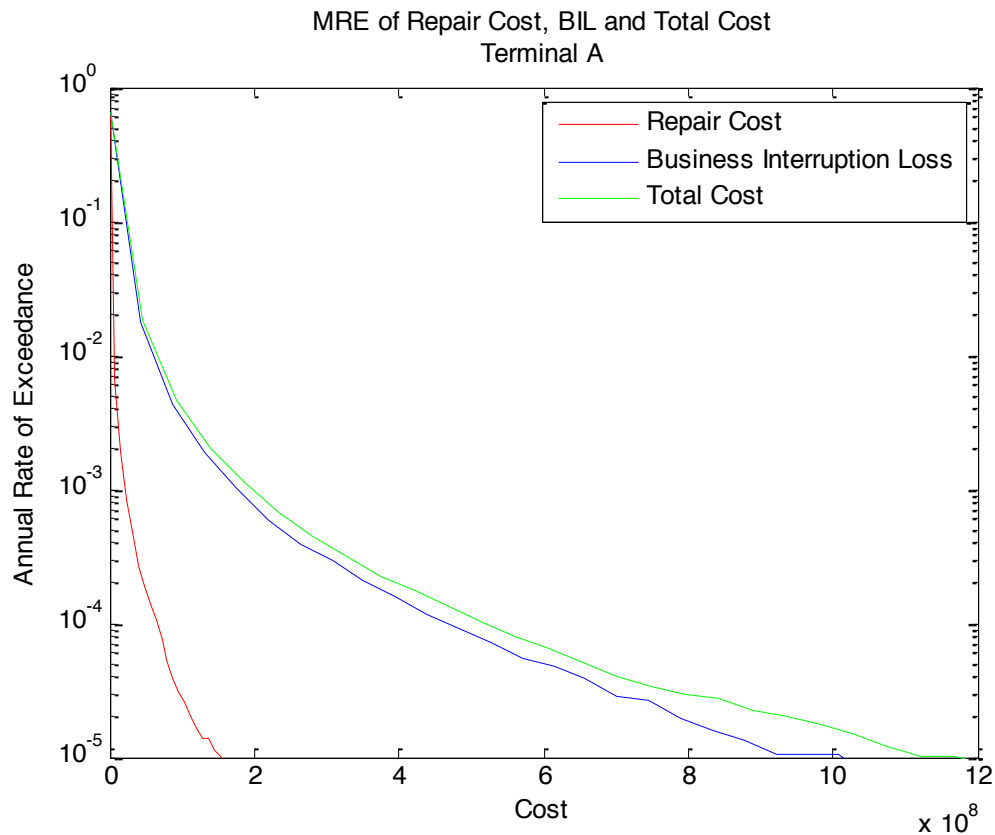


Figure 4.18 – Comparison of RC, BIL, and TC Exceedance Curves: Terminal A

When these costs are compared simultaneously (Figure 4.18) the MRE curves confirm that business interruption losses make up the majority of the total cost (as discussed in 4.3.1.3). This figure only shows a comparison of Terminal A, but the remainder of the terminals plot in the same manner. Notice how at larger annual rates of exceedance and smaller costs the total cost and BIL curves are nearly equal. Only as the exceedance rates decrease and the repair cost grows larger does an apparent separation grow between total cost and BIL.

4.4.2.1 Repair Cost Exceedance Curves

The following curves compare repair costs among the port terminals:

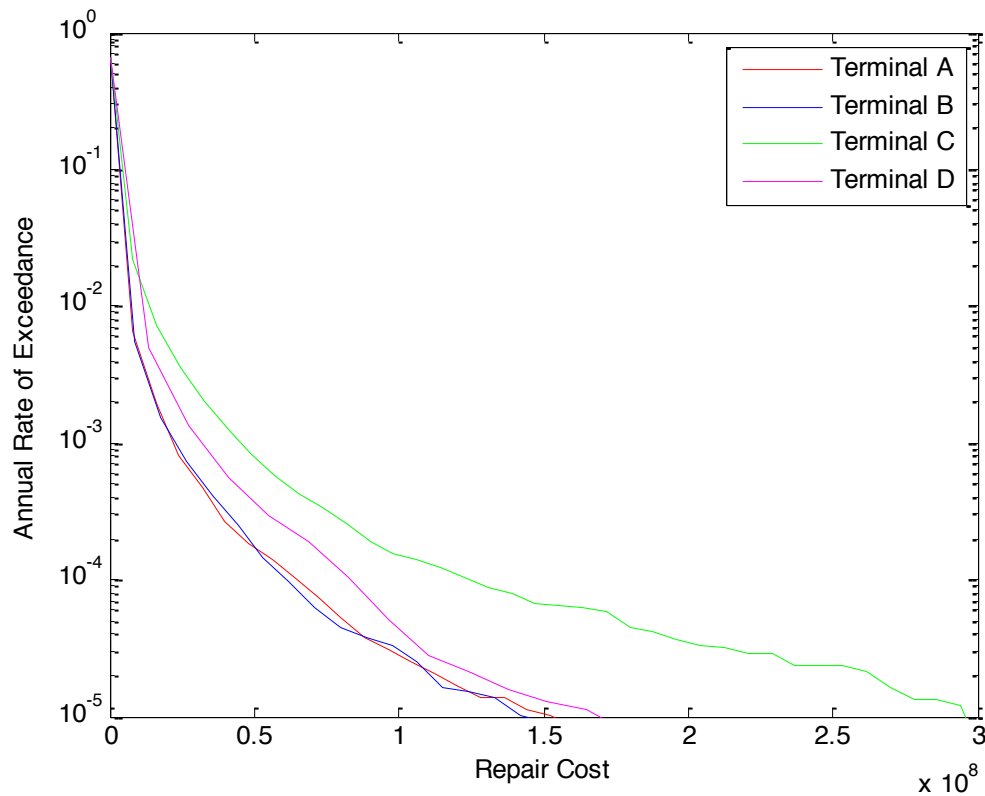


Figure 4.19 - Repair Cost Exceedance Curves: All Terminals

Repair cost exceedance rates vary by terminal. For instance in Figure 4.19 if the exceedance rates are compared at a repair cost of $1 \times 10^8 = \$100,000,000$, Terminal C has the smallest annual rate of exceedance at about 9×10^{-4} , Terminal D is next at 6×10^{-5} , and Terminals A and B are nearly equal at about 7×10^{-5} . In terms of return periods, a \$100,000,000 repair cost has an expected return period of 90000 years at Terminal C, 600000 years at Terminal D, and 700000 years at Terminals A and B. Using this logic with respect to repair costs, Terminal C is the most vulnerable, followed by terminal D, and then Terminals A and B. This result makes sense because wharf repair costs make up the majority of the total repair costs and the order of vulnerability also corresponds with the order of berth length from longest to shortest.

4.4.2.2 Business Interruption Loss Curves

Next the exceedance curves for business interruption losses were plotted for all terminals in Figure 4.20:

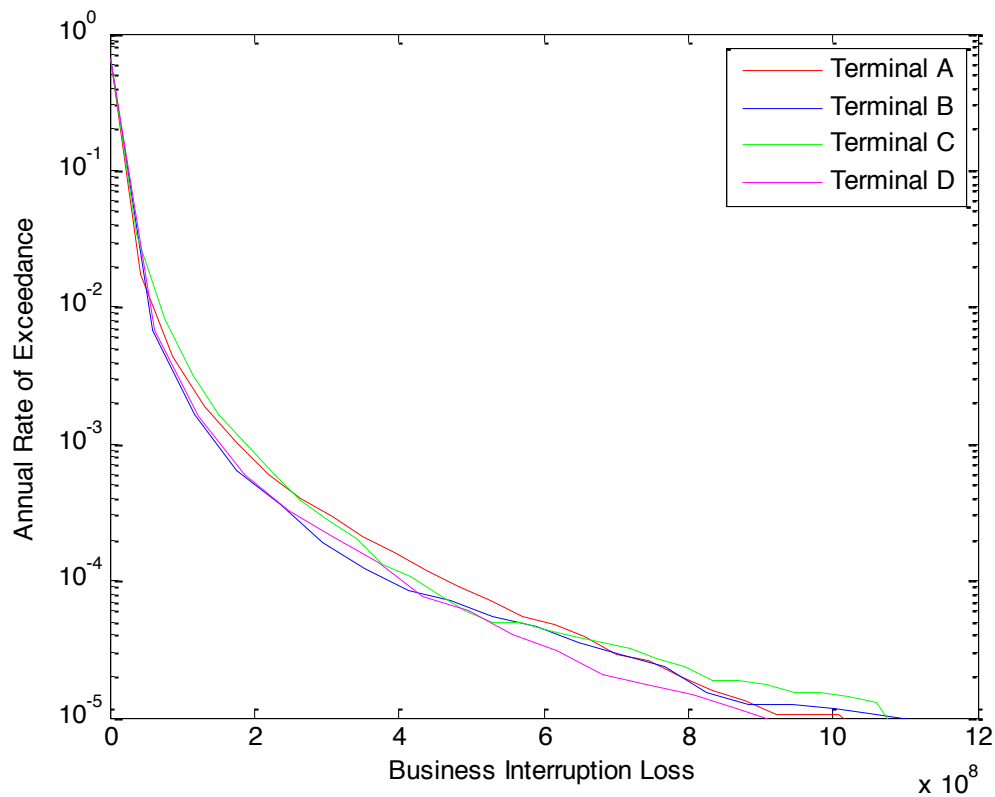


Figure 4.20- Business Interruption Loss Exceedance Curves: All Terminals

Unlike repair costs, vulnerability in terms of business interruption losses by terminal would be ordered: C, A, D and B. As described in Section 3.6, the BIL magnitude is dependent on wharf repair time, berth length, crane repair time and number of cranes, with wharf repair time being the most dominant variable. Terminal C has the highest annual rates of exceedance most likely because it is the longest berth, which means it also has the smallest inter-arrival time. Table 4.7 shows the mean inter-arrival times for each terminal calculated for the current data:

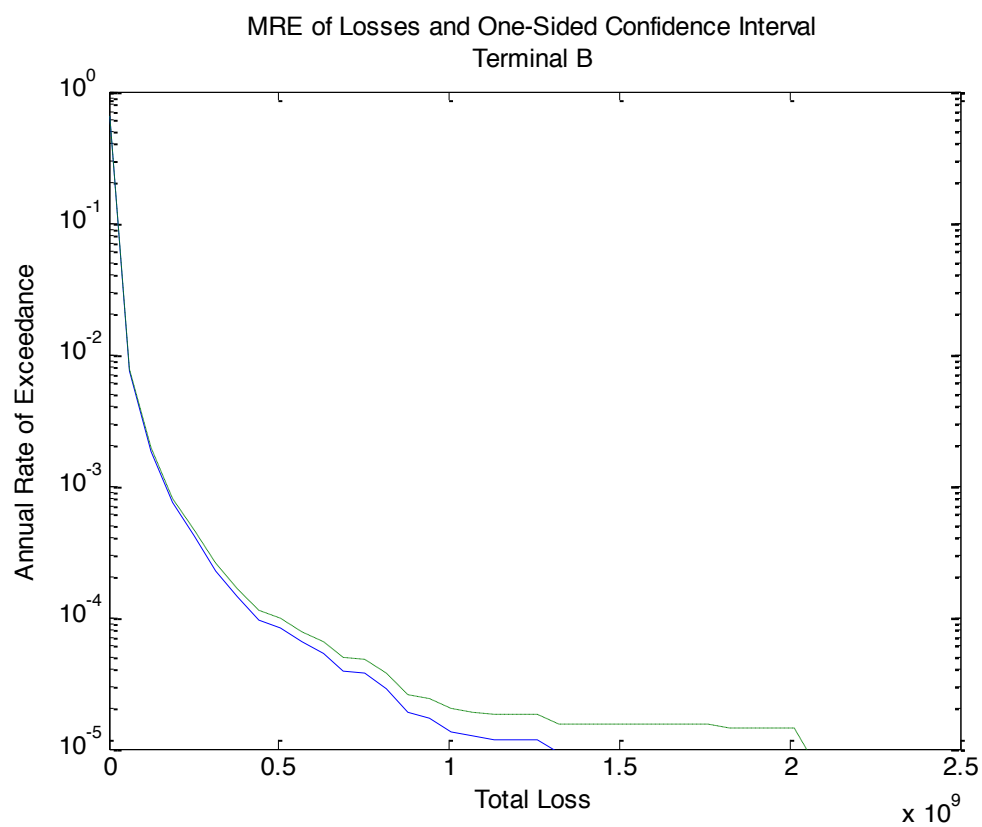
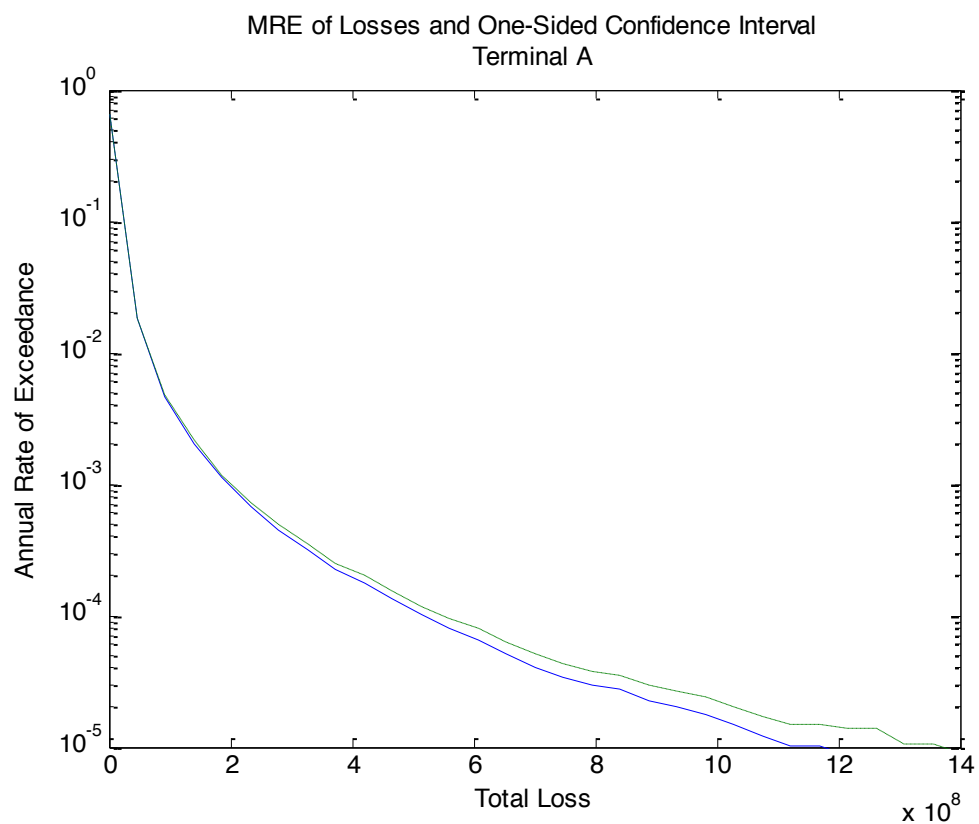
Table 4.7 – Mean Inter-arrival Times for All Terminals

Terminal	Length (ft.)	Mean Inter-Arrival Time (days)
A	2400	2.38
B	2400	2.38
C	5400	0.91
D	3600	1.47

Since more ships arrive at Terminal C as compared to any other, very large BILs can be more easily reached (i.e. larger exceedance rate) because more ships will be displaced during extreme damage. The second largest BIL is at Terminal A, which incidentally is the shortest terminal (equal to B). This terminal has high BILs because it has the most vulnerable crane type. At Terminal A, ships cannot be serviced because there are few available cranes for loading/unloading. Terminals D and B have nearly identical BILs. Each of these terminals contains the same crane type and has similar inter-arrival times.

4.4.2.3 Total Cost Curves

It is of no surprise that the exceedance curves for total cost have the same terminal vulnerability order as BIL since total cost is dominated by the business interruption loss. Figure 4.21 separates the total loss curves for each terminal and shows the mean MRE and a one-sided 90% confidence interval. Notice that the variance is small for all rates of exceedance, even the very small rates.



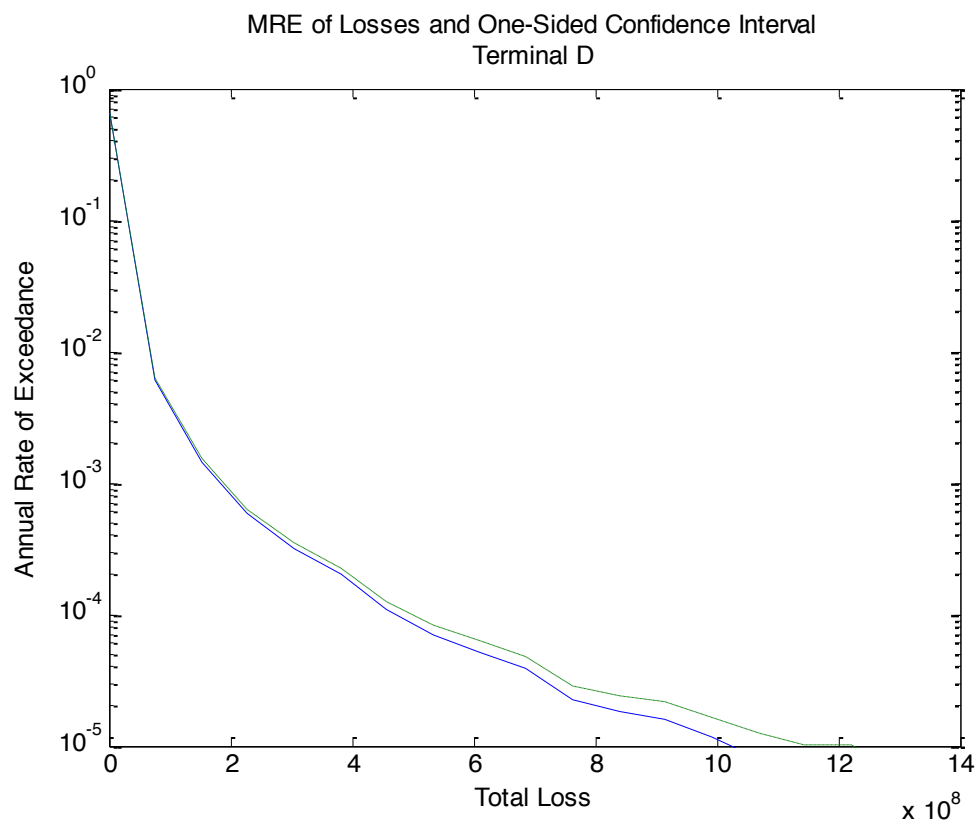
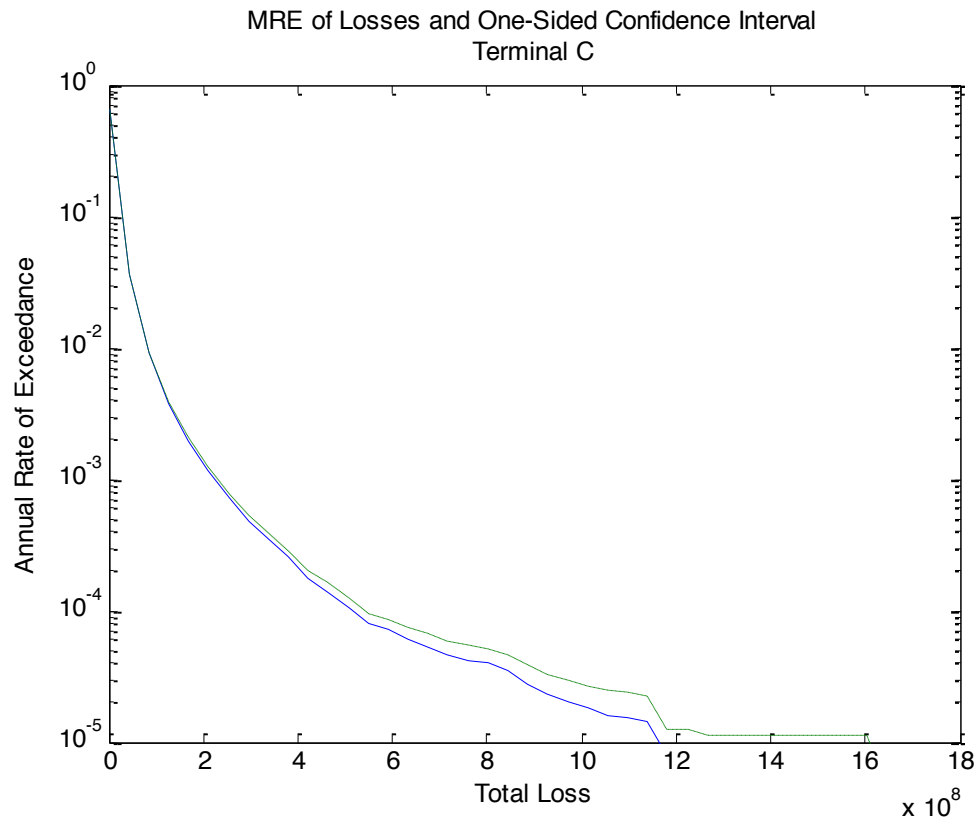


Figure 4.21 – MRE of Total Losses and One-sided Confidence Intervals: All Terminals

4.4.3 Sample Summary Statistics

As described in Section 3.7.2, the mean loss, variance of the mean, and sample variance of the earthquake sample can be calculated from the data. The following summary statistics were calculated for the baseline run: sample mean, variance of sample mean (with 90% confidence intervals), and variance of sample. Each is plotted in the figures below. Note that the variance of the mean is very small as compared to the variance of the sample.

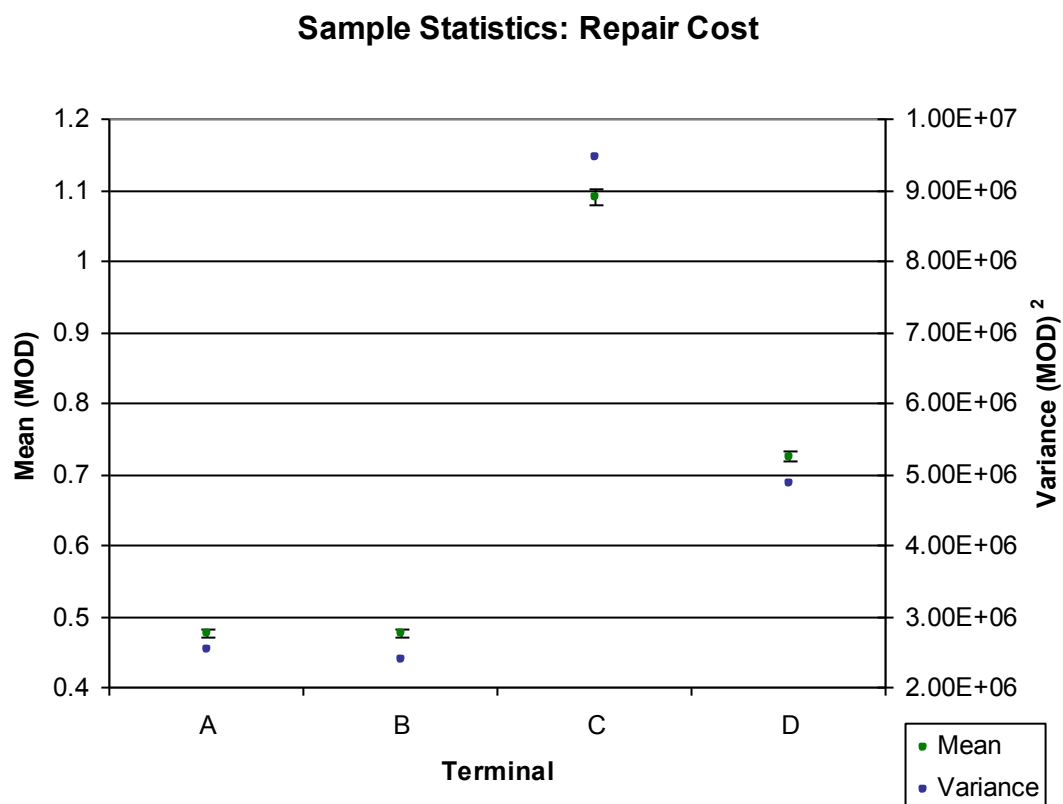


Figure 4.22 – Summary Statistics: Repair Cost

Sample Statistics: Business Interruption Loss

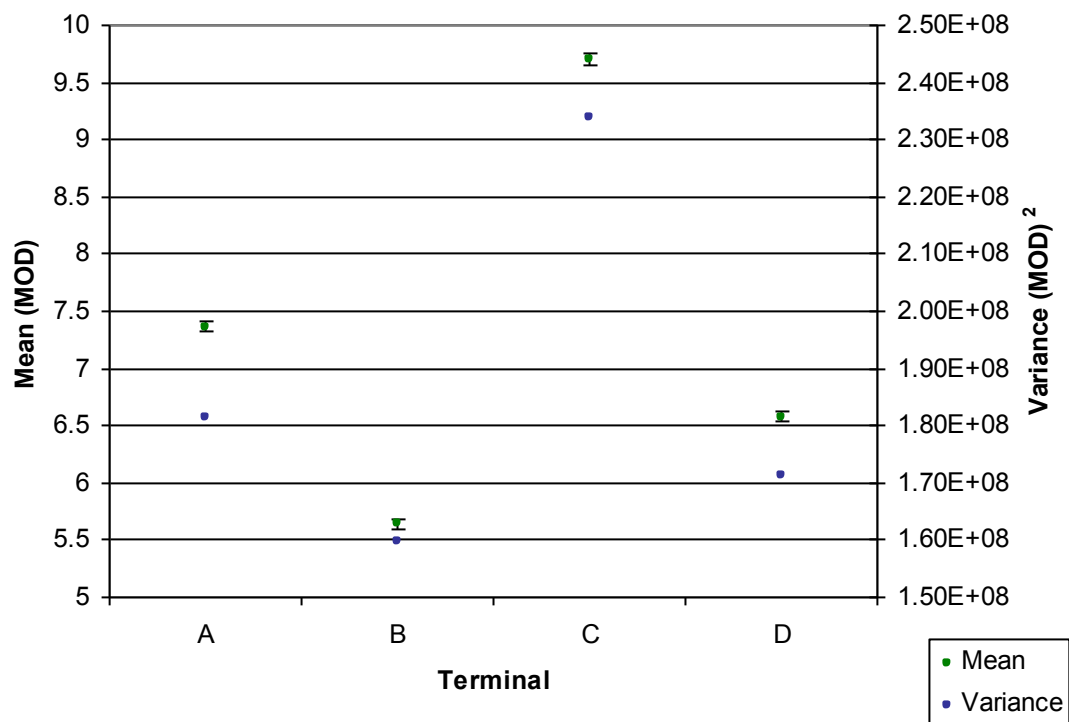


Figure 4.23 – Summary Statistics: Business Interruption Loss

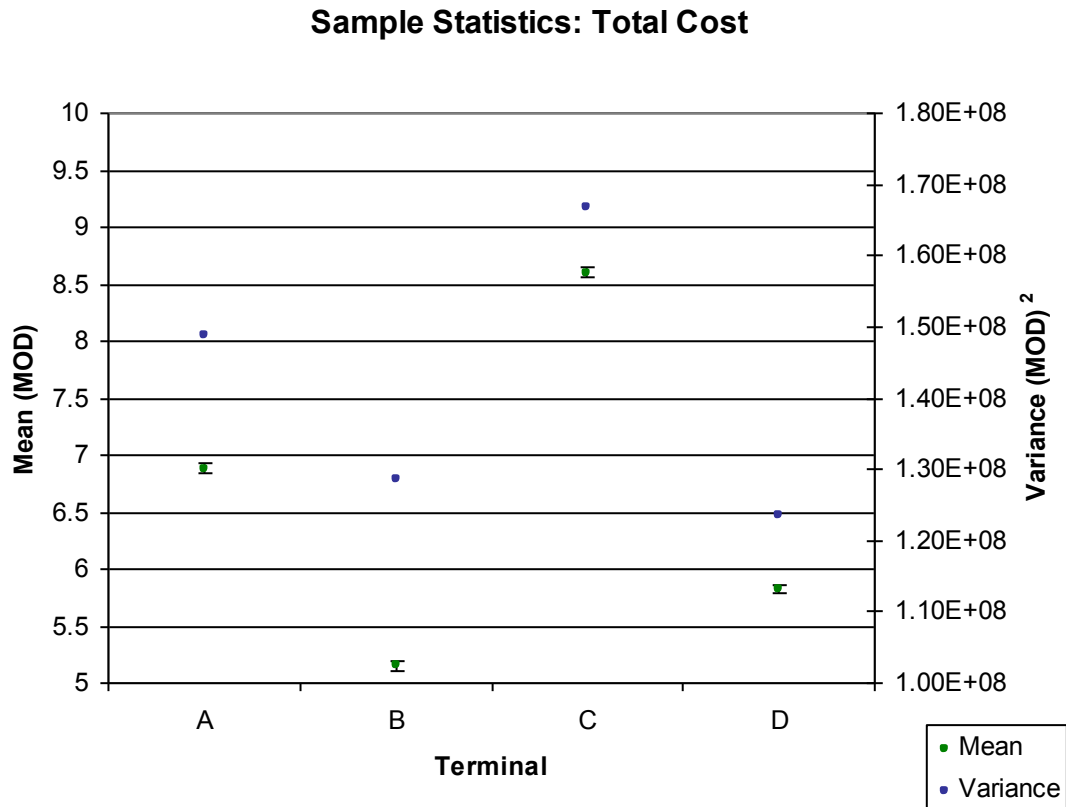


Figure 4.24 – Summary Statistics: Total Cost

4.4.4 Exceedance Curve Sample Calculations

Exceedance curves are particularly useful because they can be used to extract basic information about the port that is valuable to port stakeholders. The subsequent sections give examples of three calculations that can be made using exceedance curves and summary statistics: finding the probability of a specific loss over some exposure period, finding the loss associated with a specific return period, and finding the mean, variance, and confidence interval of the loss over some exposure period.

4.4.4.1 Probability of a Specific Loss

This example will calculate the probability of exceeding a total loss of \$200,000,000 over an exposure time of 20 years at Terminal A. To find the mean rate of exceeding the loss at Terminal A, the exceedance curve for total losses at Terminal A will

be used. The mean rate of exceedance can be found from this graph by finding the MRE associated with a loss of \$200,000,000 (Figure 4.25). For this example the $\lambda(\text{Total Loss} = \$200,000,000) = 0.01$. The probability that the loss exceeds \$200,000,000 over a 20 year time period $= 1 - e^{-\lambda t}$. So,

$$P[TL > \$200,000,000, t = 20 \text{ years}] = 1 - e^{-\lambda t} = 1 - e^{-0.001*20} = 0.0198 = 2\% .$$

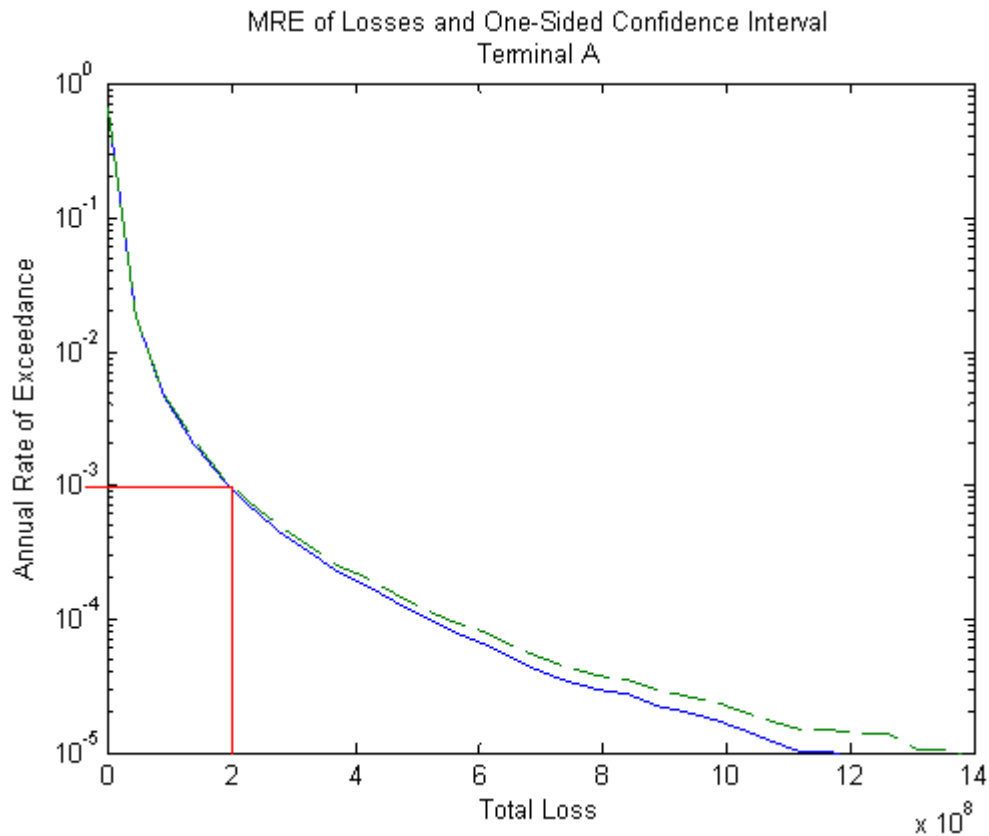


Figure 4.25 - Finding the Probability of Exceeding a Specific Loss

4.4.4.2 Loss Associated with a Specific Return Period

Port stakeholders might also be interested in finding the loss associated with a specific return period. For instance, the Port of Los Angeles uses the operating level return period of 72 years as a design measure for seismic hazards. The mean rate of exceedance associated with this return period (λ) $= 1/72 = 0.014$. To find the loss associated with this MRE at the hypothetical port at Terminal A, one would simply find

the loss associated with that specific MRE in the total loss exceedance curve (Figure 4.26). From the figure the associated loss equals approximately 0.5×10^8 , or \$50,000,000. Calculations such as this are especially useful in determining the kind of impact of a particular return period on the actual port components. For instance, in this case, calculating an actual loss for the OLE is more revealing to the earthquake's actual effect at the port than stating that no major disruption is anticipated at this level, which is typical of current practice.

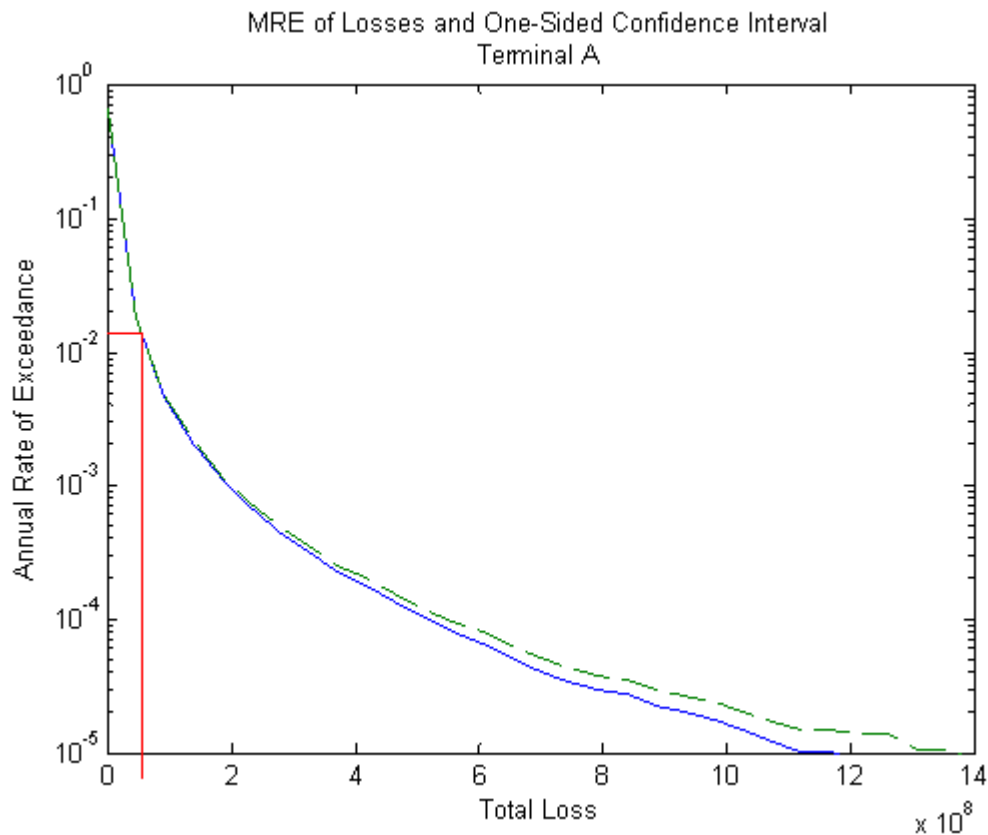


Figure 4.26 - Finding the Loss Associated with a Specific Return Period

4.4.4.3 Exposure Time Calculations

The last example uses the summary statistics (which can be calculated from the exceedance curves) to calculate the net present value of the mean, variance, and confidence intervals over some exposure time. If the mean, variance and confidence

intervals were to be calculated for the 20-year exposure time used in the first example, supposing that a conservative discount rate of 5% is used, and noting that the starting summary statistics are currently calculated in 2009 dollars, the sample mean in for the 20-year exposure time would be calculated using the following equation:

$$mean = mean_{2009} * \frac{1 - (1 + discount_rate)^{-exp_osure_time}}{discount_rate} \quad (4.2)$$

$$mean = mean_{2009} * \frac{1 - (1 + 0.05)^{-20}}{0.05} = mean_{2009} * 12.4622 \quad (4.3)$$

Likewise, the variance would be calculated as:

$$variance = variance_{2009} * \frac{1 - (1 + discount_rate)^{-2*exp_osure_time}}{discount_rate/(2 + discount_rate)} \quad (4.4)$$

$$variance = variance_{2009} * \frac{1 - (1 + 0.05)^{-2*20}}{0.05/(2 + 0.05)} = variance_{2009} * 35.1716 \quad (4.5)$$

Therefore the summary statistics for total cost for a 20-year exposure time would be:

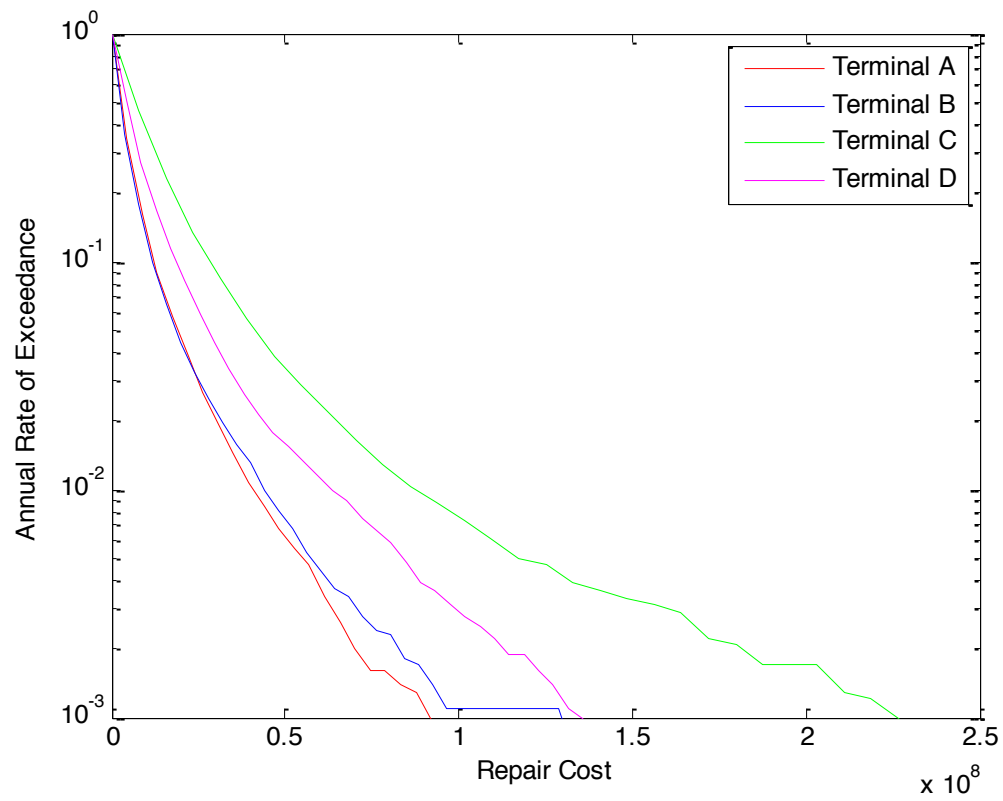
Table 4.8 – Summary Statistics for Exposure time of 20 years

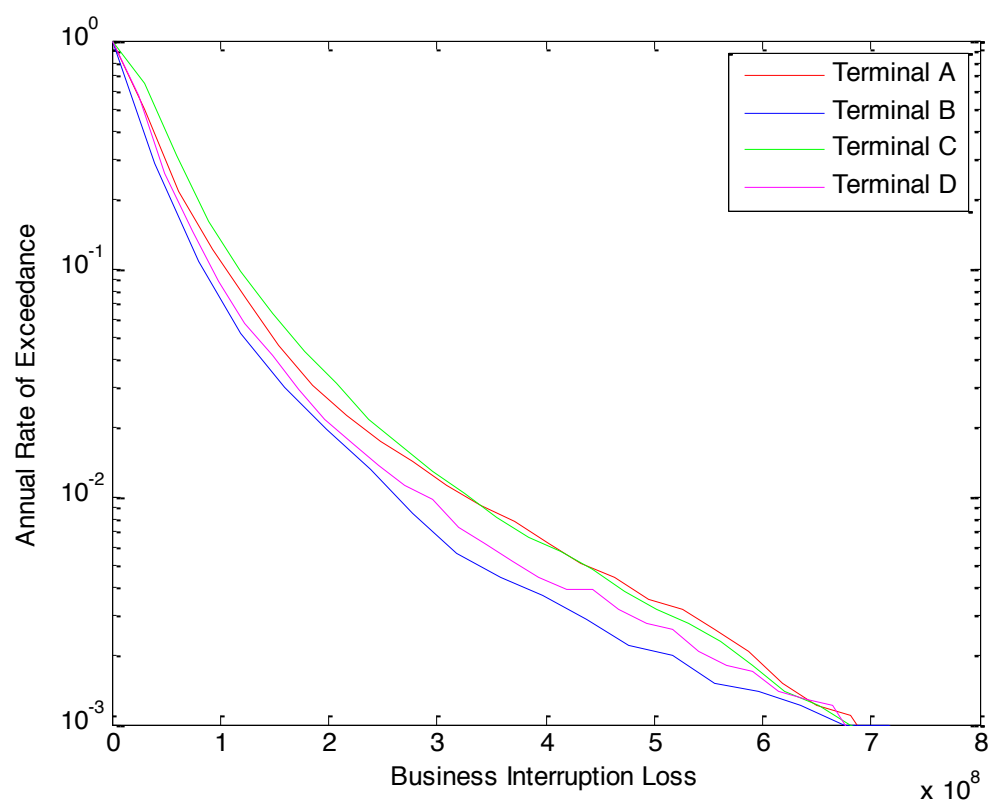
	Total Cost at Each Terminal			
	A	B	C	D
Sample mean (\$)	5.08E+07	4.11E+07	9.16E+07	5.64E+07
Variance of Mean (\$)²	1.91E+10	1.53E+10	6.09E+10	2.90E+10
CI 90% (\$)	5.05E+07	4.09E+07	9.12E+07	5.61E+07
	5.10E+07	4.13E+07	9.20E+07	5.67E+07

4.5 Scenario-Based Analysis Results

The scenario-based run on the hypothetical port tested within the risk analysis framework was modeled after the earthquake event in Port-au-Prince, Haiti in 2010. The specifics of the scenario modeled were a 10000-earthquake sample of ruptures with a

mean magnitude of 7.0 and COV of 0.2 at a distance 20-25 km from the source zone. That specific scenario produced the following repair cost, business interruption loss and total cost exceedance results (Figure 4.27):





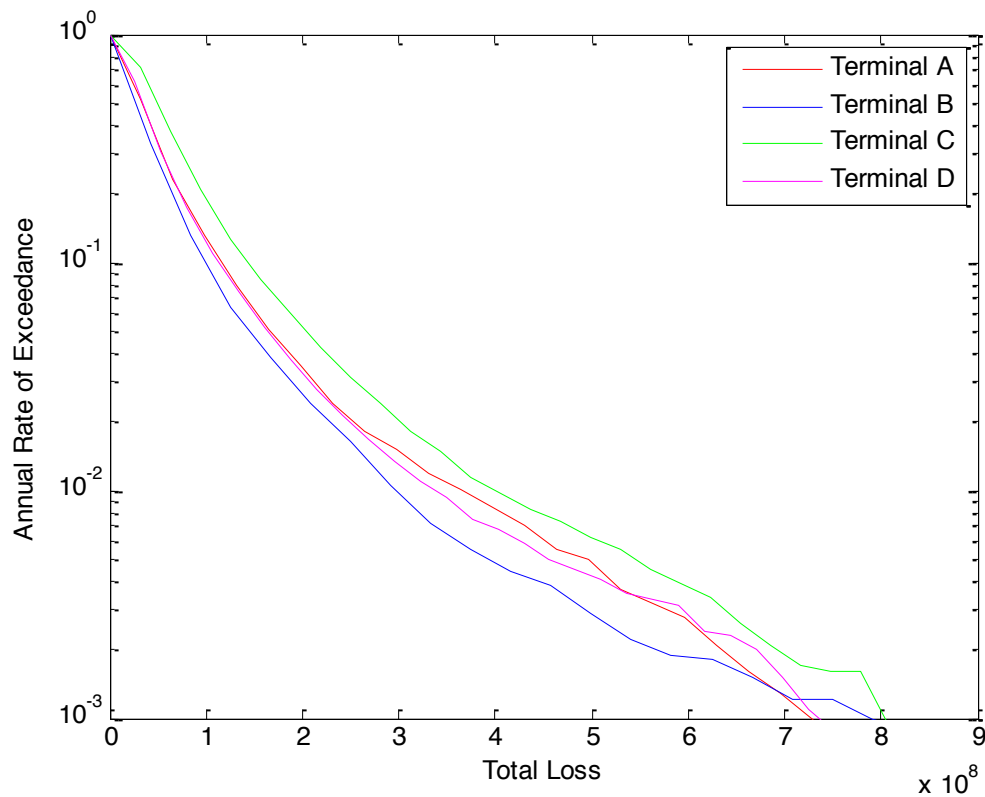


Figure 4.27 – Exceedance Results for Scenario-based example run a.) Repair Cost, b.) Business Interruption Loss, and c.) Total Loss

Exceedance curves plot as expected. Total repair costs were smaller than business interruption losses, and the orders of vulnerability of each terminal for each type of loss was consistent with what was seen for the corresponding exceedance rates in the fully probabilistic hazard method. Perhaps more enlightening for this specific type of hazard scenario are the mean annual losses calculated for the specific scenario. The mean annual losses give an estimation of the extent of damage expected at the hypothetical port if an earthquake the magnitude and distance of the 2010 Haiti earthquake were to occur. Figure 4.28 plots the mean annual loss, standard deviation of the mean, and sample variance for the scenario-based run.

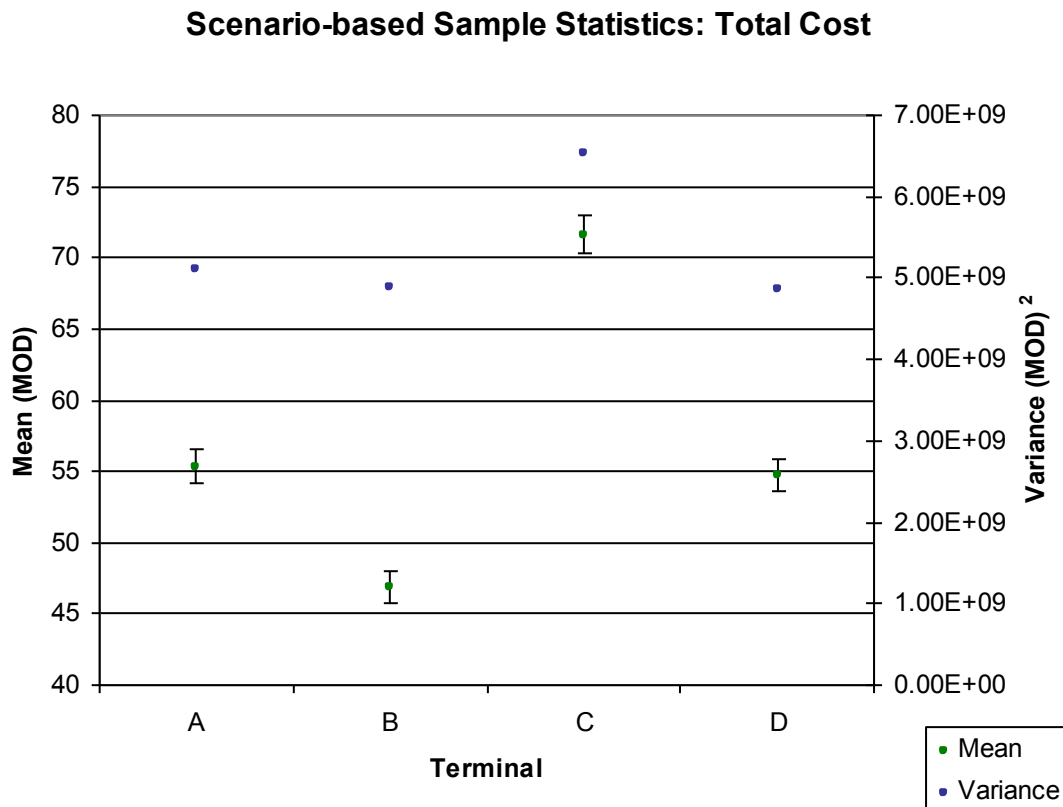


Figure 4.28 – Sample Statistics of Scenario-Based Run: Total Cost

The mean total loss at each terminal ranges between \$45-75 million dollars, with Terminal C having the highest mean and Terminal B the lowest. If an earthquake the size of the 2010 Haiti earthquake were to occur at the hypothetical port in Santa Cruz California, the mean total cost to completely repair the port would equal approximately \$229 million dollars.

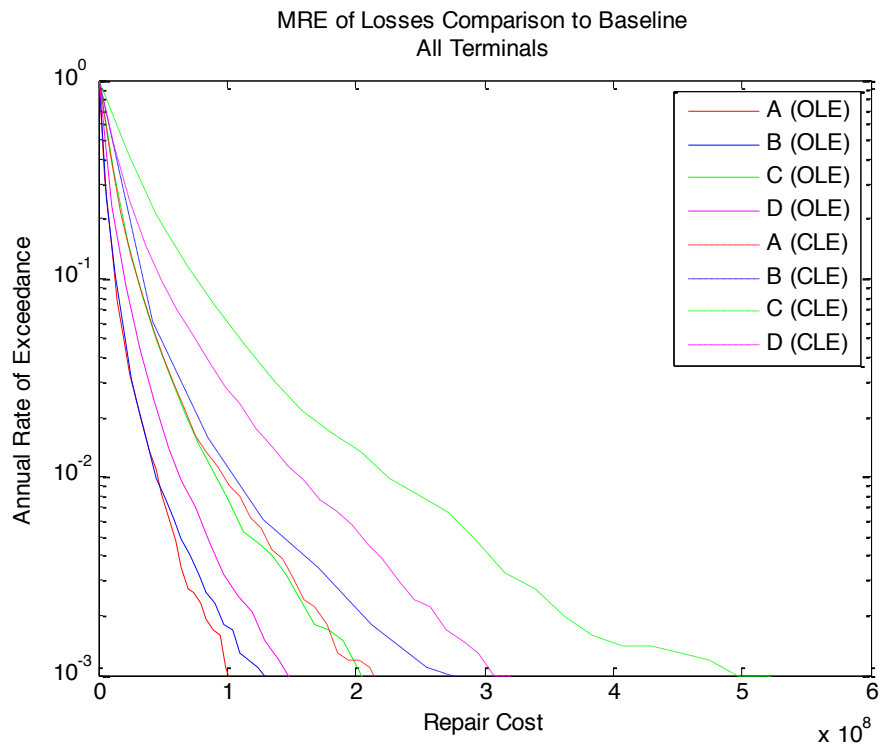
4.6 Intensity-Based Analysis Results

The intensity-based runs tested within the risk analysis framework correspond to the operating level and contingency level design earthquakes used at the Port of Los Angeles. The specific inputs for each of the scenarios can be found in Table 4.9.

Table 4.9 - Intensity Based Scenario Inputs

Earthquake	Intensity Measure	IM Value	COV	# of EQs in Sample
OLE	PGV	15 cm/s	0.2	10000
CLE	PGV	42 cm/s	0.1	10000

By using the OLE and CLE it is possible to test if the hypothetical port meets the Port of Los Angeles design requirements that no interruption occur for the OLE and an acceptable amount of disruption occur after the CLE. The following figures plot the exceedance values for repair cost, business interruption loss, and total loss (Figure 4.29):



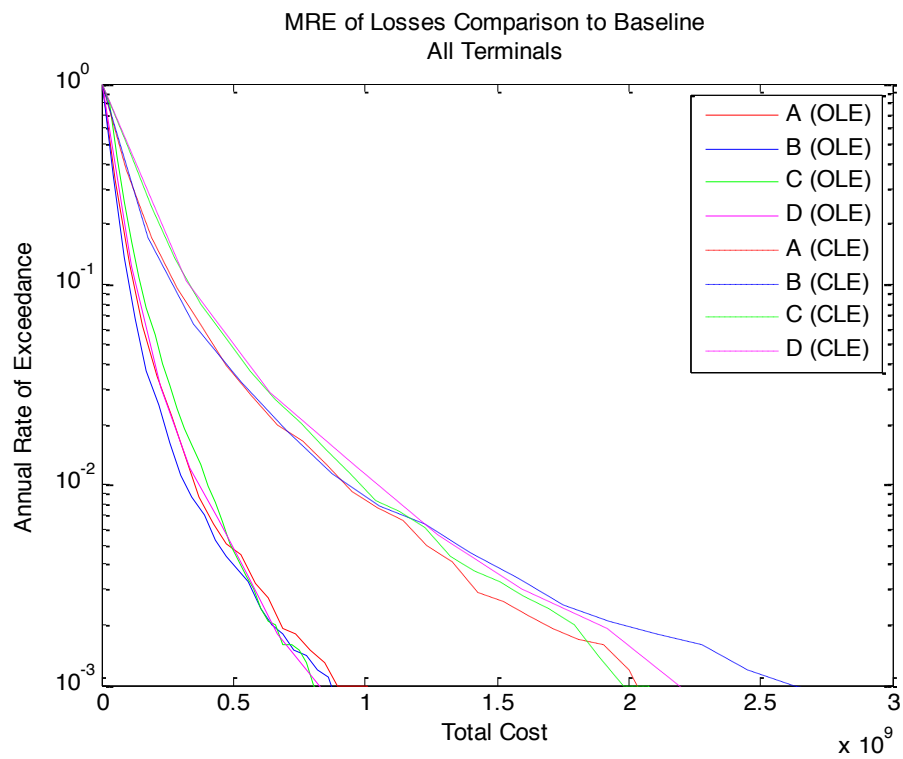
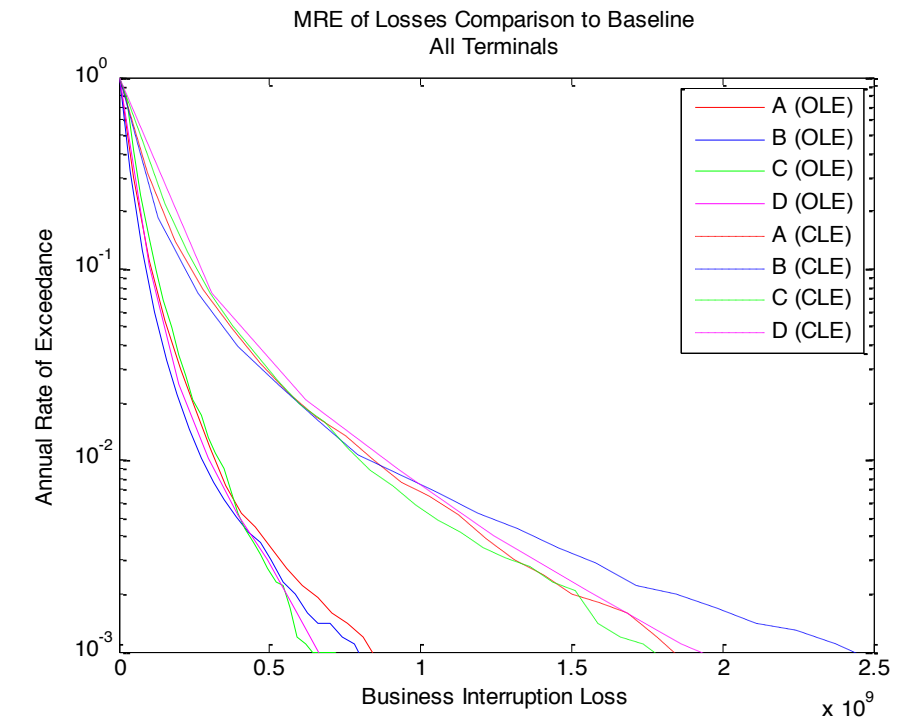
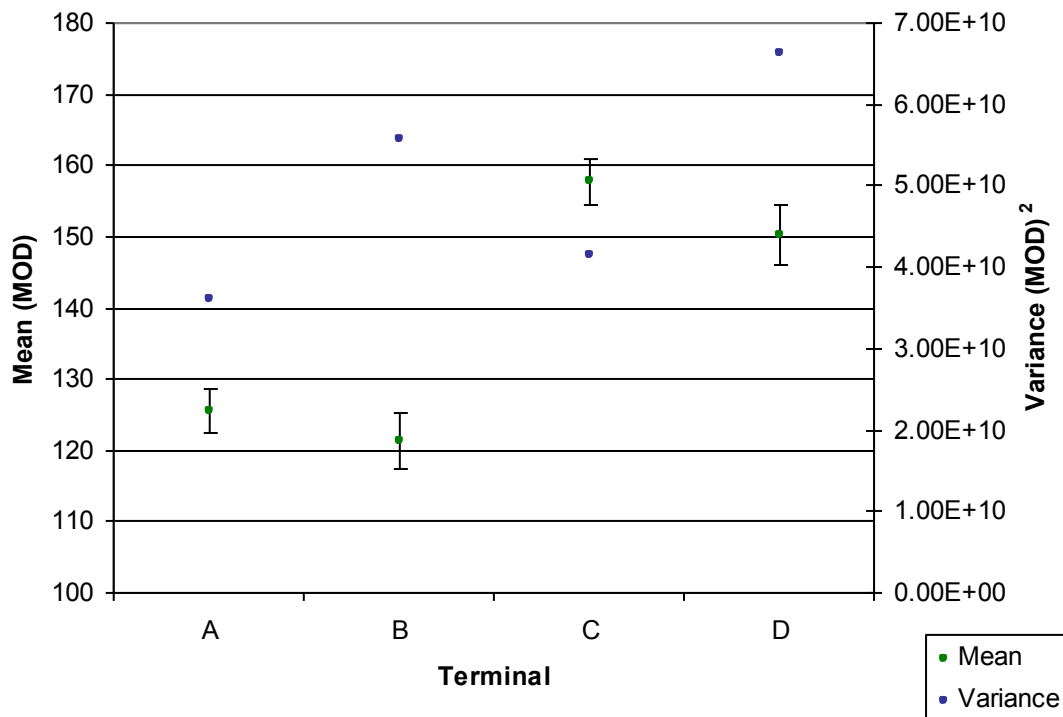


Figure 4.29 – Exceedance Results for OLE and CLE example runs a.) Repair Cost, b.) Business Interruption Loss, and c.) Total Loss

From the figures it is possible to see that the loss incurred from the OLE are much less than those from the CLE (which is expected), but both still produce rather large losses. After the OLE, the port should still be operational, but from the business interruption loss exceedance curve one can see that losses range anywhere from \$10 to \$800 million dollars. Losses that high indicate that the port is not continuing on with “normal operation”. This fact is further proved by the mean annual losses calculated for each scenario Figure 4.30:

OLE Sample Statistics: Total Cost



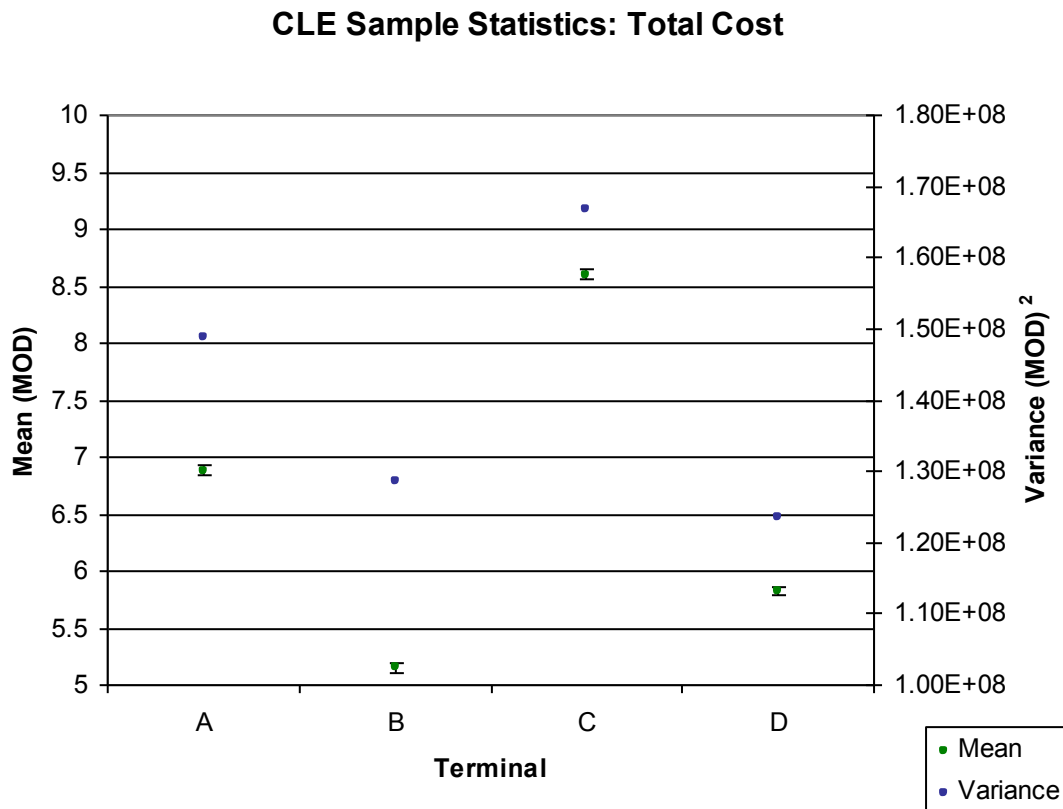


Figure 4.30 – Sample Statistics of OLE and CLE Run: Total Cost

The mean annual losses for the OLE range from \$50 – \$75 million dollars while mean losses for the CLE range from \$125-\$160 million dollars. Both of these mean total losses would indicate that extensive damage has occurred within the hypothetical port, much more than designed for according to the standards. The mean maximum repair times for the wharf and crane for each scenario further confirm this result (Table 4.10):

Table 4.10 – Mean Maximum Repair Times for OLE and CLE

	OLE		CLE	
	Wharf (days)	Crane (days)	Wharf (days)	Crane (days)
A	198	17	372	131
B	201	29	381	168
C	273	4	577	80
D	235	36	470	218

For the OLE scenario, it takes Terminal A 6.5 months to fully recover, Terminal B - slightly under seven months, Terminal C - nine months, and Terminal D – almost eight months. These repair times further indicate that the OLE would cause significant interruption within the hypothetical port. The CLE repair times are even larger so their interruption is also larger. If the hypothetical port was being tested to the standards of the Port of Los Angeles, it would need to be redesigned to reduce the physical repairs and downtime resulting from both the OLE and CLE.

4.7 Sources of Uncertainty

The risk analysis framework is fully probabilistic, which dictates that multiple sources of uncertainty are built into the framework as a whole. In an attempt to ascertain the sources of the largest uncertainties, four possible sources were identified: uncertainty associated with the ground motions, uncertainty associated with the calculated repair requirements of the crane, uncertainty associated with the calculated repair requirements of the wharf, and uncertainty within the operational regression model. The variations associated with each source were compared by conducting a series of risk analysis framework runs in which each source was isolated. The runs conducted within this analysis were as follows:

Table 4.11 – Description of Uncertainty Runs

Run	Isolated Source of Uncertainty	Description
1	None	Use the mean of all sources of uncertainty
2	Ground Motion	Allow uncertainty within ground motions
3	Spatial Correlation	Allow uncertainty within ground motions but neglect spatial correlation, allow uncertainty in all other sources
4	Crane Repair Requirements	Allow uncertainty when calculating crane repair cost and time
5	Wharf Repair Requirements	Allow uncertainty when calculating wharf repair cost and time
6	Operational Regression	Allow uncertainty when calculating TEU Loss from linear operational regression model.

4.7.1.1 Control: Using the Mean of All Sources of Uncertainty

To compare the sources of uncertainty, a “control” run had to be created where all examined sources of uncertainty were removed. Sources of uncertainty included were: ground motions, crane repair requirements, wharf repair requirements, and the operational regression. For this run for each source, the following means were employed:

- 1.) Ground Motions – The mean of the ground motions was considered as using only the arithmetic mean (\bar{Y}_{jk}) in the ground motion equation:

$$\ln(Y_{jk}) = \ln(\bar{Y}_{jk}) + \varepsilon_{jk} + \eta_k$$
 . For the true mean the inter- and intra-event residuals were neglected. However, an additional run will be conducted that examines only neglecting the spatial correlation in the residuals as compared to a baseline run.

- 2.) Crane and Wharf Repair Requirements – The mean of the repair requirements was calculated by using only the mean cost and mean time for chosen damage states when calculating repair requirements. Normally, repair requirements are chosen randomly from a lognormal distribution using the mean and a sigma value equal to the covariance matrix conditional on the specified values of intensity measures.
- 3.) Operational Regression – The multivariate regression equation that calculates the number of TEUs lost for specific damage scenarios is a mean value that is sampled as a lognormal distribution over a sigma value equal to the error associated with the equation. To make this value a mean the figure calculated from the equation is simply used and the error is ignored.

Figure 4.31 plots the MRE for total cost for a baseline run and a run only using mean values for all uncertainty sources for every terminal in the hypothetical port.

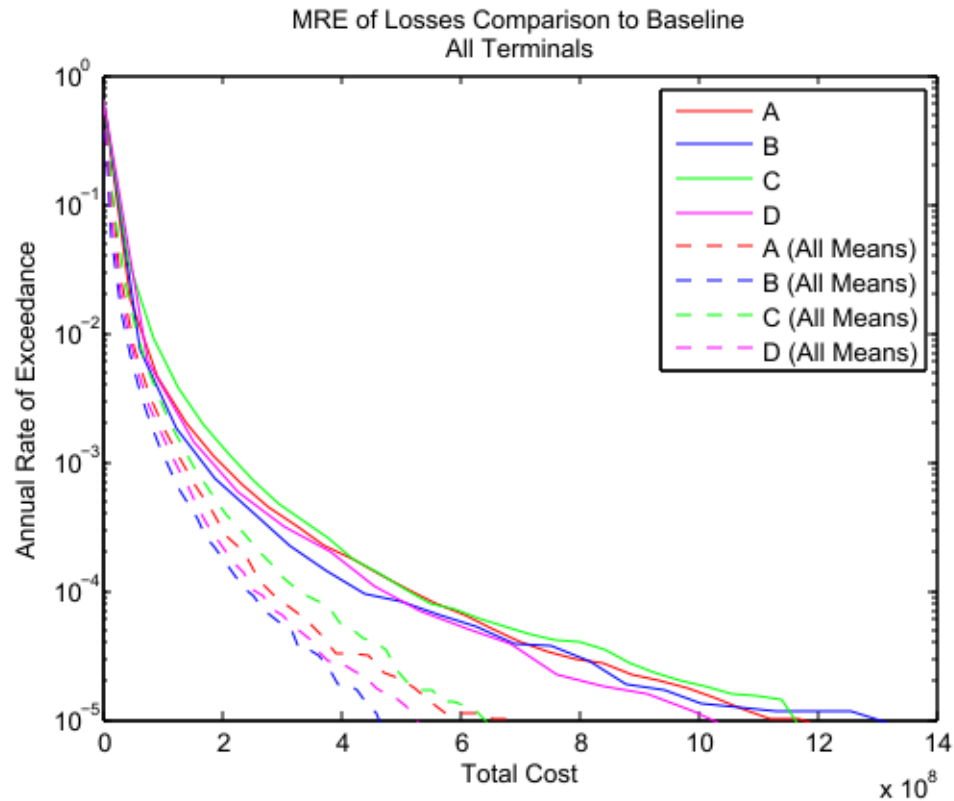


Figure 4.31 – Total Cost Uncertainty Comparison: Control – Using only Mean Values

Neglecting uncertainty significantly decreases the total cost values at equal rates of exceedance. All subsequent graphs will contain plots of each of these runs for reference. However, for ease of viewing and since the trends in every terminal are similar, all subsequent graphs will only plot comparison for Terminal A. Figure 4.40 plots total cost solely for Terminal A:

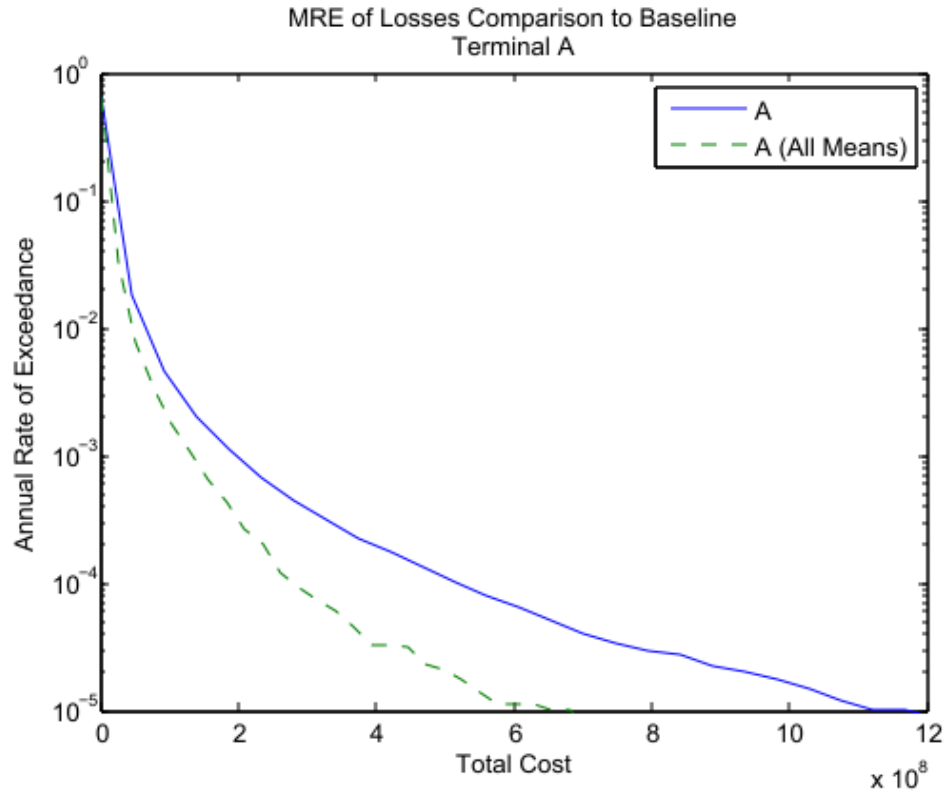


Figure 4.32 – Total Cost Uncertainty Comparison: Mean Values, Terminal A

The next figure (Figure 4.39) separates the components of total cost and plots repair cost and business interruption loss. Notice that the difference in cost between the all mean and baseline run is much smaller for repair cost than it is for business interruption loss.

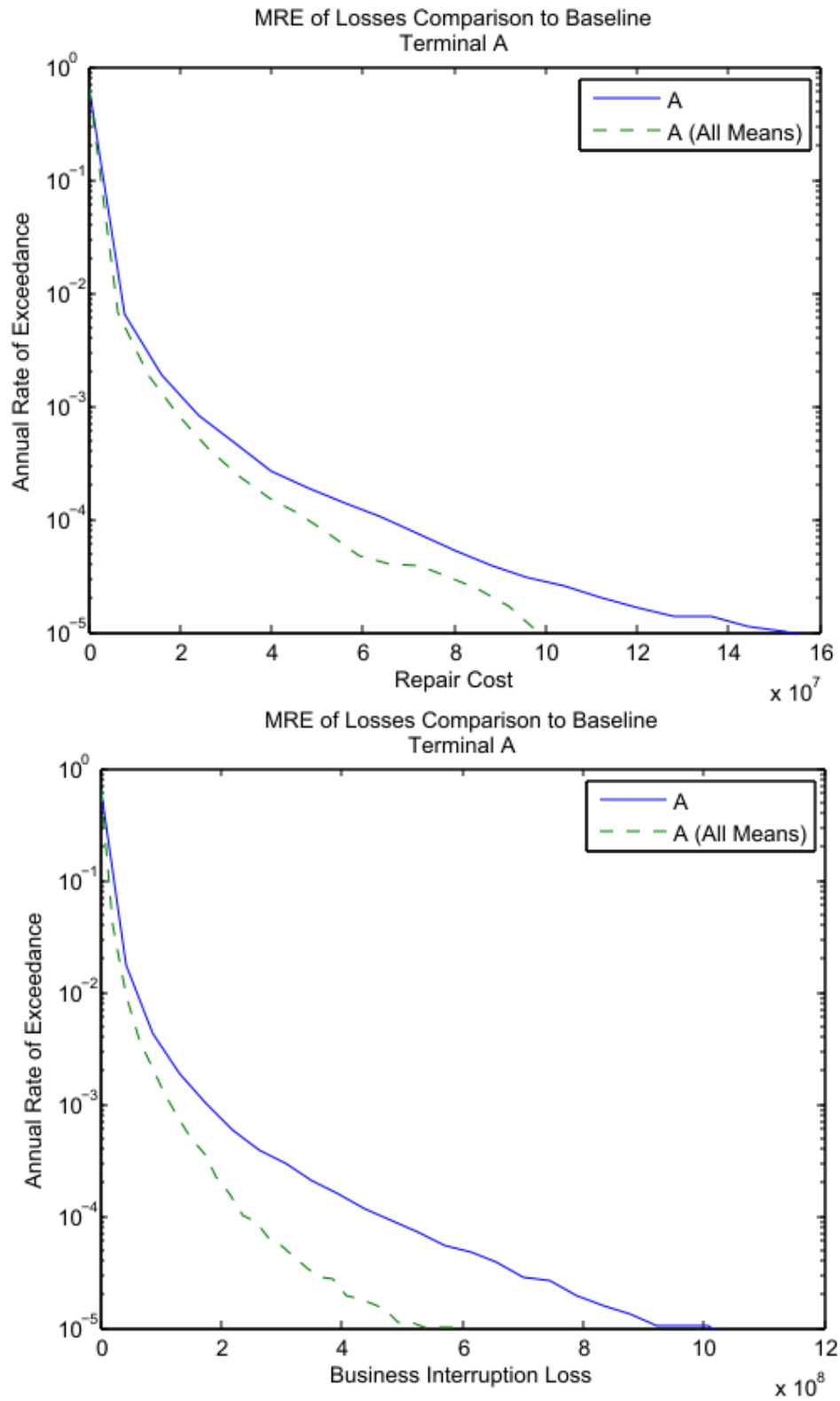


Figure 4.33 – a.) Repair Cost and b.) Business Interruption Loss Uncertainty Comparison: Mean Values, Terminal A

4.7.1.2 Ground Motion

The following section examines the effect of introducing uncertainty as developed from the ground motions into the calculation of total costs within the risk analysis program. Common convention dictates that a large amount of uncertainty can be associated with ground motions. The following run uses mean values for all uncertainty sources except for the ground motions, which are calculated in the same manner as in the baseline scenario. Figure 4.34 plots the MRE of total cost for the baseline, all means, and ground motion scenarios.

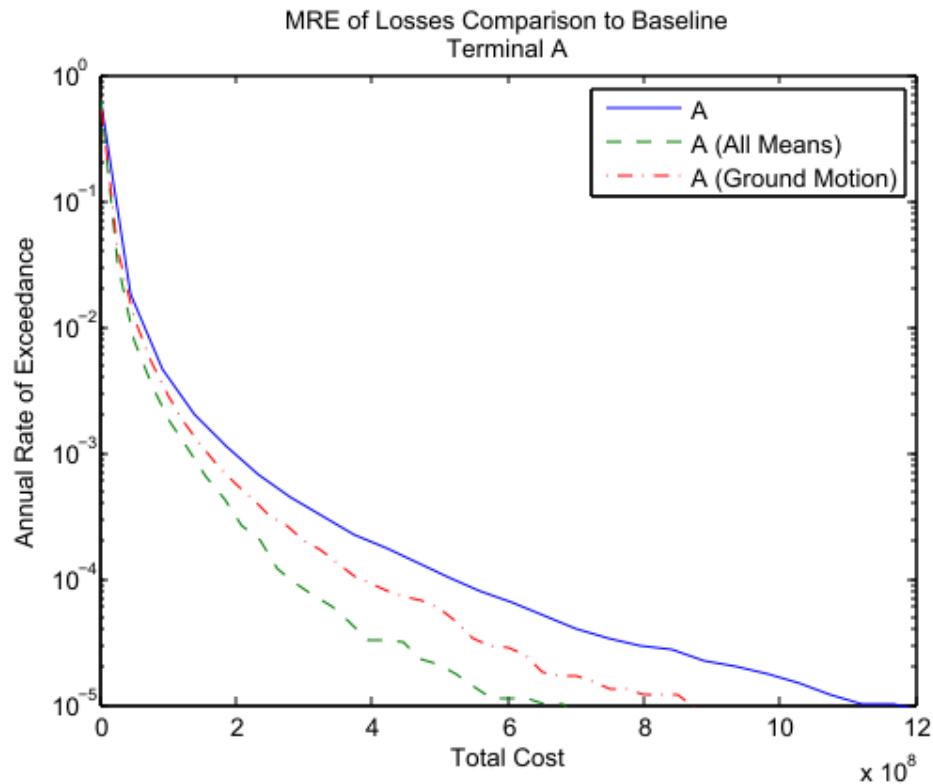


Figure 4.34 – Total Cost Uncertainty Comparison: Ground Motion

By adding uncertainty in with the ground motions it accounts for around 50% of the cost difference between the all means and baseline scenarios. The same can be seen for both the repair costs and business interruption losses (Figure 4.35):

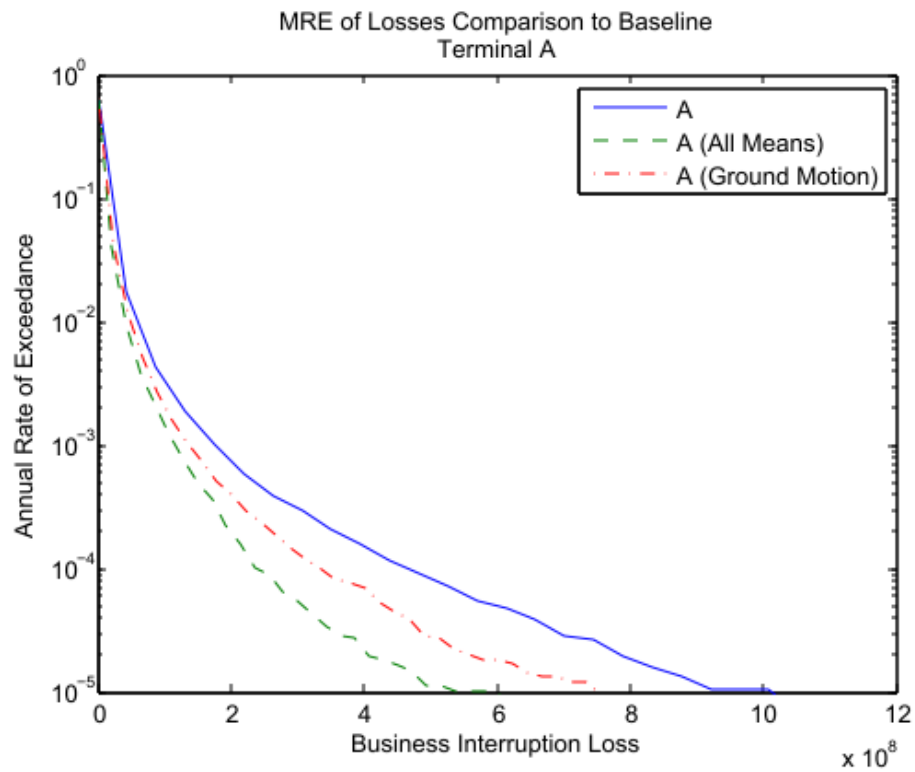
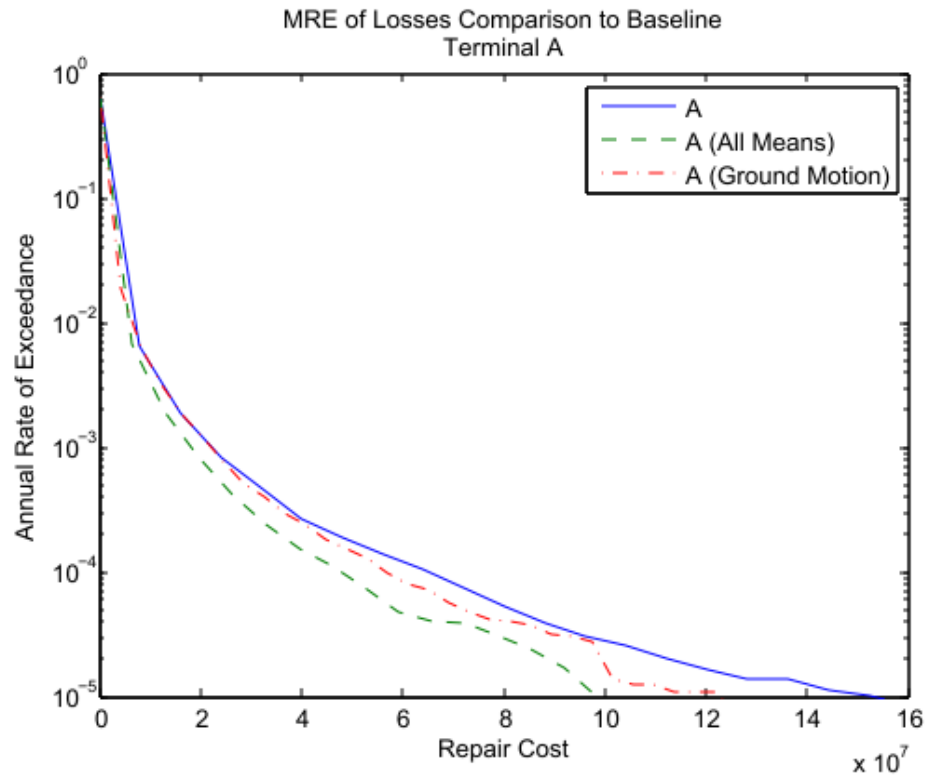


Figure 4.35 – a.) Repair Cost and b.) Business Interruption Loss Uncertainty Comparison: Ground Motion

4.7.1.3 Spatial Correlation

Park et al. (2007) showed that neglecting ground motion spatial correlation underestimated large losses and overestimated small losses in risk analyses. This statement was tested by neglecting spatial correlation within the calculation of the ground motion intensity measures in the risk analysis framework. The figures below (Figure 4.36 - Figure 4.37) plot the MRE curves that include and don't include spatial correlation. The reader should note that for all terminals, neglecting spatial correlation seemed to have little to no affect. Possible reasons for this is the small number of sites tested within the risk analysis framework. The Park study ran risk analyses that tested two portfolios of sites, one containing over 1,000 sites, and the other containing 133. The resulting MRE Loss curves produced for both portfolios displayed noticeable variations of losses for exceedance rates small than 10^{-3} . Since the hypothetical port only contains four sites, it is entirely possible that this sample was not large enough to properly capture the importance of ground motion spatial correlation.

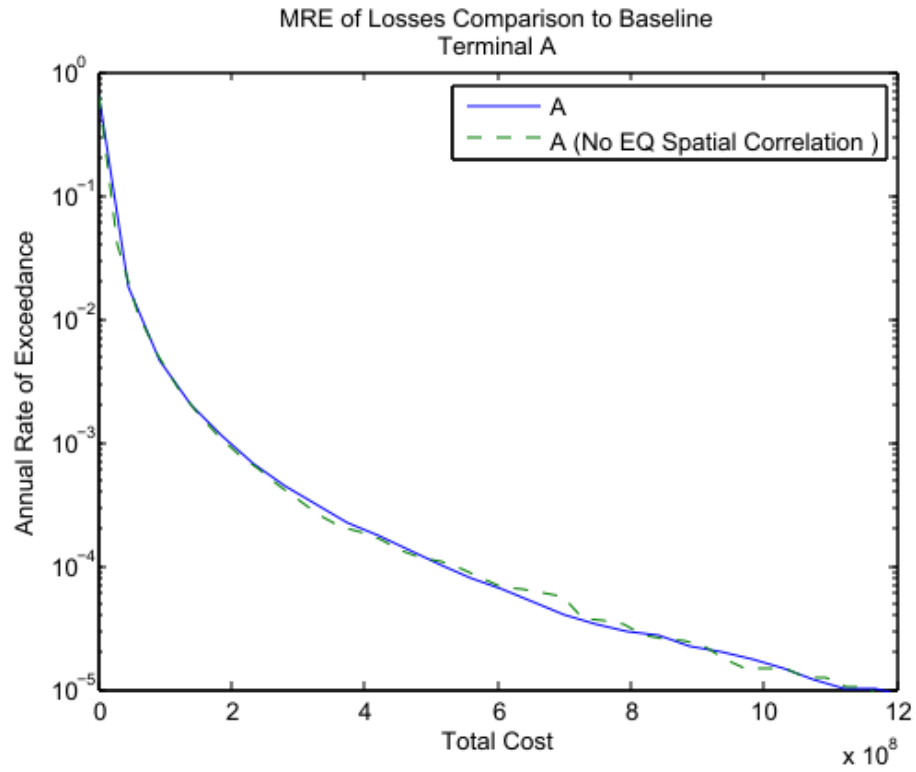
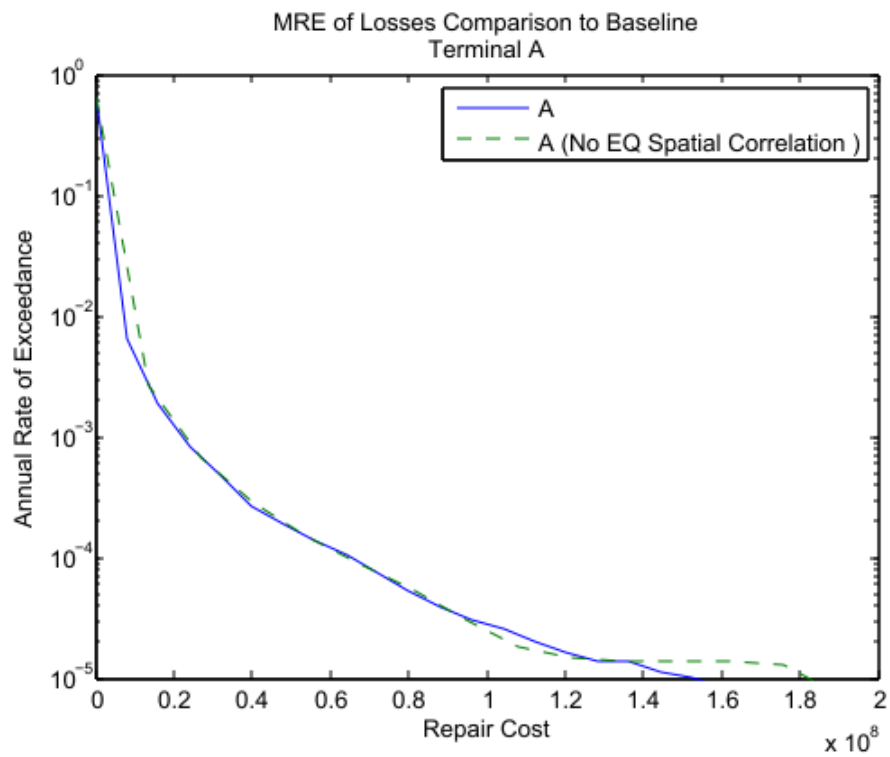


Figure 4.36 – Total Cost Uncertainty Comparison: Spatial Correlation



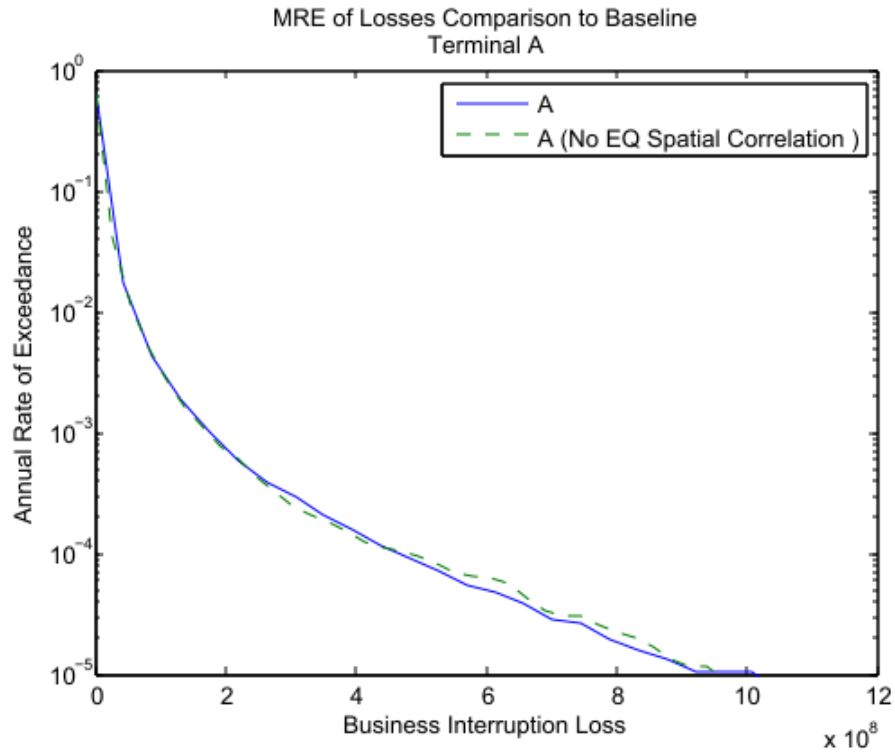


Figure 4.37 – a.) Repair Cost and b.) Business Interruption Loss Uncertainty Comparison: Spatial Correlation

4.7.1.4 Crane Repair Requirements

The crane repair requirements introduce uncertainty into the calculation of total cost in the risk analysis program because crane costs and times are randomly chosen from a lognormal distribution using the mean value and a sigma term. Figure 4.38 plots the all means and baseline scenario as compared to a scenario run where the only uncertainty allowed stemmed from the crane repair requirements:

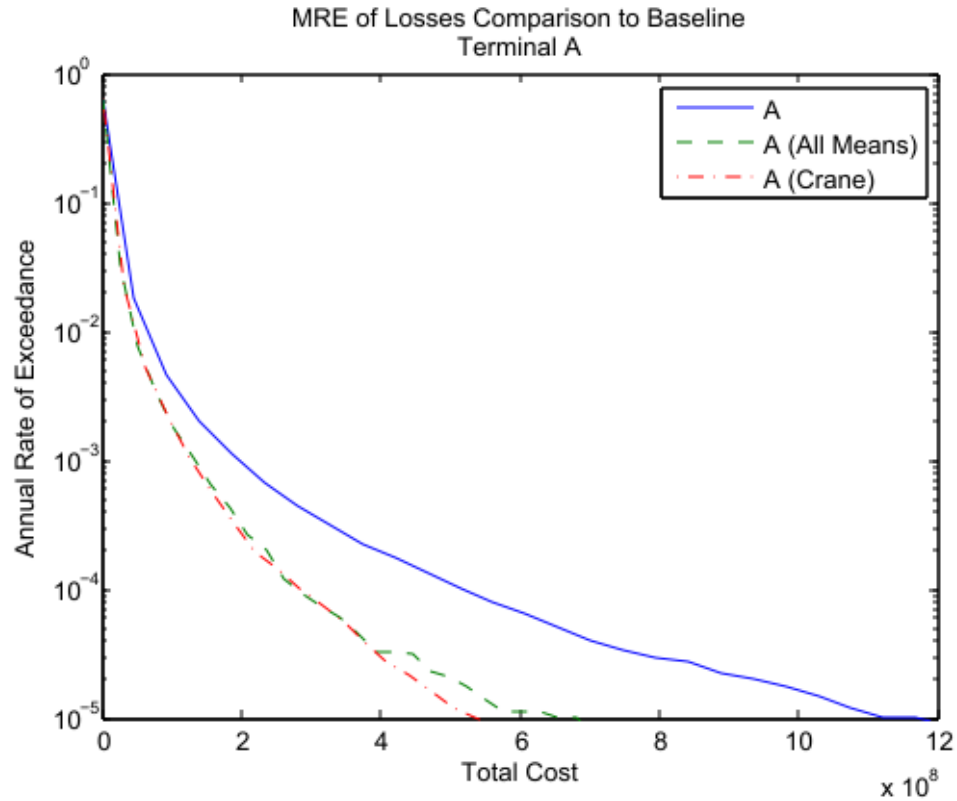


Figure 4.38 – Total Cost Uncertainty Comparison: Crane Repair Requirements

The crane repair requirement scenario is almost equal to the all means scenario. This indicates that the crane repair requirements are not large sources of uncertainty since the results including the uncertainty are almost identical to the results where it is omitted. The same conclusion applies to the repair costs and business interruption losses (Figure 4.39):

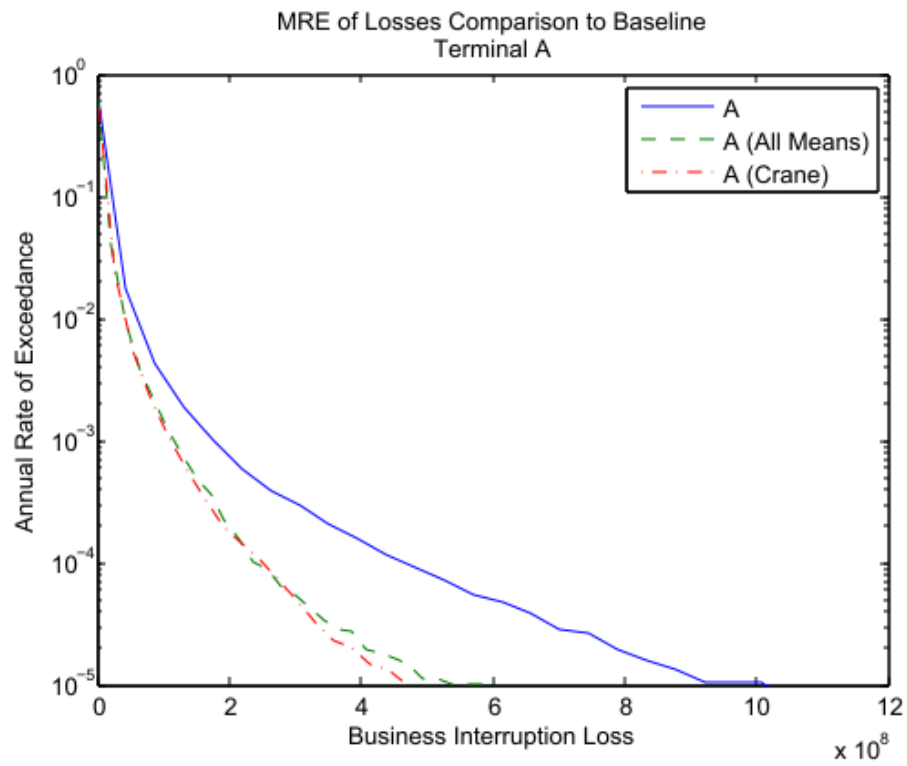
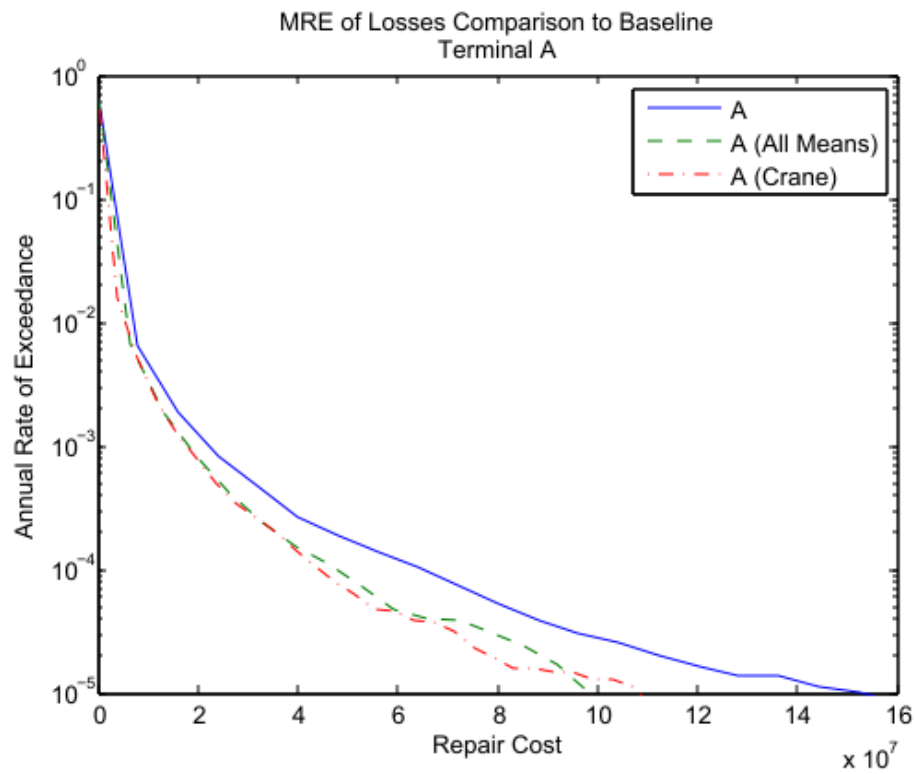


Figure 4.39 – a.) Repair Cost and b.) Business Interruption Loss Uncertainty Comparison: Crane Repair Requirements

4.7.1.5 Wharf Repair Requirements

The wharf repair requirements are calculated in the same manner as the crane repair requirements except that the sigma calculated differs from that of the cranes.

Figure 4.40 plots the baseline and all means runs and compares that to a run where the only uncertainty allowed came from the wharf repair requirements:

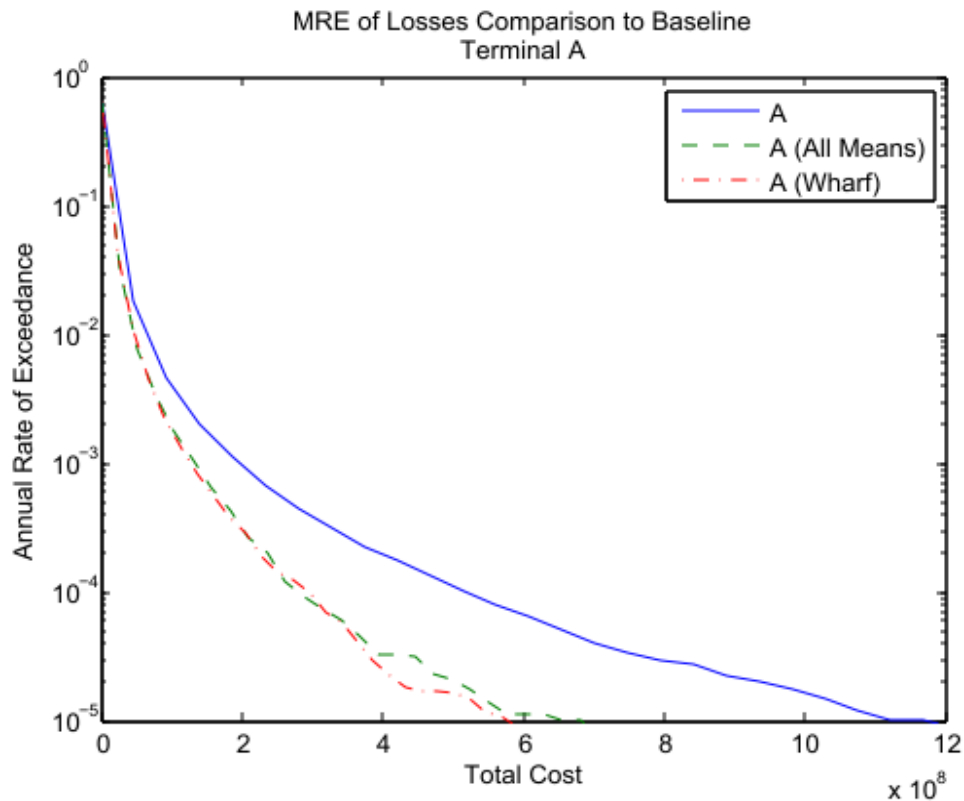


Figure 4.40 – Total Cost Uncertainty Comparison: Wharf Repair Requirements

Much like the crane repair requirements, the wharf repair requirements are not a large source of uncertainty and the results for total cost (Figure 4.40) and repair cost / business interruption loss (Figure 4.41) are almost identical to the run using only mean values.

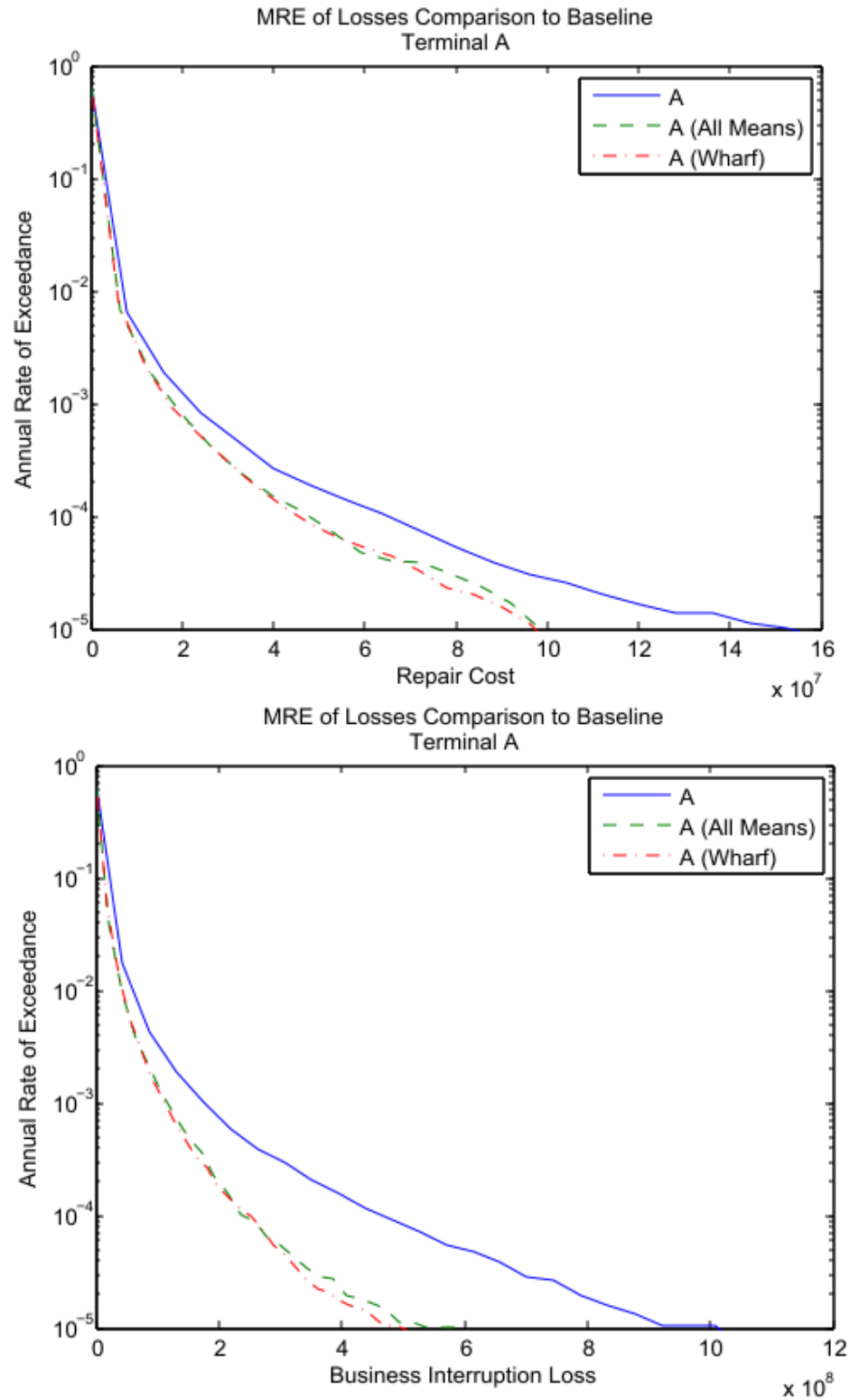


Figure 4.41 – a.) Repair Cost and b.) Business Interruption Loss Uncertainty Comparison: Wharf Repair Requirements

4.7.1.6 Operational Regression Model

The uncertainty within the operational regression model is the last source of uncertainty to be tested. Uncertainty within this model results because TEU loss values are randomly chosen according to a distribution using the mean value and an error value (Figure 4.42).

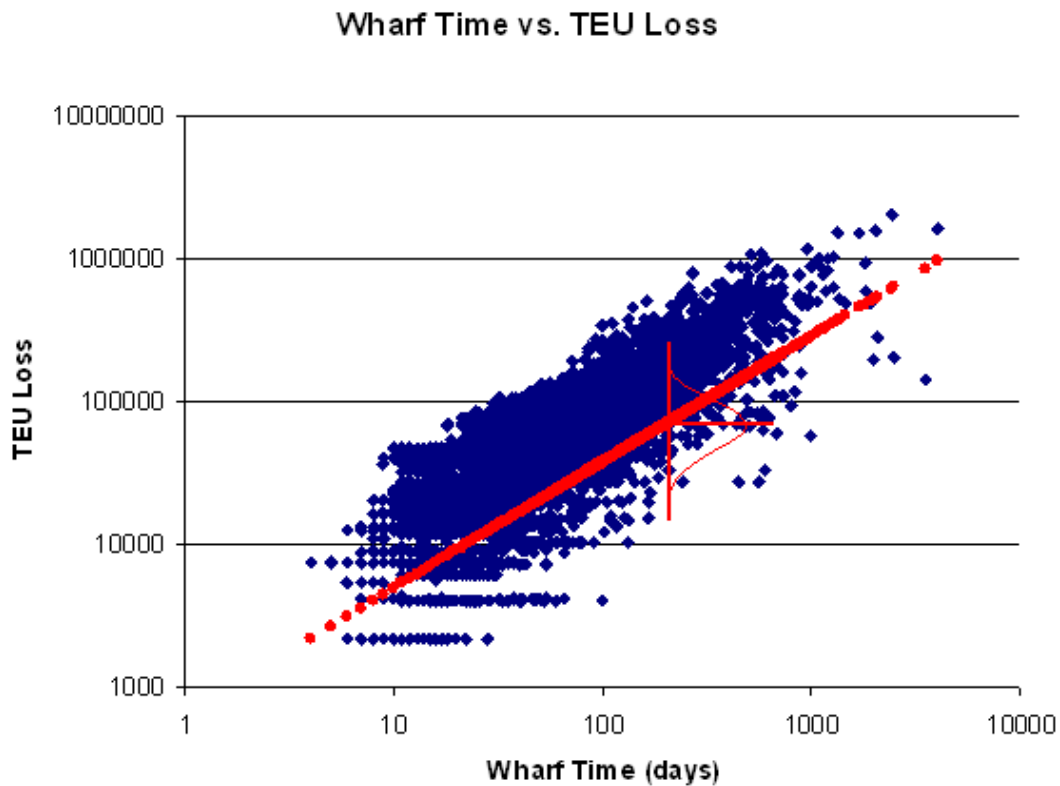


Figure 4.42 – Illustration of Uncertainty within the Operational regression Model's calculation of TEUs. (Red = mean and distribution)

Figure 4.43 plots the baseline and all means scenarios as compared to a run only allowing uncertainty in the calculation of the TEU loss within the operational regression model as previously described:

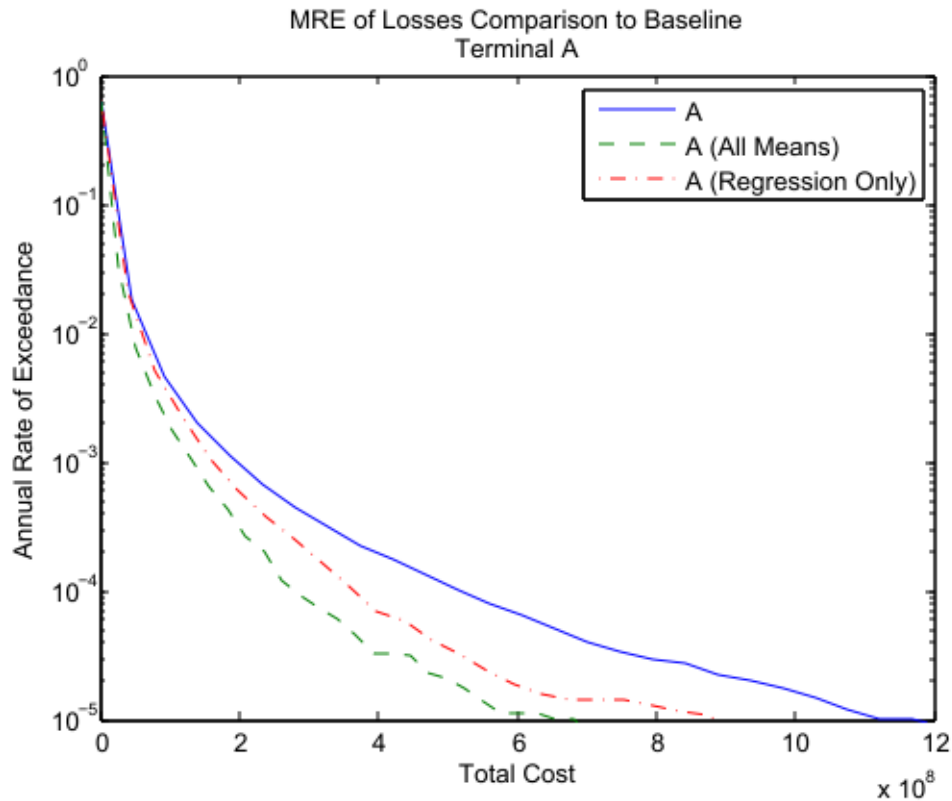


Figure 4.43 – Total Cost Uncertainty Comparison: Regression Analysis

The uncertainty within the regression analysis also accounts for a significant amount of the total uncertainty within the risk analysis. Much like the ground motions, it appears that regression uncertainty accounts for around half of the total uncertainty. Unlike the ground motions, this uncertainty is solely expressed in the calculation of the business interruption loss as seen in Figure 4.44. This result is expected since the operational regression equation has no influence on the repairs, because they are used as input into the equation.

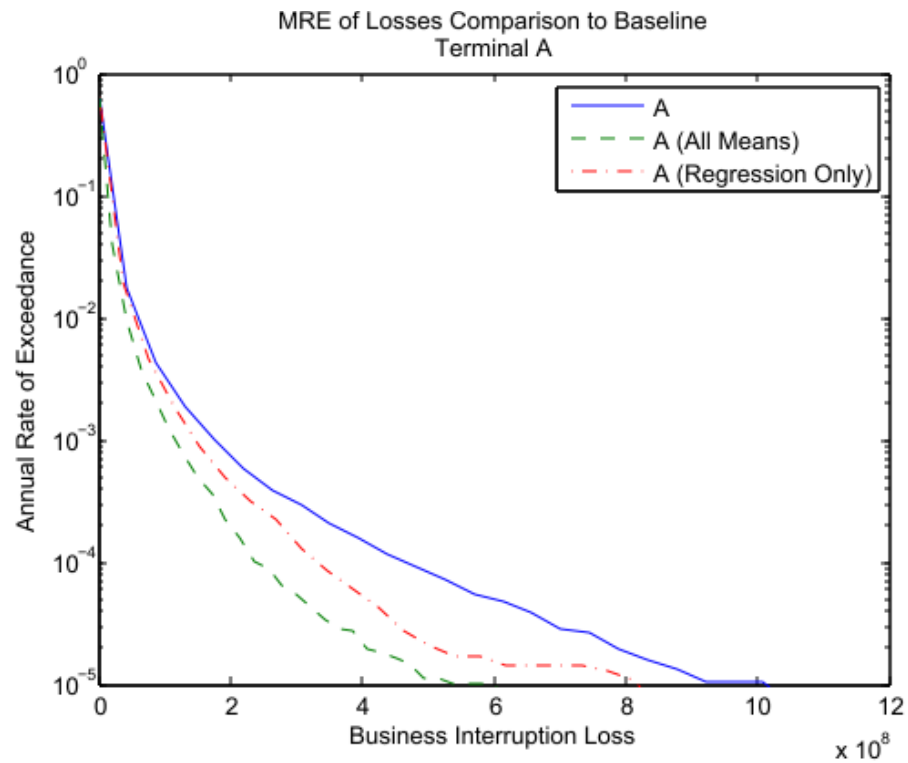
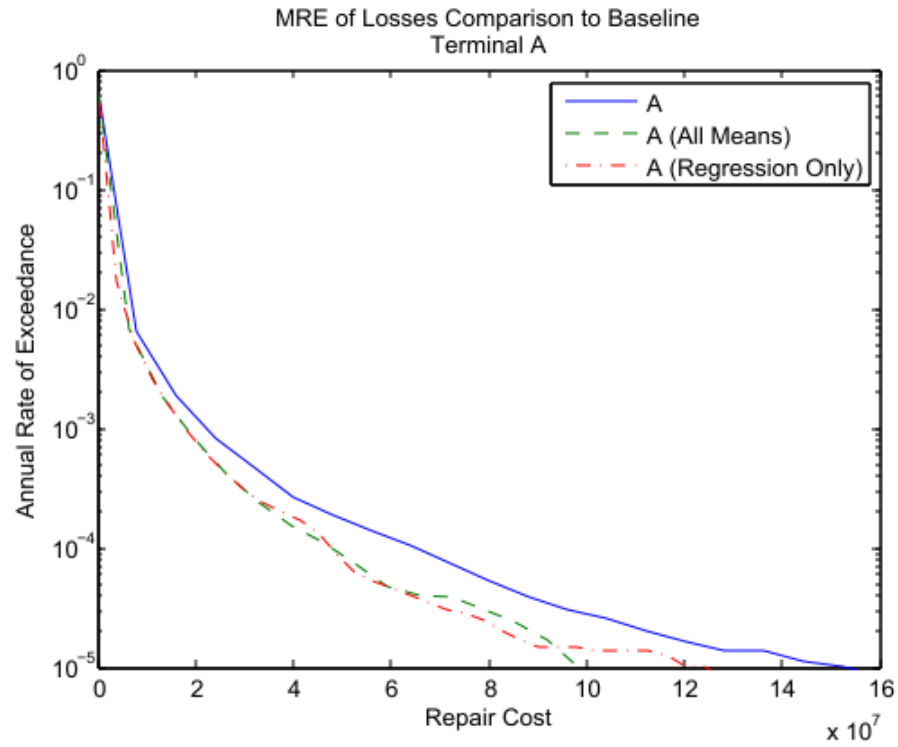
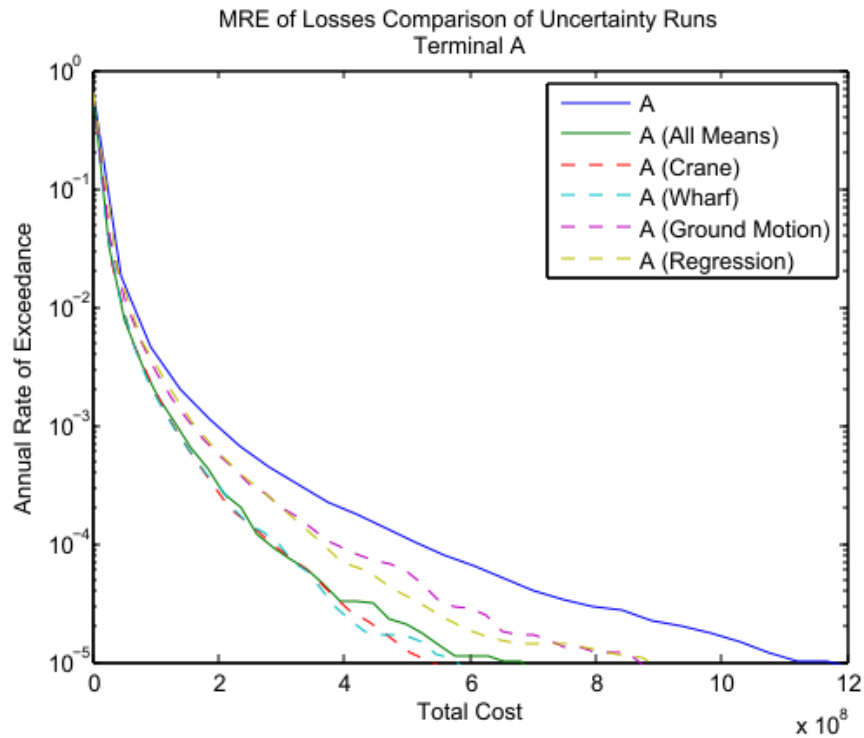
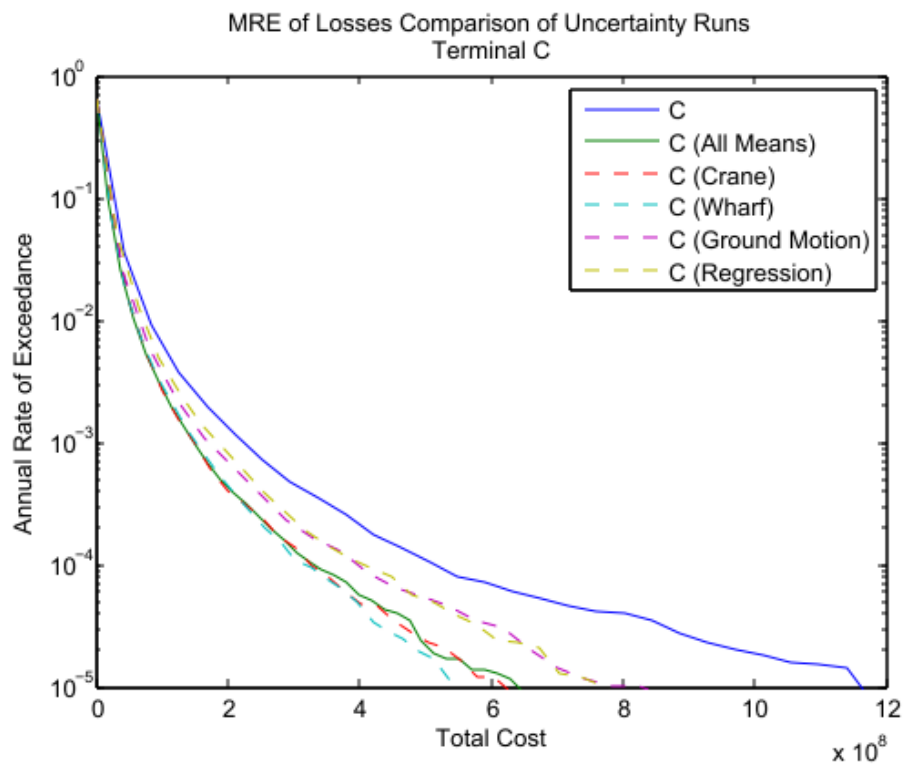
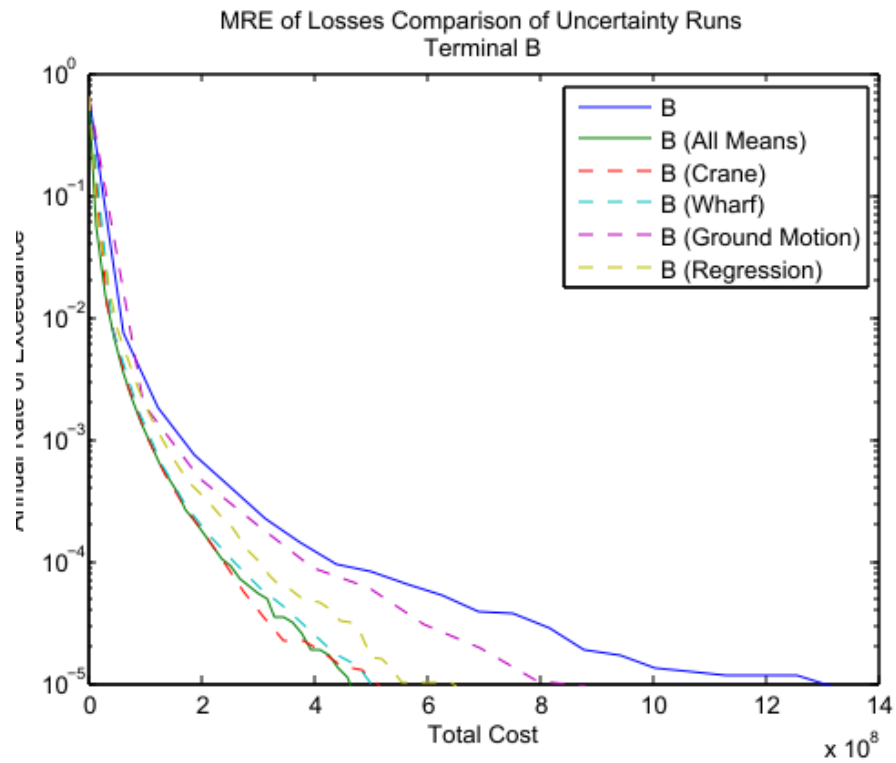


Figure 4.44 – a.) Repair Cost and b.) Business Interruption Loss Uncertainty Comparison: Regression Analysis

4.7.1.7 Comparison of All Sources of Uncertainty

The following figure (Figure 4.45) plots every source on uncertainty examined for each terminal. These plots shed light on the influences that each uncertainty source plays within the risk analysis at each terminal:





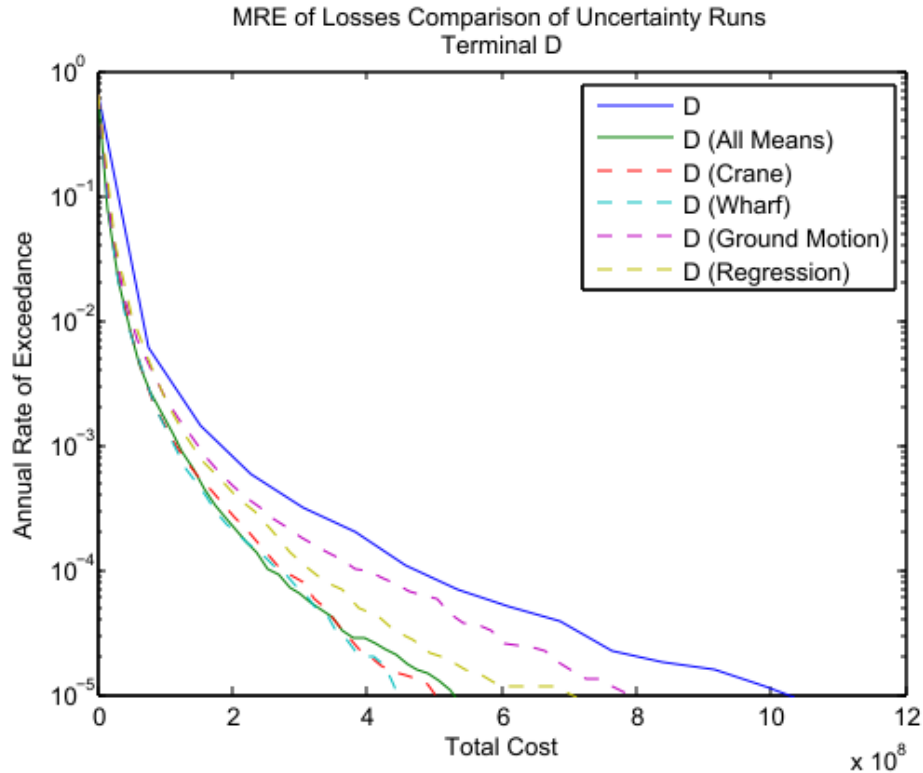


Figure 4.45 – Comparison of Uncertainty Runs Terminals A, B, C, and D

In every terminal the uncertainty associated with the wharf and crane repair requirements attributed to little if any of the overall uncertainty. Both sources were equal to or near the all mean run at every terminal. The ground motions and the regression equations were the main sources of uncertainty, but had different distributions at varying terminals. At terminals A and C their contributions were nearly equal, but at terminals B and D, the ground motions were the largest source of uncertainty.

4.8 Comparison with Previous Studies

True comparisons of the entire risk analysis program are hard to make with previous studies because the ports described in each of these studies are very different. However, some direct comparisons could be made regarding individual components of previous studies. Some comparisons as to the hazards and port components have already been made in previous sections, so this section will make comparisons regarding the

operational modeling within the risk analysis program since this is the part that differs the most as compared to all previous studies. Operational modeling at the level of the NEES Grand challenge project has yet to be employed in port risk analysis. The subsequent sections will compare the operational modeling techniques of Werner and Taylor 2004, Pachakis and Kiremidjian, and a linear calculation of BIL to the BQCSP technique used within the grand challenge project.

4.8.1 Werner and Taylor

Werner and Taylor's study estimated loss at the Port of Oakland and therefore operational policies specific to the Port of Oakland were used. For instance, in the event of an emergency, the port facility reserves the right to implement a force majeure clause in which the port is allowed to assign ships to any available berth post-disaster. Business interruption losses for each day after the earthquake are then calculated using the following formula:

$$BIL = (m - j) * \frac{22hrs}{ship} * \frac{YTEU}{hr} * \frac{\$59}{TEU} \quad (4.2)$$

This equation functions under the following assumptions: Business interruption losses are calculated by multiplying the number of ships not serviced that day by the revenue accumulated per ship. The number of ships not serviced equals the number of ships scheduled (m) – the number of ship spaces available (capacity, j). Revenue that would have been acquired (cost/ship) if the ship had been processed is estimated using average values from various sources. It should be noted that no operational consideration of the cranes is taken. This method assumes that cranes will be available for every open berth length post-earthquake.

4.8.1.1 Cost

Cost is equal to the money lost/ship. For the Port of Oakland, this is calculated as $\frac{22hrs}{ship} * \frac{YTEU}{hr} * \frac{\$59}{TEU}$. From Adams (2000), it is estimated that ships in a large vessel schedule spend on average 22 hours in port. Additionally, for the port of Oakland the number of TEUs loaded/unloaded per hour was equal to 36 in 1999, and according to income records for the port, they receive \$59 on average for each TEU handled. Multiplied out, the cost/ship equals \$46728/ship. However, because Werner and Taylor used a walkthrough method for analysis, this cost is only applicable to the year 1999. For subsequent years in the walkthrough, it is assumed that the number of TEUs handled will increase by 3% per annum, therefore $YTEU = 36 * (1.03)^j$. Here, j equals the number of years after 1999. Notice that ship capacity is neglected since the average number of TEUs/hour is considered instead.

4.8.1.2 Number of Ships Scheduled

The number of incoming ships per day is based on the average weekly demands at the Port of Oakland and data provided by Adams (2000). Daily demands are allocated proportional to the number of work hours per day of the week for San Francisco bay Area Longshoreman. As an example, the number of hours worked per day on Monday-Friday is about twice the number worked on Saturday and Sunday. Additionally, it has been assumed that weekly shipping demands will increase 5% per annum.

4.8.1.3 Port Capacity

The capacity of the port is an indication of the number of ships that can be docked, loaded and unloaded at the port at any given time. Post-earthquake, it is expected that some of the port facilities could be damaged and unusable. Port capacity was calculated by assuming that a normal container ship has a length of 970 ft., and that

were more than one ship to be docked at the same terminal, it would require 200 ft. of clearance. Available berth lengths will determine the available ship capacity for each post-earthquake day.

4.8.1.4 Comparison

To most accurately compare the Werner and Taylor BIL calculation to that of the risk analysis, the “port” confines will be limited to only terminals A and B and the force majeure scenario will be used in the risk analysis. Using equation 4.2, the business interruption loss will be calculated for the combined arrival schedule of Terminals A and B using the Werner/Taylor method and compared to the business interruption loss calculated using the force majeure combination in the risk analysis framework. From equation 4.2, and assuming that the earthquake in question takes place in the year 2011:

$$YTEU = 36 * (1.03)^{2011-1999} = 51.3274 \quad (4.3)$$

\$59/TEU would also have to be adjusted for inflation to 2011 dollars. Assuming 5% inflation, $\$59 * (1.05)^{2011-1999} = \$106/TEU$. Therefore,

$$BIL = (m - j) * \frac{22hrs}{ship} * \frac{YTEU}{hr} * \frac{\$106}{TEU} = (m - j) * \frac{\$119695}{ship} \quad (4.4)$$

The variables m and j correspond to the number of scheduled ships and berth capacity respectively. Berth capacity can be calculated from the repair requirements for given earthquakes, and the number of scheduled ships can be calculated using the arriving vessel stream.

Capacity

For this example, a moderate-sized earthquake (M6.05 from the South San Andreas fault) with moderate damage will be investigated at terminal A. Terminal A and Terminal B are both 2400 ft long and in an undamaged condition, can accommodate 4 ships according to the Werner/Taylor assumption of 970 ft ship lengths with 200 ft

clearance between them. As calculated within the risk analysis framework, Figure displays the 600 ft berths of Terminal A and Terminal B and their respective repair times:

RT = 27	RT = 32	RT = 25	RT = 22	RT = 20	RT = 21	RT = 25	RT = 31
Terminal A				Terminal B			

Figure 4.46 Terminal A and B – BIL Comparison Example

Since each berth is 600 ft in length, two consecutive berths would need to be open in order to accommodate one ship. Therefore according to these repair times and berth locations the following ship capacities are available at Terminal A and B on the following days:

Table 4.12 Ship Capacity for Comparison Example

Day	Ship Capacity
0-19	0
20	0
21	1
22	1
23-24	1
25-26	2
27-30	2
31	3
32+	4

Scheduled

Using the ship arrival schedule calculated in the risk analysis program, the number of scheduled ships can be found and compared to the capacity as in equation 4.2. Business interruption loss will be calculated by summing the number of ships that cannot be accommodated at Terminals A and B during the repair period. Table 4.13 compares the number of scheduled ships to the capacity of the port.

Table 4.13 Scheduled Arrivals vs. Capacity for Terminal A

Scheduled Arrivals (day)	Capacity on that day	Scheduled - Capacity
2.7	0	1
5.0	0	1
6.9	0	1
7.1	0	1
7.7	0	1
8.4	0	1
8.9	0	1
16.0	0	1
17.3	0	1
19.4	0	1
19.5	0	1
21.3	1	0
21.8	0	1
26.2	2	0
28.9	2	0
29.0	2	0
30.1	2	0
30.6	2	0
33.4	4	0
38.9	4	0
	SUM	12

Twelve ships will not be accommodated using this method for calculating business interruption losses, and at \$119,695/ship, that means the total business interruption loss will equal \$1,436,340. This figure is much less than the BIL = \$29,340,490 calculated using the risk analysis program.

The discrepancy between the figures can be explained by the method used to calculate the BIL and the assumptions made in doing so. One major difference is that the risk analysis program calculates losses to both the port operator and to the port terminal, at an amount of \$100 and \$150 per TEU respectively. If the \$106 per TEU increased to \$250, the BIL using the Werner/Taylor method would increase to \$3.39 million dollars. This figure is still well below the \$29 million calculated by the risk analysis program. The second major difference is that the Werner/Taylor method calculates the average lost per ship, and it assumes that all ships are 970 ft in length. Table 4.14 shows the ship

lengths and TEUs used in the ship arrival stream used in the risk analysis for the 12 ships that were not accommodated at Terminal A.

Table 4.14 Ship Arrival Stream – Ship lengths and TEUs

Scheduled Arrival (day)	Ship Length	TEUs/ship
2.7	964.3	5414
5.0	849.6	3569
6.9	964.6	6351
7.1	918.1	7358
7.7	900.9	8613
8.4	964.7	4316
8.9	1148.0	10267
16.0	964.7	3981
17.3	964.7	6070
19.4	983.3	7662
19.5	964.7	6740
21.8	902.0	4901

While most of the ships are around 970 ft in length, the number of TEUs on each ship is very different from what is assumed in the Werner/Taylor method. If it costs \$119,695 per ship and \$106 per TEU, then by division this method assumes that there are approximately $(\$119695/\$106)$ 1129.2 TEUs per ship. However, from the table it can be seen that every ship, no matter the length holds more than 1129 TEUs, and the average capacity is 6270 TEU. It is important to remember that the TEU and ship length values in the risk analysis arrival stream are sampled and calculated from actual ships in the MXSOCAL log that actually docked at the Port of Los Angeles or the Port of Long Beach. If the Werner/Taylor TEU figure were increased, it would cost $(\$106 \times 6270)$ \$664,683/ship and the BIL calculated would increase to \$7.9 million dollars. If that new TEU figure were used with the risk analysis loss of \$250/TEU instead of the \$106/TEU currently used, the BIL calculation would increase to \$18.8 million dollars. This figure is much closer to the \$29 million calculated within the risk analysis program. The additional difference in loss of \$10 million dollars could possibly be explained by the fact

that the Werner and Taylor method considers a force majeure option for the entire port of Oakland while the risk analysis framework only considers force majeure in Terminals A and B. Even though the compared arrival stream is identical, the port of Oakland has more available berths than at Terminals A and B which will reduce the overall business interruption loss. However, the risk analysis program method for calculating business interruption loss does seem to be more accurate than the Werner/Taylor method which uses port and ship assumptions that contributes to an underestimation the business interruption loss figure.

4.8.2 Pachakis and Kiremidjian

The operational modeling within this study is more representative of the approach taken within the Grand Challenge operational modeling. Here, loss is calculated as the difference between revenue generated during some time period and revenue generated during that same time period conditional on damage caused by an earthquake. Calculated revenue for the operational model of Pachakis and Kiremidjian is dependent on the fees collected from craneage, wharfage, and dockage revenues. Definitions of each of these fees can be found in Section 2.4.2.

4.8.2.1 Ship Traffic

Ship arrivals were assumed to have exponentially distributed inter-arrival times, and modeled as a random process with different traffic intensities for each month (nonhomogeneous Poisson arrivals). Properties associated with the ships (quantity of cargo, capacity, minimum and maximum number of cranes to be used) are generated from distributions based on collected data. Once the traffic stream is generated, ships are distributed to each terminal according to actual percentages seen in practice.

4.8.2.2 Berth Assignment and Crane Allocation

Once a ship enters the port, it is assigned a terminal and berth. Berths are assigned by examining all berth sets within the port that can accommodate the ship's length and capacity. Actual berth assignment goes to the berth set with the largest number of available cranes. Each berth accepts ships into an individual queuing model. If the model exceeds some maximum number of ships within its queue, the incoming ship is diverted to others berths or terminals. The number of cranes used to load/unload a ship depends on the capacity of the ship itself. From observed data, Pachakis and Kiremidjian estimated that one crane is used for every 400 TEUs to be handled. An algorithm uses this average, the number of available cranes, and the ship capacities to assign cranes within the operational model. Algorithms for both berth and crane assignment minimize the waiting time and service time for each ship.

4.8.2.3 Service Times

The service time, or time the ship spends at the dock being loaded and unloaded, is calculated as a lognormal distribution with varying parameters dependent on the handling system (cranes, storage equipment, etc.).

The main differences between the Pachakis and Kiremidjian (PK) model and that used in the Grand Challenge occur in the algorithms that assign berths and cranes. The GC model uses rolling horizon's to plan for incoming arrival streams much as a port official would in real life. The queuing model suggested by Pachakis and Kiremidjian does not allow for future planning. Once the ship enters the queue, it must be dealt with before another ship can be planned for. The GC model more closely mimics real-life situations and is therefore more suitable. Furthermore, there are also slight differences in how ship data is stored and used within the models. The GC model samples ships from a database of actual ships and therefore the ship properties are fixed and inherent to each ship. On

the other hand, the PK model randomly samples ship lengths and the properties are then sampled from distributions based on that length. While either method is acceptable, the GC method utilizes actual west coast ships.

4.8.3 Linear Calculation of BIL

An additional comparison of BIL calculation will be made using a linear calculation of the TEU Loss ($= \text{BIL}/\$250$) based on the availability of port structures during the repair period of the port. From observation it is apparent that business interruption losses are a function of the availability of berths and cranes given some ship arrival schedule. For the linear calculation it will be assumed that TEU Loss is calculated as a fraction of the berths and cranes available on a given day.

The specific examples used will be the five earthquake examples in section 3.5.2.1. The linear BIL calculation procedure will be described using earthquake #3, and then calculated TEU Losses will be compared for each of the five earthquakes in the aforementioned example. Recall for each earthquake example that a 3000 ft terminal was examined and repair requirements for each of the 600 ft berths and six cranes were specified. Figure 4.47 shows the repair requirements for Earthquake #3, which will be used in the linear BIL calculation procedure example. Earthquake #3 represents a moderate sized earthquake with moderate wharf damage and mild crane damage

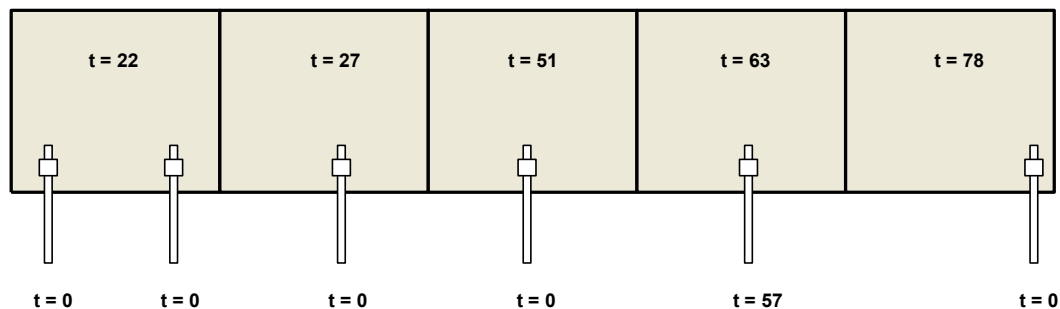


Figure 4.47 Wharf and Crane Repair Times for Example Earthquake Scenario #3

For this example, the maximum repair time equals 78 days for berth 5, which equals 11.1 weeks. Therefore, it will be assumed that no business interruption losses will occur past week 12. The following figure plots the TEUs handled per week within the port for a no damage state (normal operation) and for BQCSP calculated operation after Earthquake 3 (EQ 3) (Figure 4.48). When the number of handled TEUs during EQ 3 operation is subtracted from the number of TEUs handled during normal operation, which in this case equals 70943 TEUs. Business interruption loss (BIL) would be calculated by multiplying the TEU loss by a figure of \$250 Lost/ TEU (BIL = \$17,735,750). For the rest of this example, loss figures will not be dollar amounts. Instead, TEU Loss will be the measure of reduced throughput.

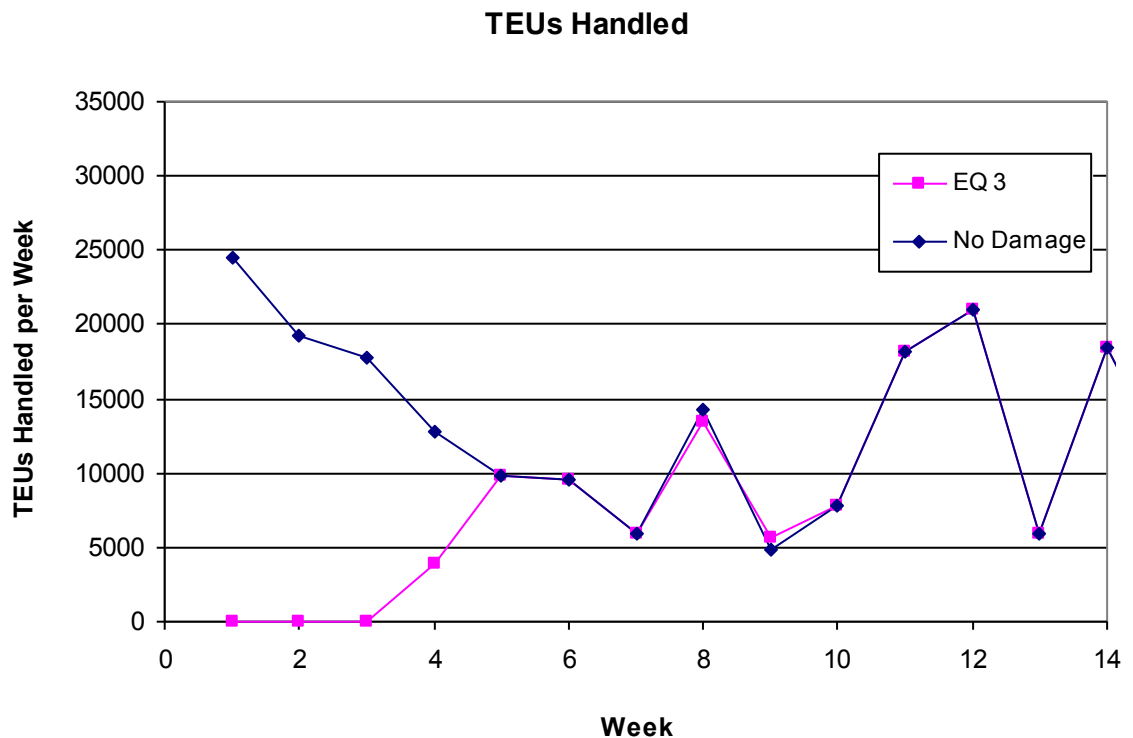


Figure 4.48 – TEUs Handled per Week in EQ 3 and No Damage Scenarios

TEU Loss can be calculated in a linear manner according to the availability of port structures. In this calculation, the TEUs handled per week in the no damage condition will be multiplied by the fraction of components not available per given week. This calculation assumes that all components at the port are used equally and that when components are not available for use, the TEUs handled per week will be reduced by a factor equal to the number of unavailable components over the total number of components. Figure 4.49 is a replica of Figure 4.48 showing the TEUs handled per week for EQ 3 but with the availability of the components (berths, cranes) during weeks when repairs are made. Repair times were rounded up to the nearest week, so for week 4 one can see that 1 of 5 berths are available and 5 of 6 cranes are available.

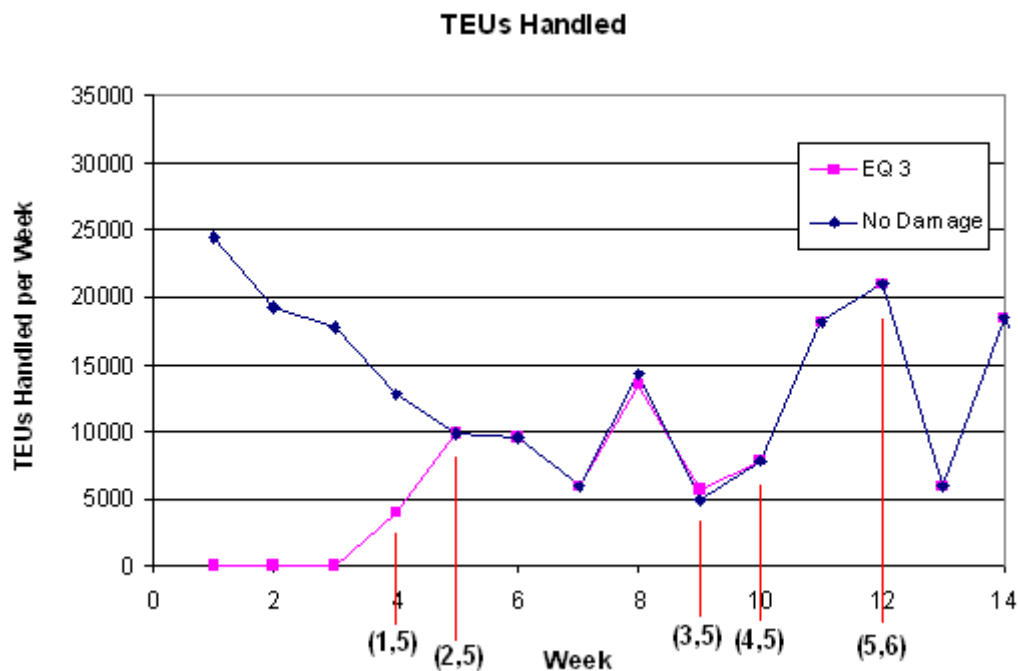


Figure 4.49 TEUs Handled per Week with (berth,crane) Availability: Earthquake 3

Table 4.15 calculates the TEUs lost per week using the linear calculation based on the total components and compares that to the TEUs lost per week using the BQCSP model. For instance, for week 4, 1 of 5 berths and 5 of 6 cranes are available, so the

linear calculation of TEU loss would equal the normal TEUs handled * 5/11 components that are unavailable. In addition, a linear TEU loss was also calculated separately for the number of berths and number of cranes not available as the multiplier times the normal TEUs handled.

Table 4.15 Calculation of Linear TEU Losses Using Components and Berths Not Available – Earthquake #3

Week	Normal TEUs Handled	Components Not Available	Linear TEU Loss	BQCSP TEU Loss	Berths Not Available	Linear TEU Loss	Cranes Not Available	Linear TEU Loss
1	24500	6/11	13,364	25,111	5/5	24,500	1/6	4,083
2	19208	6/11	10,477	20,628	5/5	19,208	1/6	3,201
3	17836	6/11	9,729	16,474	5/5	41,034	1/6	2,973
4	12740	5/11	5,791	8,731	4/5	10,192	1/6	2,123
5	9800	4/11	3,564	0	3/5	5,880	1/6	1,633
6	9604	4/11	3,492	0	3/5	5,762	1/6	1,601
7	5880	4/11	2,138	0	3/5	3,528	1/6	980
8	14308	4/11	5,203	0	3/5	8,585	1/6	2,385
9	4900	1/11	445	0	2/5	1,960	1/6	817
10	7840	1/11	713	0	1/5	1,568	1/6	1,307
11	18228	1/11	0	0	1/5	0	1/6	3,038
12	20972	0/11	0	0	0/5	0	0/6	0
Total			54,916	70,943	Total	122,217	Total	24,141

It is apparent from the table that for EQ 3, using the components not available or the cranes not available underestimates the TEU Loss, and using the number of berths not available overestimates the TEU Loss. This result is expected. TEU losses are a direct result of the number of ships that have to turn away from the port because they cannot be serviced at the port. While the number of ships that can be serviced is a function of the wharf and crane availability, more often than not, the damage of one component dominates the other. In this instance, there is far more wharf damage than crane damage. The average of the linearly calculated TEU loss from only the berth and only the crane components provides a reasonable estimate of TEU Loss (TEU Loss = 73,179). This figure is the closest of all linear estimations to the BQCSP calculated TEU Loss (= 70,943).

These linear estimations and which combination of components / computation method was further investigated using the other four earthquakes within the example. The following figures (Figure 4.50 - Figure 4.53) show the TEUs handled and component availability for the other four earthquake examples:

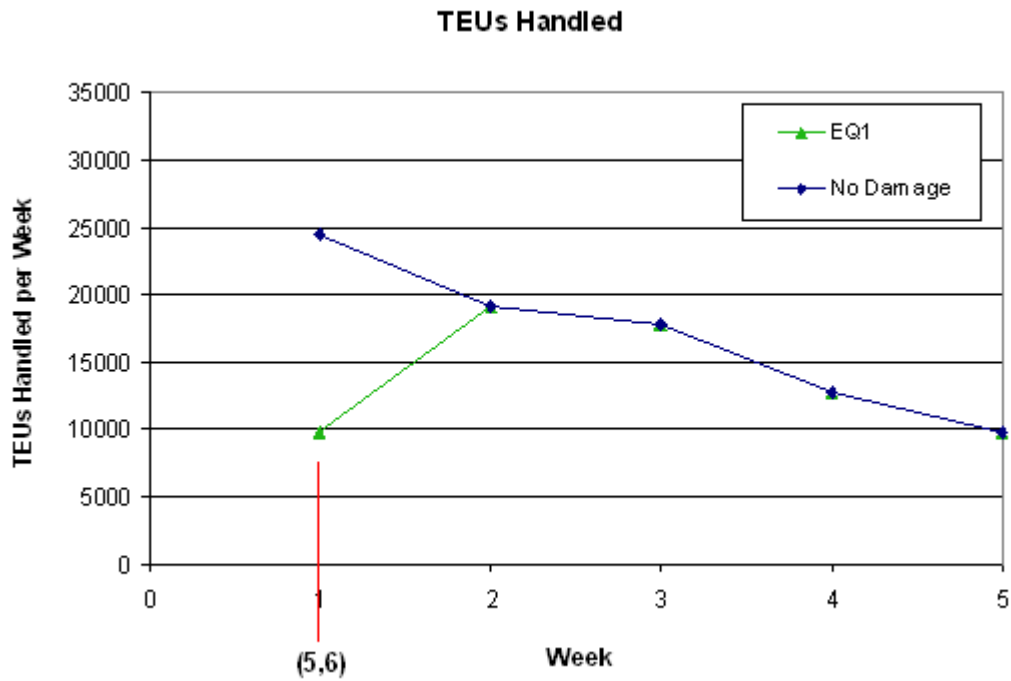


Figure 4.50 TEUs Handled per Week: Earthquake 1

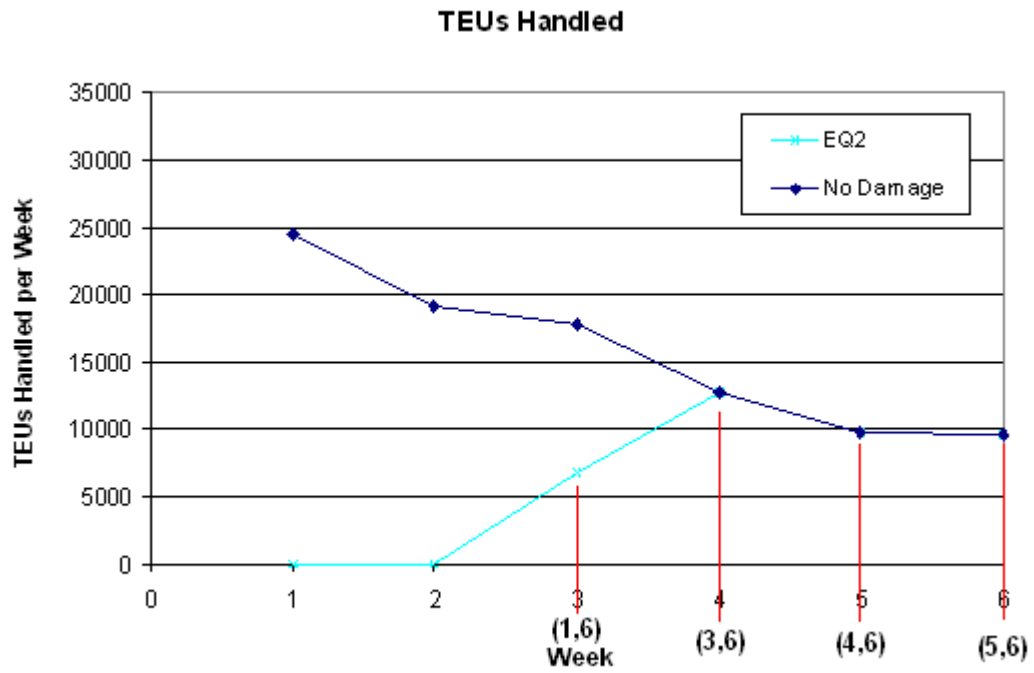


Figure 4.51 TEUs Handled per Week: Earthquake 2

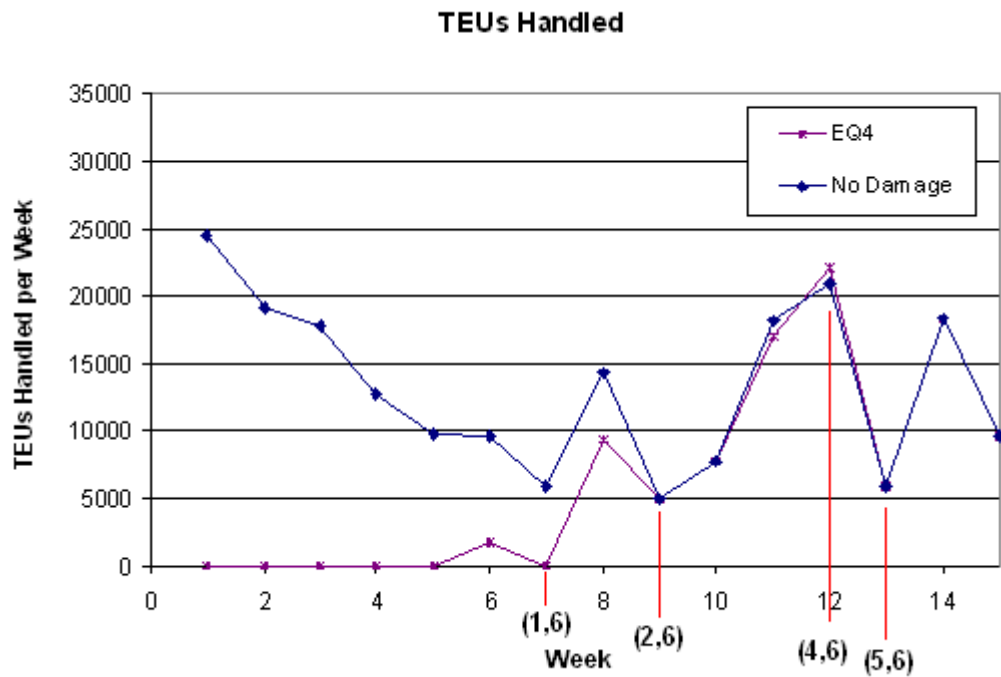


Figure 4.52 TEUs Handled per Week: Earthquake 4

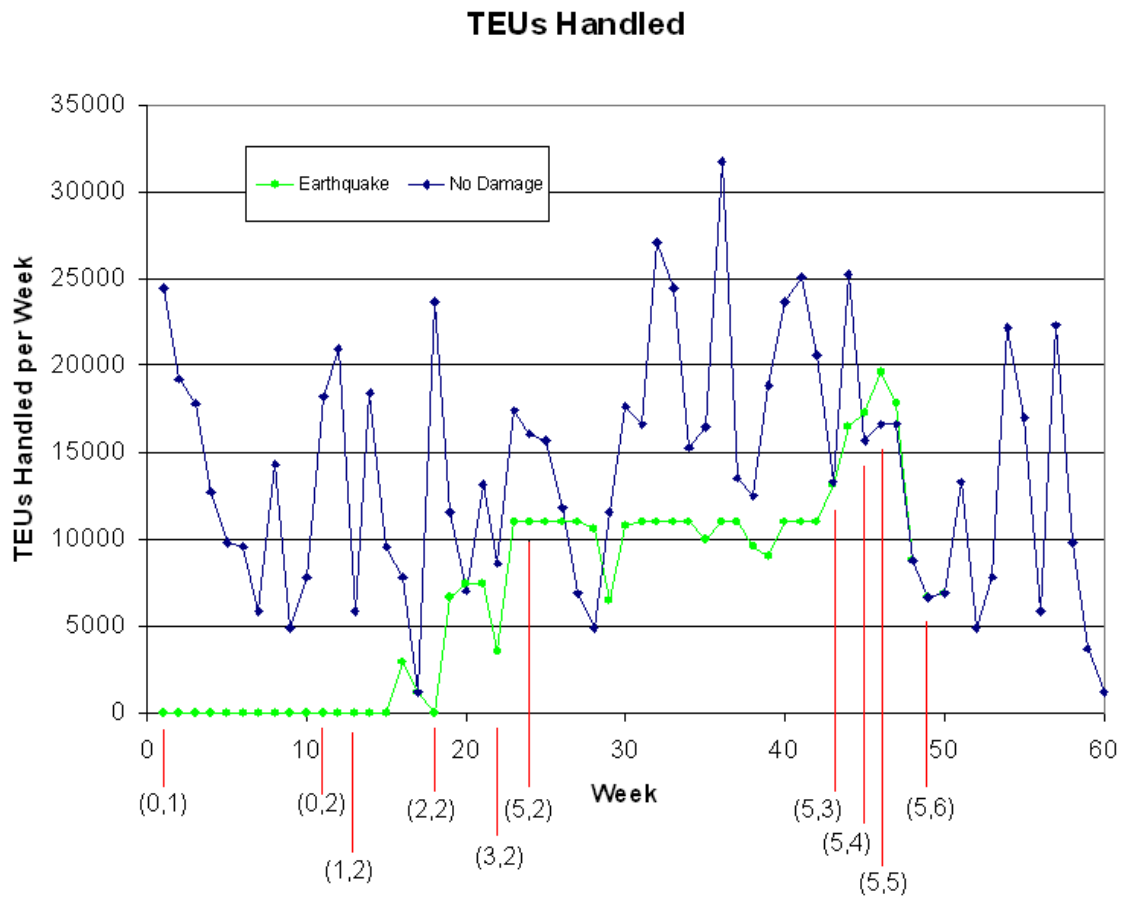


Figure 4.53 TEUs Handled per Week: Earthquake 5

The other four earthquake examples vary in the degree of damage at the terminal. Earthquake 1 results in very minor damage, while Earthquake 5 results in extensive damage. In the same manner as the Earthquake 3 example, linear loss calculations were made for the previous four earthquake examples using the total number of components, solely the berths not available, and solely the cranes not available. Results for all five earthquakes are listed in Table 4.16:

Table 4.16 Comparison of TEU Losses Using Different Component Indicators

Earthquake	BQCSP TEU Loss	Linear TEU Loss (Total Comp)	Linear TEU Loss (Berth)	Linear TEU Loss (Cranes)	Linear TEU Loss (Avg B & C)
1	14847	11136	24500	0	12250
2	55276	29560	63073	0	31536
3	70943	54916	122217	24141	73179
4	103805	53401	132614	0	66307
5	385069	1010330911	235827	477064	356446

It can be seen from Table 4.16 that for earthquakes where both berth and crane damage occurs, the average of the TEU loss for the berth and the loss for the crane provides the best estimate. For Earthquake 5, the total component estimate severely overestimated the loss. This resulted from the long time period during which repairs continued. For instance as seen in Figure 4.53, while it only took 23 weeks to repair all of the berths, the cranes were not all functional until week 49. So from week 24-49 the total component linear model was calculating TEU losses that were probably not consistent with those actually occurring at the port. After week 11 there were two cranes available. The BQCSP estimation is much lower because those two cranes worked constantly to load/unload all the cargo entering the port so that little TEU loss actually occurred. On the other hand, Table 4.16 shows that for earthquakes where only one component type of damage occurs, the average does not provide the best estimation. Instead, the calculation using the damaged component provides the best estimation, and in the case of Earthquakes 1, 2, and 4, that component is the wharf. The only exception to this is Earthquake 1, which can be explained through rounding. The berths in Earthquake 1 received minor damage and all but one was repaired by day 4 of week one. However, the linear calculation rounds up to the nearest week, so all of the berth sections are considered unusable and every TEU that arrived during week one is lost. This problem could easily be remedied by calculated the linear TEUs lost per day instead of per week. However, if a linear TEU Loss calculation were to be made, it would be best

to base it on the average of the TEU losses calculated for each separate component unless one of the component types remains undamaged, in which case it would be best to calculate the loss based on the fraction of the damaged component unavailable. Still, the use of the BQCSP model would provide even better data since it calculates TEU Loss resulting from its actual source: the number of ships displaced from the port after an earthquake.

5 MITIGATION OPTIONS

The mitigation options discussed in previous chapters will be compared to the baseline configuration in the subsequent sections. It is important to note that mitigation options will only be compared in a monetary sense. However, every mitigation option may also have additional environmental or social benefits with their implementation that will not and cannot be quantified monetarily in this section. Mitigation options to be considered include: upgrade of cranes to J100 models, installation of vertical drains in the wharf backfill, reducing repair time with repair incentives, and implementation of a force majeure policy.

5.1 Geotechnical Options

Much of the damage to the wharves was caused by the lateral movement of the soil during liquefaction. The next mitigation run models the situation in which vertically drains are installed within the backfill to prevent liquefaction. Liquefaction prevention should lessen the wharf repair costs and reducing total cost. First the exceedance curves for the wharf repair cost will be checked to ensure that the drains are in fact reducing liquefaction and the overall wharf damage (Figure 5.1 - Figure 5.4):

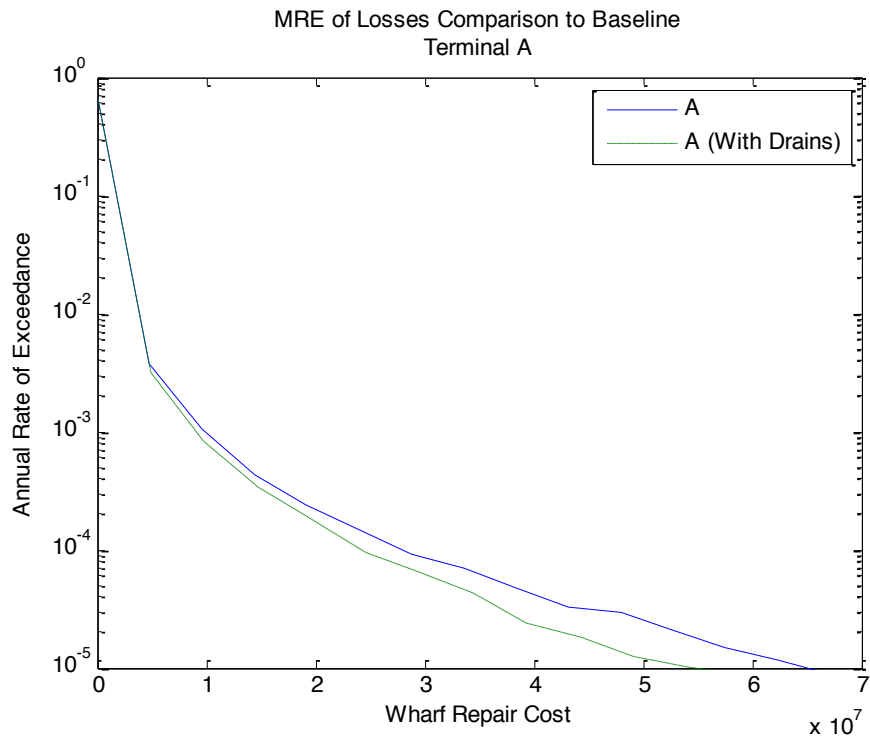


Figure 5.1 – MRE of Wharf Repair Costs With and Without Drains: Terminal A

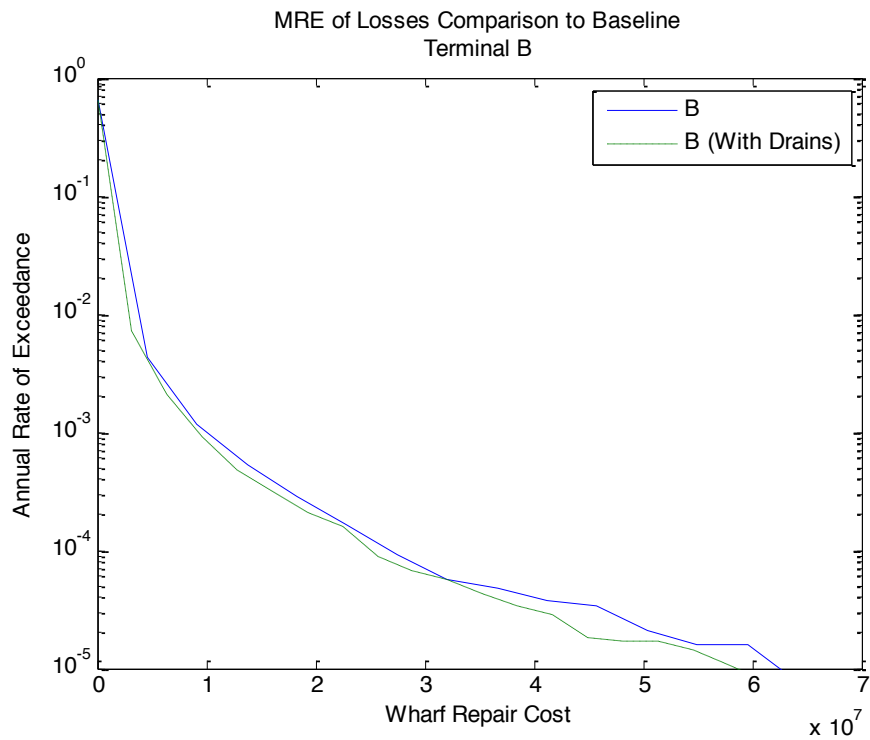


Figure 5.2 – MRE of Wharf Repair Costs With and Without Drains: Terminal B

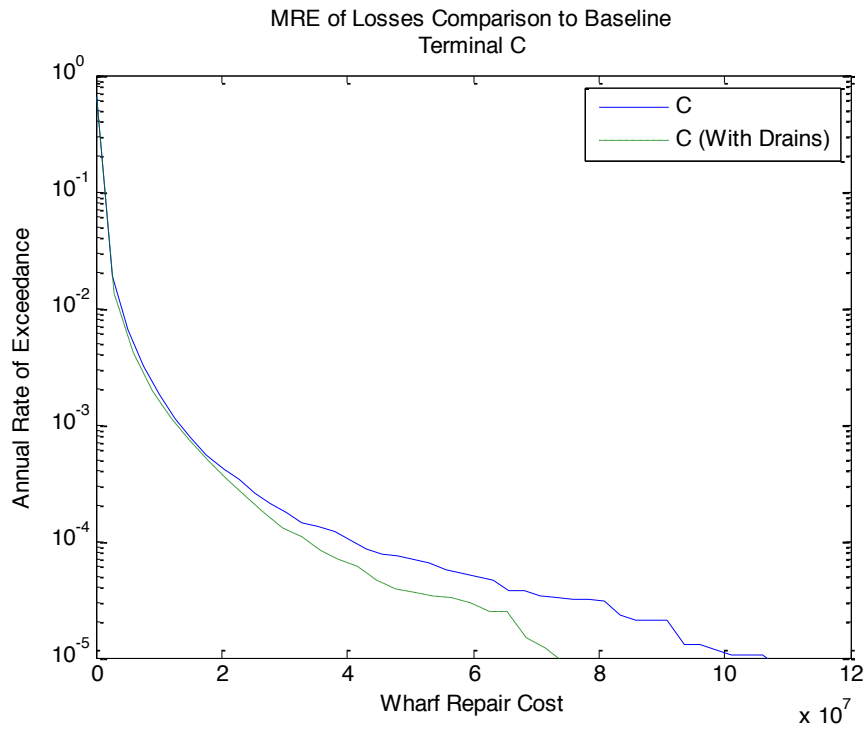


Figure 5.3 – MRE of Wharf Repair Costs With and Without Drains: Terminal C

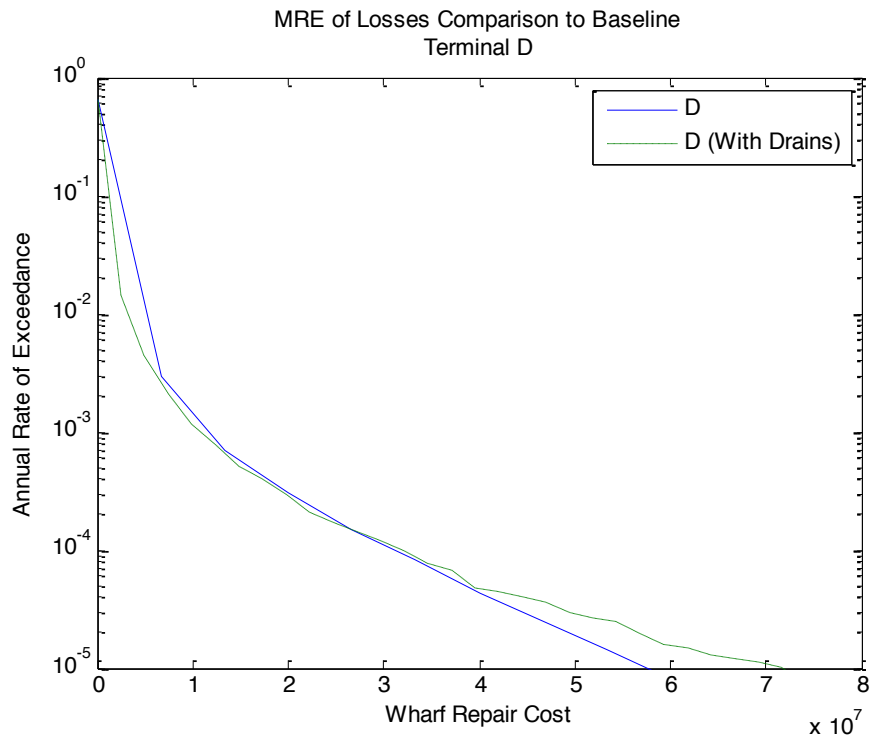


Figure 5.4 – MRE of Wharf Repair Costs With and Without Drains: Terminal D

While only slightly decreasing the exceedance values, terminals with drains have smaller exceedance values than terminals without drains. Figure 5.5 shows that drains also slightly reduce the overall repair cost:

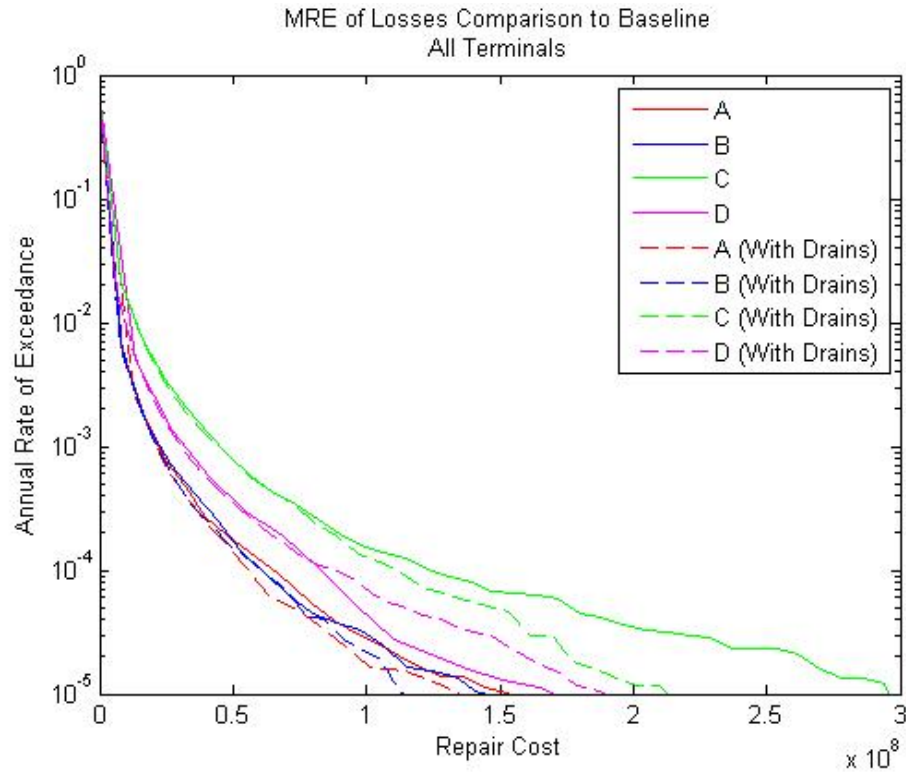


Figure 5.5 – MRE of Repair Costs With and Without Drains: All Terminals

This exceedance reduction in repair costs may also translate into a decrease in exceedance rates for business interruption losses (Figure 5.6):

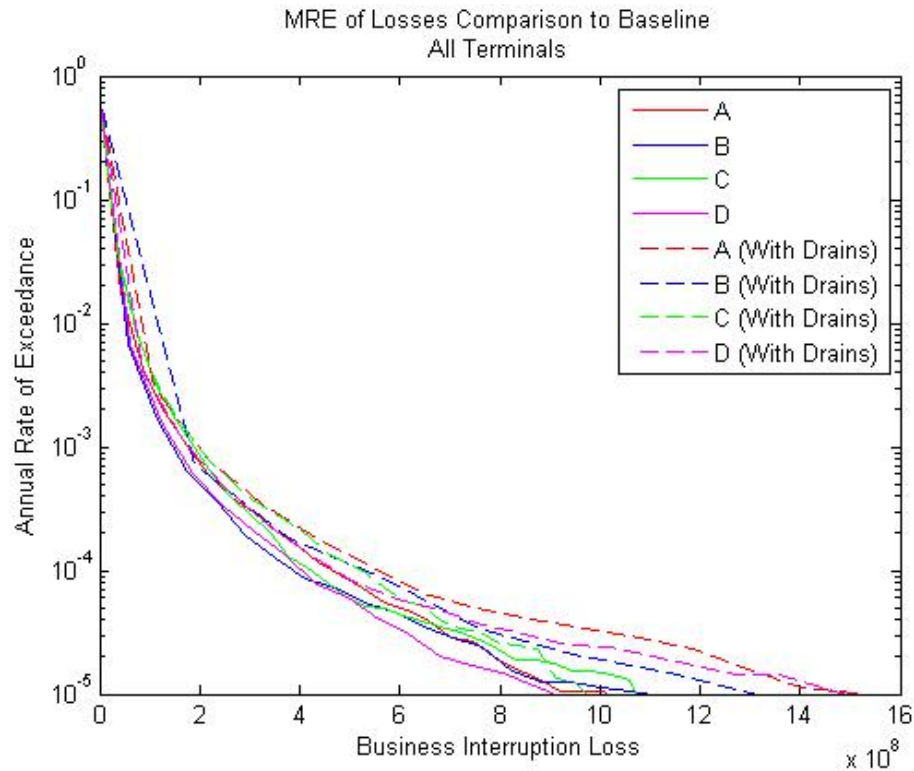


Figure 5.6 – MRE of Business Interruption Losses With and Without Drains: All Terminals

However, in examining Figure 5.6 business interruption loss exceedance values are only slightly reduced in Terminals A, B, and D, and almost equal at Terminal C. Since business interruption losses comprise the majority of the total cost, the same magnitude of exceedance reductions should also be present in the MRE curves for total cost (Figure 5.7 - Figure 5.11):

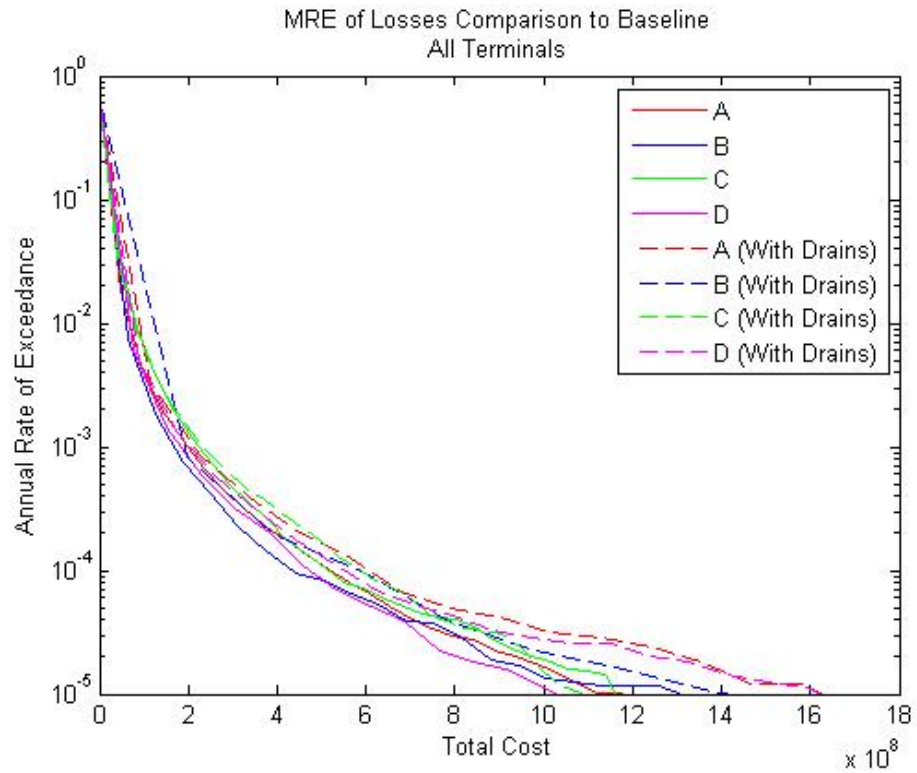


Figure 5.7 – MRE of Total Losses With and Without Drains: All Terminals

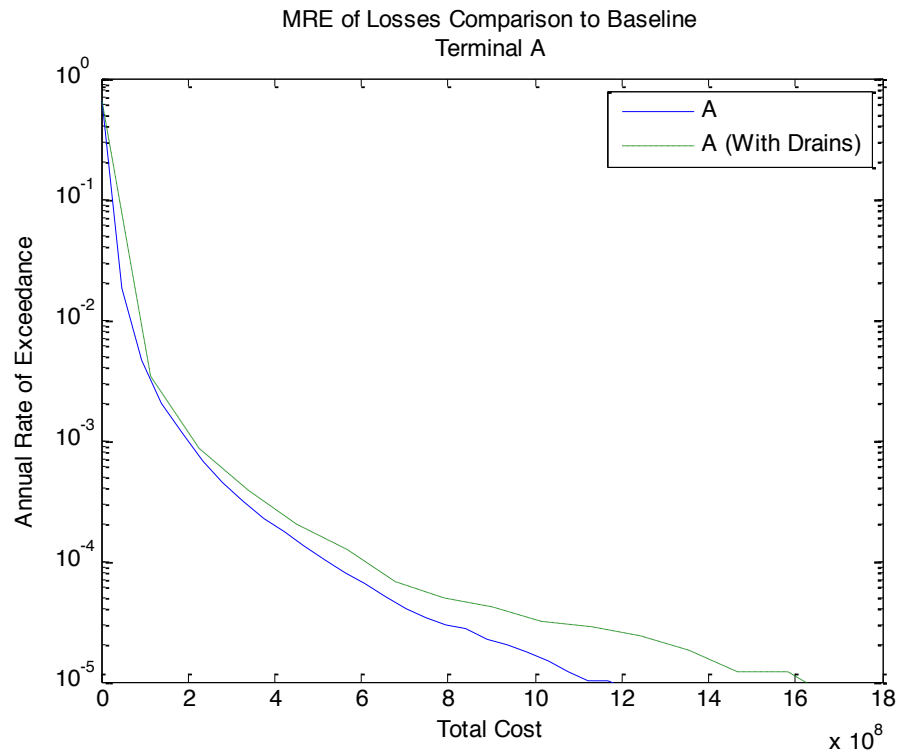


Figure 5.8 – MRE of Total Losses With and Without Drains: Terminal A

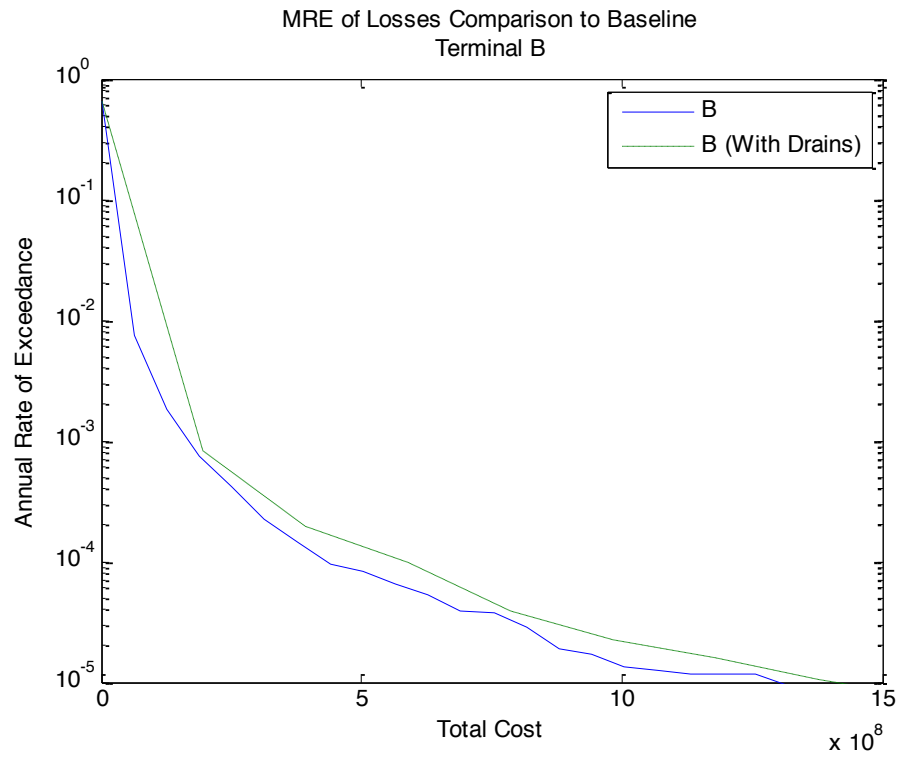


Figure 5.9 – MRE of Total Losses With and Without Drains: Terminal B

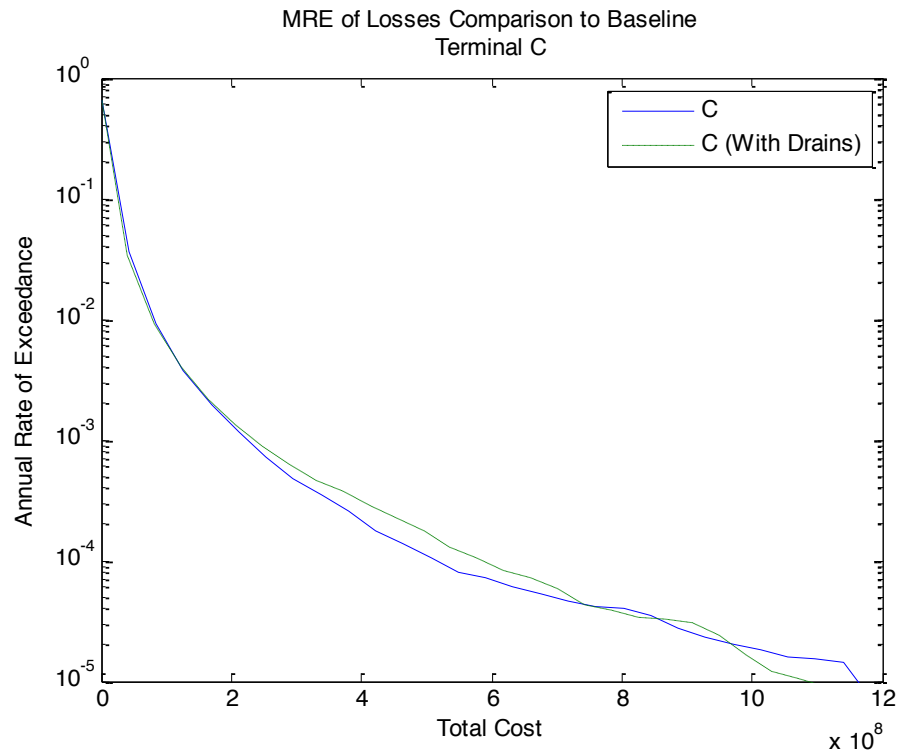


Figure 5.10 – MRE of Total Losses With and Without Drains: Terminal C

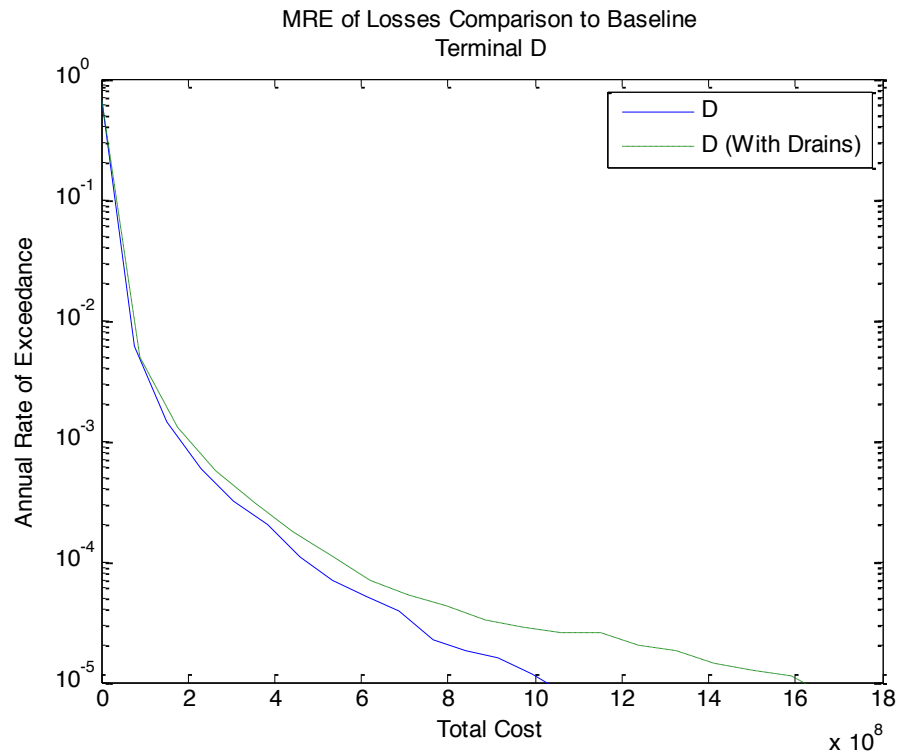


Figure 5.11 – MRE of Total Losses With and Without Drains: Terminal D

While it is apparent that the installation of vertical drains does have an effect in reducing the wharf repair costs, the reduction in exceedance is so small that it has only a slight affect in reducing the overall total cost.

5.2 Structural Options

5.2.1 Crane Improvements

Three different crane types existed in the baseline configuration. To illustrate the effect of crane improvements, the cranes at terminals A, B, and D were replaced with J100 cranes. These are the newest and least seismically vulnerable of the cranes tested within the scope of this risk analysis. The following figures (Figure 5.12 - Figure 5.14) plot the annual rate of exceedance for crane repair costs at terminals A, B, and D for the baseline configuration and a configuration with upgraded cranes: (Terminal C was omitted because a J100 crane already existed in the baseline configuration.)

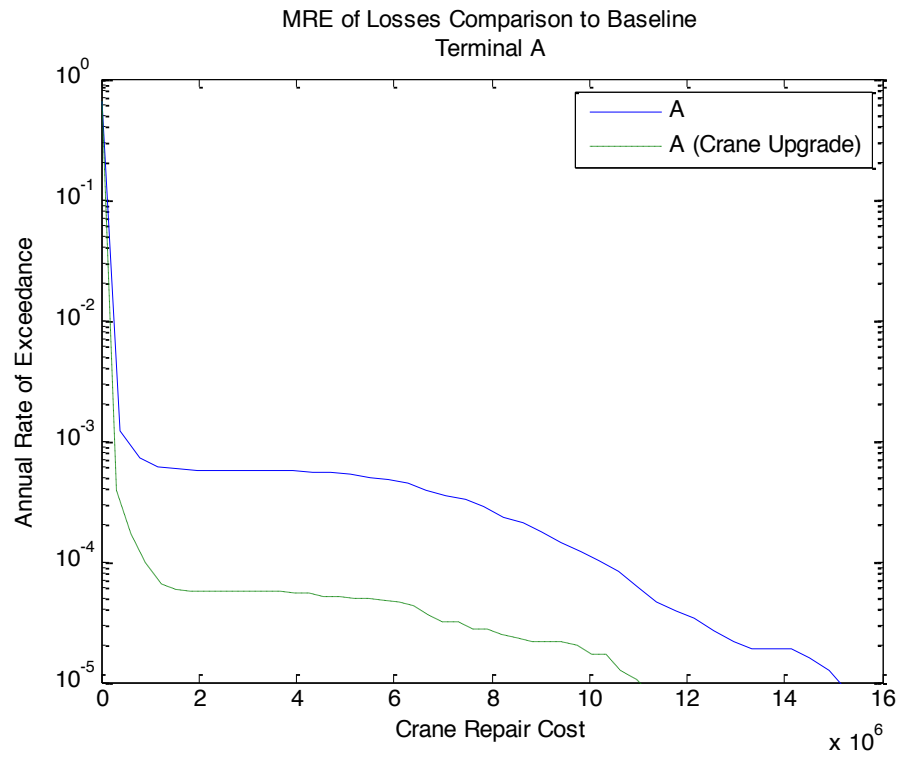


Figure 5.12 – MRE of Crane Repair Costs With and Without Crane Upgrade: Terminal A

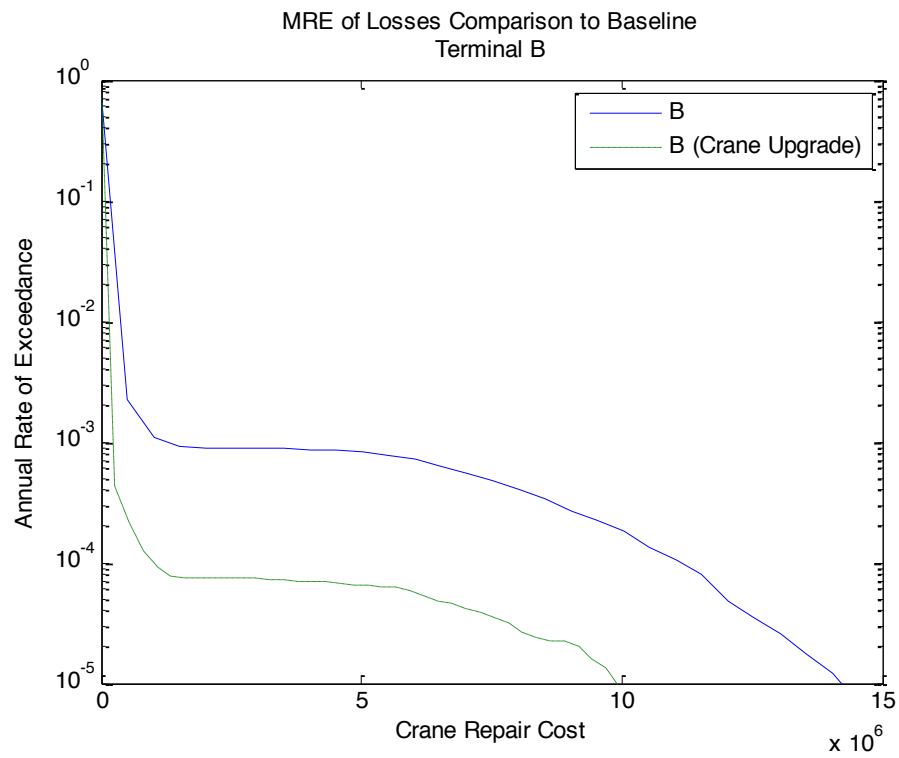


Figure 5.13 – MRE of Crane Repair Costs With and Without Crane Upgrade: Terminal B

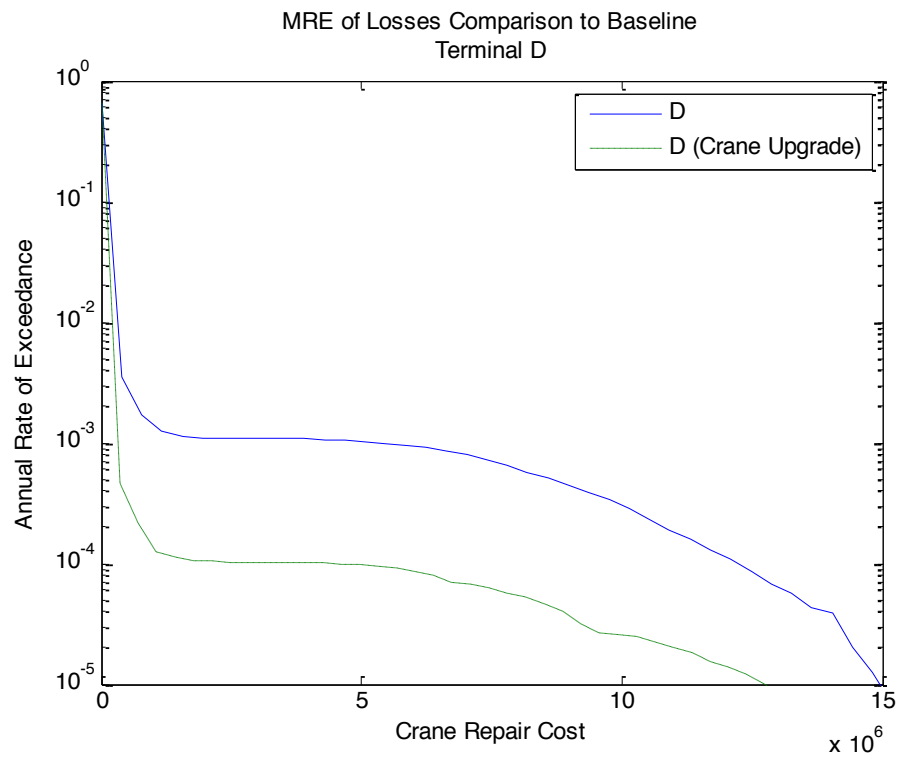


Figure 5.14 – MRE of Crane Repair Costs With and Without Crane Upgrade: Terminal D

In every case, replacing the current crane with the J100 upgrade decreased the exceedance rate for crane repair costs. Comparatively (

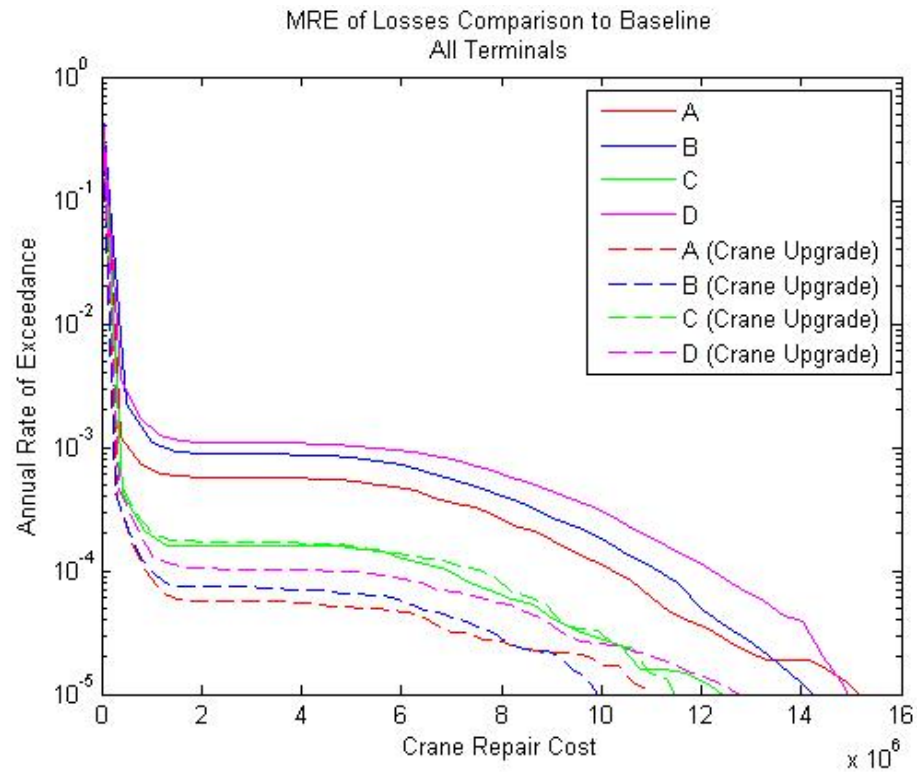


Figure 5.15), terminals B and D, which correspond to the LD100 crane, show the largest difference in exceedance rates for repair costs between all the terminals:

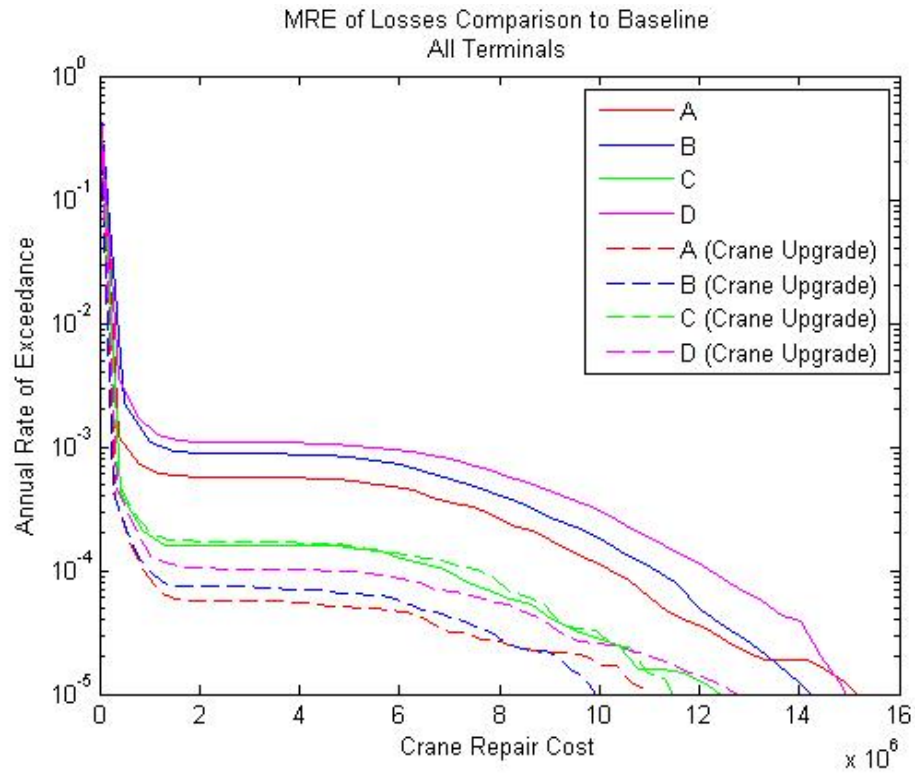


Figure 5.15 - MRE of Crane Repair Costs With and Without Crane Upgrade: All Terminals

It is obvious that crane repair costs are lowered by updating all the current cranes. However, replacement of the cranes would need to lower the total cost at each terminal in order to be cost effective overall. Figure 5.16 compares exceedance rates for total cost between all the terminals:

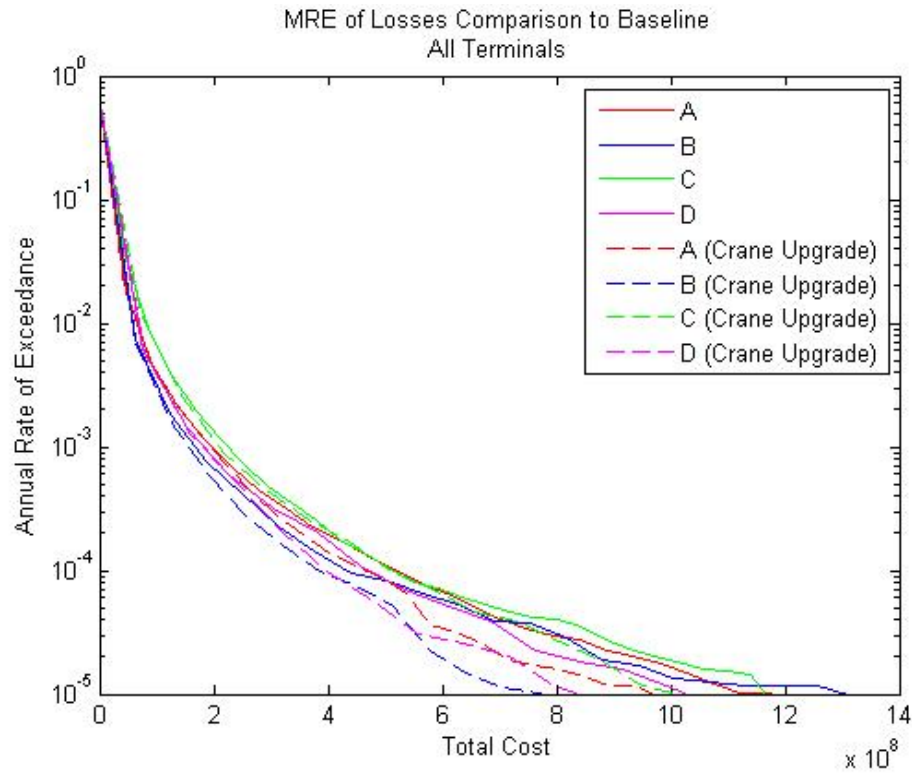


Figure 5.16 - MRE of Total Costs With and Without Crane Upgrade: All Terminals

Terminals A, B and D all show decreased exceedance rates for total cost. This decrease can be attributed partially to the decrease in crane repair cost, but is mostly attributed to the decrease in business interruption losses that can be seen in Figure 5.17 - Figure 5.19:

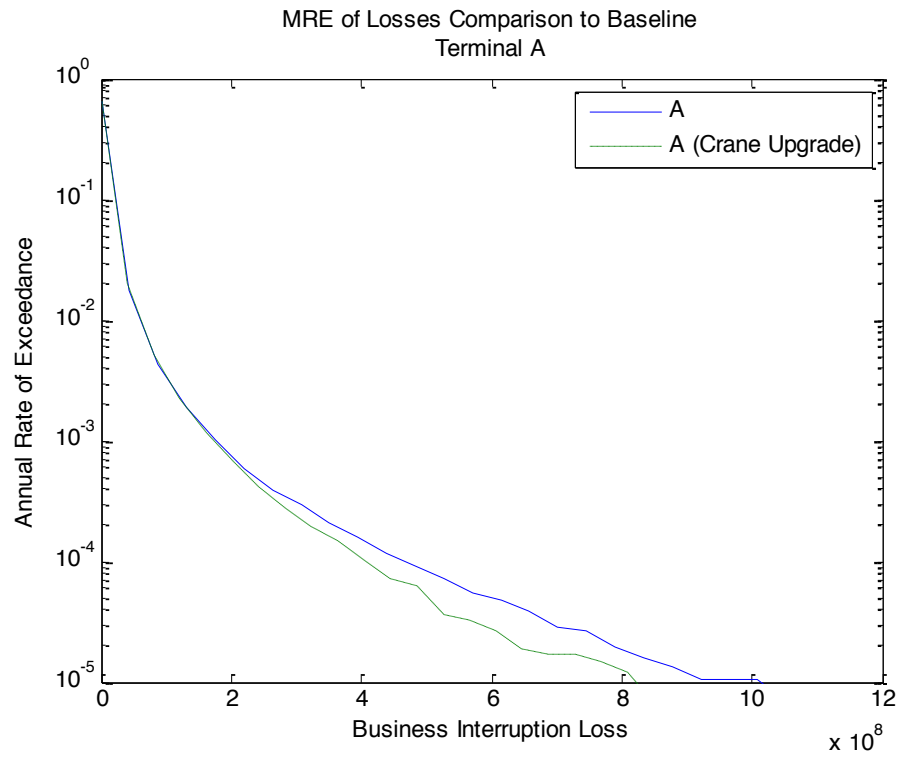


Figure 5.17 - MRE of BIL With and Without Crane Upgrade: Terminal A

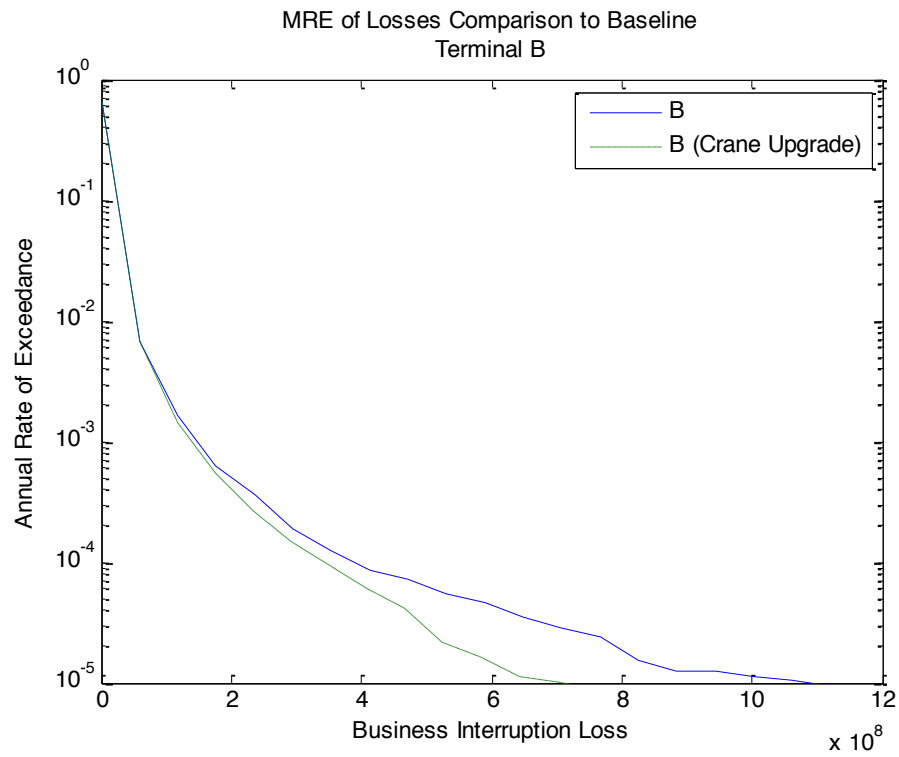


Figure 5.18 - MRE of BIL With and Without Crane Upgrade: Terminal B

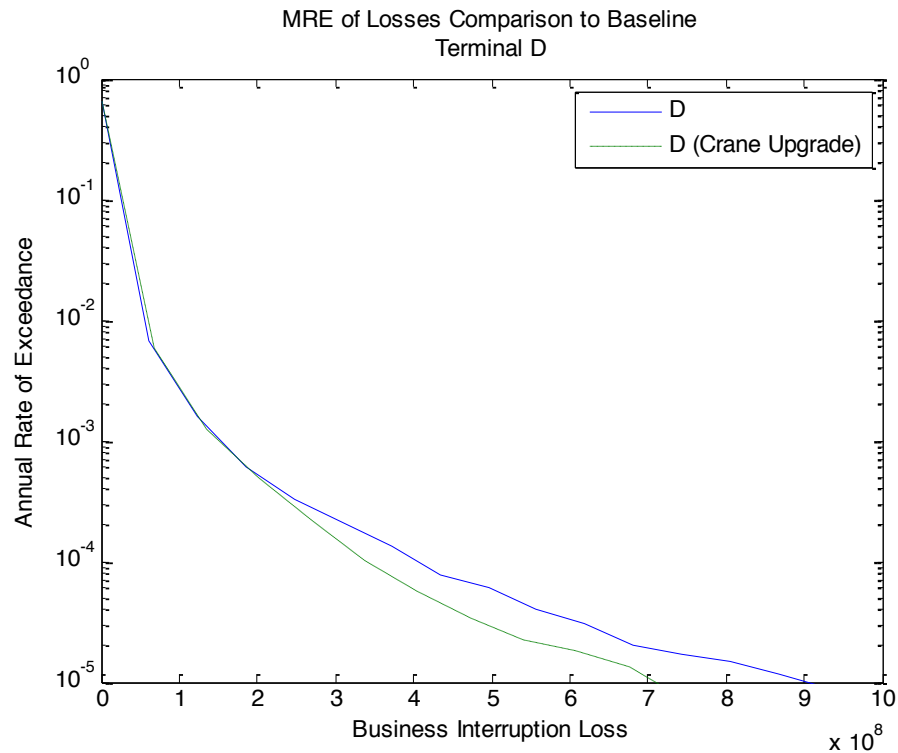


Figure 5.19 - MRE of BIL With and Without Crane Upgrade: Terminal D

Using this information, if crane upgrades were to be planned, it would be best to update the LD100 cranes in Terminals B and D first, and then the LD50 cranes at Terminal A since the crane repair cost is reduced the most for the LD100 cranes.

5.3 Repair Options

As seen in Section 4.5.3, business interruption losses comprise the majority of the overall total cost. Operational mitigation options provide a means to decrease the business interruption losses within the port. Multiple operational scenarios will be run to study the effect of operational changes on the total cost. Introducing repair incentives and implementing a force majeure option will be studied as mitigation options. Additionally, runs will also be conducted that vary the mobilization time and the repair sequence in order to examine those variables effect on total cost.

5.3.1 Repair Incentives

The following program run offers a repair incentive to the construction workers repairing the physical port damage. By offering a repair incentive, the effect of decreasing the overall downtime can be examined. In this scenario repair time will be reduced by 50% and the corresponding repair costs will be doubled. For example, a repair scenario that took 14 days and cost \$450,000 in the baseline configuration will now take 7 days but cost \$900,000. This scenario is a simple rough estimate of real life repair incentives. Obviously the repair time of every job cannot be cut in half, and it may cost more or less than double the original cost. However, this estimate should still provide excellent insight into the affect that repair time and cost has on the port system.

The first plot of exceedance rates for repair costs checks to make sure that repair costs are being increased within the risk analysis program. If every cost for each of the 100,000 earthquakes is doubled, the exceedance rates for the run with decreased repair times should be much higher than the baseline run:

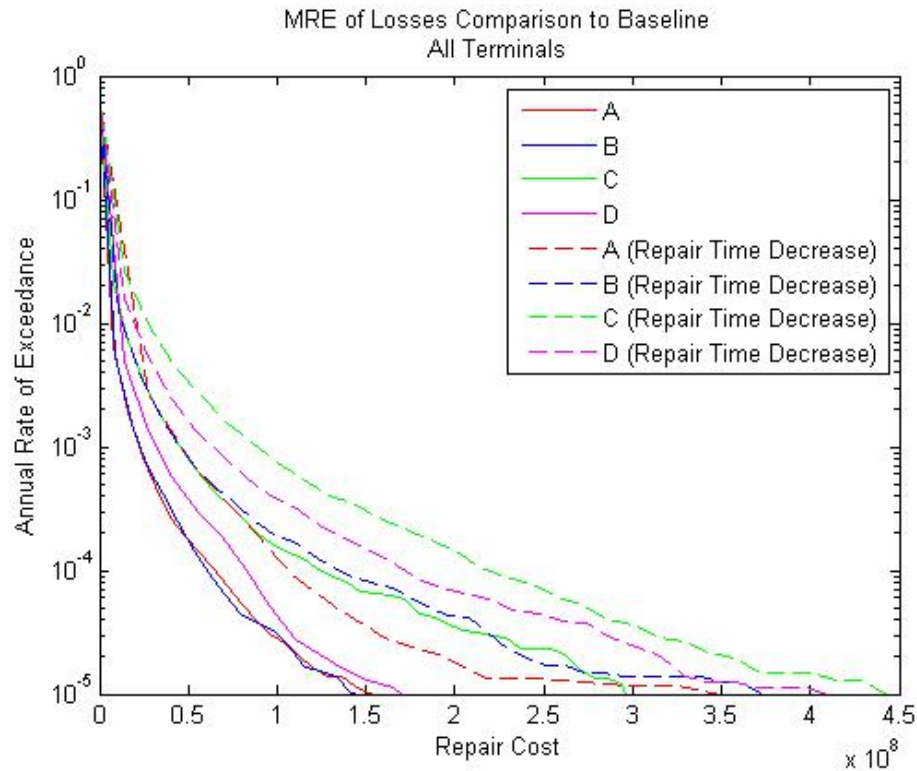


Figure 5.20 – MRE of Repair Costs Baseline and Repair Time Decrease: All Terminals

Figure 5.20 shows that exceedance values of repair costs with the repair time decrease are in fact higher than that of the baseline run. Therefore the program is calculating repair costs correctly. Likewise, repair time reductions can be checked by examining the exceedance values of the business interruption losses. When repair times are reduced, fewer ships will be displaced at the hypothetical port and business interruption losses will be reduced, reducing the exceedance rates (Figure 5.21):

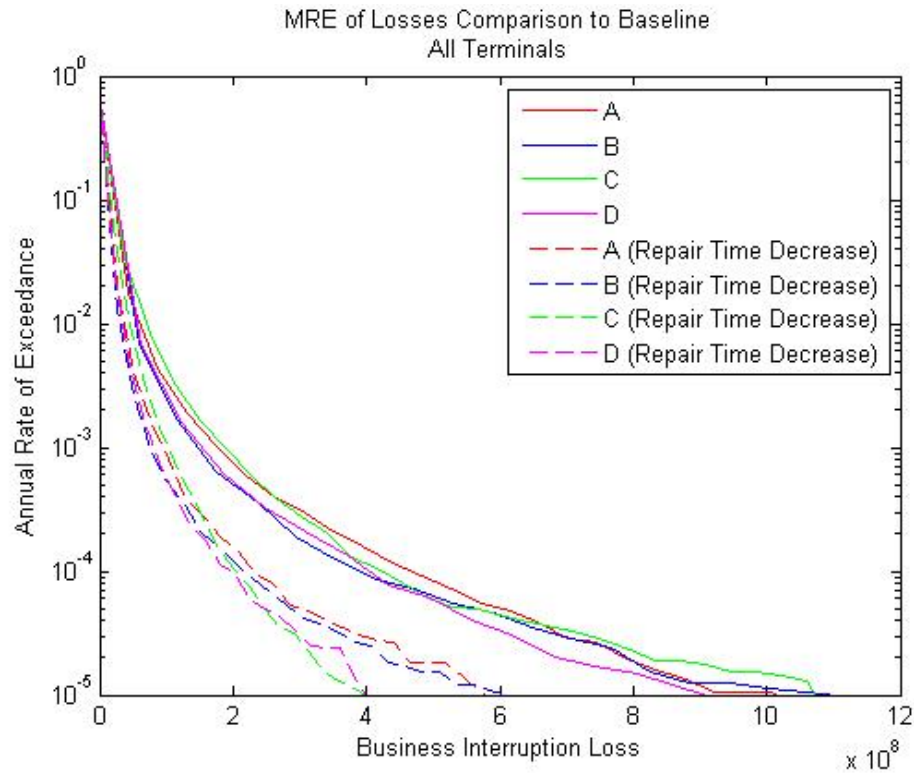


Figure 5.21– MRE of BIL Baseline and Repair Time Decrease: All Terminals

Exceedance rates for the repair time decrease scenario are all smaller than the baseline exceedance rates. Therefore, the program is properly implementing the reduction in repair time. The overall effect of the reduction of repair time and the increase in repair cost will be determined by the exceedance rates for total cost (Figure 5.22 - Figure 5.26):

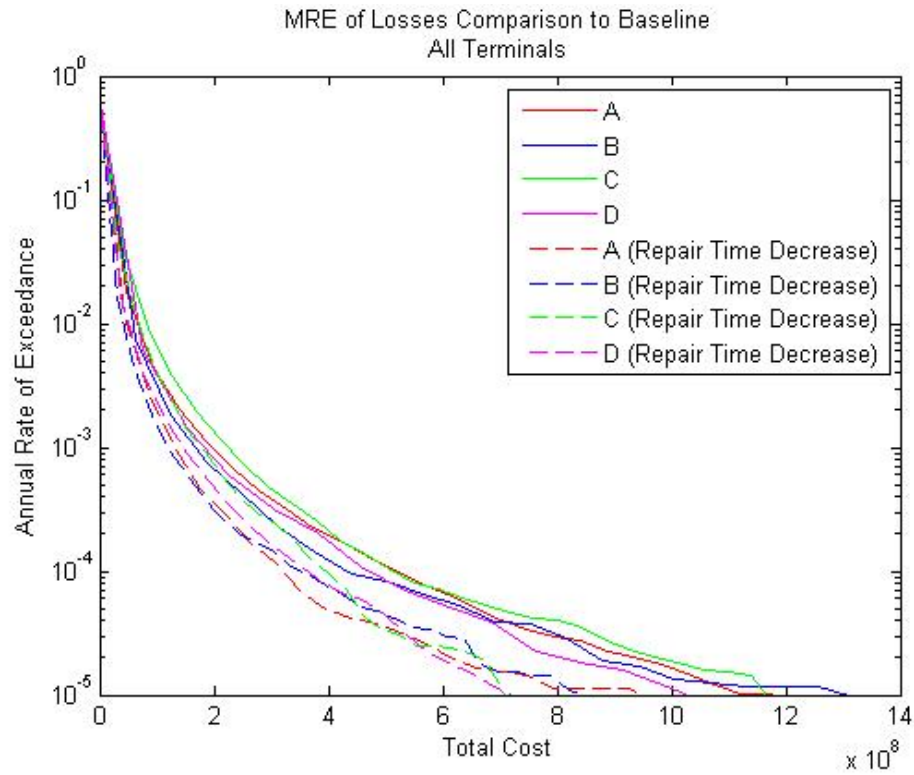


Figure 5.22 – MRE of Total Cost Baseline and Repair Time Decrease: All Terminals

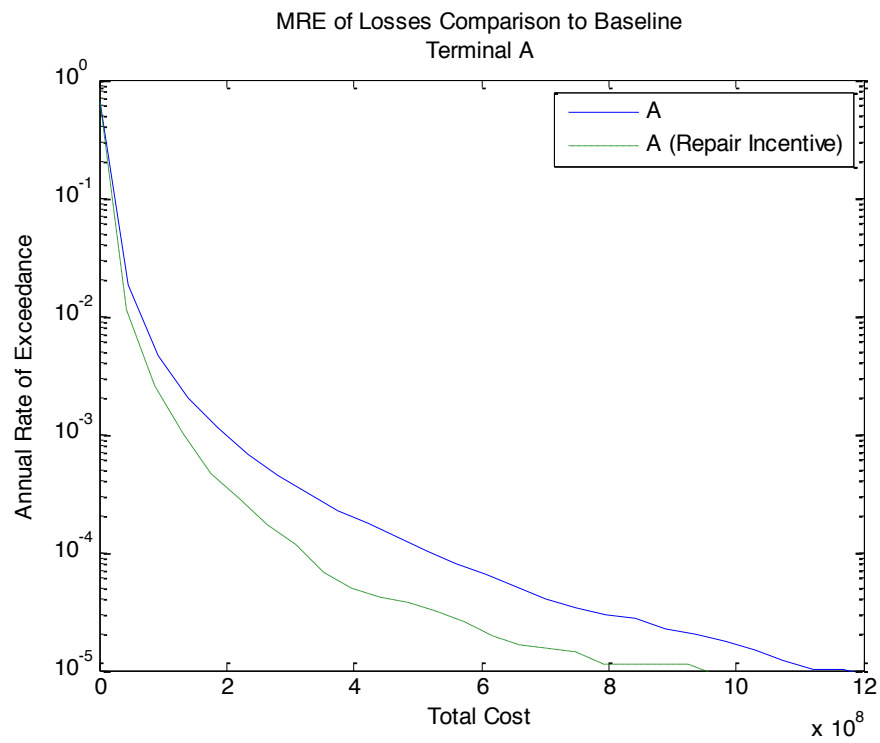


Figure 5.23 – MRE of Total Cost Baseline and Repair Time Decrease: Terminal A

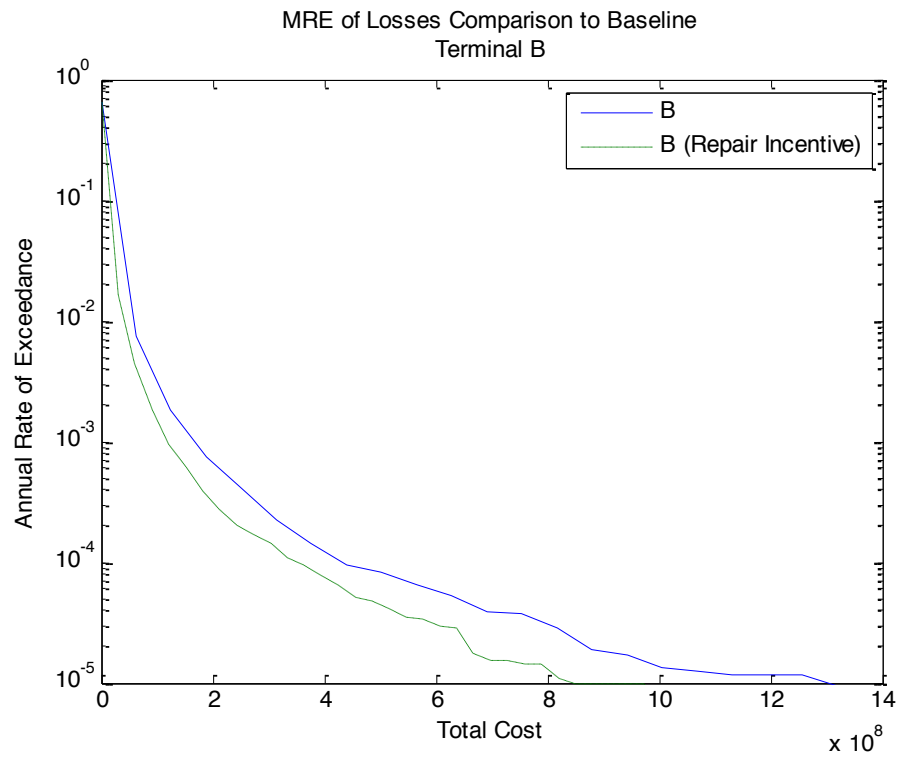


Figure 5.24 – MRE of Total Cost Baseline and Repair Time Decrease: Terminal B

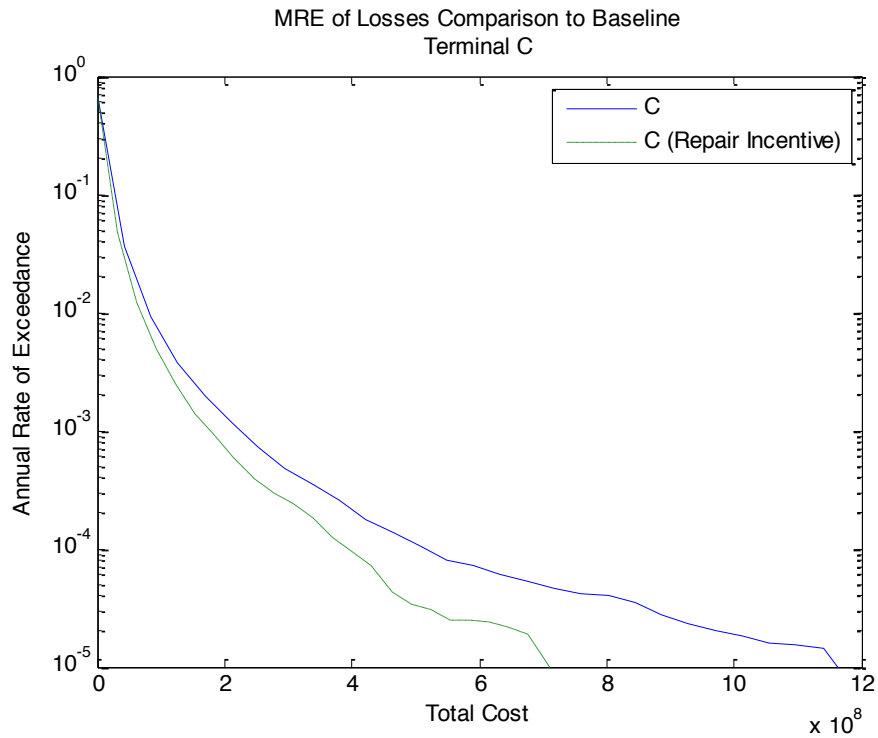


Figure 5.25 – MRE of Total Cost Baseline and Repair Time Decrease: Terminal C

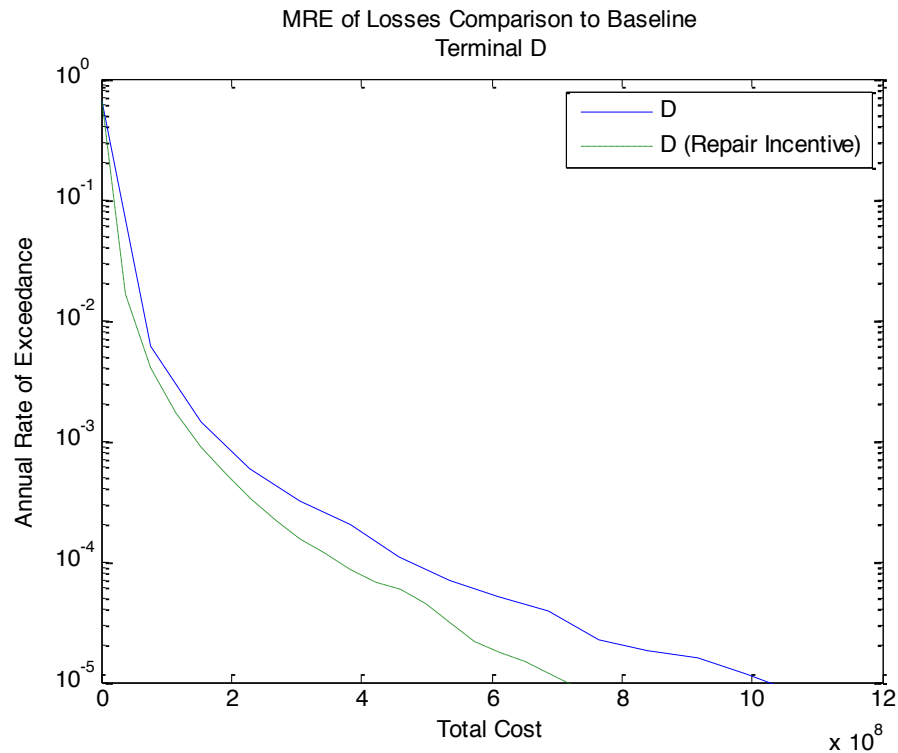


Figure 5.26 – MRE of Total Cost Baseline and Repair Time Decrease: Terminal D

Despite the increase in repair costs, the decrease in repair time decreased the exceedance rates for the overall total cost. In fact, the decrease in exceedance rates is clearly visible at every terminal. This result reiterates the significance of business interruption loss in calculating the total cost.

5.3.2 Varying Mobilization Time

Mobilization time refers to the amount of time it takes to get the supplies and workers needed to begin port repair. The mobilization time within the baseline run is a function of the earthquake magnitude. For earthquakes less than 6.0 mobilization is assumed to take place within a week, or take 7 days. Earthquakes M 6.0 – 7.0 are assumed to have mobilization times of 14 days, and earthquakes above a M 7.0 are assumed to have mobilization times of 28 days. It was apparent from the reduction of repair time run that decreases in repair time have significant effects on the total cost.

Therefore two additional runs were completed to test the effect of varying the mobilization time. In one run, mobilization time was decreased to 10 days independent of the earthquake magnitude, and in the second run mobilization time was increased to 60 days independent of the earthquake size. Figure 5.27 uses business interruption loss to compare the increase and decrease of mobilization time to the baseline run for Terminal A:

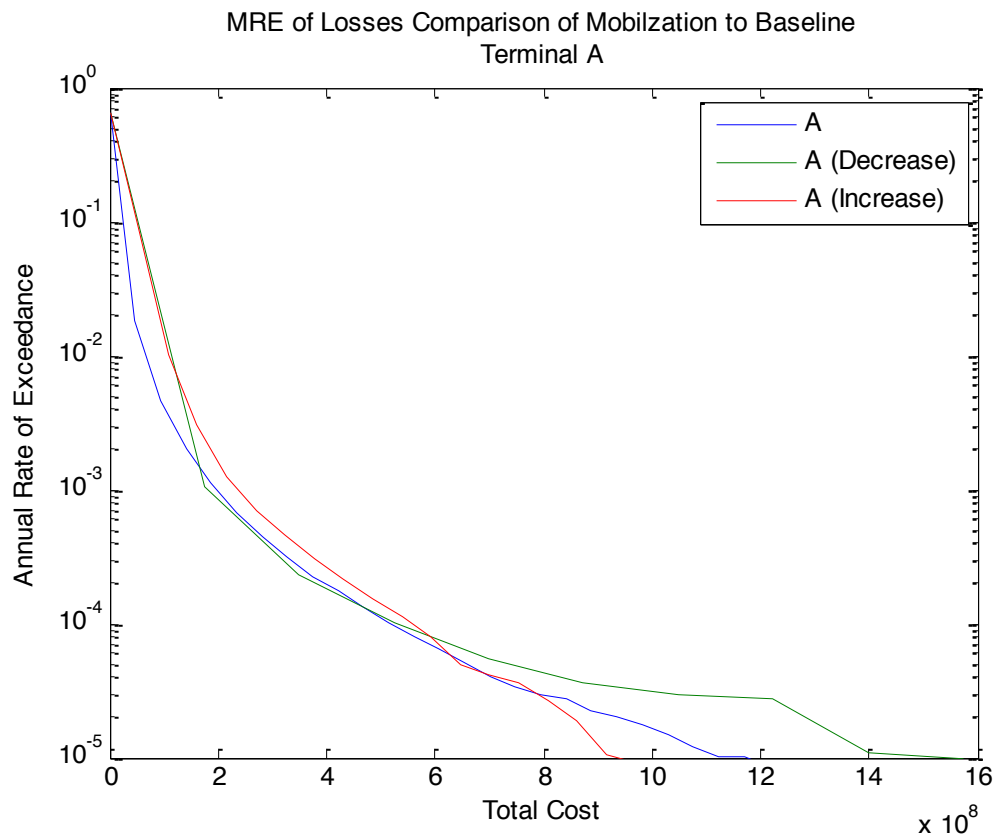


Figure 5.27 – MRE of Total Cost Baseline and Mobilization Variation: Terminal A

Differences in total cost are negligible for exceedance rates larger than 10^{-4} (10000 year return period). Since only data above the 10^{-4} is considered well defined, it is possible to say that adjusting mobilization time will not provide a significant effect in increasing or reducing the total cost. This is further confirmed by the MRE curves generated for total cost for the other terminals (Figure 5.28 - Figure 5.30):

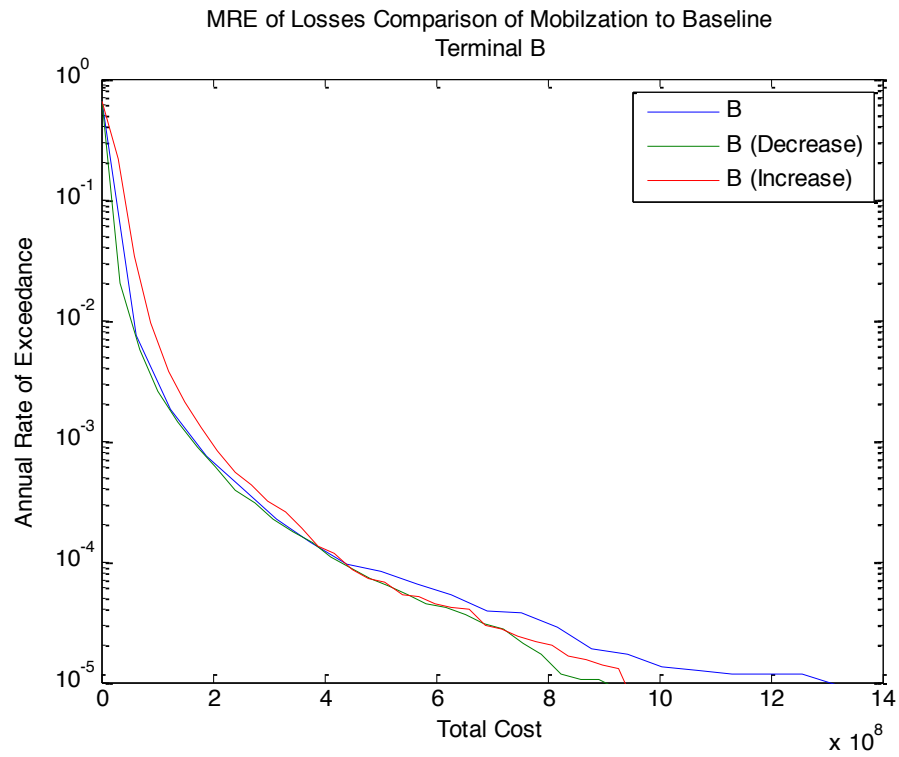


Figure 5.28 – MRE of Total Cost Baseline and Mobilization Variation: Terminal B

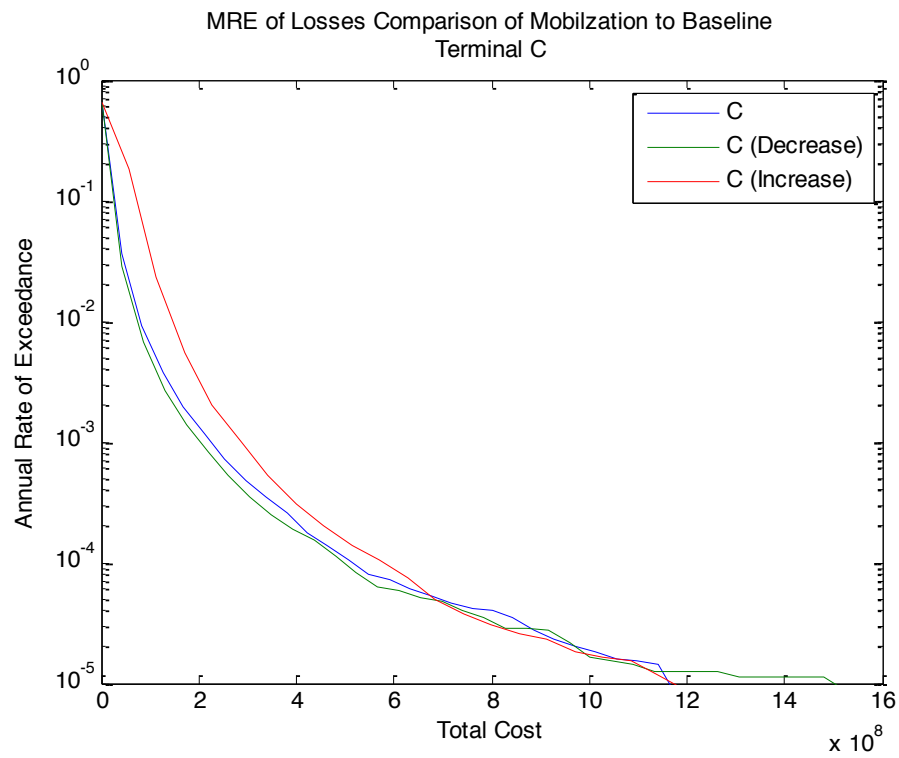


Figure 5.29 – MRE of Total Cost Baseline and Mobilization Variation: Terminal C

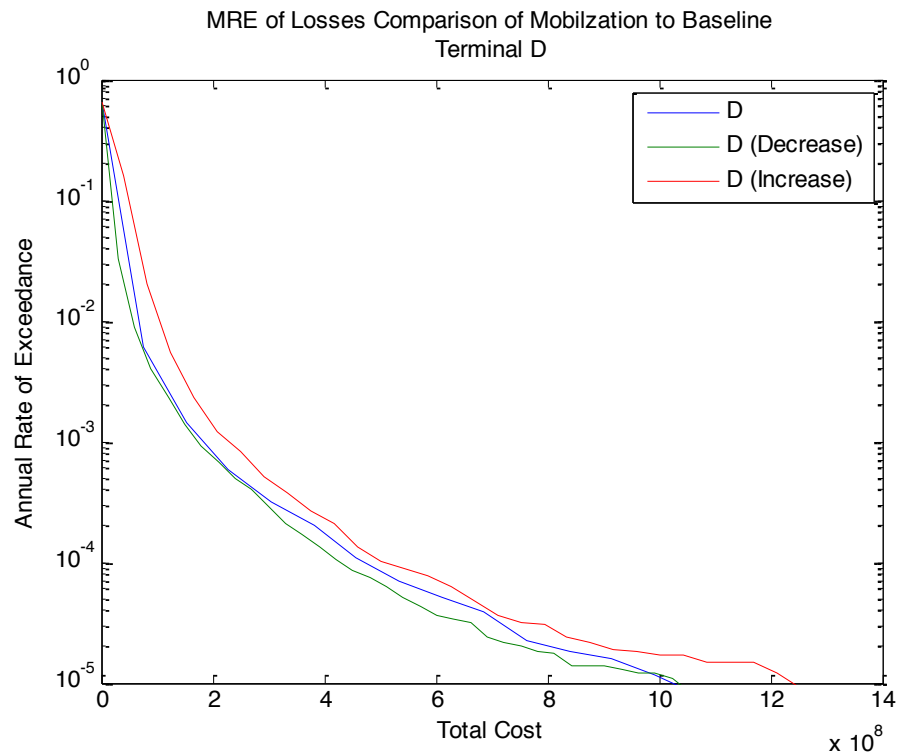


Figure 5.30 – MRE of Total Cost Baseline and Mobilization Variation: Terminal D

5.3.3 Repair Sequencing

It is assumed in the baseline scenario that wharf and crane repairs will be done simultaneously (in parallel). As an example, take the following terminal with the following repair times for each berth and crane (Figure 5.31):

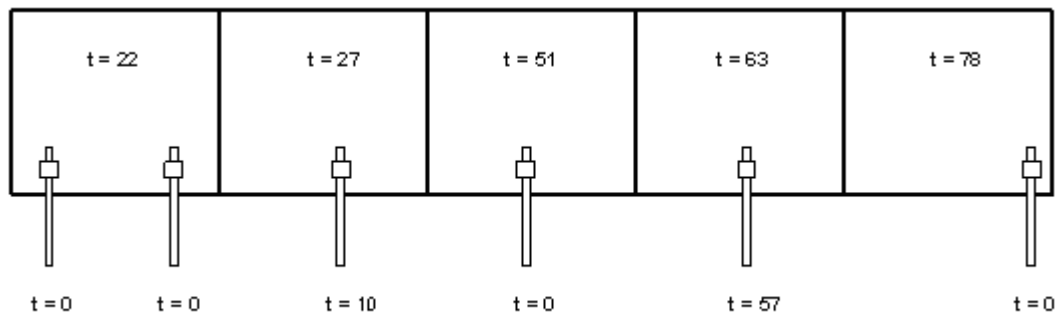


Figure 5.31 – Terminal Example: Repair Sequencing

In the baseline scenario the total repair time would equal 78 days for the wharf and 57 days for the crane because it is assumed that workers would be making repairs on the entire wharf from day 1. This scenario is used for the baseline runs because it is not unreasonable to assume that workers would repair more than one berth in a terminal at a time. It would be extremely conservative to assume that the workers would only work consecutively on only one berth or crane at a time. In that case, the repair time would increase from 78 days to $22+27+51+63+78 = 241$ days for the wharf and 67 days for the cranes. A program run was conducted that implemented the “series” scenario and it had a large influence on the business interruption loss (Figure 5.32):

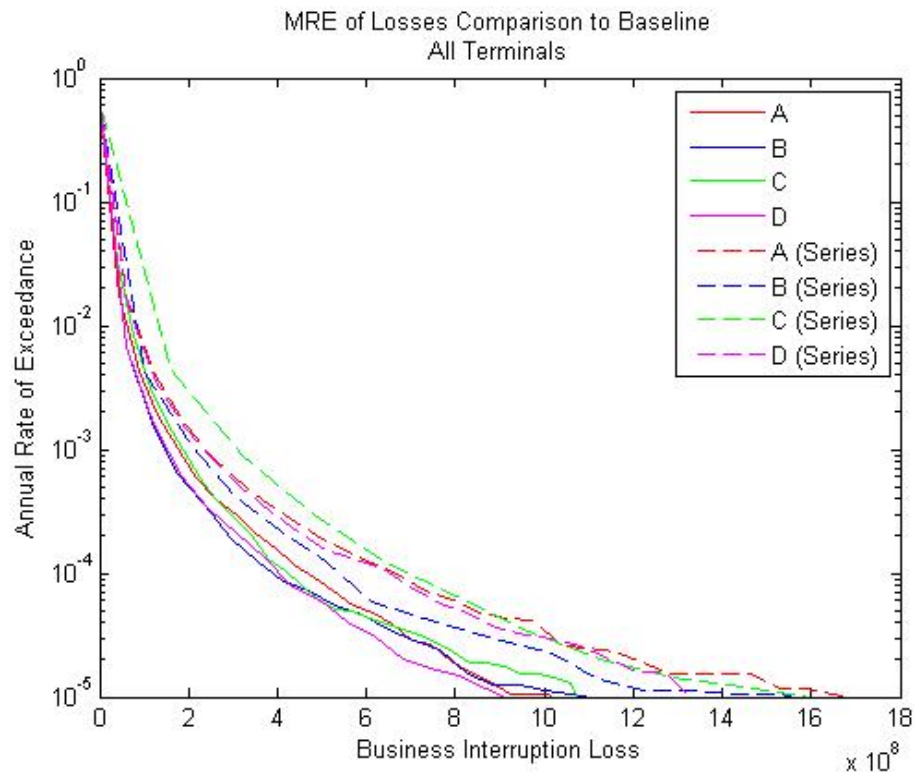


Figure 5.32 – MRE of BIL Baseline and Repair Sequencing Variation: All Terminals

Figure 5.32 shows significant increases in exceedance were present at every terminal. Subsequently this affected the total cost in the same manner (Figure 5.33):

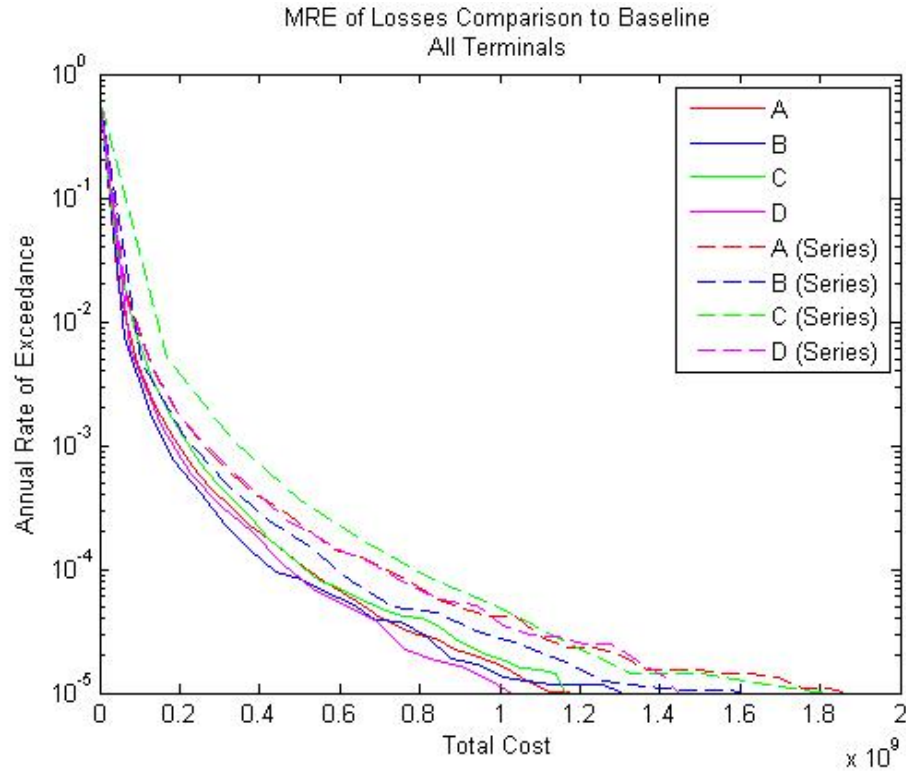


Figure 5.33 – MRE of Total Cost Baseline and Repair Sequencing Variation: All Terminals

5.4 Operational Options

In an emergent situation it is common for a port to implement a force majeure policy in which ships of varying companies are allowed to dock at any wharf to which they are assigned. To test this scenario the ship arrivals of terminals A and B will be combined and incoming ships will be allowed to dock at any of the open berths within the two terminals. In a force majeure situation and earthquake would occur and damage would result at terminals A and B. The repairs to each terminal would be calculated normally and the repair costs would remain the same. However, business interruption losses would differ because there are now a larger number of berths that the incoming ships could possibly dock at. If the BQCSP operational model was used to calculate BIL it would have to be rewritten to account for the larger number of combined berths and

cranes. However, the regression operational model estimates BIL using the following variables: berth length, number of cranes, and the wharf and crane repair times.

If force majeure was enacted, it could be represented by one of two methods using the regression equation. First, terminals A and B could be combined into a “superberth” with a length of $(2400+2400)$ 4800 ft, $(4+5)$ 9 cranes. However, the repair times would have to be set to either that of terminal A or B. It was decided that repair times would be set to the minimum of the two maximum repair times for the wharf under the assumption that by the minimum max repair time incoming ships could at least fully utilize the repaired terminal, and business interruption losses should not exceed past that date. The second method for calculating BIL in a force majeure situation uses the commutative property ($BIL_{AB} = BIL \text{ for Terminal A} + BIL \text{ for Terminal B}$) and the fact that using the minimum of the max repair times in the superberth essentially means that now each terminal can have the BILs calculated separately as long as the repair times for each are the minimum max repair time of the two terminals. When calculated separately, a series of if statements can be added within the risk analysis framework to ensure that if the BIL of say Terminal A was zero before force majeure, it will remain zero after force majeure.

Remember, the operational regression equation first determines if the BIL for a particular earthquake equals zero, if it does not, it calculates the BIL. So for method one with the superberth, the regression would determine if $BIL = 0$, and if not calculate the BIL. However, it is possible that for a given earthquake that originally had BILs equal to zero for both terminals, that a $BIL > 0$ could have been calculated for the superberth. This result is unacceptable because it is not representative of reality. Therefore it was prevented by separating the terminals, finding the BIL using the minimum max repair time if the original BIL was > 0 , and then adding the terminals together to get the BIL for the combined terminal. When plotted, the MREs for method one and method two were quite similar, but it was decided to use method two because it was more realistic. Figure plots the MRE for total cost for 100,000 stratified sample earthquakes using force

majeure method 2 and compares that to the sum of the total costs if Terminals A and B were calculated separately.

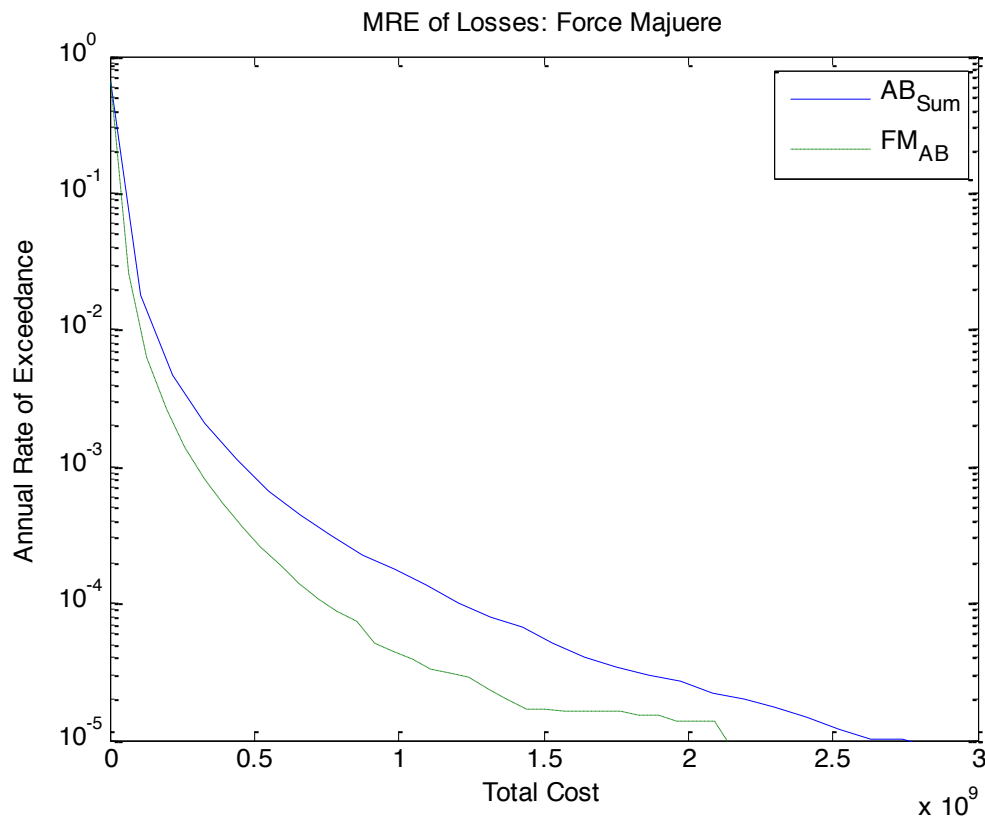


Figure 5.34 – MRE of Losses: Force Majeure

Force majeure reduces annual rates of exceedance especially for the very small values. Therefore, it would be a good mitigation option to reduce the business interruption losses at ports. This is particularly true since it has no initial costs.

5.5 Economic Analysis of Alternative Options

One of the real benefits to the vast functionality of the risk analysis program and all of the data that it can produce is that it can be used to assess seismic vulnerability in ports and be applied in various economic analyses evaluating mitigation options. Recent studies have found that in some higher-hazard ports in the US, no plans to assess seismic vulnerability have been made, and many have no or only informal seismic mitigation plans (Scharks et al.). Unlike engineers, port stakeholders are more likely to use financial

data rather than force or displacement data to make important port decisions such as retrofitting a component or changing an operational routine. The risk analysis framework marries the two by using engineering data to estimate financial losses that could be used to make important port decisions. The following sections highlight some of the ways in which the risk analysis can be utilized to economically evaluate mitigation options, plan for emergency response, and calibrate the current seismic design.

5.6 Economic Analysis

Several economic analyses could be used with the risk analysis to evaluate mitigation options. The methods discussed in the following section will include cost benefit analysis, mean-variance, and stochastic dominance. Several mitigation options will be examined within the scope of the hypothetical port using the aforementioned methods.

5.6.1 Cost Benefit Analysis

One of the most commonly used methods for economic analysis is cost benefit analysis (Sullivan et al. 2003). This method can be used to assess whether a project is worth completing or to choose between several different options. The basic principal involves comparing the total expected cost of an option against the total expected benefits to determine if the benefits outweigh the cost:

$$B - C = \frac{PV(\text{benefits of proposed project})}{PV(\text{total cost of proposed project})} \quad (5.1)$$

Using this equation, if the ratio $B-C > 1$, then the benefits outweigh the costs and the project is a good investment. However, if $B-C < 1$, the benefits do not outweigh the cost and the project is not a good investment.

For the port system cost benefit analysis will be used to compare the cost/benefit of installing vertical drains in the embankment at each terminal. Costs associated with this scenario include:

- Cost of installing vertical drains at each terminal

Benefits associated with this scenario will include:

- Money saved in business interruption losses by decreasing the TEU loss during earthquakes with the installation of the vertical drains.
- Money saved in wharf repair costs during earthquakes with the installation of the vertical drains.
- Money saved in crane repair costs during earthquakes with the installation of the vertical drains.

Annual maintenance and operating costs for the port are being excluded in this analysis because each would be relatively equal with or without the presence of vertical drains at the terminals. The cost benefit analysis will be conducted over an exposure time of 20 years using a discount rate of 5% per year to determine whether the installation of vertical drains is a good investment.

5.6.1.1 Cost of Installing Vertical Drains

Vertical drains installed within the wharf embankment will span the length of the terminal and treat the embankment 100 ft. inland of the landside crane rail (Rathje 2010). Each corrugated drain is 3 inches in diameter with a spacing of 3.3 ft. Therefore for each 100 ft of terminal length there are $30 \times 30 = 900$ drains. Drains will be extended the full depth of the liquefiable soil layer (60 ft.). Therefore there would be $900 \times 60 \text{ ft.} = 54000$ linear ft. of drains per 100 ft. of terminal length.

Scott Ellington, a prefabricated vertical drain contractor at Ellington-Cross suggests that drain installation roughly costs about \$4 per linear foot (Ellington 2010). Therefore, $\$4/\text{ft} \times 54000 \text{ ft} = \$216,000$ per 100 ft of terminal will be used to calculate the total cost of drain installation at each terminal:

Table 5.1 – Installation Costs per Terminal for PVDs

Terminal	Terminal Length (ft.)	Drain Installation Cost (\$)
A	2400	5,184,000
B	2400	5,184,000
C	5400	11,664,000
D	3600	7,776,000

5.6.1.2 Calculation of Benefits

To calculate the money saved through the implementation of vertical drains, wharf repair costs, crane repair costs, and business interruption losses were calculated by the program for the scenario where drains have been installed in the port in addition to the baseline scenario. Repair costs and BIL with drains (Table 5.2) and Repair costs and BIL for the baseline (Table 5.3) were calculated at each terminal:

Table 5.2 – Average Repair Costs and BIL with Drains

Terminal	Repair Cost (\$)	BIL (\$)
A	480,948	6,494,950
B	486,619	4,818,660
C	1,094,360	8,074,470
D	740,625	5,457,780

Table 5.3 – Average Repair Costs and BIL: Baseline

Terminal	Repair Cost (\$)	BIL (\$)
A	476,348	6,881,400
B	475,937	5,153,050
C	1,090,270	8,604,650
D	725,274	5,825,250

The money saved can then be calculated by subtracting the losses for repair and business interruption for the scenario run with drains from the baseline scenario (Table 5.4):

Table 5.4 – Wharf Repair Costs and BIL Saved Through Drain Upgrade

Terminal	Wharf Repair Cost (\$)	BIL (\$)	Total (\$)
A	-4,600	386,450	381,850
B	-10,682	334,390	323,708
C	-4,090	530,180	526,090
D	-15,351	367,470	352,119

5.6.1.3 Calculation of Cost/Benefit

The benefit cost ratio will be calculated for each terminal using the costs and benefits calculated above in the following equation where i = discount rate and N = study period (Sullivan et al, 2003):

$$B - C = \frac{PV(\text{benefits of proposed project})}{PV(\text{total cost of proposed project})} = \frac{\text{Total Benefit} * \frac{i(1+i)^N}{(1+i)^N - 1}}{\text{Installation Cost}} \quad (5.2)$$

Table shows the result of the calculation of the above equation for each terminal:

Table 5.5 – B-C Ratio for PVD Installation

Terminal	B-C Ratio
A	0.006
B	0.005
C	0.004
D	0.004

5.6.1.4 Conclusion

From the ratios, it is apparent that cost of installing vertical drains is not exceeded by the benefits of installation for any of the terminals in the hypothetical port. Therefore, it can be said that while the installation of vertical drains in the wharf backfill does

reduce the wharf and crane repair costs during earthquake events, overall it is not cost effective and is not recommended as a mitigation option.

5.6.2 Mean-Variance Analysis

Mean-variance is a method of decision making borrowed from modern portfolio theory that aims to make “portfolios” mean/variance efficient. In other words, portfolios should have the highest level of return per unit of risk and the lowest level of risk per unit of return (Lintner 1965). Translated for the port, mean-variance criterion evaluates the “investment” of a seismic mitigation option and how it affects the return (or profit) of the port system and the variance of the returns associated with that mitigation option. The goal for a port system would be to apply a mitigation option that offers a large reduction in overall loss, and also is fairly consistent (i.e., minimum variance) in producing that result.

Calculation of the mean total cost of the investment option will be taken from the exceedance curves for total cost, and the variance will be calculated from the mean according to the equation:

$$Variance = \left(\sum_{i=0}^N \left(p_i^2 * \frac{Var(X)}{N} \right) \right) * total\ rate^2 \quad (5.3)$$

where N is the total number of strata from stratified sampling, p_i is the probability of an earthquake being in strata i , and the total rate is the sum of all mean rates of occurrence for the earthquakes sampled. $Var(X) = \int (x - \mu)^2 f(x) dx$ where μ is the mean expected value calculated from:

$$mean = \left(\sum_{i=0}^N (p_i * [mean(x_i)]) \right) * total\ rate \quad (5.4)$$

The following figure (Figure 5.35) plots the mean total costs and standard deviations of that total cost in Terminal B for three of the previously discussed mitigation options: the addition of prefabricated vertical drains in the embankment backfill, the

upgrade to solely J100 cranes at Terminals A, B, and D, and the reduction of wharf and crane repair times by half while doubling the repair costs:

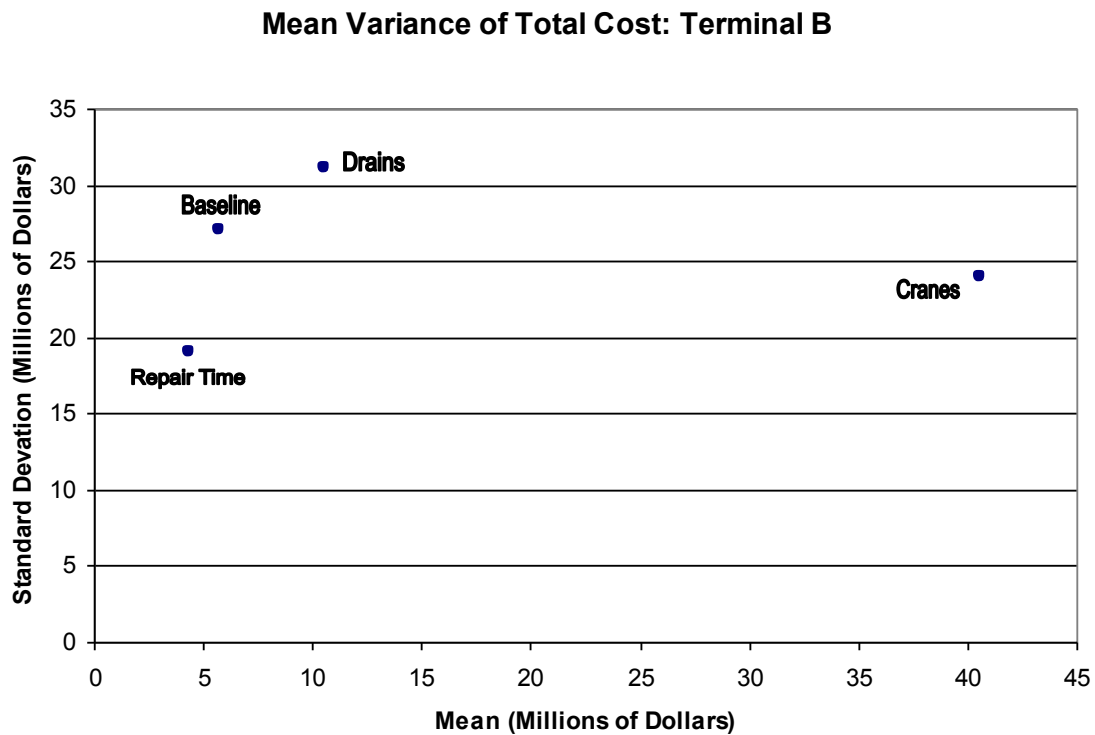


Figure 5.35 – Mean Variance of Total Cost: Terminal B

In examining the means in Figure 5.35 it is apparent that the largest decrease in total cost came from the repair time decrease option. The implementation of PVDs or a crane upgrade had higher mean costs than the baseline scenario because the initial costs for the mitigation options are so large. The repair time mitigation option produced the largest decrease in variance, followed by the drain option. The variance for the crane mitigation option was slightly higher than the baseline. From Figure the mitigation option involving the repair time would be good to implement and the drain mitigation might be considered if the reduction in variance was worth the increase in mean cost. However if a mitigation option were to be implemented, it is apparent that the best to

worst option of the three shown would be: repair time decrease, installation of vertical drains, and upgrade of cranes.

5.6.3 Stochastic Dominance

Stochastic dominance is commonly used in decision analysis in reference to ranking gambles (probability distributions over a number of possible outcomes) as superior to other gambles. For the port system, the gambles will be taken as the entire cumulative distribution function of total loss for the different mitigation options at the port. Using stochastic dominance, options can be ranked. First order dominance would be preferential where A is dominated by B if the $CDF_A \geq CDF_B$ at every point. If this is not the case and $\int x dCDF_A = \int x dCDF_B$, the options will be ranked using second order dominance criteria. Here, A is dominated by B if $\int u(x) dCDF_A \leq \int u(x) dCDF_B$ for every weakly increasing concave utility function u . This translates to B being more dominant over A if B is more predictable (has a lower risk aversion) and has at least as high of a mean.

10,000 earthquake conventional Monte Carlo samples were run to get the total loss data used to create cumulative distribution functions for the stochastic dominance comparison. Monte Carlo sampling was chosen over stratified sampling because the total cost data generated in the program from stratified sampling is not representative of the earthquake distribution of the ERF. To accurately compare the total costs generated by the earthquakes in the samples, the earthquakes themselves need to be representative of the ERF. The following figure compares cumulative distribution function of the total cost (in millions of dollars) for the following mitigation options: configuration with drains, all terminals with upgraded J100 cranes, and a 50% decrease in repair time (with a doubled repair cost) for Terminal B (Figure 5.36):

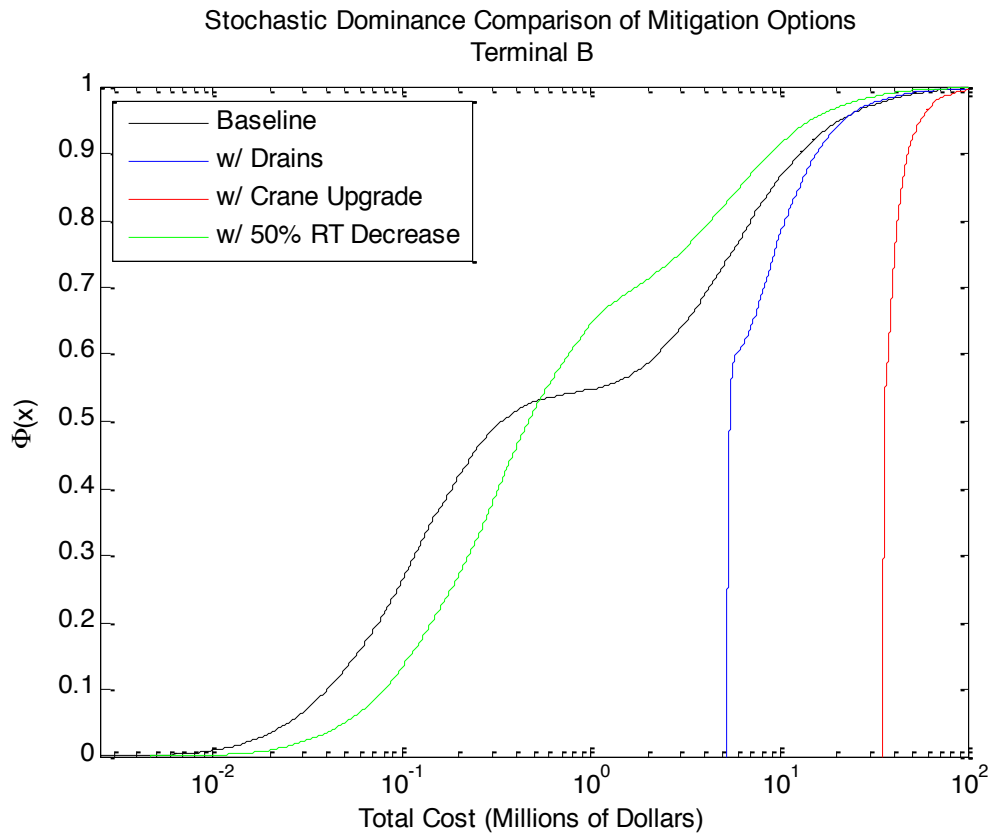


Figure 5.36 – Stochastic Dominance Comparison of Mitigation Options: Terminal B

The cumulative distribution functions show the same order as the mitigation option comparison using mean variance: the repair time decrease has the smallest total cost values in its cumulative distribution function, installation of drains follows, and lastly the crane upgrade option.

5.7 Planning for Port Emergency Response Operations

As seen in Port-au-prince, Haiti, for ports are vital components in emergency response reactions (Green et al. 2010; Werner et al. 2010). In order for a port to operate at a maximum functionality after earthquake disasters, emergency response preparations should be made before the earthquake event. The risk analysis program could be used to estimate the port's operational capacity after an earthquake event and test various mitigation options that might help increase capacity (such as force majeure).

5.8 Calibration of Current Seismic Design

The risk analysis program could be used to calibrate the current seismic design within west coast ports. For instance, the contingency level earthquake (CLE) and the operating level earthquake (OLE) at the Port of Los Angeles (POLA) have return periods of 475 and 72 years, respectively. If the terminal locations, and terminal parameters (terminal length, wharf type, number of cranes, crane type, etc.) for the Port of Los Angeles were input into the risk analysis program, it could be used to calculate the repair times and repair costs at the port. Those could then be input into an operational model and for the CLE it would be possible to estimate if:

- 1.) “CLE forces and deformations, including permanent embankment deformations, [resulted] in controlled inelastic structural behavior and limited permanent deformation.” (Port of Los Angeles 2007)
- 2.) “All damage requiring repair [was] located where visually observable and accessible for repairs.” (Port of Los Angeles 2007)
- 3.) “Temporary loss of operations [was] restorable within an acceptable period of time.” (Port of Los Angeles 2007)

For the OLE it would be possible to estimate if:

- 1.) “OLE forces and deformations, including permanent embankment deformations, [did not result] in significant structural damage.” (Port of Los Angeles 2007)
- 2.) “All damage requiring repair [was] located where visually observable and accessible for repairs.” (Port of Los Angeles 2007)
- 3.) “Repairs [did] not interrupt wharf operations.” (Port of Los Angeles 2007)

If these requirements were met, no calibration would be needed. However, if they were not, the risk analysis program could be used to estimate appropriate exceedance values for the specified level of damage or test mitigation options that would improve

port performance to the specified level of damage. While it is not possible to estimate requirements 1 and 2 for either of the earthquake levels because the location and components in the hypothetical port differ from those of the POLA, the hypothetical port will be used to estimate operations after OLE and CLE events. For the OLE, the baseline port scenario will be run for a design earthquake with an annual rate of occurrence = 1.3×10^{-2} and the CLE for an exceedance rate = 2.1×10^{-3} . The program will calculate average total losses, business interruption losses, and repair costs for a sample of specific intensity measures. The reference curve in Figure 5.37 was used to determine that an exceedance rate of 0.013 (OLE) corresponded to a PGV of 15 cm/s and that an exceedance rate of 0.002 (CLE) corresponded to a PGV of 42 cm/s:

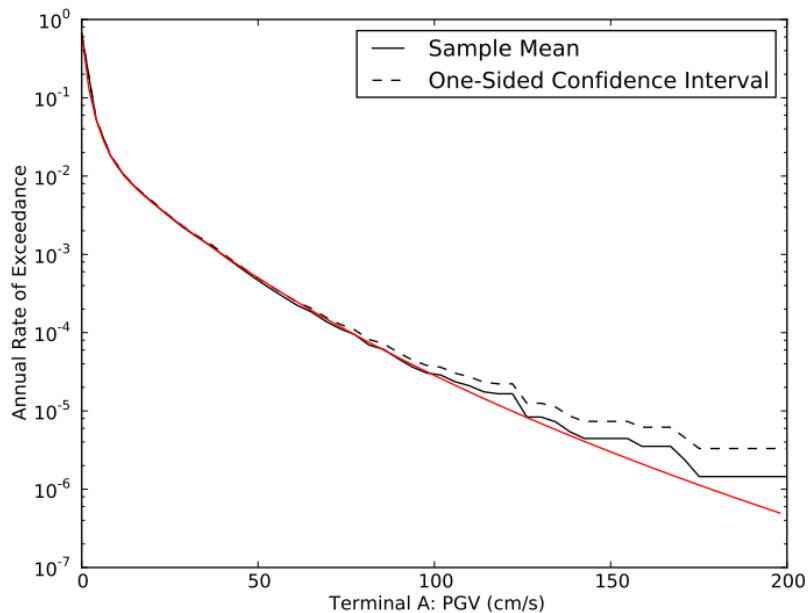


Figure 5.37 – Reference curve for PGV vs. Annual Rate of Exceedance

The operating level earthquake was run in the program as a 10,000 earthquake sample from the ERF with a mean PGV of 15 cm/s and a COV = 0.2 ($\sigma = \pm 3$ cm/s). The contingency level earthquake was run in the same manner with a PGV of 42 cm/s and a coefficient of variation = 0.1 ($\sigma = \pm 4.2$ cm/s). While Figure 5.37 is calculated

specifically for Terminal A, similar graphs for each of the other terminals were also examined. For an exceedance rate of 0.002, PGV values were generally in the 40-45 cm/s range and it is expected that relative intensities for both earthquake levels at all terminals will be included within the specified variances.

Table 5.6 shows the average repair costs and times, business interruption losses, and total losses for each of the terminals in a baseline hypothetical port that were calculated by running an intensity-based sample of 10,000 earthquakes.

Table 5.6 – Repair Costs and Times for OLE and CLE at hypothetical port

OLE	Max Repair Time		Costs		
Terminal	Wharf	Crane	Repair Cost	BIL	Total Loss
A	198	17	\$5,733,480	\$51,886,500	\$58,174,900
B	201	29	\$5,920,040	\$42,953,800	\$49,910,400
C	273	4	\$13,309,500	\$61,048,000	\$74,510,200
D	235	37	\$8,915,830	\$48,686,200	\$59,165,800

CLE	Max Repair Time		Costs		
Terminal	Wharf	Crane	Repair Cost	BIL	Total Loss
A	372	131	\$13,060,100	\$107,690,000	\$125,609,000
B	381	168	\$13,754,100	\$99,453,600	\$121,239,000
C	577	80	\$33,433,400	\$120,290,000	\$157,701,000
D	470	218	\$21,371,100	\$114,107,000	\$150,204,000

Granted, the baseline configuration of the hypothetical port was designed to be the most seismically vulnerable configuration tested, the damage sustained during either the operating or contingency level earthquakes are still quite large. For instance, the wharf damage at Terminal C after the OLE would take 9 months to repair. In those nine months, there is \$61 million of business interruption losses. When displaced, the port and terminal operators combined lose anywhere from \$300,000 to \$2,747,000 per ship. Assuming an average value per ship of \$1.5 million, a BIL of \$65 million would translate into approximately 43 displaced ships on average for an operating level earthquake. This statistic does not coincide with the no interruption in wharf operations expected. The

same sentiment applies to the CLE which has average wharf repair times at every terminal greater than one year. The POLA code does not specifically mention what an “acceptable period of time” is for the restoration of port operations, but it is more than likely less than one year.

Again it should be noted that the hypothetical port is in a different geographic location than the POLA, and wharf structures, soil conditions, and port configurations at the POLA are not exactly the same as for the hypothetical port. However, it is apparent that if the risk analysis framework were applied specifically to the Port of Los Angeles it could be extremely useful in calibrating current seismic design.

6 APPLICATION OF RISK ANALYSIS FRAMEWORK TO OTHER PORTS

As explained in Chapter 3, the risk analysis framework was specifically designed for use at the hypothetical port in Santa Cruz, California. However, aspects specific to the hypothetical port or its location can be changed so that the risk analysis framework could be applied to other actual or hypothetical ports in the US. The following chapter discusses the issues and makes suggestions as to how one would go about applying the risk analysis framework to another port location or configuration. Specific categories include: hazard-related, component-related, and system-related issues.

6.1 Hazard-related Issues

The hazard-related issues in within the risk analysis program are all contingent upon the location of the port to be analyzed. The hypothetical port was located in Santa Cruz, California and this location determined the latitudes and longitudes of each of the terminals, the earthquake rupture forecast used, and the ground motion prediction equation chosen with in the analysis. For ports located in different locations, the following must be considered:

Port Location: Rupture distances are determined using the latitudes and longitudes of the earthquake rupture to the latitudes and longitudes of the terminal locations. The details of each should be known.

Earthquake Rupture Forecast: For the hypothetical port, the ERF is pulled from the Uniform California Earthquake Rupture Forecast, Version 2 (WGCEP 2008) according to those ruptures that possibly affect the chosen Santa Cruz port site. Relevant earthquakes are determined using the OPENSHA program (Feild et al. 2009). If the ERF were repopulated based on location, these references could be used for other California sites, but port locations outside California would require different methods in acquiring ruptures for the generation of the ERF. The USGS earthquake hazard program is one

possible source for rupture sites, because it has hazards mapped for the 48 conterminous states, Alaska, Hawaii, Puerto Rico and the Virgin Islands.

Ground Motion Prediction Equation: The OpenSHA program has the capability of using one of the following attenuation relationships to calculate the median intensity measures at the terminal sites: Abrahamson and Silva (1997), Abrahamson and Silva (2008), Abrahamson (2000), Boore and Atkinson (2008), Boore, Joyner, and Fumal (1997), Campbell and Bozorgnia (2003), Campbell and Bozorgnia (2008), Campbell (1997), Chiou and Youngs (2008), Field (2000), Sadigh et al.(1997), ShakeMap (2003), Spudich et al. (1999), and USGS Combined (2004). In addition, OpenSHA also accommodates the following intensity measure types (in relation to each ground motion): peak ground acceleration (PGA), peak ground velocity (PGV), peak ground displacement (PGD), spectral acceleration (SA), and modified Mercalli intensity (MMI). If the OpenSHA program does not contain a ground motion prediction equation applicable to the port site, the intensity measures must be calculated manually for every rupture to terminal site distance according to the required GMPE.

6.2 Component-related Issues

The Grand Challenge risk analysis framework focused on modeling pile-supported marginal wharves, which are the most common type of wharf structure in the US, and light-duty 50 ft gage (LD50), light-duty 100 ft gage (LD100), and jumbo 100 ft gage (J100) cranes, which are the three most commonly found crane types in the US. However, specific wharf and crane configurations will vary from port to port depending on local practice, soil conditions, age of the structures, etc. The following sections discuss the issues involved in modeling wharf and crane structures other than those used for the hypothetical port.

6.2.1 Wharf and Embankment

As mentioned, embankments and wharf types vary from port to port as a factor of local practices, soil conditions, etc. Therefore, the embankment/wharf model currently used in the risk analysis program will not be applicable to another port. The following section discusses alternative wharf and embankment types and the main issues involved in implementing a model using these alternative configurations.

6.2.1.1 Other possible embankments

The embankment in the hypothetical port is a sloped embankment consisting of hydraulically placed sand fill over native soils. While this embankment type is common within US ports, the back fill could also consist exclusively of native soils, be a combination of rock and sand dike with a backland fill, or consist of a sea wall or bulkhead (Werner 1998).

6.2.1.2 Embankment Performance in Past Earthquakes

Generally, embankments have not performed well during seismic excitation. Most failures are caused by embankment foundations on top of weak underlying soils or the embankment being constructed of loose sandy fills that are prone to strength loss during excitation. Common failure modes include: severe lateral ground deformations, excessive settlements due to the densification of loose sandy soils, slumping of embankments, slope failures through embankment, and catastrophic failures of the underlying foundation soils which lead to deep-seated embankment failures (Werner 1998).

6.2.1.3 Embankment Modeling

Proper modeling of the embankment is important because slope failures and the resulting displacements can exert significant forces onto piles, cause displacement of the crane rail, or displacement of the wharf itself. Seismic analysis of the embankment

should therefore focus on the stability of the embankment itself and also the global stability of the embankment including the embankment, backfill, and foundation soils (Werner 1998). In choosing the type of analysis, consideration should be taken as to the potential for liquefaction. For embankments without hydraulically placed backfill more traditional pseudostatic rigid body methods would suffice for modeling. However, if liquefaction is a potential problem, the user should at least choose a two-dimensional numerical model that calculates both porewater pressures and displacements within the embankment at multiple points along the wharf piles/walls. OPENSEES (McKenna and McGann 2010) or FLAC (Itasca 2011) provide an excellent medium through which to conduct these analyses.

6.2.1.4 Other Possible Wharf Configurations

The wharf modeled for the hypothetical port was a 1960's pile-supported marginal wharf categorized by the 2 sets of batter piles on the landside and seaside of the wharf (Section 3.4.3.1). This wharf type is one of the pile-supported marginal wharves commonly found in US ports and the design was replaced by more modern designs without batter piles. Additional wharf models and fragility curves will need to be generated for wharf types that differ from the type used in the hypothetical port. Some typical wharf configurations aside from pile supported marginal wharves include pile walls and gravity walls (quay walls). Figure 6.1 shows some of the typical pier and wall structures used around the world (PIANC 2001). The pile supported wharf types are typically found in the US while the quay walls are more common elsewhere. For instance quay walls were the most common wharf structure in the port of Kobe.

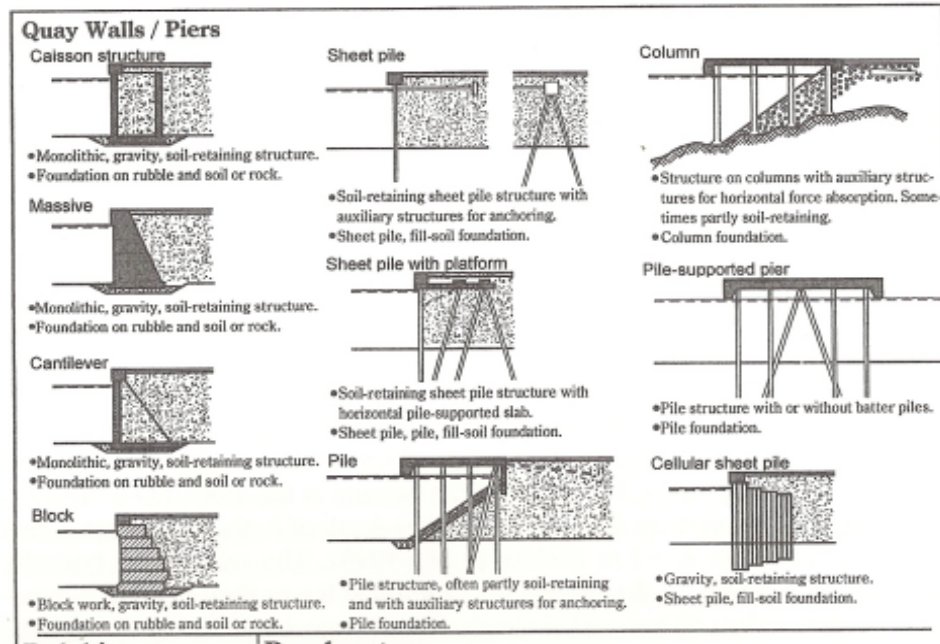


Figure 6.1 – Common Wharf Structures (from (PIANC 2001))

6.2.1.5 Wharf Performance in Past Earthquakes

Past earthquakes have demonstrated several key vulnerabilities in pile-supported marginal wharf performance. The presence of batter piles has been seen to have poor earthquake performance. Batter piles provide large amounts of lateral stiffness which mobilizes large lateral seismic forces at pile caps and deck connections. This has led to severe cracking and fracture of piles in addition to the damage of the pile caps and decking (Werner 1998). Wharves containing solely vertical piles have fared much better during past earthquake excitation because they are more flexible laterally than batter piles. However, vertical piles still do not have the ductility or anchorage needed to perform well in liquefiable soils.

6.2.1.6 Developing Fragility Curves

The physical modeling of the wharf, especially at a liquefiable site, will require at least a two dimensional finite element analysis that integrates the embankment results into the wharf model as input through some type of soil-structure interaction model. The

wharf model used in the hypothetical port analysis used OPENSEES and integrated the soil-structure interaction through the use of a macroelement model which uses a Bouc-Wen type hysteresis model to capture the effects of liquefiable soil. This resource is currently available in the current version of OPENSEES.

When developing fragility curves, attention needs to be paid to modeling the parts of the wharf that are prone to damage so that the assessment of damage states is accurate. For pile-supported wharves, common damage modes include:

- 1.) Pile Damage – Include minimally spalled and moderately damaged vertical piles (above or below the water level), broken batter piles (if applicable), and broken piles below the ground surface.
- 2.) Deck Damage – Include damage to the underside of the deck above the piles, ruptured concrete shear keys, and ruptured deck caused by punch through
- 3.) Displacements – Include the relative movement between the crane rails and the collector trench and the relative movement between the crane rail and the wharf deck

Repair costs and times for each of these failure modes can be found in Section 3.4.3.3. Damage states and the corresponding repair costs and times will be selected from this data by modeling the displacements (piles, deck, etc.) and the relative movement of various wharf components (wharf deck to crane rail, crane rail to collector trench, etc.), the rotation of the pile deck connections due to torsional forces, and the curvature ductility demands of the piles.

While it is highly recommended that fragility curves be developed conducting a wharf model analysis like the one presented in Shafieezadeh (2011) If it is not possible to conduct a finite element analysis for the particular type of wharf examined, fragility curves for various wharf types are available, the most commonly used being those from HAZUS. HAZUS defines five damage states: none (ds_1), slight/minor (ds_2), moderate (ds_3), extensive (ds_4) and complete (ds_5), and for waterfront structures (wharves /

seawalls), the following damage and “restoration” (repair time) functions are defined for waterfront structures (FEMA 2003):

Table 6.1 Damage and Repair Time Fragility Curves from (FEMA 2003)

Permanent Ground Deformation			
Components	Damage State	Median (in)	β
Waterfront Structures (PWSI)	slight/minor	5	0.50
	moderate	12	0.50
	extensive	17	0.50
	complete	43	0.50

Restoration Functions (All Normal Distributions)			
Classification	Damage State	Mean (Days)	σ
Buildings, Waterfront Structures	slight/minor	0.6	0.2
	moderate	3.5	3.5
	extensive	22	22
	complete	85	73
Cranes/Cargo Handling Equipment	slight/minor	0.4	0.35
	moderate	6	6
	extensive	30	30
	complete	75	55

6.2.2 Crane

6.2.2.1 Other Possible Crane Configurations

Container cranes are operationally defined by their outreach, which determines the widest ship that the crane can accommodate during loading/unloading. The ship’s width dictates the number of rows of containers on board. Ships range in width from 12 – 24 containers wide (Kosbab 2010). The following histogram presents the maximum container width of a survey of 313 US container cranes (Schleiffarth 2008).

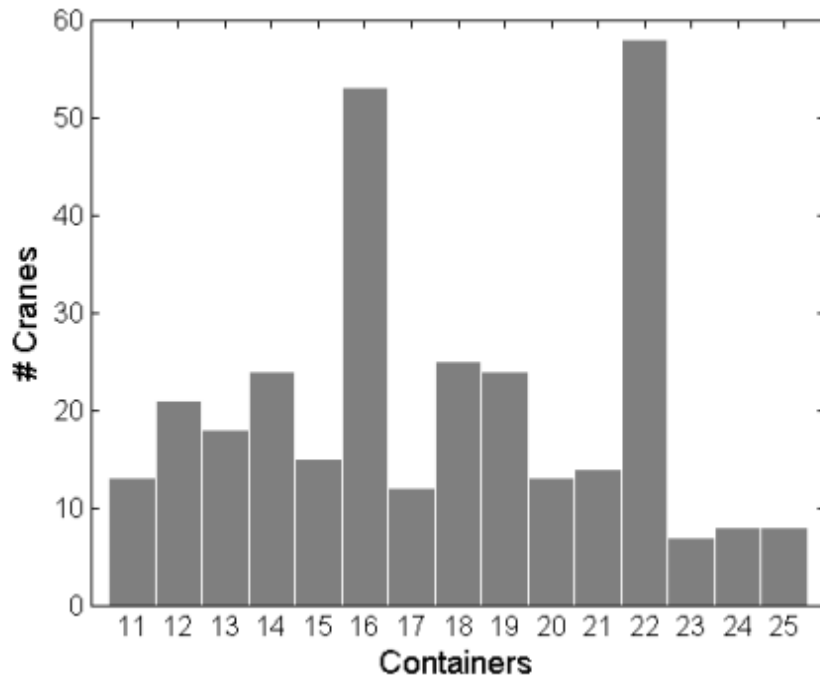


Figure 6.2 – Histogram of the Maximum Width (# of containers) of Surveyed US Container Cranes.

From Figure 6.2, cranes at US ports could range in maximum outreaches from 11 to 25 containers. Additionally, these cranes would have gage lengths of either 50 or 100 feet (most common gage widths in US ports). The three cranes chosen for the hypothetical port configuration represent the majority of cranes currently in use, and span a range of expected seismic behavior. The set chosen within the NEES Grand Challenge project was intended to provide enough example information that any given A-frame crane of typical construction could be seismically modeled and evaluated and fragility curves could be produced (Kosbab 2010).

6.2.2.2 Crane Performance in Past Earthquakes

Past performance of cranes during earthquakes has showed minor damage even for larger ground motions provided the crane foundation supports do not fail. However, collapse has been seen during some large motions and significant damage has occurred in conjunction with foundation failures (Werner 1998). Derailment is the most common

mode of crane damage because cranes are allowed to uplift during excitation. Within the risk analysis program the damage states for cranes include: derailment, slight crane damage (to the crane portal), moderate damage, and complete collapse.

6.2.2.3 Developing Fragility Curves

Fragility curves can be generated for any A-frame crane of typical construction using the examples of the portal uplift theory seismic demand model outlined in Kosbab (2010). If these methods are not used, it is recommended that the crane model developed should calculate portal drift as a function of spectral acceleration to determine one of four damage states: derailment, immediate use, structural damage, complete collapse. If neither of the previous options are obtainable, the lognormal fragility curves described in the HAZUS Technical Manual (2003) could be used.

Table 6.2 – Fragility and Restoration Parameters of HAZUS Damage States for Unanchored/Rail Mounted Port Cranes from (FEMA 2003)

	Fragility			Restoration	
	PGA median (g)	PGD median (in)	β	Mean (days)	σ
slight/minor	0.15	2	0.6	0.4	0.35
moderate	0.35	4	0.6	6	6
extensive	0.8	10	0.7	30	30
complete	0.8	10	0.7	75	55

Note: Because fragility functions are defined for both PGA and PGD, a simple multi-hazard analysis must be conducted to determine the damage state probabilities.

6.3 System-related Issues

System-related issues for the seismic risk analysis revolve around the specific system input characteristics of the port analyzed. For the hypothetical port, the arrival stream, incoming ships, delay threshold, repair sequencing, and TEU costs are specific to

the hypothetical port. The use of another port within the risk analysis framework would require the user to gather system information that accurately describes operations at that particular port. If the port analyzed is an actual port, it should not be that difficult to gather this information. The arrival stream would be based on the mean inter-arrival times for that port which could be calculated using an incoming ship log in a similar manner to how it was calculated in section 3.5.1. Incoming ship lengths and TEU capacities would be sampled from the same incoming ship log. The delay threshold and cost per TEU would need to be set specific to the port analyzed and could be found by asking port officials. Lastly, the repair sequencing would need to be tailored to the policies of the actual port. The risk analysis program already accommodates repair in parallel or in series from smallest to largest repair time, any other sequencing would need to be programmed in by the user. If the port examined is not an actual port and instead hypothetical like the port examined in this study, the same considerations of system issues is required, but tailored to the specific port location. For instance, the arrival streams for California ports differ from that of Northwestern ports. Therefore, at a minimum, arrival logs for similar ports in the location of question would need to be retrieved to develop the arrival stream and an incoming ship database.

In addition, it should be noted that the aforementioned system issues apply to the BQCSP model. If the user would like to apply the operational regression model, the regression equations would need to be recalculated using the BQCSP data of a couple thousand earthquakes that employs the new arrival stream and incoming ship data as described in section 3.6. The current operational regression model within the risk analysis framework is only applicable to the arrival stream, incoming ship data, and port configuration (wharves and cranes) specific to the hypothetical port.

7 SUMMARY, CONCLUSIONS, AND FUTURE WORK

7.1 Summary and Conclusions

Ports are extremely important in this era of global trade and historical examples have shown that earthquake disruption can cause significant economic impacts. The Port of Kobe is just one case study of the possible disruption to ports after an earthquake, and its fall from the 6th to 55th largest port in the world even after complete repair is a testament to the lasting effects of that disruption. The main objective of this thesis was to create and investigate the validity of a risk framework that uses state-of-the-art techniques to model earthquake disruption in container port systems and the resulting physical and operational losses.

The risk analysis framework probabilistically calculates losses using a modified PEER framework that starts with intensity measures and uses conditional variables to arrive at monetary losses within the port. First, earthquake scenarios are sampled from an earthquake rupture forecast. This sampling can be conducted using Monte Carlo techniques with or without stratified (importance) sampling, scenario-based, or intensity-based sampling. Next, intensity measures from the sampled earthquakes are spatially correlated between terminals. These intensity measures are then applied to previously calculated fragility models of wharves and cranes based on typical structures at west coast ports. The fragility models, which were extensively studied by numerous researchers within the scope of the NEES Grand Challenge project, use the intensity measures to calculate the probability that said intensity measure will result in a particular damage state for the wharf or crane. Once the damage state is known, the repair requirements for the wharf and crane can be calculated. Repair requirements within the framework are defined as physical repair cost of a component and the repair time (in days) it will take to fix the component. Repair cost translated directly into a monetary loss, however, repair time is used as input in an operational model that assigns berths and

cranes to arriving ships post-earthquake in a port whose capacity has been reduced by physical damage. Due to the reduced capacity, oftentimes, incoming ships will be displaced because the port does not have sufficient resources to service the ships within a reasonable amount of time. The shipping containers (measured in twenty-foot equivalent units or TEUs) on ships that are displaced are summed over the repair period and are used to calculate the business interruption loss resulting from the earthquake. Business interruption losses and repair costs can be added together to get the total loss per terminal resulting from earthquake disruption. The risk analysis framework can make this calculation for large numbers of randomly sampled earthquakes and then calculate loss exceedance curves for annual exceedance probabilities as small as 10^{-4} .

This thesis developed and used the risk analysis framework in several different capacities. First a baseline port configuration was run that was expected to cause the greatest damage of any of the scenarios studied. The baseline scenario was then dissected to make sure that the methods used within the framework were providing reasonable results. The following findings resulted from the study of the baseline configuration:

- Business interruption losses make up the largest portion of the total losses experienced at port systems. Risk analyses that neglect or underestimate the business interruption losses will significantly underestimate the total losses experienced at a port due to earthquake disruption, especially for large earthquakes.
- It is possible that business interruption losses equal zero for a given earthquake. This was especially true for earthquakes that caused little to no disruption. However, some larger earthquakes still resulted in relatively long repair times and no business interruption loss. No business interruption loss for larger earthquakes was more common at larger terminals because some portions would remain

undamaged and so incoming ships could still be serviced without having to be displaced.

- The downtime associated with wharf repair had the largest influence on determining whether or not business interruption losses occurred. Most earthquakes required some form of wharf repair, while very few earthquakes required crane repair.

After the baseline configuration was studied, the risk analysis framework was re-run using configurations that implemented various mitigation options. The mitigation option configurations were run to see which options were the most effective and to test what variables within the framework have the most influence on the total loss. Upon completion of runs for a wharf upgrade, crane upgrade, installation of prefabricated vertical drains, implementation of a repair incentive, and implementation of a force majeure policy, the following conclusions were reached:

- Mitigation options that reduce the repair times within the framework have the greatest effect in decreasing the overall total cost. The repair incentive mitigation was the most successful option when economically compared to the others. Force majeure (allowing ships to dock at other terminals other than the one to which they are assigned) was also effective in reducing total cost. These results occurred because reducing repair times has a direct correlation to the business interruption loss, which makes up the majority of the total losses in port systems.
- The physical mitigation options studied (wharf and crane upgrades, installation of drains) were the least successful in reducing total losses. Physical mitigation options showed significant reductions in loss at very small exceedance rates, and only very small loss reductions in larger exceedance rates. While each option reduced overall total losses, the implementation costs were so large that overall, the options were not cost effective.

Overall, the risk analysis framework presented in this work is extremely versatile and extremely useful in examining risk-related port decisions. Not only can the framework capture risk scenarios using Monte Carlo sampling of possible earthquake ruptures, but it also has the ability to examine specific intensity measure ranges or specific faults. These features make it possible to examine specific earthquake scenarios and subsequently that data could be used for emergency preparedness planning or to calibrate current seismic designs.

7.2 Impact of Research

The primary impact of this research is that it provides a state-of-the-art risk analysis framework to model the effect of earthquake disruption in container port systems. It has previously been established that ports are an integral transportation hub; the loss of which results in significant economic losses. The benefits and contributions of such a risk analysis framework include:

- The framework itself is currently the best model available for assessing seismic risk in container port system. Current port codes solely focus on the response of individual port components such as the wharves or the cranes to ground motions with arbitrary return periods. The seismic risk framework considers how those components work together as a system probabilistically over a large range of earthquake intensity measures that could cause disruption. By looking at the entire system, the risk analysis framework can calculate port metrics such as total loss that are meaningful to the port stakeholders that make investment decisions for the port.
- The risk analysis framework offers a valuable tool for evaluating mitigation options. One or more mitigation option can be applied to a port system and the resulting losses can be compared to the port “as is”. This data can be

economically analyzed by the port stakeholders and used to make sound financial decisions.

- Emergency preparedness planning in ports would be possible using the risk analysis framework. Stakeholders could apply intensity-based hazards within the program to examine post-earthquake operations. These results could be used to create an action plan in the event that an earthquake of that intensity was to actually occur.
- The risk analysis framework could also be used to calibrate the current seismic design criteria in ports. The model run at specific intensities could validate (or contradict) the current assumptions made in current design codes with respect to responses to components and the operational functionality of the port for the specified return periods.

7.3 Recommendations for Future Work

The currently defined scope of the port system for this risk analysis framework provides ample opportunity to expand and additional research would be suggested in the following areas:

- Port Configurations - Currently, component fragility curves are only defined for a late 1960's type wharf. Future research might include additional commonly used West Coast wharves. Along the same line, it would be beneficial to include other soil profiles within the embankment model in addition to the highly liquefaction susceptible soil profile used herein. For example, a non-liquefiable soil, or a soil that includes one or more soil improvement measures might also be appropriate to model. The risk analysis framework could also be used to model specific west coast ports, and their exact components and locations.
- Mitigation Options – Additional mitigation options could be implemented within the risk analysis framework to examine their success in reducing total losses. For

example, no structural retrofit options were examined within the scope of this project. Retrofit options often cost less than the replacement options studied. Perhaps they would be more cost-effective in reducing total loss within the port system. Several mitigation options that could be recommended include crane retrofits, pile-deck connection retrofits, and a retrofit to tie the crane-rail to the wharf. Injection of colloidal silica gel in the wharf backfill was also suggested as a soil improvement option yet never implemented. The monetary losses calculated in scenarios with mitigation options only apply to physical losses to the port. Mitigation options might also impart environmental or social benefits that are not being accounted for within the current risk analysis framework. The monetary equivalence of these additional benefits could be a source of study.

- BQCSP Operational Model – The BQCSP operational model was a significant advancement over operational models in previous risk analyses. However, it required significant computing times that were not feasible because of the need to use large numbers of earthquakes in the Monte Carlo simulations. Future work should include the time to use the BQCSP model to its fullest extent within large earthquake samples. In addition, some possible improvements to the code might include the ability to save and retrieve the operational statistics for any earthquake within the sample and the inclusion of crane blocking within the scheduling program.
- Extend the port system parameters – Lastly, future research might include an extension of the port system parameters. As it stands, the risk analysis only calculates repair requirements for the wharves and cranes. Additional components could cause losses that are not currently being considered. For instance, business interruption losses, which make up the majority of the total losses within the port could result from loss of communications, damage to the roadways within the port, or loss of port utilities. Furthermore, it would be

interesting to try to estimate the effects of port disruption on larger economic systems on the local, state, or national level.

APPENDIX A – CALIBRATION OF OPERATIONAL MODEL

One of the challenges in integrating the BQCSP operational modeling into the risk analysis program was calibration. The run time needed to be efficient, but the results should still be statistically representative of actual crane operations. The berth and crane assignments generated after one earthquake could take anywhere from several seconds to several minutes to run depending on how the stopping criteria within the operational program were defined. Knowing that risk analysis scenarios would contain at least 1000 earthquakes, it was important to scale the runtime down to something manageable.

A.1 Stopping Criteria within the Operational Model

When the BQCSP operational model runs, the sub-optimal tabu search examines a number of possible solutions to the berth and crane scheduling problem at a specific time period, compares them to a stored best solution for that time period, and then after a certain number of solutions are examined, the program accepts the best solution and moves on to the next time period. The point at which the model decides it has the “best solution” can be controlled by a number of stopping criteria. Two stopping criteria were examined within the operational model to reduce runtime: 1.) limiting the number of solutions examined at each time period, and 2.) limiting the number of time periods.

A.1.1 Full vs. Half Stopping Criteria

The first stopping criteria examined was the number of solutions examined at each time period. Examining fewer solutions would reduce runtime, but it is also important to make certain that enough solutions are examined to adequately solve the operational problem. The original operational program took around two minutes to run one earthquake. So, to reduce the runtime, the number of solutions examined at each

time period by the operational model was cut in half. The statistics generated from the half-stopping criteria were then compared with those of the full-stopping criteria to assure that adequate solutions were still developed. The utilization statistics for earthquakes 1-4 for the full and half stopping criteria are compared in Figure A.1 - Figure A.5. Figure A.1 and Figure A.2, which show the utilization and TEU statistics for earthquake scenario #1:

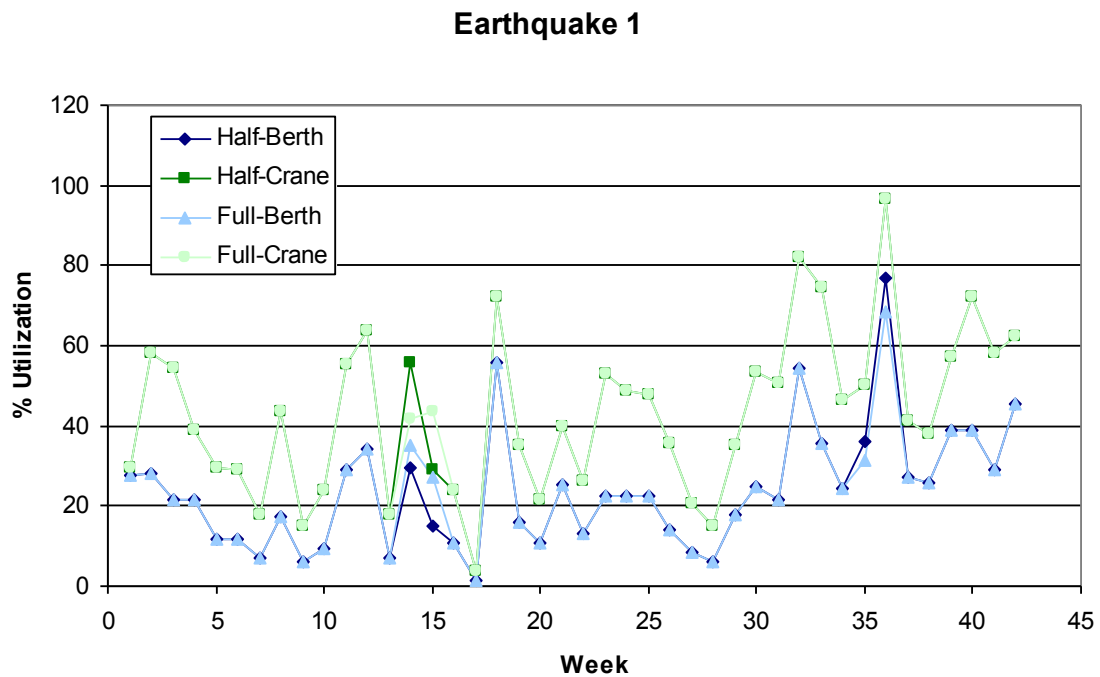


Figure A.1 Earthquake 1: Utilization statistics for full and half stopping criteria

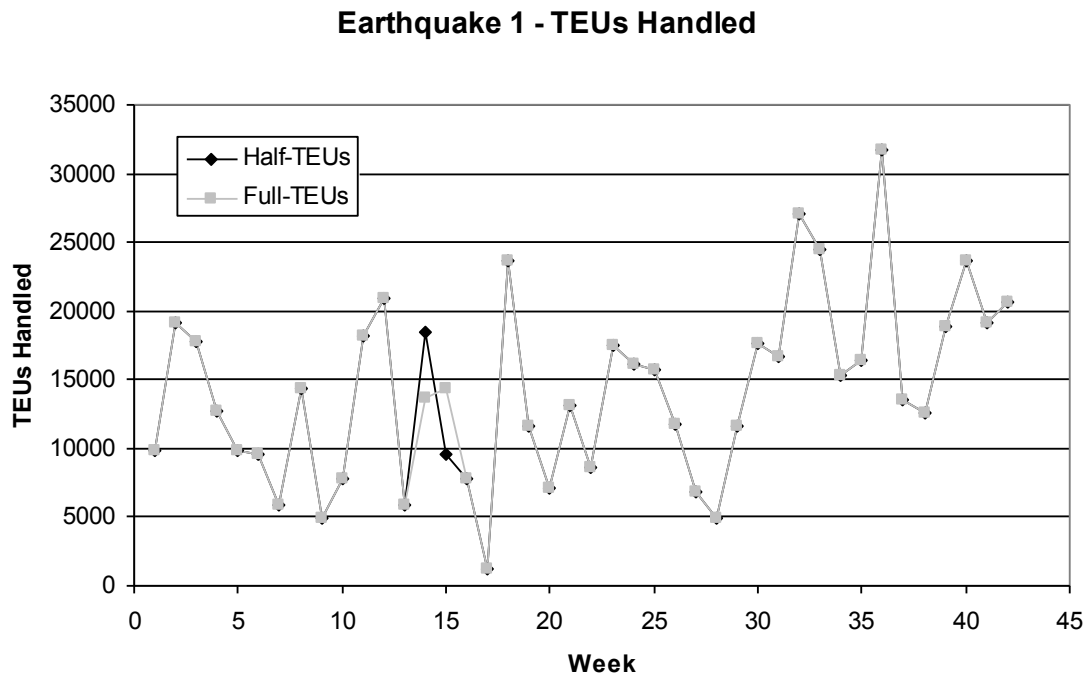


Figure A.2 Earthquake 1: TEU statistics for full and half stopping criteria

It can be seen in Figure A.1 that the half stopping criteria resulted in a differing solution in weeks 14-15 and 35-36 for berth utilization, and weeks 14-15 for crane utilization. It should be noted that one solution is not necessarily better than the other. This can be assumed because both solutions still handle the same number of TEUs during the weeks where the differences occur (Figure A.2). During weeks 35-36, the number of TEUs handled is exactly the same for both weeks, and during weeks 14-15, the total number of TEUs handled over the two-week period is equal. Similar small difference can be seen between the full and half stopping criteria statistics of the other earthquakes (Figure A.3- Figure A.5). However, since the TEUs handled in each situation are equal like in Figure A.2; it can be said that the full stopping criteria is no better than the half stopping criteria. Furthermore, since the half stopping criteria took far less computation time, it was ultimately used within the risk analysis.

Earthquake 2

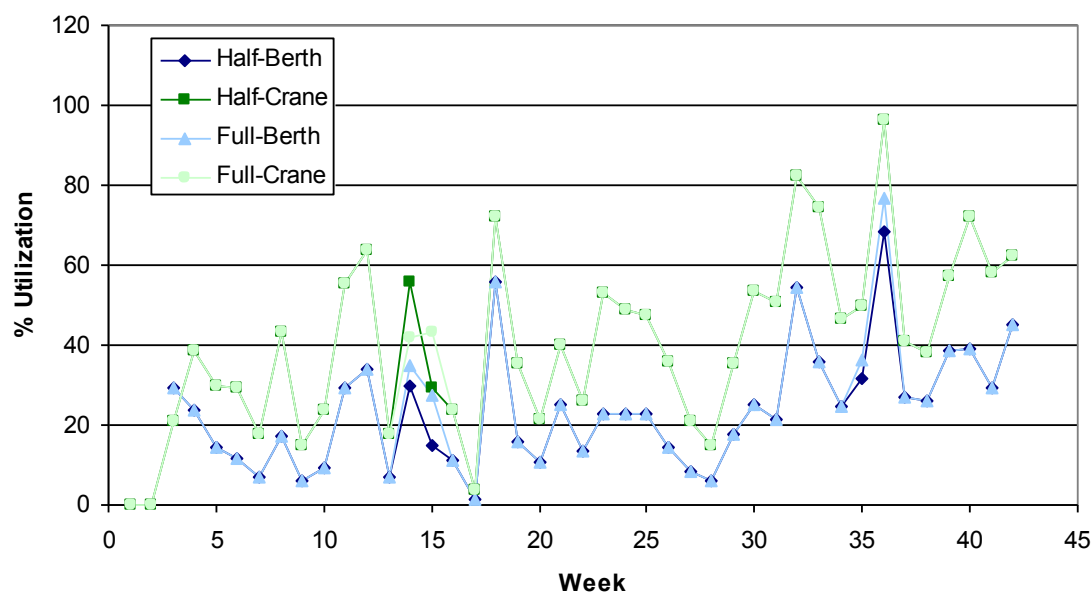


Figure A.3 Earthquake 2: Utilization statistics for full and half stopping criteria

Earthquake 3

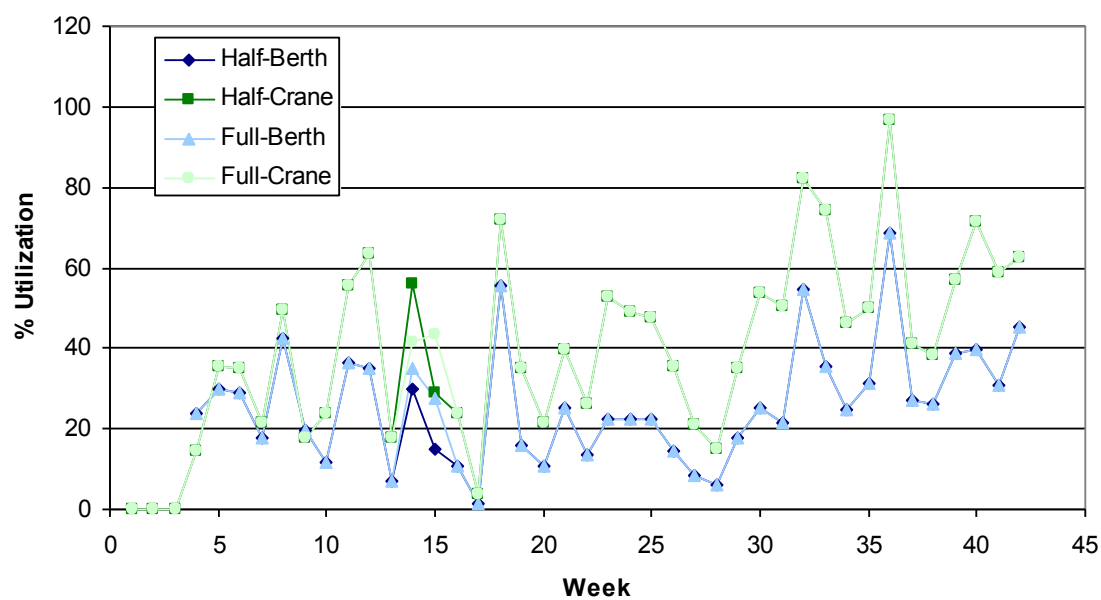


Figure A.4 Earthquake 3: Utilization statistics for full and half stopping criteria

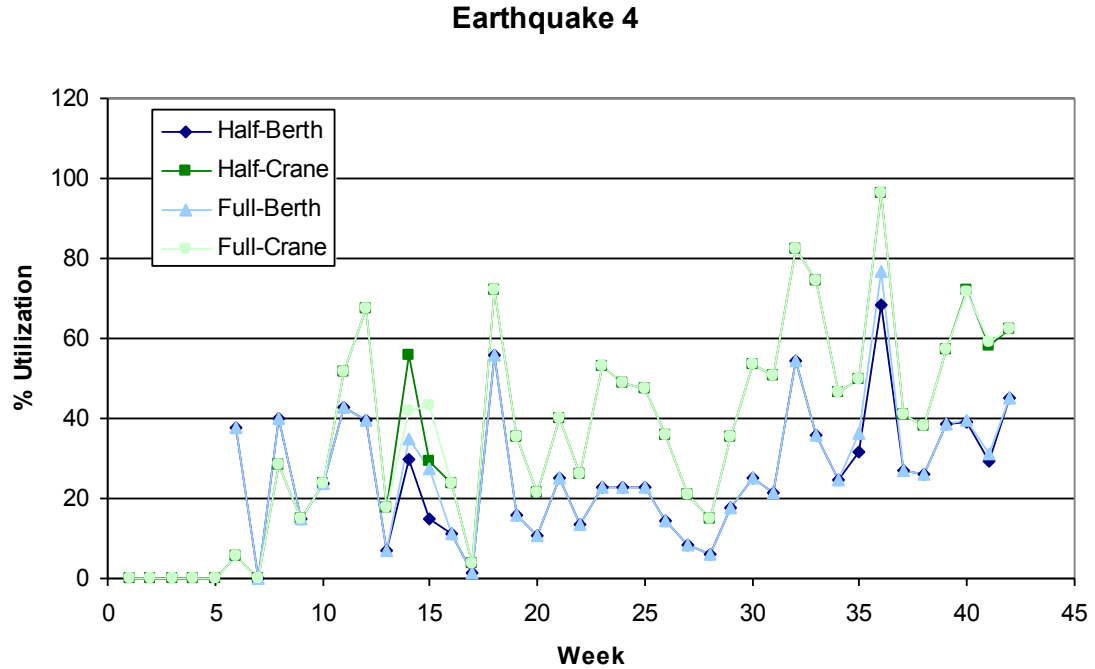


Figure A.5 Earthquake 4: Utilization statistics for full and half stopping criteria

A.2 Stopping Criteria Based on Repair Periods

The next method used to decrease the run time of the operational model was to limit the number of time periods over which the berth and crane assignments were run. For the earthquake scenarios (1-5) run, the same ship arrival schedule was used so that the results could be comparable. In addition, a “calibration” scenario was also run within the operational model under the parameters that no berth or crane damage occurred. In this manner, earthquake scenarios could also be directly compared to the port under “normal” operations. Theoretically, during the earthquake event scenarios, once all the repairs were complete and the port caught up with the delays that may have occurred, the port operations should return to normal operations: in this case, the calibration scenario.

Figure A.6- Figure A.9 plots port statistics for earthquakes 1-4 as well as the statistics

generated from the calibration scenario. Earthquake 5 was omitted from this data simply because it has a 50-week repair period and it's easier to visually compare the data if the scale is not skewed by having to add the additional weeks to accommodate it.

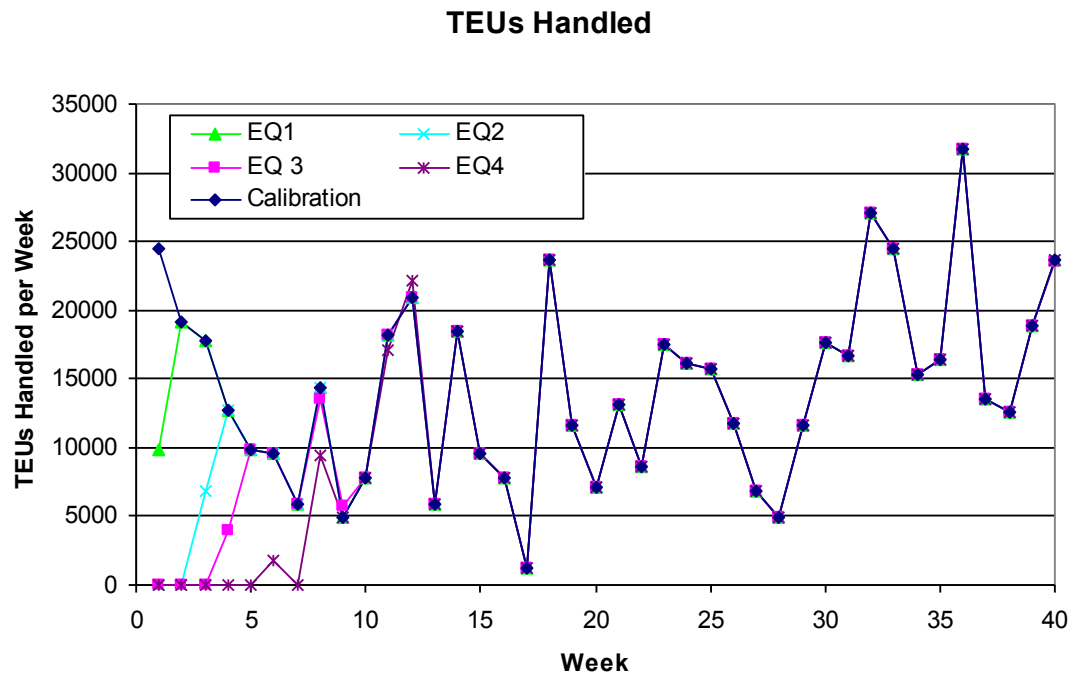


Figure A.6 TEU statistic comparison of earthquake scenarios

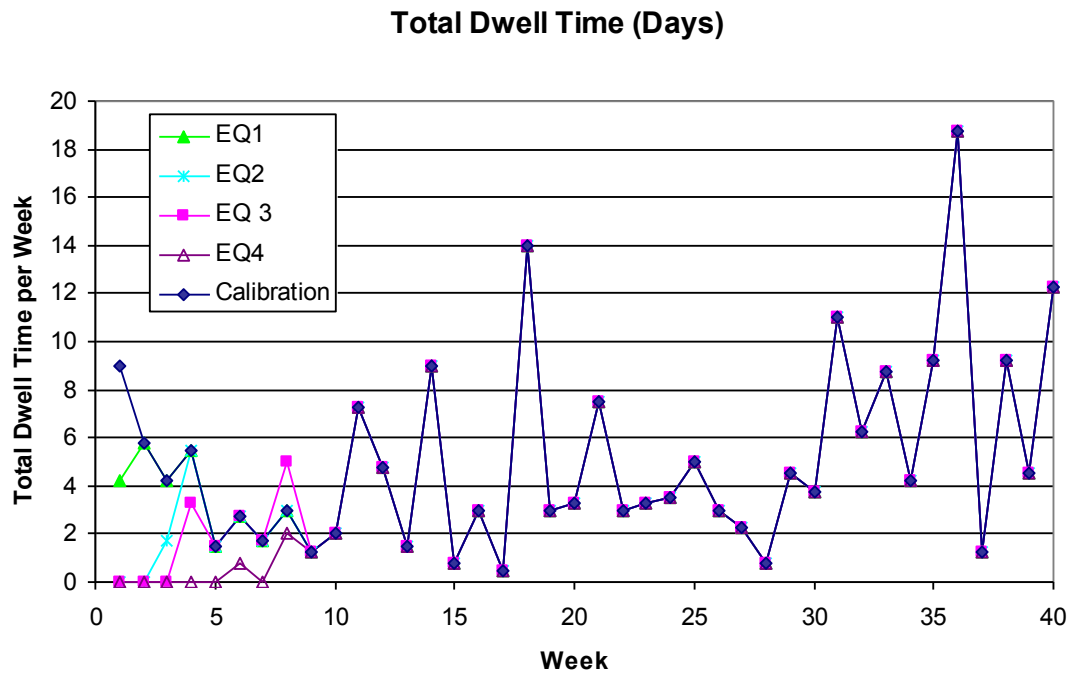


Figure A.7 Total dwell time statistic comparison of earthquake scenarios

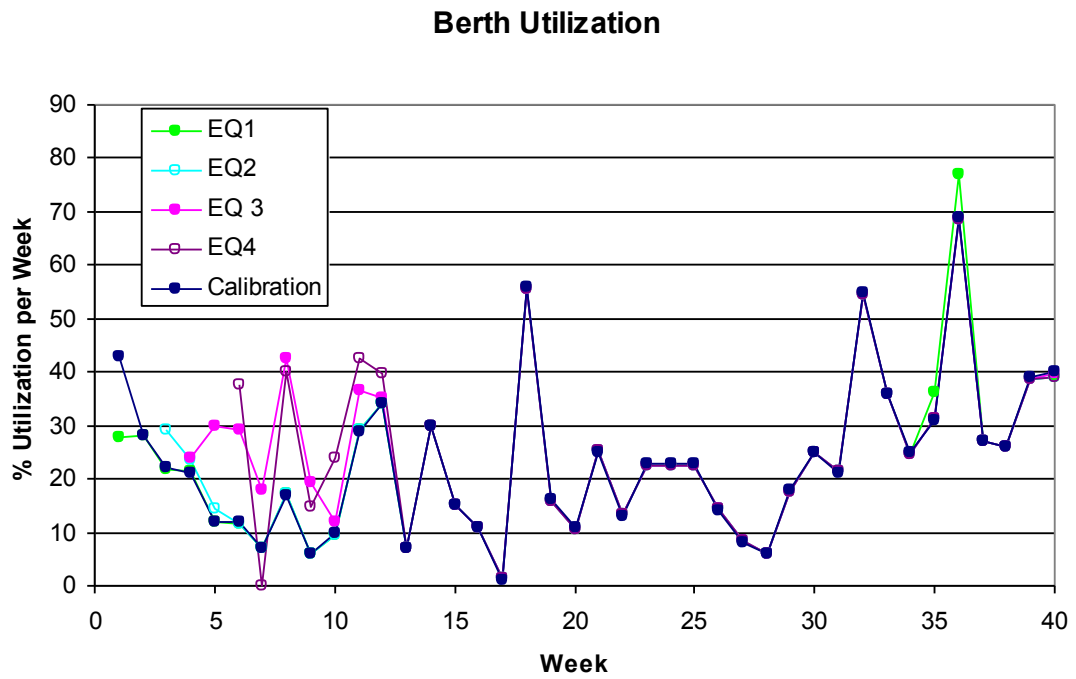


Figure A.8 Berth utilization comparison of earthquake scenarios

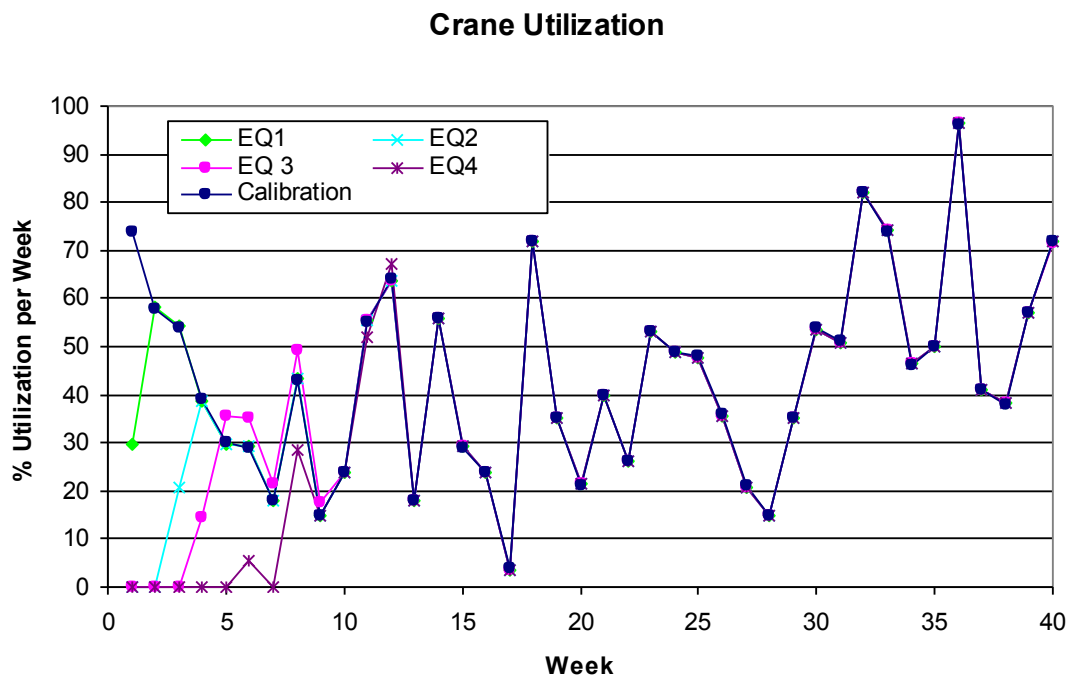


Figure A.9 Crane utilization comparison of earthquake scenarios

From Figure A.6- Figure A.9 it is apparent in every statistic that each earthquake does eventually return to normal operations. Table A.1 shows the actual repair period for each earthquake and indicates the week in which each statistic returns to its normal operation.

Table A.1 Number of Weeks Required to Return to Normal Operation

Earthquake	Repair Period (weeks)	TEUs Handled	Dwell Time	Berth Utilization	Crane Utilization
1	0.71	2	2	2	2
2	4.87	3	4	5	3
3	11.14	5	5	12	10
4	11.71	8	9	13	9

The number of weeks required to return to normal operation varies among each statistic. For instance, TEUs handled and dwell time take five weeks to recover while crane utilization takes twice that. It should also be noted that some statistics still haven't recovered even after the repair period is complete (Berth Utilization). Therefore it was decided that for each earthquake scenario the operational model would run through the repair period and for 3 additional BQCSP time periods (approximately 1 day). After this point it would be assumed that all operational statistics would be equal to those generated in the calibration scenario.

APPENDIX B – GROUND MOTIONS

The ground motions used to evaluate the fragility analysis for the wharf were discussed in Section 3.4.1, and the time histories of each can be found within this appendix. Figures contain the x and y direction time histories of three different motions. Motions are graphed respective of the records listed in the figure title. Simulated motions begin after the NGA motions in the same manner.

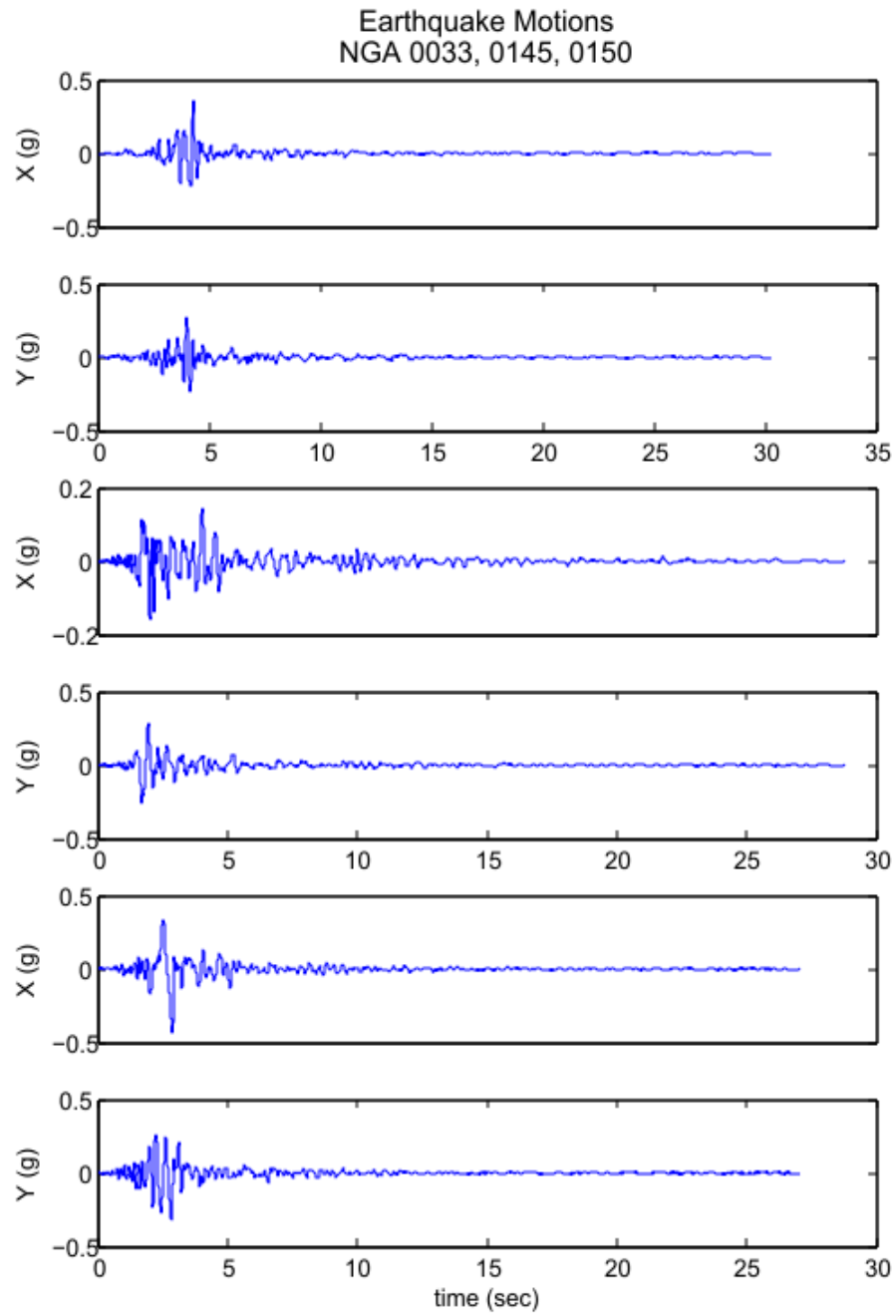


Figure B.1 NGA 0033, 0145, 0150

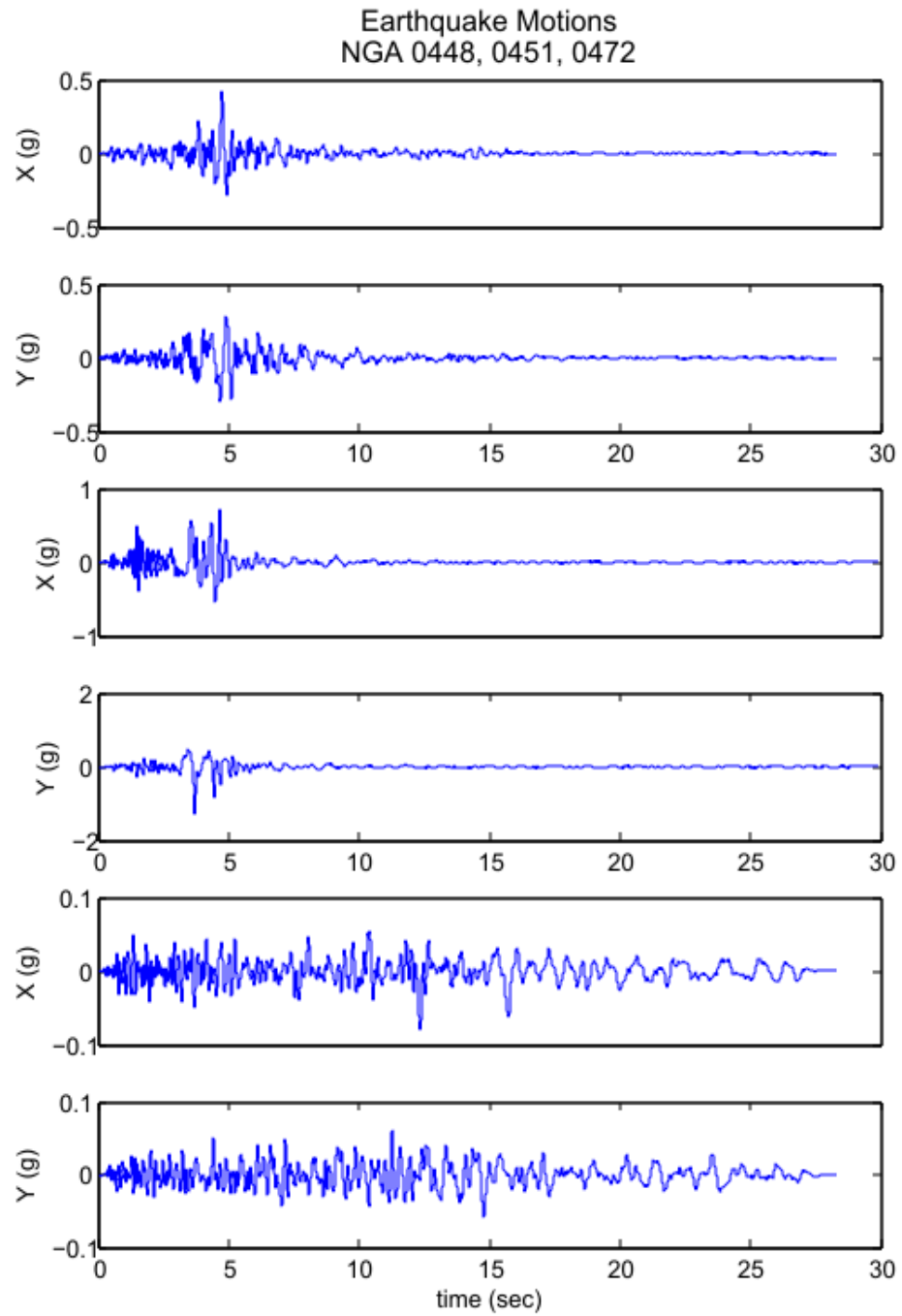


Figure B.2 NGA 0448, 0451, 0472

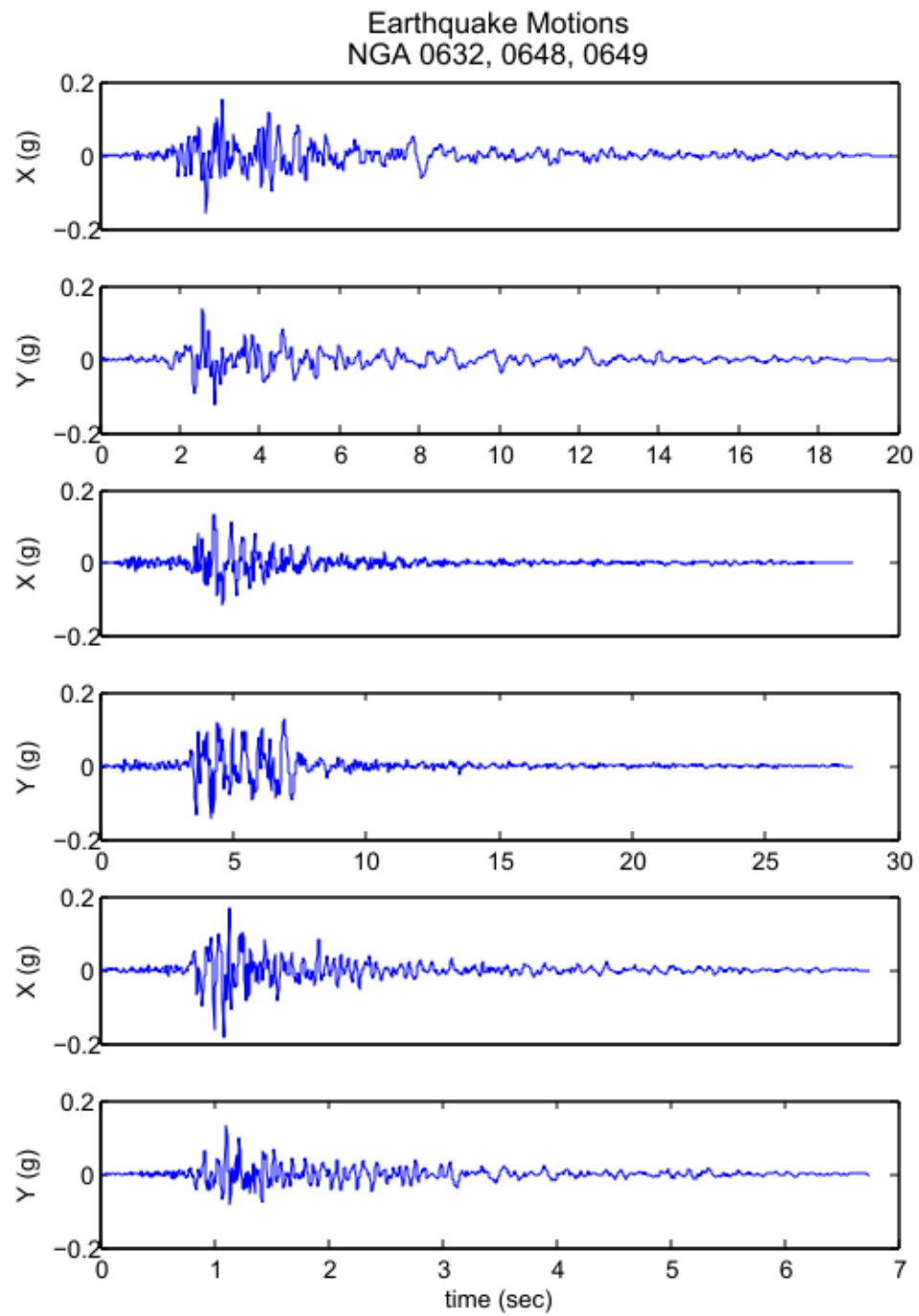


Figure B.3 NGA 0632, 0648, 0649

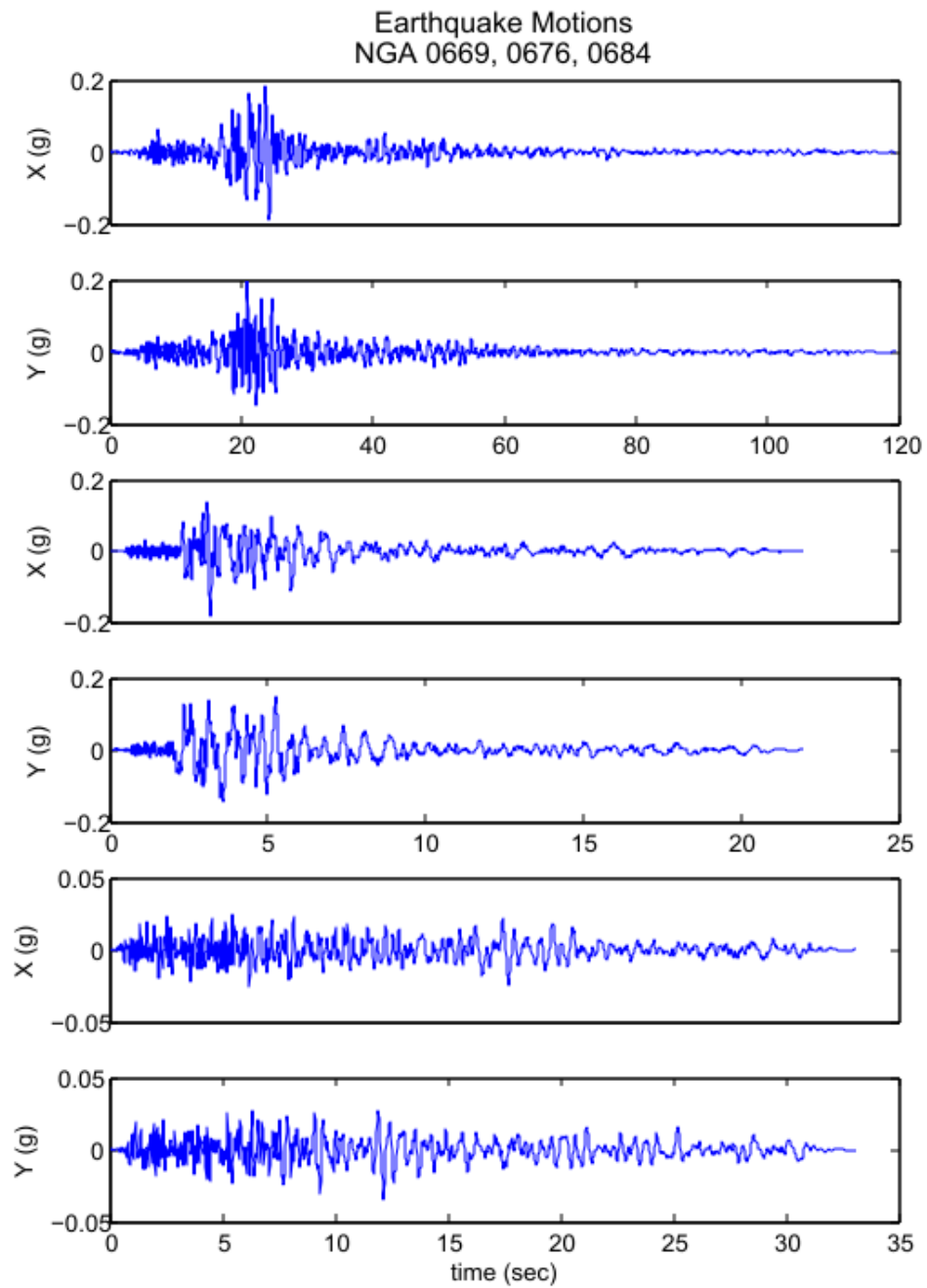


Figure B.4 NGA 0669, 0676, 0684

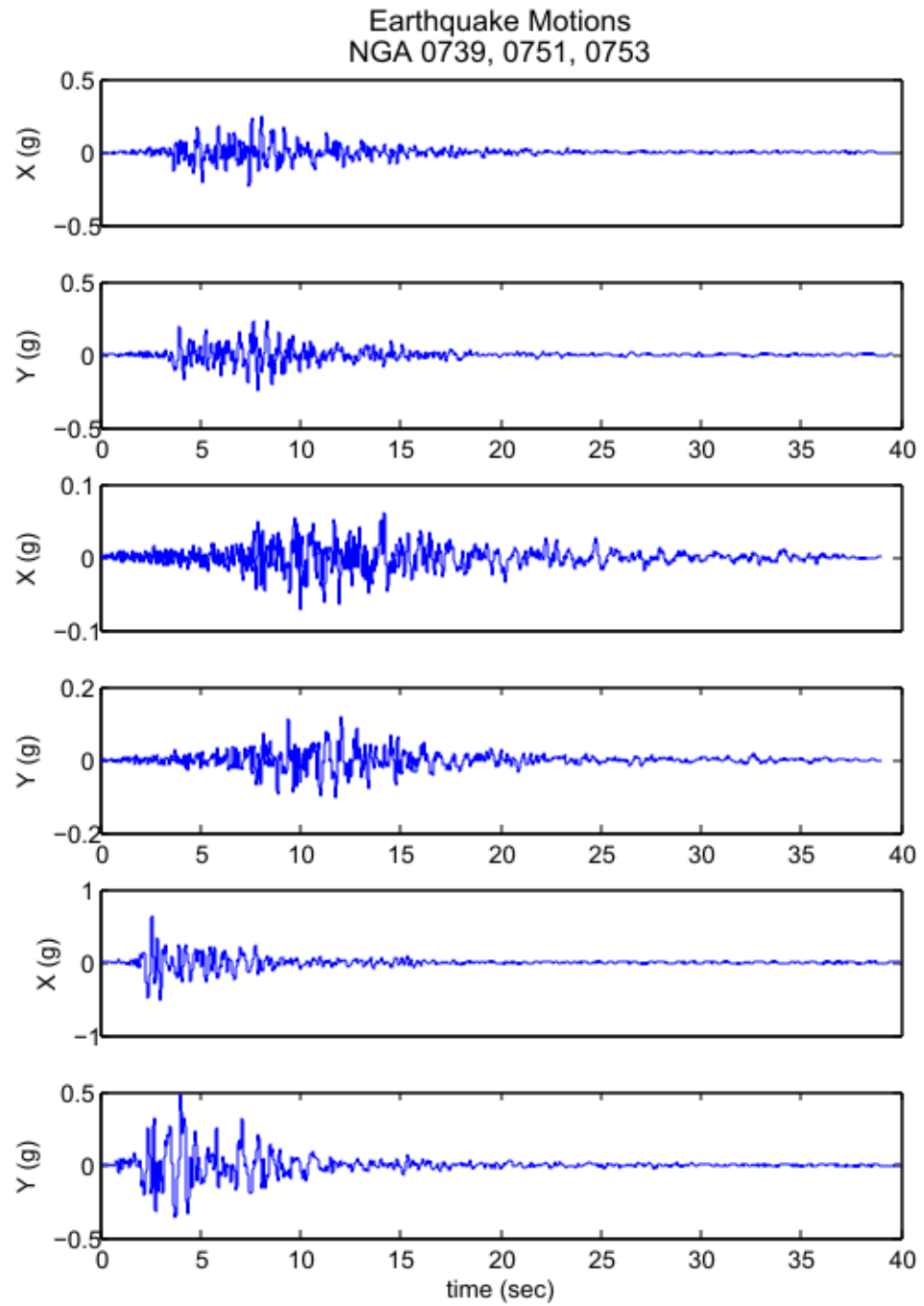


Figure B.5 NGA 0739, 0751, 0753

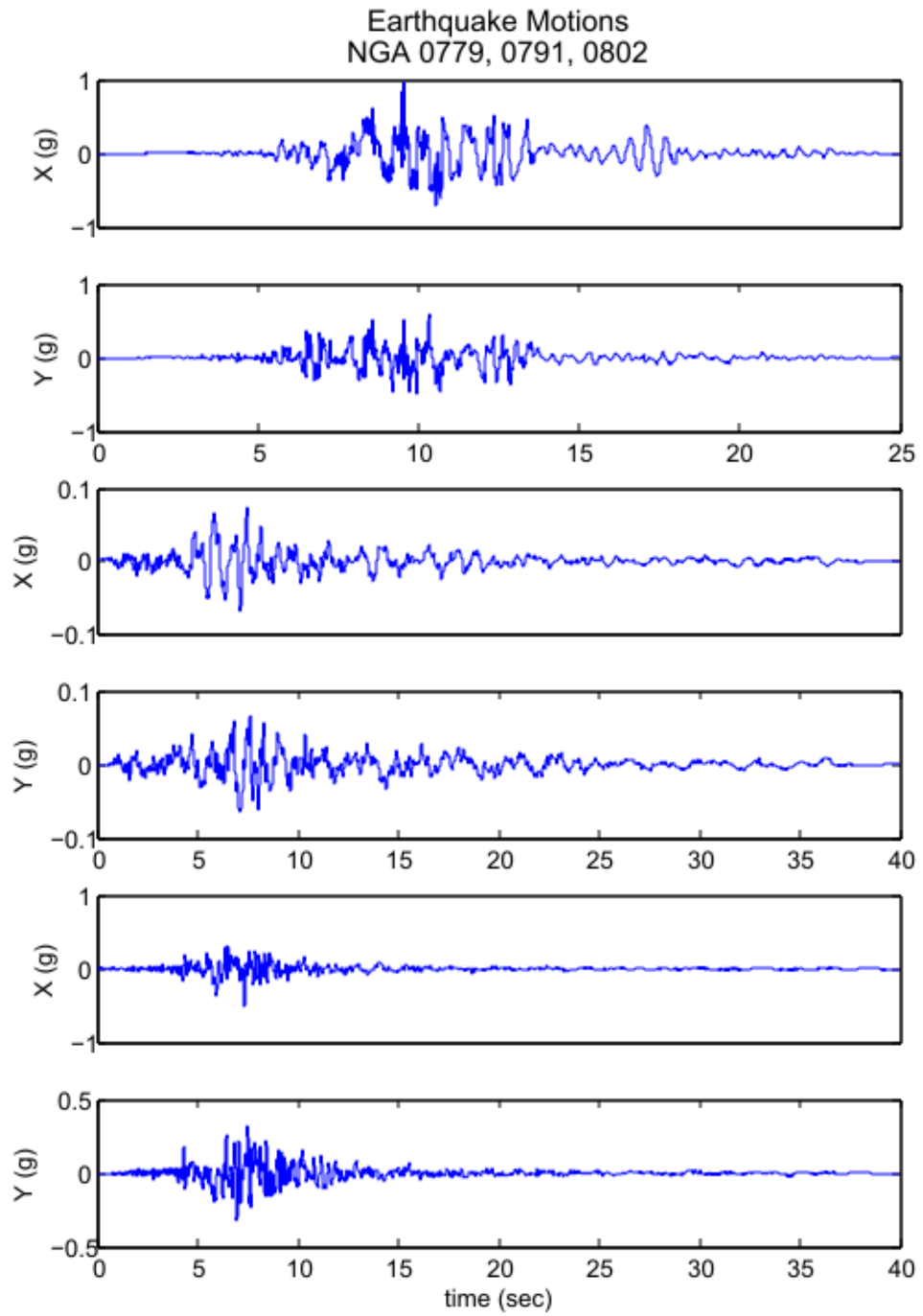


Figure B.6 NGA 0779, 0791, 0802

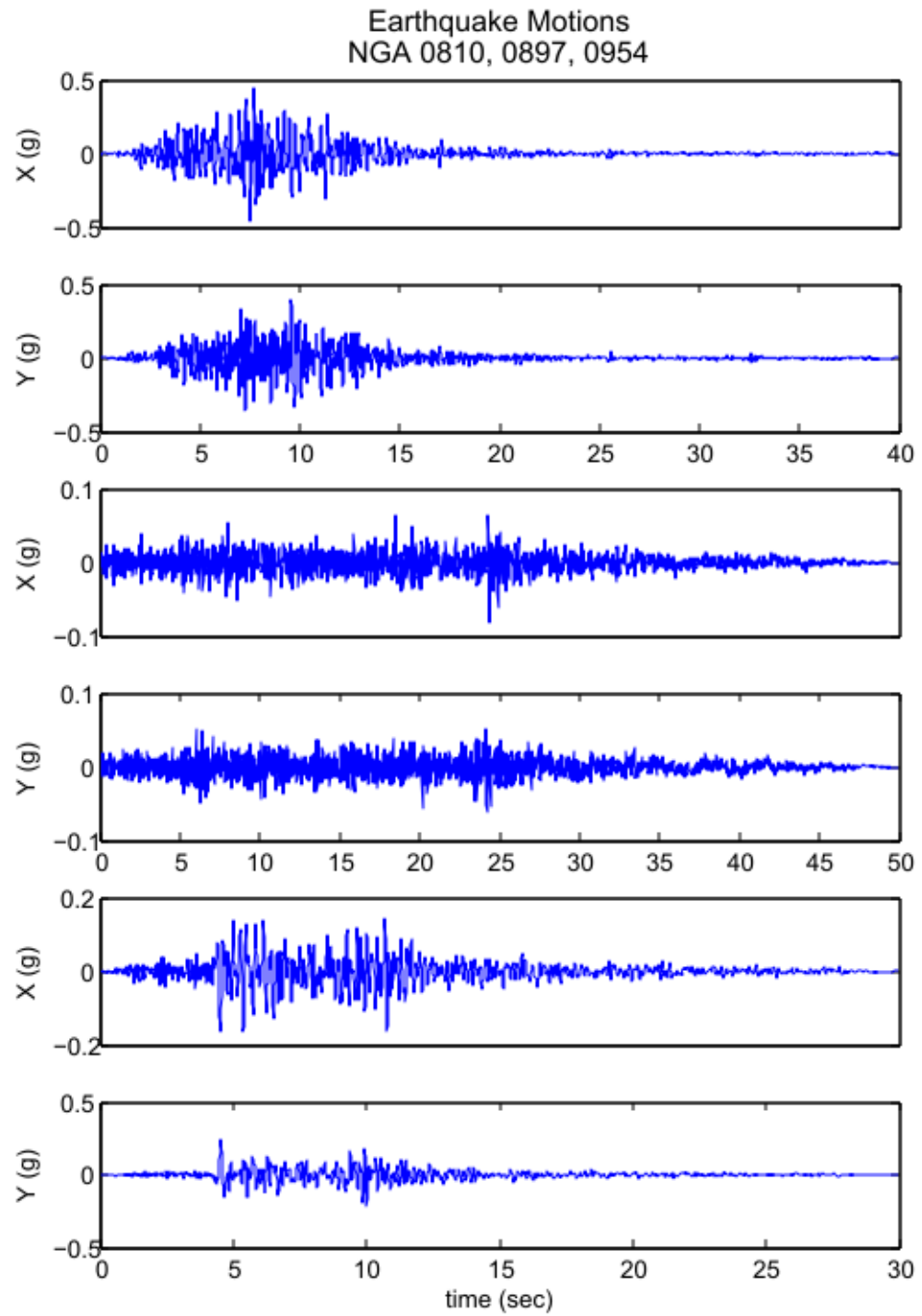


Figure B.7 NGA 0810, 0897, 0954

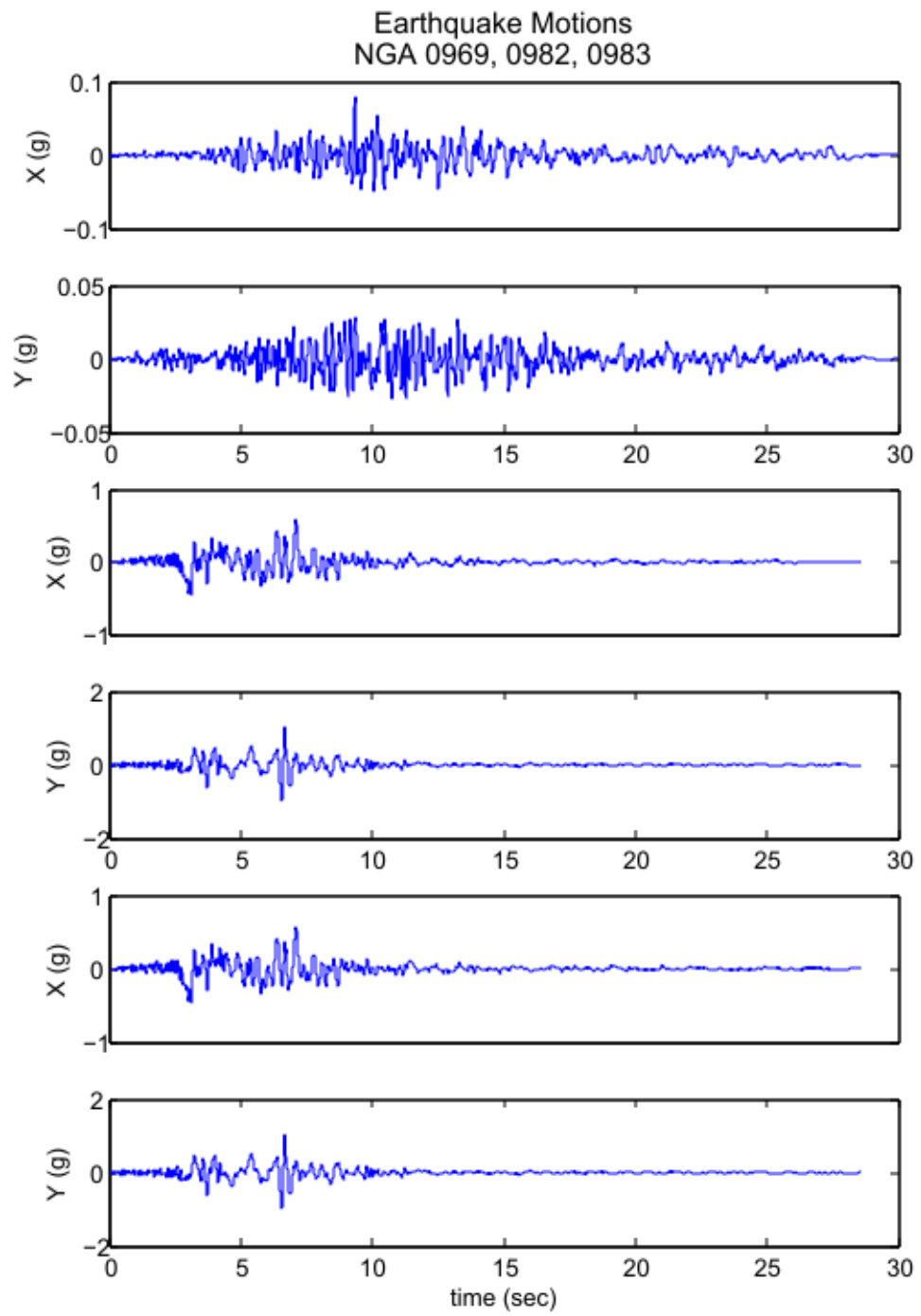


Figure B.8 NGA 0969, 0982, 0983

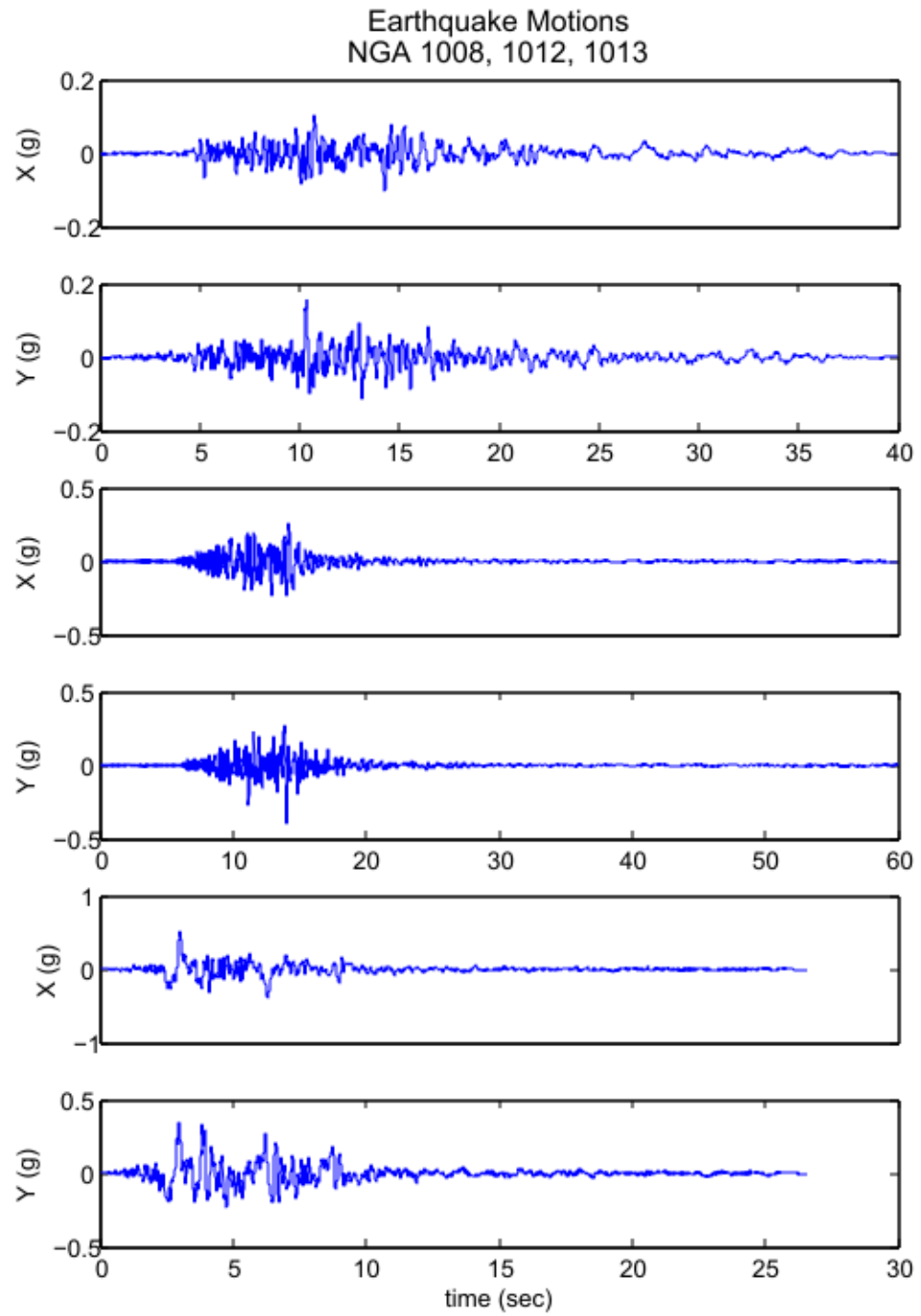


Figure B.9 NGA 1008, 1012, 1013

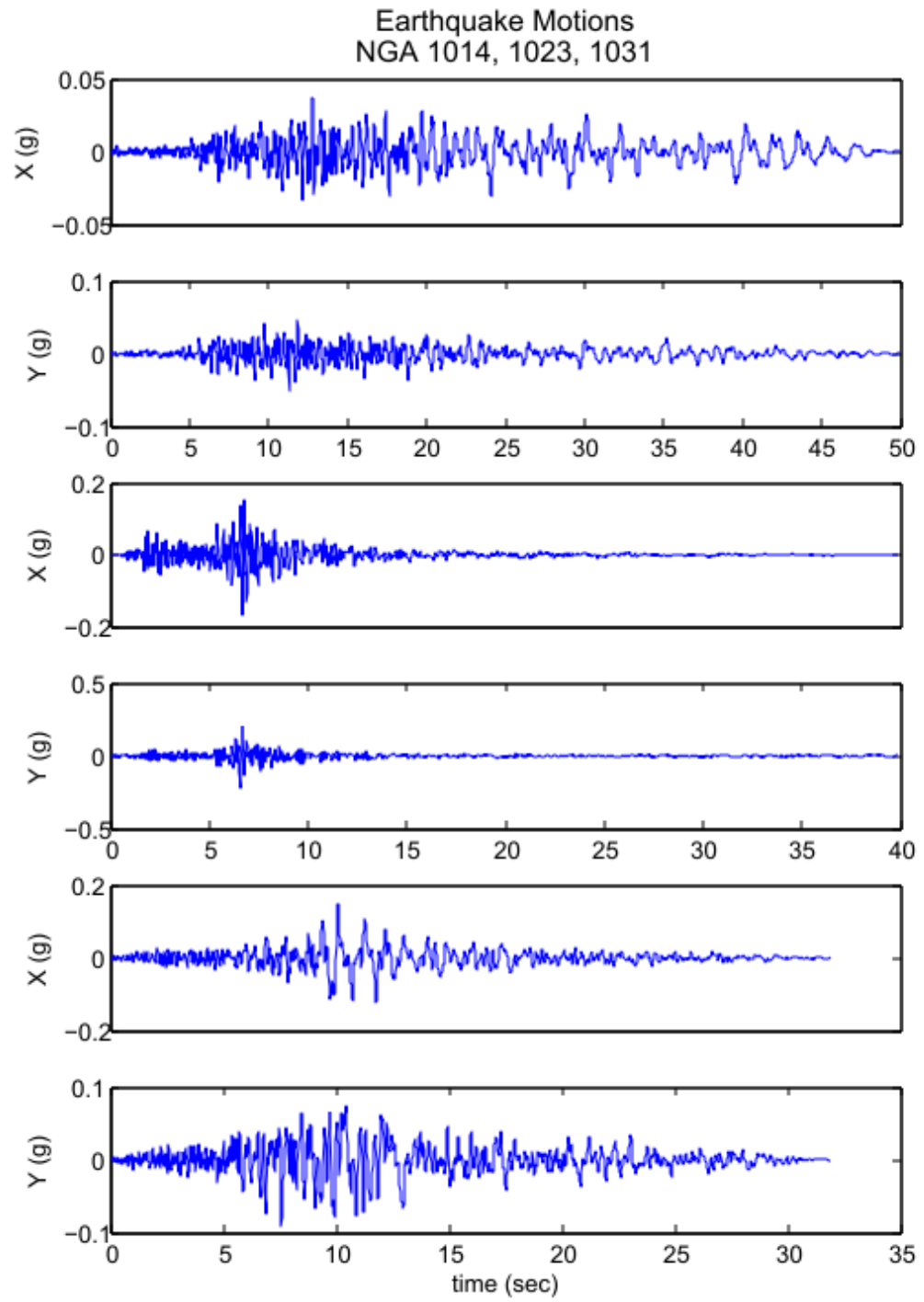


Figure B.10 NGA 1014, 1023, 1031

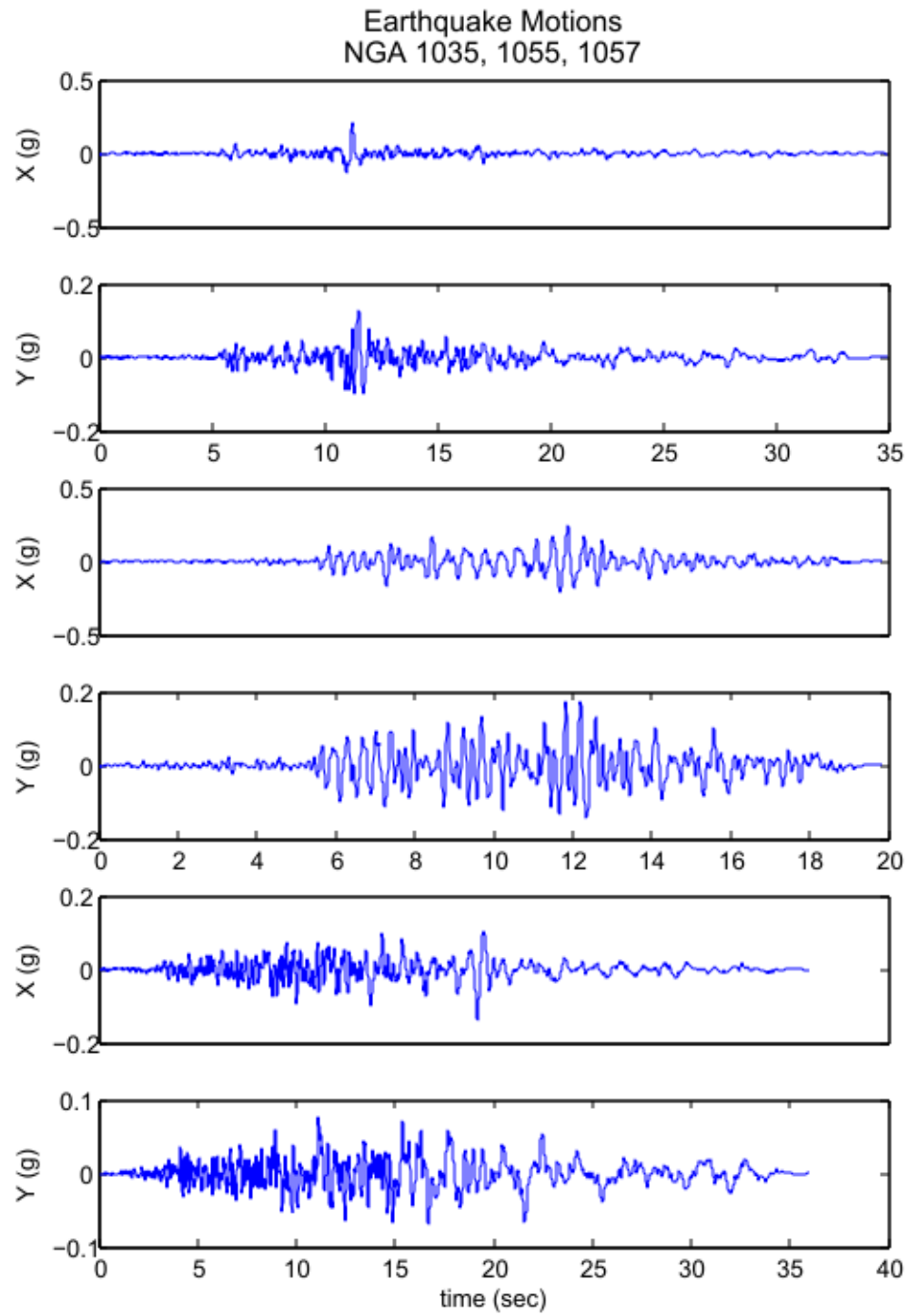


Figure B.11 NGA 1035, 1055, 1057

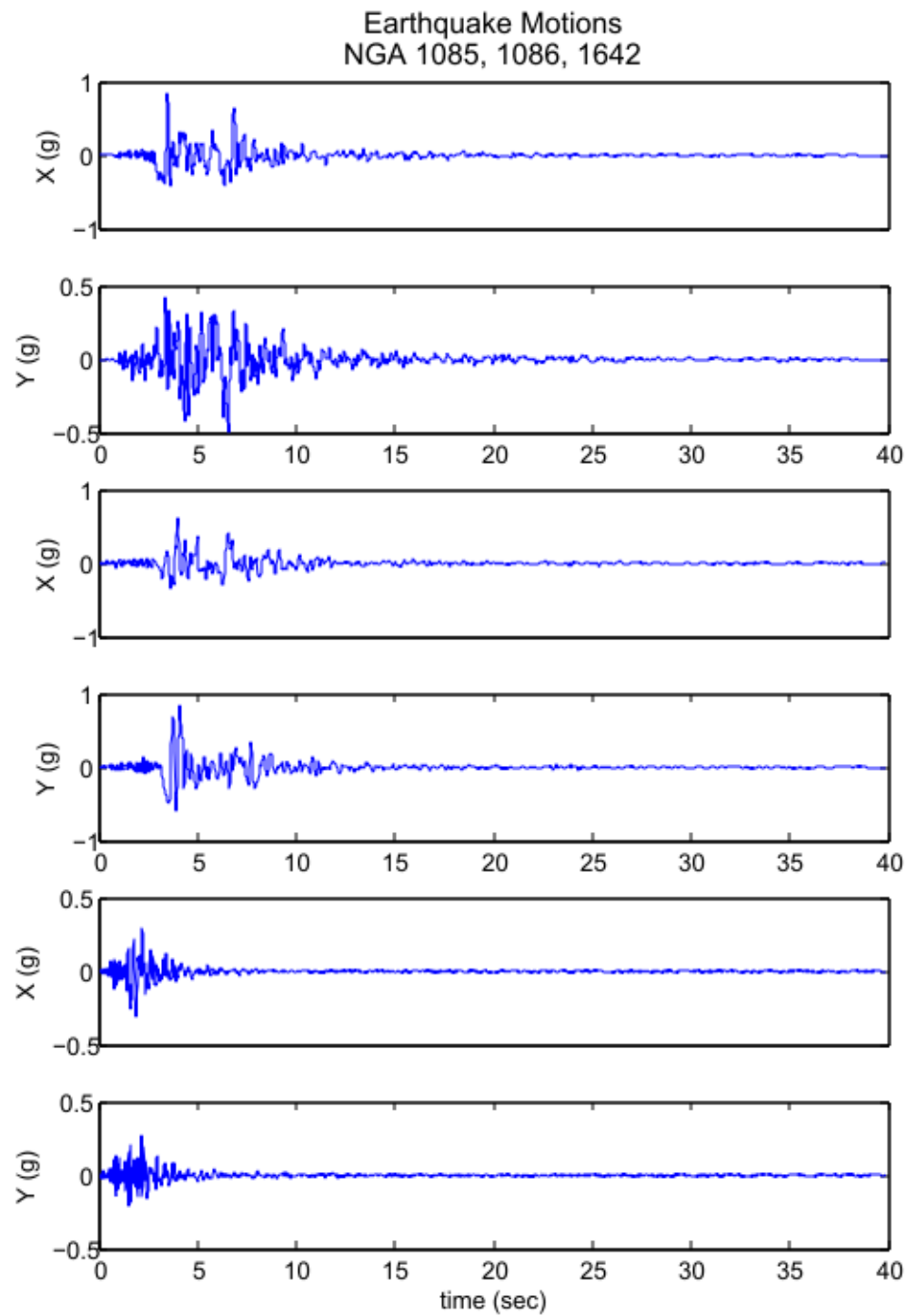


Figure B.12 NGA 1085, 1086, 1642

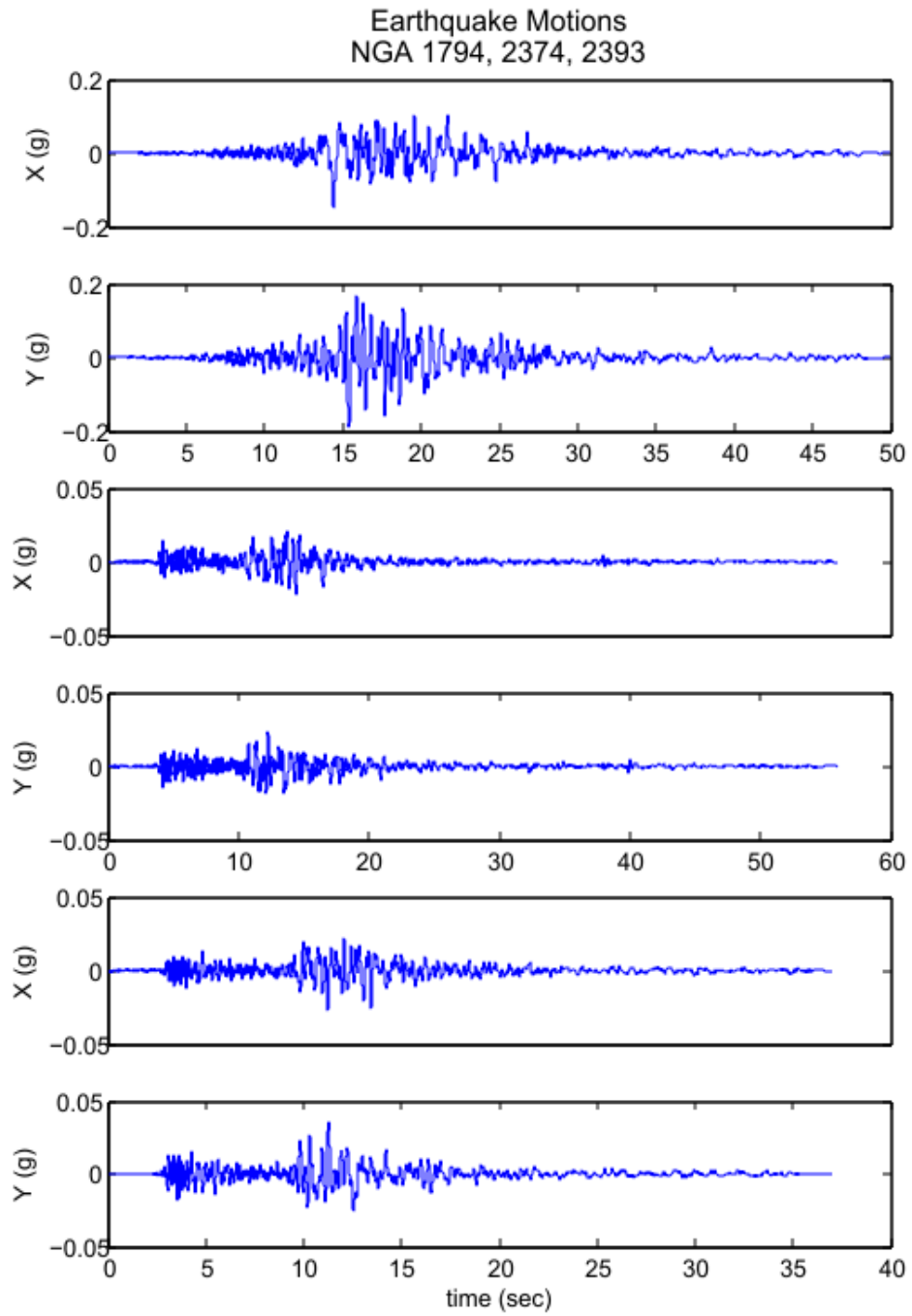


Figure B.13 NGA 1794, 2374, 2393

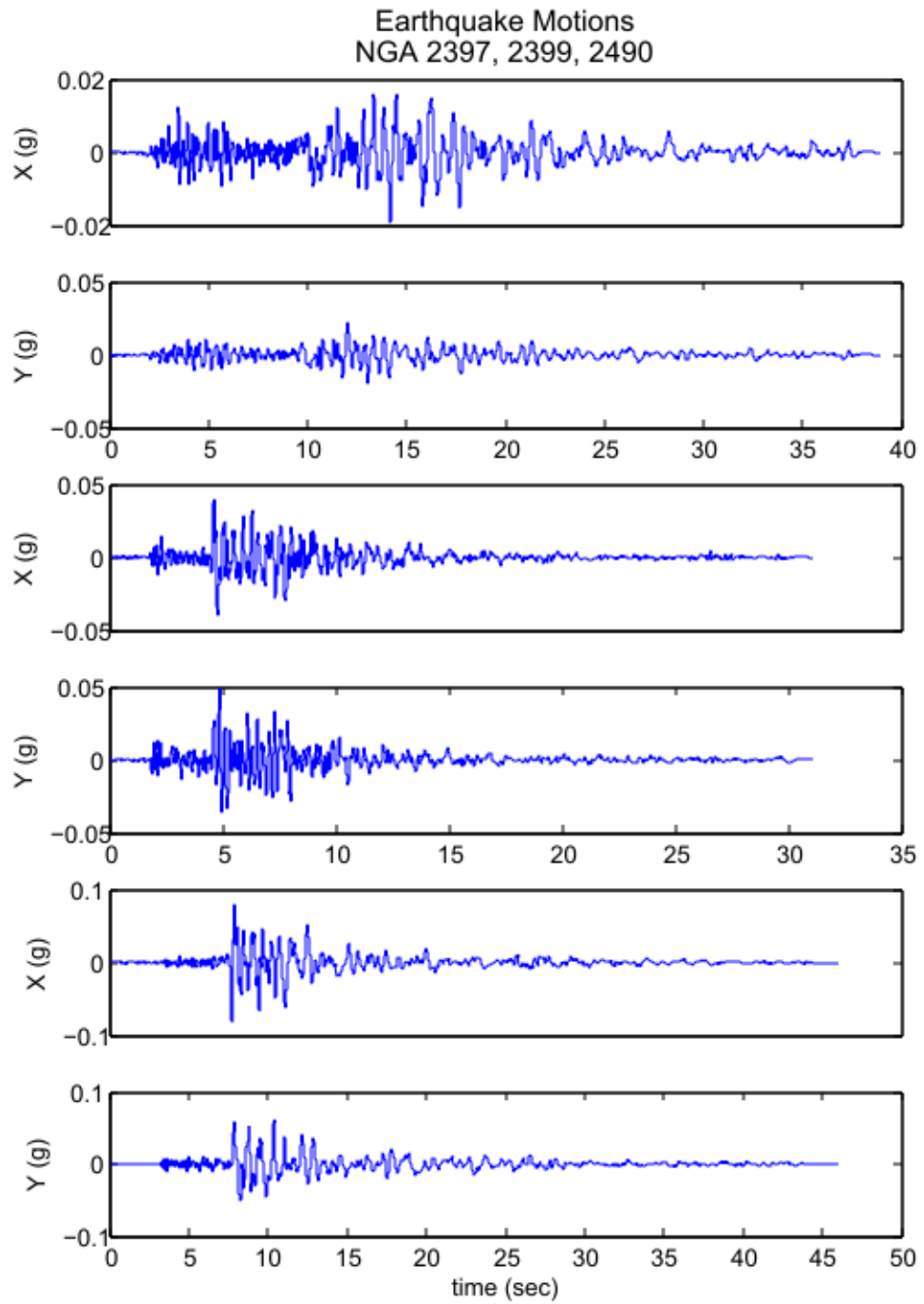


Figure B.14 NGA 2397, 2399, 2490

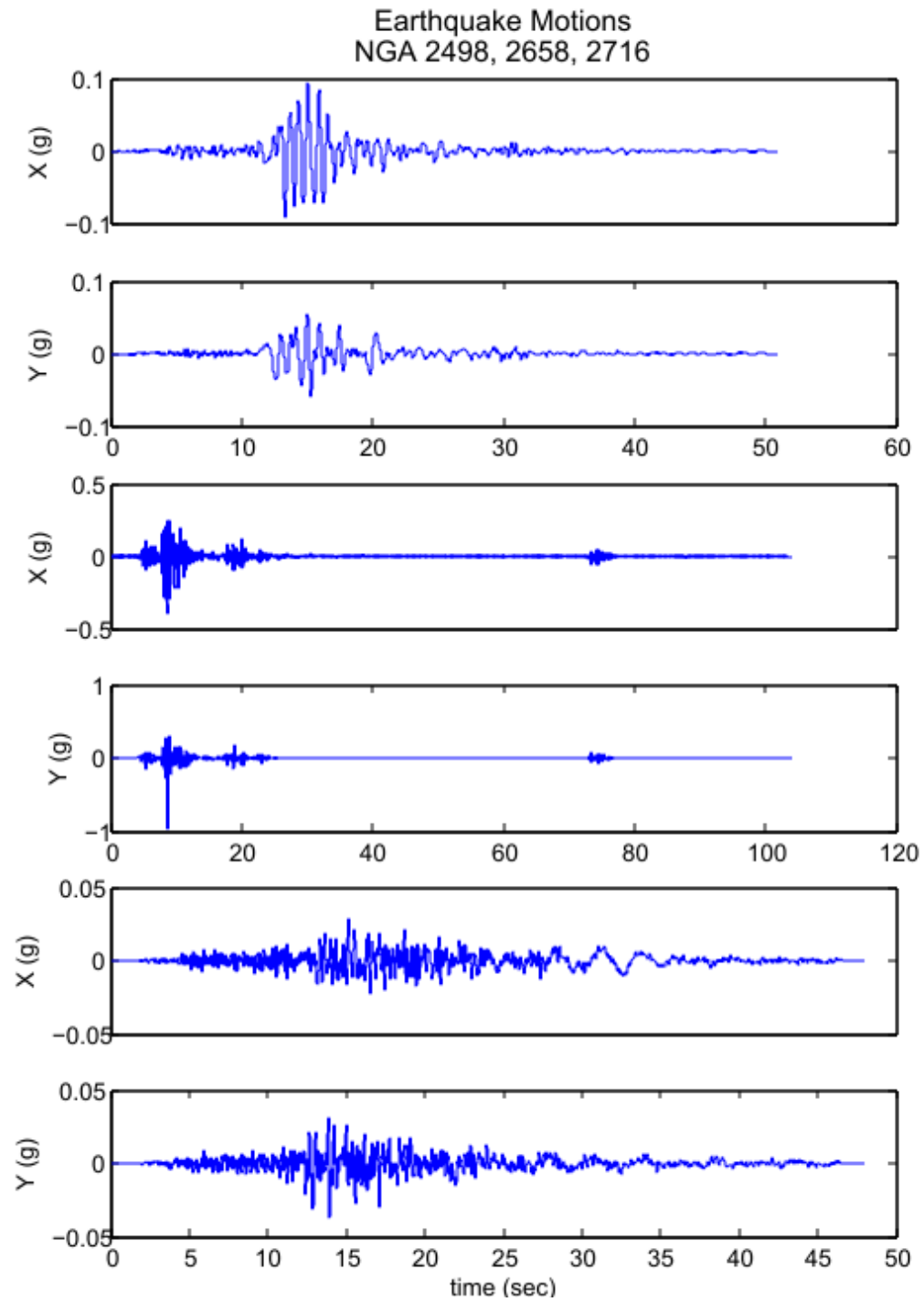


Figure B.15 NGA 2498, 2658, 2716

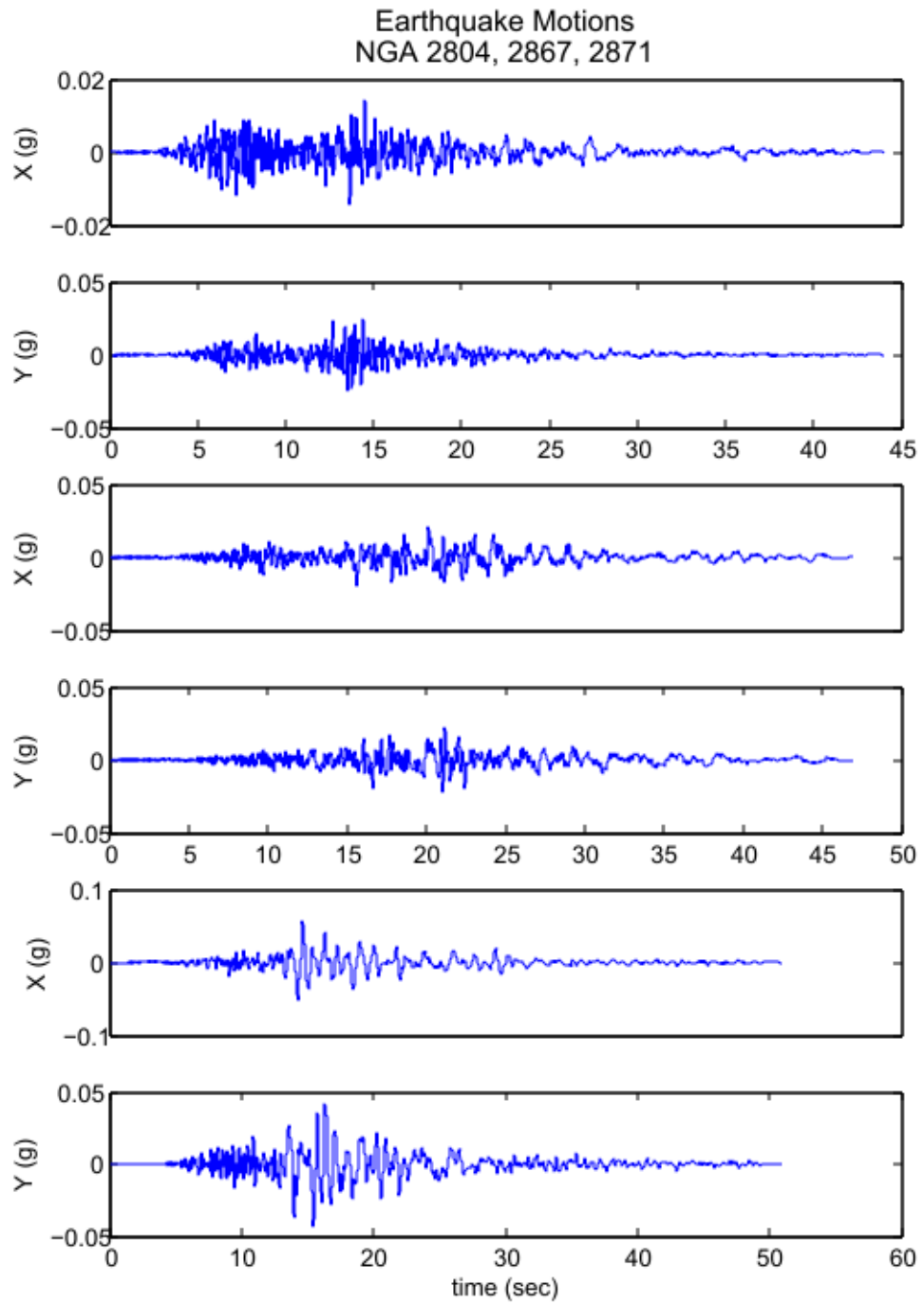


Figure B.16 NGA 2804, 2967, 2871

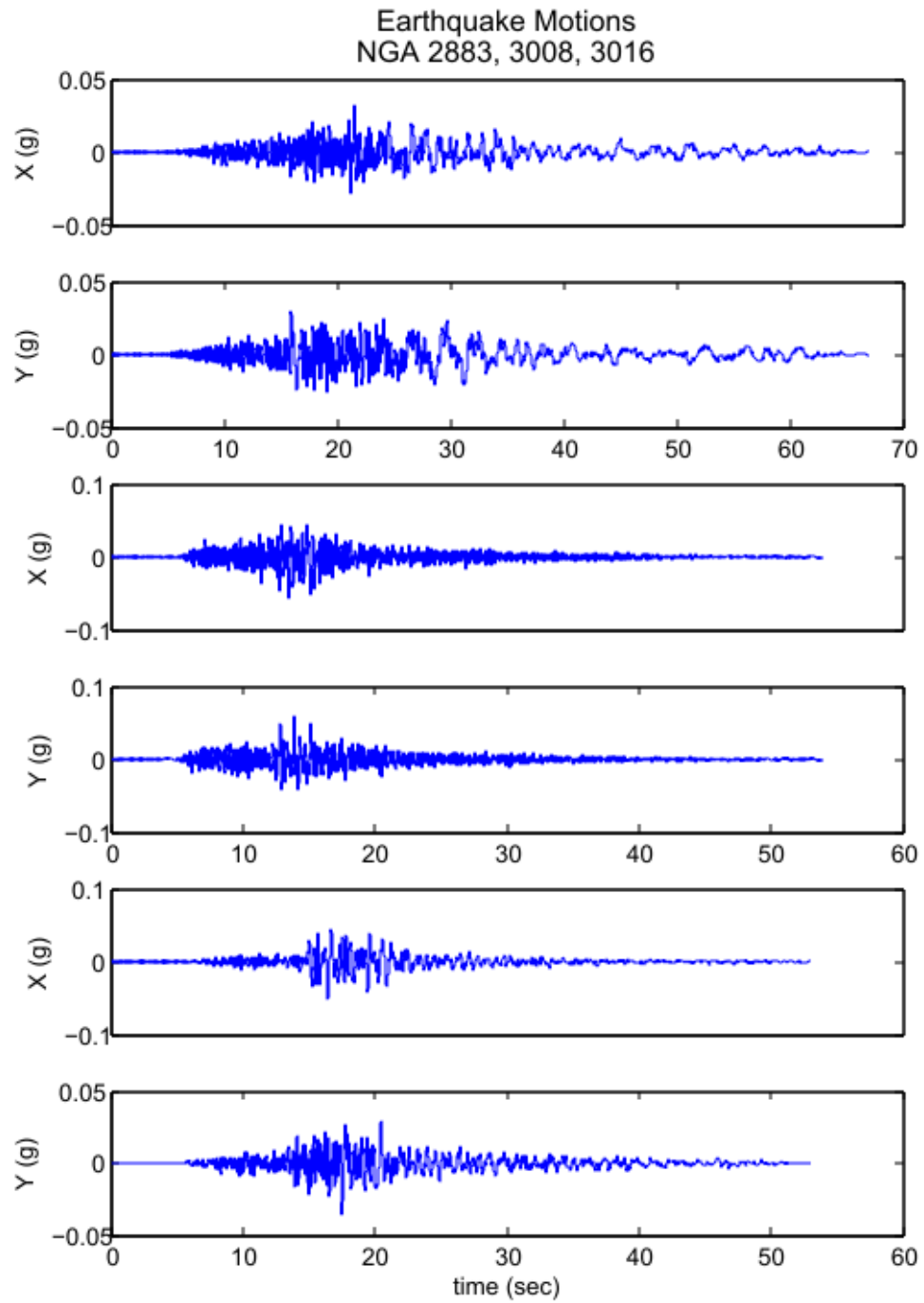


Figure B.17 NGA 2883, 3008, 3016

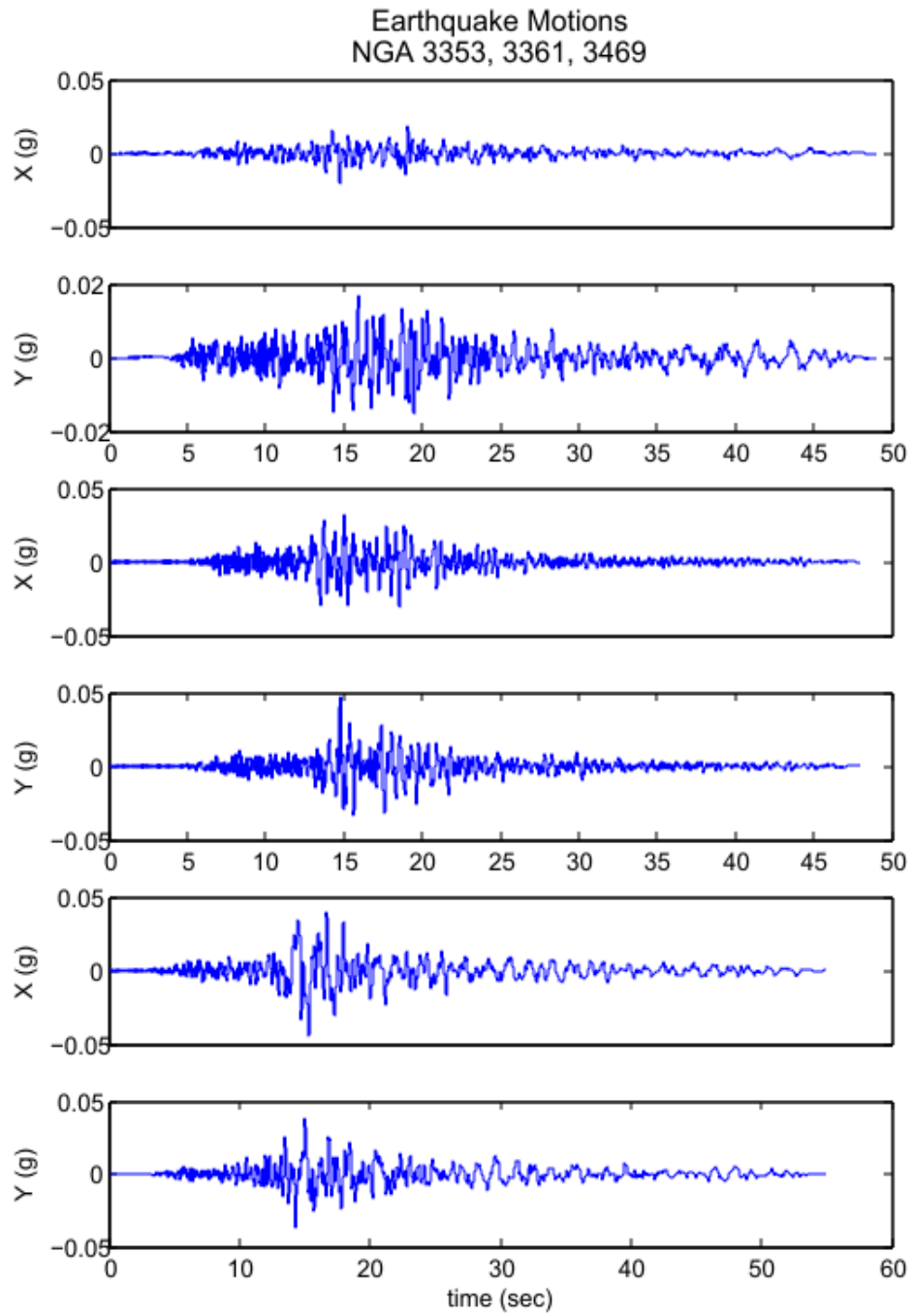


Figure B.18 NGA 3353, 3361, 3469

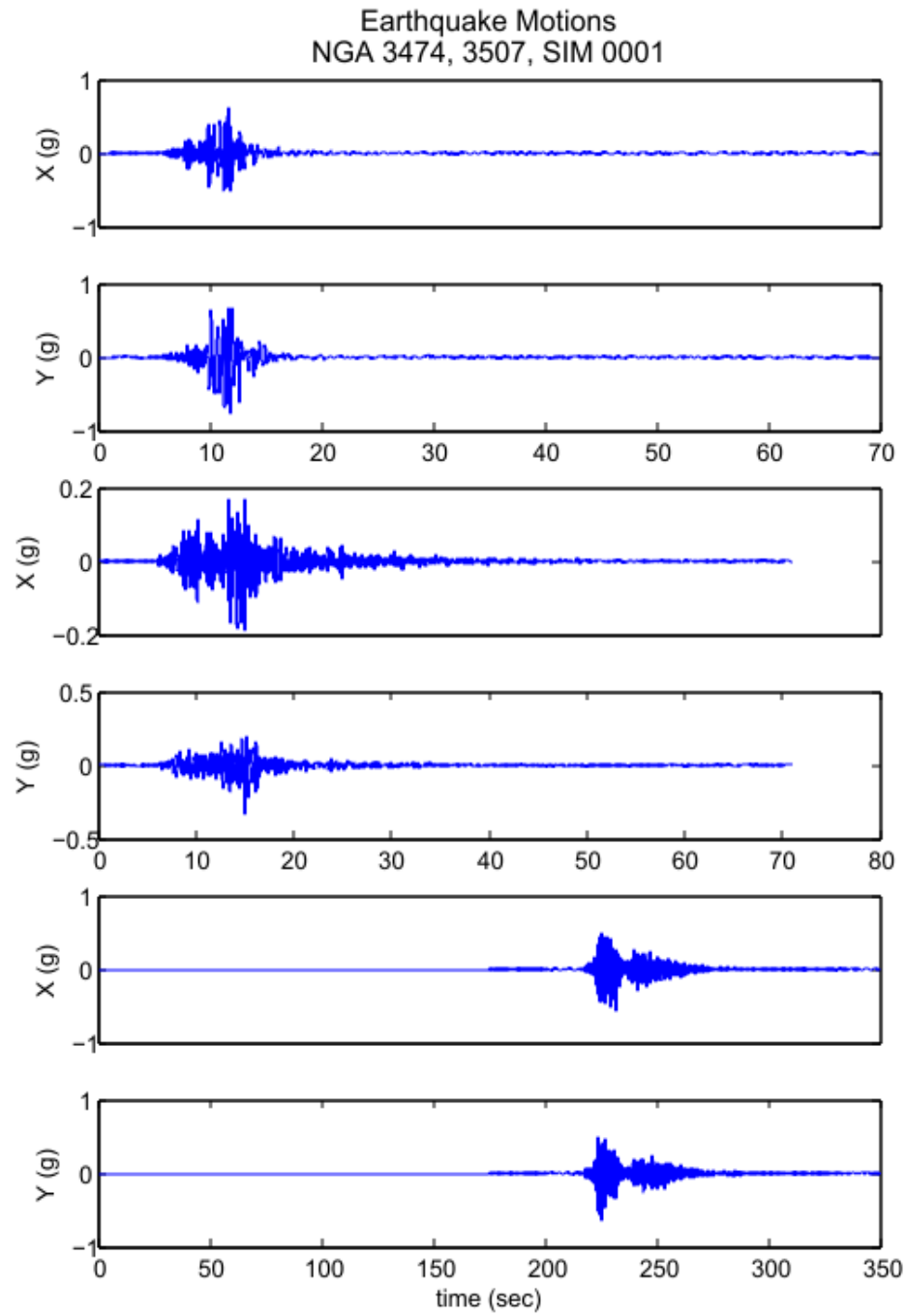


Figure B.19 NGA 3474, 3507, SIM 0001

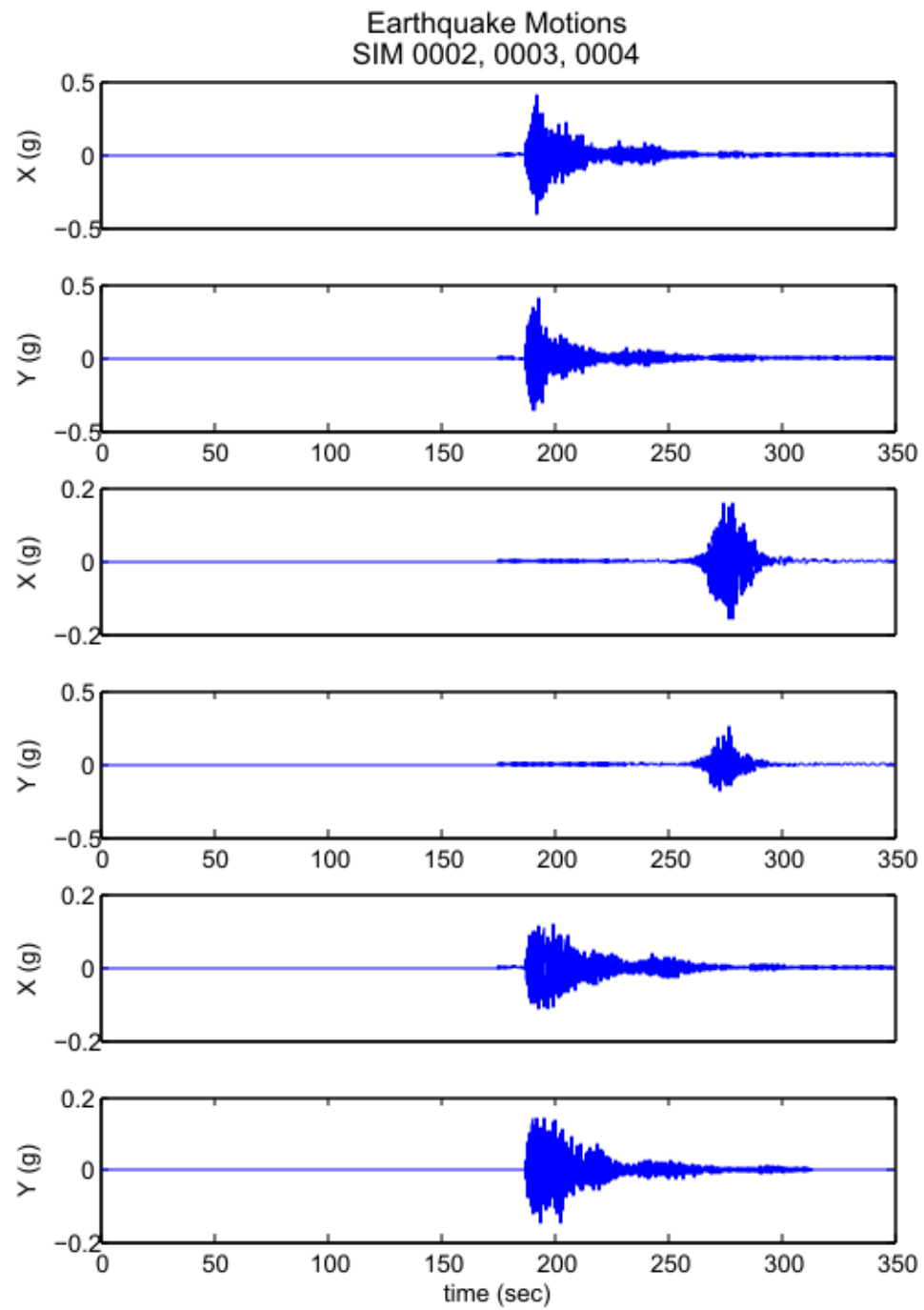


Figure B.20 SIM 0002, 0003, 0004

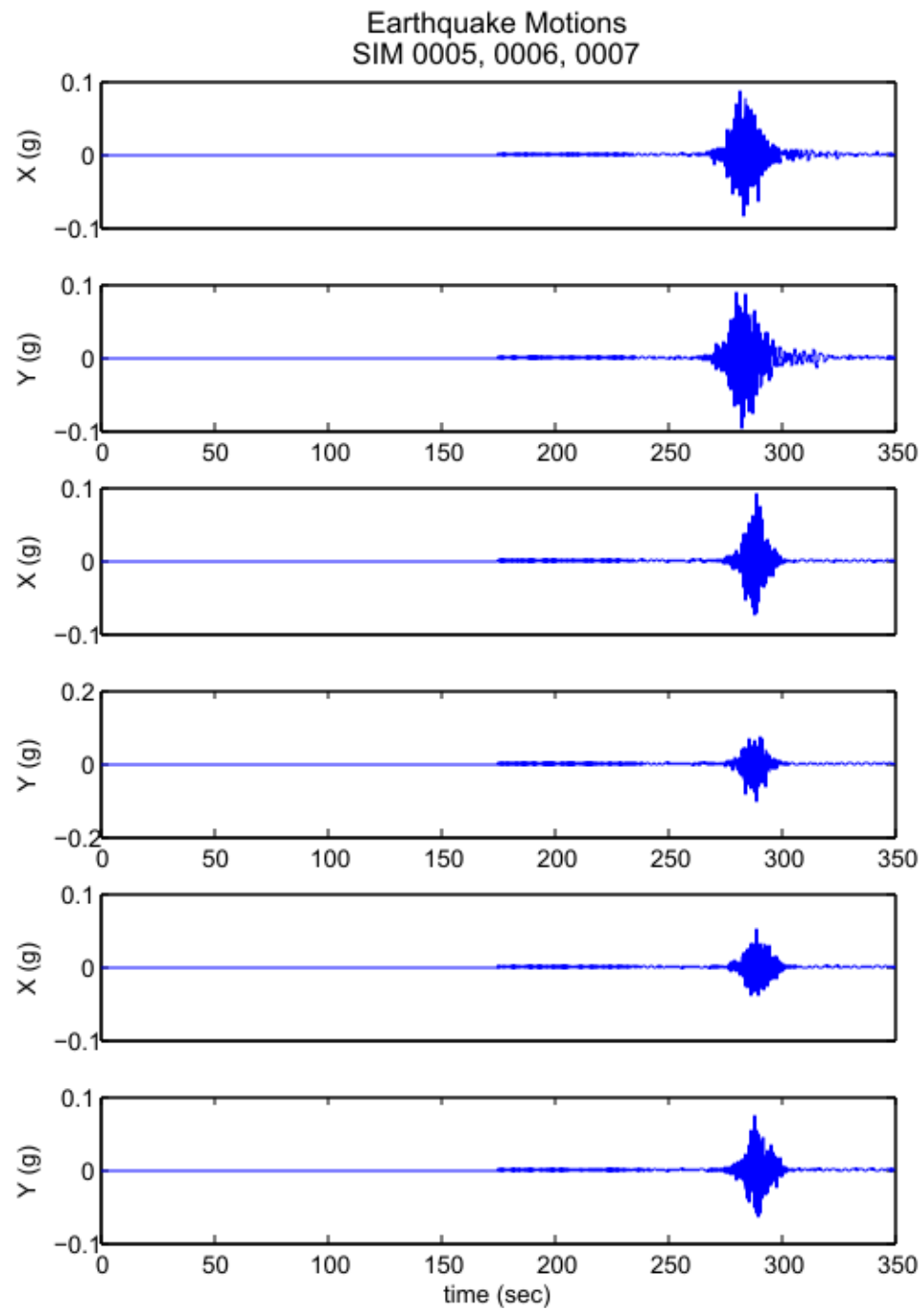


Figure B.21 SIM 0005, 0006, 0007

APPENDIX C- MARINE EXCHANGE OF SOUTHERN CALIFORNIA DATA

The following data was taken from a three month shipping log kept by the Marine Exchange of Southern California from March-August of 2008. The data was used to estimate ship arrivals and ships were sampled from this data according to the calculated arrival stream in Section 3.5.1. Data is sorted first according to berth destination, and then according to arrival date.

Vessel Name	Length (m)	TEU Capacity	Berth	Arrival	Inter-Arrival (days)	Departure	Dwell Time (hrs)	Berth Length (m)	Mean Ships /Day	StdDev Ships /Day
Xin Yan Tai	279.60	5668	100	3/16/08 16:35	3.875	3/19/2008 18:40	74:05 :00	365.76	0.124	0.323
CMA CGM America	267.70	4043	100	3/20/08 13:35	3.069	3/22/2008 19:40	54:05 :00	365.76	0.124	0.323
Xin Chi Wan	279.60	5668	100	3/23/08 15:15	6.247	3/26/2008 6:35	63:20 :00	365.76	0.124	0.323
Xin Fu Zhou	279.90	5668	100	3/29/08 21:10	6.747	4/2/2008 6:55	81:45 :00	365.76	0.124	0.323
Xin Qin Huang Dao	279.60	5668	100	4/5/08 15:05	8.014	4/8/2008 7:05	64:00 :00	365.76	0.124	0.323
CSCL Hong Kong	274.67	5551	100	4/13/08 15:25	10.563	4/17/2008 7:00	87:35 :00	365.76	0.124	0.323
Xin Yan Tai	279.60	5668	100	4/24/08 4:55	7.003	4/27/2008 6:40	73:45 :00	365.76	0.124	0.323
Xin Fu Zhou	279.90	5668	100	5/1/08 5:00	3.469	5/4/2008 17:05	84:05 :00	365.76	0.124	0.323
Xin Ning Bo	279.60	5668	100	5/4/08 16:15	9.049	5/7/2008 7:15	63:00 :00	365.76	0.124	0.323
Xin Qin Huang Dao	279.60	5668	100	5/13/08 17:25	5.986	5/17/2008 6:40	85:15 :00	365.76	0.124	0.323
CSCL Hong Kong	274.67	5551	100	5/19/08 17:05	3.955	5/22/2008 17:55	72:50 :00	365.76	0.124	0.323
CSCL Seattle	275.00	5551	100	5/23/08 16:00	8.917	5/27/2008 6:45	86:45 :00	365.76	0.124	0.323
Xin Yan Tai	279.60	5668	100	6/1/08 14:00	11.632	6/4/2008 17:55	75:55 :00	365.76	0.124	0.323
Xin Ya Zhou	334.00	8530	100	6/13/08 5:10	11.368	6/17/2008 18:45	109:3 5:00	365.76	0.124	0.323
Xin Yang Zhou	263.20	4051	100	6/24/08 14:00	11.635	6/27/2008 13:45	71:45 :00	365.76	0.124	0.323
Xin Wei Hai	263.23	4250	100	7/6/08 5:15	7.392	7/8/2008 20:35	63:20 :00	365.76	0.124	0.323
Xin Ou Zhou	335.00	8530	100	7/13/08 14:40	7.017	7/19/2008 6:30	135:5 0:00	365.76	0.124	0.323
Xin Ya Zhou	334.00	8530	100	7/20/08 15:05	6.955	7/25/2008 20:45	125:4 0:00	365.76	0.124	0.323
Xin Yang Zhou	263.20	4051	100	7/27/08 14:00	9.649	7/29/2008 15:40	49:40 :00	365.76	0.124	0.323

Xin Xia Men	279.90	5668	100	8/6/08 5:35	1.979	8/8/2008 5:20	47:45 :00	365.76	0.124	0.323
Xin Chong Qing	263.23	4051	100	8/8/08 5:05	10.993	8/10/2008 17:45	60:40 :00	365.76	0.124	0.323
Xin Su Zhou	263.20	4051	100	8/19/08 4:55	5.094	8/21/2008 18:45	61:50 :00	365.76	0.124	0.323
Xin Tai Cang	262.33	4253	100	8/24/08 7:10	6.382	8/26/2008 20:40	61:30 :00	365.76	0.124	0.323
Xin Yan Tai	279.90	5668	100	8/30/08 16:20				365.76	0.124	0.323
YM March	278.94	5570	121	3/1/08 15:05	8.212	3/4/2008 19:30	76:25 :00	1066.8	0.366	0.545
YM Wealth	275.00	5551	121	3/9/08 20:10	6.403	3/12/2008 18:20	70:10 :00	1066.8	0.366	0.545
YM Success	275.00	5551	121	3/16/08 5:50	6.017	3/19/2008 6:50	73:00 :00	1066.8	0.366	0.545
YM Great	278.94	5570	121	3/22/08 6:15	3.455	3/25/2008 19:10	84:55 :00	1066.8	0.366	0.545
YM Initiative	172.70	1799	121	3/25/08 17:10	4.531	3/26/2008 18:30	25:20 :00	1066.8	0.366	0.545
YM Fountain	275.00	5551	121	3/30/08 5:55	2.927	4/2/2008 5:05	71:10 :00	1066.8	0.366	0.545
Ville D'Aquarius	259.35	3940	121	4/2/08 4:10	3.448	4/5/2008 18:10	86:00 :00	1066.8	0.366	0.545
YM March	278.94	5570	121	4/5/08 14:55	3.632	4/8/2008 19:00	76:05 :00	1066.8	0.366	0.545
YM Ideals	171.90	1805	121	4/9/08 6:05	4.299	4/10/2008 7:00	24:55 :00	1066.8	0.366	0.545
YM Wealth	275.00	5551	121	4/13/08 13:15	2.885	4/16/2008 7:20	66:05 :00	1066.8	0.366	0.545
YM Instruction	172.70	1805	121	4/16/08 10:30	3.090	4/17/2008 19:45	33:15 :00	1066.8	0.366	0.545
YM Success	275.00	5551	121	4/19/08 12:40	3.726	4/22/2008 18:30	77:50 :00	1066.8	0.366	0.545
YM Increment	172.70	1805	121	4/23/08 6:05	1.378	4/24/2008 7:55	25:50 :00	1066.8	0.366	0.545
YM Europe	275.70	3604	121	4/24/08 15:10	2.080	4/26/2008 18:25	51:15 :00	1066.8	0.366	0.545
YM Great	278.94	5570	121	4/26/08 17:05	3.552	4/29/2008 17:55	72:50 :00	1066.8	0.366	0.545
YM Initiative	172.70	1799	121	4/30/08 6:20	3.941	5/1/2008 7:15	24:55 :00	1066.8	0.366	0.545
YM Fountain	275.00	5551	121	5/4/08 4:55	3.049	5/7/2008 7:20	74:25 :00	1066.8	0.366	0.545
YM Inception	172.70	1805	121	5/7/08 6:05	3.368	5/8/2008 7:35	25:30 :00	1066.8	0.366	0.545
YM March	278.94	5570	121	5/10/08 14:55	3.628	5/13/2008 18:40	75:45 :00	1066.8	0.366	0.545
YM Ideals	171.90	1805	121	5/14/08 6:00	3.243	5/15/2008 5:30	23:30 :00	1066.8	0.366	0.545
YM Wealth	275.00	5551	121	5/17/08 11:50	4.764	5/20/2008 18:50	79:00 :00	1066.8	0.366	0.545
YM Instruction	172.70	1805	121	5/22/08 6:10	3.243	5/23/2008 7:35	25:25 :00	1066.8	0.366	0.545

YM Success	275.00	5551	121	5/25/08 12:00	6.076	5/28/2008 18:40	78:40 :00	1066.8	0.366	0.545
YM Great	278.94	5570	121	5/31/08 13:50	3.688	6/4/2008 7:05	89:15 :00	1066.8	0.366	0.545
YM Initiative	172.70	1799	121	6/4/08 6:20	3.247	6/5/2008 6:45	24:25 :00	1066.8	0.366	0.545
YM Fountain	275.00	5551	121	6/7/08 12:15	7.118	6/11/2008 6:45	90:30 :00	1066.8	0.366	0.545
YM March	278.94	5570	121	6/14/08 15:05	6.865	6/18/2008 7:00	87:55 :00	1066.8	0.366	0.545
YM Wealth	275.00	5551	121	6/21/08 11:50	5.101	6/25/2008 7:45	91:55 :00	1066.8	0.366	0.545
CSCS Shanghai	274.67	5551	121	6/26/08 14:15	2.160	6/29/2008 20:35	78:20 :00	1066.8	0.366	0.545
YM Success	275.00	5551	121	6/28/08 18:05	3.497	7/2/2008 7:10	85:05 :00	1066.8	0.366	0.545
YM Increment	172.70	1805	121	7/2/08 6:00	5.319	7/3/2008 9:00	27:00 :00	1066.8	0.366	0.545
YM Great	278.94	5570	121	7/7/08 13:40	5.601	7/10/2008 17:55	76:15 :00	1066.8	0.366	0.545
YM South	275.70	3725	121	7/13/08 4:05	4.122	7/15/2008 20:35	64:30 :00	1066.8	0.366	0.545
YM Fountain	275.00	5551	121	7/17/08 7:00	2.962	7/20/2008 7:00	72:00 :00	1066.8	0.366	0.545
YM East	275.70	3725	121	7/20/08 6:05	5.434	7/22/2008 18:10	60:05 :00	1066.8	0.366	0.545
YM March	278.94	5570	121	7/25/08 16:30	5.563	7/29/2008 18:50	98:20 :00	1066.8	0.366	0.545
YM Wealth	275.00	5551	121	7/31/08 6:00	6.924	8/3/2008 8:40	74:40 :00	1066.8	0.366	0.545
YM Success	275.00	5551	121	8/7/08 4:10	3.580	8/10/2008 18:00	85:50 :00	1066.8	0.366	0.545
YM West	275.68	3725	121	8/10/08 18:05	3.507	8/13/2008 8:00	61:55 :00	1066.8	0.366	0.545
YM Great	278.94	5570	121	8/14/08 6:15	3.465	8/17/2008 17:50	83:35 :00	1066.8	0.366	0.545
YM South	275.70	3725	121	8/17/08 17:25	6.566	8/20/2008 8:00	62:35 :00	1066.8	0.366	0.545
YM Fountain	275.00	5551	121	8/24/08 7:00		8/28/2008 7:10	96:10 :00	1066.8	0.366	0.545
YM Increment	172.70	1805	126	3/19/08 6:00	2.174	3/20/2008 8:40	26:40 :00	1066.8	0.366	0.545
YM Europe	275.70	3604	126	3/21/08 10:10	2.830	3/23/2008 18:50	56:40 :00	1066.8	0.366	0.545
YM America	275.70	3604	126	3/24/08 6:05	8.000	3/26/2008 8:45	50:40 :00	1066.8	0.366	0.545
YM Immense	172.70	1805	126	4/1/08 6:05	1.003	4/2/2008 7:00	24:55 :00	1066.8	0.366	0.545
YM Inception	172.70	1805	126	4/2/08 6:10	5.396	4/3/2008 5:55	23:45 :00	1066.8	0.366	0.545
YM Asia	275.70	3604	126	4/7/08 15:40	7.924	4/9/2008 18:55	51:15 :00	1066.8	0.366	0.545
YM Prosperity	269.68	3266	126	4/15/08 13:50	7.080	4/17/2008 17:55	52:05 :00	1066.8	0.366	0.545

CMA CGM America	267.70	4043	126	4/22/08 15:45	6.601	4/25/2008 6:20	62:35 :00	1066.8	0.366	0.545
YM America	275.70	3604	126	4/29/08 6:10	5.962	5/1/2008 7:40	49:30 :00	1066.8	0.366	0.545
YM Yantian	275.70	3918	126	5/5/08 5:15	7.424	5/7/2008 19:10	61:55 :00	1066.8	0.366	0.545
YM Asia	275.70	3604	126	5/12/08 15:25	7.899	5/15/2008 4:45	61:20 :00	1066.8	0.366	0.545
YM Prosperi ty	269.68	3266	126	5/20/08 13:00	6.708	5/22/2008 18:00	53:00 :00	1066.8	0.366	0.545
YM Europe	275.70	3604	126	5/27/08 6:00	6.000	5/29/2008 17:55	59:55 :00	1066.8	0.366	0.545
YM America	275.70	3604	126	6/2/08 6:00	7.007	6/4/2008 18:40	60:40 :00	1066.8	0.366	0.545
YM Yantian	275.70	3918	126	6/9/08 6:10	5.455	6/11/2008 7:05	48:55 :00	1066.8	0.366	0.545
YM Inceptio n	172.70	1805	126	6/14/08 17:05	1.552	6/15/2008 19:05	26:00 :00	1066.8	0.366	0.545
YM Asia	275.70	3604	126	6/16/08 6:20	3.052	6/18/2008 7:50	49:30 :00	1066.8	0.366	0.545
YM Ideals	171.90	1805	126	6/19/08 7:35	4.194	6/20/2008 7:55	24:20 :00	1066.8	0.366	0.545
YM Prosperi ty	269.68	3266	126	6/23/08 12:15	2.740	6/25/2008 16:50	52:35 :00	1066.8	0.366	0.545
YM Instructi on	172.70	1805	126	6/26/08 6:00	4.424	6/27/2008 7:50	25:50 :00	1066.8	0.366	0.545
YM Europe	275.70	3604	126	6/30/08 16:10	5.653	7/2/2008 20:00	51:50 :00	1066.8	0.366	0.545
YM West	275.68	3725	126	7/6/08 7:50	20.927	7/8/2008 6:50	47:00 :00	1066.8	0.366	0.545
YM Zenith	275.70	3725	126	7/27/08 6:05	7.000	7/29/2008 7:45	49:40 :00	1066.8	0.366	0.545
YM North	275.70	3725	126	8/3/08 6:05	20.986	8/5/2008 8:10	50:05 :00	1066.8	0.366	0.545
YM East	275.70	3725	126	8/24/08 5:45	7.021	8/26/2008 8:00	50:15 :00	1066.8	0.366	0.545
YM Zenith	275.70	3725	126	8/31/08 6:15				1066.8	0.366	0.545
YM Interacti on	171.90	1805	127	4/2/08 6:05		4/4/2008 17:55	59:50 :00	1066.8	0.366	0.545
Mol Express	294.00	4646	139	3/3/08 15:10	6.722	3/5/2008 19:30	52:20 :00	1234.44	0.319	0.466
Mol Solution	278.94	5220	139	3/10/08 8:30	1.854	3/12/2008 6:15	45:45 :00	1234.44	0.319	0.466
Mol Innovati on	294.11	4369	139	3/12/08 5:00	0.969	3/13/2008 3:10	22:10 :00	1234.44	0.319	0.466
USL Condor	161.30	1347	139	3/13/08 4:15	3.622	3/14/2008 6:45	26:30 :00	1234.44	0.319	0.466
Mol Proficie ncy	293.20	6350	139	3/16/08 19:10	3.809	3/18/2008 19:00	47:50 :00	1234.44	0.319	0.466
Mol Confide nce	275.00	4411	139	3/20/08 14:35	3.021	3/23/2008 6:05	63:30 :00	1234.44	0.319	0.466
Mol Prosperi ty	293.19	6350	139	3/23/08 15:05	6.997	3/25/2008 9:20	42:15 :00	1234.44	0.319	0.466

Mol Partner	293.20	6350	139	3/30/08 15:00	7.188	4/1/2008 19:05	52:05 :00	1234.44	0.319	0.466
Mol Paradise	293.19	6350	139	4/6/08 19:30	1.976	4/8/2008 19:15	47:45 :00	1234.44	0.319	0.466
Mol Efficiency	294.09	4646	139	4/8/08 18:55	4.851	4/10/2008 18:00	47:05 :00	1234.44	0.319	0.466
Mol Presence	279.77	6350	139	4/13/08 15:20	3.497	4/15/2008 19:10	51:50 :00	1234.44	0.319	0.466
Mol Expeditor	294.00	4646	139	4/17/08 3:15	1.069	4/17/2008 18:10	14:55 :00	1234.44	0.319	0.466
Mol Confidence	275.00	4411	139	4/18/08 4:55	2.490	4/20/2008 5:55	49:00 :00	1234.44	0.319	0.466
Mol Proficiency	293.20	6350	139	4/20/08 16:40	2.528	4/22/2008 18:50	50:10 :00	1234.44	0.319	0.466
Mol Advantage	278.94	5220	139	4/23/08 5:20	4.413	4/25/2008 6:50	49:30 :00	1234.44	0.319	0.466
Mol Prosperity	293.19	6350	139	4/27/08 15:15	2.128	4/29/2008 18:15	51:00 :00	1234.44	0.319	0.466
Mol Enterprise	294.13	4646	139	4/29/08 18:20	6.455	4/30/2008 16:15	21:55 :00	1234.44	0.319	0.466
Mol Partner	293.20	6350	139	5/6/08 5:15	5.406	5/8/2008 5:30	48:15 :00	1234.44	0.319	0.466
Mol Paradise	293.19	6350	139	5/11/08 15:00	3.583	5/13/2008 18:00	51:00 :00	1234.44	0.319	0.466
Mol Confidence	275.00	4411	139	5/15/08 5:00	3.503	5/17/2008 6:50	49:50 :00	1234.44	0.319	0.466
Mol Presence	279.77	6350	139	5/18/08 17:05	1.972	5/20/2008 16:45	47:40 :00	1234.44	0.319	0.466
Mol Endowment	294.12	5078	139	5/20/08 16:25	2.670	5/21/2008 17:50	25:25 :00	1234.44	0.319	0.466
Mol Wave	231.00	3554	139	5/23/08 8:30	2.333	5/25/2008 6:25	45:55 :00	1234.44	0.319	0.466
Mol Proficiency	293.20	6350	139	5/25/08 16:30	2.938	5/27/2008 18:50	50:20 :00	1234.44	0.319	0.466
Trieste	270.00	3876	139	5/28/08 15:00	3.962	5/30/2008 4:40	37:40 :00	1234.44	0.319	0.466
Mol Prosperity	293.19	6350	139	6/1/08 14:05	1.677	6/3/2008 6:30	40:25 :00	1234.44	0.319	0.466
Mol Innovation	294.11	4369	139	6/3/08 6:20	1.250	6/4/2008 6:25	24:05 :00	1234.44	0.319	0.466
Mol Discovery	253.27	3054	139	6/4/08 12:20	1.889	6/6/2008 4:25	40:05 :00	1234.44	0.319	0.466
Mol Wind	231.00	3554	139	6/6/08 9:40	2.229	6/12/2008 23:25	157:4 5:00	1234.44	0.319	0.466
Mol Partner	293.20	6350	139	6/8/08 15:10	2.990	6/10/2008 19:00	51:50 :00	1234.44	0.319	0.466
Mol Liberty	246.30	2522	139	6/11/08 14:55	4.024	6/13/2008 2:55	36:00 :00	1234.44	0.319	0.466
Mol Paradise	293.19	6350	139	6/15/08 15:30	3.028	6/17/2008 20:05	52:35 :00	1234.44	0.319	0.466

Mol Miracle	244.78	2996	139	6/18/08 16:10	3.917	6/21/2008 15:30	71:20 :00	1234.44	0.319	0.466
Mol Presenc e	279.77	6350	139	6/22/08 14:10	3.035	6/24/2008 19:20	53:10 :00	1234.44	0.319	0.466
Trieste	270.00	3876	139	6/25/08 15:00	2.955	6/27/2008 5:45	38:45 :00	1234.44	0.319	0.466
Mol Proficie ncy	293.20	6350	139	6/28/08 13:55	2.611	6/30/2008 17:55	52:00 :00	1234.44	0.319	0.466
Mol Excellen ce	294.00	4646	139	7/1/08 4:35	1.003	7/1/2008 18:25	13:50 :00	1234.44	0.319	0.466
Mol Discove ry	253.27	3054	139	7/2/08 4:40	3.938	7/3/2008 18:10	37:30 :00	1234.44	0.319	0.466
Mol Prosperi ty	293.19	6350	139	7/6/08 3:10	2.451	7/8/2008 6:20	51:10 :00	1234.44	0.319	0.466
Mol Enduran ce	294.13	4646	139	7/8/08 14:00	0.965	7/9/2008 6:40	16:40 :00	1234.44	0.319	0.466
Mol Liberty	246.30	2522	139	7/9/08 13:10	3.045	7/11/2008 7:00	41:50 :00	1234.44	0.319	0.466
Mol Partner	293.20	6350	139	7/12/08 14:15	3.969	7/15/2008 6:30	64:15 :00	1234.44	0.319	0.466
Mol Miracle	244.78	2996	139	7/16/08 13:30	3.375	7/18/2008 3:50	38:20 :00	1234.44	0.319	0.466
Mol Paradise	293.19	6350	139	7/19/08 22:30	2.653	7/21/2008 20:20	45:50 :00	1234.44	0.319	0.466
Mol Enterpri se	294.13	4646	139	7/22/08 14:10	1.045	7/23/2008 8:15	18:05 :00	1234.44	0.319	0.466
Trieste	270.00	3876	139	7/23/08 15:15	1.993	7/25/2008 4:50	37:35 :00	1234.44	0.319	0.466
Mol Fortune	226.42	2701	139	7/25/08 15:05	1.563	7/27/2008 3:55	36:50 :00	1234.44	0.319	0.466
Mol Presenc e	279.77	6350	139	7/27/08 4:35	3.021	7/29/2008 19:00	62:25 :00	1234.44	0.319	0.466
Mol Discove ry	253.27	3054	139	7/30/08 5:05	4.003	7/31/2008 18:50	37:45 :00	1234.44	0.319	0.466
Mol Proficie ncy	293.20	6350	139	8/3/08 5:10	2.976	8/5/2008 19:00	61:50 :00	1234.44	0.319	0.466
Mol Liberty	246.30	2522	139	8/6/08 4:35	2.351	8/7/2008 19:05	38:30 :00	1234.44	0.319	0.466
Mol Wonder	231.00	3554	139	8/8/08 13:00	2.056	8/10/2008 6:00	41:00 :00	1234.44	0.319	0.466
Mol Prosperi ty	293.19	6350	139	8/10/08 14:20	2.597	8/12/2008 19:10	52:50 :00	1234.44	0.319	0.466
Mol Miracle	244.78	2996	139	8/13/08 4:40	2.389	8/14/2008 19:00	38:20 :00	1234.44	0.319	0.466
Mol World	232.03		139	8/15/08 14:00	1.660	8/17/2008 6:00	40:00 :00	1234.44	0.319	0.466
Mol Partner	293.20	6350	139	8/17/08 5:50	3.385	8/19/2008 17:50	60:00 :00	1234.44	0.319	0.466
Trieste	270.00	3876	139	8/20/08 15:05	1.979	8/22/2008 4:55	37:50 :00	1234.44	0.319	0.466
Mol Wind	231.00	3554	139	8/22/08 14:35	1.986	8/24/2008 5:55	39:20 :00	1234.44	0.319	0.466
Mol Paradise	293.19	6350	139	8/24/08 14:15	2.351	8/26/2008 20:30	54:15 :00	1234.44	0.319	0.466

Mol Discover y	253.27	3054	139	8/26/08 22:40	2.639	8/28/2008 18:55	44:15 :00	1234.44	0.319	0.466
Mol Fortune	226.42	2701	139	8/29/08 14:00	1.642	8/31/2008 5:20		1234.44	0.319	0.466
Mol Presenc e	279.77	6350	139	8/31/08 5:25				1234.44	0.319	0.466
OOCL Busan	259.80	4500	212	2/29/08 5:35	4.476	3/2/2008 18:10	60:35 :00	1767.84	0.422	0.593
Santa Barbara	253.28	3054	212	3/4/08 17:00	2.552	3/6/2008 19:00	50:00 :00	1767.84	0.422	0.593
OOCL Seattle	280.54	5888	212	3/7/08 6:15	5.368	3/10/2008 10:25	76:10 :00	1767.84	0.422	0.593
Katsura gi	292.30	3613	212	3/12/08 15:05	7.007	3/15/2008 7:30	64:25 :00	1767.84	0.422	0.593
NYK Deneb	294.12	4922	212	3/19/08 15:15	8.003	3/22/2008 20:15	77:00 :00	1767.84	0.422	0.593
OOCL Dubai	280.54	5888	212	3/27/08 15:20	3.528	3/30/2008 19:20	76:00 :00	1767.84	0.422	0.593
OOCL Japan	276.16	5344	212	3/31/08 4:00	2.549	4/2/2008 18:25	62:25 :00	1767.84	0.422	0.593
OOCL Busan	259.80	4526	212	4/2/08 17:10	7.514	4/6/2008 11:05	89:55 :00	1767.84	0.422	0.593
OOCL Seattle	280.54	5888	212	4/10/08 5:30	6.434	4/13/2008 10:10	76:40 :00	1767.84	0.422	0.593
MISC Merlion	294.06	4281	212	4/16/08 15:55	9.389	4/19/2008 19:00	75:05 :00	1767.84	0.422	0.593
NYK Deneb	294.12	4922	212	4/26/08 1:15	5.965	4/28/2008 21:05	67:50 :00	1767.84	0.422	0.593
OOCL Dubai	280.54	5888	212	5/2/08 0:25	6.622	5/4/2008 18:20	65:55 :00	1767.84	0.422	0.593
OOCL Busan	259.80	4526	212	5/8/08 15:20	6.594	5/11/2008 5:00	61:40 :00	1767.84	0.422	0.593
OOCL Seattle	280.54	5888	212	5/15/08 5:35	5.309	5/18/2008 6:20	72:45 :00	1767.84	0.422	0.593
Santa Monica	254.28	3054	212	5/20/08 13:00	2.424	5/22/2008 17:30	52:30 :00	1767.84	0.422	0.593
OOCL China	276.02	5344	212	5/22/08 23:10	5.785	5/25/2008 16:15	65:05 :00	1767.84	0.422	0.593
NYK Deneb	294.12	4922	212	5/28/08 18:00	2.990	5/31/2008 17:20	71:20 :00	1767.84	0.422	0.593
NYK Androm eda	299.80	6214	212	5/31/08 17:45	4.559	6/3/2008 10:20	64:35 :00	1767.84	0.422	0.593
OOCL Dubai	280.54	5888	212	6/5/08 7:10	5.306	6/8/2008 4:50	69:40 :00	1767.84	0.422	0.593
Hansa Africa	243.00	3424	212	6/10/08 14:30	3.896	6/12/2008 18:50	52:20 :00	1767.84	0.422	0.593
NYK Athena	299.90	6492	212	6/14/08 12:00	3.167	6/17/2008 13:50	73:50 :00	1767.84	0.422	0.593
Santa Barbara	253.28	3054	212	6/17/08 16:00	3.583	6/19/2008 17:50	49:50 :00	1767.84	0.422	0.593
NYK Argus	299.90	6492	212	6/21/08 6:00	10.378	6/24/2008 4:15	70:15 :00	1767.84	0.422	0.593
OOCL China	276.02	5344	212	7/1/08 15:05	4.997	7/4/2008 19:15	76:10 :00	1767.84	0.422	0.593
NYK Phoenix	299.95	6586	212	7/6/08 15:00	2.771	7/9/2008 9:15	66:15 :00	1767.84	0.422	0.593
Santa Cruz	251.50	2850	212	7/9/08 9:30	4.219	7/11/2008 3:50	42:20 :00	1767.84	0.422	0.593
OOCL Dubai	280.54	5888	212	7/13/08 14:45	6.038	7/17/2008 19:50	101:0 5:00	1767.84	0.422	0.593
NYK Atlas	299.90	6492	212	7/19/08 15:40	3.934	7/23/2008 15:15	95:35 :00	1767.84	0.422	0.593

Santa Barbara	253.28	3054	212	7/23/08 14:05	6.080	7/25/2008 17:25	51:20 :00	1767.84	0.422	0.593
Santa Monica	254.28	3054	212	7/29/08 16:00	4.597	7/31/2008 17:50	49:50 :00	1767.84	0.422	0.593
NYK Argus	299.90	6492	212	8/3/08 6:20	3.212	8/6/2008 12:45	78:25 :00	1767.84	0.422	0.593
NYK Springtide	253.28	3054	212	8/6/08 11:25	3.191	8/8/2008 6:30	43:05 :00	1767.84	0.422	0.593
NYK Lodestar	299.80	6178	212	8/9/08 16:00	3.073	8/12/2008 18:40	74:40 :00	1767.84	0.422	0.593
Santa Cruz	251.50	2850	212	8/12/08 17:45	4.184	8/14/2008 20:05	50:20 :00	1767.84	0.422	0.593
NYK Athena	299.90	6492	212	8/16/08 22:10	3.878	8/20/2008 16:25	90:15 :00	1767.84	0.422	0.593
NYK Starlight	251.00	2850	212	8/20/08 19:15	3.865	8/22/2008 19:10	47:55 :00	1767.84	0.422	0.593
NYK Andromeda	299.80	6214	212	8/24/08 16:00		8/28/2008 5:15	85:15 :00	1767.84	0.422	0.593
NYK Starlight	251.00	2850	214	2/29/08 16:15	1.698	3/2/2008 9:40	41:25 :00	1767.84	0.422	0.593
NYK Phoenix	299.95	6586	214	3/2/08 9:00	7.319	3/4/2008 19:55	58:55 :00	1767.84	0.422	0.593
NYK Andromeda	299.80	6214	214	3/9/08 16:40	5.931	3/12/2008 18:50	74:10 :00	1767.84	0.422	0.593
NYK Atlas	299.90	6492	214	3/15/08 15:00	3.576	3/18/2008 18:25	75:25 :00	1767.84	0.422	0.593
NYK Springtide	253.28	3054	214	3/19/08 4:50	3.056	3/21/2008 5:50	49:00 :00	1767.84	0.422	0.593
NYK Athena	299.90	6492	214	3/22/08 6:10	3.417	3/25/2008 9:05	74:55 :00	1767.84	0.422	0.593
Santa Cruz	251.50	2850	214	3/25/08 16:10	4.455	3/27/2008 17:45	49:35 :00	1767.84	0.422	0.593
NYK Argus	299.90	6492	214	3/30/08 3:05	4.837	4/2/2008 3:55	72:50 :00	1767.84	0.422	0.593
NYK Starlight	251.00	2850	214	4/3/08 23:10	1.743	4/5/2008 17:35	42:25 :00	1767.84	0.422	0.593
NYK Lodestar	299.80	6178	214	4/5/08 17:00	4.958	4/8/2008 17:50	72:50 :00	1767.84	0.422	0.593
Santa Barbara	253.28	3054	214	4/10/08 16:00	1.958	4/12/2008 9:40	41:40 :00	1767.84	0.422	0.593
NYK Phoenix	299.95	6586	214	4/12/08 15:00	3.090	4/15/2008 17:45	74:45 :00	1767.84	0.422	0.593
Santa Monica	254.28	3054	214	4/15/08 17:10	3.955	4/17/2008 18:00	48:50 :00	1767.84	0.422	0.593
NYK Andromeda	299.80	6214	214	4/19/08 16:05	4.413	4/22/2008 18:00	73:55 :00	1767.84	0.422	0.593
NYK Springtide	253.28	3054	214	4/24/08 2:00	2.417	4/26/2008 2:55	48:55 :00	1767.84	0.422	0.593
NYK Atlas	299.90	6492	214	4/26/08 12:00	3.542	4/29/2008 17:45	77:45 :00	1767.84	0.422	0.593
Santa Cruz	251.50	2850	214	4/30/08 1:00	3.170	5/2/2008 0:20	47:20 :00	1767.84	0.422	0.593
NYK Athena	299.90	6492	214	5/3/08 5:05	3.330	5/6/2008 4:05	71:00 :00	1767.84	0.422	0.593

NYK Starlight	251.00	2850	214	5/6/08 13:00	4.045	5/8/2008 17:25	52:25 :00	1767.84	0.422	0.593
NYK Argus	299.90	6492	214	5/10/08 14:05	2.997	5/13/2008 3:30	61:25 :00	1767.84	0.422	0.593
Santa Barbara	253.28	3054	214	5/13/08 14:00	4.458	5/15/2008 18:20	52:20 :00	1767.84	0.422	0.593
NYK Lodestar	299.80	6178	214	5/18/08 1:00	6.608	5/20/2008 16:40	63:40 :00	1767.84	0.422	0.593
NYK Phoenix	299.95	6586	214	5/24/08 15:35	2.979	5/27/2008 3:40	60:05 :00	1767.84	0.422	0.593
NYK Springtide	253.28	3054	214	5/27/08 15:05	7.045	5/29/2008 17:40	50:35 :00	1767.84	0.422	0.593
Santa Cruz	251.50	2850	214	6/3/08 16:10	3.861	6/5/2008 17:55	49:45 :00	1767.84	0.422	0.593
NYK Atlas	299.90	6492	214	6/7/08 12:50	6.972	6/10/2008 9:30	68:40 :00	1767.84	0.422	0.593
NYK Vesta	338.17	9012	214	6/14/08 12:10	4.170	6/18/2008 4:20	88:10 :00	1767.84	0.422	0.593
OOCL Seattle	280.54	5888	214	6/18/08 16:15	5.934	6/22/2008 3:50	83:35 :00	1767.84	0.422	0.593
Santa Monica	254.28	3054	214	6/24/08 14:40	5.181	6/26/2008 17:10	50:30 :00	1767.84	0.422	0.593
NYK Lodestar	299.80	6178	214	6/29/08 19:00	2.934	7/2/2008 18:45	71:45 :00	1767.84	0.422	0.593
NYK Springtide	253.28	3054	214	7/2/08 17:25	4.660	7/4/2008 17:00	47:35 :00	1767.84	0.422	0.593
NYK Venus	338.17	9012	214	7/7/08 9:15	5.837	7/10/2008 18:05	80:50 :00	1767.84	0.422	0.593
NYK Andromeda	299.80	6214	214	7/13/08 5:20	3.986	7/16/2008 17:50	84:30 :00	1767.84	0.422	0.593
NYK Starlight	251.00	2850	214	7/17/08 5:00	2.080	7/19/2008 3:50	46:50 :00	1767.84	0.422	0.593
NYK Vesta	338.17	9012	214	7/19/08 6:55	7.347	7/23/2008 16:55	106:0 0:00	1767.84	0.422	0.593
NYK Lyra	299.80	6178	214	7/26/08 15:15	7.632	7/29/2008 17:35	74:20 :00	1767.84	0.422	0.593
Busan Express	300.00	6750	214	8/3/08 6:25	2.955	8/6/2008 3:55	69:30 :00	1767.84	0.422	0.593
OOCL Long Beach	322.97	8063	214	8/6/08 5:20	4.997	8/9/2008 18:05	84:45 :00	1767.84	0.422	0.593
OOCL Southampton	323.00	8063	214	8/11/08 5:15	5.420	8/15/2008 3:50	94:35 :00	1767.84	0.422	0.593
OOCL Shenzhen	323.00	8063	214	8/16/08 15:20	5.590	8/20/2008 17:30	98:10 :00	1767.84	0.422	0.593
NYK Vesta	338.17	9012	214	8/22/08 5:30	9.063	8/26/2008 5:45	96:15 :00	1767.84	0.422	0.593
NYK Atlas	299.90	6492	214	8/31/08 7:00				1767.84	0.422	0.593
Ever Ulysses	285.00	5652	227	3/1/08 13:25	3.823	3/3/2008 3:45	38:20 :00	1432.56	0.665	0.603
Ever Result	294.13	4229	227	3/5/08 9:10	3.208	3/6/2008 6:40	21:30 :00	1432.56	0.665	0.603
Ever Uberty	285.00	5364	227	3/8/08 14:10	5.993	3/10/2008 17:40	51:30 :00	1432.56	0.665	0.603

Ever Urban	280.00	5652	227	3/14/08 14:00	1.639	3/16/2008 4:50	38:50 :00	1432.56	0.665	0.603
Hatsu Excel	300.00	6332	227	3/16/08 5:20	1.993	3/17/2008 20:25	39:05 :00	1432.56	0.665	0.603
Ever Decent	294.13	4211	227	3/18/08 5:10	3.021	3/19/2008 4:35	23:25 :00	1432.56	0.665	0.603
Ever Reach	294.03	4229	227	3/21/08 5:40	1.313	3/22/2008 5:35	23:55 :00	1432.56	0.665	0.603
Ever Unific	285.00	5652	227	3/22/08 13:10	2.851	3/24/2008 20:25	55:15 :00	1432.56	0.665	0.603
Ever Useful	285.00	5652	227	3/25/08 9:35	4.271	3/26/2008 19:25	33:50 :00	1432.56	0.665	0.603
Ever Uranus	285.00	5652	227	3/29/08 16:05	5.538	3/31/2008 17:45	49:40 :00	1432.56	0.665	0.603
Ever Dainty	294.13	4211	227	4/4/08 5:00	0.979	4/5/2008 5:35	24:35 :00	1432.56	0.665	0.603
Aramis	230.82	2728	227	4/5/08 4:30	2.997	4/6/2008 6:25	25:55 :00	1432.56	0.665	0.603
Ital Lunare	294.05	5060	227	4/8/08 4:25	1.986	4/9/2008 19:25	39:00 :00	1432.56	0.665	0.603
Hatsu Eagle	300.00	6332	227	4/10/08 4:05	6.010	4/12/2008 18:00	61:55 :00	1432.56	0.665	0.603
Ever Divine	294.13	4211	227	4/16/08 4:20	3.448	4/17/2008 4:35	24:15 :00	1432.56	0.665	0.603
Hatsu Excel	300.00	6332	227	4/19/08 15:05	2.576	4/21/2008 20:05	53:00 :00	1432.56	0.665	0.603
Ever Dynam ic	294.13	4211	227	4/22/08 4:55	4.420	4/23/2008 6:05	25:10 :00	1432.56	0.665	0.603
Ever Union	285.00	5652	227	4/26/08 15:00	2.503	4/28/2008 19:45	52:45 :00	1432.56	0.665	0.603
Ever Useful	285.00	5652	227	4/29/08 3:05	4.090	4/30/2008 20:45	41:40 :00	1432.56	0.665	0.603
Ever Deluxe	294.13	4211	227	5/3/08 5:15	1.490	5/3/2008 19:05	13:50 :00	1432.56	0.665	0.603
Ever Uranus	285.00	5652	227	5/4/08 17:00	2.510	5/6/2008 9:30	40:30 :00	1432.56	0.665	0.603
Hatsu Envoy	300.00	6332	227	5/7/08 5:15	2.958	5/9/2008 6:40	49:25 :00	1432.56	0.665	0.603
Ever Shine	300.00	7024	227	5/10/08 4:15	3.035	5/12/2008 5:20	49:05 :00	1432.56	0.665	0.603
Ever Delight	294.13	4211	227	5/13/08 5:05	1.955	5/14/2008 4:50	23:45 :00	1432.56	0.665	0.603
Hatsu Eagle	300.00	6332	227	5/15/08 4:00	4.524	5/17/2008 17:35	61:35 :00	1432.56	0.665	0.603
Ever Racer	294.13	4229	227	5/19/08 16:35	2.483	5/20/2008 19:15	26:40 :00	1432.56	0.665	0.603
Ever Safety	299.99	7124	227	5/22/08 4:10	3.410	5/24/2008 4:35	48:25 :00	1432.56	0.665	0.603
Ever Dynam ic	294.13	4211	227	5/25/08 14:00	2.434	5/26/2008 4:30	14:30 :00	1432.56	0.665	0.603
Ever Useful	285.00	5652	227	5/28/08 0:25	0.615	5/30/2008 5:30	53:05 :00	1432.56	0.665	0.603
Ever Result	294.13	4229	227	5/28/08 15:10	0.642	5/29/2008 7:50	16:40 :00	1432.56	0.665	0.603
Ever Union	285.00	5652	227	5/29/08 6:35	3.931	5/31/2008 17:30	58:55 :00	1432.56	0.665	0.603
Ever Divine	294.13	4211	227	6/2/08 4:55	1.698	6/3/2008 7:40	26:45 :00	1432.56	0.665	0.603
Ever Respect	294.13	4229	227	6/3/08 21:40	3.722	6/4/2008 19:00	21:20 :00	1432.56	0.665	0.603
Hatsu Envoy	300.00	6332	227	6/7/08 15:00	2.087	6/9/2008 18:05	51:05 :00	1432.56	0.665	0.603

Ever Decent	294.13	4211	227	6/9/08 17:05	0.997	6/10/2008 18:20	25:15 :00	1432.56	0.665	0.603
Ever Diamond	294.13	4211	227	6/10/08 17:00	1.517	6/11/2008 7:15	14:15 :00	1432.56	0.665	0.603
Ital Lunare	294.05	5060	227	6/12/08 5:25	8.944	6/14/2008 17:50	60:25 :00	1432.56	0.665	0.603
Hatsu Eagle	300.00	6332	227	6/21/08 4:05	3.042	6/23/2008 6:30	50:25 :00	1432.56	0.665	0.603
Ever Dainty	294.13	4211	227	6/24/08 5:05	1.962	6/25/2008 6:30	25:25 :00	1432.56	0.665	0.603
Ever Useful	285.00	5652	227	6/26/08 4:10	2.000	6/28/2008 4:45	48:35 :00	1432.56	0.665	0.603
Ever Safety	299.99	7124	227	6/28/08 4:10	4.545	6/30/2008 17:30	61:20 :00	1432.56	0.665	0.603
Ever Result	294.13	4229	227	7/2/08 17:15	0.493	7/3/2008 5:45	12:30 :00	1432.56	0.665	0.603
Ever Union	285.00	5652	227	7/3/08 5:05	5.177	7/5/2008 9:00	51:55 :00	1432.56	0.665	0.603
Ever Racer	294.13	4229	227	7/8/08 9:20	1.240	7/9/2008 6:15	20:55 :00	1432.56	0.665	0.603
Ever Decent	294.13	4211	227	7/9/08 15:05	1.028	7/10/2008 4:30	13:25 :00	1432.56	0.665	0.603
Ever Elite	300.00	6332	227	7/10/08 15:45	3.583	7/12/2008 20:05	52:20 :00	1432.56	0.665	0.603
Ever Shine	300.00	7024	227	7/14/08 5:45	2.979	7/16/2008 9:30	51:45 :00	1432.56	0.665	0.603
Ital Lunare	294.05	5060	227	7/17/08 5:15	3.413	7/19/2008 20:10	62:55 :00	1432.56	0.665	0.603
Ever Unific	285.00	5652	227	7/20/08 15:10	3.104	7/22/2008 16:30	49:20 :00	1432.56	0.665	0.603
Ever Develop	294.13	4211	227	7/23/08 17:40	0.889	7/24/2008 8:30	14:50 :00	1432.56	0.665	0.603
Ever Respect	294.13	4229	227	7/24/08 15:00	0.611	7/25/2008 6:15	15:15 :00	1432.56	0.665	0.603
Hatsu Eagle	300.00	6332	227	7/25/08 5:40	3.389	7/27/2008 19:40	62:00 :00	1432.56	0.665	0.603
Ever Dainty	294.13	4211	227	7/28/08 15:00	0.566	7/29/2008 4:40	13:40 :00	1432.56	0.665	0.603
Ever Diamond	294.13	4211	227	7/29/08 4:35	1.976	7/30/2008 6:30	25:55 :00	1432.56	0.665	0.603
Ever Useful	285.00	5652	227	7/31/08 4:00	7.059	8/2/2008 18:05	62:05 :00	1432.56	0.665	0.603
Ever Union	285.00	5652	227	8/7/08 5:25	7.399	8/9/2008 17:45	60:20 :00	1432.56	0.665	0.603
Ever Ursula	285.00	5652	227	8/14/08 15:00	3.406	8/17/2008 4:50	61:50 :00	1432.56	0.665	0.603
Ever Elite	300.00	6332	227	8/18/08 0:45	3.240	8/19/2008 20:45	44:00 :00	1432.56	0.665	0.603
Ital Lunare	294.05	5060	227	8/21/08 6:30	4.358	8/23/2008 19:05	60:35 :00	1432.56	0.665	0.603
Hatsu Eagle	300.00	6332	227	8/25/08 15:05	2.587	8/27/2008 18:35	51:30 :00	1432.56	0.665	0.603
Ever Urban	280.00	5652	227	8/28/08 5:10	3.399	8/30/2008 20:35		1432.56	0.665	0.603
Ever Diamond	294.13	4211	227	8/31/08 14:45				1432.56	0.665	0.603
Ital Lunare	294.05	5060	230	3/3/08 0:25	0.622	3/4/2008 5:35	29:10 :00	1432.56	0.665	0.603
Ever Dynamic	294.13	4211	230	3/3/08 15:20	2.531	3/4/2008 17:30	26:10 :00	1432.56	0.665	0.603

Hatsu Eagle	300.00	6332	230	3/6/08 4:05	2.462	3/8/2008 13:30	57:25 :00	1432.56	0.665	0.603
Ital Libera	294.10	5060	230	3/8/08 15:10	4.587	3/10/2008 9:45	42:35 :00	1432.56	0.665	0.603
Ever Safety	299.99	7124	230	3/13/08 5:15	2.497	3/15/2008 6:20	49:05 :00	1432.56	0.665	0.603
Ever Deluxe	294.13	4211	230	3/15/08 17:10	5.170	3/16/2008 18:10	25:00 :00	1432.56	0.665	0.603
Ever Ethic	300.00	6332	230	3/20/08 21:15	3.691	3/23/2008 4:45	55:30 :00	1432.56	0.665	0.603
Ever Delight	294.13	4211	230	3/24/08 13:50	1.625	3/25/2008 18:20	28:30 :00	1432.56	0.665	0.603
Ever Develop	294.13	4211	230	3/26/08 4:50	0.976	3/27/2008 5:25	24:35 :00	1432.56	0.665	0.603
Hatsu Envoy	300.00	6332	230	3/27/08 4:15	4.465	3/29/2008 18:15	62:00 :00	1432.56	0.665	0.603
Ever Diadem	294.13	4211	230	3/31/08 15:25	2.542	4/1/2008 18:30	27:05 :00	1432.56	0.665	0.603
Ever Shine	300.00	7024	230	4/3/08 4:25	2.538	4/5/2008 17:45	61:20 :00	1432.56	0.665	0.603
Ever Ursula	285.00	5652	230	4/5/08 17:20	2.455	4/7/2008 19:00	49:40 :00	1432.56	0.665	0.603
Ever Result	294.13	4229	230	4/8/08 4:15	1.108	4/9/2008 3:30	23:15 :00	1432.56	0.665	0.603
Ever Reward	294.13	4229	230	4/9/08 6:50	3.260	4/10/2008 5:20	22:30 :00	1432.56	0.665	0.603
Ever Uberty	285.00	5364	230	4/12/08 13:05	2.635	4/15/2008 0:30	59:25 :00	1432.56	0.665	0.603
Ever Urban	280.00	5652	230	4/15/08 4:20	1.993	4/17/2008 5:10	48:50 :00	1432.56	0.665	0.603
Ever Safety	299.99	7124	230	4/17/08 4:10	4.458	4/19/2008 17:30	61:20 :00	1432.56	0.665	0.603
Ever Decent	294.13	4211	230	4/21/08 15:10	2.528	4/22/2008 19:00	27:50 :00	1432.56	0.665	0.603
Ever Ethic	300.00	6332	230	4/24/08 3:50	2.559	4/26/2008 18:40	62:50 :00	1432.56	0.665	0.603
Trieste	270.00	3876	230	4/26/08 17:15	2.038	4/27/2008 20:00	26:45 :00	1432.56	0.665	0.603
Ever Develop	294.13	4211	230	4/28/08 18:10	2.413	4/29/2008 18:30	24:20 :00	1432.56	0.665	0.603
Ever Unicorn	285.00	5652	230	5/1/08 4:05	4.455	5/3/2008 18:35	62:30 :00	1432.56	0.665	0.603
Ever Dainty	294.13	4211	230	5/5/08 15:00	2.549	5/6/2008 18:30	27:30 :00	1432.56	0.665	0.603
Ever Ursula	285.00	5652	230	5/8/08 4:10	4.767	5/11/2008 2:55	70:45 :00	1432.56	0.665	0.603
Ever Reward	294.13	4229	230	5/12/08 22:35	1.111	5/13/2008 18:05	19:30 :00	1432.56	0.665	0.603
Ital Lunare	294.05	5060	230	5/14/08 1:15	3.201	5/15/2008 20:35	43:20 :00	1432.56	0.665	0.603
Ever Uberty	285.00	5364	230	5/17/08 6:05	2.733	5/19/2008 5:30	47:25 :00	1432.56	0.665	0.603
Ever Urban	280.00	5652	230	5/19/08 23:40	4.184	5/21/2008 9:40	34:00 :00	1432.56	0.665	0.603
Hatsu Excel	300.00	6332	230	5/24/08 4:05	7.490	5/26/2008 4:20	48:15 :00	1432.56	0.665	0.603
Ever Ethic	300.00	6332	230	5/31/08 15:50	4.514	6/2/2008 10:10	42:20 :00	1432.56	0.665	0.603
Ever Elite	300.00	6332	230	6/5/08 4:10	3.052	6/7/2008 18:10	62:00 :00	1432.56	0.665	0.603
Ever Uranus	285.00	5652	230	6/8/08 5:25	2.406	6/10/2008 9:10	51:45 :00	1432.56	0.665	0.603
Ever Shine	300.00	7024	230	6/10/08 15:10	3.670	6/12/2008 20:10	53:00 :00	1432.56	0.665	0.603

Ever Ursula	285.00	5652	230	6/14/08 7:15	2.264	6/16/2008 6:05	46:50 :00	1432.56	0.665	0.603
Ever Delight	294.13	4211	230	6/16/08 13:35	0.649	6/17/2008 5:30	15:55 :00	1432.56	0.665	0.603
Ever Develop	294.13	4211	230	6/17/08 5:10	1.969	6/18/2008 10:25	29:15 :00	1432.56	0.665	0.603
Ever Urban	280.00	5652	230	6/19/08 4:25	3.424	6/21/2008 18:25	62:00 :00	1432.56	0.665	0.603
Ever Uberty	285.00	5364	230	6/22/08 14:35	4.608	6/24/2008 10:15	43:40 :00	1432.56	0.665	0.603
Hatsu Excel	300.00	6332	230	6/27/08 5:10	2.007	6/29/2008 6:05	48:55 :00	1432.56	0.665	0.603
Ever Diadem	294.13	4211	230	6/29/08 5:20	2.181	6/29/2008 18:30	13:10 :00	1432.56	0.665	0.603
Ever Reward	294.13	4229	230	7/1/08 9:40	1.267	7/2/2008 5:45	20:05 :00	1432.56	0.665	0.603
Ever Ethic	300.00	6332	230	7/2/08 16:05	3.563	7/4/2008 18:15	50:10 :00	1432.56	0.665	0.603
Ever Unison	285.00	5652	230	7/6/08 5:35	2.813	7/8/2008 4:40	47:05 :00	1432.56	0.665	0.603
Hatsu Envoy	300.00	6332	230	7/9/08 1:05	7.167	7/11/2008 5:40	52:35 :00	1432.56	0.665	0.603
Ever Ursula	285.00	5652	230	7/16/08 5:05	2.382	7/18/2008 6:00	48:55 :00	1432.56	0.665	0.603
Sun Right	294.03	4229	230	7/18/08 14:15	5.413	7/19/2008 4:15	14:00 :00	1432.56	0.665	0.603
Ever Urban	280.00	5652	230	7/24/08 0:10	2.712	7/26/2008 17:55	65:45 :00	1432.56	0.665	0.603
Hatsu Excel	300.00	6332	230	7/26/08 17:15	3.306	7/29/2008 4:30	59:15 :00	1432.56	0.665	0.603
Ever Safety	299.99	7124	230	7/30/08 0:35	3.194	8/1/2008 4:00	51:25 :00	1432.56	0.665	0.603
Ever Ethic	300.00	6332	230	8/2/08 5:15	2.413	8/4/2008 5:45	48:30 :00	1432.56	0.665	0.603
Ever Reach	294.03	4229	230	8/4/08 15:10	0.576	8/5/2008 4:35	13:25 :00	1432.56	0.665	0.603
Ever Delight	294.13	4211	230	8/5/08 5:00	1.017	8/6/2008 6:25	25:25 :00	1432.56	0.665	0.603
Ever Unison	285.00	5652	230	8/6/08 5:25	3.406	8/8/2008 4:35	47:10 :00	1432.56	0.665	0.603
Hatsu Envoy	300.00	6332	230	8/9/08 15:10	1.993	8/11/2008 9:45	42:35 :00	1432.56	0.665	0.603
Ever Racer	294.13	4229	230	8/11/08 15:00	2.569	8/12/2008 7:20	16:20 :00	1432.56	0.665	0.603
Ever Diadem	294.13	4211	230	8/14/08 4:40	1.434	8/14/2008 19:20	14:40 :00	1432.56	0.665	0.603
Ever Shine	300.00	7024	230	8/15/08 15:05	3.563	8/17/2008 20:00	52:55 :00	1432.56	0.665	0.603
Ever Deluxe	294.13	4211	230	8/19/08 4:35	1.000	8/20/2008 5:35	25:00 :00	1432.56	0.665	0.603
Ever Unific	285.00	5652	230	8/20/08 4:35	3.542	8/22/2008 5:25	48:50 :00	1432.56	0.665	0.603
Sun Round	294.03	4229	230	8/23/08 17:35	1.892	8/24/2008 5:50	12:15 :00	1432.56	0.665	0.603
Ever Respect	294.13	4229	230	8/25/08 15:00	0.569	8/26/2008 5:15	14:15 :00	1432.56	0.665	0.603
Ever Decent	294.13	4211	230	8/26/08 4:40	1.028	8/27/2008 5:55	25:15 :00	1432.56	0.665	0.603
Hatsu Excel	300.00	6332	230	8/27/08 5:20	3.486	8/29/2008 20:40		1432.56	0.665	0.603
Ever Safety	299.99	7124	230	8/30/08 17:00				1432.56	0.665	0.603
APL Colima	166.15	1296	302	3/5/08 5:10	13.507	3/6/2008 1:25	20:15 :00	1219.2	0.67	0.746

APL Brazil	260.88	4132	302	3/18/08 17:20	1.497	3/19/2008 9:50	16:30 :00	1219.2	0.67	0.746
Horizon Enterprise	247.89	2139	302	3/20/08 5:15	4.375	3/21/2008 5:45	24:30 :00	1219.2	0.67	0.746
APL Korea	276.30	4832	302	3/24/08 14:15	7.031	3/26/2008 19:10	52:55 :00	1219.2	0.67	0.746
APL Thailand	276.30	4832	302	3/31/08 15:00	7.014	4/3/2008 10:15	67:15 :00	1219.2	0.67	0.746
APL Singapore	276.30	4832	302	4/7/08 15:20	28.563	4/9/2008 19:55	52:35 :00	1219.2	0.67	0.746
APL Jade	294.00	4392	302	5/6/08 4:50	15.576	5/6/2008 23:35	18:45 :00	1219.2	0.67	0.746
Ines	149.64	1012	302	5/21/08 18:40	5.618	5/22/2008 18:15	23:35 :00	1219.2	0.67	0.746
APL Arabia	293.99	4843	302	5/27/08 9:30	0.813	5/28/2008 4:25	18:55 :00	1219.2	0.67	0.746
APL Mendoza	128.86	831	302	5/28/08 5:00	8.372	5/29/2008 7:05	26:05 :00	1219.2	0.67	0.746
Ines	149.64	1012	302	6/5/08 13:55	6.635	6/6/2008 19:15	29:20 :00	1219.2	0.67	0.746
APL Mendoza	128.86	831	302	6/12/08 5:10	4.410	6/13/2008 3:20	22:10 :00	1219.2	0.67	0.746
APL Singapore	276.30	4832	302	6/16/08 15:00	7.694	6/18/2008 16:30	49:30 :00	1219.2	0.67	0.746
APL Turquoise	294.11	4369	302	6/24/08 7:40	1.931	6/25/2008 3:55	20:15 :00	1219.2	0.67	0.746
APL Philippines	276.30	4832	302	6/26/08 6:00	1.958	6/28/2008 5:45	47:45 :00	1219.2	0.67	0.746
APL Holland	277.26	5514	302	6/28/08 5:00	5.132	6/29/2008 19:40	38:40 :00	1219.2	0.67	0.746
Hyundai Integral	294.10	4922	302	7/3/08 8:10	1.104	7/5/2008 4:55	44:45 :00	1219.2	0.67	0.746
APL Costa Rica	292.15	4324	302	7/4/08 10:40	4.771	7/8/2008 23:20	108:4 0:00	1219.2	0.67	0.746
APL Holland	277.26	5514	302	7/9/08 5:10	3.000	7/10/2008 23:30	42:20 :00	1219.2	0.67	0.746
APL Belgium	277.00	5514	302	7/12/08 5:10	3.035	7/13/2008 17:40	36:30 :00	1219.2	0.67	0.746
APL Thailand	276.30	4832	302	7/15/08 6:00	3.969	7/17/2008 5:45	47:45 :00	1219.2	0.67	0.746
APL Canada	277.00	5762	302	7/19/08 5:15	7.000	7/20/2008 22:30	41:15 :00	1219.2	0.67	0.746
APL England	277.00	5514	302	7/26/08 5:15	3.010	7/28/2008 0:25	43:10 :00	1219.2	0.67	0.746
APL Jade	294.00	4392	302	7/29/08 5:30	0.990	7/30/2008 3:55	22:25 :00	1219.2	0.67	0.746
APL Canada	277.00	5762	302	7/30/08 5:15	7.024	7/31/2008 19:10	37:55 :00	1219.2	0.67	0.746
APL England	277.00	5514	302	8/6/08 5:50	4.427	8/7/2008 19:10	37:20 :00	1219.2	0.67	0.746
APL Holland	277.26	5514	302	8/10/08 16:05	2.545	8/12/2008 4:45	36:40 :00	1219.2	0.67	0.746
APL Scotland	277.26	5514	302	8/13/08 5:10	2.997	8/14/2008 18:05	36:55 :00	1219.2	0.67	0.746
APL Sweden	277.22	5762	302	8/16/08 5:05	2.997	8/17/2008 19:10	38:05 :00	1219.2	0.67	0.746

APL Arabia	293.99	4843	302	8/19/08 5:00	1.333	8/20/2008 5:25	24:25 :00	1219.2	0.67	0.746
Hyundai Voyager	294.12	4922	302	8/20/08 13:00	4.684	8/23/2008 4:30	63:30 :00	1219.2	0.67	0.746
APL Singapore	276.30	4832	302	8/25/08 5:25	4.986	8/27/2008 5:05	47:40 :00	1219.2	0.67	0.746
APL Canada	277.00	5762	302	8/30/08 5:05				1219.2	0.67	0.746
APL Sweden	277.22	5762	303	3/1/08 5:30	3.073	3/4/2008 2:20	68:50 :00	1219.2	0.67	0.746
APL Arabia	293.99	4843	303	3/4/08 7:15	3.920	3/4/2008 20:45	13:30 :00	1219.2	0.67	0.746
APL Belgium	277.00	5514	303	3/8/08 5:20	4.201	3/11/2008 5:55	72:35 :00	1219.2	0.67	0.746
APL Acajutla	132.59	660	303	3/12/08 10:10	2.795	3/13/2008 4:40	18:30 :00	1219.2	0.67	0.746
APL Canada	277.00	5762	303	3/15/08 5:15	3.743	3/18/2008 16:45	83:30 :00	1219.2	0.67	0.746
APL China	276.30	4832	303	3/18/08 23:05	3.250	3/21/2008 6:10	55:05 :00	1219.2	0.67	0.746
APL England	277.00	5514	303	3/22/08 5:05	3.191	3/25/2008 8:05	75:00 :00	1219.2	0.67	0.746
Hyundai Commo dore	275.00	4651	303	3/25/08 9:40	3.816	3/27/2008 17:30	55:50 :00	1219.2	0.67	0.746
APL Scotland	277.26	5514	303	3/29/08 5:15	3.340	4/1/2008 5:45	72:30 :00	1219.2	0.67	0.746
APL Turquoise	294.11	4369	303	4/1/08 13:25	3.660	4/2/2008 3:20	13:55 :00	1219.2	0.67	0.746
APL Holland	277.26	5514	303	4/5/08 5:15	4.000	4/8/2008 4:40	71:25 :00	1219.2	0.67	0.746
Hyundai Baron	275.10	4651	303	4/9/08 5:15	2.993	4/11/2008 16:30	59:15 :00	1219.2	0.67	0.746
APL Sweden	277.22	5762	303	4/12/08 5:05	3.288	4/15/2008 3:45	70:40 :00	1219.2	0.67	0.746
Hyundai Duke	275.00	4651	303	4/15/08 12:00	5.840	4/18/2008 6:00	66:00 :00	1219.2	0.67	0.746
Ines	149.64	1012	303	4/21/08 8:10	1.604	4/22/2008 19:15	35:05 :00	1219.2	0.67	0.746
APL China	276.30	4832	303	4/22/08 22:40	2.656	4/24/2008 19:15	44:35 :00	1219.2	0.67	0.746
APL Colima	166.15	1296	303	4/25/08 14:25	0.622	4/26/2008 3:55	13:30 :00	1219.2	0.67	0.746
APL Canada	277.00	5762	303	4/26/08 5:20	3.003	4/29/2008 4:45	71:25 :00	1219.2	0.67	0.746
APL Korea	276.30	4832	303	4/29/08 5:25	4.021	5/1/2008 5:05	47:40 :00	1219.2	0.67	0.746
APL England	277.00	5514	303	5/3/08 5:55	3.743	5/6/2008 6:00	72:05 :00	1219.2	0.67	0.746
Hyundai Baron	275.10	4651	303	5/6/08 23:45	3.219	5/9/2008 18:40	66:55 :00	1219.2	0.67	0.746
APL Scotland	277.26	5514	303	5/10/08 5:00	3.385	5/13/2008 5:35	72:35 :00	1219.2	0.67	0.746
APL Singapore	276.30	4832	303	5/13/08 14:15	3.618	5/15/2008 19:25	53:10 :00	1219.2	0.67	0.746
APL Holland	277.26	5514	303	5/17/08 5:05	3.406	5/20/2008 5:55	72:50 :00	1219.2	0.67	0.746
Hyundai Dynasty	294.12	4922	303	5/20/08 14:50	3.590	5/22/2008 19:45	52:55 :00	1219.2	0.67	0.746

APL Sweden	277.22	5762	303	5/24/08 5:00	3.424	5/27/2008 5:45	72:45 :00	1219.2	0.67	0.746
Hyundai Voyager	294.12	4922	303	5/27/08 15:10	3.569	5/30/2008 2:20	59:10 :00	1219.2	0.67	0.746
APL Belgium	277.00	5514	303	5/31/08 4:50	7.017	6/3/2008 5:20	72:30 :00	1219.2	0.67	0.746
APL Canada	277.00	5762	303	6/7/08 5:15	3.406	6/10/2008 5:10	71:55 :00	1219.2	0.67	0.746
Hyundai Goodwill	294.12	4922	303	6/10/08 15:00	3.597	6/13/2008 6:35	63:35 :00	1219.2	0.67	0.746
APL England	277.00	5514	303	6/14/08 5:20	3.097	6/17/2008 7:25	74:05 :00	1219.2	0.67	0.746
Hyundai Dynasty	294.12	4922	303	6/17/08 7:40	3.910	6/20/2008 3:55	68:15 :00	1219.2	0.67	0.746
APL Scotland	277.26	5514	303	6/21/08 5:30	5.514	6/24/2008 5:50	72:20 :00	1219.2	0.67	0.746
APL Mendoza	128.86	831	303	6/26/08 17:50	4.524	6/27/2008 17:55	24:05 :00	1219.2	0.67	0.746
APL China	276.30	4832	303	7/1/08 6:25	5.219	7/3/2008 6:05	47:40 :00	1219.2	0.67	0.746
Ines	149.64	1012	303	7/6/08 11:40	1.764	7/7/2008 13:50	26:10 :00	1219.2	0.67	0.746
APL Korea	276.30	4832	303	7/8/08 6:00	2.104	7/10/2008 6:15	48:15 :00	1219.2	0.67	0.746
APL Los Angeles	267.17	4250	303	7/10/08 8:30	4.861	7/13/2008 1:25	64:55 :00	1219.2	0.67	0.746
Hyundai Dynasty	294.12	4922	303	7/15/08 5:10	3.007	7/17/2008 19:25	62:15 :00	1219.2	0.67	0.746
APL Argentina	260.66	4038	303	7/18/08 5:20	2.785	7/20/2008 18:35	61:15 :00	1219.2	0.67	0.746
APL Singapore	276.30	4832	303	7/21/08 0:10	2.208	7/22/2008 16:00	39:50 :00	1219.2	0.67	0.746
APL Belgium	277.00	5514	303	7/23/08 5:10	3.198	7/24/2008 18:40	37:30 :00	1219.2	0.67	0.746
APL Spain	280.54	5888	303	7/26/08 9:55	3.889	7/29/2008 17:45	79:50 :00	1219.2	0.67	0.746
APL Philippines	276.30	4832	303	7/30/08 7:15	2.910	8/1/2008 3:50	44:35 :00	1219.2	0.67	0.746
APL Scotland	277.26	5514	303	8/2/08 5:05	2.014	8/3/2008 19:00	37:55 :00	1219.2	0.67	0.746
APL China	276.30	4832	303	8/4/08 5:25	4.410	8/6/2008 5:05	47:40 :00	1219.2	0.67	0.746
APL Denver	256.42	4250	303	8/8/08 15:15	2.701	8/11/2008 5:25	62:10 :00	1219.2	0.67	0.746
APL Korea	276.30	4832	303	8/11/08 8:05	2.889	8/13/2008 6:40	46:35 :00	1219.2	0.67	0.746
Hyundai Dynasty	294.12	4922	303	8/14/08 5:25	3.993	8/16/2008 2:35	45:10 :00	1219.2	0.67	0.746
APL Thailand	276.30	4832	303	8/18/08 5:15	4.222	8/20/2008 5:15	48:00 :00	1219.2	0.67	0.746
APL Ireland	279.70	5588	303	8/22/08 10:35	4.788	8/26/2008 2:35	88:00 :00	1219.2	0.67	0.746
APL Sweden	277.22	5762	303	8/27/08 5:30	2.767	8/28/2008 17:35		1219.2	0.67	0.746
APL Australia	282.10	4389	303	8/29/08 23:55				1219.2	0.67	0.746

APL Singapore	276.30	4832	304	3/3/08 19:00	2.924	3/5/2008 23:55	52:55 :00	1219.2	0.67	0.746
Hyundai Admiral	275.10	4651	304	3/6/08 17:10	3.896	3/8/2008 17:35	48:25 :00	1219.2	0.67	0.746
APL Philippines	276.30	4832	304	3/10/08 14:40	7.597	3/12/2008 19:15	52:35 :00	1219.2	0.67	0.746
Hyundai Duke	275.00	4651	304	3/18/08 5:00	7.149	3/20/2008 20:20	63:20 :00	1219.2	0.67	0.746
APL Malaysia	293.99	4843	304	3/25/08 8:35	4.639	3/26/2008 14:30	29:55 :00	1219.2	0.67	0.746
APL Colima	166.15	1296	304	3/29/08 23:55	7.212	3/30/2008 16:40	16:45 :00	1219.2	0.67	0.746
Ines	149.64	1012	304	4/6/08 5:00	1.073	4/7/2008 3:40	22:40 :00	1219.2	0.67	0.746
Hyundai Admiral	275.10	4651	304	4/7/08 6:45	4.667	4/9/2008 5:40	46:55 :00	1219.2	0.67	0.746
APL Colima	166.15	1296	304	4/11/08 22:45	2.694	4/12/2008 19:20	20:35 :00	1219.2	0.67	0.746
APL Philippines	276.30	4832	304	4/14/08 15:25	2.576	4/16/2008 18:40	51:15 :00	1219.2	0.67	0.746
APL Topaz	275.80	3502	304	4/17/08 5:15	1.997	4/19/2008 3:10	45:55 :00	1219.2	0.67	0.746
APL Belgium	277.00	5514	304	4/19/08 5:10	3.083	4/22/2008 5:55	72:45 :00	1219.2	0.67	0.746
APL Egypt	293.99	4843	304	4/22/08 7:10	2.347	4/23/2008 3:45	20:35 :00	1219.2	0.67	0.746
Hyundai Dynasty	294.12	4922	304	4/24/08 15:30	6.760	4/26/2008 19:30	52:00 :00	1219.2	0.67	0.746
Hyundai Voyager	294.12	4922	304	5/1/08 9:45	4.823	5/3/2008 10:15	48:30 :00	1219.2	0.67	0.746
APL Thailand	276.30	4832	304	5/6/08 5:30	5.653	5/8/2008 9:25	51:55 :00	1219.2	0.67	0.746
APL Colima	166.15	1296	304	5/11/08 21:10	2.434	5/12/2008 18:25	21:15 :00	1219.2	0.67	0.746
Hyundai Goodwill	294.12	4922	304	5/14/08 7:35	5.927	5/16/2008 18:05	58:30 :00	1219.2	0.67	0.746
APL Philippines	276.30	4832	304	5/20/08 5:50	6.385	5/22/2008 4:55	47:05 :00	1219.2	0.67	0.746
APL China	276.30	4832	304	5/26/08 15:05	7.007	5/28/2008 18:45	51:40 :00	1219.2	0.67	0.746
APL Korea	276.30	4832	304	6/2/08 15:15	3.118	6/4/2008 19:45	52:30 :00	1219.2	0.67	0.746
Hyundai Baron	275.10	4651	304	6/5/08 18:05	4.622	6/8/2008 6:20	60:15 :00	1219.2	0.67	0.746
APL Brazil	260.88	4132	304	6/10/08 9:00	0.854	6/11/2008 4:20	19:20 :00	1219.2	0.67	0.746
APL Thailand	276.30	4832	304	6/11/08 5:30	5.972	6/13/2008 5:55	48:25 :00	1219.2	0.67	0.746
APL Malaysia	293.99	4843	304	6/17/08 4:50	3.767	6/18/2008 9:10	28:20 :00	1219.2	0.67	0.746
Ines	149.64	1012	304	6/20/08 23:15	3.649	6/21/2008 22:45	23:30 :00	1219.2	0.67	0.746
Hyundai Voyager	294.12	4922	304	6/24/08 14:50	2.608	6/27/2008 4:45	61:55 :00	1219.2	0.67	0.746
APL Australia	282.10	4389	304	6/27/08 5:25	7.403	6/29/2008 17:15	59:50 :00	1219.2	0.67	0.746
APL Sweden	277.22	5762	304	7/4/08 15:05	3.997	7/7/2008 6:00	62:55 :00	1219.2	0.67	0.746

Hyundai Goodwill	294.12	4922	304	7/8/08 15:00	6.569	7/11/2008 5:10	62:10 :00	1219.2	0.67	0.746
APL Egypt	293.99	4843	304	7/15/08 4:40	1.021	7/16/2008 4:10	23:30 :00	1219.2	0.67	0.746
APL Sweden	277.22	5762	304	7/16/08 5:10	6.021	7/18/2008 4:15	47:05 :00	1219.2	0.67	0.746
Hyundai Voyager	294.12	4922	304	7/22/08 5:40	6.979	7/24/2008 17:35	59:55 :00	1219.2	0.67	0.746
Hyundai Integral	294.10	4922	304	7/29/08 5:10	4.458	7/31/2008 18:20	61:10 :00	1219.2	0.67	0.746
APL General	274.66	5551	304	8/2/08 16:10	2.958	8/5/2008 4:45	60:35 :00	1219.2	0.67	0.746
Hyundai Goodwill	294.12	4922	304	8/5/08 15:10	11.049	8/7/2008 18:40	51:30 :00	1219.2	0.67	0.746
APL India	277.00	5762	304	8/16/08 16:20	3.910	8/19/2008 13:00	68:40 :00	1219.2	0.67	0.746
APL Holland	277.26	5514	304	8/20/08 14:10	3.271	8/21/2008 19:15	29:05 :00	1219.2	0.67	0.746
APL Belgium	277.00	5514	304	8/23/08 20:40	3.972	8/25/2008 5:40	33:00 :00	1219.2	0.67	0.746
Hyundai Integral	294.10	4922	304	8/27/08 20:00		8/30/2008 9:45		1219.2	0.67	0.746
APL Colima	166.15	1296	305	3/19/08 17:00	47.816	3/20/2008 19:35	26:35 :00	1219.2	0.67	0.746
Ines	149.64	1012	305	5/6/08 12:35		5/7/2008 18:05	29:30 :00	1219.2	0.67	0.746
Maersk Dallas	294.10	5026	401	3/1/08 5:00	2.010	3/1/2008 20:00	15:00 :00	2191.51 2	1.108	0.863
Maersk Florence	134.44	868	401	3/3/08 5:15	3.000	3/3/2008 20:30	15:15 :00	2191.51 2	1.108	0.863
Majestic Maersk	294.12	4640	401	3/6/08 5:15	4.205	3/7/2008 3:50	22:35 :00	2191.51 2	1.108	0.863
Maersk Fremantle	134.44	868	401	3/10/08 10:10	2.503	3/11/2008 2:20	16:10 :00	2191.51 2	1.108	0.863
Maersk Danbury	294.10	4900	401	3/12/08 22:15	4.361	3/13/2008 18:40	20:25 :00	2191.51 2	1.108	0.863
Maersk Fortaleza	134.44	868	401	3/17/08 6:55	2.924	3/17/2008 22:30	15:35 :00	2191.51 2	1.108	0.863
Maersk Dolores	294.15	5042	401	3/20/08 5:05	4.003	3/20/2008 22:35	17:30 :00	2191.51 2	1.108	0.863
Maersk Florence	134.44	868	401	3/24/08 5:10	6.997	3/25/2008 0:55	19:45 :00	2191.51 2	1.108	0.863
Maersk Fremantle	134.44	868	401	3/31/08 5:05	3.000	3/31/2008 18:30	13:25 :00	2191.51 2	1.108	0.863
Maersk MESSOLONGI	294.12	4640	401	4/3/08 5:05	3.958	4/3/2008 19:40	14:35 :00	2191.51 2	1.108	0.863
Maersk Fortaleza	134.44	868	401	4/7/08 4:05	3.042	4/7/2008 18:40	14:35 :00	2191.51 2	1.108	0.863
Marie Maersk	294.12	4640	401	4/10/08 5:05	4.017	4/11/2008 5:15	24:10 :00	2191.51 2	1.108	0.863
Maersk Florence	134.44	868	401	4/14/08 5:30	2.997	4/14/2008 18:40	13:10 :00	2191.51 2	1.108	0.863
Maersk Dhaka	294.10	5060	401	4/17/08 5:25	3.983	4/18/2008 3:50	22:25 :00	2191.51 2	1.108	0.863
Maersk Fremantle	134.44	868	401	4/21/08 5:00	3.007	4/21/2008 18:00	13:00 :00	2191.51 2	1.108	0.863

Maersk Mykonos	294.11	4640	401	4/24/08 5:10	1.410	4/25/2008 4:05	22:55 :00	2191.51 2	1.108	0.863
Sofie Maersk	346.98	8680	401	4/25/08 15:00	5.295	4/27/2008 17:50	50:50 :00	2191.51 2	1.108	0.863
Maersk Fortaleza	134.44	868	401	4/30/08 22:05	7.108	5/2/2008 5:55	31:50 :00	2191.51 2	1.108	0.863
Anna Maersk	352.00	9310	401	5/8/08 0:40	3.986	5/10/2008 10:30	57:50 :00	2191.51 2	1.108	0.863
Sealand Comet	292.15	4065	401	5/12/08 0:20	4.622	5/14/2008 16:30	64:10 :00	2191.51 2	1.108	0.863
Soroe Maersk	346.98	8680	401	5/16/08 15:15	1.094	5/18/2008 19:00	51:45 :00	2191.51 2	1.108	0.863
Helsinki Express	259.01	3322	401	5/17/08 17:30	5.917	5/18/2008 18:00	24:30 :00	2191.51 2	1.108	0.863
Charlotte Maersk	346.98	8890	401	5/23/08 15:30	6.993	5/25/2008 17:55	50:25 :00	2191.51 2	1.108	0.863
Svendborg Maersk	346.98	8680	401	5/30/08 15:20	6.965	6/1/2008 16:00	48:40 :00	2191.51 2	1.108	0.863
Sally Maersk	346.98	8680	401	6/6/08 14:30	7.000	6/9/2008 4:40	62:10 :00	2191.51 2	1.108	0.863
Clifford Maersk	346.98	8680	401	6/13/08 14:30	2.642	6/15/2008 17:05	50:35 :00	2191.51 2	1.108	0.863
Maersk Florence	134.44	868	401	6/16/08 5:55	11.378	6/16/2008 18:10	12:15 :00	2191.51 2	1.108	0.863
Svend Maersk	346.98	8680	401	6/27/08 15:00	6.889	6/30/2008 4:25	61:25 :00	2191.51 2	1.108	0.863
Caroline Maersk	346.98	8660	401	7/4/08 12:20	7.111	7/7/2008 20:25	80:05 :00	2191.51 2	1.108	0.863
Susan Maersk	347.00	8680	401	7/11/08 15:00	4.684	7/14/2008 5:15	62:15 :00	2191.51 2	1.108	0.863
NYK Nebula	294.00	4882	401	7/16/08 7:25	2.476	7/17/2008 19:00	35:35 :00	2191.51 2	1.108	0.863
Cornelia Maersk	346.98	8890	401	7/18/08 18:50	0.844	7/21/2008 5:50	59:00 :00	2191.51 2	1.108	0.863
London Express	294.04	4616	401	7/19/08 15:05	6.000	7/20/2008 18:10	27:05 :00	2191.51 2	1.108	0.863
Sofie Maersk	346.98	8680	401	7/25/08 15:05	7.007	7/28/2008 6:30	63:25 :00	2191.51 2	1.108	0.863
Skagen Maersk	346.98	8680	401	8/1/08 15:15	2.524	8/4/2008 4:20	61:05 :00	2191.51 2	1.108	0.863
Maersk Fremantle	134.44	868	401	8/4/08 3:50	1.469	8/4/2008 18:45	14:55 :00	2191.51 2	1.108	0.863
Kiel Express	294.00	4639	401	8/5/08 15:05	3.024	8/6/2008 22:40	31:35 :00	2191.51 2	1.108	0.863
Anna Maersk	352.00	9310	401	8/8/08 15:40	2.587	8/11/2008 5:40	62:00 :00	2191.51 2	1.108	0.863
Sealand Meteor	292.15	4000	401	8/11/08 5:45	4.396	8/13/2008 6:05	48:20 :00	2191.51 2	1.108	0.863
Soroe Maersk	346.98	8680	401	8/15/08 15:15	2.549	8/18/2008 4:20	61:05 :00	2191.51 2	1.108	0.863
Maersk Florence	134.44	868	401	8/18/08 4:25	3.035	8/18/2008 19:10	14:45 :00	2191.51 2	1.108	0.863
Majestic Maersk	294.12	4640	401	8/21/08 5:15	1.590	8/22/2008 3:30	22:15 :00	2191.51 2	1.108	0.863
Charlotte Maersk	346.98	8890	401	8/22/08 19:25	5.413	8/25/2008 2:00	54:35 :00	2191.51 2	1.108	0.863
Maersk Danbury	294.10	4900	401	8/28/08 5:20	1.406	8/28/2008 18:45		2191.51 2	1.108	0.863

Svendborg Maersk	346.98	8680	401	8/29/08 15:05				2191.51 2	1.108	0.863
Grasmere Maersk	292.08	4338	402	3/4/08 5:15	10.417	3/5/2008 3:45	22:30 :00	2191.51 2	1.108	0.863
Clifford Maersk	346.98	8680	402	3/14/08 15:15	9.010	3/16/2008 19:00	51:45 :00	2191.51 2	1.108	0.863
Carsten Maersk	346.98	8660	402	3/23/08 15:30	3.646	3/25/2008 18:30	51:00 :00	2191.51 2	1.108	0.863
Glasgow Maersk	292.06	4338	402	3/27/08 7:00	1.333	3/28/2008 12:45	29:45 :00	2191.51 2	1.108	0.863
Svend Maersk	346.98	8680	402	3/28/08 15:00	9.003	3/30/2008 18:10	51:10 :00	2191.51 2	1.108	0.863
Caroline Maersk	346.98	8660	402	4/6/08 15:05	11.997	4/8/2008 20:20	53:15 :00	2191.51 2	1.108	0.863
Cornelia Maersk	346.98	8890	402	4/18/08 15:00	9.601	4/20/2008 19:05	52:05 :00	2191.51 2	1.108	0.863
Sealand Meteor	292.15	4000	402	4/28/08 5:25	6.948	4/29/2008 19:00	37:35 :00	2191.51 2	1.108	0.863
Sealand Lightning	292.15	4062	402	5/5/08 4:10	4.462	5/6/2008 17:45	37:35 :00	2191.51 2	1.108	0.863
Maersk Saigon	332.00	8402	402	5/9/08 15:15	5.583	5/12/2008 12:40	69:25 :00	2191.51 2	1.108	0.863
Dirch Maersk	292.12	4324	402	5/15/08 5:15	4.003	5/16/2008 3:50	22:35 :00	2191.51 2	1.108	0.863
Sealand Intrepid	292.15	4062	402	5/19/08 5:20	6.997	5/20/2008 17:50	36:30 :00	2191.51 2	1.108	0.863
Sealand Charger	292.15	4065	402	5/26/08 5:15	7.010	5/27/2008 18:30	37:15 :00	2191.51 2	1.108	0.863
Sealand Meteor	292.15	4000	402	6/2/08 5:30	6.993	6/3/2008 17:50	36:20 :00	2191.51 2	1.108	0.863
Sealand Lightning	292.15	4062	402	6/9/08 5:20	2.990	6/10/2008 18:40	37:20 :00	2191.51 2	1.108	0.863
Maersk Dolores	294.15	5042	402	6/12/08 5:05	4.010	6/13/2008 6:05	25:00 :00	2191.51 2	1.108	0.863
Sealand Comet	292.15	4065	402	6/16/08 5:20	4.382	6/18/2008 6:00	48:40 :00	2191.51 2	1.108	0.863
Carsten Maersk	346.98	8660	402	6/20/08 14:30	2.656	6/23/2008 6:05	63:35 :00	2191.51 2	1.108	0.863
Sealand Intrepid	292.15	4062	402	6/23/08 6:15	3.451	6/24/2008 18:55	36:40 :00	2191.51 2	1.108	0.863
Santiago Express	206.00	2182	402	6/26/08 17:05	6.378	6/27/2008 19:50	26:45 :00	2191.51 2	1.108	0.863
Marie Maersk	294.12	4640	402	7/3/08 2:10	1.441	7/4/2008 6:05	27:55 :00	2191.51 2	1.108	0.863
Oakland Express	294.06	4890	402	7/4/08 12:45	2.698	7/6/2008 19:40	54:55 :00	2191.51 2	1.108	0.863
Sealand Meteor	292.15	4000	402	7/7/08 5:30	4.052	7/8/2008 17:30	36:00 :00	2191.51 2	1.108	0.863
Iwaki	193.03	1613	402	7/11/08 6:45	2.941	7/12/2008 5:45	23:00 :00	2191.51 2	1.108	0.863
Sealand Lightning	292.15	4062	402	7/14/08 5:20	2.003	7/16/2008 4:55	47:35 :00	2191.51 2	1.108	0.863
Maersk Kokura	318.24	7908	402	7/16/08 5:25	4.983	7/19/2008 4:45	71:20 :00	2191.51 2	1.108	0.863
Sealand Comet	292.15	4065	402	7/21/08 5:00	3.010	7/22/2008 18:05	37:05 :00	2191.51 2	1.108	0.863
Maersk Gironde	292.08	4824	402	7/24/08 5:15	2.406	7/25/2008 18:40	37:25 :00	2191.51 2	1.108	0.863

Tokyo Express	294.17	4864	402	7/26/08 15:00	1.545	7/28/2008 4:45	37:45 :00	2191.51 2	1.108	0.863
Maersk Florence	134.44	868	402	7/28/08 4:05	3.038	7/29/2008 1:50	21:45 :00	2191.51 2	1.108	0.863
Maersk Moncton	294.11	4640	402	7/31/08 5:00	4.014	8/1/2008 3:45	22:45 :00	2191.51 2	1.108	0.863
Sealand Charger	292.15	4065	402	8/4/08 5:20	3.000	8/5/2008 19:50	38:30 :00	2191.51 2	1.108	0.863
Dirch Maersk	292.12	4324	402	8/7/08 5:20	2.420	8/8/2008 6:05	24:45 :00	2191.51 2	1.108	0.863
Leverku sen Express	294.01	4639	402	8/9/08 15:25	1.458	8/10/2008 17:35	26:10 :00	2191.51 2	1.108	0.863
Maersk Fortaleza	134.44	868	402	8/11/08 2:25	3.115	8/11/2008 22:30	20:05 :00	2191.51 2	1.108	0.863
Maersk Dallas	294.10	5026	402	8/14/08 5:10	2.410	8/15/2008 2:25	21:15 :00	2191.51 2	1.108	0.863
Albert Maersk	346.00	9310	402	8/16/08 15:00	5.597	8/19/2008 19:05	76:05 :00	2191.51 2	1.108	0.863
Maersk Klaipeda	299.90	6802	402	8/22/08 5:20	2.944	8/25/2008 2:20	69:00 :00	2191.51 2	1.108	0.863
Maersk Fremantle	134.44	868	402	8/25/08 4:00	2.049	8/25/2008 18:40	14:40 :00	2191.51 2	1.108	0.863
Maersk Karlskrona	318.24	7908	402	8/27/08 5:10	4.410	8/30/2008 6:15		2191.51 2	1.108	0.863
Seoul Express	294.17	4864	402	8/31/08 15:00				2191.51 2	1.108	0.863
Maersk Kyrenia	299.90	6802	403	3/5/08 5:00	7.014	3/7/2008 18:25	61:25 :00	2191.51 2	1.108	0.863
Knud Maersk	318.24	7908	403	3/12/08 5:20	6.997	3/14/2008 19:55	62:35 :00	2191.51 2	1.108	0.863
Maersk Kimi	299.90	6674	403	3/19/08 5:15	4.955	3/21/2008 18:20	61:05 :00	2191.51 2	1.108	0.863
Karen Maersk	318.24	7908	403	3/24/08 4:10	9.028	3/26/2008 19:45	63:35 :00	2191.51 2	1.108	0.863
Maersk Klaipeda	299.90	6802	403	4/2/08 4:50	5.028	4/4/2008 18:45	61:55 :00	2191.51 2	1.108	0.863
Kate Maersk	318.24	7908	403	4/7/08 5:30	8.997	4/9/2008 19:35	62:05 :00	2191.51 2	1.108	0.863
Maersk Karachi	299.90	6674	403	4/16/08 5:25	6.986	4/18/2008 18:05	60:40 :00	2191.51 2	1.108	0.863
Maersk Kure	138.24	7908	403	4/23/08 5:05	7.184	4/25/2008 18:50	61:45 :00	2191.51 2	1.108	0.863
Maersk Kalmar	299.90	6674	403	4/30/08 9:30	6.816	5/2/2008 19:50	58:20 :00	2191.51 2	1.108	0.863
Maersk Kokura	318.24	7908	403	5/7/08 5:05	7.010	5/9/2008 17:50	60:45 :00	2191.51 2	1.108	0.863
Maersk Kyrenia	299.90	6802	403	5/14/08 5:20	7.000	5/16/2008 19:30	62:10 :00	2191.51 2	1.108	0.863
Maersk Kotka	318.24	6477	403	5/21/08 5:20	7.000	5/23/2008 5:00	47:40 :00	2191.51 2	1.108	0.863
Maersk Kampala	299.99	6802	403	5/28/08 5:20	6.990	5/30/2008 4:50	47:30 :00	2191.51 2	1.108	0.863
Maersk Kawasaki	318.24	7908	403	6/4/08 5:05	7.000	6/6/2008 17:35	60:30 :00	2191.51 2	1.108	0.863
Maersk Klaipeda	299.90	6802	403	6/11/08 5:05	7.000	6/13/2008 20:15	63:10 :00	2191.51 2	1.108	0.863

Maersk Karlskrona	318.24	7908	403	6/18/08 5:05	7.132	6/20/2008 6:35	49:30 :00	2191.51 2	1.108	0.863
Maersk Kimi	299.90	6674	403	6/25/08 8:15	4.285	6/27/2008 5:40	45:25 :00	2191.51 2	1.108	0.863
Sealand Charger	292.15	4065	403	6/29/08 15:05	2.583	6/30/2008 18:55	27:50 :00	2191.51 2	1.108	0.863
CMA CGM Orfeo	350.00	9661	403	7/2/08 5:05	4.059	7/5/2008 9:05	76:00 :00	2191.51 2	1.108	0.863
Ipanema	193.03	1613	403	7/6/08 6:30	2.965	7/7/2008 18:45	36:15 :00	2191.51 2	1.108	0.863
Maersk Kalmar	299.90	6674	403	7/9/08 5:40	3.389	7/11/2008 17:15	59:35 :00	2191.51 2	1.108	0.863
Albert Maersk	346.00	9310	403	7/12/08 15:00	10.583	7/16/2008 18:00	99:00 :00	2191.51 2	1.108	0.863
Maersk Kyrenia	299.90	6802	403	7/23/08 5:00	3.497	7/25/2008 19:50	62:50 :00	2191.51 2	1.108	0.863
Ikoma	193.03	1631	403	7/26/08 16:55	1.514	7/27/2008 9:40	16:45 :00	2191.51 2	1.108	0.863
Sealand Intrepid	292.15	4062	403	7/28/08 5:15	6.281	7/30/2008 4:00	46:45 :00	2191.51 2	1.108	0.863
Izumo	193.03	1613	403	8/3/08 12:00	1.517	8/4/2008 2:45	14:45 :00	2191.51 2	1.108	0.863
Maersk Kotka	318.24	6477	403	8/5/08 0:25	4.632	8/8/2008 12:00	83:35 :00	2191.51 2	1.108	0.863
Columbine Maersk	346.98	8890	403	8/9/08 15:35	3.573	8/12/2008 20:10	76:35 :00	2191.51 2	1.108	0.863
Maersk Kawasaki	318.24	7908	403	8/13/08 5:20	4.090	8/15/2008 19:15	61:55 :00	2191.51 2	1.108	0.863
Imari	193.03	1613	403	8/17/08 7:30	4.924	8/18/2008 1:00	17:30 :00	2191.51 2	1.108	0.863
E.R. Cape Town	184.70	1728	403	8/22/08 5:40	2.986	8/22/2008 17:45	12:05 :00	2191.51 2	1.108	0.863
Sealand Comet	292.15	4065	403	8/25/08 5:20	6.028	8/27/2008 10:50	53:30 :00	2191.51 2	1.108	0.863
Ikaruga	193.03	1613	403	8/31/08 6:00		8/31/2008 16:50		2191.51 2	1.108	0.863
Maersk Bentonville	294.10	4300	404	3/2/08 15:00	7.007	3/4/2008 17:25	50:25 :00	2191.51 2	1.108	0.863
Maersk Baltimore	294.10	4300	404	3/9/08 15:10	7.545	3/11/2008 14:35	47:25 :00	2191.51 2	1.108	0.863
Maersk Boston	294.10	4300	404	3/17/08 4:15	13.458	3/18/2008 19:35	39:20 :00	2191.51 2	1.108	0.863
Maersk Buffalo	294.10	4300	404	3/30/08 15:15	12.111	4/1/2008 18:25	51:10 :00	2191.51 2	1.108	0.863
Susan Maersk	347.00	8680	404	4/11/08 17:55	1.885	4/13/2008 19:20	49:25 :00	2191.51 2	1.108	0.863
Maersk Baltimore	294.10	4300	404	4/13/08 15:10	7.014	4/15/2008 16:50	49:40 :00	2191.51 2	1.108	0.863
Maersk Boston	294.10	4300	404	4/20/08 15:30	2.524	4/22/2008 17:40	50:10 :00	2191.51 2	1.108	0.863
Sealand Charger	292.15	4065	404	4/23/08 4:05	5.007	4/24/2008 22:10	42:05 :00	2191.51 2	1.108	0.863
Columbine Maersk	346.98	8890	404	4/28/08 4:15	3.052	4/30/2008 18:10	61:55 :00	2191.51 2	1.108	0.863
Maersk Gironde	292.08	4824	404	5/1/08 5:30	3.406	5/2/2008 5:30	24:00 :00	2191.51 2	1.108	0.863

Albert Maersk	346.00	9310	404	5/4/08 15:15	3.573	5/7/2008 0:15	57:00 :00	2191.51 2	1.108	0.863
Maersk Mandra ki	294.11	4640	404	5/8/08 5:00	5.292	5/9/2008 4:30	23:30 :00	2191.51 2	1.108	0.863
Clementine Maersk	346.98	8890	404	5/13/08 12:00	5.125	5/16/2008 19:20	79:20 :00	2191.51 2	1.108	0.863
Cornelius Maersk	346.98	8660	404	5/18/08 15:00	3.590	5/21/2008 18:50	75:50 :00	2191.51 2	1.108	0.863
Maersk Dallas	294.10	5026	404	5/22/08 5:10	3.479	5/23/2008 3:10	22:00 :00	2191.51 2	1.108	0.863
CMA CGM Orfeo	350.00	9661	404	5/25/08 16:40	3.514	5/28/2008 20:00	75:20 :00	2191.51 2	1.108	0.863
Majestic Maersk	294.12	4640	404	5/29/08 5:00	2.424	5/30/2008 4:10	23:10 :00	2191.51 2	1.108	0.863
Columbine Maersk	346.98	8890	404	5/31/08 15:10	4.587	6/3/2008 19:15	76:05 :00	2191.51 2	1.108	0.863
Maersk Danbury	294.10	4900	404	6/5/08 5:15	5.000	6/6/2008 4:40	23:25 :00	2191.51 2	1.108	0.863
Albert Maersk	346.00	9310	404	6/10/08 5:15	5.010	6/13/2008 5:40	72:25 :00	2191.51 2	1.108	0.863
Sovereign Maersk	346.98	8680	404	6/15/08 5:30	4.066	6/18/2008 7:05	73:35 :00	2191.51 2	1.108	0.863
Glasgow Maersk	292.06	4338	404	6/19/08 7:05	6.924	6/20/2008 6:00	22:55 :00	2191.51 2	1.108	0.863
Maersk Messologi	294.12	4640	404	6/26/08 5:15	1.104	6/26/2008 19:30	14:15 :00	2191.51 2	1.108	0.863
Cornelius Maersk	346.98	8660	404	6/27/08 7:45	4.903	6/30/2008 5:30	69:45 :00	2191.51 2	1.108	0.863
Maersk Kure	318.24	7908	404	7/2/08 5:25	4.014	7/4/2008 10:40	53:15 :00	2191.51 2	1.108	0.863
Columbine Maersk	346.98	8890	404	7/6/08 5:45	3.976	7/9/2008 19:50	86:05 :00	2191.51 2	1.108	0.863
Maersk Dhaka	294.10	5060	404	7/10/08 5:10	1.250	7/10/2008 18:40	13:30 :00	2191.51 2	1.108	0.863
Lisbon Express	216.13	2400	404	7/11/08 11:10	2.705	7/12/2008 19:40	32:30 :00	2191.51 2	1.108	0.863
Maersk Fremantle	134.44	868	404	7/14/08 4:05	3.094	7/15/2008 0:25	20:20 :00	2191.51 2	1.108	0.863
Maersk Darmstadt	294.10	4944	404	7/17/08 6:20	2.625	7/18/2008 4:00	21:40 :00	2191.51 2	1.108	0.863
Izu	193.03	1631	404	7/19/08 21:20	1.642	7/21/2008 1:25	28:05 :00	2191.51 2	1.108	0.863
Maersk Fortaleza	134.44	868	404	7/21/08 12:45	4.326	7/22/2008 4:35	15:50 :00	2191.51 2	1.108	0.863
Milan Express	216.21	2808	404	7/25/08 20:35	1.358	7/26/2008 18:35	22:00 :00	2191.51 2	1.108	0.863
Sovereign Maersk	346.98	8680	404	7/27/08 5:10	6.010	7/30/2008 19:20	86:10 :00	2191.51 2	1.108	0.863
Cornelius Maersk	346.98	8660	404	8/2/08 5:25	4.115	8/5/2008 19:55	86:30 :00	2191.51 2	1.108	0.863

CMA CGM Force	339.62	8750	404	8/6/08 8:10	4.670	8/9/2008 19:30	83:20 :00	2191.51 2	1.108	0.863
Maersk Kampala	299.99	6802	404	8/11/08 0:15	4.632	8/14/2008 5:50	77:35 :00	2191.51 2	1.108	0.863
Kobe Express	293.94	4616	404	8/15/08 15:25	2.580	8/16/2008 17:45	26:20 :00	2191.51 2	1.108	0.863
Sealand Lightning	292.15	4062	404	8/18/08 5:20	5.413	8/19/2008 18:15	36:55 :00	2191.51 2	1.108	0.863
Paris Express	294.00	4639	404	8/23/08 15:15	2.729	8/24/2008 18:30	27:15 :00	2191.51 2	1.108	0.863
Maersk Seville	335.00	8452	404	8/26/08 8:45	4.854	8/29/2008 19:25	82:40 :00	2191.51 2	1.108	0.863
Sovereign Maersk	346.98	8680	404	8/31/08 5:15				2191.51 2	1.108	0.863
Horizon Spirit	272.30	665	405	3/6/08 5:55	2.392	3/8/2008 5:15	47:20 :00	2191.51 2	1.108	0.863
Sealand Intrepid	292.15	4062	405	3/8/08 15:20	6.990	3/10/2008 6:40	39:20 :00	2191.51 2	1.108	0.863
Sealand Charger	292.15	4065	405	3/15/08 15:05	4.622	3/17/2008 6:15	39:10 :00	2191.51 2	1.108	0.863
Horizon Spirit	272.30	665	405	3/20/08 6:00	2.257	3/22/2008 4:35	46:35 :00	2191.51 2	1.108	0.863
Sealand Meteor	292.15	4000	405	3/22/08 12:10	9.722	3/24/2008 6:30	42:20 :00	2191.51 2	1.108	0.863
Sealand Lightning	292.15	4062	405	4/1/08 5:30	2.031	4/2/2008 17:50	36:20 :00	2191.51 2	1.108	0.863
Horizon Spirit	272.30	665	405	4/3/08 6:15	2.382	4/5/2008 4:10	45:55 :00	2191.51 2	1.108	0.863
Sealand Comet	292.15	4065	405	4/5/08 15:25	4.590	4/7/2008 3:45	36:20 :00	2191.51 2	1.108	0.863
Horizon Reliance	272.30	665	405	4/10/08 5:35	2.406	4/12/2008 4:35	47:00 :00	2191.51 2	1.108	0.863
Sealand Intrepid	292.15	4062	405	4/12/08 15:20	4.608	4/14/2008 6:45	39:25 :00	2191.51 2	1.108	0.863
Horizon Spirit	272.30	665	405	4/17/08 5:55	6.997	4/19/2008 4:55	47:00 :00	2191.51 2	1.108	0.863
Horizon Reliance	272.30	665	405	4/24/08 5:50	7.135	4/26/2008 4:25	46:35 :00	2191.51 2	1.108	0.863
Horizon Spirit	272.30	665	405	5/1/08 9:05	6.844	5/3/2008 4:30	43:25 :00	2191.51 2	1.108	0.863
Horizon Reliance	272.30	665	405	5/8/08 5:20	7.024	5/10/2008 4:35	47:15 :00	2191.51 2	1.108	0.863
Horizon Spirit	272.30	665	405	5/15/08 5:55	6.983	5/17/2008 5:00	47:05 :00	2191.51 2	1.108	0.863
Horizon Reliance	272.30	665	405	5/22/08 5:30	3.375	5/24/2008 4:40	47:10 :00	2191.51 2	1.108	0.863
Valencia Express	216.13	2400	405	5/25/08 14:30	3.625	5/26/2008 18:35	28:05 :00	2191.51 2	1.108	0.863
Horizon Spirit	272.30	665	405	5/29/08 5:30	7.007	5/31/2008 4:55	47:25 :00	2191.51 2	1.108	0.863
Horizon Reliance	272.30	665	405	6/5/08 5:40	2.997	6/7/2008 4:45	47:05 :00	2191.51 2	1.108	0.863
Humboldt Express	206.00	2181	405	6/8/08 5:35	11.087	6/9/2008 3:10	21:35 :00	2191.51 2	1.108	0.863
Horizon Reliance	272.30	665	405	6/19/08 7:40	3.865	6/21/2008 5:05	45:25 :00	2191.51 2	1.108	0.863
Maersk Fremantle	134.44	868	405	6/23/08 4:25	3.059	6/23/2008 20:05	15:40 :00	2191.51 2	1.108	0.863

Horizon Spirit	272.30	665	405	6/26/08 5:50	7.007	6/28/2008 4:40	46:50 :00	2191.51 2	1.108	0.863
Horizon Reliance	272.30	665	405	7/3/08 6:00	2.542	7/5/2008 5:35	47:35 :00	2191.51 2	1.108	0.863
Ikoma	193.03	1631	405	7/5/08 19:00	4.444	7/6/2008 19:30	24:30 :00	2191.51 2	1.108	0.863
Horizon Spirit	272.30	665	405	7/10/08 5:40	2.594	7/12/2008 6:00	48:20 :00	2191.51 2	1.108	0.863
Izumo	193.03	1613	405	7/12/08 19:55	4.465	7/13/2008 19:10	23:15 :00	2191.51 2	1.108	0.863
Horizon Reliance	272.30	665	405	7/17/08 7:05	3.031	7/19/2008 4:30	45:25 :00	2191.51 2	1.108	0.863
IGA	193.03	1613	405	7/20/08 7:50	3.910	7/20/2008 19:10	11:20 :00	2191.51 2	1.108	0.863
Horizon Spirit	272.30	665	405	7/24/08 5:40	2.566	7/26/2008 4:40	47:00 :00	2191.51 2	1.108	0.863
Imari	193.03	1613	405	7/26/08 19:15	4.444	7/27/2008 6:30	11:15 :00	2191.51 2	1.108	0.863
Horizon Reliance	272.30	665	405	7/31/08 5:55	2.434	8/2/2008 4:30	46:35 :00	2191.51 2	1.108	0.863
E.R. Cape Town	184.70	1728	405	8/2/08 16:20	3.323	8/3/2008 5:00	12:40 :00	2191.51 2	1.108	0.863
Valencia Express	216.13	2400	405	8/6/08 0:05	1.236	8/7/2008 5:05	29:00 :00	2191.51 2	1.108	0.863
Horizon Spirit	272.30	665	405	8/7/08 5:45	2.087	8/9/2008 5:05	47:20 :00	2191.51 2	1.108	0.863
IGA	193.03	1613	405	8/9/08 7:50	1.264	8/10/2008 5:30	21:40 :00	2191.51 2	1.108	0.863
Ikaruga	193.03	1613	405	8/10/08 14:10	3.663	8/11/2008 1:55	11:45 :00	2191.51 2	1.108	0.863
Horizon Reliance	272.30	665	405	8/14/08 6:05	4.330	8/16/2008 4:30	46:25 :00	2191.51 2	1.108	0.863
Ipanema	193.03	1613	405	8/18/08 14:00	2.656	8/19/2008 4:15	14:15 :00	2191.51 2	1.108	0.863
Horizon Spirit	272.30	665	405	8/21/08 5:45	2.014	8/23/2008 4:50	47:05 :00	2191.51 2	1.108	0.863
Iwaki	193.03	1613	405	8/23/08 6:05	4.990	8/23/2008 16:55	10:50 :00	2191.51 2	1.108	0.863
Horizon Reliance	272.30	665	405	8/28/08 5:50	1.965	8/30/2008 4:45		2191.51 2	1.108	0.863
Humboldt Express	206.00	2181	405	8/30/08 5:00	1.451	8/31/2008 7:00		2191.51 2	1.108	0.863
Izu	193.03	1631	405	8/31/08 15:50				2191.51 2	1.108	0.863
Lisbon Express	216.13	2400	406	4/30/08 15:10	4.576	5/1/2008 8:30	17:20 :00	2191.51 2	1.108	0.863
Maersk Florence	134.44	868	406	5/5/08 5:00	6.990	5/5/2008 17:15	12:15 :00	2191.51 2	1.108	0.863
Maersk Fremantle	134.44	868	406	5/12/08 4:45	8.399	5/12/2008 17:15	12:30 :00	2191.51 2	1.108	0.863
Maersk Fortaleza	134.44	868	406	5/20/08 14:20	5.583	5/21/2008 5:15	14:55 :00	2191.51 2	1.108	0.863
Maersk Florence	134.44	868	406	5/26/08 4:20	6.986	5/26/2008 19:05	14:45 :00	2191.51 2	1.108	0.863
Maersk Fremantle	134.44	868	406	6/2/08 4:00	6.997	6/2/2008 18:15	14:15 :00	2191.51 2	1.108	0.863
Maersk Fortaleza	134.44	868	406	6/9/08 3:55	21.014	6/9/2008 17:30	13:35 :00	2191.51 2	1.108	0.863

Maersk Fortalez a	134.44	868	406	6/30/08 4:15	7.444	6/30/2008 19:35	15:20 :00	2191.51 2	1.108	0.863
Maersk Florence	134.44	868	406	7/7/08 14:55		7/8/2008 4:55	14:00 :00	2191.51 2	1.108	0.863
Zim Piraeus	294.10	5042	A92	3/12/08 13:40	2.958	3/13/2008 20:15	30:35 :00	1097.28	0.476	0.633
Valencia Express	216.13	2400	A92	3/15/08 12:40	3.135	3/16/2008 19:25	30:45 :00	1097.28	0.476	0.633
Zim Mediterranean	294.10	4839	A92	3/18/08 15:55	4.628	3/19/2008 17:40	25:45 :00	1097.28	0.476	0.633
MSC Debra	294.10	5060	A92	3/23/08 7:00	2.358	3/24/2008 10:55	27:55 :00	1097.28	0.476	0.633
Zim California	294.00	4839	A92	3/25/08 15:35	18.323	3/26/2008 18:45	27:10 :00	1097.28	0.476	0.633
Santiago Express	206.00	2182	A92	4/12/08 23:20	7.198	4/14/2008 5:00	29:40 :00	1097.28	0.476	0.633
Milan Express	216.21	2808	A92	4/20/08 4:05	18.167	4/21/2008 5:00	24:55 :00	1097.28	0.476	0.633
MSC Valencia	334.07	7928	A92	5/8/08 8:05	4.528	5/11/2008 8:30	72:25 :00	1097.28	0.476	0.633
MSC Ornella	294.05	5048	A92	5/12/08 20:45	17.122	5/14/2008 16:25	43:40 :00	1097.28	0.476	0.633
MSC Tanzania	294.10	4545	A92	5/29/08 23:40	3.122	5/31/2008 19:30	43:50 :00	1097.28	0.476	0.633
MSC Fabienne	294.00	5050	A92	6/2/08 2:35	4.462	6/3/2008 5:00	26:25 :00	1097.28	0.476	0.633
MSC Debra	294.10	5060	A92	6/6/08 13:40	11.625	6/7/2008 20:25	30:45 :00	1097.28	0.476	0.633
Zim Piraeus	294.10	5042	A92	6/18/08 4:40	15.066	6/19/2008 8:30	27:50 :00	1097.28	0.476	0.633
MSC Lucy	324.85	8089	A92	7/3/08 6:15	5.760	7/6/2008 18:55	84:40 :00	1097.28	0.476	0.633
MSC Emma	294.05	5048	A92	7/9/08 0:30	6.188	7/10/2008 5:00	28:30 :00	1097.28	0.476	0.633
MSC Ornella	294.05	5048	A92	7/15/08 5:00	31.167	7/17/2008 4:25	47:25 :00	1097.28	0.476	0.633
MSC Debra	294.10	5060	A92	8/15/08 9:00	11.219	8/16/2008 19:50	34:50 :00	1097.28	0.476	0.633
Zim Haifa	294.10	5026	A92	8/26/08 14:15	2.726	8/28/2008 19:00	52:45 :00	1097.28	0.476	0.633
MSC Poh Lin	294.17	5050	A92	8/29/08 7:40		8/31/2008 5:05		1097.28	0.476	0.633
MSC Fabienne	294.00	5050	A94	3/11/08 20:55	1.344	3/13/2008 5:05	32:10 :00	1097.28	0.476	0.633
MSC Tamara	265.00	4250	A94	3/13/08 5:10	9.917	3/15/2008 6:30	49:20 :00	1097.28	0.476	0.633
MSC Carolina	274.67	5919	A94	3/23/08 3:10	4.128	3/25/2008 20:55	65:45 :00	1097.28	0.476	0.633
MSC Kenya	294.10	4545	A94	3/27/08 6:15	5.392	3/27/2008 18:25	12:10 :00	1097.28	0.476	0.633
Zim Beijing	294.15	5026	A94	4/1/08 15:40	4.733	4/2/2008 17:25	25:45 :00	1097.28	0.476	0.633
MSC Fiammetta	277.30	5762	A94	4/6/08 9:15	2.299	4/8/2008 16:40	55:25 :00	1097.28	0.476	0.633
Zim New York	294.10	4839	A94	4/8/08 16:25	1.319	4/9/2008 19:30	27:05 :00	1097.28	0.476	0.633

MSC Poh Lin	294.17	5050	A94	4/10/08 0:05	12.510	4/11/2008 3:55	27:50 :00	1097.28	0.476	0.633
MSC Lisa	294.10	5048	A94	4/22/08 12:20	1.865	4/23/2008 19:50	31:30 :00	1097.28	0.476	0.633
MSC Lucy	324.85	8089	A94	4/24/08 9:05	1.549	4/26/2008 19:20	58:15 :00	1097.28	0.476	0.633
MSC Kyoto	269.78	3876	A94	4/25/08 22:15	4.264	4/27/2008 19:15	45:00 :00	1097.28	0.476	0.633
Zim Shanghai	294.12	4839	A94	4/30/08 4:35	1.184	5/1/2008 5:00	24:25 :00	1097.28	0.476	0.633
MSC Busan	324.80	8089	A94	5/1/08 9:00	5.278	5/4/2008 6:30	69:30 :00	1097.28	0.476	0.633
Zim Panama	294.00	4839	A94	5/6/08 15:40	13.972	5/7/2008 20:00	28:20 :00	1097.28	0.476	0.633
Zim Haifa	294.10	5026	A94	5/20/08 15:00	7.021	5/21/2008 19:00	28:00 :00	1097.28	0.476	0.633
Zim Virginia	294.00	4839	A94	5/27/08 15:30	7.628	5/28/2008 18:55	27:25 :00	1097.28	0.476	0.633
Zim Shenzhen	294.10	4839	A94	6/4/08 6:35	6.385	6/5/2008 4:50	22:15 :00	1097.28	0.476	0.633
Zim Qingdao	260.62	4253	A94	6/10/08 15:50	6.889	6/11/2008 16:45	24:55 :00	1097.28	0.476	0.633
MSC Poh Lin	294.17	5050	A94	6/17/08 13:10	14.111	6/18/2008 19:15	30:05 :00	1097.28	0.476	0.633
Zim California	294.00	4839	A94	7/1/08 15:50	13.990	7/2/2008 20:30	28:40 :00	1097.28	0.476	0.633
Zim New York	294.10	4839	A94	7/15/08 15:35	1.594	7/16/2008 20:30	28:55 :00	1097.28	0.476	0.633
MSC Charleston	324.80	8089	A94	7/17/08 5:50	5.413	7/20/2008 5:10	71:20 :00	1097.28	0.476	0.633
Zim Pusan	294.10	4839	A94	7/22/08 15:45	7.535	7/23/2008 17:35	25:50 :00	1097.28	0.476	0.633
Zim Barcelona	294.12	5042	A94	7/30/08 4:35	1.080	7/31/2008 4:30	23:55 :00	1097.28	0.476	0.633
MSC Tanzania	294.10	4545	A94	7/31/08 6:30	5.656	8/1/2008 18:50	36:20 :00	1097.28	0.476	0.633
MSC Fabienné	294.00	5050	A94	8/5/08 22:15	6.656	8/7/2008 4:05	29:50 :00	1097.28	0.476	0.633
Zim Panama	294.00	4839	A94	8/12/08 14:00	7.000	8/13/2008 19:00	29:00 :00	1097.28	0.476	0.633
Zim Savannah	294.10	5026	A94	8/19/08 14:00	7.639	8/20/2008 18:00	28:00 :00	1097.28	0.476	0.633
CMA CGM Hugo	334.08	8328	A94	8/27/08 5:20		8/30/2008 7:00		1097.28	0.476	0.633
MSC Ela	294.10	5048	A96	3/1/08 18:20	3.438	3/3/2008 5:00	34:40 :00	1097.28	0.476	0.633
Zim Qingdao	260.62	4253	A96	3/5/08 4:50	2.031	3/6/2008 1:50	21:00 :00	1097.28	0.476	0.633
Helsinki Express	259.01	3322	A96	3/7/08 5:35	4.003	3/8/2008 6:15	24:40 :00	1097.28	0.476	0.633
MSC Toronto	324.80	8089	A96	3/11/08 5:40	6.396	3/14/2008 5:15	71:35 :00	1097.28	0.476	0.633
MSC Kyoto	269.78	3876	A96	3/17/08 15:10	6.628	3/19/2008 5:20	38:10 :00	1097.28	0.476	0.633

MSC Texas	334.07	8238	A96	3/24/08 6:15	6.378	3/27/2008 5:50	71:35 :00	1097.28	0.476	0.633
Humboldt Express	206.00	2181	A96	3/30/08 15:20	1.951	3/31/2008 18:50	27:30 :00	1097.28	0.476	0.633
MSC Alyssa	273.70	4340	A96	4/1/08 14:10	6.778	4/3/2008 17:50	51:40 :00	1097.28	0.476	0.633
CMA CGM Hugo	334.08	8328	A96	4/8/08 8:50	5.017	4/12/2008 7:25	94:35 :00	1097.28	0.476	0.633
MSC Malta	276.20	5527	A96	4/13/08 9:15	6.830	4/15/2008 18:15	57:00 :00	1097.28	0.476	0.633
Zim Pusan	294.10	4839	A96	4/20/08 5:10	2.010	4/21/2008 3:50	22:40 :00	1097.28	0.476	0.633
Zim Barcelona	294.12	5042	A96	4/22/08 5:25	7.983	4/23/2008 2:55	21:30 :00	1097.28	0.476	0.633
MSC Texas	334.07	8238	A96	4/30/08 5:00	3.951	5/3/2008 19:00	86:00 :00	1097.28	0.476	0.633
MSC Emma	294.05	5048	A96	5/4/08 3:50	2.097	5/5/2008 4:45	24:55 :00	1097.28	0.476	0.633
Pacific Link	334.00	8238	A96	5/6/08 6:10	7.389	5/8/2008 19:25	61:15 :00	1097.28	0.476	0.633
Zim Savannah	294.10	5026	A96	5/13/08 15:30	3.736	5/14/2008 20:10	28:40 :00	1097.28	0.476	0.633
MSC Ela	294.10	5048	A96	5/17/08 9:10	1.934	5/18/2008 17:05	31:55 :00	1097.28	0.476	0.633
MSC Toronto	324.80	8089	A96	5/19/08 7:35	2.497	5/21/2008 19:40	60:05 :00	1097.28	0.476	0.633
MSC Beijing	324.80	8089	A96	5/21/08 19:30	7.660	5/24/2008 20:15	72:45 :00	1097.28	0.476	0.633
MSC Lucy	324.85	8089	A96	5/29/08 11:20	3.750	6/1/2008 5:00	65:40 :00	1097.28	0.476	0.633
MSC Texas	334.07	8238	A96	6/2/08 5:20	3.167	6/5/2008 8:40	75:20 :00	1097.28	0.476	0.633
MSC Busan	324.80	8089	A96	6/5/08 9:20	5.660	6/8/2008 5:05	67:45 :00	1097.28	0.476	0.633
MSC Kenya	294.10	4545	A96	6/11/08 1:10	1.715	6/12/2008 5:00	27:50 :00	1097.28	0.476	0.633
MSC Charleston	324.80	8089	A96	6/12/08 18:20	4.427	6/15/2008 5:45	59:25 :00	1097.28	0.476	0.633
CMA CGM Hugo	334.08	8328	A96	6/17/08 4:35	5.990	6/20/2008 8:55	76:20 :00	1097.28	0.476	0.633
MSC Lisa	294.10	5048	A96	6/23/08 4:20	1.476	6/24/2008 5:10	24:50 :00	1097.28	0.476	0.633
Zim Mediterranean	294.10	4839	A96	6/24/08 15:45	2.639	6/25/2008 20:45	29:00 :00	1097.28	0.476	0.633
MSC Beijing	324.80	8089	A96	6/27/08 7:05	3.875	6/29/2008 22:00	62:55 :00	1097.28	0.476	0.633
CMA CGM Vivaldi	334.06	8238	A96	7/1/08 4:05	3.924	7/4/2008 10:35	78:30 :00	1097.28	0.476	0.633
MSC Donata	257.87	4132	A96	7/5/08 2:15	3.538	7/7/2008 5:00	50:45 :00	1097.28	0.476	0.633
Zim Beijing	294.15	5026	A96	7/8/08 15:10	1.580	7/9/2008 19:35	28:25 :00	1097.28	0.476	0.633
MSC Busan	324.80	8089	A96	7/10/08 5:05	4.372	7/13/2008 7:10	74:05 :00	1097.28	0.476	0.633
Pacific Link	334.00	8238	A96	7/14/08 14:00	8.601	7/17/2008 19:30	77:30 :00	1097.28	0.476	0.633

MSC Ela	294.10	5048	A96	7/23/08 4:25	6.028	7/24/2008 6:00	25:35 :00	1097.28	0.476	0.633
MSC Toronto	324.80	8089	A96	7/29/08 5:05	3.174	8/1/2008 8:20	75:15 :00	1097.28	0.476	0.633
MSC Beijing	324.80	8089	A96	8/1/08 9:15	4.267	8/4/2008 5:25	68:10 :00	1097.28	0.476	0.633
Zim Shanghai	294.12	4839	A96	8/5/08 15:40	1.625	8/6/2008 16:45	25:05 :00	1097.28	0.476	0.633
MSC Lucy	324.85	8089	A96	8/7/08 6:40	3.941	8/9/2008 18:55	60:15 :00	1097.28	0.476	0.633
MSC Texas	334.07	8238	A96	8/11/08 5:15	3.010	8/13/2008 18:35	61:20 :00	1097.28	0.476	0.633
MSC Busan	324.80	8089	A96	8/14/08 5:30	4.594	8/16/2008 19:00	61:30 :00	1097.28	0.476	0.633
MSC Kenya	294.10	4545	A96	8/18/08 19:45	2.399	8/19/2008 19:25	23:40 :00	1097.28	0.476	0.633
MSC Charleston	324.80	8089	A96	8/21/08 5:20	6.139	8/23/2008 19:00	61:40 :00	1097.28	0.476	0.633
CMA CGM Courage	339.62	8600	A96	8/27/08 8:40				1097.28	0.476	0.633
Manukai	217.00	2890	C62	3/2/08 7:45	5.135	3/5/2008 13:55	78:10 :00	548.64	0.216	0.412
Mahima hi	262.14	3027	C62	3/7/08 11:00	1.816	3/8/2008 12:40	25:40 :00	548.64	0.216	0.412
Manulan i	217.00	2890	C62	3/9/08 6:35	7.059	3/12/2008 14:00	79:25 :00	548.64	0.216	0.412
Maunaw ili	217.00	2890	C62	3/16/08 8:00	5.063	3/19/2008 14:00	78:00 :00	548.64	0.216	0.412
Mahima hi	262.14	3027	C62	3/21/08 9:30	1.854	3/22/2008 12:55	27:25 :00	548.64	0.216	0.412
Maunale i	207.60	2890	C62	3/23/08 6:00	7.010	3/26/2008 13:00	79:00 :00	548.64	0.216	0.412
R.J. Pfeiffer	217.48	1970	C62	3/30/08 6:15	3.365	4/2/2008 14:00	79:45 :00	548.64	0.216	0.412
Mahima hi	262.14	3027	C62	4/2/08 15:00	3.615	4/5/2008 4:25	61:25 :00	548.64	0.216	0.412
Manukai	217.00	2890	C62	4/6/08 5:45	7.031	4/9/2008 14:25	80:40 :00	548.64	0.216	0.412
Manulan i	217.00	2890	C62	4/13/08 6:30	5.115	4/16/2008 14:00	79:30 :00	548.64	0.216	0.412
Mahima hi	262.14	3027	C62	4/18/08 9:15	3.451	4/19/2008 12:20	27:05 :00	548.64	0.216	0.412
Maunaw ili	217.00	2890	C62	4/21/08 20:05	5.931	4/23/2008 14:00	41:55 :00	548.64	0.216	0.412
Maunale i	207.60	2890	C62	4/27/08 18:25	4.455	4/30/2008 13:25	67:00 :00	548.64	0.216	0.412
Mahima hi	262.14	3027	C62	5/2/08 5:20	2.000	5/3/2008 12:20	31:00 :00	548.64	0.216	0.412
R.J. Pfeiffer	217.48	1970	C62	5/4/08 5:20	7.188	5/7/2008 13:10	79:50 :00	548.64	0.216	0.412
Manukai	217.00	2890	C62	5/11/08 9:50	4.955	5/14/2008 14:15	76:25 :00	548.64	0.216	0.412
Mahima hi	262.14	3027	C62	5/16/08 8:45	1.934	5/17/2008 12:45	28:00 :00	548.64	0.216	0.412
Manulan i	217.00	2890	C62	5/18/08 7:10	7.076	5/21/2008 13:55	78:45 :00	548.64	0.216	0.412
Maunaw ili	217.00	2890	C62	5/25/08 9:00	4.979	5/28/2008 13:50	76:50 :00	548.64	0.216	0.412
Mahima hi	262.14	3027	C62	5/30/08 8:30	1.885	5/31/2008 12:20	27:50 :00	548.64	0.216	0.412
Maunale i	207.60	2890	C62	6/1/08 5:45	6.986	6/4/2008 14:00	80:15 :00	548.64	0.216	0.412

R.J. Pfeiffer	217.48	1970	C62	6/8/08 5:25	5.149	6/11/2008 15:30	82:05 :00	548.64	0.216	0.412
Mahima hi	262.14	3027	C62	6/13/08 9:00	1.868	6/14/2008 12:00	27:00 :00	548.64	0.216	0.412
Manukai Manulani	217.00	2890	C62	6/15/08 5:50	6.979	6/18/2008 14:30	80:40 :00	548.64	0.216	0.412
Mahima hi	217.00	2890	C62	6/22/08 5:20	5.149	6/25/2008 14:30	81:10 :00	548.64	0.216	0.412
Maunawili	262.14	3027	C62	6/27/08 8:55	2.132	6/28/2008 13:05	28:10 :00	548.64	0.216	0.412
Mokihana	217.00	2890	C62	6/29/08 12:05	4.944	7/2/2008 13:40	73:35 :00	548.64	0.216	0.412
Maunalei	262.14	3027	C62	7/4/08 10:45	1.802	7/5/2008 6:30	19:45 :00	548.64	0.216	0.412
Mahima hi	207.60	2890	C62	7/6/08 6:00	5.115	7/9/2008 5:05	71:05 :00	548.64	0.216	0.412
R.J. Pfeiffer	262.14	3027	C62	7/11/08 8:45	1.858	7/12/2008 18:05	33:20 :00	548.64	0.216	0.412
Manukai Mahima hi	217.48	1970	C62	7/13/08 5:20	7.010	7/16/2008 5:05	71:45 :00	548.64	0.216	0.412
Manulani	217.00	2890	C62	7/20/08 5:35	5.167	7/23/2008 5:10	71:35 :00	548.64	0.216	0.412
Maunawili	262.14	3027	C62	7/25/08 9:35	1.819	7/26/2008 17:45	32:10 :00	548.64	0.216	0.412
Mahima hi	217.00	2890	C62	7/27/08 5:15	7.000	7/30/2008 4:55	71:40 :00	548.64	0.216	0.412
Maunalei	217.00	2890	C62	8/3/08 5:15	5.149	8/6/2008 5:15	72:00 :00	548.64	0.216	0.412
R.J. Pfeiffer	262.14	3027	C62	8/8/08 8:50	3.274	8/9/2008 17:00	32:10 :00	548.64	0.216	0.412
Mahima hi	207.60	2890	C62	8/11/08 15:25	5.583	8/13/2008 5:15	37:50 :00	548.64	0.216	0.412
Manoa	217.48	1970	C62	8/17/08 5:25	5.066	8/20/2008 5:05	71:40 :00	548.64	0.216	0.412
Manulani	262.14	3027	C62	8/22/08 7:00	1.931	8/23/2008 10:40	27:40 :00	548.64	0.216	0.412
Hyundai Highness	262.14	3027	C62	8/24/08 5:20	7.003	8/27/2008 5:35	72:15 :00	548.64	0.216	0.412
Hyundai Discovery	217.00	2890	C62	8/31/08 5:25				548.64	0.216	0.412
Hyundai Independence	274.65	5551	E26	2/29/08 5:15	14.014	3/3/2008 17:10	83:55 :00	640.08	0.135	0.342
Hyundai Confidence	274.60	5551	E26	3/14/08 5:35	7.976	3/17/2008 17:30	83:55 :00	640.08	0.135	0.342
Hyundai Freedom	274.60	5550	E26	3/22/08 5:00	6.010	3/25/2008 8:10	75:10 :00	640.08	0.135	0.342
Hyundai Highness	274.67	5680	E26	3/28/08 5:15	6.997	3/31/2008 18:00	84:45 :00	640.08	0.135	0.342
Hyundai Independence	274.65	5551	E26	4/4/08 5:10	7.003	4/7/2008 18:55	85:45 :00	640.08	0.135	0.342
Hyundai Discovery	274.66	5551	E26	4/11/08 5:15	6.990	4/14/2008 16:35	83:20 :00	640.08	0.135	0.342
Hyundai Independence	274.60	5551	E26	4/18/08 5:00	7.003	4/21/2008 17:50	84:50 :00	640.08	0.135	0.342
Hyundai Independence	274.60	5550	E26	4/25/08 5:05	7.021	4/28/2008 16:30	83:25 :00	640.08	0.135	0.342

Hyundai Confidence	274.67	5680	E26	5/2/08 5:35	7.003	5/5/2008 17:35	84:00 :00	640.08	0.135	0.342
Hyundai Highness	274.65	5551	E26	5/9/08 5:40	6.986	5/12/2008 19:40	86:00 :00	640.08	0.135	0.342
Hyundai Freedom	274.66	5551	E26	5/16/08 5:20	6.993	5/19/2008 18:50	85:30 :00	640.08	0.135	0.342
Hyundai Discovery	274.60	5551	E26	5/23/08 5:10	6.510	5/26/2008 17:40	84:30 :00	640.08	0.135	0.342
Hyundai Independence	274.60	5550	E26	5/29/08 17:25	7.497	6/2/2008 4:50	83:25 :00	640.08	0.135	0.342
Hyundai Confidence	274.67	5680	E26	6/6/08 5:20	6.403	6/9/2008 3:45	70:25 :00	640.08	0.135	0.342
Hyundai Highness	274.65	5551	E26	6/12/08 15:00	7.000	6/16/2008 3:40	84:40 :00	640.08	0.135	0.342
Hyundai Freedom	274.66	5551	E26	6/19/08 15:00	7.323	6/23/2008 2:40	83:40 :00	640.08	0.135	0.342
Hyundai Discovery	274.60	5551	E26	6/26/08 22:45	6.694	6/30/2008 17:05	90:20 :00	640.08	0.135	0.342
Hyundai Independence	274.60	5550	E26	7/3/08 15:25	6.990	7/7/2008 19:45	100:2 0:00	640.08	0.135	0.342
Hyundai Confidence	274.67	5680	E26	7/10/08 15:10	7.580	7/14/2008 4:00	84:50 :00	640.08	0.135	0.342
Hyundai Highness	274.65	5551	E26	7/18/08 5:05	6.424	7/21/2008 4:45	71:40 :00	640.08	0.135	0.342
Hyundai Freedom	274.66	5551	E26	7/24/08 15:15	6.990	7/28/2008 4:50	85:35 :00	640.08	0.135	0.342
Hyundai Discovery	274.60	5551	E26	7/31/08 15:00	7.063	8/4/2008 5:00	86:00 :00	640.08	0.135	0.342
Hyundai Independence	274.60	5550	E26	8/7/08 16:30	7.535	8/11/2008 1:25	80:55 :00	640.08	0.135	0.342
Hyundai Confidence	274.67	5680	E26	8/15/08 5:20	6.997	8/18/2008 5:25	72:05 :00	640.08	0.135	0.342
Hyundai Highness	274.65	5551	E26	8/22/08 5:15	7.003	8/25/2008 2:35	69:20 :00	640.08	0.135	0.342
Hyundai Freedom	274.66	5551	E26	8/29/08 5:20				640.08	0.135	0.342
NYK Kai	288.31	3808	F8	3/1/08 18:00	5.917	3/5/2008 3:20	81:20 :00	838.2	0.141	0.347
OOCL Ningbo	323.00	8063	F8	3/7/08 16:00	6.979	3/12/2008 5:45	109:4 5:00	838.2	0.141	0.347
OOCL Hamburg	322.97	8063	F8	3/14/08 15:30	7.007	3/19/2008 4:20	108:5 0:00	838.2	0.141	0.347
OOCL Tianjin	322.97	8063	F8	3/21/08 15:40	7.014	3/26/2008 4:30	108:5 0:00	838.2	0.141	0.347

OOCL Long Beach	322.97	8063	F8	3/28/08 16:00	6.983	4/2/2008 5:40	109:4 0:00	838.2	0.141	0.347
OOCL Rotterdam	323.00	8063	F8	4/4/08 15:35	7.986	4/9/2008 4:45	109:1 0:00	838.2	0.141	0.347
OOCL Ningbo	323.00	8063	F8	4/12/08 15:15	6.024	4/16/2008 5:30	86:15 :00	838.2	0.141	0.347
OOCL Hamburg	322.97	8063	F8	4/18/08 15:50	7.000	4/23/2008 3:50	108:0 0:00	838.2	0.141	0.347
OOCL Tianjin	322.97	8063	F8	4/25/08 15:50	7.580	4/30/2008 3:15	107:2 5:00	838.2	0.141	0.347
OOCL Long Beach	322.97	8063	F8	5/3/08 5:45	6.417	5/7/2008 4:55	95:10 :00	838.2	0.141	0.347
OOCL Rotterdam	323.00	8063	F8	5/9/08 15:45	6.986	5/14/2008 5:10	109:2 5:00	838.2	0.141	0.347
OOCL Ningbo	323.00	8063	F8	5/16/08 15:25	7.003	5/21/2008 3:45	108:2 0:00	838.2	0.141	0.347
OOCL Hamburg	322.97	8063	F8	5/23/08 15:30	7.003	5/28/2008 2:00	106:3 0:00	838.2	0.141	0.347
OOCL Tianjin	322.97	8063	F8	5/30/08 15:35	7.003	6/4/2008 5:10	109:3 5:00	838.2	0.141	0.347
OOCL Long Beach	322.97	8063	F8	6/6/08 15:40	7.003	6/11/2008 4:10	108:3 0:00	838.2	0.141	0.347
OOCL Rotterdam	323.00	8063	F8	6/13/08 15:45	7.003	6/18/2008 2:00	106:1 5:00	838.2	0.141	0.347
OOCL Ningbo	323.00	8063	F8	6/20/08 15:50	7.007	6/25/2008 4:35	108:4 5:00	838.2	0.141	0.347
OOCL Hamburg	322.97	8063	F8	6/27/08 16:00	6.986	7/2/2008 4:20	108:2 0:00	838.2	0.141	0.347
OOCL Tianjin	322.97	8063	F8	7/4/08 15:40	7.014	7/9/2008 5:35	109:5 5:00	838.2	0.141	0.347
OOCL Asia	322.90	8063	F8	7/11/08 16:00	6.986	7/16/2008 3:50	107:5 0:00	838.2	0.141	0.347
OOCL Rotterdam	323.00	8063	F8	7/18/08 15:40	6.997	7/23/2008 4:45	109:0 5:00	838.2	0.141	0.347
OOCL Ningbo	323.00	8063	F8	7/25/08 15:35	7.007	7/30/2008 4:20	108:4 5:00	838.2	0.141	0.347
OOCL Hamburg	322.97	8063	F8	8/1/08 15:45	7.052	8/6/2008 4:30	108:4 5:00	838.2	0.141	0.347
OOCL Tianjin	322.97	8063	F8	8/8/08 17:00	6.958	8/13/2008 4:35	107:3 5:00	838.2	0.141	0.347
OOCL Asia	322.90	8063	F8	8/15/08 16:00	9.965	8/20/2008 2:55	106:5 5:00	838.2	0.141	0.347
OOCL Rotterdam	323.00	8063	F8	8/25/08 15:10	4.014	8/28/2008 16:20	73:10 :00	838.2	0.141	0.347
OOCL Ningbo	323.00	8063	F8	8/29/08 15:30				838.2	0.141	0.347
Ikoma	193.03	1631	G227	3/1/08 5:20	2.917	3/1/2008 20:45	15:25 :00	1944.31 92	0.541	0.624
Essen Express	293.99	4639	G227	3/4/08 3:20	2.594	3/5/2008 16:30	37:10 :00	1944.31 92	0.541	0.624
Maruba Zonda	176.41	1372	G227	3/6/08 17:35	1.490	3/7/2008 6:30	12:55 :00	1944.31 92	0.541	0.624

Izumo	193.03	1613	G227	3/8/08 5:20	1.285	3/8/2008 17:55	12:35 :00	1944.31 92	0.541	0.624
Cap Maleas	175.00	1740	G227	3/9/08 12:10	1.837	3/10/2008 19:30	31:20 :00	1944.31 92	0.541	0.624
CSAV Mexico	207.00	2764	G227	3/11/08 8:15	2.868	3/11/2008 17:55	9:40: 00	1944.31 92	0.541	0.624
Izu	193.03	1631	G227	3/14/08 5:05	0.962	3/14/2008 19:50	14:45 :00	1944.31 92	0.541	0.624
IGA	193.03	1613	G227	3/15/08 4:10	5.278	3/15/2008 17:35	13:25 :00	1944.31 92	0.541	0.624
Ikoma	193.03	1631	G227	3/20/08 10:50	2.222	3/21/2008 16:20	29:30 :00	1944.31 92	0.541	0.624
Imari	193.03	1613	G227	3/22/08 16:10	1.559	3/23/2008 6:45	14:35 :00	1944.31 92	0.541	0.624
Gloria	184.70	1728	G227	3/24/08 5:35	5.476	3/24/2008 20:00	14:25 :00	1944.31 92	0.541	0.624
E.R. Cape Town	184.70	1728	G227	3/29/08 17:00	1.542	3/30/2008 5:40	12:40 :00	1944.31 92	0.541	0.624
Cap Maleas	175.00	1740	G227	3/31/08 6:00	2.139	3/31/2008 17:35	11:35 :00	1944.31 92	0.541	0.624
Hansa Flensbu rg	175.00	1740	G227	4/2/08 9:20	4.778	4/3/2008 15:45	30:25 :00	1944.31 92	0.541	0.624
Maruba Zonda	176.41	1372	G227	4/7/08 4:00	3.059	4/7/2008 18:20	14:20 :00	1944.31 92	0.541	0.624
Polynesi a	157.16	1122	G227	4/10/08 5:25	6.990	4/11/2008 17:20	35:55 :00	1944.31 92	0.541	0.624
E.R. Cape Town	184.70	1728	G227	4/17/08 5:10	6.438	4/18/2008 4:20	23:10 :00	1944.31 92	0.541	0.624
Cap Matatul a	158.75	1129	G227	4/23/08 15:40	2.559	4/25/2008 4:35	36:55 :00	1944.31 92	0.541	0.624
Izu	193.03	1631	G227	4/26/08 5:05	7.424	4/26/2008 18:10	13:05 :00	1944.31 92	0.541	0.624
Dresden Express	294.00	4639	G227	5/3/08 15:15	6.865	5/4/2008 17:20	26:05 :00	1944.31 92	0.541	0.624
Iwaki	193.03	1613	G227	5/10/08 12:00	2.208	5/11/2008 5:35	17:35 :00	1944.31 92	0.541	0.624
Cap Maleas	175.00	1740	G227	5/12/08 17:00	1.962	5/13/2008 5:40	12:40 :00	1944.31 92	0.541	0.624
Gloria	184.70	1728	G227	5/14/08 16:05	2.552	5/15/2008 6:45	14:40 :00	1944.31 92	0.541	0.624
IGA	193.03	1613	G227	5/17/08 5:20	0.983	5/17/2008 17:45	12:25 :00	1944.31 92	0.541	0.624
Izu	193.03	1631	G227	5/18/08 4:55	1.118	5/19/2008 4:55	24:00 :00	1944.31 92	0.541	0.624
Libra Santos	220.00	3104	G227	5/19/08 7:45	3.448	5/20/2008 7:55	24:10 :00	1944.31 92	0.541	0.624
Norasia Alya	220.00	3104	G227	5/22/08 18:30	3.976	5/23/2008 6:50	12:20 :00	1944.31 92	0.541	0.624
Gloria	184.70	1728	G227	5/26/08 17:55	2.483	5/27/2008 17:50	23:55 :00	1944.31 92	0.541	0.624
Maruba Zonda	176.41	1372	G227	5/29/08 5:30	4.194	5/29/2008 20:00	14:30 :00	1944.31 92	0.541	0.624
CSAV Mexico	207.00	2764	G227	6/2/08 10:10	5.035	6/3/2008 5:25	19:15 :00	1944.31 92	0.541	0.624
Ikaruga	193.03	1613	G227	6/7/08 11:00	1.750	6/8/2008 18:55	31:55 :00	1944.31 92	0.541	0.624
Maruba Zonda	176.41	1372	G227	6/9/08 5:00	6.976	6/9/2008 19:55	14:55 :00	1944.31 92	0.541	0.624
Ipanem a	193.03	1613	G227	6/16/08 4:25	2.066	6/16/2008 18:05	13:40 :00	1944.31 92	0.541	0.624

Maruba Zonda	176.41	1372	G227	6/18/08 6:00	2.962	6/18/2008 19:00	13:00 :00	1944.31 92	0.541	0.624
E.R. Cape Town	184.70	1728	G227	6/21/08 5:05	1.021	6/21/2008 18:40	13:35 :00	1944.31 92	0.541	0.624
Cap Matatula	158.75	1129	G227	6/22/08 5:35	7.979	6/24/2008 0:20	42:45 :00	1944.31 92	0.541	0.624
Maruba Zonda	176.41	1372	G227	6/30/08 5:05	7.490	6/30/2008 19:20	14:15 :00	1944.31 92	0.541	0.624
Gloria	184.70	1728	G227	7/7/08 16:50	6.556	7/8/2008 19:05	26:15 :00	1944.31 92	0.541	0.624
Cap Maleas	175.00	1740	G227	7/14/08 6:10	2.201	7/14/2008 17:40	11:30 :00	1944.31 92	0.541	0.624
Gloria	184.70	1728	G227	7/16/08 11:00	4.792	7/17/2008 5:40	18:40 :00	1944.31 92	0.541	0.624
Maruba Zonda	176.41	1372	G227	7/21/08 6:00	2.292	7/21/2008 20:05	14:05 :00	1944.31 92	0.541	0.624
Cap Maleas	175.00	1740	G227	7/23/08 13:00	4.674	7/24/2008 4:40	15:40 :00	1944.31 92	0.541	0.624
Gloria	184.70	1728	G227	7/28/08 5:10	2.042	7/28/2008 18:40	13:30 :00	1944.31 92	0.541	0.624
Maruba Zonda	176.41	1372	G227	7/30/08 6:10	3.455	7/30/2008 18:00	11:50 :00	1944.31 92	0.541	0.624
Libra Santos	220.00	3104	G227	8/2/08 17:05	1.503	8/3/2008 17:35	24:30 :00	1944.31 92	0.541	0.624
Cap Maleas	175.00	1740	G227	8/4/08 5:10	5.243	8/5/2008 4:30	23:20 :00	1944.31 92	0.541	0.624
Norasia Alya	220.00	3104	G227	8/9/08 11:00	1.781	8/10/2008 17:30	30:30 :00	1944.31 92	0.541	0.624
Maruba Zonda	176.41	1372	G227	8/11/08 5:45	1.396	8/11/2008 19:40	13:55 :00	1944.31 92	0.541	0.624
Norman die Bridge	276.52	3720	G227	8/12/08 15:15	2.851	8/14/2008 18:35	51:20 :00	1944.31 92	0.541	0.624
Cap Maleas	175.00	1740	G227	8/15/08 11:40	0.688	8/16/2008 5:25	17:45 :00	1944.31 92	0.541	0.624
Williamsburg Bridge	275.08	3484	G227	8/16/08 4:10	6.083	8/18/2008 5:45	49:35 :00	1944.31 92	0.541	0.624
Maruba Zonda	176.41	1372	G227	8/22/08 6:10		8/22/2008 16:40	10:30 :00	1944.31 92	0.541	0.624
Ipanema	193.03	1613	G229	2/29/08 16:10	2.545	3/1/2008 2:30	10:20 :00	1944.31 92	0.541	0.624
Gloria	184.70	1728	G229	3/3/08 5:15	3.413	3/3/2008 19:45	14:30 :00	1944.31 92	0.541	0.624
Iwaki	193.03	1613	G229	3/6/08 15:10	2.552	3/7/2008 6:45	15:35 :00	1944.31 92	0.541	0.624
Rialto Bridge	245.00	3473	G229	3/9/08 4:25	3.069	3/13/2008 21:00	112:3 5:00	1944.31 92	0.541	0.624
Gloria	184.70	1728	G229	3/12/08 6:05	4.024	3/13/2008 5:50	23:45 :00	1944.31 92	0.541	0.624
San Pedro Bridge	232.06	3681	G229	3/16/08 6:40	2.962	3/18/2008 6:10	47:30 :00	1944.31 92	0.541	0.624
Cap Maleas	175.00	1740	G229	3/19/08 5:45	2.983	3/19/2008 19:30	13:45 :00	1944.31 92	0.541	0.624
Dong Hai Bridge	268.80	4252	G229	3/22/08 5:20	4.497	3/24/2008 5:45	48:25 :00	1944.31 92	0.541	0.624
Izumo	193.03	1613	G229	3/26/08 17:15	1.622	3/27/2008 6:20	13:05 :00	1944.31 92	0.541	0.624
New York Express	294.06	4890	G229	3/28/08 8:10	3.427	3/29/2008 18:45	34:35 :00	1944.31 92	0.541	0.624

Williams burg Bridge	275.08	3484	G229	3/31/08 18:25	2.372	4/2/2008 17:55	47:30 :00	1944.31 92	0.541	0.624
CSAV Rio Petrohu e	207.40	2474	G229	4/3/08 3:20	2.576	4/4/2008 19:50	40:30 :00	1944.31 92	0.541	0.624
Concord Bridge	275.80	3484	G229	4/5/08 17:10	7.451	4/7/2008 18:30	49:20 :00	1944.31 92	0.541	0.624
Rialto Bridge	245.00	3473	G229	4/13/08 4:00	3.313	4/15/2008 5:45	49:45 :00	1944.31 92	0.541	0.624
Cap Van Diemen	194.06	1876	G229	4/16/08 11:30	3.694	4/17/2008 4:45	17:15 :00	1944.31 92	0.541	0.624
Clifton Bridge	276.52	3456	G229	4/20/08 4:10	7.000	4/22/2008 6:10	50:00 :00	1944.31 92	0.541	0.624
Dong Hai Bridge	268.80	4252	G229	4/27/08 4:10	3.087	4/29/2008 15:15	59:05 :00	1944.31 92	0.541	0.624
Cap Maleas	175.00	1740	G229	4/30/08 6:15	2.899	4/30/2008 19:15	13:00 :00	1944.31 92	0.541	0.624
Ikoma	193.03	1631	G229	5/3/08 3:50	0.507	5/3/2008 16:45	12:55 :00	1944.31 92	0.541	0.624
Norasia Polaris	220.42	3104	G229	5/3/08 16:00	0.510	5/4/2008 4:40	12:40 :00	1944.31 92	0.541	0.624
Williams burg Bridge	275.08	3484	G229	5/4/08 4:15	4.469	5/6/2008 5:35	49:20 :00	1944.31 92	0.541	0.624
Maruba Zonda	176.41	1372	G229	5/8/08 15:30	2.031	5/9/2008 14:35	23:05 :00	1944.31 92	0.541	0.624
Concord Bridge	275.80	3484	G229	5/10/08 16:15	5.955	5/12/2008 19:50	51:35 :00	1944.31 92	0.541	0.624
Kobe Express	293.94	4616	G229	5/16/08 15:10	2.642	5/17/2008 18:30	27:20 :00	1944.31 92	0.541	0.624
Maruba Zonda	176.41	1372	G229	5/19/08 6:35	2.979	5/19/2008 18:45	12:10 :00	1944.31 92	0.541	0.624
Cap Maleas	175.00	1740	G229	5/22/08 6:05	1.969	5/22/2008 18:25	12:20 :00	1944.31 92	0.541	0.624
Clifton Bridge	276.52	3456	G229	5/24/08 5:20	3.413	5/26/2008 5:30	48:10 :00	1944.31 92	0.541	0.624
Seoul Express	294.17	4864	G229	5/27/08 15:15	3.993	5/29/2008 4:45	37:30 :00	1944.31 92	0.541	0.624
Dong Hai Bridge	268.80	4252	G229	5/31/08 15:05	4.587	6/2/2008 18:40	51:35 :00	1944.31 92	0.541	0.624
Gloria	184.70	1728	G229	6/5/08 5:10	2.146	6/5/2008 18:00	12:50 :00	1944.31 92	0.541	0.624
Williams burg Bridge	275.08	3484	G229	6/7/08 8:40	6.896	6/9/2008 18:35	57:55 :00	1944.31 92	0.541	0.624
Concord Bridge	275.80	3484	G229	6/14/08 6:10	7.389	6/16/2008 19:40	61:30 :00	1944.31 92	0.541	0.624
Rialto Bridge	245.00	3473	G229	6/21/08 15:30	4.569	6/23/2008 20:10	52:40 :00	1944.31 92	0.541	0.624
Gloria	184.70	1728	G229	6/26/08 5:10	1.951	6/26/2008 17:25	12:15 :00	1944.31 92	0.541	0.624
Clifton Bridge	276.52	3456	G229	6/28/08 4:00	3.347	6/30/2008 5:40	49:40 :00	1944.31 92	0.541	0.624
Libra Rio	221.00	3104	G229	7/1/08 12:20	1.292	7/2/2008 4:35	16:15 :00	1944.31 92	0.541	0.624
Cap Maleas	175.00	1740	G229	7/2/08 19:20	3.510	7/3/2008 16:00	20:40 :00	1944.31 92	0.541	0.624
Dong Hai Bridge	268.80	4252	G229	7/6/08 7:35	2.583	7/8/2008 17:05	57:30 :00	1944.31 92	0.541	0.624

Maruba Zonda	176.41	1372	G229	7/8/08 21:35	3.278	7/9/2008 17:20	19:45 :00	1944.31 92	0.541	0.624
Williamsburg Bridge	275.08	3484	G229	7/12/08 4:15	3.514	7/14/2008 5:50	49:35 :00	1944.31 92	0.541	0.624
Montevideo	207.40	2500	G229	7/15/08 16:35	3.490	7/16/2008 18:30	25:55 :00	1944.31 92	0.541	0.624
Concord Bridge	275.80	3484	G229	7/19/08 4:20	3.323	7/21/2008 4:40	48:20 :00	1944.31 92	0.541	0.624
Cap Matatula	158.75	1129	G229	7/22/08 12:05	4.118	7/24/2008 3:40	39:35 :00	1944.31 92	0.541	0.624
Rialto Bridge	245.00	3473	G229	7/26/08 14:55	6.552	7/28/2008 20:00	53:05 :00	1944.31 92	0.541	0.624
Clifton Bridge	276.52	3456	G229	8/2/08 4:10	11.535	8/4/2008 5:40	49:30 :00	1944.31 92	0.541	0.624
Polynesia	157.16	1122	G229	8/13/08 17:00	11.542	8/18/2008 20:00	123:0 0:00	1944.31 92	0.541	0.624
CSAV Mexico	207.00	2764	G229	8/25/08 6:00	1.372	8/26/2008 2:40	20:40 :00	1944.31 92	0.541	0.624
E.R. Wilhelmshaven	211.85	2496	G229	8/26/08 14:55	2.597	8/28/2008 19:40	52:45 :00	1944.31 92	0.541	0.624
Maersk Phuket	210.10	2890	G229	8/29/08 5:15		8/31/2008 5:00		1944.31 92	0.541	0.624
Cosco Hamburg	280.00	5440	J245	3/2/08 5:05	6.000	3/4/2008 6:00	48:55 :00	1798.32	1.157	0.971
Cosco Tianjin	278.90	5570	J245	3/8/08 5:05	5.389	3/10/2008 6:00	48:55 :00	1798.32	1.157	0.971
Cosco Qingdao	280.00	5440	J245	3/13/08 14:25	2.628	3/16/2008 5:25	63:00 :00	1798.32	1.157	0.971
Cosco Rotterdam	280.00	5440	J245	3/16/08 5:30	3.000	3/18/2008 6:00	48:30 :00	1798.32	1.157	0.971
Jinhe	280.00	5440	J245	3/19/08 5:30	3.997	3/21/2008 17:15	59:45 :00	1798.32	1.157	0.971
Cosco Shanghai	280.00	5440	J245	3/23/08 5:25	4.399	3/25/2008 6:35	49:10 :00	1798.32	1.157	0.971
Cosco Hong Kong	280.00	5440	J245	3/27/08 15:00	2.597	3/30/2008 5:35	62:35 :00	1798.32	1.157	0.971
Cosco Felixstowe	280.00	5440	J245	3/30/08 5:20	5.406	4/1/2008 5:40	48:20 :00	1798.32	1.157	0.971
Chuanhe	280.00	5440	J245	4/4/08 15:05	4.597	4/7/2008 6:25	63:20 :00	1798.32	1.157	0.971
Yuehe	280.00	5440	J245	4/9/08 5:25	3.993	4/11/2008 18:50	61:25 :00	1798.32	1.157	0.971
Luhe	280.00	5440	J245	4/13/08 5:15	4.014	4/15/2008 5:55	48:40 :00	1798.32	1.157	0.971
Cosco Qingdao	280.00	5440	J245	4/17/08 5:35	2.969	4/19/2008 16:00	58:25 :00	1798.32	1.157	0.971
Cosco Rotterdam	280.00	5440	J245	4/20/08 4:50	6.031	4/22/2008 5:20	48:30 :00	1798.32	1.157	0.971
Cosco Yokohama	300.00	7455	J245	4/26/08 5:35	4.986	4/28/2008 18:40	61:05 :00	1798.32	1.157	0.971
Cosco Hong Kong	280.00	5440	J245	5/1/08 5:15	3.483	5/3/2008 18:25	61:10 :00	1798.32	1.157	0.971

Cosco Felixstowe	280.00	5440	J245	5/4/08 16:50	6.514	5/6/2008 17:20	48:30 :00	1798.32	1.157	0.971
Cosco Hamburg	280.00	5440	J245	5/11/08 5:10	4.368	5/13/2008 6:10	49:00 :00	1798.32	1.157	0.971
Yuehe	280.00	5440	J245	5/15/08 14:00	2.635	5/18/2008 5:30	63:30 :00	1798.32	1.157	0.971
Luhe	280.00	5440	J245	5/18/08 5:15	3.372	5/20/2008 5:30	48:15 :00	1798.32	1.157	0.971
Cosco Qingdao	280.00	5440	J245	5/21/08 14:10	8.101	5/23/2008 17:45	51:35 :00	1798.32	1.157	0.971
Cosco Yokohama	300.00	7455	J245	5/29/08 16:35	2.955	6/1/2008 16:55	72:20 :00	1798.32	1.157	0.971
Cosco Shanghai	280.00	5440	J245	6/1/08 15:30	2.990	6/3/2008 18:00	50:30 :00	1798.32	1.157	0.971
Cosco Hong Kong	280.00	5440	J245	6/4/08 15:15	4.038	6/7/2008 6:40	63:25 :00	1798.32	1.157	0.971
Cosco Felixstowe	280.00	5440	J245	6/8/08 16:10	7.545	6/10/2008 18:20	50:10 :00	1798.32	1.157	0.971
Chuanhe	280.00	5440	J245	6/16/08 5:15	3.094	6/18/2008 6:05	48:50 :00	1798.32	1.157	0.971
Yuehe	280.00	5440	J245	6/19/08 7:30	2.903	6/21/2008 19:15	59:45 :00	1798.32	1.157	0.971
Luhe	280.00	5440	J245	6/22/08 5:10	6.333	6/24/2008 6:00	48:50 :00	1798.32	1.157	0.971
Cosco Qingdao	280.00	5440	J245	6/28/08 13:10	7.208	7/1/2008 6:15	65:05 :00	1798.32	1.157	0.971
Cosco Yokohama	300.00	7455	J245	7/5/08 18:10	6.465	7/8/2008 19:25	73:15 :00	1798.32	1.157	0.971
Cosco Hong Kong	280.00	5440	J245	7/12/08 5:20	7.997	7/14/2008 18:15	60:55 :00	1798.32	1.157	0.971
Cosco Hamburg	280.00	5440	J245	7/20/08 5:15	3.024	7/22/2008 5:50	48:35 :00	1798.32	1.157	0.971
Cosco Long Beach	300.07	7455	J245	7/23/08 5:50	3.979	7/26/2008 6:30	72:40 :00	1798.32	1.157	0.971
Luhe	280.00	5440	J245	7/27/08 5:20	2.003	7/29/2008 5:30	48:10 :00	1798.32	1.157	0.971
Yuehe	280.00	5440	J245	7/29/08 5:25	6.090	7/31/2008 5:30	48:05 :00	1798.32	1.157	0.971
Cosco Napoli	334.00	8204	J245	8/4/08 7:35	2.903	8/6/2008 18:30	58:55 :00	1798.32	1.157	0.971
Cosco Qingdao	280.00	5440	J245	8/7/08 5:15	3.997	8/9/2008 6:00	48:45 :00	1798.32	1.157	0.971
Cosco Shanghai	280.00	5440	J245	8/11/08 5:10	3.010	8/13/2008 5:30	48:20 :00	1798.32	1.157	0.971
Cosco Yokohama	300.00	7455	J245	8/14/08 5:25	2.990	8/16/2008 17:35	60:10 :00	1798.32	1.157	0.971
Cosco Felixstowe	280.00	5440	J245	8/17/08 5:10	3.042	8/19/2008 6:00	48:50 :00	1798.32	1.157	0.971
Cosco Hong Kong	280.00	5440	J245	8/20/08 6:10	3.958	8/22/2008 6:25	48:15 :00	1798.32	1.157	0.971

Cosco Hamburg	280.00	5440	J245	8/24/08 5:10	4.330	8/26/2008 6:15	49:05 :00	1798.32	1.157	0.971
Cosco Long Beach	300.07	7455	J245	8/28/08 13:05	2.684	8/31/2008 5:20		1798.32	1.157	0.971
Luhe	280.00	5440	J245	8/31/08 5:30				1798.32	1.157	0.971
CMA CGM Blue Whale	294.11	5040	J247	5/12/08 4:00	42.090	5/12/2008 18:05	14:05 :00	1798.32	1.157	0.971
CMA CGM Kingfish	283.81	5042	J247	6/23/08 6:10	20.438	6/23/2008 18:25	12:15 :00	1798.32	1.157	0.971
Cosco Felixstowe	280.00	5440	J247	7/13/08 16:40	24.556	7/16/2008 6:30	61:50 :00	1798.32	1.157	0.971
CMA CGM White Shark	294.11	5040	J247	8/7/08 6:00		8/7/2008 22:15	16:15 :00	1798.32	1.157	0.971
CMA CGM Hugo	334.08	8328	J266	3/4/08 4:30	5.024	3/6/2008 17:55	61:25 :00	1798.32	1.157	0.971
Cosco Sydney	215.45	2702	J266	3/9/08 5:05	8.295	3/11/2008 5:10	48:05 :00	1798.32	1.157	0.971
CMA CGM Vivaldi	334.06	8238	J266	3/17/08 12:10	13.708	3/20/2008 17:30	77:20 :00	1798.32	1.157	0.971
Pacific Link	334.00	8238	J266	3/31/08 5:10	4.014	4/2/2008 17:30	60:20 :00	1798.32	1.157	0.971
Manoa	262.14	3027	J266	4/4/08 5:30	3.983	4/5/2008 5:00	23:30 :00	1798.32	1.157	0.971
Cosco Hamburg	280.00	5440	J266	4/8/08 5:05	6.163	4/10/2008 5:20	48:15 :00	1798.32	1.157	0.971
MSC Toronto	324.80	8089	J266	4/14/08 9:00	8.122	4/17/2008 4:30	67:30 :00	1798.32	1.157	0.971
CMA CGM Vivaldi	334.06	8238	J266	4/22/08 11:55	4.722	4/25/2008 19:35	79:40 :00	1798.32	1.157	0.971
Cosco Shanghai	280.00	5440	J266	4/27/08 5:15	1.958	4/29/2008 4:00	46:45 :00	1798.32	1.157	0.971
CMA CGM Kingfish	283.81	5042	J266	4/29/08 4:15	1.465	4/29/2008 16:30	12:15 :00	1798.32	1.157	0.971
USL Condor	161.30	1347	J266	4/30/08 15:25	4.528	5/2/2008 17:55	50:30 :00	1798.32	1.157	0.971
CMA CGM Orca	294.10	5040	J266	5/5/08 4:05	5.052	5/5/2008 19:20	15:15 :00	1798.32	1.157	0.971
Chuanhe	280.00	5440	J266	5/10/08 5:20	2.563	5/12/2008 18:30	61:10 :00	1798.32	1.157	0.971
CMA CGM Hugo	334.08	8328	J266	5/12/08 18:50	3.729	5/15/2008 18:25	71:35 :00	1798.32	1.157	0.971
CMA CGM Africa	334.00	8468	J266	5/16/08 12:20	7.774	5/19/2008 18:10	77:50 :00	1798.32	1.157	0.971
USL Kiwi	157.12	1122	J266	5/24/08 6:55	2.253	5/25/2008 4:00	21:05 :00	1798.32	1.157	0.971

CMA CGM Vivaldi	334.06	8238	J266	5/26/08 13:00	6.628	5/30/2008 6:55	89:55 :00	1798.32	1.157	0.971
CMA CGM Dolphin	294.12	5040	J266	6/2/08 4:05	2.594	6/2/2008 18:25	14:20 :00	1798.32	1.157	0.971
Francois e Gilot	161.30	1341	J266	6/4/08 18:20	4.413	6/6/2008 5:40	35:20 :00	1798.32	1.157	0.971
Pacific Link	334.00	8238	J266	6/9/08 4:15	5.448	6/12/2008 4:40	72:25 :00	1798.32	1.157	0.971
Cosco Hamburg	280.00	5440	J266	6/14/08 15:00	3.958	6/17/2008 7:00	64:00 :00	1798.32	1.157	0.971
CMA CGM Africa	334.00	8468	J266	6/18/08 14:00	4.684	6/21/2008 18:30	76:30 :00	1798.32	1.157	0.971
MSC Toronto	324.80	8089	J266	6/23/08 6:25	6.955	6/25/2008 19:15	60:50 :00	1798.32	1.157	0.971
CMA CGM Orca	294.10	5040	J266	6/30/08 5:20	2.000	6/30/2008 17:20	12:00 :00	1798.32	1.157	0.971
USL Kea	154.46	1221	J266	7/2/08 5:20	4.375	7/4/2008 3:10	45:50 :00	1798.32	1.157	0.971
Cosco Shanghai	280.00	5440	J266	7/6/08 14:20	3.149	7/8/2008 19:15	52:55 :00	1798.32	1.157	0.971
MSC Texas	334.07	8238	J266	7/9/08 17:55	5.594	7/13/2008 4:40	82:45 :00	1798.32	1.157	0.971
CMA CGM Swordfish	294.12	5042	J266	7/15/08 8:10	6.295	7/16/2008 4:30	20:20 :00	1798.32	1.157	0.971
CMA CGM Hugo	334.08	8328	J266	7/21/08 15:15	3.059	7/24/2008 18:00	74:45 :00	1798.32	1.157	0.971
CMA CGM Africa	334.00	8468	J266	7/24/08 16:40	3.587	7/27/2008 18:30	73:50 :00	1798.32	1.157	0.971
CMA CGM Dolphin	294.12	5040	J266	7/28/08 6:45	14.997	7/28/2008 16:50	10:05 :00	1798.32	1.157	0.971
CMA CGM Marlin	294.12	5042	J266	8/12/08 6:40	7.330	8/12/2008 16:25	9:45: 00	1798.32	1.157	0.971
Pacific Link	334.00	8238	J266	8/19/08 14:35		8/22/2008 5:35	63:00 :00	1798.32	1.157	0.971
USL Kiwi	157.12	1122	J270	4/4/08 5:45	4.979	4/5/2008 5:15	23:30 :00	1798.32	1.157	0.971
Varamo	166.15	1296	J270	4/9/08 5:15	7.003	4/11/2008 19:55	62:40 :00	1798.32	1.157	0.971
Francois e Gilot	161.30	1341	J270	4/16/08 5:20	7.990	4/18/2008 5:10	47:50 :00	1798.32	1.157	0.971
Eagle 2	147.87	1118	J270	4/24/08 5:05	21.010	4/25/2008 19:20	38:15 :00	1798.32	1.157	0.971
USL Kea	154.46	1221	J270	5/15/08 5:20	13.420	5/16/2008 2:35	21:15 :00	1798.32	1.157	0.971
Varamo	166.15	1296	J270	5/28/08 15:25	11.625	5/30/2008 16:40	49:15 :00	1798.32	1.157	0.971
CMA CGM White Shark	294.11	5040	J270	6/9/08 6:25	3.323	6/9/2008 18:55	12:30 :00	1798.32	1.157	0.971
Eagle 2	147.87	1118	J270	6/12/08 14:10	3.663	6/19/2008 3:25	157:1 5:00	1798.32	1.157	0.971

CMA CGM Marlin	294.12	5042	J270	6/16/08 6:05	2.958	6/16/2008 17:15	11:10 :00	1798.32	1.157	0.971
USL Condor	161.30	1347	J270	6/19/08 5:05	19.073	6/20/2008 19:20	38:15 :00	1798.32	1.157	0.971
CMA CGM Blue Whale	294.11	5040	J270	7/8/08 6:50	5.934	7/8/2008 18:55	12:05 :00	1798.32	1.157	0.971
USL Kiwi	157.12	1122	J270	7/14/08 5:15	2.455	7/15/2008 17:20	36:05 :00	1798.32	1.157	0.971
Varamo	166.15	1296	J270	7/16/08 16:10	4.580	7/18/2008 22:35	54:25 :00	1798.32	1.157	0.971
CMA CGM Tarpon	294.12	5042	J270	7/21/08 6:05	15.392	7/21/2008 17:20	11:15 :00	1798.32	1.157	0.971
CMA CGM Vivaldi	334.06	8238	J270	8/5/08 15:30	0.493	8/8/2008 19:55	76:25 :00	1798.32	1.157	0.971
USL Condor	161.30	1347	J270	8/6/08 3:20	15.559	8/9/2008 5:30	74:10 :00	1798.32	1.157	0.971
USL Kea	154.46	1221	J270	8/21/08 16:45		8/23/2008 3:20	34:35 :00	1798.32	1.157	0.971
Hanjin Ottawa	278.08	5774	T134	3/7/08 4:20	1.045	3/9/2008 6:45	50:25 :00	1524	0.757	0.87
Cape Santiag o	158.75	1129	T134	3/8/08 5:25	3.948	3/9/2008 6:25	25:00 :00	1524	0.757	0.87
Wan Hai 510	268.80	4252	T134	3/12/08 4:10	4.493	3/14/2008 4:40	48:30 :00	1524	0.757	0.87
Cape Santiag o	158.75	1129	T134	3/16/08 16:00	2.510	3/17/2008 11:25	19:25 :00	1524	0.757	0.87
Kota Salam	268.80	4252	T134	3/19/08 4:15	5.788	3/21/2008 6:45	50:30 :00	1524	0.757	0.87
Cape Santiag o	158.75	1129	T134	3/24/08 23:10	1.208	3/25/2008 20:15	21:05 :00	1524	0.757	0.87
Wan Hai 505	268.80	4252	T134	3/26/08 4:10	7.927	3/28/2008 6:30	50:20 :00	1524	0.757	0.87
Cape Santiag o	158.75	1129	T134	4/3/08 2:25	6.076	4/3/2008 19:25	17:00 :00	1524	0.757	0.87
Wan Hai 501	268.80	4252	T134	4/9/08 4:15	3.462	4/11/2008 6:40	50:25 :00	1524	0.757	0.87
Cape Santiag o	158.75	1129	T134	4/12/08 15:20	9.573	4/13/2008 6:30	15:10 :00	1524	0.757	0.87
Cape Santiag o	158.75	1129	T134	4/22/08 5:05	1.333	4/22/2008 18:20	13:15 :00	1524	0.757	0.87
Kota Salam	268.80	4252	T134	4/23/08 13:05	6.632	4/25/2008 6:00	40:55 :00	1524	0.757	0.87
Wan Hai 505	268.80	4252	T134	4/30/08 4:15	7.014	5/2/2008 18:30	62:15 :00	1524	0.757	0.87
Wan Hai 509	268.80	4352	T134	5/7/08 4:35	4.028	5/9/2008 5:25	48:50 :00	1524	0.757	0.87
Cape Santiag o	158.75	1129	T134	5/11/08 5:15	2.958	5/11/2008 20:30	15:15 :00	1524	0.757	0.87
Wan Hai 501	268.80	4252	T134	5/14/08 4:15	5.455	5/16/2008 6:30	50:15 :00	1524	0.757	0.87
Cape Santiag o	158.75	1129	T134	5/19/08 15:10	1.538	5/20/2008 5:15	14:05 :00	1524	0.757	0.87

Wan Hai 510	268.80	4252	T134	5/21/08 4:05	7.465	5/23/2008 5:50	49:45 :00	1524	0.757	0.87
Cape Santiago	158.75	1129	T134	5/28/08 15:15	6.559	5/29/2008 4:00	12:45 :00	1524	0.757	0.87
Wan Hai 505	268.80	4252	T134	6/4/08 4:40	2.066	6/6/2008 5:25	48:45 :00	1524	0.757	0.87
Cape Santiago	158.75	1129	T134	6/6/08 6:15	4.934	6/7/2008 6:25	24:10 :00	1524	0.757	0.87
Wan Hai 509	268.80	4352	T134	6/11/08 4:40	4.031	6/13/2008 6:25	49:45 :00	1524	0.757	0.87
Cape Santiago	158.75	1129	T134	6/15/08 5:25	2.997	6/15/2008 19:15	13:50 :00	1524	0.757	0.87
Wan Hai 501	268.80	4252	T134	6/18/08 5:20	5.990	6/20/2008 6:05	48:45 :00	1524	0.757	0.87
Cape Santiago	158.75	1129	T134	6/24/08 5:05	0.997	6/24/2008 22:20	17:15 :00	1524	0.757	0.87
Wan Hai 510	268.80	4252	T134	6/25/08 5:00	6.927	6/27/2008 5:20	48:20 :00	1524	0.757	0.87
Kota Salam	268.80	4252	T134	7/2/08 3:15	7.517	7/4/2008 7:00	51:45 :00	1524	0.757	0.87
Wan Hai 505	268.80	4252	T134	7/9/08 15:40	6.549	7/11/2008 18:40	51:00 :00	1524	0.757	0.87
Wan Hai 509	268.80	4352	T134	7/16/08 4:50	3.431	7/18/2008 19:40	62:50 :00	1524	0.757	0.87
Cape Santiago	158.75	1129	T134	7/19/08 15:10	3.590	7/20/2008 6:30	15:20 :00	1524	0.757	0.87
Wan Hai 501	268.80	4252	T134	7/23/08 5:20	2.017	7/25/2008 5:55	48:35 :00	1524	0.757	0.87
Hanjin Taipei	274.67	5447	T134	7/25/08 5:45	3.389	7/27/2008 16:55	59:10 :00	1524	0.757	0.87
Cape Santiago	158.75	1129	T134	7/28/08 15:05	1.573	7/29/2008 14:55	23:50 :00	1524	0.757	0.87
Wan Hai 510	268.80	4252	T134	7/30/08 4:50	6.997	8/1/2008 5:50	49:00 :00	1524	0.757	0.87
Kota Salam	268.80	4252	T134	8/6/08 4:45	2.413	8/8/2008 6:35	49:50 :00	1524	0.757	0.87
CSCL Fos	207.92	2672	T134	8/8/08 14:40	4.604	8/10/2008 18:30	51:50 :00	1524	0.757	0.87
Wan Hai 505	268.80	4252	T134	8/13/08 5:10	2.747	8/15/2008 6:00	48:50 :00	1524	0.757	0.87
Cape Santiago	158.75	1129	T134	8/15/08 23:05	5.253	8/16/2008 20:20	21:15 :00	1524	0.757	0.87
Wan Hai 509	268.80	4352	T134	8/21/08 5:10	2.795	8/23/2008 5:35	48:25 :00	1524	0.757	0.87
Hanjin Philadelphia	282.10	4367	T134	8/24/08 0:15	3.198	8/25/2008 18:35	42:20 :00	1524	0.757	0.87
Wan Hai 501	268.80	4252	T134	8/27/08 5:00		8/29/2008 20:30		1524	0.757	0.87
Hanjin Amsterdam	278.80	5608	T136	3/14/08 5:25	7.003	3/16/2008 7:10	49:45 :00	1524	0.757	0.87
Portland Senator	294.13	4545	T136	3/21/08 5:30	7.000	3/23/2008 12:00	54:30 :00	1524	0.757	0.87
Peking Senator	294.10	4545	T136	3/28/08 5:30	4.972	3/30/2008 7:00	49:30 :00	1524	0.757	0.87
Wan Hai 509	268.80	4352	T136	4/2/08 4:50	3.427	4/3/2008 19:45	38:55 :00	1524	0.757	0.87

Hanjin Pretoria	282.10	4367	T136	4/5/08 15:05	2.590	4/7/2008 6:45	39:40 :00	1524	0.757	0.87
Hanjin Beijing	279.00	5302	T136	4/8/08 5:15	3.010	4/10/2008 7:15	50:00 :00	1524	0.757	0.87
Hanjin Athens	278.80	5774	T136	4/11/08 5:30	4.955	4/13/2008 6:40	49:10 :00	1524	0.757	0.87
Wan Hai 510	268.80	4252	T136	4/16/08 4:25	3.035	4/18/2008 5:35	49:10 :00	1524	0.757	0.87
Hanjin Helsinki	274.00	5447	T136	4/19/08 5:15	6.007	4/21/2008 6:40	49:25 :00	1524	0.757	0.87
Hanjin Rome	279.00	5302	T136	4/25/08 5:25	5.410	4/27/2008 10:30	53:05 :00	1524	0.757	0.87
Cape Santiago	158.75	1129	T136	4/30/08 15:15	2.576	5/1/2008 6:30	15:15 :00	1524	0.757	0.87
Hanjin Taipei	274.67	5447	T136	5/3/08 5:05	6.007	5/5/2008 6:45	49:40 :00	1524	0.757	0.87
Hanjin Brussels	278.80	5608	T136	5/9/08 5:15	8.420	5/11/2008 7:05	49:50 :00	1524	0.757	0.87
Hanjin Praha	282.10	4367	T136	5/17/08 15:20	6.000	5/19/2008 6:45	39:25 :00	1524	0.757	0.87
Penang Senator	294.10	4545	T136	5/23/08 15:20	4.535	5/25/2008 6:35	39:15 :00	1524	0.757	0.87
Kota Salam	268.80	4252	T136	5/28/08 4:10	2.135	5/30/2008 6:45	50:35 :00	1524	0.757	0.87
Hanjin Ottawa	278.08	5774	T136	5/30/08 7:25	6.920	6/1/2008 6:30	47:05 :00	1524	0.757	0.87
Hanjin Amsterdam	278.80	5608	T136	6/6/08 5:30	6.990	6/8/2008 6:55	49:25 :00	1524	0.757	0.87
Portland Senator	294.13	4545	T136	6/13/08 5:15	7.007	6/14/2008 20:25	39:10 :00	1524	0.757	0.87
Peking Senator	294.10	4545	T136	6/20/08 5:25	6.986	6/22/2008 6:55	49:30 :00	1524	0.757	0.87
Hanjin Beijing	279.00	5302	T136	6/27/08 5:05	6.712	6/29/2008 5:40	48:35 :00	1524	0.757	0.87
Hanjin Athens	278.80	5774	T136	7/3/08 22:10	7.705	7/6/2008 20:40	70:30 :00	1524	0.757	0.87
Hanjin Helsinki	274.00	5447	T136	7/11/08 15:05	17.049	7/13/2008 18:25	51:20 :00	1524	0.757	0.87
CSCL Hong Kong	274.67	5551	T136	7/28/08 16:15	3.333	7/31/2008 6:25	62:10 :00	1524	0.757	0.87
Hanjin Brussels	278.80	5608	T136	8/1/08 0:15	5.167	8/3/2008 6:35	54:20 :00	1524	0.757	0.87
Cape Santiago	158.75	1129	T136	8/6/08 4:15	2.788	8/6/2008 22:30	18:15 :00	1524	0.757	0.87
Hanjin Paris	279.00	5302	T136	8/8/08 23:10	6.271	8/11/2008 4:45	53:35 :00	1524	0.757	0.87
Penang Senator	294.10	4545	T136	8/15/08 5:40	7.413	8/17/2008 6:30	48:50 :00	1524	0.757	0.87
Hanjin Ottawa	278.08	5774	T136	8/22/08 15:35	2.323	8/24/2008 20:30	52:55 :00	1524	0.757	0.87
Cape Santiago	158.75	1129	T136	8/24/08 23:20	4.653	8/25/2008 19:35	20:15 :00	1524	0.757	0.87
Hanjin Amsterdam	278.80	5608	T136	8/29/08 15:00		8/31/2008 20:40		1524	0.757	0.87
Hanjin Boston	300.08	7455	T138	3/5/08 22:45	3.313	3/8/2008 20:35	69:50 :00	1524	0.757	0.87
Hanjin Pretoria	282.10	4367	T138	3/9/08 6:15	3.375	3/10/2008 20:30	38:15 :00	1524	0.757	0.87

Hanjin Yantian	300.07	7455	T138	3/12/08 15:15	2.587	3/15/2008 5:40	62:25 :00	1524	0.757	0.87
CSCL Seattle	275.00	5551	T138	3/15/08 5:20	4.743	3/18/2008 6:30	73:10 :00	1524	0.757	0.87
Hanjin Baltimore	300.07	7455	T138	3/19/08 23:10	4.247	3/22/2008 20:35	69:25 :00	1524	0.757	0.87
Xin Xia Men	279.90	5668	T138	3/24/08 5:05	9.747	3/26/2008 18:00	60:55 :00	1524	0.757	0.87
Hanjin Miami	300.00	7455	T138	4/2/08 23:00	7.670	4/5/2008 20:40	69:40 :00	1524	0.757	0.87
Hanjin Boston	300.08	7455	T138	4/10/08 15:05	5.038	4/14/2008 6:35	87:30 :00	1524	0.757	0.87
Xin Chang Shu	279.90	5668	T138	4/15/08 16:00	4.938	4/18/2008 6:30	62:30 :00	1524	0.757	0.87
CSCL Shanghai	274.67	5551	T138	4/20/08 14:30	3.615	4/23/2008 6:30	64:00 :00	1524	0.757	0.87
Hanjin Philadelphia	282.10	4367	T138	4/24/08 5:15	3.413	4/25/2008 20:45	39:30 :00	1524	0.757	0.87
CSCL Kobe	277.30	5762	T138	4/27/08 15:10	5.587	4/30/2008 19:40	76:30 :00	1524	0.757	0.87
Hanjin Phoenix	282.10	4367	T138	5/3/08 5:15	4.003	5/4/2008 18:25	37:10 :00	1524	0.757	0.87
Xin Pu Dong	279.00	5668	T138	5/7/08 5:20	4.670	5/10/2008 15:35	82:15 :00	1524	0.757	0.87
CSCL Los Angeles	277.30	5762	T138	5/11/08 21:25	4.118	5/14/2008 6:20	56:55 :00	1524	0.757	0.87
Hanjin Paris	279.00	5302	T138	5/16/08 0:15	6.611	5/17/2008 23:40	47:25 :00	1524	0.757	0.87
Hanjin Boston	300.08	7455	T138	5/22/08 14:55	3.389	5/25/2008 18:20	75:25 :00	1524	0.757	0.87
Hanjin Philadelphia	282.10	4367	T138	5/26/08 0:15	5.906	5/27/2008 18:35	42:20 :00	1524	0.757	0.87
Xin Xia Men	279.90	5668	T138	5/31/08 22:00	3.302	6/3/2008 20:25	70:25 :00	1524	0.757	0.87
Hanjin Yantian	300.07	7455	T138	6/4/08 5:15	4.003	6/6/2008 21:00	63:45 :00	1524	0.757	0.87
Hanjin Pretoria	282.10	4367	T138	6/8/08 5:20	7.392	6/9/2008 20:25	39:05 :00	1524	0.757	0.87
Hanjin Praha	282.10	4367	T138	6/15/08 14:45	9.601	6/17/2008 6:35	39:50 :00	1524	0.757	0.87
Xin Qin Huang Dao	279.60	5668	T138	6/25/08 5:10	3.417	6/28/2008 6:35	73:25 :00	1524	0.757	0.87
Hanjin Phoenix	282.10	4367	T138	6/28/08 15:10	2.583	6/30/2008 6:30	39:20 :00	1524	0.757	0.87
CSCL Kobe	277.30	5762	T138	7/1/08 5:10	2.049	7/3/2008 7:45	50:35 :00	1524	0.757	0.87
Cape Santiago	158.75	1129	T138	7/3/08 6:20	8.378	7/4/2008 4:20	22:00 :00	1524	0.757	0.87
Cape Santiago	158.75	1129	T138	7/11/08 15:25	6.997	7/12/2008 6:30	15:05 :00	1524	0.757	0.87
Hanjin Rome	279.00	5302	T138	7/18/08 15:20	4.580	7/21/2008 6:40	63:20 :00	1524	0.757	0.87
Hanjin Dallas	300.04	7455	T138	7/23/08 5:15	3.000	7/26/2008 5:30	72:15 :00	1524	0.757	0.87

Hanjin Philadelphia	282.10	4367	T138	7/26/08 5:15	4.000	7/28/2008 17:35	60:20 :00	1524	0.757	0.87
Hanjin Miami	300.00	7455	T138	7/30/08 5:15	7.392	8/1/2008 20:45	63:30 :00	1524	0.757	0.87
Hanjin Boston	300.08	7455	T138	8/6/08 14:40	5.028	8/8/2008 20:35	53:55 :00	1524	0.757	0.87
Xin Qing Dao	279.90	5668	T138	8/11/08 15:20	8.576	8/13/2008 18:10	50:50 :00	1524	0.757	0.87
Hanjin Baltimore	300.07	7455	T138	8/20/08 5:10	4.785	8/22/2008 6:55	49:45 :00	1524	0.757	0.87
Xin Tian Jin	279.60	5668	T138	8/25/08 0:00	5.212	8/28/2008 7:40	79:40 :00	1524	0.757	0.87
Hanjin Phoenix	282.10	4367	T138	8/30/08 5:05				1524	0.757	0.87
Penang Senator	294.10	4545	T140	2/29/08 15:00	7.590	3/2/2008 6:35	39:35 :00	1524	0.757	0.87
CSC Los Angeles	277.30	5762	T140	3/8/08 5:10	6.764	3/11/2008 6:35	73:25 :00	1524	0.757	0.87
Hanjin Praha	282.10	4367	T140	3/14/08 23:30	4.656	3/16/2008 20:35	45:05 :00	1524	0.757	0.87
Xin Da Lian	279.60	5668	T140	3/19/08 15:15	2.625	3/22/2008 6:55	63:40 :00	1524	0.757	0.87
Hanjin Philadelphia	282.10	4367	T140	3/22/08 6:15	4.375	3/24/2008 6:55	48:40 :00	1524	0.757	0.87
Hanjin Dallas	300.04	7455	T140	3/26/08 15:15	3.326	3/29/2008 6:45	63:30 :00	1524	0.757	0.87
Hanjin Phoenix	282.10	4367	T140	3/29/08 23:05	4.663	3/31/2008 19:30	44:25 :00	1524	0.757	0.87
Xin Yan Tian	279.60	5668	T140	4/3/08 15:00	4.590	4/6/2008 20:45	77:45 :00	1524	0.757	0.87
Xin Lian Yun Gang	279.60	5668	T140	4/8/08 5:10	6.417	4/10/2008 20:30	63:20 :00	1524	0.757	0.87
Hanjin Praha	282.10	4367	T140	4/14/08 15:10	10.587	4/16/2008 6:35	39:25 :00	1524	0.757	0.87
Hanjin Yantian	300.07	7455	T140	4/25/08 5:15	5.410	4/27/2008 20:40	63:25 :00	1524	0.757	0.87
Hanjin Baltimore	300.07	7455	T140	4/30/08 15:05	6.997	5/3/2008 11:40	68:35 :00	1524	0.757	0.87
Hanjin Dallas	300.04	7455	T140	5/7/08 15:00	3.003	5/10/2008 6:45	63:45 :00	1524	0.757	0.87
Hanjin Pretoria	282.10	4367	T140	5/10/08 15:05	6.372	5/12/2008 11:40	44:35 :00	1524	0.757	0.87
Hanjin Miami	300.00	7455	T140	5/17/08 0:01	14.635	5/19/2008 18:35	66:34 :00	1524	0.757	0.87
Hanjin Phoenix	282.10	4367	T140	5/31/08 15:15	4.024	6/2/2008 6:15	39:00 :00	1524	0.757	0.87
Xin Da Lian	279.60	5668	T140	6/4/08 15:50	6.628	6/7/2008 20:40	76:50 :00	1524	0.757	0.87
Hanjin Baltimore	300.07	7455	T140	6/11/08 6:55	6.941	6/13/2008 22:05	63:10 :00	1524	0.757	0.87
Hanjin Dallas	300.04	7455	T140	6/18/08 5:30	6.403	6/20/2008 20:40	63:10 :00	1524	0.757	0.87
Hanjin Philadelphia	282.10	4367	T140	6/24/08 15:10	1.993	6/26/2008 6:00	38:50 :00	1524	0.757	0.87
Hanjin Miami	300.00	7455	T140	6/26/08 15:00	5.594	6/28/2008 20:30	53:30 :00	1524	0.757	0.87

Hanjin Boston	300.08	7455	T140	7/2/08 5:15	5.997	7/4/2008 20:05	62:50 :00	1524	0.757	0.87
Hanjin Pretoria	282.10	4367	T140	7/8/08 5:10	1.750	7/9/2008 20:25	39:15 :00	1524	0.757	0.87
Hanjin Yantian	300.07	7455	T140	7/9/08 23:10	4.264	7/12/2008 7:00	55:50 :00	1524	0.757	0.87
Hanjin Wilming ton	289.50	4024	T140	7/14/08 5:30	2.403	7/16/2008 6:40	49:10 :00	1524	0.757	0.87
Hanjin Baltimor e	300.07	7455	T140	7/16/08 15:10	2.993	7/19/2008 6:55	63:45 :00	1524	0.757	0.87
Hanjin Praha	282.10	4367	T140	7/19/08 15:00	4.007	7/21/2008 17:30	50:30 :00	1524	0.757	0.87
Xin Yan Tian	279.60	5668	T140	7/23/08 15:10	6.021	7/27/2008 20:15	101:0 5:00	1524	0.757	0.87
Xin Yang Zhou	263.20	4051	T140	7/29/08 15:40	3.563	7/30/2008 20:40	29:00 :00	1524	0.757	0.87
Hanjin Phoenix	282.10	4367	T140	8/2/08 5:10	6.007	8/4/2008 6:20	49:10 :00	1524	0.757	0.87
Xin Xia Men	279.90	5668	T140	8/8/08 5:20	1.413	8/9/2008 6:25	25:05 :00	1524	0.757	0.87
Hanjin Pretoria	282.10	4367	T140	8/9/08 15:15	3.997	8/11/2008 6:25	39:10 :00	1524	0.757	0.87
Hanjin Yantian	300.07	7455	T140	8/13/08 15:10	2.993	8/15/2008 20:40	53:30 :00	1524	0.757	0.87
Hanjin Praha	282.10	4367	T140	8/16/08 15:00	4.240	8/18/2008 7:05	40:05 :00	1524	0.757	0.87
Xin Chang Shu	279.90	5668	T140	8/20/08 20:45	6.354	8/23/2008 19:30	70:45 :00	1524	0.757	0.87
Hanjin Dallas	300.04	7455	T140	8/27/08 5:15		8/30/2008 6:30		1524	0.757	0.87

REFERENCES

- AAPA (2009). Port Industry Statistics, American Association of Port Authorities.
- Abrahamson, N. (1999). RSPM - Spectral Matching Program.
- Abrahamson, N. (2000). Effects of rupture directivity on probabilistic seismic hazard analysis. Proceedings of the 6th International Conference on Seismic Zonation, Palm Springs, CA, Earthquake Engineering Research Institute (EERI).
- Abrahamson, N. and W. Silva (1997). "Empirical Response Spectral Attenuation Relations for Shallow Crustal earthquakes." Sesmological Research Letters **68**(1): 94-127.
- Abrahamson, N. and W. Silva (2008). "Summary of the Abrahamson & Silva NGA Ground-Motion Relations." Earthquake Spectra **24**(1): 67-97.
- Ak, A. (2008). Berth and Quay Crane Scheduling: Problems, Models, and Solution Methods. PhD, Georgia Institute of Technology.
- Algermissen, S. T. and D. M. Perkins (1976). A probabilistic estimate of maximum acceleration in rock in the contiguous United States, U.S. Geological Survey Open-File Report 76-416: 45 pp.
- American Society of Civil Engineers (2000). Prestandard and commentary for the seismic rehabilitation of buildings. FEMA Publication 356. Reston, Virginia, ASCE.
- Andrews, D. C. A. and G. R. Martin (2000). Criteria for Liquefaction of Silty Soils. Proceedings of the 12th World Conference on Earthquake Engineering, Auckland, New Zealand.
- Applied Technology Council (1978). Tentative Provisions for the Development of Seismic Regulations for Buildings. A. T. Council. Redwood City, NSF 78-8.
- Applied Technology Council (1996). Seismic Evaluation and retrofit of concrete buildings. ATC-40. Redwood City, California, Applied Technology Council.

- Applied Technology Council (1997). NEHRP commentary on the guidelines for the seismic rehabilitation of buildings. FEMA Publication 274. Redwood City, California, Applied Technology Council.
- Applied Technology Council (1997). NEHRP Guidelines for the Seismic Rehabilitation of Buildings. FEMA Publication 273. Redwood City, California, Applied Technology Council.
- Applied Technology Council (2006). Next-Generation Performance-Based Design Guidelines: Program Plan for New and Existing Buildings. H. S. FEMA, Prepared by Applied Technology Council.
- ASCE (2005). ASCE 7-05 Minimum Design Loads for Buildings and Other Structures. Reston, VA, American Society of Civil Engineers.
- ASCE (2011). Seismic Design of Pile-Supported Piers and Wharves, To be Published, American Society of Civil Engineers: 80.
- Associated Press (2010). Haiti's port system chokes supply lines and commerce. St. Petersburg Times. St. Petersburg, McClatchy Newspapers.
- Baker, J. W. and N. Jayaram (2008). "Correlation of Spectral Acceleration Values from NGA Ground Motion Models." Earthquake Spectra **24**(1): 299-317.
- BBC News (2010) "Haiti port opening raises hopes for quake victims." February 2010 2010.
- Bierwirth, C. and F. Meisel (2009). "A survey of berth allocation and quay crane scheduling problems in container terminals." European Journal of Operations Research **202**(3): 615-627.
- Boore, D. M. and G. M. Atkinson (2008). "Ground-Motion Prediction Equations for the Average Horizontal Component of PGA, PGV, and 5%-Damped PSA at Spectral Periods between 0.01 s and 10 s." Earthquake Spectra **24**(1): 99-138.
- Boore, D. M., J. Gibbs, W. B. Joyner, J. Tinsley and D. Ponti (2003). "Estimated ground motion from the 1994 Northridge California earthquake at the site of the Interstate

- 10 and La Cienega Boulevard bridge collapse." Seismological Society of America **93**(6): 2737-2751.
- Boore, D. M., W. B. Joyner and T. E. Fumal (1997). "Equations for estimating horizontal response spectra and peak acceleration from western North American earthquakes: A summary of recent work." Seismological Research Letters **68**(1): 128-153.
- Boore, D. M., W. B. Joyner and T. E. Fumal (1997). "Equations for Estimating Horizontal Response Spectra and Peak Acceleration from western North American Earthquakes: A summary of recent work." Seismological Research Letters **68**(127): 40 pp.
- Boulanger, R. and I. M. Idriss (2006). "Liquefaction Susceptibility Criteria for Silts and Clays." ASCE, Journal of Geotechnical and Geoenvironmental Engineering **132**(11).
- Boulanger, R. W., B. L. Kutter, D. W. Wilson and C. J. Curras (1999). "Seismic soil-pile structure interaction experiments and analyses." Journal of Geotechnical and Geoenvironmental Engineering **125**: 750-759.
- Brackman, E. (2009). Performance tools for piles and pile-to-wharf connections, M.S. Thesis, University of Washington.
- Bray, J. D. and R. B. Sancio (2006). "Assessment of the Liquefaction Susceptibility of Fine-Grained Soils." ASCE, Journal of Geotechnical and Geoenvironmental Engineering **132**(9).
- California State Land Commission (2010). California Code of Regulations, Part 2, California building Code, Chapter 31F, Title 24 (Marine Oil Terminal Engineering and Maintenance Standards (MOTEMS)).
- Campbell, K. W. (1997). "Empirical near-source attenuation relationships for horizontal and vertical components of peak ground acceleration, peak ground velocity, and

- pseudo-absolute acceleration response spectra." Seismological Research Letters **68**(1): 154-179.
- Campbell, K. W. and Y. Bozorgnia (2003). "Updated near-source ground motion (attenuation) relations for the horizontal and vertical components of peak ground acceleration and acceleration response spectra." Bulletin of the Seismological Society of America **93**(1): 314-331.
- Campbell, K. W. and Y. Bozorgnia (2008). "NGA ground motion model for the geometric mean horizontal component of PGA, PGV, PGD and 5% damped linear elastic response spectra for periods ranging from 0.01 to 10s." Earthquake Spectra **24**(1): 139-171.
- Canonaco, P., P. Legato, R. Mazza and R. Musmanno (2007). "A queuing network model for the management of berth crane operations." Computers and Operations Research **35**(8): 2432-2446.
- Chang, S., M. Shinozuka and J. E. Moore (2000). "Probabilistic earthquake Scenarios: Extending Risk Analysis Methodologies to Spatially Distributed Systems." Earthquake Spectra **16**(3): 557-572.
- Chiou, B., R. Darragh, N. Gregor and W. Silva (2008). "NGA Project Strong-Motion Database." Earthquake Spectra **24**(1): 23-44.
- CNN News (2010) "Haiti peir opens, road laid into Port-au-Prince." CNN World.
- Cornell, C. A. (1968). "Engineering Seismic Risk Analysis." Bulletin of Seismology I Soc. of America **58**: 1583-1606.
- Dafalias, Y. F. and M. T. Manzari (2004). "Simple Plasticity Sand Model Accounting for Fabric Change Effects." Journal of Engineering Mechanics: pp. 662-634.
- Deierlein, G., H. Krawinkler and C. A. Cornell (2003). A framework for performance-based earthquake engineering. 2003 Pacific Conference on Earthquake Engineering. Christchurch, New Zealand.

- DesRoches, R. D., M. Comerio, M. Eberhard, W. Mooney and G. Rix (2011). "Overview of the 2010 Haiti Earthquake." Earthquake Spectra **27**(S1): 1-21.
- Earthquake Engineering Research Institute (EERI) (1990). Earthquake Reconnaissance Report. Supplement to Volume 6 of Earthquake Spectra. El Cerrito, Oakland, CA. **Volume 90-01**.
- Ellington, S. (2010). Conversation about PVD Costs. G. Rix, Georgia Institute of Technology.
- Ellingwood, B. R. and A. H.-S. Ang (1974). "Risk-based evaluation of design criteria." Journal of the Structural Division **100**(9): 1771-1778.
- Federal Emergency Management Agency (FEMA) (2003). Multi-hazard loss estimation methodology, Earthquake Model. HAZUS-MH MR4 Technical Manual. Washington, DC.
- Feild, E. H., T. H. Jordan and C. A. Cornell (2009). IM Event Set Calculator. OpenSHA, University of Southern California.
- FEMA (2003). HAZUS MH-MR4 Technical Manual. Washington, DC, Department of Homeland Security.
- Field, E. H. (2000). "A modified ground-motion attenuation relationship for southern California that accounts for detailed site classification and a basin-depth effect." Bulletin of the Seismological Society of America **90**(6b): 209-221.
- Gallagher, P. M. (2000). Passive site remediation for mitigation of liquefaction risk, Virginia Polytechnic Institute.
- Gallagher, P. M. and J. K. Mitchell (2002). "Influence of colloidal silica grout on liquefaction potential and cyclic undrained behavior of loose sand." Soil Dynamics and Earthquake Engineering **22**(1): 1017-1026.
- Gazetas, G. and N. Makris (1991). "Dynamic pile-soil-pile interaction Part I: Analysis of axial vibration." Earthquake Engineering and Structural Dynamics **20**: 115-132.

- Green, R., S. Olson, B. Cox, G. Rix, E. Rathje, J. Bachhuber, J. French, S. Lasley and N. Martin (2011). "Geotechnical Aspects of Failures at Port-au-Prince during the 12 January 2010 Haiti Earthquake." Earthquake Spectra **27**(1): 43-66.
- Hamada, M., R. Isoyama and K. Wakamatsu (1996). "Liquefaction-induced ground displacement and its related damage to lifeline facilities." Soils and Foundations (special): 81-97.
- Howell, R., E. Rathje, R. Kamai and W. B. Ross (2011). "Centrifuge modeling of prefabricated vertical drains for liquefaction remediation." to be published in ASCE Journal of Geotechnical and Geoenvironmental Engineering.
- Ishihara, K. (1996). Soil Behaviour in Earthquake Geotechnics. New York, NY, Oxford University Press Inc.
- Itasca (2011). FLAC - Fast Lagrangian Analysis of Continua, User's Manual. Minneapolis, Minnesota, Itasca Consulting Group.
- Jacobs, L. (2010). Shake table experiments for the determination of the seismic response of jumbo container cranes. Ph.D. Thesis, Civil and Environmental Engineering, Georgia Institute of Technology.
- Jayaram, N. and J. W. Baker (2009). Correlation model for spatially distributed ground-motion intensities. Earthquake Engineering and Structural Dynamics, John Wiley & Sons, Ltd.
- Jayaram, N. and J. W. Baker (2010). "Efficient Sampling and data reduction techniques for probabilistic seismic lifeline risk assessment." Earthquake Engineering and Structural Dynamics **39**: 1109-1131.
- Johnson, R. A. (1992). Statistics: Principles and Methods. New York, J. Wiley.
- Kia, M., E. Shayan and F. Ghotb (2000). "The importance of information technology in port terminal operations." International Journal of Physical Distribution & Logistics Management **30**(3/4): 331-344.

- Kia, M., E. Shayan and F. Ghotb (2002). "Investigation of port capacity under a new approach by computer simulation." Computers and Industrial Engineering **42**: 533-540.
- Kosbab, B. (2010). Seismic Performance Evaluation of Port Container Cranes Allowed to Uplift. Ph.D. Thesis, Civil and Environmental Engineering, Georgia Institute of Technology.
- Kosbab, B., L. Jacobs and R. DesRoches (2009). Analysis and Testing of Container Cranes under EQ Loads. Technical Council on Lifeline Earthquake Engineering (TCLEE) Conference 2009. Oakland, CA.
- Kramer, S. L. (2008). Performance-Based Earthquake Engineering: Opportunities and Implications for Geotechnical Engineering Practice. Geotechnical Earthquake Engineering and Soil Dynamics IV. Sacramento, CA, ASCE.
- Kramer, S. L. and R. A. Mitchell (2006). "Ground Motion Intensity Measures for Liquefaction Hazard Evaluation." Earthquake Spectra **22**(2): 413-438.
- Kuo, T., W. Huang, S. Wu and P. Cheng (2006). "A case study of inter-arrival time distributions of container ships." Journal of Marine Science and Technology **14**(3): 155-164.
- Lai, C. and G. Rix (1998). Simultaneous Inversion of Rayleigh Phase velocity and Attenuation for Near-Surface Site Characterization. Atlanta, GA, Georgia Institute of Technology, School of Civil and Environmental Engineering, Report No. GIT-CEE/GEO-98-2
- Lehman, D., C. Roeder, A. Jellin and E. Brackman (2009). Improving the Seismic Performance of Pile-to-Wharf Connections. Technical Council on Lifeline Earthquake Engineering (TCLEE) Conference 2009. Oakland, CA.
- Liftech Inc. (2008). "On the Mend". Oakland, CA.

- Lintner (1965). "The valuation of risk assets and the selection of risky investments in stock portfolios and capital budgets." The Review of Economics and Statistics **47**(1): 13-37.
- Lysmer and Kuhlemeyer (1969). "Finite dynamic model for infinite media." Journal of Engineering Mechanics Division, ASCE **95**(1).
- Makris, N. and G. Gazetas (1992). "Dynamic pile-soil-pile interaction Part II: Lateral and seismic response." Earthquake Engineering and Structural Dynamics **21**: 145-162.
- Marine Exchange of Southern California (2008). Monthly Database Access Reports.
- Martin, G. R. and M. Lew, Eds. (1999). Recommended Procedures for Implementation of DMG special Publication 117, Guidelines for Analyzing and Mitigating Liquefaction Hazards in California. Southern California Earthquake Center, University of Southern California.
- McGann, C., H. Shin, P. Arduino and P. Machenzie-Helnwein (2011). Effective Stress Site Response Analysis of a Layered Soil Column, University of Washington.
- McKenna, F. and C. McGann (2010). OpenSees Laboratory,
<http://nees.org/resources/openseeslab>.
- McKenna, F. and G. P. Rodgers (2010). OpenSees Source Code / Not for Direct Execution.
- Na, U. J., S. R. Chaudhuri and M. Shinozuka (2008). "Probabilistic assessment for seismic performance of port structures." Soil Dynamics and Earthquake Engineering(28): 147-158.
- Na, U. J. and M. Shinozuka (2009). "Simulation-based seismic loss estimation of seaport transportation system." Reliability Engineering and System Safety **84**: 722-731.
- NEHRP (2009). Research Required to Support Full Implementation of Performance-Based Seismic Design. US Department of Commerce. Washington, D.C., National Institute of Standards and Technology (NIST).

- Newmark, N. and W. J. Hall (1982). Engineering Monographs on Earthquake Criteria, Structural Design, and Strong Motion Records. Earthquake Spectra and Design. Oakland, CA, Earthquake Engineering Research Institute. **3**.
- Nigram and Jennings (1969). "Calculation of Response Spectra from Strong-Motion Earthquake Records." Bulletin of Seismological Society of America **59**(2): 909-922.
- NIST (2011). NIST/SEMATECH e-Handbook of Statistical Methods, <http://www.itl.nist.gov/div898/handbook/>. [accessed 8/9/11].
- Pachakis, D. and A. S. Kiremidjian (2004). "Estimation of Downtime-Related Revenue Losses in Seaports Following Scenario Earthquakes." Earthquake Spectra **20**(2): 427-449.
- Park, J., P. Bazzurro and J. Baker (2007). Modeling spatial correlation of ground motion intensity measures for regional seismic hazard and portfolio loss estimation. Tenth International Conference on Application of Statistic and Probability in Civil Engineering (ICASP10), Tokyo, Japan.
- PIANC (2001). Seismic Design Guidelines for Port Structures. Tokyo, A. A. Balkema Publishers.
- Port of Long Beach. (2010). "TEUs Archive Since 1995." Retrieved 10/11, 2010, from http://www.polb.com/economics/stats/teus_archive.asp.
- Port of Los Angeles (2007). The Port of Los Angeles Seismic Code for Port Structures. Port of Los Angeles and ASCE. **POLA Code 07**.
- Port of Los Angeles. (2010, 9/13/2010). "Port of Los Angeles Container Statistics 2008." Retrieved 10/11, 2010, from http://www.portoflosangeles.org/stats/stats_2008.htm.
- Porter, K. (2006). An Overview of PEER's Performance-Based Earthquake Engineering Methodology. 9th International Conference on Applications of Statistics and Probability in Civil Engineering (ICASP9). San Francisco.

- Rathje, E. (2010). Conversation about Vertical Drains. A. Vytiniotis. Ph D Thesis, Massachusetts Institute of Technology.
- Reuters. (2011, 3/16/2011). "Japanese earthquake could cost \$3.4 billion a day in lost seaborne trade." Retrieved 3/18, 2011, from http://www.porttechnology.org/news/japanese_earthquake_could_cost_3.4_billion_a_day_in_lost_trade.
- Reuters. (2011). "Some Japanese port re-opened; others operational by end of today." Retrieved 3/18, 2011, from http://www.porttechnology.org/news/some_japanese_ports_re_open_within_the_next_few_days?utm_source=Port+Technology+Newsletter&utm_campaign=356be6657c-PortTechnology_Newsletter17_03_2011&utm_medium=email.
- Riddle, R. J. (2010) "First Person: Reopening the port at Port-au-Prince." www.army.mil, July 28, 2010.
- Rubinstein and Kroese (2007). Simulation and the Monte Carlo Method. Hoboken, New Jersey, John Wiley & Sons, Inc.
- Sadigh, K., C. Y. Chang, J. A. Egan, F. Makdisi and R. R. Youngs (1997). "Attenuation relationships for shallow crustal earthquakes based on California strong motion data." Seismological Research Letters **68**(1): 180-189.
- Scharks, T., A. Bostrom, L. Reimann-Garetson and D. G. Rix "Risk Decision making and Seismic Risk Preparedness at North American Seaports: Analysis of a System-Wide Survey," Submitted to Earthquake Spectra, August 2011.
- Schleiffarth, L. (2008). Survey of global Container Crane Sizes. Atlanta, GA, Georgia Institute of Technology.
- SEAOC (1959). Recommended Lateral Force Requirements and Commentary (SEAOC Blue Book). Sacramento, California, Structural Engineers Association of California.

- SEAOC (1995). Vision 2000: Performance-Based Seismic Engineering of Buildings. S. E. A. o. California. Sacramento, California.
- Seed, R. B., K. O. Cetin, R. E. S. Moss, Krammerer, J. Wu, Pestana, Riemer, Sancio, J. D. Bray, R. E. Kayen and Faris (2003). Recent Advances in Soil Liquefaction Engineering: A Unified Consistent Framework
26th Annual ASCE Los Angeles Section Spring Seminar. Long Beach, California.
- Seeds, N. (2011). Conversation about Delay Threshold. G. Rix. Atlanta, GA, Georgia Institute of Technology.
- Shafieezadeh, A. (2011). Seismic Vulnerability Assessment of Wharf Structures. Ph.D. Thesis, Georgia Institute of Technology.
- Shafieezadeh, A., R. D. DesRoches, S. D. Werner and G. J. Rix (2009). Seismic Response of Pile-Supported Container Wharves. Technical Council on Lifeline Earthquake Engineering (TCLEE) Conference 2009. Oakland, CA.
- Shipping China (2009). ZPMC's era of Heavy Industry. Shanghai, China, Kaiji Press Co., Ltd.
- Soderburg, E., J. Hsieh and A. Cix (2009). Seismic guidelines for Container Ports. TCLEE 2009 Conference. Oakland, CA.
- Spencer, L. (2010). Evaluation of Colloidal Silicia Gel as a Method to Mitigate Liquefaction. Ph.D. Thesis, Georgia Institute of Technology.
- Spudich, P., W. B. Joyner, A. G. Lindh, D. M. Boore, B. M. Margaris, and J. B. Fletcher (1999). "SEA99: A revised ground motion prediction relation for use in extensional tectonic regimes." Bulletin of the Seismological Society of America **89**(1): 1156-1170.
- Sullivan, W., E. Wicks and J. Luxhoj (2003). Engineering Economy. Upper Saddle River, NJ, Prentice Hall.
- Taylor, C., S. Werner and S. Jakubowski (2001). "Walkthrough Method for Catastrophe Decision Making." Natural Hazards Review **2**(4): 193-202.

- Taylor, J. (2010). Vital hours for rescuers as supplies trickle in. The Independent. London.
- Towhata and K. Ishihara (1985). Modeling soil behavior under principle axes rotation. Fifth International Conference on Numerical Methods in Geomechanics: 523-530.
- USGS (2003). USGS ShakeMap.
- USGS (2004). "USGS Combined."
- Varun, V. (2010). A non-linear dynamic macroelement for soil structure interaction analyses of piles in liquefiable sites. Ph.D. Thesis, Georgia Institute of Technology.
- Varun, V. and D. Assimaki (2008). A nonlinear dynamic macroelement for soil-structure interaction analyses of pile-supported wharfs. Geotechnical Earthquake Engineering and Soil Dynamics IV, Special Publication No. 181. Reston, VA, American Society of Civil Engineers: 10 pp.
- Vytiniotis, A. (2005). Numerical Simulation of the Response of Sandy Soils Treated with Pre-Fabricated Vertical Drains. Master of Science, Massachusetts Institute of Technology.
- Vytiniotis, A. (2010). Effect of Apex correction and return to bounding surface correction schemes. Boston, MA, Massachuttes Institute of Technology: 8.
- Vytiniotis, A., A. Whittle and E. Kausel (2011). Effects of Seismic Motion Characteristics on Cyclic Mobility and Liquefaction. 5th International Conference on earthquake geotechnical Engineering. Santiago, Chile.
- Werner, S. and G. Rix (2008). Wharf fragility models for container ports. Proceedings of 6th Annual NEES Meeting, The Value of Earthquake Engineering, Portland, OR.
- Werner, S. and C. Taylor (2004). Seismic-Risk-Reduction Planning evaluations for Wharf and Embankment Strengthening Program, Port of Oakland. Oakland, California, Seismic Systems & Engineering Consultants.

- Werner, S. D., Ed. (1998). Seismic Guidelines for Ports. Reston, VA, American Society of Civil Engineers.
- Werner, S. D. and W. C. Cooke (2009). Wharf Repair Estimates for Use in Demonstration Seismic Risk Analysis of Port Systems Oakland CA, Seismic Systems & Engineering Consultants.
- Werner, S. D. and S. E. Dickenson (1996). Hyogo-ken-Nanbu Earthquake of January 17, 1995: A Post-earthquake Reconnaissance of Port Facilities. Reston, VA, American Society of Civil Engineers.
- Werner, S. D., N. McCullough, W. Bruin, A. Augustine, G. Rix, B. Crowder and J. Tomblin (2011). "Seismic Performance of Port de Port-au-Prince during the Haiti Earthquake and Post-Earthquake Restoration of Cargo Throughput." Earthquake Spectra **27**(1): 387-410.
- WGCEP (2008). The Uniform California Earthquake Rupture Forecast, Version 2 (UCERF 2). U.S. Geological Survey Open File Report 2007-1437 and California Geological Survey Special Report 203.
- WGCEP. (2008). The Uniform California Earthquake Rupture Forecast, Version 2 (UCERF 2). U.S. Geological Survey Open File Report 2007-1437 and California Geological Survey Special Report 203.
- Youd, T. L., I. M. Idriss, Andrus, Arango, Christian, R. Dobry, W. D. Finn, Harder, Hynes, K. Ishihara, L. Koester, S. Liao, Marcuson, Martin, J. K. Mitchell, Moriwaki, Power, Robertson, R. B. Seed and K. Stokoe (2001). "Liquefaction Resistance of Soils: Summary report from the 1996 NCEER and 1998 NCEEF/NSF Workshops on the Evaluation of Liquefaction Resistance of Soils." ASCE, Journal of Geotechnical and Geoenvironmental Engineering **127**(10).